Chiral Perturbation Theory for Lattice QCD

H A B I L I T A T I O N S S C H R I F T

zur Erlangung der Lehrbefähigung
für das Fach Theoretische Physik

vorgelegt dem Fakultätsrat der
Mathematisch-Naturwissenschaftlichen Fakultät I
der Humboldt-Universität zu Berlin

von
Dr. Oliver Bär
geboren am 28.12.1967 in Frankfurt am Main

Prof. Dr. Dr. h.c. Christoph Markschies
Präsident der der Humboldt-Universität zu Berlin

Prof. Dr. Andreas Herrmann
Dekan der Mathematisch-Naturwissenschaftlichen Fakultät I

Berlin, den 21.07.2010

Gutachter:
1. Prof. Dr. M. Golterman
2. Prof. Dr. H. Leutwyler
3. Prof. Dr. U. Wolff

Hinweis

Diese Version stimmt mit der beurteilten Habilitationsschrift überein. Es wurden lediglich einige Layoutänderungen vorgenommen, um den Anforderungen der Universitätsbibliothek der Humboldt Universität zu genügen.

Remark

This version agrees with the assessed Habilitation thesis. It differes from the original version only by some minor changes in the layout in order to comply with the requirements of the library at the Humboldt University.

Zusammenfassung

Diese Schrift enthält die schriftlichen Habilitationsleistungen gemäß §2 Absatz (1), der Habilitationsordnung der Mathematisch-Naturwissenschaftlichen Fakultät I der Humboldt Universität zu Berlin. Im einzelnen sind dies

- eine Monographie (in englischer Sprache) mit dem Titel *Chiral Perturbation Theory for Lattice QCD*,
- die Nachdrucke von dreizehn Veröffentlichungen, publiziert in internationalen Fachjournalen,
- eine Erklärung zum eigenen Anteil an den Veröffentlichungen (gemäß §2 Absatz (2) Satz 2 der Habilitationsordnung).

Schlagwörter:
Chirale Störungstheorie, Gitter-QCD, Effektive Feldtheorie, Gitterartifakte

Abstract

This composition contains the written 'Habilitationsleistungen' required according to the Habilitation statutes §2 article (1) of the Faculty of Mathematics and Natural Sciences I, Humboldt University, Berlin. It contains

- the monograph *Chiral Perturbation Theory for Lattice QCD*,
- reprints of thirteen papers, published in international journals,
- a statement about my own contributions to the published papers (according to the Habilitation statutes §2 article (2) sentence 2).

Keywords:
Chiral Perturbation Theory, Lattice QCD, Effective Field Theory, Lattice artifacts

Contents

Part I.

List of publications and statements about own contributions

List of publications

The following is a list of the publications which are handed in as part of the written *Habilitationsleistung* according to the Habilitation statutes §2 article (1) sentence 1b. Each entry is followed by a brief description of my own contributions to the projects, as required by the Habilitation statutes §2 article (2) sentence 2. The label in front of each entry coincides with the one used in the monograph in part II to refer to these papers.

[1] **Simulations with different lattice Dirac operators for valence and sea quarks,**
with G. Rupak and N. Shoresh, Phys. Rev. D **67**, 114505 (2003).

The idea for this project emerged from discussions I had with N. Shoresh. All calculations were done independently by myself and N. Shoresh and finally cross-checked by G. Rupak. The first draft for the paper was written by N. Shoresh and finalized by myself.

[2] **Chiral perturbation theory at $O(a^2)$ for lattice QCD,**
with G. Rupak and N. Shoresh, Phys. Rev. D **70**, 034508 (2004).

This is a follow-up project of [1]. All calculations were independently done by all three collaborators. I wrote the first draft and the final version of the paper.

[3] **Chiral perturbation theory at non-zero lattice spacing,**
Nucl. Phys. Proc. Suppl. **140** (2005) 106.

These are the proceedings of a plenary talk I gave at *Lattice 2004*. It provides a review of chiral perturbation theory for lattice QCD which summarizes the status in 2004. Preparing the talk and writing the proceedings was done completely by myself.

[4] **Twisted-mass QCD, O(a) improvement and Wilson chiral perturbation theory,**
with S. Aoki, Phys. Rev. D **70**, 116011 (2004).

The idea for this project emerged from discussions with S. Aoki. Our contributions were complimentary: S. Aoki contributed the lattice QCD part (culminating in section II of the paper), I contributed the WChPT part (sections III and IV of the paper). All parts were independently cross-checked by each other. I wrote the first draft and final version of the entire paper.

[5] Chiral perturbation theory for staggered sea quarks and Ginsparg-Wilson valence quarks,
with C. Bernard, G. Rupak and N. Shoresh, Phys. Rev. D **72**, 054502 (2005).

This is a follow-up project of [1, 2]. The idea for this project emerged from discussions I and N. Shoresh had with C. Bernard while he was visiting MIT in fall 2002. The contributions were complimentary: N. Shoresh and I contributed the construction of the mixed action chiral lagrangian (section II and the appendix of the paper). I wrote the draft of these parts for the paper. C. Bernard contributed the calculation of the pion masses and the decay constant (section III of the paper). He also wrote this part of the paper. All calculations were independently cross-checked by G. Rupak.

[6] Pseudo scalar meson masses in Wilson chiral perturbation theory for 2+1 flavors,
with S. Aoki, T. Ishikawa and S. Takeda, Phys. Rev. D **73**, 014511 (2006).

Follow-up project of [2]. I contributed the construction of the chiral lagrangian and the power countings for 2+1 flavor. The calculation of the pseudo scalar masses was done primarily by S. Aoki's student S. Takeda and partly by T. Ishikawa. These calculations were cross-checked by S. Aoki and myself. I wrote the first draft and the final version of the paper.

[7] Vector meson masses in 2+1 flavor Wilson chiral perturbation theory,
with S. Aoki and S. Takeda, Phys. Rev. D **73**, 094501 (2006).

Follow-up project of [6]. I contributed the construction of the vector meson chiral lagrangian and the power countings. The calculation of the vector meson masses was done primarily by S. Takeda and independently checked by myself and S. Aoki. I wrote the first draft and the final version of the paper.

[8] Automatic O(a) improvement for twisted-mass QCD in the presence of spontaneous symmetry breaking,
with S. Aoki, Phys. Rev. D **74**, 034511 (2006).

Follow-up project of [4]. The contributions were again complimentary: S. Aoki contributed the lattice QCD part (culminating in section II of the paper), I contributed the WChPT part (section III of the paper). All parts were independently cross-checked by each other. I wrote the first draft and the final version of the entire paper.

[9] WChPT analysis of twisted-mass lattice data,
with S. Aoki Eur. Phys. J. A **31**, 481 (2007).

I had the idea for applying the results in [4, 8] to data generated by the European Twisted Mass Collaboration (ETMC). I did the main analysis of the data. I wrote the first draft and the final version of the paper. I also presented the results at the conference *Lattice 2005* and a Ringberg workshop in 2006.

[10] Pion scattering in Wilson chiral perturbation theory,
with S. Aoki and B. Biedermann, Phys. Rev. D **78**, 114501 (2008).

The idea of applying WChPT to pion scattering emerged in discussions with S. Aoki. I did most of the calculations together with my student B. Biedermann. The results were independently checked by S. Aoki. I wrote the first draft and the final version of the paper.

[11] The epsilon regime with Wilson fermions,
with S. Necco and S. Schaefer, JHEP **0903**, 006 (2009).

The idea for this project emerged from discussions with S. Schaefer. I did most of the conceptional work (power counting and epsilon expansion) and also did all calculations in the GSM* regime. These were independently cross-checked by S. Necco. I wrote the first draft and the final version of the paper. The numerical analysis was done by S. Schaefer who also wrote this part of the paper (section 5.2).

[12] Vector and Axial Currents in Wilson chiral perturbation theory,
with S. Aoki and S. Sharpe, Phys. Rev. D **80**, 014506 (2009).

I had the main idea that the renormalization condition for the lattice currents may induce additional lattice spacing corrections in the effective currents. All calculations were independently done by myself and by S. Aoki. S. Sharpe cross-checked the final results, in particular the calculation of the renormalization condition. I wrote the first draft of the paper which was finalized by S. Sharpe. I also prepared a poster that was presented at the conference *Lattice 2009*.

[13] The epsilon regime with twisted mass Wilson fermions,
with S. Necco and A. Shindler, JHEP **1004**, 053 (2010).

Follow-up project of [11]. The conceptual work generalizing the results of [11] to twisted masses was done by myself. The corrections in the GSM* were independently calculated by all three collaborators. I wrote the first draft of the paper, which was completed mainly by A. Shindler.

Part II.

Chiral perturbation theory for lattice QCD

1. Introduction

Lattice Quantum Chromodynamics (QCD) is popular mainly for two reasons. First of all, the replacement of continuous space-time by a discrete space-time grid ('lattice') provides a regulator that makes QCD ultraviolet finite and nonperturbatively well-defined. In fact, to date lattice QCD is the only nonperturbative definition of QCD. Secondly, the discrete formulation of QCD is well suited for nonperturbative computations of observables by numerical Monte Carlo simulations.

These numerical simulations of lattice QCD pose numerous 'technical problems'. One of the many obstacles one faces is the so-called *chiral extrapolation*. It refers to a limitation concerning the quark masses in an actual lattice simulation. Obviously, the values for the quark masses should be chosen according to their actual physical values. For various reasons this is out of reach, at least at the time these lines are written. The 'numerical cost' (i.e. computer time) of a simulation increases rapidly the smaller the quark masses are, and simulating the small up and down type quark masses is simply too demanding numerically. The standard workaround for this problem are simulations with various heavier quark masses than in nature followed by the (chiral) extrapolation of the results to the smaller physical quark masses.

This procedure raises the question about the quark mass dependence of the observables one is interested in. The standard tool one usually invokes is chiral perturbation theory (ChPT). This low-energy effective theory for QCD predicts the quark mass dependence of various physical quantities. Well-known examples are the following expressions for the pion mass and decay constant (in the 1-loop approximation for $N_f = 2$ and degenerate quark masses $m_u = m_d \equiv m$):

$$\frac{M_\pi^2}{2Bm} = 1 + \frac{2Bm}{32\pi^2 f^2} \ln \frac{2Bm}{\Lambda_3^2}\,, \qquad \frac{f_\pi}{f} = 1 - \frac{2Bm}{16\pi^2 f^2} \ln \frac{2Bm}{\Lambda_4^2}\,. \tag{1.1}$$

Although $f, B, \Lambda_{3,4}$ are unknown constants, the functional form of the quark mass dependence is a prediction of ChPT, in particular the nonanalytic logarithmic dependence. Therefore, ChPT seems to provide the necessary input for the chiral extrapolation of lattice QCD data.

As mentioned before, ChPT is a low-energy effective theory of QCD. Its predictions are expected to be reliable for sufficiently small quark masses. Hence, before using ChPT results one should make sure that ChPT is indeed applicable. Here the proof of the pudding is in the eating: one checks if the lattice data follow the predicted quark mass dependence. In particular, one looks for the logarithmic quark mass dependence because this is the characteristic prediction of ChPT that is not captured by a simple-minded polynomial ansatz. Once the lattice data shows the characteristic curvature of the chiral

logarithm one gains confidence that ChPT can be applied.

There is a potential problem with this line of argument. The construction of ChPT is based on the characteristic symmetry properties of *continuum* QCD. Unfortunately, lattice QCD does not respect all of these symmetries. In particular, the formulations with 'traditional' lattice fermions (Wilson and staggered) compromise chiral symmetry in some respects, and this symmetry is at the heart of ChPT. Consequently, the continuum limit of the lattice data has to be taken first before results like the ones in (1.1) can be employed for the chiral extrapolation.

However, there are various reasons why one may like to reverse this order. For example, as long as data for only one lattice spacing is available the continuum limit cannot be taken. Performing the chiral extrapolation first is also simpler in practice. Whatever the reasons might be, the reversed order requires to formulate ChPT for lattice QCD, taking into account the particular breaking of chiral symmetry. Otherwise one introduces an uncontrolled error in the chiral extrapolation. Even worse, the modifications of the continuum ChPT results might be so severe that the lattice data are not described at all by the continuum results, and the chiral extrapolation cannot be performed.

The main idea for ChPT formulated for lattice QCD goes back to two papers [14, 15] published about a decade ago. Since then a lot has been learned about the chiral extrapolation at nonzero lattice spacing. Many formulae for masses, decay constants and other observables have been derived that include explicitly the contributions due to a nonvanishing lattice spacing. These formulae are the proper expressions one should use when the chiral extrapolation is performed before the continuum limit is taken.

The aim of this write-up is to provide an introduction to ChPT for lattice QCD. The focus is on the concepts and the method for the construction, not on reviewing all the results that have been derived so far. Wherever possible I present results for the simplest case only, namely ChPT for two quark flavors with a degenerate mass term. These are usually sufficient to explain and highlight the differences to continuum ChPT, but not necessarily the ones appropriate for actual data analysis. The main point here is to develop an understanding for the general features of ChPT at nonzero lattice spacing, those that hold universally and irrespectively of the particular lattice QCD formulation.

This write-up partly overlaps with two lecture notes, although the emphasis here is quite different. S. Sharpe's Nara lecture notes [16] provide a very readable introduction to continuum ChPT as well as the formulation for lattice QCD, although it focuses on Wilson fermions with a twisted mass term. M. Golterman's Les Houches lecture notes [17] covers continuum ChPT as well. In addition it provides a very accessible introduction to ChPT for lattice QCD, covering, among other topics, staggered fermions and mixed action theories. The reader interested in complementary presentations of the subject is urged to consult these two references.

This write-up is neither an introduction to continuum ChPT nor to lattice QCD. There are many useful lecture notes and reviews available that cover these subjects on various levels of depth. To give just a few examples the reader is referred to [18, 19, 20] for introductions to continuum ChPT. There are also quite a few text books on lattice QCD on the market [21, 22, 23]. However, giving these references should not suggest that the reader is expected to be an expert on both subjects. On the contrary, I sincerely

hope that a reader with a general knowledge of QCD and field theory will benefit from this introduction.

2. Spontaneous chiral symmetry breaking in QCD and ChPT

2.1. Spontaneous chiral symmetry breaking in QCD

Asymptotic freedom and *confinement* are the most prominent properties of QCD, the theory of the strong interaction between quarks and gluons. The first one refers to the running coupling constant $\alpha_s(Q^2)$ that becomes small for large momenta Q^2; and confinement commonly summarizes the fact that the particle spectrum of QCD consists of color singlet states (hadrons) and not of colored quarks.

Notwithstanding the importance of these two properties for explaining a variety of experimental observations, *spontaneous chiral symmetry breaking* in QCD plays an important rôle as well. For example, it explains why the lightest hadron, the pion with a mass of about 140 MeV, is so much lighter than, for instance, the ρ meson with a mass of 770 MeV. The quark content of both hadrons is the same, but the spins of the two quarks add up to zero in case of the pion and to one in case of the ρ meson. The spin-spin interaction, however, cannot explain the large mass difference. The mechanism at work behind the mass difference is the spontaneous breaking of chiral symmetry in QCD.

In order to discuss this let us consider QCD with $N_f = 3$ flavors, the up, down and strange quark. The heavier charm, bottom and top quarks do not play a relevant rôle in the following. The fermion part of the QCD lagrangian (in euclidean space-time) is

$$\mathcal{L}_{\text{QCD,quark}} = \overline{q}\,[\not{D} + M]\,q \tag{2.1}$$

$$= \overline{q}_L \not{D} q_L + \overline{q}_R \not{D} q_R + \overline{q}_L M q_R + \overline{q}_R M^\dagger q_L\,, \tag{2.2}$$

where $q_X = (q_{u,X}, q_{d,X}, q_{s,X})^T, X = L, R$ contains the chiral components of the three quark fields. The anti-quark fields are defined analogously and the decomposition into chiral components is obtained with the standard left- and right-handed projection operators. The mass matrix M contains the three quark masses, $M = \text{diag}(m_u, m_d, m_s)$, which we assume to be real and positive. In this case $M^\dagger = M$, but keeping $M^\dagger$ in (2.1) will be convenient later on.

The massless part of the lagrangian (2.1) is invariant under the transformations

$$\begin{aligned} q_L &\to L q_L\,, & \overline{q}_L &\to \overline{q}_L L^\dagger\,, \\ q_R &\to R q_R\,, & \overline{q}_R &\to \overline{q}_R R^\dagger\,, \end{aligned} \tag{2.3}$$

with L, R being elements of $\text{SU}(3)_{L,R}$. In other words, the symmetry group of massless

QCD is[1]

$$G = \mathrm{SU}(3)_L \times \mathrm{SU}(3)_R \,. \tag{2.4}$$

Of course, this symmetry is explicitly broken by a nonvanishing mass matrix. However, it is by now widely accepted that this symmetry is also *spontaneously* broken down to the diagonal subgroup

$$H = \mathrm{SU}(3)_{L=R} \,, \tag{2.5}$$

where $L = R$. This conviction is supported by a variety of experimental observations that can be explained by assuming the spontaneous symmetry breakdown and working out the consequences. The simplest is the aforementioned small pion mass. If all quark masses were zero the Goldstone theorem would predict eight massless Goldstone bosons. With quark masses sufficiently light such that the explicit symmetry breaking by the quark masses is small compared to the spontaneous breaking, the Goldstone bosons receive a mass that can be arbitrarily small compared to the typical hadron masses. So the small pion and (moderately small) kaon masses are naturally explained by their Goldstone boson character and small quark masses.

2.2. Chiral perturbation theory

The Goldstone boson character of the pions implies that their coupling is proportional to their momentum.[2] For example, pion scattering becomes weaker the smaller the exchanged momentum is. The weak coupling makes it possible to describe them perturbatively by a low-energy effective field theory, so-called chiral perturbation theory (ChPT) [24, 25, 26] This effective theory is given by an effective (chiral) lagrangian and effective operators. The key principle for their construction are the symmetries of the underlying theory one wishes to describe, since the effective theory must respect these symmetries. This requirement poses strong constraints on the allowed terms in the effective lagrangian. Further constraints come from the fact that we perform a derivative expansion in a low-energy effective theory. Both constraints are usually sufficient to end up with an effective theory that is useful in practice.

Let us demonstrate this for massless QCD. The Goldstone theorem tells us that the massless excitations (the Goldstone bosons) are described by fields 'living' in the coset space G/H. For G and H of the last section, G/H is isomorphic to SU(3), so the Goldstone bosons can be described by an SU(3) valued field $\Sigma(x)$. The physical pion, kaon and eta fields are contained in Σ according to

$$\Sigma = \exp\left(2i\pi/f\right), \tag{2.6}$$

[1] The symmetry group is even larger by two U(1) groups. One is baryon number while the other (axial) U(1) is anomalous. These groups are not essential in the following and we ignore them.

[2] For brevity we often use the term 'pion' to refer to all (pseudo) Goldstone bosons, including the kaons and the eta.

with

$$\pi = \frac{1}{\sqrt{2}} \begin{pmatrix} \frac{\pi^0}{\sqrt{2}} + \frac{\eta}{\sqrt{6}} & \pi^+ & K^+ \\ \pi^- & -\frac{\pi^0}{\sqrt{2}} + \frac{\eta}{\sqrt{6}} & K^0 \\ K^- & \overline{K}^0 & -\frac{2\eta}{\sqrt{6}} \end{pmatrix} . \tag{2.7}$$

The dimensionful constant f can be shown to be the pion decay constant (see below).

For the construction of the chiral lagrangian we need the transformation behaviour of Σ under the symmetries of the QCD lagrangian. Transformations in G act on Σ as

$$\Sigma \xrightarrow{G} L\Sigma R^\dagger \, . \tag{2.8}$$

The other relevant symmetries are O(4) invariance[3] and the two discrete symmetries parity (P) and charge conjugation (C), which are given by

$$\Sigma \xrightarrow{P} \Sigma^\dagger \, , \qquad \Sigma \xrightarrow{C} \Sigma^{\mathrm{T}} . \tag{2.9}$$

These transformation laws are most easily understood by inspecting (2.7) and noting that the Goldstone boson fields are pseudo scalars.

The chiral effective lagrangian is now constructed from the field Σ and its partial derivatives. It must be an O(4) scalar and a singlet under G, P and C. Restricting the number of derivatives to two there is only one term possible,

$$\mathcal{L}_2 = \frac{f^2}{4} \langle \partial_\mu \Sigma \partial_\mu \Sigma^\dagger \rangle \, . \tag{2.10}$$

The angled brackets are a short hand notation for taking the trace in flavor space, $\langle \ldots \rangle = \mathrm{tr}\{\ldots\}$. Although the structure of the term in $\mathcal{L}_2$ is fixed by symmetries, its 'strength', i.e. its prefactor, is not. This prefactor is called a *low-energy coupling* (LEC) of the theory. The LECs of an effective theory are determined by the underlying theory. The requirement is that the effective theory has to reproduce the low-energy physics of the underlying theory. However, it is a different question how to get the LECs in practice. In some effective theories the LECs can be computed perturbatively by matching correlation functions calculated perturbatively in both theories. In case of QCD and ChPT this matching can only be done nonperturbatively with results from lattice QCD simulations, or one resorts to comparing with experimental data.

Expanding Σ in powers of the pion fields we recover at first nontrivial order the standard kinetic terms of pseudo scalar fields,

$$\mathcal{L}_2 = \partial_\mu \pi^+ \partial_\mu \pi^- + \frac{1}{2} \partial_\mu \pi^0 \partial_\mu \pi^0 + \partial_\mu K^+ \partial_\mu K^- + \ldots \, . \tag{2.11}$$

The correct normalization of the fields has been put in by hand. It explains a posteriori the use of the same constant f in (2.6) and (2.10).

Expanding Σ further one finds terms involving four or more pion fields. These describe

[3] In Minkowski space time it corresponds to Lorentz invariance.

the interactions between the pions. Independently of the concrete form we can say that all terms involve derivatives. Hence, the interaction is proportional to the four-momentum of the pions and therefore vanishes in the zero momentum limit. We already mentioned this feature of Goldstone boson scattering at the beginning of this section. However, expanding $\mathcal{L}_2$ does not produce all interaction terms. In order to be complete one has to take into account consistently the higher contributions $\mathcal{L}_k, k = 4, 6, \ldots$, in the effective lagrangian. For example, the $\mathcal{L}_4$ part contains all invariants with four derivatives. It turns out that there are three such terms [26],

$$\mathcal{L}_4 = -L_1\langle\partial_\mu\Sigma\partial_\mu\Sigma^\dagger\rangle^2 - L_2\langle\partial_\mu\Sigma\partial_\nu\Sigma^\dagger\rangle\langle\partial_\mu\Sigma\partial_\nu\Sigma^\dagger\rangle - L_3\langle(\partial_\mu\Sigma\partial_\mu\Sigma^\dagger)^2\rangle\,. \tag{2.12}$$

Each term comes with its own LEC L_k, usually called (at this order) *Gasser-Leutwyler coefficient*. The expansion of Σ in $\mathcal{L}_4$ starts with four pion fields and these are the remaining interaction terms at this order. In order to get all interaction terms involving six derivatives one needs $\mathcal{L}_2, \mathcal{L}_4$ and $\mathcal{L}_6$. The generalization to $2n$ derivatives is obvious.

Apparently, there are infinitely many interaction terms in the complete chiral lagrangian, each associated with its own coupling. Hence, the effective theory is clearly nonrenormalizable. This is expected from a theory that is supposed to give an effective description of the physics at low energies, i.e. below a cut-off scale Λ. In the present case the scale Λ is of the order 1 Gev as the typical QCD scale. The organizing principle that renders the effective theory useful is the *derivative expansion*, the expansion in the momenta of the pions. The dimensionless expansion parameter is the ratio

$$r_p = \frac{p^2}{\Lambda^2}\,. \tag{2.13}$$

Working to a fixed order r_p^n one takes into account the interaction terms with $2n$ or less derivatives only. This is a finite number and once all couplings are known (by comparing with experiment, for instance) the theory starts to become predictive. Obviously one wants $r_p \ll 1$ so that a small value for n is sufficient. State of the art calculations in ChPT go up to $n = 3$, i.e. to $\mathrm{O}(p^6)$.[4]

So far we considered massless QCD. In the case of non-vanishing quark masses chiral symmetry is also explicitly broken and the pions are not massless. As long as this explicit breaking and the acquired pion masses are small compared to the masses of the other particles (in other words, small compared to the scale Λ), the effective theory can still be used to describe the pions and their interactions. Important is that the symmetry breaking due to the mass matrix M is properly included in the effective theory. The key observation here is that the massive QCD lagrangian is invariant under transformations in G, P, C provided the mass matrix transforms nontrivially as well, namely

$$M \xrightarrow{G} LMR^\dagger\,, \qquad M \xrightarrow{C} M^T\,, \qquad M \xrightarrow{P} M^\dagger\,. \tag{2.14}$$

Note that this implies $M^\dagger \longrightarrow RM^\dagger L^\dagger$, and this explains why we wrote $\overline{q}_R M^\dagger q_L$ in (2.1).

[4]For a brief status report of these calculations see [27].

Of course, the quark masses do not transform, but imposing this transformation law in an intermediate step allows us to find the proper chiral lagrangian in the presence of nonzero quark masses. We write down the most general lagrangian compatible with the symmetries G, P and C, constructed with Σ, its derivatives *and* the mass matrix M, which transforms according to (2.14). This prescription, often called *spurion analysis*, guarantees that the way the mass term breaks chiral symmetry in QCD is correctly carried over to the effective theory.

To first nontrivial order the chiral lagrangian reads [25, 26]

$$\mathcal{L}_2 = \frac{f^2}{4}\langle \partial_\mu \Sigma \partial_\mu \Sigma^\dagger \rangle - \frac{f^2 B}{2}\langle \Sigma M^\dagger + M\Sigma^\dagger \rangle \,. \tag{2.15}$$

The second term involving M gives rise to mass terms for the pions. Expanding to quadratic order in the fields one finds

$$\begin{aligned}\mathcal{L}_2 = {} & \partial_\mu \pi^+ \partial_\mu \pi^- + m^2_{\pi^\pm}\pi^+\pi^- + \frac{1}{2}\partial_\mu \pi^0 \partial_\mu \pi^0 + \frac{1}{2} m^2_{\pi^0}\pi^0\pi^0 \\ & + \partial_\mu K^+ \partial_\mu K^- + m^2_{K^\pm} K^+ K^- + \dots \,.\end{aligned} \tag{2.16}$$

where the pion and kaon masses are given by

$$M^2_{\pi^\pm} = B(m_u + m_d)\,, \qquad M^2_{\pi^0} = B(m_u + m_d)\,, \tag{2.17}$$

$$M^2_{K^\pm} = B(m_u + m_s)\,, \qquad M^2_{K^0} = B(m_d + m_s)\,. \tag{2.18}$$

Expanding further one obtains interaction terms involving four or more pion fields. All these terms are associated with one power of a quark mass, which is equivalent to one power of a squared pion mass. Consequently, these interactions do contribute even in the zero four momentum limit.

There are more invariants we can write down. These, however, involve more than one power of the quark mass matrix. The organizing principle for including them in the chiral lagrangian is again the low-energy expansion. The expansion parameters are the ratios

$$r_m = \frac{M^2_{\mathrm{GB}}}{\Lambda^2}\,, \tag{2.19}$$

with M^2_{GB} being the various Goldstone boson masses. Λ is of the order 1 Gev while the pion and kaon masses are about 140 and 500 MeV, respectively. Hence, $M^2_{\mathrm{GB}}/\Lambda^2$ is about 0.02 and 0.25. The latter is not terribly small but one still expects a reasonably well-behaved expansion.

Since we have two expansion parameters, the momentum of the Goldstone boson and its mass, we need to fix a counting rule that tells us the relative size of the terms with derivatives and with the mass matrix. Such a counting is called a *power counting scheme*. The standard scheme counts one Goldstone boson mass as one power of momentum, i.e. $r_p \sim r_m$. Formulated in terms of the quark mass matrix this is equivalent to counting two derivatives as one mass matrix. For this reason, $\mathcal{L}_2$ given in (2.15) is the consistent

leading order (LO) lagrangian containing all possible terms with two derivatives and one power of M.

The corresponding next-to-leading order (NLO) lagrangian $\mathcal{L}_4$ involves all terms with four derivatives, two powers of M or two derivatives and one power of M. In short, all terms of $\mathrm{O}(p^4, p^2M, M^2)$. It is convenient to introduce the scaled mass matrix

$$\hat{M} \equiv 2BM\,, \tag{2.20}$$

and the $\mathcal{L}_4$ lagrangian reads [26]

$$\begin{aligned}\mathcal{L}_4 = &- L_1\langle\partial_\mu\Sigma\partial_\mu\Sigma^\dagger\rangle^2 - L_2\langle\partial_\mu\Sigma\partial_\nu\Sigma^\dagger\rangle\langle\partial_\mu\Sigma\partial_\nu\Sigma^\dagger\rangle - L_3\langle(\partial_\mu\Sigma\partial_\mu\Sigma^\dagger)^2\rangle \\ &+ L_4\langle\partial_\mu\Sigma\partial_\mu\Sigma^\dagger\rangle\langle\hat{M}\Sigma^\dagger + \Sigma\hat{M}^\dagger\rangle + L_5\langle\partial_\mu\Sigma\partial_\mu\Sigma^\dagger(\hat{M}\Sigma^\dagger + \Sigma\hat{M}^\dagger)\rangle \\ &- L_6\langle\hat{M}\Sigma^\dagger + \Sigma\hat{M}^\dagger\rangle^2 - L_7\langle\hat{M}\Sigma^\dagger - \Sigma\hat{M}^\dagger\rangle^2 - L_8\langle\hat{M}\Sigma^\dagger\hat{M}\Sigma^\dagger + \Sigma\hat{M}^\dagger\Sigma\hat{M}^\dagger\rangle\,. \end{aligned} \tag{2.21}$$

All LECs L_i here are dimensionless because $\hat{M}$ has mass dimension two. The number of independent LECs is ten (eight plus the LO coefficients f and B). The number of LECs grows rapidly at higher order in the expansion. The lagrangian $\mathcal{L}_6$ contains already more than one hundred unknown coefficients [28]. However, the number of independent coefficients in observables is much less, since different terms in the lagrangian lead to the same contribution in an observable, and only particular linear combinations of LECs are independent. Nevertheless, the chiral expansion is practically of limited use beyond the next-to-next-to-leading order (NNLO) approximation.

Some simplifications occur if we describe only the pions and neglect the kaons [25]. Apart from the replacement $\mathrm{SU}(3) \to \mathrm{SU}(2)$ the mathematics is essentially unchanged. Σ is an SU(2) field with the matrix in (2.7) being restricted to its upper left block (with η set to zero). The lagrangian $\mathcal{L}_2$ is the same, but the eight terms in $\mathcal{L}_4$ are no longer independent. Instead, making use of Cayley-Hamilton relations $\mathcal{L}_4$ reduces to[5]

$$\begin{aligned}\mathcal{L}_4 = &- L_{13}\langle\partial_\mu\Sigma\partial_\mu\Sigma^\dagger\rangle^2 - L_2\langle\partial_\mu\Sigma\partial_\nu\Sigma^\dagger\rangle\langle\partial_\mu\Sigma\partial_\nu\Sigma^\dagger\rangle \\ &+ L_{45}\langle\partial_\mu\Sigma\partial_\mu\Sigma^\dagger\rangle\langle\hat{M}\Sigma^\dagger + \Sigma\hat{M}^\dagger\rangle - L_{68}\langle\hat{M}\Sigma^\dagger + \Sigma\hat{M}^\dagger\rangle^2\,. \end{aligned} \tag{2.22}$$

with

$$L_{13} = L_1 + \frac{L_3}{2}\,, \qquad L_{45} = L_4 + \frac{L_5}{2}\,, \qquad L_{68} = L_6 + \frac{L_8}{2}\,. \tag{2.23}$$

In computing observables to a given order in the chiral expansion one encounters loop diagrams that result in nonanalytic corrections, so-called *chiral logarithms*. Let us illustrate these for the simplest example, the 1-loop result for the pion mass. For simplicity we consider SU(2) ChPT with the additional simplification that the up and down type quark masses are degenerate, $m_u = m_d \equiv m$. The result reads [25]

$$M_\pi^2 = M_0^2\left(1 + \frac{M_0^2}{32\pi^2 f^2}\ln\frac{M_0^2}{\mu^2} - \frac{16M_0^2}{f^2}(L_{45} - 2L_{68})\right) \tag{2.24}$$

[5] Also the lagrangian $\mathcal{L}_6$ simplifies: it contains 'only' 56 terms [29].

with M_0 being the LO (tree-level) pion mass,

$$M_0^2 = 2Bm\,, \tag{2.25}$$

stemming from $\mathcal{L}_2$. The contribution proportional to $M_0^2 \ln M_0^2/\mu^2$ originates in the interaction terms of $\mathcal{L}_2$ that couple four pion fields. Two of them are contracted and result in a loop correction to the self-energy of the pion. This contribution needs to be renormalized and leads to the renormalization scale μ in (2.24). This scale, although not explicitly indicated, is also present in the $\mathcal{L}_4$ correction proportional to the combination $L_{45} - 2L_{68}$ of LECs. The coefficients L_i in (2.24) are no longer the (bare) coefficients in $\mathcal{L}_4$. Instead, they refer to the renormalized and μ-dependent LECs, $L_i = L_i^r(\mu)$, but for simplicity we continue to write L_i. However, the scale dependence of the LECs is such that it compensates the scale dependence of the chiral logarithm, leading to a scale independent pion mass.

Note that the interaction terms of $\mathcal{L}_2$ lead to a renormalization of the coefficients L_i in the higher order lagrangian $\mathcal{L}_4$, and not to a renormalization of LO coefficients f and B. This continues to be so beyond the 1-loop approximation and it signals again the non-renormalizability of the chiral effective theory.

So far we have discussed the QCD lagrangian and its matching to the lagrangian of the chiral effective theory. However, one is often interested in correlation functions of operators, hence, these operators in QCD need to be transcribed to the effective theory as well.

The most prominent operators are the vector and axial vector currents and the scalar and pseudo scalar densities, which in QCD read

$$V_\mu^a(x) = \overline{q}(x)\gamma_\mu T^a q(x)\,, \qquad A_\mu^a(x) = \overline{q}(x)\gamma_\mu\gamma_5 T^a q(x)\,, \tag{2.26}$$

$$S^a(x) = \overline{q}(x) T^a q(x)\,, \qquad P^a(x) = \overline{q}(x)\gamma_5 T^a q(x)\,, \tag{2.27}$$

where the T^a denote the eight hermitian group generators of SU(3), which we normalize as usual, $\mathrm{tr}(T^a T^b) = \delta^{ab}/2$. Restricting the index a to $1, 2, 3$ one obtains the expressions for the SU(2) case.

As discussed before, the QCD lagrangian is invariant under chiral symmetry transformations (c.f. eq. (2.3)) if all quark masses vanish. In this case the vector and axial vector currents are conserved as a consequence of this symmetry. For nonvanishing quark masses $m_u = m_d \equiv m$ we find (in the SU(2) case) the Ward identities (WIs)

$$\partial_\mu V_\mu^a(x) = 0\,, \qquad \partial_\mu A_\mu^a(x) = 2mP^a(x)\,, \tag{2.28}$$

where these equations are meant to hold in correlation functions with other local operators. There are even more Ward identities stemming from the non-abelian character of the symmetry group (sometimes referred to as 'current algebra'). All these Ward identities are particular properties of QCD, and the currents and densities in the chiral effective theory must be constructed in such a way that all Ward identities are properly reproduced (to the order in the derivative expansion one works to).

A very convenient method to achieve this is by constructing and matching the generating functional for correlation functions [25, 26]. It involves a source term in the effective action where sources are coupled to the currents and densities. Correlation functions of currents and densities are then obtained by functional derivatives of the generating functional with respect to the sources. The generating functional in the effective theory is again strongly constrained by the symmetries of the corresponding one in QCD. Together with the derivative expansion one obtains a systematic method to compute correlation functions of the currents and densities in the chiral effective theory.

A more pedestrian way for reaching the same results is the following. The QCD currents and densities in (2.26), (2.27) have well-defined transformation properties under the chiral symmetry group, charge conjugation and parity. One can simply write down the most general expressions in the effective theory that transform the same way. Organizing principle for all terms is again the derivative expansion, the LO expressions have the least number of derivatives and powers of the quark mass matrix. This is completely analogous to the construction of the effective lagrangian described before.

The expressions found that way have their own LECs. Not all of them are independent, though. All Ward identities must be reproduced, which implies relations among the various LECs, and imposing a few WIs usually fixes them. The LO expressions for the currents are obtained even simpler, since these are just the Noether currents associated with chiral symmetry. For later reference we quote here the LO expressions for the currents and densities:[6]

$$V^a_{\mu,\mathrm{LO}} = \frac{f^2}{2}\mathrm{tr}\left[T^a(\Sigma^\dagger\partial_\mu\Sigma + \Sigma\partial_\mu\Sigma^\dagger)\right], \quad A^a_{\mu,\mathrm{LO}} = \frac{f^2}{2}\mathrm{tr}\left[T^a(\Sigma^\dagger\partial_\mu\Sigma - \Sigma\partial_\mu\Sigma^\dagger)\right], \tag{2.29}$$

$$S^a_{\mathrm{LO}} = \frac{f^2B}{2}\mathrm{tr}\left[T^a(\Sigma + \Sigma^\dagger)\right], \qquad P^a_{\mathrm{LO}} = \frac{f^2B}{2}\mathrm{tr}\left[T^a(\Sigma - \Sigma^\dagger)\right]. \tag{2.30}$$

A prominent observable involving the axial vector current is the pion decay constant f_π, defined by

$$\langle 0|A^a_\mu(x)|\pi^b(p)\rangle = \delta^{ab} f_\pi p_\mu e^{-ipx}. \tag{2.31}$$

The right hand side makes use of O(4) symmetry and translation symmetry of the left hand side. To LO one finds $f_\pi = f$, hence justifying the identification of this LEC with the pion decay constant. To one loop we obtain [25]

$$f_\pi = f\left(1 - \frac{M_0^2}{16\pi^2 f^2}\ln\frac{M_0^2}{\mu^2} + \frac{8M_0^2}{f^2}L_{45}\right). \tag{2.32}$$

The structure is the same as for the pion mass in (2.24). Again, the dependence on the scale μ cancels and f_π is scale independent.

The results (2.24) and (2.32) demonstrate how lattice QCD simulations may be employed to obtain the LECs of ChPT. By computing M_π^2 and f_π for various quark masses and comparing with the ChPT predictions one obtains estimates for the various LECs involved. For the current status on this see the review [30]. We remark that the LECs

[6] Note that various conventions for the overall normalization can be found in the literature.

are often given in a slightly different form. For example, introducing Λ_3 and Λ_4 by the definitions

$$8L_{45} = \frac{1}{16\pi^2}\ln\frac{\Lambda_4^2}{\mu^2}\,, \qquad 16(L_{45}-2L_{68}) = \frac{1}{32\pi^2}\ln\frac{\Lambda_3^2}{\mu^2}\,, \tag{2.33}$$

the 1-loop results for the pion mass and decay constant can be written as

$$M_\pi^2 = M_0^2\left(1+\frac{M_0^2}{32\pi^2 f^2}\ln\frac{M_0^2}{\Lambda_3^2}\right)\,, \tag{2.34}$$

$$f_\pi = f\left(1-\frac{M_0^2}{16\pi^2 f^2}\ln\frac{M_0^2}{\Lambda_4^2}\right)\,. \tag{2.35}$$

These are the results already mentioned in the introduction, cf. (1.1). Very often $\Lambda_{3,4}$ are quoted in the literature. Alternatively, the form $\bar{l}_{3,4} \equiv \ln(\Lambda_{3,4}^2/M_{\pi,\mathrm{phys}}^2)$ is used, where $M_{\pi,\mathrm{phys}} = 139.6$ MeV denotes the physical pion mass.

3. Lattice QCD and the Symanzik effective theory

3.1. Lattice QCD

Lattice QCD refers to QCD formulated on a discrete space-time grid, with the quark and gluon fields appropriately discretized. The lattice spacing a provides a momentum cut-off $\Lambda_{\mathrm{UV}} \sim a^{-1}$ that makes the theory finite and well-defined. In contrast to other known regulators the lattice is nonperturbative and does not break the $\mathrm{SU}(3)_{\mathrm{color}}$ gauge symmetry. Of course, in order to get physical results the cut-off has to be removed in the end by sending the lattice spacing to zero.

Lattice QCD offers a second, more practical advantage: Physical results can be obtained by numerical methods. The path integrals one is typically interested in can be computed by Monte Carlo integration. Although afflicted with statistical errors this is to date the only known method to obtain nonperturbative QCD results from first principles.

Numerical simulations of QCD necessarily require a nonzero lattice spacing a and a finite space-time volume V. The corrections caused by a finite volume are usually exponentially suppressed and it is often legitimate to ignore them. The corrections caused by a nonzero lattice spacing are not quite as innocuous. Lattice spacings in present day simulations typically cover the range $0.05 \ldots 0.1$ fm, which corresponds to a momentum cut-off between 2 and 4 GeV, which is not that much larger than the QCD scale.

In practice the continuum limit is taken by computing physical observables at various lattice spacings and then extrapolating the results to $a = 0$. For a reliable extrapolation it is obviously advantageous if not necessary to know how the observables depend on a. The theoretical tool to study the continuum limit is provided by the Symanzik effective theory.

3.2. Continuum limit and Symanzik effective theory

Suppose we have properly discretized QCD such that we recover continuum QCD in the continuum limit. For small but nonzero a we expect the lattice theory to be 'close' to continuum QCD, with small corrections that vanish with powers of a.

This naive expectation has been put on firmer theoretical grounds by K. Symanzik [31, 32], who showed that a lattice field theory can be described by an effective continuum theory in which the dependence on the lattice spacing is made explicit. This type of effective theory is collectively called *Symanzik effective theory*, and it is another example

for a low-energy effective field theory. The relevant ratio of scales that one expands in is $\Lambda_{\mathrm{QCD}}/\Lambda_{\mathrm{UV}} \sim a\Lambda_{\mathrm{QCD}}$.

Also the Symanzik effective theory is defined by an effective action and effective operators. The construction principles are again symmetries and the low-energy expansion. Both effective action and effective operators are the most general expressions compatible with the symmetries of the underlying lattice theory, and the expansion in powers of a gives an organizing principle for all allowed terms. Quite generally, the structure of the Symanzik effective action is

$$S_{\mathrm{Sym}} = S_0 + aS_1 + a^2 S_2 + \dots \,, \tag{3.1}$$

$$S_k = \sum_i \int d^4x\, \bar{c}_i^{(k+4)} O_i^{(k+4)} \,, \tag{3.2}$$

where the $O_i^{(n)}$ are local operators of dimension n, constructed from the gauge and quark fields and their derivatives. The constants $\bar{c}_i^{(n)}$ are unknown coefficients, the low-energy couplings of the Symanzik effective theory. The first term S_0 is, by construction, the usual continuum QCD action.

We mention two sources of simplification that help in writing down the Symanzik effective theory. First, since all that matters is the effective action, terms that are related by partial integration can be dropped in S_{Sym}. Second, terms that are related by using the field equations (equations of motion, or EOM for short) can be ignored in S_{Sym} as long as one is interested in an effective description of on-shell correlation functions. This is usually sufficient if one is interested in physical properties like hadron masses, decay constants, scattering amplitudes etc., all of which can be obtained by studying on-shell correlation functions of appropriately chosen operators.

The effective operators, here generically denoted by Φ and also constructed from the gauge and quark fields, have a similar looking expansion,

$$\Phi_{\mathrm{Sym}} = \Phi_0 + a\Phi_1 + a^2\Phi_2 + \dots \,, \tag{3.3}$$

$$\Phi_k = \sum_i \bar{c}_i^{(k)} \phi_i^{(k)} \,. \tag{3.4}$$

with Φ_0 being the continuum field. The terms in Φ_k are again restricted by the transformation properties of the corresponding lattice operator under the various symmetries of the underlying lattice theory. Moreover, $a^k\Phi_k$ must have the same dimension as Φ_0, i.e. $[\Phi_k] = [\Phi_0] + k$. The constants $\bar{c}_i^{(n)}$ are again unknown couplings. It should be mentioned that not all a dependence is explicit in (3.1) and (3.3). The coefficients $\bar{c}_i^{(n)}$ are functions of the gauge coupling g^2 and are therefore expected to show a logarithmic a dependence. This dependence is expected to be much milder than the polynomial a dependence. Hence, it is usually ignored.

The number of terms present in S_k and Φ_k and also their concrete form is not universal

and depends on the details of the lattice theory. The decisive factor in this respect is the fermion discretization one uses for the quark fields. The reason is that all fermion discretizations compromise one or more symmetries of continuum QCD. Most obvious is the breaking of O(4) symmetry, which shows up in S_2 in form of O(4) violating operators O_i^6. More severe is the explicit breaking of chiral symmetry by Wilson fermions, which gives rise to (chiral symmetry breaking) terms at O(a) in S_1. Staggered fermions, on the other hand, do have enough symmetry such that O(a) terms are excluded (i.e. $S_1 = 0$). However, their particular breaking of the flavor symmetry shows up at O(a^2) in form of flavor violating terms. Finally, although overlap or domain-wall fermions preserve chiral and flavor symmetry, their Symanzik expansion still starts at O(a^2) with terms compatible with these symmetries.

The various symmetry transformations and the Symanzik expansions for most of the lattice fermions mentioned before have been worked out a long time ago and can be found in the literature. We do not reiterate all the results here. Instead, we first discuss in detail the simplest nontrivial case, namely Wilson fermions. This instructive example illustrates the main features needed in section 4.3, where the corresponding results for the other lattice fermions are summarized.

3.3. Example: Effective action for Wilson fermions

Let us consider lattice QCD with Wilson fermions [33]. Their explicit chiral symmetry breaking leads to a Symanzik expansion for the effective action that starts already at O(a). In fact, it even starts at O(a^{-1}), because the term $O^{(-1)} = \overline{q}q/a$ is compatible with all symmetries and should therefore appear in (3.1). However, this term has the form of a mass term and can be absorbed in the renormalization of the quark masses in S_0. Hence, in terms of the renormalized quark masses the Symanzik expansion starts with S_0 instead of S_{-1}.

Using the equations of motion there is essentially only one term in S_1, the Pauli term [34]

$$S_1 = \overline{c}_{\mathrm{SW}} \int d^4x \, \overline{q}(x) \, i\sigma_{\mu\nu} G_{\mu\nu}(x) q(x) \tag{3.5}$$

with $G_{\mu\nu}$ being the field strength tensor. Note that this term breaks chiral symmetry, as expected. Moreover, the Pauli term has a simple interpretation because it describes a color-magnetic moment: the leading artifact of the space-time lattice is the assignment of an anomalous color-magnetic moment to the quarks [35].

The complete list of dimension six operators in S_2 can be found in Ref. [34]. Among the terms with fermions (fermion bilinears and 4-fermion operators) are operators which break chiral symmetry and others which preserve it. It is also at this order in the Symanzik action that the lattice structure of the underlying theory shows up in form of a quark bilinear that breaks the O(4) symmetry. In total there are fifteen different terms at O(a^2) for the case with degenerate quark masses, and even more for the most general case with all quark masses being different.

The transformation properties of the individual terms in S_k under chiral symmetry

determine their impact on the construction of lattice ChPT. For example, the integrand of the Pauli term can be written as $\overline{q}_L i\sigma_{\mu\nu}G_{\mu\nu}q_R + \overline{q}_R i\sigma_{\mu\nu}G_{\mu\nu}q_L$ in terms of the chiral components of the fermion fields. This makes the breaking of chiral symmetry explicit, since this term couples left- and right-handed fields. Moreover, we see that the Pauli term breaks chiral symmetry exactly as a (flavor degenerate) mass term. This already tells us that the effect of S_1 on the pions is a shift of the pion masses; a result we will establish explicitly shortly.

Although chiral symmetry is broken in S_1 it can be 'restored' if we allow the overall coefficient $a\bar{c}_{\mathrm{SW}}$ of the Pauli term to transform nontrivially. This is a generalization of the spurion analysis discussed in section 2.1, where we introduced the transformation law (2.14) for the quark mass matrix. Here we replace $a\bar{c}_{\mathrm{SW}}$ by a spurion field A that transforms under G, C and P according to

$$A \xrightarrow{G} LAR^\dagger\,, \qquad A \xrightarrow{C} A^T\,, \qquad A \xrightarrow{P} A^\dagger\,. \tag{3.6}$$

Obviously, the term $\overline{q}_L iA\sigma_{\mu\nu}G_{\mu\nu}q_R + \overline{q}_R i\sigma_{\mu\nu}G_{\mu\nu}A^\dagger q_L$ is now invariant under G, and we recover the correct 'physical' Pauli term of the Symanzik theory by substituting $A \to a\bar{c}_{\mathrm{SW}}$.

The same procedure can be applied to the chiral symmetry breaking terms at $\mathrm{O}(a^2)$, as has been shown in [2]. For each term the coefficient (including the factor a^2) is promoted to a spurion field with appropriately chosen transformation behaviour such that chiral symmetry, charge conjugation and parity are restored. The correct Symanzik effective action is recovered with the proper 'physical value' for each spurion field.

3.4. Example: Effective operators for Wilson fermions

In principle, the Symanzik expansion of the effective operators follows the same lines as for the effective action. However, a difference arises for operators that renormalize non-trivially, for example nonconserved currents. In this case the particular renormalization conditions have to be taken into account for a proper matching to the operators in the Symanzik theory.

Let us discuss this for the vector current. Recall that continuum QCD is invariant under vector chiral symmetry transformations provided the quark masses are degenerate. Consequently, a conserved vector current exists, cf. (2.26) and (2.28). The same is true for lattice QCD with Wilson fermions. The conserved current can be obtained by the usual Noether procedure. Since it involves quark fields at neighboring lattice points this current is often called 'point-split' vector current [36]. We do not quote the explicit expression for this current because it is not relevant in the following. Important is that this current does not renormalize because it is conserved.

Current conservation is a (particularly simple) WI, and any WI in the lattice theory must be reproduced in the Symanzik effective theory. Hence, in order to get the correct vector current in the Symanzik theory one can start with the general expansion (3.3), (3.4) for a vector current but one insists on a vanishing divergence of this expression. This provides a constraint on the terms that appear on the right hand side.

Besides the conserved current there exist other vector currents in the lattice theory. All of them differ by terms of $\mathrm{O}(a)$, hence they have the same continuum limit. Mostly used in practice is the local current, that is the direct analogue of the continuum current in (2.26) (all quark fields reside on the same lattice point x, hence the name 'local'). This current is not conserved though. Consequently, its renormalization involves a nontrivial renormalization factor[1]

$$V^a_{\mu,\mathrm{ren,Loc}} = Z_{\mathrm{V,Loc}}\, V^a_{\mu,\mathrm{Loc}}\,. \tag{3.7}$$

The renormalization is finite with $Z_{\mathrm{V}} \neq 1$. The Z-factor can be fixed by imposing some continuum WI which the current has to satisfy in the continuum limit [36, 38, 39]. This guarantees the proper normalization of the current. For example, one could impose the condition [40, 41, 42]

$$Z_{\mathrm{V,Loc}}\langle\pi^a(\vec{p})|V^b_{\mu,\mathrm{Loc}}(0)|\pi^c(\vec{p})\rangle = \epsilon^{abc} 2p_\mu\,, \tag{3.8}$$

where $|\pi(\vec{p})\rangle$ denotes a single pion state with momentum p_μ. There are other conditions that one can equally well choose, and depending on the particular choice one usually gets different results for the Z-factor. However, the main point here is the following: Any condition or property an operator satisfies in the fundamental theory must be satisfied in the effective theory as well. This can either be an exact WI that follows from a symmetry, or any (renormalization) condition that is imposed by hand. The impact of particular renormalization conditions on the vector and axial vector currents has been studied in [12], and a brief account of these results is given in section 6.5.

[1] For an introduction see the lecture notes [37] by R. Sommer, for example.

4. ChPT for Lattice QCD

4.1. Strategy

The basic strategy for constructing ChPT for lattice QCD at nonzero lattice spacing is a two-step matching to effective theories [14, 15]. We first construct the Symanzik effective theory, which describes the lattice theory close to the continuum limit. As discussed before, the cut-off effects appear in terms of higher dimensional operators in the effective action and the effective operators, multiplied by powers of the lattice spacing a. In the second step we derive the chiral lagrangian for this effective theory using the standard arguments of ChPT. This results in a chiral expansion in which the dependence on the lattice spacing is made explicit.

The main rôle of the Symanzik effective theory in this two-step procedure is that it provides a systematic expansion of the lattice theory around the continuum limit. It organizes the nonzero lattice spacing effects in powers of a and therefore according to their importance when the continuum limit is approached. The structure of the higher dimensional operators in the Symanzik action determines if and how the cut-off effects break the symmetries of the corresponding continuum theory. In particular, the way chiral symmetry is broken by the lattice spacing effects is made transparent, which is crucial for constructing the chiral lagrangian. Finally, Symanzik's effective theory is a continuum theory, and the well-established derivation of ChPT from continuum QCD is readily extended to this effective theory with additional symmetry breaking parameters.

4.2. Example: ChPT for QCD with Wilson fermions

The leading term in the Symanzik expansion (3.1) is the continuum QCD action. We therefore expect the lattice theory to show the same spontaneous symmetry breaking pattern as in the continuum, provided both the quark masses and the lattice spacing are small. In that case the low-energy physics is, as described in section 2, dominated by pseudo Goldstone bosons. These acquire a nonzero mass due to the explicit chiral symmetry breaking by the quark masses and, additionally, by the chiral symmetry breaking terms in S_k, $k > 0$.

The low-energy chiral effective theory for these bosons is nowadays called *Wilson ChPT* (WChPT). In order to construct the effective lagrangian we follow the principles described before: We write down the most general lagrangian that is invariant under the symmetries of the underlying theory, here the Symanzik theory. Symmetry breaking terms are consistently included performing a spurion analysis. This procedure is completely analogous to the way the quark masses are incorporated in continuum ChPT.

Here, however, we have to perform a spurion analysis for each symmetry breaking term in eq. (3.1), also those associated with the nonzero lattice spacing. The low-energy expansion in small momenta and Goldstone boson masses is extended by an expansion in small powers of the lattice spacing.

The Pauli term (3.5) is a particularly simple example to illustrate this procedure. We have seen that S_1 is invariant under G, C and P after we have introduced the spurion field A, c.f. eq. (3.6). This must be carried over to the effective theory by including all invariant terms in the effective action that can be constructed with A and the other 'building blocks' Σ, its partial derivatives and M. The simplest invariant with only one power of A is $\langle A^\dagger\Sigma + \Sigma^\dagger A\rangle$.[1] After setting $A \to a\bar{c}_{\mathrm{SW}}$ it leads to the term

$$\mathcal{L}_a = -\frac{f^2 W_0}{2}\, a\bar{c}_{\mathrm{SW}}\langle\Sigma + \Sigma^\dagger\rangle\,. \tag{4.1}$$

The coefficient W_0 is another LEC not determined by symmetries. This term resembles a (degenerate) mass term with a and $\bar{c}_{\mathrm{SW}}W_0$ playing the rôle of m and B.[2] This is expected since (4.1) is a consequence of the Pauli term which breaks chiral symmetry just like a degenerate mass term. And this is all that matters for the Goldstone bosons, although on the quark level a Pauli term is certainly not equivalent to a mass term.

Because (4.1) is essentially a mass term for the Goldstone bosons it is convenient to combine this term with the standard mass term in $\mathcal{L}_2$. This is achieved by defining the so-called *shifted mass* m' according to [14]

$$Bm' = Bm + W_0\bar{c}_{\mathrm{SW}}a\,. \tag{4.2}$$

Recall that m includes already the dominant additive mass renormalization proportional to $1/a$. The shifted mass includes, in addition, the subdominant shift of $\mathrm{O}(a)$. It is matter of taste which mass is used for parametrizing the chiral lagrangian. Physical results do not depend on this choice. In the following we will exclusively work with the shifted mass, and for simplicity we drop the prime and denote it by m from now on.

The term (4.1) describes the leading lattice spacing correction of $\mathrm{O}(a)$ to the continuum chiral lagrangian. Subleading terms of $\mathrm{O}(ap^2, am)$ stem from the invariants with one power of A and either two partial derivatives or one power of the mass spurion M [43]. Other higher corrections are the terms of $\mathrm{O}(a^2)$, originating in invariants with two powers of A or genuine $\mathrm{O}(a^2)$ spurion fields associated with the chiral symmetry breaking terms in S_2 of the Symanzik effective action [2]. The main result of the complete spurion analysis is easily summarized: Take any term in the Gasser-Leutwyler lagrangian $\mathcal{L}_4$ containing M and replace M by A, this gives all terms of $\mathrm{O}(ap^2, am)$. In the case of degenerate quark masses the corresponding lagrangians $\mathcal{L}_{ap^2}$ and $\mathcal{L}_{am}$ read [43]

$$\mathcal{L}_{ap^2} = \hat{a}\bar{c}_{\mathrm{SW}}\Big[W_4\langle\partial_\mu\Sigma\partial_\mu\Sigma^\dagger\rangle\langle\Sigma^\dagger + \Sigma\rangle + W_5\langle\partial_\mu\Sigma\partial_\mu\Sigma^\dagger(\Sigma^\dagger + \Sigma)\rangle\Big]\,, \tag{4.3}$$

[1] The invariant $\langle A^\dagger M + MA\rangle$ reduces to a constant in the effective action, hence it is dropped.

[2] In contrast to B the mass dimension of W_0 is three instead of one, so both combinations Bm and $W_0 a$ are of mass dimension two.

$$\mathcal{L}_{am} = -\hat{a}\hat{m}\bar{c}_{\mathrm{SW}}\Big[W_6\langle\Sigma^\dagger+\Sigma\rangle^2 + W_7\langle\Sigma^\dagger-\Sigma\rangle^2 + W_8\langle\Sigma^\dagger\Sigma^\dagger+\Sigma\Sigma\rangle\Big]\,. \tag{4.4}$$

Each term comes with a new unknown LEC. For convenience we introduced the scaled variables (both of mass dimension two)

$$\hat{m} = 2Bm\,, \qquad \hat{a} = 2W_0 a\,. \tag{4.5}$$

Performing the same replacement in the terms quadratic in M yields the terms of $\mathrm{O}(a^2)$ [2]:[3]

$$\mathcal{L}_{a^2} = -\hat{a}^2\Big[W_6'\langle\Sigma^\dagger+\Sigma\rangle^2 + W_7'\langle\Sigma^\dagger-\Sigma\rangle^2 + W_8'\langle\Sigma^\dagger\Sigma^\dagger+\Sigma\Sigma\rangle\Big]\,. \tag{4.6}$$

Although simple this final result is not obvious. Some 4-quark operators in S_2 break chiral symmetry in a different way than a mass term. Moreover, rotational $\mathrm{O}(4)$ symmetry is broken at $\mathrm{O}(a^2)$. However, the spurion analysis shows that the spurion field A (and powers of it) is sufficient to generate all terms in the chiral lagrangian through $\mathrm{O}(a^2)$, and the $\mathrm{O}(4)$ symmetry breaking terms enter at a higher order in the chiral expansion [2].

Significant simplification take place for $\mathrm{SU}(2)$ WChPT. In this case $\langle\Sigma^\dagger-\Sigma\rangle = 0$, so the W_7, W_7' terms are absent. Moreover, using Cayley-Hamilton relations the other terms are not independent, and the lagrangians reduce to

$$\mathcal{L}_{ap^2} = \hat{a}\bar{c}_{\mathrm{SW}}W_{45}\langle\partial_\mu\Sigma\partial_\mu\Sigma^\dagger\rangle\langle\Sigma^\dagger+\Sigma\rangle\,, \tag{4.7}$$

$$\mathcal{L}_{am} = -\hat{a}\hat{m}\bar{c}_{\mathrm{SW}}W_{68}\langle\Sigma^\dagger+\Sigma\rangle^2\,, \tag{4.8}$$

$$\mathcal{L}_{a^2} = -\hat{a}^2W_{68}'\langle\Sigma^\dagger+\Sigma\rangle^2\,. \tag{4.9}$$

Only three LECs enter compared with with eight LECs in the general $\mathrm{SU}(N_f)$ case.

The order counting in WChPT requires some care. The generalized low-energy expansion is a simultaneous expansion in powers of small momenta, masses and lattice spacings. More precisely, using the notation of section 2.2, it is an expansion in the small ratios r_p, r_m and

$$r_a = \frac{aW_0}{\Lambda^2}. \tag{4.10}$$

In lattice ChPT there are two sources of explicit chiral symmetry breaking present, the quark masses and the lattice spacing. The nontrivial question is the relative size of these two sources, or, in other words, the relative size of r_m and r_a. And the relative size of these two expansion parameters determines the order a term appears in the chiral lagrangian. Note that r_m and r_a are not fixed numbers in lattice ChPT, since we are, at least in principle, free to choose the quark masses and the lattice spacing at will.

The literature distinguishes two different regimes. One can invent other schemes as well but these two are believed to be the relevant ones for analyzing current lattice

[3] In $\mathcal{L}_{a^2}$ we have absorbed the dependence on $\bar{c}_{\mathrm{SW}}$ in the definition of the LECs W_i'. The dependence is not just a simple overall factor $\bar{c}_{\mathrm{SW}}^2$. The reason for this absorption will become clear in section 4.3.1.

QCD data. The GSM (*generically small masses*) regime [44] assumes that the breaking of chiral symmetry due to the quark mass and the lattice spacing is of equal size, i.e. $r_m \sim r_a$. Instead of $r_m \sim r_a$ one often writes $m \sim a\Lambda_{\mathrm{QCD}}^2$ (setting all dimensionful constants equal to the QCD scale Λ_{QCD}), or simplistic $m \sim a$. This assumption implies the following order counting:

GSM regime:

$$\begin{aligned} \mathrm{LO}: &\quad p^2,\, m \\ \mathrm{NLO}: &\quad p^4,\, p^2m,\, m^2,\, p^2a,\, ma,\, a^2\,. \end{aligned} \tag{4.11}$$

In terms of the lagrangians we discussed so far it means

GSM regime:

$$\mathcal{L}_{\mathrm{LO}} = \mathcal{L}_2 \tag{4.12}$$

$$\mathcal{L}_{\mathrm{NLO}} = \mathcal{L}_4 + \mathcal{L}_{ap^2} + \mathcal{L}_{am} + \mathcal{L}_{a^2}\,. \tag{4.13}$$

Recall that we use the shifted mass, hence the term $\mathcal{L}_a$ in (4.1) is included in $\mathcal{L}_2$.

Let us assume we are in the GSM regime. Lowering the quark mass by keeping the lattice spacing fixed we will eventually reach the LCE (*large cut-off effects*) regime [10] where $r_m \sim r_a^2$ ($m \sim a^2\Lambda_{\mathrm{QCD}}^3$ or even $m \sim a^2$ for short). This implies that we have to take the $\mathrm{O}(a^2)$ term at LO, and the LO lagrangian consists of the terms of $\mathrm{O}(p^2, m, a^2)$:

LCE regime:

$$\mathcal{L}_{\mathrm{LO}} = \mathcal{L}_2 + \mathcal{L}_{a^2}\,. \tag{4.14}$$

The higher order terms contribute according to the following scheme:

LCE regime:

$$\begin{aligned} \mathrm{LO}: &\quad p^2,\, m,\, a^2 \\ \mathrm{NLO}: &\quad p^2a,\, ma,\, a^3 \\ \mathrm{NNLO}: &\quad p^4,\, p^2m,\, m^2,\, p^2a^2,\, ma^2,\, a^4\,. \end{aligned} \tag{4.15}$$

The standard NLO terms of continuum ChPT appear here at NNLO, a consequence of the $\mathrm{O}(p^2a, ma, a^3)$ terms not present in continuum ChPT. Note that all terms in (4.11) are also present in (4.15), even though reshuffled. This already indicates, that a result obtained in the LCE regime yields the corresponding result in the GSM regime by dropping appropriate terms.

As mentioned before, one can define other regimes. The power counting will be different depending on the relative size of the mass and the lattice spacing. The smaller the lattice spacing compared to the mass the higher the order where the lattice spacing corrections enter and the more 'continuum-like' is the resulting effective theory.

The construction of the effective operators follows the same steps. Starting point is the Symanzik expansion (3.3). The leading term Φ_0 is in general the standard continuum QCD expression, hence it maps to the usual effective operator known in continuum ChPT. The symmetry breaking terms in $\Phi_1, \Phi_2, \ldots$ are taken into account by a spurion analysis, just as in the construction of the chiral lagrangian. As a concrete example consider the local axial vector current. In this case Φ_0 equals the continuum expression

given in (2.26). Φ_1 consists of one term only, the derivative of the pseudo scalar density, $\Phi_1 = \bar{c}_{\rm A}\partial_\mu P^a$, with P^a being the continuum pseudo scalar density of (2.27). Through $\mathrm{O}(a)$ the axial vector in the Symanzik effective theory therefore reads

$$A^a_{\mu,\mathrm{Sym,Loc}} = A^a_\mu + a\bar{c}_{\rm A}\partial_\mu P^a\,. \tag{4.16}$$

Note that this is the Symanzik current *without* the renormalization factor $Z_{\rm A}$ and without the correction factor $1+\bar{b}_{\rm A}am$ [12]. These are overall factors and can be included after one has mapped the current into the chiral effective theory. We come back to this issue in section 6.5 where the renormalization of the axial vector current is discussed in more detail. Here we focus on the effective current $A^a_{\mu,\mathrm{eff}}$ that corresponds to the Symanzik current (4.16).

The leading term A^a_μ is the difference of the right-handed and left-handed currents. The $\mathrm{O}(a)$ correction, on the other hand, has not this structure and couples directly right- and left-handed fields. However, promoting the coefficient $a\bar{c}_{\rm A}$ to a spurion field $C_{\rm A}$ with appropriate transformation behaviour [12], the Symanzik current $A^a_{\mu,\mathrm{Sym,Loc}}$ can be made transform as the continuum axial vector current. The counterpart in WChPT is now obtained by writing down the most general axial vector current, made of Σ and all spurion fields, including $C_{\rm A}$. One finds [12], after setting all spurion fields to their proper final value (including $C_{\rm A}\to a\bar{c}_{\rm A}$):

$$A^a_{\mu,\mathrm{eff}} = A^a_{\mu,\mathrm{LO}}\left(1+\frac{4}{f^2}\hat{a}W_{45}\bar{c}_{\rm SW}\langle\Sigma+\Sigma^\dagger\rangle\right) + 4\hat{a}W_{\rm A}\bar{c}_{\rm A}\partial_\mu\langle T^a(\Sigma-\Sigma^\dagger)\rangle\,, \tag{4.17}$$

$A^a_{\mu,\mathrm{LO}}$ denotes the LO current (2.29) of continuum ChPT. At $\mathrm{O}(a)$ there are two corrections. The one involving $W_{45}\bar{c}_{\rm SW}$ stems from the Pauli term (3.5), as is easily understood from the coefficient $\bar{c}_{\rm SW}$. The second correction proportional to $\bar{c}_{\rm A}$ originates in the $\mathrm{O}(a)$ correction in (4.16). It comes with a new LEC $W_{\rm A}$ not present in the chiral lagrangian.

A similar construction can be carried out for the scalar and pseudo scalar density and for the vector current. The result for the latter is given in Ref. [12].

Based on the chiral effective lagrangian and the effective operators of this section results for the pseudo scalar masses, decay constants and scattering lengths have been computed [10, 12, 6]. The results for these observables will be presented in section 6. Here we briefly discuss a necessary prerequisite for such calculations, namely the vacuum configuration of the theory.

Correlation functions in ChPT are usually computed by a standard saddle point expansion, where the field Σ is expanded according to

$$\Sigma(x) = \Sigma_{\rm vac}^{1/2}\exp\left(\frac{2i\pi(x)}{f}\right)\Sigma_{\rm vac}^{1/2}\,. \tag{4.18}$$

Here $\Sigma_{\rm vac}$ is the *vacuum configuration* (also called *ground state*) that minimizes the classical potential energy. In continuum ChPT one finds $\Sigma_{\rm vac}=1$ (identity matrix), at least for the standard choice of positive quark masses, and we have already used this result in (2.6) without mentioning. $\Sigma_{\rm vac}=1$ remains true in WChPT in the GSM regime,

since the LO lagrangian is as in continuum ChPT. However, in the LCE regime the $\mathrm{O}(a^2)$ lagrangian $\mathcal{L}_{a^2}$ is of LO too and the competition between this term and the mass term can result in nontrivial vacuum states $\Sigma_{\mathrm{vac}} \neq 1$. This is most easily demonstrated for SU(2) in the mass degenerate case, where the potential energy is read off from the LO chiral lagrangian in (4.14) as

$$V = -\frac{f^2}{2} Bm \langle \Sigma + \Sigma^\dagger \rangle + \frac{f^2}{16} c_2 a^2 \langle \Sigma + \Sigma^\dagger \rangle^2 \,. \tag{4.19}$$

Here we introduced the short hand notation

$$c_2 = -64 W'_{68} \frac{W_0^2}{f^2} \tag{4.20}$$

for the particular combination of LECs in $\mathcal{L}_{a^2}$. The potential (4.19) is easily minimized and reveals an interesting phase structure depending on the sign of c_2 [14]. If c_2 is negative the ground state is found to be

$$\Sigma_{\mathrm{vac}} = \begin{cases} +1\,, & m > 0 \\ -1\,, & m < 0 \end{cases} \qquad \text{for } c_2 < 0\,. \tag{4.21}$$

There is a first order phase transition at $m = 0$ where the ground state changes its sign discontinuously. This discontinuity shows itself in the pion mass, which at tree-level reads

$$M^2_{\pi,\mathrm{LO}} = 2B|m| - 2c_2 a^2 \,. \tag{4.22}$$

All three pions are massive for all quark masses, and the pion mass assumes its minimal value

$$M^2_{\pi,\mathrm{LO,min}} = 2|c_2| a^2 \tag{4.23}$$

at $m = 0$.

On the other hand, if c_2 is positive, the ground state is given by

$$\Sigma_{\mathrm{vac}} = \begin{cases} +1\,, & Bm \;\geq\; c_2 a^2 \\ \exp(i\vec{\phi}\cdot\vec{\sigma})\,, \quad \cos|\vec{\phi}| = \dfrac{Bm}{c_2 a^2}\,, & |Bm| \;<\; c_2 a^2 \\ -1\,, & Bm \;\leq\; -c_2 a^2 \end{cases} \qquad \text{for } c_2 > 0\,. \tag{4.24}$$

For masses with $0 \leq |m| < c_2 a^2/B$ the ground state is given by a nontrivial SU(2) element $\exp(i\vec{\phi}\cdot\vec{\sigma})$. The SU(2) flavor symmetry is spontaneously broken to U(1) (rotations around the direction of $\vec{\phi}$). As a consequence of the Goldstone theorem two pions, which we can choose to be the charged ones, are exactly massless throughout the region $0 \leq |m| < c_2 a^2/B$. The ground state varies continuously at $|m| = c_2 a^2/B$, hence the phase transition at these masses is second order. Aoki anticipated the existence of such a spontaneously broken phase with massless pions long ago [45]. His arguments for such a phase were completely different, but we see that WChPT predicts the existence of such a phase very naturally. However, the magnitude and the sign of c_2 depend on

the details of the underlying lattice theory, i.e. what particular lattice action has been chosen. Moreover, it is not a simple task to measure c_2 numerically. We will repeatedly come back to this issue in later sections.

To date the phase structure for SU(N_f), $N_f > 2$, has not been solved. This case is much more difficult since $\mathcal{L}_{a^2}$ consists of three different terms with three unknown LECs.

4.3. ChPT for other lattice fermions

The steps discussed in the last section can be and have been applied to lattice QCD with other fermion discretizations. The details differ because the symmetry properties of the various lattice fermions are different. Hence, the associated chiral effective theory will be different as well. However, the main idea, in particular the two-step matching

$$\textit{Lattice QCD} \longrightarrow \textit{Symanzik effective theory} \longrightarrow \textit{ChPT},$$

remains the same.

In the following we will briefly discuss the chiral effective theories for Wilson fermions with a twisted mass term, Ginsparg-Wilson fermions and staggered fermions. The discussion will not be as thorough as for Wilson fermions, but we will provide enough details to understand the results presented in the following sections.

4.3.1. O(a) improved Wilson fermions

The idea of O(a) improvement goes back to Symanzik [31, 32], and it is a widely employed concept in lattice QCD. In fact, standard unimproved Wilson fermions are hardly used in practice.

The main idea of O(a) improvement is a modification of the lattice action and the lattice operators in such a way that the approach to the continuum limit is of O(a^2) instead of O(a). For example, a so-called clover term is added to the standard Wilson fermion action. This clover term is essentially the lattice version of the Pauli term in (3.5) with a prefactor c_{SW}. If this prefactor is properly tuned (as a function of the coupling constant), the coefficient $\overline{c}_{\mathrm{SW}}$ in the corresponding Symanzik effective action will vanish, i.e. $S_1 = 0$ and the lattice spacing corrections start with O(a^2).

In addition to the action the lattice operators need to be improved as well. For example, one adds a correction to the axial vector current in the lattice theory. Again, the coefficient of this correction, c_{A}, needs to be properly tuned such that the coefficient $\overline{c}_{\mathrm{A}}$ in (4.16) vanishes.

How this tuning is done in practice is somewhat nontrivial.[4] However, the details are not relevant for the following. We are interested in the construction of the chiral effective theory, and it is based entirely on the Symanzik effective theory. If the Symanzik theory is free of terms of O(a), there will be no O(a) terms in WChPT as well. Formally this

[4] For an introduction see the lecture notes by M. Lüscher [35], for example.

is achieved by setting $\bar{c}_{\mathrm{SW}} = \bar{c}_{\mathrm{A}} = 0$ in all previously given formulae. This amounts to dropping the contributions $\mathcal{L}_{ap^2}$ and $\mathcal{L}_{am}$ in the chiral lagrangian and the $\mathrm{O}(a)$ correction in the axial vector current in (4.17).

This simple prescription finally explains why we kept the coefficients $\bar{c}_{\mathrm{SW}}, \bar{c}_{\mathrm{A}}$ explicit in the contributions linear in a, even though they are always accompanied by another unknown coefficient W_i. The $\mathrm{O}(a^2)$ terms are not simply proportional to these coefficients and therefore do not vanish for $\bar{c}_{\mathrm{SW}} = \bar{c}_{\mathrm{A}} = 0$.

4.3.2. Wilson twisted mass fermions

Consider lattice QCD with two Wilson quarks. In case of degenerate quarks the standard mass term is of the form $M = m_0\, 1$. The subscript in the mass highlights the fact that this is the bare quark mass. In twisted mass lattice QCD the mass term is generalized to [46, 47]

$$M_0 = m_0\, 1 + i\mu_0\gamma_5\sigma_3\,, \tag{4.25}$$

where μ_0 is the bare *twisted quark mass*. At first sight the twisted mass does not appear to be a mass term. In continuum QCD one can show [46] that, under a flavor non-singlet transformation of the quark fields, (4.25) is equivalent to a standard degenerate mass term with mass $\tilde{m}_0 = \sqrt{{m_0}^2 + {\mu_0}^2}$. However, on the lattice, with the additional Wilson term to remove the fermion doublers, this is not the case.

Historically the first reason to introduce a twisted mass term was that it provides a strict lower bound on the spectrum of the Wilson-Dirac operator, $D^\dagger D \geq \mu_0^2$. Hence, the problems with exceptional configurations were circumvented and smaller quark masses could be simulated in numerical calculations. However, the main reason for such a mass term is that twisted mass fermions show scaling violations of $\mathrm{O}(a^2)$ at *maximal twist*, i.e. they are *automatically $O(a)$ improved* without going through the steps of the Symanzik improvement program mentioned before [48, 49]. A precise definition of maximal twist will be given later, but it essentially means that the (renormalized!) untwisted quark mass m is set to zero.

The mass term (4.25) singles out the σ_3 direction and breaks the SU(2) flavor symmetry. On the other hand, the symmetries of the massless theory are obviously the same as for massless Wilson fermions with a standard mass term. Hence, the chiral effective theory, and in particular the chiral effective lagrangian, is the same as for standard Wilson fermions, except for the mass term which in the effective theory reads

$$M = m\, 1 + i\mu\sigma_3\,. \tag{4.26}$$

It involves no γ_5 since the degrees of freedom are bosons. In addition, (4.26) contains the renormalized quark masses. Note that the twisted quark mass is only multiplicatively renormalized, $\mu = Z_\mu\mu_0/a$ [46], in contrast to the standard mass $m = Z_m(m_0 - m_{\mathrm{cr}})/a$. As in the untwisted case the leading effect of the Pauli term can be (and usually is) absorbed by an $\mathrm{O}(a)$ shift of m.

The mass term (4.26) and the modifications because of a nonzero μ seem innocuous. However, a nonzero μ has crucial impact on the vacuum configuration, which has a

nonvanishing contribution pointing into the σ_3 direction,

$$\Sigma_{\text{vac}} = \exp\left(i\phi\sigma_3\right) . \tag{4.27}$$

ϕ is called the *vacuum angle*, and it depends on m, μ and a. The nonconstant nature of the vacuum angle has nontrivial consequences for observables, which will be discussed in section 8.

4.3.3. Ginsparg-Wilson fermions

Ginsparg-Wilson fermions is the generic name for lattice fermions with a Dirac operator satisfying the Ginsparg-Wilson relation [50],

$$\gamma_5 D + D\gamma_5 = aD\gamma_5 D\,. \tag{4.28}$$

Explicit examples are domain-wall [51, 52] and overlap fermions [53, 54]. The Ginsparg-Wilson relation implies exact chiral symmetry at nonzero lattice spacing [55] with all its beneficial consequences. For instance, there exists an unambiguous definition for the topological charge and an exact index theorem [56, 57].

Exact chiral symmetry results in a Symanzik expansion that starts at $\mathrm{O}(a^2)$, i.e. $S_1 = 0$. Also S_{-1} is excluded and the mass is only multiplicatively renormalized. Moreover, all terms in S_2 are compatible with chiral symmetry. Consequently, the chiral lagrangian is essentially as in continuum ChPT but with the LECs being lattice spacing dependent: $f = f(a^2)\,, B = B(a^2)$ and so forth. In the continuum limit they assume their continuum values, of course.

The only nontrivial but small modification is due to O(4) symmetry violating terms in S_2 of the Symanzik theory, for instance the $\mathrm{O}(a^2)$ term [34]

$$O^{(6)}_{\text{break}} = \overline{q}\gamma_\mu D_\mu D_\mu D_\mu q\,. \tag{4.29}$$

In principle, this term can be mapped into ChPT by promoting its coefficient to a spurion field that transforms under O(4) transformations in such a way that $O^{(6)}_{\text{break}}$ is a O(4) scalar. But even without carrying out the details one can easily conclude that the effects are highly suppressed in the chiral expansion: In order to break the O(4) symmetry, while still preserving the discrete hypercubic symmetry, an operator must carry at least four space-time indices. In the chiral lagrangian these are provided by the partial derivative ∂_μ, hence the operator is at least of $\mathrm{O}(p^4)$. Adding the fact that it is also an $\mathrm{O}(a^2)$ effect, we conclude that the leading O(4) symmetry breaking terms in the chiral lagrangian are of $\mathrm{O}(a^2p^4)$ (an example is the term $a^2\sum_\mu \langle\partial_\mu\partial_\mu\Sigma\partial_\mu\partial_\mu\Sigma^\dagger\rangle$). Hence, even in the LCE regime this term is of NNLO, and it is usually ignored. Note that this term is also present in the Symanzik effective action for Wilson and for staggered fermions (and ignored for the same reason).

4.3.4. Staggered fermions

Staggered (or Kogut-Susskind) fermions [58, 59] used to be and still are very popular for dynamical simulations. They are numerically very fast to simulate compared with other lattice fermions. In addition, they possess an exact axial U(1) symmetry at nonzero lattice spacing which protects the quark mass from an additive renormalization. As a result, lattice QCD simulations with staggered fermions used to reach significantly smaller quark masses than those using Wilson fermions, although recent algorithmic developments improved the performance of the latter significantly [60, 61, 62, 63, 64, 65]. The major disadvantage of staggered fermions is that they do not solve the fermion doubling problem completely: One staggered field describes four degenerate fermions in the continuum limit [66]. It is customary to refer to these extra degrees of freedom as 'taste', in contrast to the standard label 'flavor' for the different quark fields.

In order to reduce the number of tastes one usually employs the so-called 'fourth-root-trick': The fermion determinant of the staggered Dirac operator D_{Stag} is replaced by $\sqrt[4]{\det D_{\text{Stag}}}$ in numerical lattice simulations. This trick legitimately raises the question whether the rooted theory correctly describes QCD in the continuum limit. Perturbatively this seems to be a correct procedure, since the factor 1/4 correctly reduces the contributions from loop diagrams. However, the question is trickier nonperturbatively: Taking the fourth root spoils locality and all known universality arguments can no longer be naively applied. Hence it is questionable whether the rooted lattice theory has the correct continuum limit.

Even if the fourth-root-trick is correct in this respect, we still have a problem in setting up the chiral effective theory for a rooted lattice theory. The factor 1/4 is introduced by hand and modifies the sea quarks only. This needs to be implemented appropriately in the chiral effective theory, and a separation between sea and valence quark contributions must be introduced. This is done with the concept of *partial quenching*, which we discuss in the next section.

To separate the various issues we consider first unrooted staggered fermions. To those the principles we have discussed so far can be directly applied. Once we have discussed partial quenching we briefly come back to the rooted theory in section 5.3.

Consider lattice QCD with N_f flavors of staggered fermions. This is a local field theory and the Symanzik effective theory can be constructed as usual. The leading term S_0 is just the continuum QCD action with $4N_f$ fermions. Each flavor is fourfold degenerate because of the taste degree of freedom. In other words, S_0 has N_f $\mathrm{U}(4)_{\text{taste}}$ symmetries, one for each flavor. If we choose the same mass for all fermion flavors we also find an $\mathrm{SU}(N_f)$ flavor symmetry. In the massless theory we find the even larger symmetry group

$$G = \mathrm{SU}(4N_f)_L \times \mathrm{SU}(4N_f)_R \,. \tag{4.30}$$

The higher order terms in the Symanzik effective action are restricted by the symmetries of the lattice theory. All symmetries are discussed in detail in [66].[5] In addition to the

[5] We mention in passing that for the construction of the Symanzik effective theory it is very useful to rewrite the standard staggered fermion action: Instead of the formulation with one component fields

standard symmetries like O(4) symmetry, charge conjugation and parity there are two symmetries that are key to the restriction of the higher order terms in the Symanzik theory: an axial U(1) symmetry and the so-called *shift symmetry* that refers to translations by one lattice spacing. For example, the chiral U(1) excludes immediately a term $O^{(-1)} = \overline{q}q/a$, so the quark mass does not receive an additive renormalization. Moreover, the symmetries also forbid any term in S_1 [73], so the lattice spacing corrections start with the $O(a^2)$ corrections in S_2.

The S_2 part of the Symanzik effective action contains a large number of terms [15, 74]. There is no need to list them here and we make a few qualitative remarks only. As for all lattice fermions, the hypercubic O(4) symmetry is broken at this order. More importantly for staggered fermions is the taste symmetry breaking at this order. This symmetry is explicitly broken at $O(a^2)$, a feature that will become important later on. In any case, the transformation properties of each term in S_2 under G, P and C can be studied. Spurion fields for the noninvariant terms can be introduced as before, and these are used in the construction of the chiral effective theory, called *staggered ChPT* (SChPT).

The crucial assumption is, as before, the spontaneous breaking of (4.30) down to the diagonal subgroup

$$H = \mathrm{SU}(4N_f)_{L=R}\,, \tag{4.31}$$

associated with the existence of light (pseudo) Goldstone boson fields. The main difference to the theories discussed before is the larger field content because of additional taste degrees of freedom and larger symmetry groups. The number of Goldstone bosons is $(4N_f)^2 - 1$, so for the 3-flavor theory we have 143 instead of 8 Goldstone bosons! This is reflected in bigger Σ fields which are elements of G/H, and this manifold is of dimension $(4N_f)^2 - 1$. However, the exact taste symmetry in the continuum limit suggests a compact notation which hides most of the large field content. For example, setting $N_f = 3$ we may introduce the U(12) [sic] matrix $\Sigma = \exp(2i\pi/f)$, with

$$\pi = \begin{pmatrix} U & \pi^+ & K^+ \\ \pi^- & D & K^0 \\ K^- & \overline{K}^0 & S \end{pmatrix}\,. \tag{4.32}$$

Here U, π^+, K^+, etc. are 4×4 matrices that take into account the taste degree of freedom. We can write

$$U = \sum_{b=1}^{16} U_b \frac{T_b}{2}\,, \tag{4.33}$$

(and similarly for $\pi^+, K^+, \ldots$) where

$$T_b = \{\xi_5, i\xi_\mu\xi_5, i\xi_\mu\xi_\nu, \xi_\mu, \xi_I\} \tag{4.34}$$

at each lattice site one collects the fields on a hypercube with sixteen sites to a standard Dirac fermion (with sixteen components). The explicit construction can be found in [67, 68, 69, 70]. The symmetries of staggered fermions, formulated in terms of these hypercube fields, are given in [71, 72].

are the sixteen $\mathrm{U}(4)_{\mathrm{taste}}$ generators in the form of Euclidean gamma matrices (ξ_I denotes the 4×4 identity matrix).

Since Σ is an element of U(12) it contains one unwanted degree of freedom, the singlet field. This can be removed by first introducing a separate mass term for this singlet field, which is proportional to the singlet mass m_{sing}. Eventually the singlet can be removed from the theory by taking the limit $m_{\mathrm{sing}} \to \infty$. Although here one could directly impose the constraint $\mathrm{tr}\,\pi = 0$ in order to obtain an SU(12) element Σ, the procedure with keeping the singlet in intermediate calculations is very convenient in partially quenched theories [75], so we mention it already here. Of course, not only the singlet field receives a mass term but the other fields as well. The mass matrix in the 3-flavor theory reads

$$M = \begin{pmatrix} m_u\xi_I & 0 & 0 \\ 0 & m_d\xi_I & 0 \\ 0 & 0 & m_s\xi_I \end{pmatrix} . \tag{4.35}$$

The transformation behaviour of Σ and M under the relevant symmetries is as before, cf. eqs. (2.8), (2.9) and (2.14). It is therefore not surprising that the $\mathcal{L}_2$ and $\mathcal{L}_4$ lagrangian, stemming from the leading part S_0 in the Symanzik effective action, are just as in (2.15) and (2.21).[6]

Differences show up at $\mathrm{O}(a^2)$ originating in S_2. Here the particular symmetry properties of staggered fermions start to enter, leading to a lagrangian $\mathcal{L}_{a^2}$ that is very different from the one given in (4.6) for Wilson fermions. If we write

$$\mathcal{L}_{a^2} = a^2(\mathcal{V} + \mathcal{V}') \tag{4.36}$$

one finds four terms in each of the two potentials $\mathcal{V}$ and $\mathcal{V}'$ [74, 15, 76],

$$\begin{aligned} \mathcal{V} = {} & C_1\langle\xi_5\Sigma\xi_5\Sigma^\dagger\rangle + C_3\frac{1}{2}\sum_\nu\Big[\langle\xi_\nu\Sigma\xi_\nu\Sigma\rangle + \mathrm{h.c.}\Big] \\ & + C_4\frac{1}{2}\sum_\nu\Big[\langle\xi_{\nu5}\Sigma\xi_{5\nu}\Sigma\rangle + \mathrm{h.c.}\Big] + C_6\sum_{\mu<\nu}\langle\xi_{\mu\nu}\Sigma\xi_{\nu\mu}\Sigma^\dagger\rangle\,, \end{aligned} \tag{4.37}$$

$$\begin{aligned} \mathcal{V}' = {} & C_{2V}\frac{1}{4}\sum_\nu\Big[\langle\xi_\nu\Sigma\rangle\langle\xi_\nu\Sigma\rangle + \mathrm{h.c.}\Big] + C_{2A}\frac{1}{4}\sum_\nu\Big[\langle\xi_{\nu5}\Sigma\rangle\langle\xi_{5\nu}\Sigma\rangle + \mathrm{h.c.}\Big] \\ & + C_{5V}\frac{1}{2}\sum_\nu\Big[\langle\xi_\nu\Sigma\rangle\langle\xi_\nu\Sigma^\dagger\rangle\Big] + C_{5A}\frac{1}{2}\sum_\nu\Big[\langle\xi_{\nu5}\Sigma\rangle\langle\xi_{5\nu}\Sigma^\dagger\rangle\Big]\,. \end{aligned} \tag{4.38}$$

The C_x are unknown LECs and h.c. stands for *hermitian conjugate*.[7] The splitting of $\mathcal{L}_{a^2}$ in two potentials and the somewhat peculiar labelling of LECs has historical reasons only, but since it is standard convention in the SChPT literature we follow this notation.[8]

The explicit appearance of the taste symmetry generators in the potential makes it

[6] As mentioned before we should add the singlet mass term $m_{\mathrm{sing}}\langle\pi\rangle^2/6$.

[7] Note that it is not customary to introduce a scaled variable $\hat{a}$ of mass dimension two in SChPT. Hence the coefficients C_x are of mass dimension six instead of being dimensionless.

[8] See ref. [74] for the historical development of $\mathcal{L}_{a^2}$.

apparent that the taste symmetry is broken by $\mathcal{L}_{a^2}$. This is expected, because, as we remarked earlier, the taste symmetry is broken by the S_2 part in the Symanzik effective action. However, $\mathcal{L}_{a^2}$ does not break the $\mathrm{U}(4)_{\mathrm{taste}}$ symmetry completely but it retains an SO(4) subgroup of it [15]. This remnant SO(4) subgroup is accidental. It is broken by higher order terms of $\mathrm{O}(a^2p^2, a^2m)$, as discussed below.

Before continuing with the higher order corrections we need to make some remarks concerning the power counting. It is slightly simpler than for Wilson fermions because there are no corrections linear in a in staggered ChPT. Nevertheless, it is the relative size of the quark mass and the lattice spacing corrections that determines at what order the latter enter the chiral expansion. Let us assume first that $m^2 \sim (a\Lambda_{\mathrm{QCD}}^2)^2$, or, in short, $m^2 \sim a^2$. This corresponds to the GSM regime for Wilson fermions in (4.11), with the exception that there are no terms linear in a:

GSM regime:

$$\begin{aligned} \text{LO}: &\quad p^2,\, m \\ \text{NLO}: &\quad p^4,\, p^2m,\, m^2,\, a^2\,. \end{aligned} \tag{4.39}$$

We should mention that it is not customary in the context of staggered ChPT to refer to this scheme by the name GSM regime. This has a practical reason only: current lattice data of the MILC collaboration, which is essentially the only collaboration that carries out large scale simulations with (rooted) staggered quarks, favors a different counting where $m \sim a^2\Lambda_{\mathrm{QCD}}^3$. This corresponds to the LCE regime for Wilson fermions and the order counting is as:

LCE regime:

$$\begin{aligned} \text{LO}: &\quad p^2,\, m,\, a^2 \\ \text{NLO}: &\quad p^4,\, p^2m,\, m^2,\, p^2a^2,\, ma^2,\, a^4\,. \end{aligned} \tag{4.40}$$

We emphasize again that size of the lattice spacing corrections and the appropriate power counting depends on the details of the lattice theory. Most of the MILC simulations were done with Asqtad staggered fermions [77], a highly improved version of staggered fermions (Asqtad stands for *a-squared tadpole improved*). But even for these improved fermions the $\mathrm{O}(a^2)$ corrections are sizeable for a lattice spacing with approximately 0.1 fm. It turns out that the appropriate power counting is as in (4.40), as we discuss shortly.

Recently, so-called *highly improved staggered quarks* (HISQ) [78, 79, 80] were also used in simulations, which are another variant of (highly improved) staggered fermions. These show significantly smaller $\mathrm{O}(a^2)$ cut-off effects [81] and for smaller lattice spacings it might be appropriate to consider the scheme (4.39). However, in the following we exclusively assume the counting (4.40) for our discussion.

Taking $\mathcal{L}_{a^2}$ at LO it contributes to the tree level pseudo scalar masses. As usual these are found by expanding the Σ field to quadratic order in the pion fields. For the charged pion mass one finds [74]

$$M_{\pi_b^\pm}^2 = 2B(m_u + m_d) + a^2\Delta(\xi_b)\,. \tag{4.41}$$

The taste label $b = 5, \mu 5, \mu\nu, \mu, I$ distinguishes the sixteen different taste partners. The shift $a^2\Delta(\xi_b)$ caused by $\mathcal{L}_{a^2}$ is flavor independent and reads [74]

$$\begin{aligned}
\Delta(\xi_5) &\equiv \Delta_P = 0\,, \\
\Delta(\xi_{\mu 5}) &\equiv \Delta_A = \frac{16}{f^2}\left(C_1 + 3C_3 + C_4 + 3C_6\right)\,, \\
\Delta(\xi_{\mu\nu}) &\equiv \Delta_T = \frac{16}{f^2}\left(2C_3 + 2C_4 + 4C_6\right)\,, \\
\Delta(\xi_{\mu}) &\equiv \Delta_V = \frac{16}{f^2}\left(C_1 + C_3 + 3C_4 + 3C_6\right)\,, \\
\Delta(\xi_I) &\equiv \Delta_I = \frac{16}{f^2}\left(4C_3 + 4C_4\right)\,.
\end{aligned} \tag{4.42}$$

Note that the potential $\mathcal{V}'$ does not contribute to the charged (flavor non-singlet) pions and kaons. However, it does give a correction to the neutral (flavor singlet) pseudo scalars [74].

As expected, the mass shifts depend on taste and the $\mathrm{U}(4)_{\text{taste}}$ symmetry is broken. However, the accidental SO(4) taste symmetry of $\mathcal{L}_{a^2}$ implies that the mass shift $\Delta(\xi_i)$ is the same for all ξ_μ, all $\xi_{5\mu}$, and all $\xi_{\mu\nu}$. The shift $\Delta(\xi_5)$ is zero as a consequence of the exact axial U(1) symmetry. Hence, this pseudo scalar is called the *Goldstone pion* $\pi_5^\pm$.

The chiral effective theory does not say anything about the mass shifts $\Delta(\xi_i)$, neither the sign nor the size. A negative shift would imply a vanishing meson mass before the chiral limit and the existence of nontrivial phases, similar to the Aoki phase for Wilson fermions [82]. However, the masses of all pions are easily measured and the mass shifts observed by the MILC collaboration are all positive [83]. Moreover, the shifts are fairly large and the lattice spacing contribution $a^2\Delta(\xi_i)$ to the pion masses is of the same size as the quark mass contribution $2B(m_u + m_d)$. For example, for Asqtad staggered quarks at $a \approx 0.09$ fm one finds an average taste splitting of about $(320\ \text{MeV})^2$, while the Goldstone pion has masses between 240 and 600 MeV [84, 85]. Hence, the data directly tells us to use the counting (4.40) with the contribution $a^2\mathcal{V}$ in the leading order lagrangian.[9]

The full NLO lagrangian has been constructed in [87]. At this order the accidental SO(4) taste symmetry of $\mathcal{L}_2$ is broken by terms of $\mathrm{O}(p^2a^2)$, and the symmetry group of the effective theory coincides with the one of the underlying lattice theory. The number of terms in the NLO lagrangian is fairly large, more than 200 operators enter $\mathcal{L}_4$, and each comes with its own unknown LEC. Fortunately, the number of unknown parameters in observables is much smaller, since many of the NLO terms contribute to a given observable in the same way. For example, the NLO results for the Goldstone pion mass and decay constant were calculated in refs. [74, 88]. Only two combinations of NLO LECs enter the final results, one for each observable. If it was different SChPT would be practically useless.[10]

[9] For the HISQ action one typically finds the taste splitting reduced by a factor of 3 [86].
[10] We remark that two combinations of LO LECs in $\mathcal{V}'$ also enter the NLO result [74, 88].

5. Partial quenching and mixed action theories

5.1. General remarks

Partial quenching refers to the situation with the masses for the sea quarks (those entering the effective action) being different from the valence quarks (defining the correlation function). In this case one speaks of *partially quenched QCD* (PQQCD). It is operationally straightforward to choose the masses differently. For example, consider a loop diagram in perturbative QCD and simply take the quark mass in internal quark propagators different from the one in external lines. Similarly in numerical simulations of lattice QCD where the mass in the fermion determinant is chosen different from the one in the quark propagators. In fact, the idea of partial quenching was born because of limitations in numerical lattice simulations: the quark mass enters the fermion determinant and influences the generation of the gauge field ensembles. Once the gauge field ensemble is at hand one calculates quark propagators in this gauge field background. This second step is less time consuming than the generation of the gauge field ensemble. So why not calculating the quark propagator for various different quark masses, all (except one) being different from the quark mass used in the fermion determinant? That way one obtains more data and (hopefully) more information from the numerically expensive and therefore precious gauge field ensembles. This is still the main motivation for doing partially quenched lattice simulations.

One can go even further and choose the whole Dirac operator to be different for the sea and the valence quarks. In this case one speaks of *mixed action QCD* (MAQCD). If the valence Dirac operator is chosen to satisfy the Ginsparg-Wilson relation this mixed action setup simplifies significantly the computation of weak matrix elements because the operator mixing is as in continuum QCD. On the other hand, the generation of the gauge field ensembles may still involve numerically cheap Wilson or staggered fermions, making the mixed action setup a cost efficient alternative to full dynamical simulations with Ginsparg-Wilson fermions in both the sea and the valence sector.

For both variants of (lattice) QCD one can construct the associated chiral effective theory, called *partially quenched ChPT* (PQChPT) [89, 90] and *mixed action ChPT* (MAChPT) [1, 5]. As usual these rest on the assumption of spontaneous chiral symmetry breaking and the existence of light pseudo Goldstone bosons. These effective theories play an important rôle in analyzing the modifications due to different quark masses and/or different Dirac operators in the sea and valence sector.

In this section we briefly summarize the steps for the construction of the chiral lagrangian for both PQChPT and MAChPT. A discussion of the results for the pion mass

and the decay constant follows in section 10.

5.2. Partial quenching

The field theoretic formulation of partially quenched theories goes back to Morel [91]. His idea was to enlarge the field content of a given theory by adding valence and ghost fields, where the latter are chosen in such a way that their contribution to the effective action cancels the one of the valence fields.

To be specific let us consider continuum PQQCD with N_s sea quarks $q_{\mathrm{s},i}$. In addition, there are N_v valence quarks $q_{\mathrm{v},i}$ and N_v ghosts $\tilde{q}_i$. The latter are described by *commuting* spin 1/2 fields, so they are bosons, and this explains their name ghosts. The fermionic part of the QCD lagrangian in (2.1) is generalized to (the summation over the flavor indices is suppressed)

$$\begin{aligned}\mathcal{L}_{\mathrm{PQQCD,quark}} &= \overline{q}_\mathrm{s}\,[\not{D}_\mathrm{s} + M_\mathrm{s}]\,q_\mathrm{s} + \overline{q}_\mathrm{v}\,[\not{D}_\mathrm{v} + M_\mathrm{v}]\,q_\mathrm{v} + \tilde{q}^\dagger\,[\not{D}_\mathrm{v} + M_\mathrm{v}]\,\tilde{q}\,, &(5.1)\\ &= \overline{Q}\,[\not{D} + \mathcal{M}]\,Q\,. &(5.2)\end{aligned}$$

For the second line we combined all fields into $Q = (q_\mathrm{s}, q_\mathrm{v}, \tilde{q})^T$ and $\overline{Q} = (\overline{q}_\mathrm{s}, \overline{q}_\mathrm{v}, \tilde{q}^\dagger)$.[1] Consequently, the Dirac operator $\not{D}$ and the mass matrix $\mathcal{M}$ read

$$\not{D} = \begin{pmatrix} \not{D}_\mathrm{s} & 0 & 0 \\ 0 & \not{D}_\mathrm{v} & 0 \\ 0 & 0 & \not{D}_\mathrm{v} \end{pmatrix}, \qquad \mathcal{M} = \begin{pmatrix} M_\mathrm{s} & 0 & 0 \\ 0 & M_\mathrm{v} & 0 \\ 0 & 0 & M_\mathrm{v} \end{pmatrix}. \tag{5.3}$$

We wrote $\not{D}_\mathrm{s}$ and $\not{D}_\mathrm{v}$, leaving open the possibility that the Dirac operator is different in the sea and the valence sector. This does not make much sense in continuum PQQCD, since we have only one Dirac operator available in continuum QCD. In lattice PQQCD this notation is of much more use because of the various existing lattice Dirac operators. We come to this in section 5.4.

Introducing the standard measure terms for the quark and ghost fields and performing the integrations over these degrees of freedom, the partition function for PQQCD reads (formally!)

$$Z_\mathrm{PQQCD} = \int \mathcal{D}[A_\mu]\,\det\,[\not{D}_\mathrm{s} + M_\mathrm{s}]\exp(-S_\mathrm{gauge})\,. \tag{5.4}$$

The functional integration over the gluon fields A_μ has not been performed yet. The main observation here is that the valence quarks and ghosts do not contribute to the effective action. The 'wrong' statistics of the ghost fields leads to an exact cancellation of the fermion determinant stemming from the valence quarks (as long as the valence quark and the ghost masses are the same, something we always assume in the following). The same cancellation takes place in correlation functions involving sea quark fields only. Hence, sea correlation functions are identical to those of standard ('unquenched') QCD with N_s quarks only.

[1] Note that the fields $\tilde{q}^\dagger$ and $\tilde{q}$ are, as bosonic fields, not independent.

Correlation functions involving valence quark fields are different. Gauge invariant operators made of valence quark (and anti quark) fields will always result in valence quark propagators, and the propagator involves the valence quark masses in $M_{\rm v}$. So the lagrangian (5.1) (plus the usual gauge field part) achieves what we were after: It describes a theory where the masses of the virtual particles are different from those that appear in the 'external states'.

We use quotation marks in the previous sentence because states refer to a theory formulated in Minkowski space and the existence of a Hilbert space and a self-adjoint Hamilton operator. However, PQQCD as a euclidean field theory is not unitary and an operator representation does not exist. This is almost obvious since the theory contains spin 1/2 fields that are quantized as bosons. Only for equal sea and valence masses will the theory be unitary, because in this case the theory has an exact flavor symmetry between the sea and the valence quarks. Hence, any correlation function involving valence fields will be identical to an analogous one involving sea fields only. And the latter is, as remarked above, a correlation function of standard (and therefore unitary) QCD with $N_{\rm s}$ sea quarks. In other words, PQQCD contains standard QCD as a special case for degenerate sea and valence quark masses.

The usefulness of PQQCD rests on the assumption that chiral symmetry is spontaneously broken, leading to (pseudo) Goldstone bosons that can be described by an effective theory, partially quenched ChPT.[2] Except for some differences concerning the symmetry groups the construction of PQChPT mirrors the procedure for standard ChPT. For vanishing sea and valence masses the lagrangian (5.1) is symmetric under transformations in

$$G = \mathrm{SU}(N_{\rm s}+N_{\rm v}|N_{\rm v})_L \times \mathrm{SU}(N_{\rm s}+N_{\rm v}|N_{\rm v})_R\,. \tag{5.5}$$

The appearance of the *graded* group $\mathrm{SU}(N_{\rm s}+N_{\rm v}|N_{\rm v})$ is again a consequence of the boson character of the spin 1/2 ghost fields. An element U of the graded group $\mathrm{SU}(N_{\rm s}+N_{\rm v}|N_{\rm v})$ can be represented by a square matrix of dimension $N_{\rm s}+2N_{\rm v}$. If we write it in block form as

$$U = \begin{pmatrix} A & C \\ D & B \end{pmatrix}, \tag{5.6}$$

the matrix elements of the $(N_{\rm s}+N_{\rm v})\times(N_{\rm s}+N_{\rm v})$ matrix A and the $N_{\rm v}\times N_{\rm v}$ matrix B are commuting numbers, while the (rectangular) matrices C and D contain anticommuting matrix elements.

G is assumed to be spontaneously broken to the diagonal subgroup

$$H = \mathrm{SU}(N_{\rm s}+N_{\rm v}|N_{\rm v})_{R=L}\,. \tag{5.7}$$

The associated Goldstone boson fields are described, as usual, by fields Σ 'living' in

[2] As for standard QCD there exists no proof for this assumption. Some arguments in support of it are summarized in [17].

the coset space G/H, which here is isomorphic to $\mathrm{SU}(N_\mathrm{s}+N_\mathrm{v}|N_\mathrm{v})$ and has dimension $2(N_\mathrm{s}+2N_\mathrm{v})^2-1$. Σ can be written as an exponential of a field Φ,

$$\Sigma = \exp\left(2i\Phi/f\right) . \tag{5.8}$$

Φ plays the rôle of the field π in (2.6) and it contains all the pion fields. If we follow the convention introduced in (5.6) and write Φ in block form according to

$$\Phi = \begin{pmatrix} \phi & \eta \\ \overline{\eta} & \tilde{\phi} \end{pmatrix} , \tag{5.9}$$

the matrix ϕ contains all pion fields made out of two fermionic quarks (sea and/or valence) and the matrix $\tilde{\phi}$ consists of the pions made out of two ghost quarks. Both fields are bosonic fields, since they consist of either two fermions or two bosons. The upper left $N_\mathrm{s}\times N_\mathrm{s}$ submatrix in ϕ can be identified (for $N_\mathrm{s}=3$) with the matrix π in (2.6). On the other hand, the matrices η, $\overline{\eta}$ contain the pion fields made out of a fermionic quark and a bosonic ghost, hence these fields describe fermions.

The transformation properties of Σ under chiral transformations, parity and charge conjugation are analogous to the ones in standard ChPT, given in (2.8) and (2.9). Also the transformation of the mass spurion field $\mathcal{M}$ is as in (2.14). Since these transformation laws determine the form of the chiral lagrangian it is no surprise that the PQChPT lagrangian has the same form as the standard ChPT lagrangian. Besides the larger field content there is essentially only one crucial difference: The angled brackets $\langle\ldots\rangle$ stand for taking the *supertrace* in flavor space, since the supertrace is the appropriate invariant for graded groups. The supertrace of the matrix Φ in (5.9) is defined as

$$\mathrm{str}(\Phi) = \mathrm{tr}(\phi) - \mathrm{tr}(\tilde{\phi}) . \tag{5.10}$$

Note that it involves a relative sign between the quark and the ghost degrees of freedom. In Feynman graphs this eventually leads to a cancellation between valence and ghost pion loops.

The crucial property of PQChPT is that it contains standard unquenched ChPT as a special case when the sea and valence quark masses are chosen equal. That has to be the case since the underlying theory has this property. An immediate and important consequence is that the LECs in PQChPT are exactly the ones of standard ChPT, simply because the LECs in the chiral lagrangian do not depend on the masses. This feature finally explains why partial quenching is useful, despite the loss of unitarity and the lack of an operator representation. By monitoring the quark mass dependence of correlation functions in PQQCD and matching them to PQChPT we have a handle on the *physical* LECs of *physical* ChPT. And for this it is irrelevant that both PQQCD and PQChPT are not unitary. S. Sharpe and N. Shoresh succinctly summarized this fact by saying 'physical results from unphysical simulations' [92].

In order to illustrate this let us have a look at the 1-loop result for the mass and decay constant of a pion made of two valence quarks. For simplicity we consider the case with

$N_\mathrm{s} = N_\mathrm{v} = 2$ and degenerate quark masses in both the sea and valence sector. The results read [92]

$$M^2_{\mathrm{vv,NLO}} = M^2_{0,\mathrm{vv}} \left(1 + \frac{1}{32\pi^2 f^2} \left[(M^2_{0,\mathrm{vv}} - M^2_{0,\mathrm{ss}}) + (2M^2_{0,\mathrm{vv}} - M^2_{0,\mathrm{ss}}) \ln \frac{M^2_{0,\mathrm{vv}}}{\mu^2} \right] \right.$$
$$\left. - \frac{8}{f^2} \left[(L_5 - 2L_8) M^2_{0,\mathrm{vv}} + 2(L_4 - 2L_6) M^2_{0,\mathrm{ss}} \right] \right) , \tag{5.11}$$

$$\frac{f_{\mathrm{vv,NLO}}}{f} = 1 - \frac{M^2_{0,\mathrm{vs}}}{16\pi^2 f^2} \ln \left(\frac{M^2_{0,\mathrm{vs}}}{\mu^2} \right) + \frac{4}{f^2} \left[L_5 M^2_{0,\mathrm{vv}} + 2L_4 M^2_{0,\mathrm{ss}} \right] , \tag{5.12}$$

where $M^2_{0,\mathrm{vv}}, M^2_{0,\mathrm{ss}}$ and $M^2_{0,\mathrm{vs}}$ are the tree-level masses for the various pions,

$$M^2_{0,\mathrm{vv}} = 2Bm_\mathrm{v} , \qquad M^2_{0,\mathrm{ss}} = 2Bm_\mathrm{s} , \qquad M^2_{0,\mathrm{vs}} = B(m_\mathrm{v} + m_\mathrm{s}) , \tag{5.13}$$

Setting $m_\mathrm{s} = m_\mathrm{v}$ we recover the unquenched results in (2.24) and (2.32), as expected. The LECs in these expressions are the same as in (2.24) and (2.32). However, the partially quenched result is more difficult in the sense that instead of one $\mathrm{O}(m^2)$ term there are now separate terms of $\mathrm{O}(m_\mathrm{v}^2)$ and of $\mathrm{O}(m_\mathrm{v} m_\mathrm{s})$. By monitoring the dependence of the pion mass on m_v (at fixed m_s, for example) we have, at least in principle, a handle on the two combinations $L_5 - 2L_8$ and $L_4 - 2L_6$. In contrast, in the unquenched theory we can only extract the linear combination $L_5 - 2L_8 + 2(L_4 - 2L_6)$. Hence, partial quenching not only admits the determination of physical LECs, it even allows the separate determination of LECs which otherwise would be 'locked' in fixed linear combinations.

So far we discussed partial quenching in continuum QCD and continuum ChPT, but the discussion goes through essentially unchanged for lattice QCD as well [76, 74, 2]. One introduces additional valence quarks and ghosts, whose contributions to the effective action exactly cancel in the partition function.[3] The construction of the corresponding chiral effective theory follows again the two-step procedure via the Symanzik effective theory. There is essentially no change except for the larger field content. For instance, the leading term in the expansion (3.1) is now (by construction) the action of PQQCD. This leads to PQChPT as the leading continuum part of the chiral effective theory. The lattice spacing corrections are again taken into account by a spurion analysis, and their concrete form depends on the lattice fermions under consideration. The final result of this analysis is easily quoted: The chiral lagrangian of the partially quenched lattice theory has the same form as the unquenched one. The difference is in the definition of the angled brackets, which in the partially quenched case denote supertraces, and in the interpretation of the field Σ and the mass matrix M. These need to be appropriately redefined to reflect the larger flavor content of the partially quenched theory.

[3] There is a subtlety with the introduction of Wilson ghosts: The spectrum of the Wilson Dirac operator cannot be shown to be strictly positiv. Hence the functional integral over the bosonic ghost fields is not guaranteed to converge for arbitrary gauge fields. This can be remedied by introducing a small twisted quark mass [93].

We mentioned in the beginning that partially quenched QCD is not unitary and therefore 'sick' as a euclidean field theory. How does this sickness show up in partially quenched ChPT? A clear sign for the unphysical effects in PQChPT is the *double pole* contribution in the flavor neutral propagator [89].

Let us simplify the discussion by considering PQChPT with two degenerate sea quarks and two degenerate valence quarks and ghosts. The flavor neutral propagator is the two-point function

$$G^N_{ab}(x-y) = \langle \Phi_{aa}(x)\Phi_{bb}(y)\rangle \,. \tag{5.14}$$

The computation of G^N is slightly nontrivial even at tree level [92], but the final result is easily quoted in momentum space:

$$G^N_{ab}(p) = \frac{\epsilon_a \delta_{ab}}{p^2 + M^2_{0,aa}} - \frac{1}{2}\frac{p^2 + M^2_{0,\mathrm{ss}}}{(p^2 + M^2_{0,aa})(p^2 + M^2_{0,bb})} \,. \tag{5.15}$$

Here $M^2_{0,aa}$ refers to the appropriate tree level pion masses, depending on the values for the flavor index a. For example, $M^2_{0,aa} = M^2_{0,\mathrm{ss}} = 2Bm_\mathrm{s}$ if a corresponds to a sea flavor or $M^2_{0,\mathrm{vv}} = 2Bm_\mathrm{v}$ if it refers to a valence quark or a ghost. For the latter we also have $\epsilon_a = -1$ (a consequence of the bosonic character of the ghosts), otherwise ϵ_a is equal to $+1$. For arbitrary (and nondegenerate) sea and valence quark flavors the second ('double pole') contribution in (5.15) is a fraction involving even more terms, and the prefactor $1/2$ is replaced by $1/N_\mathrm{s}$ [92].

When a or b denotes a sea quark flavor the second term in the neutral propagator simplifies because the numerator cancels with one factor in the denominator. In this case the neutral propagator reduces to a single pole term. This is what one expects in a 'healthy' field theory. On the other hand, if $a = b$ denote valence quark flavors the double pole remains, unless the quark masses are tuned appropriately. This is easier seen by slightly rewriting (5.15) as (using $M_{0,aa} = M_{0,bb} = M_{0,\mathrm{vv}}$)

$$G^N_{ab}(p) = \left(\delta_{ab} - \frac{1}{2}\right)\frac{1}{p^2 + M^2_{0,\mathrm{vv}}} - \frac{(M^2_{0,\mathrm{ss}} - M^2_{0,\mathrm{vv}})/2}{(p^2 + M^2_{0,\mathrm{vv}})^2} \,. \tag{5.16}$$

The residue of the double pole is proportional to the difference of the squared sea and valence pion masses. Consequently, the double pole vanishes if the quark masses satisfy $m_\mathrm{s} = m_\mathrm{v}$, i.e. in the unquenched case.

The presence of the double pole in the flavor neutral propagator leads to unphysical effects in various observables. The most prominent ones are the isospin $I = 0$ pion scattering length [94], the nucleon-nucleon potential [95] and the $I = 1$ scalar correlator [96, 97] that one needs to compute in order to get the mass of the lightest scalar meson, the a_0. Lattice simulations of the latter have directly shown the 'sickness' of partial quenching: the scalar correlator turns negative for $m_\mathrm{v} < m_\mathrm{s}$ [98], something that cannot happen in a unitary field theory.

5.3. Staggered ChPT and the fourth-root-trick

Partial quenching is a very useful tool for implementing the modifications caused by the fourth-root-trick for staggered fermions. First, it is straightforward to formulate the partially quenched theory for unrooted staggered fermions. Additional staggered valence and ghost quarks are introduced as before. The quark masses in the sea and valence sector can be chosen different or equal. The main modification is an increase in sea quark fields: Each sea quark field is 'replicated' n_r times such that there are $n_r N_s$ flavors of staggered sea quarks. The introduction of n_r is for bookkeeping reasons only. $n_r = 1$ recovers the standard partially quenched theory. However, in intermediate steps one keeps n_r arbitrary and adjusts it in the end to the desired value.

Taking into account the additional taste degree of freedom one ends up with $4n_r N_s$ sea quarks in the continuum limit. The construction of PQChPT in section 5.2 goes through essentially unchanged except for the replacement $N_s \to n_r N_s$. The calculation of observables in this replicated and partially quenched theory poses no additional difficulties compared to the partially quenched one with $n_r = 1$. A final result for any observable will be a polynomial in n_r, and these factors of n_r arise from loop diagrams and the summation over the (replicated) flavor indices.

At this stage one can finally account for the fourth-root-trick. Recall that it amounts to giving the sea quarks a weight of $1/4$ in the effective action. Perturbatively this means a factor of $1/4$ for each sea quark loop in a Feynman diagram. This is achieved by setting $n_r = 1/4$. The main assumption is that this simple rule (sometimes called *replica rule* [85]) also works on the level of the replicated and partially quenched effective theory. The chiral effective theory one obtains with this replica rule is called *rooted staggered ChPT* (rSChPT).

It is by far not obvious that this procedure is correct. In fact, the validity of the fourth-root-trick has been controversially debated in the literature.[4] Note that there are two separate issues to address. One question is whether lattice QCD with rooted staggered quarks is in the universality class of QCD, i.e. whether the continuum limit comes out correctly. A second question is whether rSChPT is indeed the correct chiral effective theory for QCD with rooted staggered quarks, i.e. whether the replica rule works out correctly in ChPT.

Here is not the place to discuss these issues appropriately and to do justice to all the work concerning these questions. A detailed summary of all the arguments in favor of the fourth-root-trick can be found in [85], where one also finds an exhaustive list of references to original papers addressing the two questions raised before.

5.4. Mixed action theories

The mixed action approach to QCD is a generalization of partial quenching. Not only are the masses in the sea and valence sector different, the whole Dirac operator is chosen

[4] A somewhat bitter account of the controversy is [99]. More neutral and scientifically appropriate discussions are given in the reviews [100, 101, 102, 103].

not to be the same. In general this makes sense only in lattice QCD where various discretizations of the Dirac operator exist.

Mixed action theories are theoretically formulated as described in the previous section, but with $\not{D}_{\rm s} \neq \not{D}_{\rm v}$. One nevertheless expects correct physical results with such a unconventional setup. The reason is the naive argument that all proper lattice Dirac operators 'converge' to the same continuum Dirac operator, the one that has been discretized in the first place. In other words, one expects the 'difference' between two lattice Dirac operators to be of $\mathrm{O}(a)$, which therefore vanishes in the continuum limit.

There are drawbacks too in this approach. Similarly to partially quenched theories, unitarity is lost for all nonzero lattice spacings. It is even worse, since mixed action QCD does not contain standard QCD when the quark masses are chosen equal. It is only in the continuum limit that unitarity can be restored. This does not happen automatically, but one has to tune the (renormalized) sea and valence quark mass such that one recovers unquenched QCD in the continuum limit. This is an extra step in mixed action simulations. Moreover, it is not at all obvious that a 'better' Dirac operator for the valence quarks (one that has exact chiral symmetry at nonzero a) automatically implies better results for physical quantities. Analytic control of the lattice spacing artifacts is clearly desirable.

Such control can be gained by studying the chiral effective theory, mixed action ChPT. Its construction is completely analogous to PQChPT. The intermediate step is again the Symanzik effective theory. The differences are in the details of the Symanzik expansion (3.1). In particular, the terms in $S_1, S_2, \ldots$ are different for the sea quark and the valence quark/ghost fields. One can nevertheless map these terms into the chiral effective theory by the standard spurion analysis. The details and the final chiral lagrangian for Wilson sea quarks can be found in [1, 2], for staggered sea quarks in [5]. In order to illustrate the results we quote here the lagrangian $\mathcal{L}_{a^2}$ for Wilson sea quarks [2].

Since the lattice spacing corrections in mixed action theories are different in the sea and valence sector it is convenient to introduce projection operators on the sea and valence sector,

$$P_S = \mathrm{diag}(1_S, 0)\,, \qquad P_V = \mathrm{diag}(0, 1_V)\,, \tag{5.17}$$

where 1_S denotes the $N_{\rm s} \times N_{\rm s}$ identity matrix in the sea sector, and 1_V the $2N_{\rm v} \times 2N_{\rm v}$ identity matrix in the valence sector (note that it includes both valence quarks and ghosts). With these definitions the lagrangian reads

$$\begin{aligned}\mathcal{L}_{a^2} = &- \hat{a}^2\Big[W_6'\langle P_S\Sigma^\dagger + \Sigma P_S\rangle^2 + W_7'\langle P_S\Sigma^\dagger - \Sigma P_S\rangle^2 + W_8'\langle P_S\Sigma^\dagger P_S\Sigma^\dagger + \Sigma P_S\Sigma P_S\rangle\Big] \\ &- \hat{a}^2 W_{\rm Mix}\langle\tau_3\Sigma\tau_3\Sigma^\dagger\rangle\,.\end{aligned} \tag{5.18}$$

This result is easily understood. The first line on the right hand side is basically the same as in eq. (4.6), except for the replacement $\Sigma \to \Sigma P_S$. The presence of P_S in the first three terms in (5.18) makes it obvious that these are indeed the $\mathrm{O}(a^2)$ corrections stemming from the Wilson sea quarks.

There are no terms involving the projector P_V, which is a consequence of the exact chiral symmetry in the valence sector. If the valence quarks consisted of different Wilson quarks, e.g. given by a Wilson Dirac operator including a clover term, the first line in (5.18) with P_S replaced by P_V would be present too, but with different values for the LECs involved.

Finally the term involving W_{Mix}, which involves the matrix

$$\tau_3 = \text{diag}(I_S, -I_V)\,. \tag{5.19}$$

Its presence is a consequence of the reduced flavor symmetry in mixed action QCD. Because of $\not{D}_{\text{s}} \neq \not{D}_{\text{v}}$ there is no flavor symmetry between the sea and valence sector, even if the masses are chosen to be equal. Quite generally, the flavor symmetry group of mixed action theories has the form

$$G = G_{\text{Sea}} \times G_{\text{Val}}\,, \tag{5.20}$$

with $G_{\text{Sea}}, G_{\text{Val}}$ denoting the independent sea and valence flavor symmetry groups. This structure leads to the W_{Mix} term in the chiral lagrangian, which is forbidden in PQChPT with the same Dirac operator in the sea and valence sector.

A direct consequence of the W_{Mix} term is a mass splitting between the mixed pions and the sea/valence pions. Mixed pions refer to those pseudo Goldstone bosons that consist of one sea and one valence quark. For simplicity we again consider the case with $N_{\text{s}} = N_{\text{v}} = 2$ with degenerate quark masses in both sea and valence sector. At tree level we find the following masses for the sea and valence pions:

$$M^2_{0,\text{vv}} = 2Bm_{\text{v}}\,, \tag{5.21}$$

$$M^2_{0,\text{ss}} = 2Bm_{\text{s}} + \hat{a}^2\Delta_{\text{Sea}}\,, \qquad \Delta_{\text{Sea}} = \frac{16}{f^2}(2W'_6 + W'_8)\,. \tag{5.22}$$

These results reproduce (5.13) in the continuum limit, as expected. Moreover, the sea pion result reproduces the one for Wilson quarks given in (4.22) (taking into account (4.20) and $W'_{68} = W'_6 + W'_8/2$).

For the mixed pion mass we find the result

$$M^2_{0,\text{vs}} = B(m_{\text{s}} + m_{\text{v}}) + \frac{4}{f^2}\hat{a}^2\left(4W'_6 + W'_8 + 2W_{\text{Mix}}\right)\,. \tag{5.23}$$

Using the tree level results for the other pion masses this can be written as

$$M^2_{0,\text{vs}} = \frac{M^2_{0,\text{vv}} + M^2_{0,\text{ss}}}{2} + \hat{a}^2\Delta_{\text{Mix}}\,, \qquad \Delta_{\text{Mix}} = \frac{4}{f^2}(2W_{\text{Mix}} - W'_8)\,. \tag{5.24}$$

In the continuum limit the mixed pion mass is just the average of the sea and valence pion mass. The same is true for partially quenched theories as a consequence of flavor symmetry. Because this symmetry is broken in mixed action theories the mixed pion mass receives the $\text{O}(a^2)$ shift proportional to Δ_{Mix}.

This shift exemplifies the cautious remark we made earlier, namely that using a valence Dirac operator with good chiral properties does not necessarily lead to better results for physical quantities. The question whether the W_{Mix} term in the chiral lagrangian is indeed a disadvantage or not is not easily answered. If this correction is analytically under control in MAChPT it does not pose a serious problem. On the other hand, one certainly does not want the shift and the total mixed pion mass to be very large, since in this case it may give large corrections to other observables or even spoils the whole chiral expansion.[5] In this respect the mixed pion mass seems to be a suitable 'diagnostic tool' for the entire mixed action setup. Moreover, measuring the mass shift immediately tells whether one is in the GSM or LCE regime, which is necessary knowledge for the computation of other observables.

Also the flavor neutral propagator receives an $\mathrm{O}(a^2)$ correction. The result (5.16) is modified to [104]

$$G^N_{ab}(p) = \left(\delta_{ab} - \frac{1}{2}\right) \frac{1}{p^2 + M^2_{0,\mathrm{vv}}} - \frac{(M^2_{0,\mathrm{ss}} - M^2_{0,\mathrm{vv}})/2 + (16W_7'/f^2)\hat{a}^2}{(p^2 + M^2_{0,\mathrm{vv}})^2}\,. \tag{5.25}$$

where W_7' is an LEC in $\mathcal{L}_{a^2}$, see eq. (4.6). We may interpret this result as follows. In MAChPT there are two sources for the double pole in the flavor neutral propagator. One is familiar from continuum PQChPT, it is the difference in the pion masses. In addition, there is a contribution from the nonzero lattice spacing, proportional to a^2. We emphasize that the presence of this extra contribution is not the nonzero lattice spacing itself, it is once again the lack of flavor symmetry between the sea and the valence sector. In a partially quenched lattice theory with the same sea and valence quarks the W_7' term in (5.25) would be absent [104]. This is yet another example for the statement that a Dirac operator with good chiral properties in the valence sector only is not automatically better. Particular cut-off effects appear because two different Dirac operators are used.

Recall that a matching of the sea and valence masses has to be imposed for recovering unquenched QCD in the continuum limit. A variety of matching conditions are possible in principle, but the most obvious one is requiring equal masses for the sea and valence pions: $M_{\mathrm{ss}} = M_{\mathrm{vv}}$. This leads to identical sea and valence quark masses in the continuum limit. A practical advantage of this matching condition is that pion masses can be numerically computed with small errors. However, note that by imposing this condition the residue of the double pole does not vanish, and we still expect partial quenching effects of $\mathrm{O}(a^2)$. This is in contrast to the theory with the same Dirac operator in the sea and valence sector, where the residue vanishes for this matching condition.

Alternatively one could try to match in such a way that the residue of the double pole vanishes. For example, one could try to tune the masses in such a way that the unitarity violating effects in the $I = 1$ scalar correlation function vanish [105]. Although theoretically fine this matching condition lacks the precision of the condition involving the pion masses. Nevertheless, even if we could impose this condition it would mean

[5] We will see in section 10 that the mixed pion mass enters the valence pion decay constant at NLO.

that the sea and valence pion masses are different. This observation demonstrates the obvious fact that no matching condition turns the mixed action theory into a 'full' one without any sign of the two different Dirac operators in the sea and valence sector. These 'mixing effects' remain in the theory unless one takes the continuum limit.

Having discussed the results for Wilson sea quarks, the analogous results for staggered fermions in the sea sector are easily summarized. The lagrangian $\mathcal{L}_{a^2}$ is the sum of a sea part and the mixed term $a^2 W_{\text{Mix}} \langle \tau_3 \Sigma \tau_3 \Sigma^\dagger \rangle$. The sea part is essentially $\mathcal{L}_{a^2}$ of SChPT, given in (4.37), (4.38), but with Σ replaced by ΣP_S. As expected, the valence pion masses are as in (5.21) because the valence sector is the same as before. The sea pion masses, however, are as in SChPT, c.f. (4.41). The form of the tree level mixed pion mass is as in (5.23), but with $\mathrm{O}(a^2)$ correction involving the SChPT LECs C_1, C_3, C_4, C_6 instead of W_6', W_8'. In terms of the sea pion and valence pion masses one finds [5, 106]

$$M_{0,\text{vs}}^2 = \frac{M_{0,\text{vv}}^2 + \overline{M}_{0,\text{ss}}^2}{2} + \hat{a}^2 \Delta_{\text{Mix}} \,, \qquad \Delta_{\text{Mix}} = \frac{2}{f^2} W_{\text{Mix}} \,, \tag{5.26}$$

where $\overline{M}_{0,\text{ss}}^2$ denotes the *average* sea pion mass,

$$\overline{M}_{0,\text{ss}}^2 = \frac{1}{16} \sum_b M_{\pi_b^\pm}^2 \,. \tag{5.27}$$

The average is taken over all sixteen different tastes with the tree level masses in (4.41). Equation (5.26) is the analogue of (5.24).

Finally the flavor neutral propagator. Again restricting to the simple case with two degenerate sea and valence quark masses it reads [5]

$$G_{ab}^N(p) = \left(\delta_{ab} - \frac{1}{2}\right) \frac{1}{p^2 + M_{0,\text{vv}}^2} - \frac{(M_{0,\pi_I}^2 - M_{0,\text{vv}}^2)/2}{(p^2 + M_{0,\text{vv}}^2)^2} \,. \tag{5.28}$$

M_{0,π_I}^2 denotes the mass of the taste singlet pion.[6] Two important observations can be made. Firstly, the residue of the double pole can be expressed entirely as a difference of squared pion masses, i.e. there is no additional $\mathrm{O}(a^2)$ shift as for Wilson sea quarks. Secondly, it is the taste singlet sea pion mass that enters the double pole, and not, for example, the Goldstone pion π_5. This has interesting and important consequences. The residue of the double pole vanishes if the valence pion is matched to the singlet sea pion. This matching condition is also practically viable since both pion masses can be determined with small numerical uncertainties. If one instead matches the valence pion with the Goldstone pion, as is often done in practice [107, 108, 109], a remnant residue proportional to the singlet taste splitting $a^2 \Delta_I$ remains. Associated are partial quenching effects of this order. We come back to this issue in section 10 where we discuss the 1-loop results for the pion mass and decay constant in mixed action theories.

[6] We do not need to distinguish between the charged and neutral pion because we assumed degenerate sea quark masses. In general, however, it is the neutral pion that enters the flavor neutral propagator [5].

6. Wilson ChPT for 2 flavors

In previous sections we repeatedly restricted ourselves to $N_f = 2$ ChPT for Wilson fermions with a degenerate mass term. The reason was not only the simplicity of this special case. Many lattice simulations are done with two dynamical quark flavors and the corresponding WChPT results are applicable in the analysis of the data.

$N_f = 2$ WChPT results to one loop for the standard mesonic observables (pion mass, scattering lengths and pion decay constant) can be found in refs. [10, 12]. In most cases NLO results are available for both the GSM and the LCE regime. An exception is the decay constant, where only a partial NLO result for the LCE regime exists.

In the following we briefly summarize the existing results. We focus on the LCE regime for the following reason. In the LCE regime the $\mathrm{O}(a^2)$ term in the chiral lagrangian contributes at LO. Expanding the $\mathrm{O}(a^2)$ term in terms of pion fields we obtain vertices proportional to $2c_2a^2$. As part of 1-loop diagrams these lead to nonanalytic corrections proportional to $2c_2a^2 \ln M_\pi^2/\mu^2$. The presence of these additional chiral logarithms is considered to be one reason why the chiral logarithms known from continuum ChPT are not reproduced in the lattice data: The additional chiral logs obscure the nonanalytic quark mass dependence of the continuum chiral logs, and the naively expected behaviour is lost [110].

6.1. Pion mass and modified chiral logs

The modification because of additional chiral logarithms is illustrated best in the 1-loop result for the pion mass. In terms of the tree level pion mass $M_0 \equiv M_{\pi,\mathrm{LO}}$, cf. eq. (4.22), we find [10]

$$M_\pi^2 = M_0^2 \left[1 + \frac{1}{32\pi^2} \frac{M_0^2}{f^2} \ln\left(\frac{M_0^2}{\Lambda_3^2}\right) + \frac{5}{32\pi^2} \frac{2c_2a^2}{f^2} \ln\left(\frac{M_0^2}{\Xi_3^2}\right) + k_1 \frac{W_0 a}{f^2} \right] + k_3 \frac{2c_2 W_0 a^3}{f^2} + k_4 \frac{(2c_2a^2)^2}{f^2} \,. \tag{6.1}$$

The coefficients Λ_3, Ξ_3 and k_1, k_3, k_4 are combinations of previously defined LECs in the chiral Lagrangian. The exact relations between these combinations and the original LECs is not relevant in the following.[1] Note that the coefficients k_i are chosen to be dimensionless, with $k_1 = 0$ if the lattice theory is $\mathrm{O}(a)$ improved.

As expected, setting the lattice spacing to zero in (6.1) we recover the continuum ChPT result given in (2.34). This result gets modified at nonzero lattice spacing by the

[1] The exact relations can be found in [111].

anticipated chiral logarithm proportional to $c_2 a^2$ and additional corrections analytic in a. Note that the coefficient in front of the additional log is enhanced by a factor of 5 compared to the continuum log. This is better seen if we rewrite the square bracket in (6.1) as

$$\left[1 + \frac{1}{32\pi^2}\Big\{M_0^2 + 10c_2a^2\Big\}\ln\left(\frac{M_0^2}{\Lambda_3^2}\right) + \frac{10}{32\pi^2 f^2}c_2a^2\ln\left(\frac{\Lambda_3^2}{\Xi_3^2}\right) + k_1\frac{W_0 a}{f^2}\right], \tag{6.2}$$

so that the quark mass dependence comes entirely from the $\ln M_0^2/\Lambda_3^2$ term. Apparently, negative values of c_2 can render the factor $M_0^2 + 10c_2a^2$ exceptionally small such that the continuum chiral logarithm is completely diluted.

This suppression of the chiral logarithm is not unlikely. The ETM collaboration has found a negative value for c_2 in their twisted mass simulations (see ref. [112] and references therein). The calculation of the pion mass splitting provides a rough estimate for $-2c_2a^2 = M_{\pi^\pm}^2 - M_{\pi^0}^2$ (see section 8 below). The data for lattice spacings $a \approx 0.086$ fm and $M_{\pi^\pm} \approx 300$ MeV results in $-2c_2a^2 \approx (185\text{ MeV})^2$. Such a value completely suppresses the chiral log for pion masses around 400 MeV, a value not unusual in lattice simulations performed these days.

The opposite scenario with an enhanced chiral logarithm due to $c_2 > 0$ is in principle possible, but numerical lattice data does not favor this alternative.

6.2. Additive quark mass renormalization

Result (6.1) depends on the shifted quark mass m via the tree level result $M_0^2 = 2Bm - 2c_2a^2$. However, so far it is not clear how the shifted mass is related to the renormalized and the bare quark mass used in the lattice theory. In other words, the quark mass has not been matched so far, and this matching has to be done before (6.1) can be regarded as a description of the quark mass dependence of the pion mass.

The renormalized quark mass $\tilde{m}$ in lattice QCD is defined according to $\tilde{m} = Z_m(m_0 - m_{\rm cr})/a$ with m_0 and $m_{\rm cr}$ being the bare and the critical quark mass.[2] The latter predominantly accounts for the additive renormalization proportional to $1/a$, but may account for finite renormalizations of order a, a^2 etc. as well. The precise definition of $m_{\rm cr}$ is provided by specifying a renormalization condition.

To be specific let us consider a particular condition that is widely used in lattice QCD, namely the one of a vanishing pion mass, sometimes called the vector Ward identity (VWI) mass:

$$M_\pi(\tilde{m} = 0) = 0\,. \tag{6.3}$$

In words: The pion mass, as a function of the renormalized quark mass, vanishes for vanishing $\tilde{m}$. This condition fixes $m_{\rm cr}$ (but not Z_m).

We have seen in section 4.2 that the tree level pion mass vanishes if $m = c_2a^2/B$ (assuming the scenario with an Aoki phase). We therefore conclude that $\tilde{m}$ and m

[2] We use a tilde for the lattice quark mass in order to avoid confusion with the shifted quark mass m in the chiral effective theory.

are related by $\tilde{m} = m - c_2 a^2/B$. In other words both masses differ by an additive renormalization of $\mathrm{O}(a^2)$.

This tree level relation is modified at one loop. Inspecting (6.1) one easily sees that the 1-loop pion mass does not vanish for $m = c_2 a^2/B$ (equivalent to $M_0 = 0$) because of the corrections proportional to k_3, k_4. These contributions of $\mathrm{O}(a^3, a^4)$ are additional corrections to the additive mass renormalization. To be precise we define $\overline{m}$ and $\overline{M}_0^2$ by

$$\overline{M}_0^2 = 2B\overline{m} \equiv 2Bm - 2c_2 a^2 + k_3 \frac{2c_2 W_0 a^3}{f^2} + \left(k_4 \frac{(2c_2 a^2)^2}{f^2} - k_1 k_3 \frac{2c_2 W_0^2 a^4}{f^4} \right), \quad (6.4)$$

such that the quark masses $\tilde{m}$ and m differ by order a^2 and higher order terms. With this redefinition, the 1-loop result for the pion mass reads

$$M_\pi^2 = \overline{M}_0^2 \left[1 + \frac{1}{32\pi^2} \frac{\overline{M}_0^2}{f^2} \ln\left(\frac{\overline{M}_0^2}{\Lambda_3^2} \right) + \frac{5}{32\pi^2} \frac{2c_2 a^2}{f^2} \ln\left(\frac{\overline{M}_0^2}{\Xi_3^2} \right) + k_1 \frac{W_0 a}{f^2} \right]. \quad (6.5)$$

The k_3, k_4 contributions no longer appear explicitly but are absorbed in the definition of the quark mass $\overline{m}$. With this parametrization the pion mass vanishes for $\overline{m} = 0$. We therefore conclude that the mass $\overline{m}$ is proportional to the quark mass $\tilde{m}$ defined in (6.3). That both masses are not only proportional but in fact identical is a question of definition. The quark mass in ChPT appears always in form of the product Bm with the leading order LEC B. B and m are not independently defined, and any multiplicative redefinition of the quark mass is accompanied by the opposite and compensating redefinition of B.

It should be obvious that the matching differs for other definitions of the renormalized lattice quark mass. For example, another definition is through the partially conserved axial vector current (PCAC) relation. The details have not been worked out so far for this condition, but the relation between m and $\overline{m}$ will most likely be different from the one in (6.4).

The matching is greatly simplified by avoiding the notion of a quark mass dependence altogether and replacing it by the pion mass dependence. For this one computes the pion mass and any other physical observables to a given order in the chiral expansion. The pion mass result is then 'inverted' to give the shifted quark mass as a function of M_π. In a second step one obtains the pion mass dependence of the observable one is interested in. The pion mass dependence of observables is a well-defined concept since the pion mass itself is an observable and does not rely on the definition of a particular quark mass.

6.3. Order of chiral and continuum limit

The pion mass (6.5) vanishes if the chiral limit and the continuum limit are taken, irrespectively of the order one takes the limits. However, the result for the ratio $M_\pi^2/\overline{m}$ depends on the order: It converges to $2B$ if the continuum limit is taken first, but it diverges for the opposite order if the sign of c_2 is positive and exactly massless pions

exist at nonzero a.

As has been discussed in detail in ref. [113], the source of this problem is the absence of chiral symmetry in the massless limit. Recall that for $c_2 > 0$ the pions can become massless because of spontaneous breaking of the flavor symmetry, not because of spontaneous chiral symmetry breaking.

In practice the order of limits is not a problem, since one is usually interested in the physical point where the pion masses assume their physical (nonzero) values. Moreover, the pion masses one can reach in present-day numerical simulations are far from zero.

6.4. Pion scattering

The scattering amplitude for the two pion scattering process

$$\pi^\alpha(p) + \pi^\beta(k) \longrightarrow \pi^\gamma(p') + \pi^\delta(k') \tag{6.6}$$

is calculated as the residue of the four-pion pole in the four-point function. Starting from the lagrangian eq. (4.14) we obtain, expressed in terms of the standard Mandelstam variables s, t and u, the tree level result[3]

$$A(s,t,u) = \frac{1}{f^2}(s - M_\pi^2 - 2c_2a^2)\,. \tag{6.7}$$

M_π^2 denotes the tree level pion mass given in (4.22). Setting the lattice spacing to zero we recover, as expected, the familiar result of continuum ChPT [25].

Phenomenologically interesting are, besides the full scattering amplitude, the scattering lengths a_0^I for definite isospin I. Performing the standard partial wave expansion [25] we find for channels with $I = 0$ and $I = 2$ the tree level results

$$a_0^0 = \frac{7}{32\pi f^2}\left(M_\pi^2 - \frac{5}{7}\,2c_2a^2\right), \tag{6.8}$$

$$a_0^2 = -\frac{1}{16\pi f^2}\left(M_\pi^2 + 2c_2a^2\right). \tag{6.9}$$

Again, for $a = 0$ we recover the continuum results, first obtained by Weinberg [114]. For nonzero lattice spacings, however, the continuum results are modified in such a way that the scattering lengths no longer vanish in the chiral limit. Instead, they assume nonzero values of $\mathrm{O}(a^2)$. In other words, the ratio a_0^I/M_π^2 is no longer a constant but has the functional form

$$\frac{a_0^I}{M_\pi^2} = B_{0,0}^I + B_{0,1}^I\frac{a^2}{M_\pi^2}\,, \tag{6.10}$$

with $B_{0,i}^I$ being constants. Hence, the ratio a_0^I/M_π^2 diverges in the chiral limit.

This divergence has been anticipated first by Kawamoto and Smit [115]. However,

[3] Recall that the Lagrangian in eq. (4.14) is given in Euclidean space-time, so one has to Wick-rotate to Minkowski space in order to get the physical scattering amplitude.

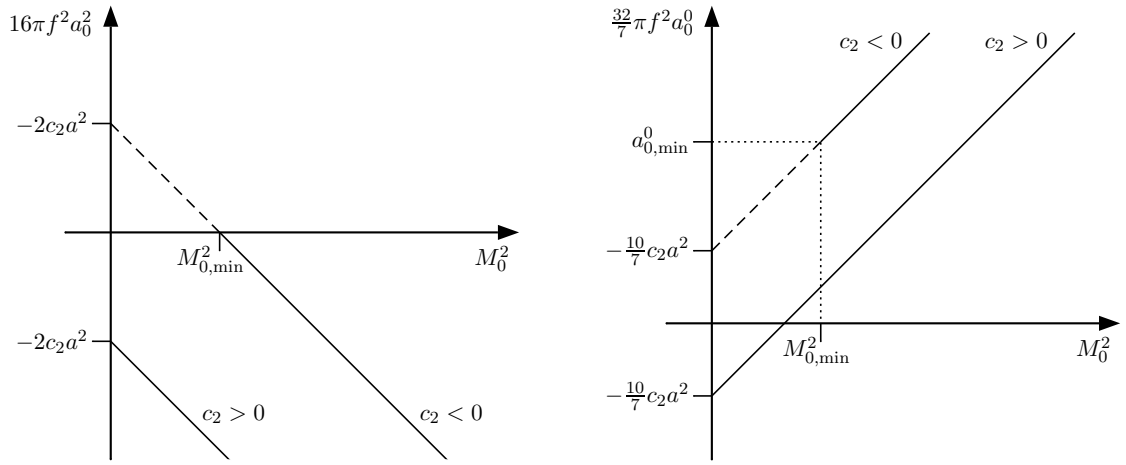

Figure 6.1.: Sketch of the scattering lengths as a function of the pion mass at nonzero lattice spacing (from Ref. [10]). The left panel shows $16\pi f^2 a_0^2$ as a function of the tree level pion mass, here denoted by M_0^2. For $c_2 < 0$ the pion mass cannot be smaller than $M^2_{0,\min}$ in eq. (4.23). Nevertheless, extrapolating to the massless point the scattering length assumes the value $-2c_2a^2$, as indicated by the dashed line. For $c_2 > 0$ the pion mass can be taken zero. At this mass the scattering length also assumes the value $-2c_2a^2$, now with the opposite sign. The right panel shows the analogous sketch for the $I = 0$ scattering length.

note that the residue of the $1/M_\pi^2$ pole is of order a^2 rather than of order a. This holds even for standard unimproved Wilson fermions, in contrast to earlier expectations [116, 117].

The reason for this 'accidental improvement' is easily understood. We have seen earlier that the leading $\mathrm{O}(a)$ correction due to the Pauli term results only in an additive renormalization of the pion mass. Since we expressed the scattering lengths as a function of the pion mass this shift is implicitly accounted for in M_π. The results for the scattering lengths excellently demonstrate that the expectation *lattice result* = *continuum result* $+O(a)$ for standard Wilson fermions is sometimes too naive. Of course, there are corrections to the scattering lengths that are linear in the lattice spacing, but these are of $\mathrm{O}(aM_\pi^2)$ and therefore suppressed in the chiral expansion [10]. Moreover, these corrections shift the constant $B^I_{0,0}$ and do not lead to a divergence proportional to $1/M_\pi^2$.

The divergence in the chiral limit will only be present if $c_2 > 0$, because only in this case can the pion indeed become massless. For the opposite sign the pion mass cannot be smaller than the minimal value quoted in eq. (4.23), resulting in the following minimal values for the scattering lengths:

$$a^0_{0,\min} = \frac{12}{32\pi f^2} 2|c_2|a^2\,, \qquad a^2_{0,\min} = 0\,. \tag{6.11}$$

Figure 6.1 sketches the pion mass dependence of the scattering lengths for the two possible signs of c_2. It seems feasible that measurements of the scattering lengths will allow to determine c_2. Extrapolating the data for a_0^2 to the chiral limit one may directly

read off c_2 as the value at vanishing pion mass, even for the $c_2 < 0$ case. A practical advantage is that this calculation of a_0^2 does not involve disconnected diagrams which usually introduce large statistical uncertainties.

The scattering amplitude and the scattering lengths have also been computed to one loop order [10]. The results are quite lengthy and we will not quote them here. However, qualitatively one finds features analogous to those in the pion mass: Besides the continuum chiral log one finds additional chiral logs proportional to $a^2 M_\pi^2 \ln M_\pi^2/\mu^2$ and $a^4 \ln M_\pi^2/\mu^2$. The presence of the latter is again a clear signal that the chiral and the continuum limit do not commute if massless pions exist at nonzero a.

6.5. Renormalization of the vector and axial vector current

In eq. (4.17) we gave the result for the axial vector current including the leading $\mathrm{O}(a)$ corrections. However, we emphasized already that eq. (4.17) is only half of the result for the axial vector current. The impact of the nontrivial current renormalization is the missing piece we still need to discuss.

Recall that the renormalized lattice currents involve a nontrivial renormalization factor and a renormalization condition that fixes it (cf. eqs. (3.7) and (3.8) for the local vector current). The renormalization condition provides a constraint that the current in the effective theory has to reproduce, and this may lead to modifications in the currents that are constructed by symmetry arguments alone.

The argument in favor of these additional modifications is easy to understand. It is quite common to impose a particular continuum chiral WI as a renormalization condition at nonzero lattice spacing [36, 38, 39]. Quite generally, a current in WChPT is the sum of the continuum current and $\mathrm{O}(a)$ corrections. The leading continuum piece satisfies, by construction, all continuum chiral WIs, while the $\mathrm{O}(a)$ correction will lead to a violation of them. The effect of the renormalization condition is now such that the renormalized current compensates for the violation of a particular chiral WI. In other words: The renormalized currents by definition absorb the violations associated with particular chiral WIs.

Let us briefly illustrate this for the axial vector current; a full account of all details (including the discussion for the vector current) can be found in ref. [12]. First of all, the renormalized axial vector current in WChPT reads,

$$A^a_{\mu,\mathrm{ren}} = Z_{\mathrm{A,eff}} A^a_{\mu,\mathrm{eff}} \,, \tag{6.12}$$

where $A^a_{\mu,\mathrm{eff}}$ refers to the expression in (4.17). The presence of the factor $Z_{\mathrm{A,eff}}$ is a remnant of imposing the renormalization condition at nonzero a, and it has the general form $Z_{\mathrm{A,eff}} = 1 + \mathrm{O}(a)$.[4] The renormalized vector current has an analogous form.

$Z_{\mathrm{A,eff}}$ is now fixed by imposing a particular WI, the same that has been imposed in the underlying lattice theory. For example, in Minkowski space there exists the well-known

[4] $Z_{\mathrm{A,eff}}$ can be thought of as the ratio of two factors, $Z_{\mathrm{A,eff}} = Z_{\mathrm{A}}/Z^0_{\mathrm{A}}$, where Z_{A} is the full renormalization factor including $\mathrm{O}(a)$ corrections, while Z^0_{A} has a perturbative expansion of the form $1 + \mathrm{O}(g(a)^2)$. These drop out in the ratio and only the $\mathrm{O}(a)$ corrections survive in the ratio [12].

('current algebra') relation stating that the commutator of two axial vector currents is equal to the vector current. The Euclidean space-time analogue of it reads [118]

$$\int_V d\vec{x}\,\epsilon^{abc}\epsilon^{cde}\langle\pi^d(\vec{p})|\left[A^a_{0,\mathrm{ren}}(y_0+t,\vec{x})-A^a_{0,\mathrm{ren}}(y_0-t,\vec{x})\right]A^b_{0,\mathrm{ren}}(y)|\pi^e(\vec{q})\rangle \\ = 2i\epsilon^{cde}\langle\pi^d(\vec{p})|V^c_{0,\mathrm{ren}}(y)|\pi^e(\vec{q})\rangle\,. \tag{6.13}$$

Note that this is a WI of the massless theory, so here we need either $\vec{p}$ or $\vec{q}$ (or both) to be nonvanishing for the right hand side to be nonzero. The right hand side needs the renormalized vector current, which can be defined using condition (3.8). Condition (6.13) determines $|Z_\mathrm{A}|$ once we have the renormalized vector current. Notice that the result can depend not only on the pion momenta but also on the Euclidean time separating the two axial currents (which traces back to the size of the region over which the axial rotation is applied).

Other renormalization conditions are sometimes used in practice, but most of them are hard to implement in the chiral effective theory. For example, matrix elements involving non-pionic states are not easily accessible in standard mesonic ChPT. Conditions involving quark states (the so-called 'RIMOM' scheme [119]) are also out of reach. In practice, only conditions involving pseudoscalar states can be treated in the chiral effective theory.

The calculation of both sides in (6.13) is straightforward but rather technical [12]. The final result reads

$$Z_{\mathrm{A,eff}} = 1-\frac{4\hat{a}}{f^2}(W_{45}\bar{c}_{\mathrm{SW}}+W_\mathrm{A}\bar{c}_\mathrm{A})z_\mathrm{A}(t)\,, \tag{6.14}$$

$$z_\mathrm{A}(t) = 1-\cosh[t(|\vec{p}|-|\vec{q}|)]\exp[-|t||\vec{p}-\vec{q}|]\,. \tag{6.15}$$

Thus, the renormalized axial vector current in WChPT is

$$A^a_{\mu,\mathrm{ren}} = \left[1-\frac{4\hat{a}}{f^2}(W_{45}\bar{c}_{\mathrm{SW}}+W_\mathrm{A}\bar{c}_\mathrm{A})z_\mathrm{A}(t)\right]A^a_{\mu,\mathrm{eff}}\,. \tag{6.16}$$

We conclude that the a dependence of $A^a_{\mu,\mathrm{eff}}$, derived using symmetries, is supplemented by an additional discretization term resulting from the application of the normalization condition. Note also that the final current depends upon the external states and on the separation t between the axial vector currents in (6.13), as expected. Concerning the t-dependence we can distinguish three cases (recalling that $\vec{p},\vec{q}\neq 0$):

1. $\vec{p}=\vec{q}$. This is the simplest case to implement practically. It leads to $z_\mathrm{A}(t)=0$ and there are no additional $\mathrm{O}(a)$ terms introduced by the current normalization.

2. $\vec{p}$ parallel to $\vec{q}$. Then, for $|t|\gg 1/|\vec{p}-\vec{q}|$, the product of cosh and exponential becomes $1/2$, and so $z_\mathrm{A}\to 1/2$.

3. All other nonvanishing $\vec{p}$ and $\vec{q}$. Here, for $|t|\gg 1/|\vec{p}-\vec{q}|$, the exponential overwhelms the cosh and $z_\mathrm{A}\to 1$.

Note that in both the second and third cases z_A depends on t for non-asymptotic values of

t. Irrespective of the various details, the main conclusion here is that the implementation of the renormalization condition leads, in general, to a nontrivial $\mathrm{O}(a)$ correction to the renormalized currents.[5]

6.6. Pion decay constant

The renormalized axial vector current can be used to compute correlation functions, for example the pion decay constant, defined in (2.31). Expanding the renormalized axial vector current in powers of the pion fields we obtain the tree level result for the pion decay constant [12]:

$$f_{\pi,\mathrm{tree}} = f\left(1 + \frac{4}{f^2}\hat{a}\left(W_{45}\overline{c}_{\mathrm{SW}} + W_{\mathrm{A}}\overline{c}_{\mathrm{A}}\right)\left[2 - z_{\mathrm{A}}(t)\right]\right) . \tag{6.17}$$

This gives the form of the discretization errors expected in a lattice calculation of f_π. Bear in mind that the result depends on the choice of renormalization condition [through $z_{\mathrm{A}}(t)$].

Various comments are in order. First, at this order in ChPT, the continuum result is simply f, which is correctly reproduced. Second, a consistency condition on the calculation is that the LECs can appear in physical quantities only in certain 'physical' combinations, and $W_{45}\overline{c}_{\mathrm{SW}} + W_{\mathrm{A}}\overline{c}_{\mathrm{A}}$ is indeed such a combination [44]. Third, the choice of underlying fermion action enters through the values of $\overline{c}_{\mathrm{SW}}$ and $\overline{c}_{\mathrm{A}}$. If only the action is Symanzik-improved then $\overline{c}_{\mathrm{SW}} = 0$, and one still finds, as expected, an $\mathrm{O}(a)$ term because $\overline{c}_{\mathrm{A}} \neq 0$. Only if both action and current are improved one finds the expected absence of the $\mathrm{O}(a)$ term – independent of the choice and details of the renormalization condition.

At one loop one finds [12]

$$f_{\pi,1-\mathrm{loop}} = f\left(1 + \frac{\hat{a}}{f^2}\tilde{W}_{\mathrm{A1}} - \frac{M_\pi^2}{16\pi^2 f^2}\left[1 + \frac{\hat{a}}{f^2}\tilde{W}_{\mathrm{A2}}\right]\ln\frac{M_\pi^2}{\Lambda_4^2} + \frac{\hat{a}M_\pi^2}{f^2}\tilde{W}_{\mathrm{A3}}\right) , \tag{6.18}$$

with $\tilde{W}_{\mathrm{A3}}$ being a new unknown LEC[6] while

$$\begin{aligned}\tilde{W}_{\mathrm{A1}} &= 4(W_{45}\overline{c}_{\mathrm{SW}} + W_{\mathrm{A}}\overline{c}_{\mathrm{A}})[2 - z_{\mathrm{A}}(t)] ,\\ \tilde{W}_{\mathrm{A2}} &= 4(W_{45}\overline{c}_{\mathrm{SW}} + W_{\mathrm{A}}\overline{c}_{\mathrm{A}})[1 - z_{\mathrm{A}}(t)] .\end{aligned} \tag{6.19}$$

This result correctly reproduces the continuum result of Gasser and Leutwyler [25] in the limit $a \to 0$. At nonzero lattice spacing, however, there appear additional terms of $\mathrm{O}(a)$, $\mathrm{O}(aM_\pi^2)$ and an additional chiral logarithm of $\mathrm{O}(aM_\pi^2 \ln M_\pi^2/\Lambda_4^2)$. Combined with the continuum term the coefficient of the chiral logarithm has the form $[1 + \hat{a}\tilde{W}_{\mathrm{A2}}/f^2]$. Hence, in contrast to the expectation expressed in [121], it not only depends on f and the number of flavors, but also on the (non-universal) lattice artifacts encoded in the

[5] This correction was missed in various papers, for example in refs. [43, 120, 44].

[6] Our notation concerning $\tilde{W}_{\mathrm{A3}}$ differs slightly from the one used in [12].

coefficient $\tilde{W}_{\mathrm{A}2}$. A peculiar exception is the third case discussed in the previous section with $z_{\mathrm{A}}(t) = 1$. Here $\tilde{W}_{\mathrm{A}2} = 0$ and the chiral logarithm is free of $\mathrm{O}(a)$ corrections.

Note that the combination L_{45} of Gasser-Leutwyler coefficients enters the 1-loop result in form of the lattice spacing dependent combination $L_{45}^{\mathrm{eff}}(a) = L_{45} + \hat{a}\tilde{W}_{\mathrm{A}3}/f^2$. In order to obtain the physically interesting part L_{45} one has to extrapolate to the continuum limit.

We close with a final remark on formula (6.18). In section 4.2 we distinguished two quark mass regimes, the GSM and the LCE regime. Formula (6.18) is not a consistent result in either of these two regimes. It is only a partial NLO result for the LCE regime since the $\mathrm{O}(a^2)$ corrections to the effective current have been ignored, simply because these have not been worked out to date. The NLO result for the GSM regime, however, can be obtained from (6.18) by dropping the corrections proportional to $\tilde{W}_{\mathrm{A}2}$ and $\tilde{W}_{\mathrm{A}3}$, which are of NNLO in this regime.

6.7. Wilson ChPT for 2+1 flavors

Eventually one is interested in lattice simulations with 2+1 flavors, two light flavors representing the (to a good approximation degenerate) up and down quark and the heavier strange quark. In order to analyze these at nonzero a the results of the previous section need to be extended to 2+1 flavor WChPT.

There is no fundamental difficulty in applying the framework of WChPT to 2+1 flavors. The main difference to the 2 flavor results is just the significantly increased complexity of the final results. This is the only reason for the lack of any results except for the pseudo scalar masses, for which NLO results exist for both the GSM and the LCE regime [6].[7] The results are rather lengthy and not very illuminating, so we refrain from presenting them here.

Qualitatively one finds the same features as in the 2 flavor case. In the LCE regime there appear additional chiral logarithms at one loop. The larger flavor content and the different masses for the pions, kaons and the eta leads to chiral logarithms of $\mathrm{O}(a^2 M_\pi^2 \ln M_\pi^2/\mu^2)$, $\mathrm{O}(a^2 M_K^2 \ln M_K^2/\mu^2)$ and $\mathrm{O}(a^2 M_\eta^2 \ln M_\eta^2/\mu^2)$. Their presence leads to a complicated quark mass dependence of the pseudo scalar masses, which does not need to resemble the dependence one expects from continuum ChPT.

[7] There exist 2+1 flavor results for vector meson masses, but this is beyond standard mesonic ChPT and will be discussed in section 11.

7. Chiral logarithms in staggered ChPT

Staggered ChPT is in some respects simpler than its Wilson counterpart. The staggered fermion quark mass renormalizes only multiplicatively, hence the chiral limit corresponds to a vanishing bare quark mass and the quark mass matching is significantly simpler than for Wilson ChPT. Moreover, in the massless limit there exists a conserved axial vector current that can be used to compute the pion decay constant. This current does not require a nontrivial renormalization constant Z_{A} and no renormalization condition needs to be imposed.

However, significant complications arise because of the extra taste degree of freedom and the breaking of the taste symmetry at nonzero a. In particular, taking the $\mathrm{O}(a^2)$ correction in $\mathcal{L}_2$ to be of leading order leads to additional interaction vertices in 1-loop calculations. In this case we expect additional chiral logarithms involving the masses in (4.41) of all taste partners.

The mass and decay constants of the Goldstone pion has been computed to one loop in refs. [74, 88]. Results are available for the most general case of three nondegenerate quark flavors. However, the final results are fairly cumbersome and hide the aspect we want to focus on here, namely the additional chiral logarithms due to taste symmetry breaking. For this reason we simplify the results by considering the case with three degenerate quark flavors, which are easily obtained from the general results. Relevant for the analysis of MILC lattice data are the 2+1 flavor expressions, which are explicitly given in [74, 88].

The squared mass of the charged Goldstone pion reads [74]

$$\begin{aligned}\frac{M^2_{\pi_5,\mathrm{NLO}}}{M^2_{\pi_5}} &= 1 + \frac{1}{48\pi^2 f^2} M^2_{\pi_I} \ln\frac{M^2_{\pi_I}}{\mu^2} - \frac{8}{f^2}\left[(L_5 - 2L_8) + 3(L_4 - 2L_6)\right] M^2_{\pi_5} + a^2\mathcal{C} \\ &\quad + \frac{1}{12\pi^2 f^2}\left\{\left[M^2_{\eta'_V}\ln\frac{M^2_{\eta'_V}}{\mu^2} - M^2_{\pi_V}\ln\frac{M^2_{\pi_V}}{\mu^2}\right] + \left[M^2_{\eta'_A}\ln\frac{M^2_{\eta'_A}}{\mu^2} - M^2_{\pi_A}\ln\frac{M^2_{\pi_A}}{\mu^2}\right]\right\}.\end{aligned} \tag{7.1}$$

The masses appearing on the right hand side (and also in the denominator on the left hand side) refer to the LO tree level masses of the pions, given in section 4.3.4, and to

$$M^2_{\eta'_V} = M^2_{\pi_V} + \frac{3a^2}{4f^2}(C_{2V} - C_{5V})\,, \qquad M^2_{\eta'_A} = M^2_{\pi_A} + \frac{3a^2}{4f^2}(C_{2A} - C_{5A})\,. \tag{7.2}$$

The LECs appearing here are those of the potential $\mathcal{V}'$, cf. (4.38). The constant $\mathcal{C}$ is the short hand notation for a combination of LECs in the $\mathrm{O}(p^2a^2, ma^2)$ chiral lagrangian.

Some remarks should be made concerning (7.1). First of all, the correct continuum limit is recovered for $a \to 0$. In the continuum limit the masses of all taste partners become degenerate, hence the second line of (7.1) vanishes while the first line reproduces the correct result of continuum ChPT [26].

Away from the continuum limit we find the anticipated additional chiral logarithms involving the η'_V, η'_A and π_V, π_A. More remarkable and perhaps surprising is the modification of the chiral logarithm that recovers the continuum chiral log. It involves the mass of the taste singlet pion $M^2_{\pi_I}$. A term proportional to $M^2_{\pi_5} \ln(M^2_{\pi_5}/\mu^2)$ that one might have naively expected does not appear at all in (7.1). Note that the appearance of $M^2_{\pi_5}$ in front of the Gasser-Leutwyler coefficients is convention. One can replace this mass by any other mass $M^2_{\pi_b}$ at the expense of a different coefficient $\mathcal{C}$.

The result for the decay constant has a similar form but differs in the details [88]:

$$\begin{aligned}\frac{f_{\pi_5}}{f} = 1 &+ \frac{3}{32\pi^2 f^2}\left\{\frac{1}{16}\sum_b M^2_{\pi_b} \ln\frac{M^2_{\pi_b}}{\mu^2}\right\} + \frac{8}{f^2}\left[L_5 + 3L_4\right] M^2_{\pi_5} + a^2\mathcal{D} \\ &- \frac{1}{12\pi^2 f^2}\left\{\left[M^2_{\eta'_V} \ln\frac{M^2_{\eta'_V}}{\mu^2} - M^2_{\pi_V} \ln\frac{M^2_{\pi_V}}{\mu^2}\right] + \left[M^2_{\eta'_A} \ln\frac{M^2_{\eta'_A}}{\mu^2} - M^2_{\pi_A} \ln\frac{M^2_{\pi_A}}{\mu^2}\right]\right\}.\end{aligned} \tag{7.3}$$

As expected, this result reproduces the correct continuum ChPT result for $a = 0$. The second line is, up to a sign, the same as in the expression for the pion mass. Slightly different is the modification of the logarithm that reproduces the continuum chiral log. It involves not only $M^2_{\pi_I}$ but all taste partners. In fact, the term $\{1/16 \ldots\}$ is the average of all sixteen chiral logs one can form with the available taste partners.

Apparently, the quark mass dependence in (7.1) and (7.3) can differ significantly from the corresponding continuum ChPT results. How big the difference is depends on the size of the mass shifts for the various pseudoscalar mesons. The results also show why it is important to systematically include the lattice spacing corrections in ChPT: The tree level masses are of the generic form $M^2 = m + a^2$, and the $\mathrm{O}(a^2)$ corrections enter the chiral logs. In the regime with $m \sim a^2$ the logarithms cannot be expanded in powers of a^2, hence there is a true nonanalytic dependence on the lattice spacing that is missed by the naive ansatz that all scaling violations are polynomial in a.

The 2+1 flavor counterparts of (7.1) and (7.3) have been used to analyze data generated by the MILC collaboration. As mentioned at the end of section 4.3.4, the taste splittings in these simulations are rather large such that the power counting $m \sim a^2$ is appropriate. The data analysis is rather involved [85]. However, quite generally one can say that the data clearly prefers the SChPT results with the $\mathrm{O}(a^2)$ corrections in the chiral logarithms. Attempts to fit the lattice data with the continuum chiral logarithms only produce very poor results. The good description of the MILC data was one of the first successes of ChPT at nonzero lattice spacing.

8. Wilson ChPT with a twisted mass term

8.1. WChPT and the *bending phenomenon*

The results of section 6 are in principle straightforwardly generalized to twisted mass WChPT, where the mass term assumes the form in (4.26). And indeed, many results have already been obtained. The discussion of the phase diagram of the theory is given in [122, 123]. The pion mass splitting between the charged and the neutral pion mass was calculated to LO in [124] (see also [120]). A complete NLO analysis of the pion masses and the decay constant in the GSM regime can be found in [44], and pion scattering in the GSM regime is discussed in [125].

In the following we will not review all these results in detail. We rather focus on one particular feature of twisted mass WChPT, which played a key rôle in the understanding of the so-called *bending phenomenon* [126]. Bending phenomenon refers to a puzzle observed in early (quenched) twisted mass lattice simulations. Employing the so-called pion mass definition for maximal twist (discussed below), one observed a strong curvature in the quark mass dependence in many observables (e.g. M_π, f_π) for small twisted quark masses μ. This unexpected observation spurred further numerical simulations with other definitions for maximal twist [127, 128, 129] as well as theoretical studies in WChPT [4, 130, 8]. It seems fair to say that nowadays the bending phenomenon is well understood, as we want to show in this section. It was very encouraging to see that WChPT describes successfully the bending phenomenon; it demonstrated that the whole set-up of WChPT seems to work.

8.2. Gap equation and ground state

Before we can perform the standard saddle point expansion in the computation of correlation functions we have to determine the ground state Σ_{vac} that minimizes the classical potential energy. Starting point is the LO lagrangian for the LCE regime in (4.14), since for larger quark masses in the GSM regime we can simply drop the c_2 term from the results. In the following we always assume c_2 to be positive, hence the charged pions become massless for $\mu = 0$ and $m = c_2 a^2/B$. The case with $c_2 < 0$ will be briefly discussed in section 8.9.

The potential energy with the mass term M in (4.26) reads

$$V = -\frac{f^2 B}{2}\langle M^\dagger \Sigma + \Sigma^\dagger M\rangle + \frac{f^2}{16} c_2 a^2 \langle \Sigma + \Sigma^\dagger\rangle^2 \,. \tag{8.1}$$

This reduces to the untwisted result (4.19) for $\mu = 0$. The twisted mass μ breaks

explicitly the SU(2) flavor symmetry. Because μ 'points' into the σ_3 direction the ground state is of the form [124, 44]

$$\Sigma_{\text{vac}} = \exp(i\phi\sigma_3)\,, \tag{8.2}$$

where ϕ is called the *vacuum angle*. With the ansatz (8.2) the potential energy becomes

$$V = f^2 2Bm_{\text{P}}\cos(\phi - \omega_L) - f^2 c_2 a^2 \cos^2\phi\,, \tag{8.3}$$

where we introduced the *polar mass* m_{P} by writing the mass term as

$$M = m\,1 + i\mu\sigma_3 = m_{\text{P}} e^{i\omega_L sigma_3}. \tag{8.4}$$

In terms of m and μ we find

$$m_{\text{P}} = \sqrt{m^2+\mu^2}\,, \qquad \tan\omega_L = \frac{\mu}{m}\,. \tag{8.5}$$

The subscript 'L' in the *twist angle* ω_L serves as a reminder that this angle relates the two mass parameters in the chiral lagrangian. It is related to but not identical with the twist angles we define later.

The ground state is given as the minimum of the potential energy. It is determined by the *gap equation* $dV/d\phi = 0$, which can be written as [4]

$$2B\mu\cos\phi = \sin\phi(2Bm - 2c_2a^2\cos\phi)\,. \tag{8.6}$$

This equation determines the vacuum angle as a function of the variable parameters in the theory, the two masses m, μ and the lattice spacing a: $\phi = \phi(m,\mu,a)$. Let us discuss the qualitative behaviour of the solution for some special cases. For this it will be convenient to introduce the short-hand notation

$$t = \cos\phi\,. \tag{8.7}$$

Particularly interesting are the solutions if two of the three parameters are constant, for example a and m or a and μ. Looking at (8.6) it is immediately obvious that t (or ϕ) cannot be constant as a function of the remaining parameter. For instance, for fixed a and m we find $t \to 0$ if $\mu \to \infty$.[1] On the other hand, for fixed a and μ we find $t \to 1$ if $m \to \infty$. There are two noteworthy exceptions: First, t is identically zero for vanishing m, independently of the values for μ and a: $\phi(m=0,\mu,a) = \pi/2$. The other special case is $\mu = 0$. This is the standard untwisted case with $t = 1$, provided $|m| > c_2a^2/B$, i.e. outside of the Aoki phase. The particular point $m = 0$ is rather special at LO in the chiral expansion: it refers to the middle of the Aoki phase.

Finally, suppose we are in the GSM regime where $m \gg c_2a^2/B$. In this case we can

[1] This is a theoretical limit to study the qualitative behaviour of the solution for the gap equation. WChPT breaks down well before this limit is reached.

drop the c_2 contribution in the gap equation and (8.6) simplifies to

$$\frac{\mu}{m} = \tan\omega_L = \tan\phi\,. \tag{8.8}$$

In the GSM regime the ground state is determined entirely by the ratio of the two quark masses.

8.3. Pion mass and decay constant

Expanding the Σ field to quadratic order in the pion fields we obtain the tree level pion masses,

$$M_{\pi^\pm}^2 = \frac{2Bm}{t} - 2c_2a^2\,, \tag{8.9}$$

$$= \frac{2B\mu}{\sqrt{1-t^2}}\,. \tag{8.10}$$

The first equation is valid for $t \neq 0$ and the second for $t \neq \pm 1$. Both are equivalent for all other values of t, as can be shown using the gap equation [4]. The explicit breaking of flavor symmetry leads to a different mass for the neutral pion. The mass splitting $\Delta M_\pi^2 \equiv M_{\pi^0}^2 - M_{\pi^\pm}^2$ is found to be given by [124]

$$\Delta M_\pi^2 = 2c_2a^2(1-t^2)\,. \tag{8.11}$$

The mass splitting is maximal for $m = 0$, since it implies $t = 0$.

An equally important observable is the pion decay constant. In twisted mass QCD one usually does not compute f_π by the matrix element involving the axial vector current. Instead, one makes use of the so-called *indirect method* [47, 131] where the decay constant is given by

$$f_\pi = \frac{2\mu}{M_{\pi^\pm}^2}\langle 0|P^\pm(0)|\pi^\mp(\vec{p})\rangle\,. \tag{8.12}$$

The benefit of this indirect method is that it does not need any renormalization factors like Z_A. On the other hand, the indirect method works at maximal twist only which we have not defined so far. For this reason, writing f_π on the left hand side of eq. (8.12) is so far just a short hand notation for the right hand side. That the right hand side has indeed something to do with the decay constant is seen once the matrix element $\langle 0|P^\pm|\pi^\mp\rangle$ is calculated. The tree level result for it is fB, and making use of (8.10) we obtain

$$f_\pi = f\sqrt{1-t^2}\,. \tag{8.13}$$

The results (8.10) and (8.13) are valid for arbitrary $t \neq \pm 1$, but for $t = 0$ they turn into the results expected from leading order continuum ChPT (with μ playing the rôle of m),

$$M_{\pi^\pm}^2 = 2B\mu\,, \qquad f_\pi = f\,. \tag{8.14}$$

In the general case there is some additional quark mass dependence implicit in t, which, as we will see shortly, can distort the functional behaviour in (8.14) significantly.

8.4. Defining maximal twist

So far we kept both masses, m and μ, as freely adjustable parameters. However, in twisted mass QCD one is mainly interested in the dependence on μ while m is tuned to some special value, the so-called *critical mass* $m_{\rm cr}$. This goes under the name *tuning to maximal twist* since one usually defines first a *twist angle* ω, which depends on m and μ, and the value $\omega = \pi/2$ defines implicitly $m_{\rm cr}$. Note that the critical mass depends in general on μ and a.

There are various ways to define a twist angle, and in the following we discuss only a few. Historically the first definition used in numerical simulations is the so-called *pion mass definition*. The untwisted quark mass is set to the value where the charged pion mass vanishes in the untwisted theory, i.e. for $\mu = 0$. Cast into an equation it can be written as

$$\underline{\text{Pion mass definition:}} \qquad M_\pi(m = m_{\rm cr}^{\rm Pion}, \mu = 0, a) = 0\,. \tag{8.15}$$

One needs to be a bit careful here. As discussed in section 4.2, depending on the sign of c_2 there are two scenarios: either there exist no massless pions at all ($c_2 < 0$) and the condition (8.15) has no solution, or there exists an Aoki phase with massless pions for all $|m| \leq c_2 a^2/B$ and the solution of (8.15) is not unique. What is usually meant in the pion mass definition is the edge of the Aoki phase. According to the discussion in 4.2 this means

$$m_{\rm cr}^{\rm Pion} = c_2 a^2/B \tag{8.16}$$

in WChPT to LO. In practice this value is obtained by performing an extrapolation of M_π^2 data, generated for various untwisted masses, to the point where the pion mass vanishes.[2]

An alternative definition is the so-called *PCAC mass definition*. In fact it refers to more than one definition. Starting point is the quark mass based on the partially conserved axial vector current (PCAC), defined by

$$m_{\rm PCAC} = \frac{\langle \partial_\mu A_\mu^a(x) P^a(0)\rangle}{2\langle P^a(x) P^a(0)\rangle}\,, \tag{8.17}$$

where a is either 1 or 2. The first definition for maximal twist and the critical mass is now simply given by a vanishing PCAC mass,

$$\underline{\text{PCAC mass definition 1:}} \qquad m_{\rm PCAC}(m = m_{\rm cr}^{\rm PCAC}, \mu, a) = 0\,. \tag{8.18}$$

[2]Note that this procedure also leads to a unique critical value for the scenario with no massless pions.

Note that $m_{\rm cr}$ does in general depend on the twisted mass and the lattice spacing: $m_{\rm cr}^{\rm PCAC}(\mu, a)$. This is slightly disadvantageous in practice, since the critical quark mass has to be readjusted once one has changed μ. This has led to a simplified definition where $m_{\rm cr}^{\rm PCAC}$ is determined once for one particular μ and then kept fixed. Proposed in the literature and also used in actual simulations is the particular value one obtains by taking the limit $\mu \to 0$,

PCAC mass definition 2: $$\tilde{m}_{\rm cr}^{\rm PCAC} = \lim_{\mu\to 0} m_{\rm cr}^{\rm PCAC}(\mu, a)\,. \tag{8.19}$$

What does the PCAC mass definition imply for the shifted mass m? The PCAC mass in (8.17) is also easily computed to LO in WChPT [4],

$$m_{\rm PCAC}^{\rm LO} = \mu \frac{t}{\sqrt{1-t^2}}\,. \tag{8.20}$$

For nonzero twisted mass this vanishes for $t = 0$, hence $m_{\rm cr}^{\rm PCAC} = 0$. This particular value is μ-independent, therefore the second PCAC mass definition has the same critical mass,

$$m_{\rm cr}^{\rm PCAC} = \tilde{m}_{\rm cr}^{\rm PCAC} = 0\,. \tag{8.21}$$

At higher order one will find that $m_{\rm cr}^{\rm PCAC}$ does depend on μ and the two version of the PCAC mass definition will lead to different critical masses.[3]

8.5. Quark mass dependence and the bending phenomenon

Depending on the definition for maximal twist, the μ-dependence of observables (at fixed a) will be different. For the PCAC mass definition (both version 1 and 2) we found $t = 0$ and the results for the pion mass and decay constant are as in (8.14). The pion mass definition is more complicated and also more interesting. Inserting (8.16) into the gap equation we obtain

$$\alpha t = \sqrt{1-t^2}(1-t)\,, \qquad \alpha = 2B\mu/2c_2a^2 \tag{8.22}$$

as the defining equation for $t(\mu, a)$. This leads to a quartic equation for t which can be solved analytically. Here it is sufficient to have a qualitative understanding of t. We know already that t vanishes for $\mu \to \infty$. One can easily conclude from (8.22) that $t \to 1$ for the opposite limit $\mu \to 0$, and that the slope $\partial t/\partial\mu$ is negative for all $\mu \geq 0$. Hence, t is a convex function that qualitatively looks like the sketch in fig. 8.1.

This implies that the decay constant in (8.13) is not a constant but rather vanishes in the chiral limit $\mu \to 0$. Also the ratio

$$R = \frac{M_{\pi^\pm}^2}{\mu} = \frac{2B}{\sqrt{1-t^2}} \tag{8.23}$$

[3] This happens once the terms of $O(\mu^2)$ are included in the calculation.

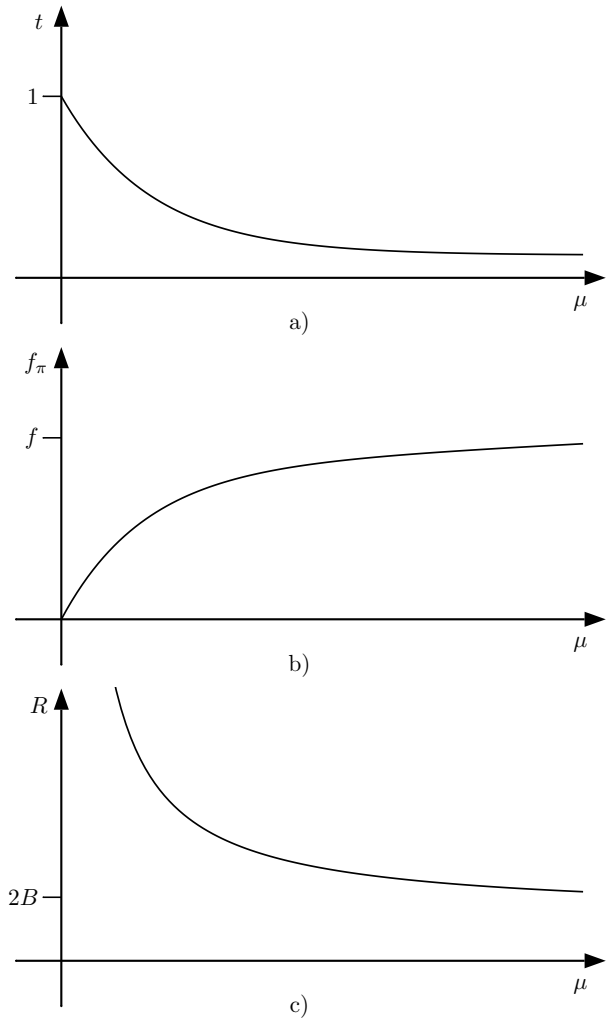

Figure 8.1.: a) Sketch of the function t as a function of μ and fixed a for the pion mass definition of maximal twist. b) and c) The resulting μ-dependence of the decay constant f_π and the ratio R defined in (8.23).

is not constant but diverges for vanishing μ. The qualitative μ-dependence is sketched in fig. 8.1. For the detailed form of the μ-dependence one has to compute $t(\mu, a)$ exactly, but at least qualitatively we expect a behaviour known as the bending phenomenon mentioned in the beginning.

These two examples teach us an important lesson. Depending on the choice for the twist angle the ground state in twisted mass WChPT is not constant but μ- (and a-) dependent. Quite generally this leads to an additional μ-dependence in observables via the function $t(\mu, a)$, which is not present in continuum ChPT. One should keep this in mind if one naively tries to extract LECs by using continuum ChPT results to analyze lattice data at nonzero a. Sometimes the data cannot be fitted at all. This was the

case for the f_π data in [126], where the observed bending of the data for small twisted masses was completely unexpected and in blunt disagreement with the predictions of continuum ChPT. More harmful is the scenario where the data can be fitted but with distorted results for the extracted LECs. For example, the factor $1/\sqrt{1-t^2}$ in R will mimic (and add to) the μ-dependence of the chiral logarithm that enters at one loop. This most probably leads to wrong fit results.

8.6. Comments on higher order corrections

So far we restricted the discussion to LO in the chiral expansion, both for the gap equation and for observables. A generalization including higher order terms has been given in [8]. Some details change but the main conclusion about the additional μ-dependence caused by $t(\mu, a)$ remains unchanged. Here we are brief and only qualitatively describe some of the changes that occur if one takes into account the terms of $\mathrm{O}(am, a\mu)$ in the chiral lagrangian and the $\mathrm{O}(a)$ corrections in the axial vector current (the latter modifies the result for the PCAC mass).

The additional terms in the chiral lagrangian modify the gap equation that determines the ground state. The most important qualitative feature is that $t = 0$ is no longer a solution for constant $m = 0$. Instead one finds a linear dependency between the twisted and the untwisted masses:

$$t = 0 \quad \Leftrightarrow \quad m = c_{68} a\mu \,, \tag{8.24}$$

where c_{68} is a combination of LECs introduced before: $c_{68} = 32 W_{68} W_0 \bar{c}_{\mathrm{SW}}/f^2$. Hence, if we want to keep the vacuum angle ϕ constant at $\pi/2$ we need to readjust m as a function of μ.

The result for the PCAC mass changes to

$$m_{\mathrm{PCAC}} = \mu \frac{t - c_{\mathrm{A}} a}{\sqrt{1-t^2}} \,, \tag{8.25}$$

and again we introduced a convenient short hand notation for a combination of previously defined LECs: $c_{\mathrm{A}} = 32 W_{\mathrm{A}} W_0 \bar{c}_{\mathrm{A}}/f^2$. Setting m_{PCAC} to zero we find the condition

$$t = c_{\mathrm{A}} a \,. \tag{8.26}$$

This can be inserted into the gap equation to find $m_{\mathrm{cr}}^{\mathrm{PCAC}}$. The explicit expression is not very illuminating and it will not be relevant in the following. Note that, in contrast to the LO analysis, the PCAC mass definition for maximal twist no longer implies the theoretically ideal case $t = 0$.

Also $m_{\mathrm{cr}}^{\mathrm{Pion}}$ changes slightly by the higher order corrections. However, the property $t(\mu, a) \to 1$ for $\mu \to 0$ is unchanged and the bending phenomenon will still occur for

small twisted masses. A careful analysis shows that for $\mu \ll c_2 a^2/B$ we have [4]

$$t = 1 - \delta\,, \qquad \delta \simeq \frac{1}{2}\left[\frac{2B\mu}{c_2 a^2}\right]^{2/3}\,. \tag{8.27}$$

The origin of the peculiar fractional exponent is the approach of the Aoki phase transition line, and the fractional power 2/3 is the mean-field critical exponent for the second order phase transition.

Finally, the additional $\mathrm{O}(a)$ corrections in the pion mass and the decay constant read ($c_{45} = 32 W_{45} W_0 \bar{c}_{\mathrm{SW}}/f^2$)

$$M_{\pi^\pm}^2 = \frac{2B\mu}{\sqrt{1-t^2}}\left[1 + (c_{68} - c_{45})at\right], \tag{8.28}$$

$$f_\pi = f\sqrt{1-t^2}\left[1 + c_{45} at\right]. \tag{8.29}$$

Obviously these are not complete NLO results since the chiral logarithms are missing. These can be added if one wishes, but for our purposes here the expressions (8.28) and (8.29) are sufficient.

8.7. Fit to lattice data

The results of the previous sections have been used to analyze quenched lattice data [9]. The data were generated by two different groups [126, 127, 128, 129], and data at two lattice spacings were available, $a \approx 0.123$ fm and $a \approx 0.093$ fm. The twisted quark mass covers the range $M_\pi = 270 \ldots 1200$ Mev, or, alternatively, $M_\pi/M_\rho \approx 0.3 - 0.8$. The untwisted bare quark mass was tuned according to the three different definitions of maximal twist: the pion mass definition, the PCAC mass definition 2 and the parity conservation definition. The latter is equivalent to the PCAC mass definition 1. In total there were 52 data points available for each of the two lattice spacings.

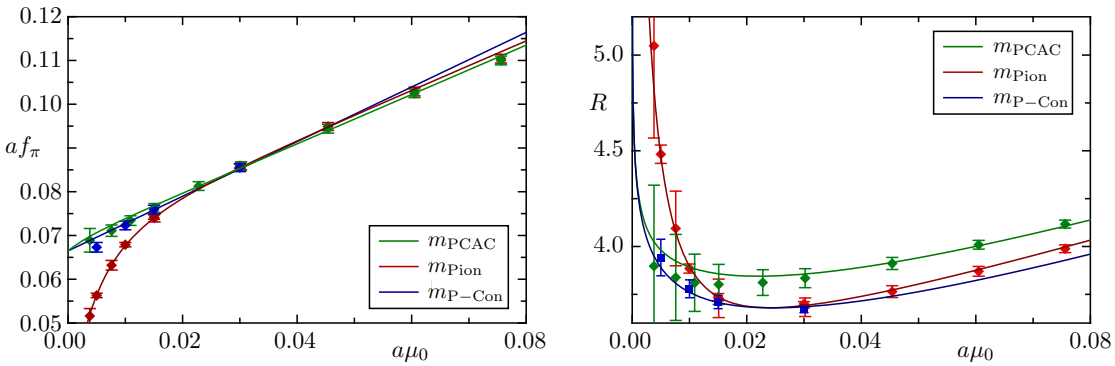

Figure 8.2.: Results of a combined fit for f_π and R at 0.093 fm (χ^2/d.o.f. = 0.23 with d.o.f. = 26). Only the data points with $a\mu_0 \leq 0.0302$ are included in the fits. Plots from ref. [9].

Figure 8.2 shows the data and the fit results for the dimensionless quantities af_π and $R = (aM_{\pi^\pm})^2/a\mu$, both as a function of the bare lattice quark mass $a\mu_0$. Clearly visible is the bending phenomenon in the data for the decay constant at small twisted masses. Also the data for R exhibits a much stronger curvature for small μ in case of the pion mass definition.

The solid lines are the fit results. Various fits have been performed, starting with all data points included and then successively removing the data points at high quark masses. In all cases good fit results were obtained with a $\chi^2/\text{d.o.f.} \approx 0.2 - 0.5$. Apparently, WChPT describes the data very well. In particular, the bending for small masses in case of the pion mass definition is perfectly reproduced. This feature is independent of the number of data points included in the fit, even though the values for the fit parameters are slightly different. Note that the curvature in the data for R with $a\mu_0 \geq 0.3$ is also well described even though the heavier data points are excluded from the fit.

The fits give reasonable values for the fit parameters. Here we only quote the estimate for the LEC c_2, obtained at $a = 0.093$ fm:

$$c_2 = \left[176 \text{ MeV}^{+17\%}_{-40\%}\right]^4. \tag{8.30}$$

The error is rather large, but it is fair to conclude that c_2 is positive and nonzero. We can conclude that for this particular lattice theory the Aoki phase scenario is realized.[4] This agrees with the observation made by the ETM collaboration who measured the pion mass splitting [132]. They found the neutral pion to be heavier than the charged one, in agreement with a positive value for c_2.

8.8. Comment on automatic O(a) improvement

Up to now we exclusively considered the quark mass dependence of observables *at fixed lattice spacing a*. We discussed how the function $t(\mu, a = \text{const.})$ modifies the naively expected quark mass dependence. We can ask the opposite question: What are the modifications in the a-dependence if we keep μ fixed? In other words we ask how the continuum limit is approached and what rôle t plays in taking it.

Consider the results (8.28) and (8.29) for the pion mass and decay constant. There are lattice corrections of O(a) as one typically expects in lattice theories with Wilson fermions. However, the corrections are associated with one power of $t(\mu, a)$, and this makes all the difference.

Consider first the PCAC mass definition for maximal twist. To LO it amounts to $t = 0$, hence the O(a) corrections vanish. To NLO we found (8.26), and inserting this in the results (8.28) and (8.29) we obtain

$$M^2_{\pi^\pm} = 2B\mu\left[1 + c_\text{A}(c_{68} - c_{45} + c_\text{A}/2)a^2\right], \tag{8.31}$$

$$f_\pi = f\left[1 + \tilde{c}_\text{A}(c_{45} - c_\text{A}/2)a^2\right]. \tag{8.32}$$

[4] Recall that the values for the LECs depend on all details of the underlying lattice theory. Choosing a different gauge and/or quark action will in general lead to different values for the LECs.

These are the continuum results plus some scaling violations of $\mathrm{O}(a^2)$. What we explicitly see here is a demonstration of the acclaimed automatic $\mathrm{O}(a)$ improvement at maximal twist [48]. It is automatic because it does not require any tuning of some coefficients in the Symanzik theory.[5] We explicitly see that the function t plays a vital rôle in this improvement since it contributes an additional power of a to the final results. In the standard theory without a twisted mass term we have $t = 1$ and the final results have scaling violations of $\mathrm{O}(a)$, as expected.

What about the pion mass definition? For large twisted masses $\mu \gg c_2 a^2/B$ we found $t \approx 0$ and the scaling violations are of $\mathrm{O}(a^2)$. However, for small twisted masses we find very different scaling violations. Using (8.27) in (8.28) and (8.29) we obtain

$$M_{\pi^\pm}^2 = (2c_2a^2)^{1/3}(2B\mu)^{2/3}\left[1 + (c_{68} - c_{45})a - (c_{68} - c_{45})a\delta\right], \tag{8.33}$$

$$f_\pi = f\sqrt{2\delta}(1 + c_{45}a - c_{45}a\delta), \tag{8.34}$$

The dependency on the lattice spacing is not polynomial at all but has fractional powers of a. This is a remnant of the fact that for $\mu \ll c_2 a^2/B$ we are close to the second order phase transition point. This is explicitly seen in the result for the pion mass: The correlation length $1/M_{\pi^\pm}$ diverges as $\mu^{-1/3}$ when the 'external field' μ vanishes, as expected from a second order phase transition.

The results (8.33) and (8.34) caused some controversy in the twisted mass community, mainly because of a misunderstanding of the results. Apparently, the scaling violations in (8.33) and (8.34) are not $\mathrm{O}(a^2)$, which led to a statement about *loss of automatic O(a) improvement* in [4, 8]. This formulation is somewhat unfortunate because it might suggest that the scaling violations are of $\mathrm{O}(a)$ instead instead of $\mathrm{O}(a^2)$. As we have discussed, this is not the case and the dependence on a is more complicated.

8.9. Comment on the $c_2 < 0$ scenario

So far we discussed the $c_2 > 0$ scenario. The reason was twofold. Firstly, the data showing the bending phenomenon suggested a positive value for c_2 because the pion mass splitting was found to be positive. Secondly, this scenario raised an immediate question for the pion mass definition: The solution of (8.15) is not unique because the charged pion mass vanishes for all values $|m| \leq c_2 a^2/B$. So what is the 'correct' condition that fixes this ambiguity?

The alternative scenario with $c_2 < 0$ can be analyzed in WChPT as well [4, 44, 130]. The details change slightly. However, the overall conclusion that the ground state can modify the quark mass dependence via the function t remains unchanged. The detailed form of the modification depends on the particular definition for the critical mass, of course. Quite generally one can show that any definition with a constant critical mass leads to a nontrivial (i.e. nonconstant) function $t(\mu, a)$, and thus to a modified quark mass dependence. For details we refer to [130] and to the appendix of [4].

[5] Note that the coefficients $\overline{c}_{\mathrm{SW}}$ and $\overline{c}_{\mathrm{A}}$ (included in the coefficients c_{45}, c_{68} and c_{A}) are not zero as in theories improved according to the Symanzik improvement program.

9. Finite volume effects: The epsilon regime with Wilson fermions

9.1. Introduction

Numerical lattice simulations are necessarily done in a finite volume, i.e. with finite temporal and spatial extent T and L. This immediately raises the question about finite size corrections, since the true physical results are those in infinite volume.

It turns out that ChPT is again a powerful tool in this respect [133, 134, 135]. The reason is that the pions are the lightest hadrons. If we imagine reducing an asymptotically large volume to smaller and smaller values, the pions will 'feel' the finiteness of the volume first. We therefore expect that ChPT can be used to describe the dominant finite volume effects on various hadronic observables.

The literature distinguishes two different finite volume regimes: (i) the p-regime where the Compton wave length of the pion, $1/M_\pi$, is much smaller than L, and (ii) the ϵ-regime with $1/M_\pi \simeq L$ or even larger. Obviously, the finite volume corrections are expected to be smaller in the p-regime. And indeed, one can show that the finite volume corrections are, for sufficiently large volumes, exponentially suppressed by factors $\exp(-M_\pi L)$. In contrast, the corrections are significantly larger in the ϵ-regime. Correlation functions are expanded in inverse powers of $1/(fL)^2$, i.e. the dependence on $1/L$ is polynomial. This is not necessarily disadvantageous. It has been pointed out that in the ϵ-regime one has a good handle on the LO LECs f and B by monitoring the volume dependence of certain correlation functions. The flip side is that numerical lattice simulations in the ϵ-regime are fairly time consuming. Small pion masses and large volumes with $M_\pi L \simeq 1$ are necessary. Moreover, it was common wisdom for a long time that the use of GW fermions with their good chiral symmetry properties is essential too for ϵ-regime simulations. Consequently, a large number of quenched simulations with these fermions in the ϵ-regime can be found in the literature [136, 137, 138, 139, 140, 141, 142, 143, 144]. The main obstacle are unquenched simulations, which are extremely demanding [145].

Having this in mind, the fairly inexpensive simulations with tree level improved Wilson fermions, performed by Hasenfratz and Schaefer in ref. [146], came as a surprise. Reweighting [147] has been used to reach small enough quark masses in order to be in the ϵ-regime, and the spatial extent L was about 2.8 fm, much larger than in all the simulations mentioned before. Even more puzzling was the observation that the explicit chiral symmetry breaking of Wilson fermions was very mild, even though the lattice spacing in these simulations was not particularly small ($a \simeq 0.11$ fm). The data for the axial vector and pseudo scalar correlation functions are very well described by the continuum ChPT predictions. A similar observation has been made before by the ETM

collaboration [148, 149]. Their data, obtained with a twisted mass term, also suggest that the ϵ-regime can be reached with Wilson fermions.

Why are the lattice artifacts so small in these simulations? A partial answer has been given with the WChPT analyses in refs. [11, 13]. It turns out that the lattice spacing corrections are in general highly suppressed and show up at higher order in the ϵ-expansion. For example, for quark masses in the GSM regime the deviations from the continuum results enter first at NNLO. We have seen the reason for this suppression before: The lattice spacing effects are either of $\mathrm{O}(a^2)$ or of $\mathrm{O}(ap^2, am)$, and these are suppressed in the chiral counting.

9.2. Continuum ChPT in infinite volume

Let us consider continuum QCD in a hypercubic volume ('box') $V = TL^3$ with periodic boundary conditions in each direction. Furthermore, we assume $T, L \gg 1/\Lambda_{\mathrm{QCD}}$, i.e. QCD is still nonperturbative and the spectrum consists of hadrons. For simplicity we consider N_f degenerate quark quarks, although later we will restrict ourselves to the case $N_f = 2$.

Strictly speaking there is no spontaneous symmetry breaking in a finite volume. Nevertheless, for sufficiently large volumes with $T, L \gg 1/\Lambda_{\mathrm{QCD}}$ the lightest hadrons are still the pions. Hence, the pions are affected most by the finite volume, and the finite size effects can be systematically studied in ChPT [133, 134, 135]. The key result here is that the lagrangian of finite volume ChPT is the same as in infinite volume [133]. In particular, the LECs are volume independent and the same as in infinite volume. The finite volume enters only through the boundary conditions for the pion fields, which means that the pion propagator is modified. In case of periodic boundary conditions the finite volume pion propagator has to be periodic as well. In terms of the infinite volume propagator $G(x) \equiv \langle \pi(x)\pi^\dagger(0)\rangle$ (flavor indices are suppressed) the finite volume propagator reads

$$G^{(\mathrm{FV})}(x) \equiv \langle \pi(x)\pi^\dagger(0)\rangle_{\mathrm{FV}} = \sum_{n_\mu} G(x + n_\mu L_\mu)\,, \tag{9.1}$$

where L_μ is the extent of the finite volume in the μ-th direction (according to our assumption in the beginning we have $L_0 \equiv T$ and $L_1 = L_2 = L_3 \equiv L$). Because of the periodic boundary conditions, the pion momenta can assume discrete values only, $p_\mu = 2\pi n_\mu / L_\mu$. Consequently, the finite volume propagator is given by the discrete sum

$$G^{(\mathrm{FV})}(x) = \frac{1}{V} \sum_{p_\mu} \frac{e^{ipx}}{p^2 + M_0^2}\,, \tag{9.2}$$

with M_0 being the (infinite volume) tree level pion mass. The vertices, on the other hand, are as in infinite volume, and it is essentially straightforward to repeat an infinite volume calculation of a particular quantity for a finite volume. Without going into details

the result of such a calculation can be summarized as follows: If the pion Compton wavelength is much smaller than the size of the finite volume, i.e. $M_\pi L \gg 1$, the finite volume result is the sum of the infinite volume result and a small finite volume correction, which is exponentially suppressed by a factor $e^{-M_\pi L}$.

There is a problem if the pion mass is so small that the pion Compton wavelength is of the same order as the extent of the box, i.e. $M_\pi L \sim 1$. This is most easily seen by inspecting the finite volume propagator. The zero-mode contribution $1/M_0^2 V$ diverges in the chiral limit and the standard perturbative expansion eventually breaks down for small enough quark masses where the zero-mode contribution is no longer small. Instead, a reordering of the perturbative series is necessary that sums up all Feynman graphs with an arbitrary number of zero-mode propagators [134]. This reordering is achieved with the so-called ϵ-*expansion*, defined by the following counting rules

$$M_0 \sim \mathrm{O}(\epsilon^2)\,, \qquad 1/L,\, 1/T,\, \partial_\mu \sim \mathrm{O}(\epsilon)\,. \tag{9.3}$$

In addition, all LECs count as O(1). With these rules the combination $1/M_0^2 V$ counts as ϵ^0. Consequently, all Feynman graphs that exclusively involve zero-mode propagators count as O(1), they are unsuppressed and all of them need to be taken into account.

It is slightly unusual to give a counting rule for the tree level pion mass. Instead, it is standard to give a counting for the quark mass. Recalling $M_0^2 = 2Bm$ we are led to the equivalent counting $m \sim \mathrm{O}(\epsilon^4)$. The key point here is, that the counting of the quark mass is dictated by the counting of L together with demanding $1/M_0^2 V = \mathrm{O}(\epsilon^0)$. We will use this in the next section in order to establish the counting rules for the ϵ-expansion in WChPT.

In practice the reordering of the perturbative expansion is not done by summing up an infinite number of Feynman graphs. Rather, the integration over the zero-mode in functional integrals is done exactly instead of perturbatively by making use of the standard saddle point expansion. This is achieved by factorizing the Σ fields as

$$\Sigma(x) = \exp\left(\frac{2i}{f}\xi(x)\right) U_0\,. \tag{9.4}$$

where the constant $U_0 \in \mathrm{SU}(N_f)$ represents the collective zero mode. The nonzero modes ξ are of order ϵ in the ϵ-expansion and satisfy

$$\int_V d^4x\, \xi(x) = 0\,, \tag{9.5}$$

because the constant mode has been separated. They can still be treated perturbatively and give rise to the usual Wick contractions.

Detailed accounts on the ϵ-regime can be found in the literature [134, 150, 151, 152], where results for various correlation functions are given. Qualitatively one can say the following. Compared to the p-regime with $M_\pi L \gg 1$ the volume corrections are enhanced in the ϵ-regime: Instead of being exponentially suppressed they are polynomial in $1/(fL)^2$.

9.3. Power countings for the epsilon regime in WChPT

Like the continuum effective theory, WChPT can also be formulated in a finite volume, either in the p- or ϵ-regime. The main task is to decide how to count the additional expansion parameter a. The general strategy is to follow the infinite volume procedure. As we have seen, the power counting depends on the relative size of m and a. At finite volume, once the counting of m is fixed by the counting of L, we obtain the counting of a.

Consider the (infinite volume) GSM regime. The LO lagrangian and the tree level pion mass M_0^2 entering the pion propagator are as in the continuum. Repeating the arguments of the previous section we conclude $m \sim \mathrm{O}(\epsilon^4)$. Since the GSM regime is defined by $m \sim a\Lambda_{\mathrm{QCD}}^2$ we are immediately led to $a \sim \mathrm{O}(\epsilon^4)$.

The LCE regime is more subtle. The tree level pion mass M_0^2, given in (4.22), is now a sum of (according to our assumption) two terms of equal order. If $c_2 < 0$, it is a sum of two positive terms. Hence, a small pion mass of order $\mathrm{O}(\epsilon^2)$ implies that both terms, $2Bm$ and $2|c_2|a^2$ are small too and of order $\mathrm{O}(\epsilon^4)$.

If c_2 is positive, the pion mass is the difference of two positive contributions. This leaves the possibility that M_0^2 is small, even though the individual terms $2Bm$ and $2|c_2|a^2$ may not be small and only their difference is. Small values for M_0^2 which we count as ϵ^4 may be obtained by the difference of two order ϵ^2 or ϵ^3 terms, for example. Even though theoretically possible, such a scenario is not very likely. Present day lattice simulations are usually done with small lattice spacings less than 0.1 fm and the $\mathrm{O}(a^2)$ corrections are expected to be small in this case. Hence, we *assume* that $a^2 \sim \mathrm{O}(\epsilon^4)$ in the Aoki regime. This assumption, together with the requirement $M_0^2 \sim \mathrm{O}(\epsilon^4)$ then also leads to $m \sim \mathrm{O}(\epsilon^4)$, the same counting as for $c_2 < 0$.

The ϵ-expansion allows to introduce yet another regime with $a \sim \mathrm{O}(\epsilon^3)$. Just by the powers of ϵ this is an intermediate regime between the GSM and LCE regime. One may think about it as the GSM regime but at a larger lattice spacing (or smaller quark mass). Its usefulness will become clear in the next section when we discuss the ϵ-expansion of correlation functions.

All three countings are perfectly fine and appropriate for a particular relative size between the mass term and the a^2 term in the chiral lagrangian. In order to be able to refer to these regimes the following nomenclature was introduced [11]:

$$\begin{aligned} \text{GSM regime:} \quad & a \sim \mathrm{O}(\epsilon^4)\,, \\ \text{GSM}^* \text{ regime:} \quad & a \sim \mathrm{O}(\epsilon^3)\,, \\ \text{LCE regime:} \quad & a \sim \mathrm{O}(\epsilon^2)\,. \end{aligned} \tag{9.6}$$

9.4. Epsilon expansion of correlation functions

The prime 'observables' in ϵ-regime calculations are correlation functions of the standard vector and axial vector currents and the scalar and pseudo scalar density. These correlators have been calculated before through NNLO in continuum ChPT [151]. In

powers of ϵ this corresponds, for example, to $\mathrm{O}(\epsilon^4)$ for the pseudo scalar correlator and $\mathrm{O}(\epsilon^8)$ for the correlator involving the axial vector current.

In order to discuss the ϵ-expansion in WChPT an operator O and the action S are split into the continuum part and a remainder proportional to powers of a,

$$O(x) = O_{\mathrm{ct}}(x) + \delta O(x)\,, \qquad S = S_{\mathrm{ct}} + \delta S\,. \tag{9.7}$$

The two-point correlator $\langle O_1(x)O_2(0)\rangle \equiv \langle O_1 O_2\rangle$ (for notational simplicity we suppress the dependence on x) can then be written according to

$$\langle O_1 O_2\rangle_W = \langle O_{1,\mathrm{ct}} O_{2,\mathrm{ct}}\rangle + \delta\langle O_1 O_2\rangle\,, \tag{9.8}$$

$$\delta\langle O_1 O_2\rangle = \langle O_{1,\mathrm{ct}}\delta O_2 + \delta O_1 O_{2,\mathrm{ct}}\rangle - \langle O_{1,\mathrm{ct}} O_{2,\mathrm{ct}}\delta S\rangle + \langle O_{1,\mathrm{ct}} O_{2,\mathrm{ct}}\rangle\langle\delta S\rangle\,. \tag{9.9}$$

The expectation value on the left hand side of (9.8), labelled with a subscript 'W' is defined with the full action S in the Boltzmann factor, while on the right hand side it is defined with S_{ct} only (for notational simplicity we suppress a subscript 'ct'). The correction to the Boltzmann factor $\exp(-\delta S)$ has been approximated by $1-\delta S$ and all higher corrections have been dropped.

Let us consider the axial vector correlator $\langle A^a_\mu(x)A^a_\mu(0)\rangle$ as a concrete example to work out the ϵ-counting for the correction $\delta\langle A^a_\mu(x)A^a_\mu(0)\rangle$. We start with the lattice corrections due to the contribution δS. It is useful to split them into two parts. The first one, denoted by δS_a, contains the terms of $\mathcal{L}_{ap^2}$ and $\mathcal{L}_{am}$ in (4.3) and (4.4). These terms start at $\mathrm{O}(\epsilon^{n_a})$ (having taken into account ϵ^{-4} stemming from the integration over space-time), where n_a counts the powers of ϵ for a. We defined three different countings in the previous section, but for now we leave n_a unspecified, write

$$\delta S_a \sim \epsilon^{n_a}\,, \tag{9.10}$$

and insert the concrete values for n_a later. Note that the symbol $\sim$ stands here just for the leading lattice contribution in the ϵ-expansion. The left hand side contains more terms that are of higher order in the ϵ-expansion.

The second contribution, δS_{a^2}, contains only the $\mathrm{O}(a^2)$ term proportional to c_2. Therefore, it counts as

$$\delta S_{a^2} \sim \epsilon^{2n_a-4}\,. \tag{9.11}$$

Finally the terms involving the discretization correction to the axial vector itself. For what matters here we can simplify the expression in (4.17). We are interested in the power counting for the ϵ-expansion, and for this we can ignore all constants which count as $\mathrm{O}(1)$. Therefore, we write[1]

$$\delta A^a_\mu \propto a\big[(\mathrm{tr}(\Sigma+\Sigma^\dagger)+1)A^a_{\mu,\mathrm{ct}} + \partial_\mu \mathrm{tr}\big(T^a(\Sigma-\Sigma^\dagger)\big)\big]\,. \tag{9.12}$$

Both, $A^a_{\mu,\mathrm{ct}}$ and $\partial_\mu\mathrm{tr}\big(T^a(\Sigma-\Sigma^\dagger)\big)$ have an open Lorentz index. Therefore, they contain at

[1] In order to avoid confusion we explicitly write tr for the trace over flavor indices in this section, instead of the earlier used notation $\langle\cdots\rangle$.

least one derivative acting on at least one power of the field $\xi(x)$. Hence, their continuum ϵ-expansion starts at $\mathrm{O}(\epsilon^2)$ and we find for the leading lattice correction

$$\delta A_\mu^a \sim \epsilon^{n_a+2} \,. \tag{9.13}$$

After these general considerations we can determine at which order the lattice spacing effects enter the correlator. In the GSM regime we set $n_a = 4$ and find $\delta\langle A_\mu^a(x) A_\mu^a(0)\rangle \sim \mathrm{O}(\epsilon^8)$. The corrections due to the lattice spacing first enter at NNLO. Up to NLO the results obtained in continuum ChPT are the appropriate ones.

In the GSM* regime we have $n_a = 3$ and obtain $\delta\langle A_\mu^a(x) A_\mu^a(0)\rangle \sim \mathrm{O}(\epsilon^6)$, hence the correction enters at NLO. Interestingly, the dominant term here stems from the correction δS_{a^2} only. The other corrections from the $\mathrm{O}(a)$ contribution in the current and δS_a enter first at ϵ^7 and are of higher order.

The modifications in the LCE regime are more pronounced. Here, cut-off effects already show up at LO. Even worse, the corrections can no longer be simply added to the continuum result. The reason is the correction δS_{a^2}, which gives a zero-mode contribution of order ϵ^0. Hence, it is no longer justified to expand completely the exponential $\exp(-S_{a^2}) \approx 1 - S_{a^2}$. The zero-mode contribution of order ϵ^0 has to be included in the leading order Boltzmann factor, which modifies in a nontrivial way the integral over the zero-mode. The other $\mathrm{O}(a)$ corrections (from δO and δS_a) are of order ϵ^2 and show up at NLO only.

What we discussed here for the axial vector correlator also holds for other correlation functions [11]. The main conclusion we can draw is that the lattice spacing corrections enter at NNLO in the GSM regime. This is quite remarkable and may explain why the numerical data of Hasenfratz and Schaefer [146] could be fitted very well using the NLO continuum expressions. Note that this suppression to NNLO holds even for the unimproved theory. If the theory is nonperturbatively improved the corrections δO and δS_a are absent, and modifications are caused by δS_{a^2} only. We have seen that this term is the dominant correction in the GSM* and LCE regime, while the others are subleading. Consequently, the ϵ-expansion is essentially unchanged for the improved theory, since only subleading terms vanish.

9.5. NLO correction in the GSM* regime

The first nontrivial modification of the continuum results at NLO appears in the GSM* regime. In ref. [11] this correction has been computed for all standard correlators for the $N_f = 2$ case. In order to illustrate the corrections we briefly summarize the result for the axial vector correlator.

The NLO correction we are looking for is caused by the constant term of the δS_{a^2} contribution,

$$\delta\langle O_1(x) O_2(y)\rangle\big|_{\mathrm{NLO,GSM}^*} = -\langle O_{1,\mathrm{ct}}^{\mathrm{LO}}(x) O_{2,\mathrm{ct}}^{\mathrm{LO}}(y) \delta S_{a^2}\rangle + \langle O_{1,\mathrm{ct}}^{\mathrm{LO}}(x) O_{2,\mathrm{ct}}^{\mathrm{LO}}(y)\rangle\langle \delta S_{a^2}\rangle \,, \tag{9.14}$$

where

$$\delta S_{a^2} = \frac{\rho}{16}\big(\mathrm{tr}(U_0 + U_0)\big)^2 \,. \tag{9.15}$$

The superscript 'LO' refers to leading order in the ϵ-expansion and we have introduced the dimensionless quantity

$$\rho = f^2 c_2 a^2 V \,. \tag{9.16}$$

For $N_f = 2$ the integral over the zero-mode leads to integrals of the type

$$\langle g(U_0)\rangle = \frac{1}{Z_0}\int_{\mathrm{SU}(2)} [dU_0]\, g(U_0)\, e^{\frac{\mu}{2}\mathrm{Tr}(U_0+U_0^\dagger)} \,, \tag{9.17}$$

where $[dU_0]$ denotes the standard Haar measure of SU(2), and Z_0 is the partition function given for $g = 1$. μ is the short hand notation for the standard combination[2]

$$\mu = f^2 BmV \,. \tag{9.18}$$

Quite generally, the integral (9.17) leads to expressions involving modified Bessel functions $I_n(z)$ with integer index n. These functions satisfy numerous recursion relations [153]. These allow us to express all integrals in terms of two Bessel functions, which we choose to be I_2 and I_1.

For the axial vector correlator we introduce the definition

$$\langle A_0^a(x) A_0^b(y)\rangle = \delta^{ab} C_{\mathrm{AA}}(x-y) \,. \tag{9.19}$$

For definiteness we consider the time-component correlator. C_{AA} at NLO can be split into a continuum part and a correction proportional to the lattice spacing,

$$C_{\mathrm{AA}}(x-y) = C_{\mathrm{AA,ct}}(x-y) + C_{\mathrm{AA},a^2}(x-y) \,. \tag{9.20}$$

For the matching with numerical results obtained in lattice simulations one is usually interested in the correlation function integrated over the spatial components,

$$C_{\mathrm{AA}}(t) = \int d^3\vec{x}\, C_{\mathrm{AA}}(x-y)|_{y=0} = C_{\mathrm{AA,ct}}(t) + C_{\mathrm{AA,a^2}}(t) \,. \tag{9.21}$$

It turns out that, at NLO, $C_{\mathrm{AA,a^2}}(t)$ does not depend on Euclidean time t [11], and it is convenient to redefine the correction by pulling out some factors:

$$C_{\mathrm{AA,a^2}} = -\frac{f^2}{2T}\rho\Delta_{\mathrm{AA}} \,. \tag{9.22}$$

For the correction Δ_{AA} one explicitly finds [11]

$$\Delta_{\mathrm{AA}} = \frac{-5\mu I_1^2(2\mu) + 10 I_1(2\mu) I_2(2\mu) + 3\mu I_2(2\mu)^2}{\mu^3 I_1^2(2\mu)} \,. \tag{9.23}$$

[2]Not to be confused with the twisted mass of section 8. Note also that one usually writes Σ for the combination $f^2 B$. It is the quark condensate in the chiral limit.

As mentioned before, the correction can be expressed in terms of the two Bessel functions I_1 and I_2 with argument μ defined in (9.18). The a dependence enters in form of the overall factor ρ, which is proportional to $c_2 a^2$. This also holds for correlators involving the vector current or the pseudo scalar density.

The result for the continuum part $C_{\mathrm{AA,ct}}(t)$ can be found in [151] (see also refs. [154, 155]). We do not give the full expression here but simply remark that it is a simple quadratic function of Euclidean time t. In a simplified form it can be written as $k_0 + k_2 t^2$, with the 'constants' k_0, k_2 being some functions of μ, L and T. The bottom line here is that the a^2 correction leads to a shift of the constant part k_0. The t-dependent piece is unaffected by the lattice spacing corrections, at least at NLO.

There is a caveat concerning the applicability of the results given so far. The correlators are given as functions of m, the shifted quark mass. As remarked before, this is the mass parameter in the chiral lagrangian and a priori not an observable. In lattice simulations one usually gives correlators as a function of the PCAC mass, defined in (8.17). The computation of the correlators in both numerator and denominator is straightforward, and to NLO in the GSM* regime one finds

$$m_{\mathrm{PCAC}} = m\left[1 + \rho\left(\frac{2}{\mu^2} - \frac{I_1(2\mu)}{\mu I_2(2\mu)}\right)\right] . \tag{9.24}$$

This result can be inverted to obtain the shifted mass as a function of the PCAC mass, and in a second step one consistently replaces m with m_{PCAC} in the correlators of interest. The resulting expressions, which differ slightly in the details, can then be used in analyzing lattice data.

9.6. Fit to lattice data

The predictions of the last section have been used to analyze the lattice data generated in [146]. Data was available for the pseudo scalar and the axial vector correlators. The data were generated with two flavors of nHYP Wilson fermions [156]. The lattice spacing was moderately small with $a \simeq 0.115$ fm, and two lattice extents were considered, $T = L = 16a \simeq 1.84$ fm and $T = L = 24a \simeq 2.8$ fm. Quark masses were such that $\mu = f^2 B m_{\mathrm{PCAC}} V \simeq 0.7 - 2.9$ for the small volume, and $\mu \simeq 2.1 - 5.0$ for the larger volume.

The data for both correlators were simultaneously fit for all available quark masses. Fit parameters are the chiral condensate $\Sigma = f^2 B$, the decay constant in the chiral limit, f, and the LEC c_2. For the larger volume one obtains [11]

$$\left[\Sigma^{\overline{\mathrm{MS}}}(\mu = 2\ \mathrm{GeV})\right]^{1/3} = 249(4)\ \mathrm{MeV}, \quad f = 88(3)\ \mathrm{MeV}, \quad c_2 = 0.02(8)\ \mathrm{GeV}^4 . \tag{9.25}$$

The data, along with the fit results, are shown in Fig. 9.1. The results for the smaller volume yields values which are consistent with eq. (9.25), but the large χ^2 of the fit indicates that the NLO formulae are not really applicable. The values of f and $\Sigma^{\overline{\mathrm{MS}}}$ are compatible with other determinations [30]. The value of c_2 is compatible with zero. This

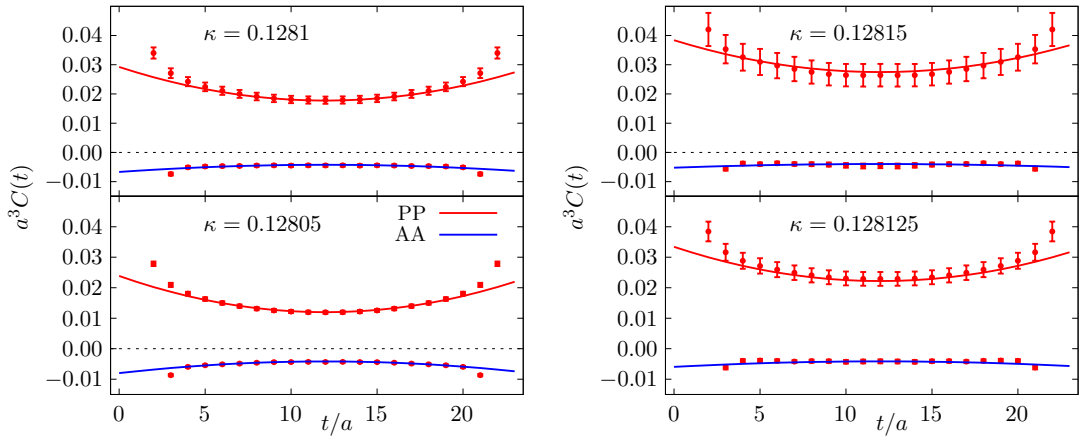

Figure 9.1.: Fit of the WChPT predictions to lattice data (from ref. [11]). All data points within the fit range of $t/a \in [6, 18]$ for the four sea quark masses are included in the combined fit. The axial vector correlator is multiplied by a factor 50 for better visibility.

is not unexpected since we had known before that the data is very well described by the continuum ChPT expressions. A continuum fit (with $c_2 = 0$) yields virtually unchanged values for f and Σ, showing that the $\mathrm{O}(a^2)$ effects have no impact on the extraction of the LECs beyond the level of the statistical uncertainties.

This is a very encouraging result. It demonstrates that simulations with Wilson fermions in the ϵ-regime are feasible and seem to be a viable alternative to time-consuming simulations with dynamical GW fermions. Lattice computations on a wide range of lattice spacings and volumes would of course be very useful to test if the predicted NLO scaling is verified.

9.7. The epsilon regime with twisted mass fermions

Recently, the discussion of the previous sections has been generalized to twisted mass Wilson fermions [13]. Most of the arguments can be carried over to the twisted mass case almost unchanged once the quark mass m is replaced by the polar mass

$$m_{\mathrm{P}} = \sqrt{m^2 + \mu^2}\,. \tag{9.26}$$

The power counting of a is determined by its relative size to m_{P}, and the three different regimes in (9.6) can be introduced as before. The discussion of the ϵ-expansion of correlation functions is essentially unchanged. It is based entirely on dimensional arguments and once m is replaced by m_{P} the entire discussion holds true for the twisted mass case as well. Hence, the order in the ϵ-expansion at which the lattice spacing effects enter is the same as for standard masses. In the GSM regime the lattice spacing corrections are suppressed and enter first at NNLO. This provides at least a qualitative explanation for the data generated by the ETM collaboration, which show small cut-off effects and can

be reasonably well described by continuum ChPT [148, 149, 157].

In the GSM* regime the cut-off corrections enter at NLO. The leading correction at this order is as in (9.14), but the Boltzmann factor in the functional integral includes a term proportional to the twisted mass μ. This difference leads to minor changes in the details of the $\mathrm{O}(a^2)$ corrections in the various correlation functions. We refrain from listing here all the corrections and refer to ref. [13].

Analyzing the ETMC data with the results in [13] is currently under way [158].

10. Pion mass and decay constant in mixed action ChPT

10.1. General considerations

In this section we present and discuss the 1-loop results for the simplest observables in mixed action ChPT, the valence pion mass and the valence pion decay constant. The lattice spacing corrections in the sea sector are quite different for either Wilson sea or staggered sea quarks, so one might expect results that are very sensitive to the details of the particular sea sector. However, this is not the case. In fact, as has been shown in [159], the calculation and the final results show many universal features and resemble closely the continuum PQChPT expressions, irrespectively of the details for the sea quark sector.

In order to discuss this important feature we again restrict ourselves to two sea and valence quark flavors, both with a degenerate quark mass. We are interested in 1-loop results for valence quark correlation functions in the LCE regime, where the $\mathrm{O}(a^2)$ terms are taken at LO. The corresponding GSM regime results are then easily obtained by dropping terms that are of higher order in this regime.

Any 1-loop calculation requires the propagators with the tree level meson masses and the appropriate interaction vertices. The tree level masses for the sea, valence and mixed pion have already been given and discussed in section 5.4. Also the flavor neutral propagator is needed, specified in (5.25) for Wilson sea quarks, and in (5.28) for staggered sea quarks. Note that almost all propagators assume their continuum form if written in terms of the meson masses, i.e. the $\mathrm{O}(a^2)$ corrections are not explicit but hidden in these meson masses. An exception is the flavor neutral propagator (5.25) for Wilson sea quarks with the explicit W_7' contribution in the residue of the double pole.

The vertices responsible for 1-loop diagrams stem from the LO lagrangian expanded in pion fields. The kinetic and the mass term lead to the same vertices as in continuum PQChPT. In addition, we have to consider the lagrangian $\mathcal{L}_{a^2}$, and here some crucial simplifications can be made. Recall that we want to compute valence correlation functions. To be specific let us assume we are interested in the 2-point function of the charged valence pion, which we denote here by $\pi^{\pm}_{\mathrm{vv}}$. Hence, the vertices we need are of the form $\pi^{+}_{\mathrm{vv}}\pi^{-}_{\mathrm{vv}}$ times a product of two more pion fields. The important observation made in [159] is, that *all these vertices can be obtained by an alternative lagrangian $\tilde{\mathcal{L}}_{a^2}$ that is equivalent to a sea quark mass term.* For example,

$$W_6'\langle P_S(\Sigma+\Sigma^\dagger)\rangle^2 \sim 2N_{\mathrm{s}}W_6'\langle P_S(\Sigma+\Sigma^\dagger)\rangle\,, \tag{10.1}$$

where '$\sim$' here means 'giving the same interaction vertices for valence correlation functions to 1-loop order'.

In order to understand how this simplification comes about consider the part $\langle P_S \Sigma \rangle$. Expanding the field Σ in powers of the pion field Φ we get a sequence of terms with the generic form $\langle P_S \Phi^n \rangle$. Here the projector P_S is crucial. It restricts one index of two Φ fields to be a sea index. For example, for $n = 2$ and 4 we obtain

$$\langle P_s \Phi^2 \rangle \longrightarrow \Phi_{sa} \Phi_{as} \,, \tag{10.2}$$

$$\langle P_s \Phi^4 \rangle \longrightarrow \Phi_{sa} \Phi_{ab} \Phi_{bc} \Phi_{cs} \,. \tag{10.3}$$

In this short hand notation we drop numerical factors involving powers of $2i/f$, and a summation over the indices is implicitly assumed. The second line contains a vertex we are after: If a, b and c are the appropriate indices of the charged valence pion field it reads $\pi^+_{\mathrm{vv}} \pi^-_{\mathrm{vv}} \sum_{\mathrm{s}} \pi_{\mathrm{sv}} \pi_{\mathrm{vs}}$ (having changed the order and made the summation over the sea index explicit).

We also see that squaring the first line does not lead to the desired vertex, simply because in this case all four Φ fields carry one sea index. This observation holds in general: The desired vertices stem from the Φ^4 contribution in $\langle P_S \Sigma \rangle$; products of lower powers do not have the appropriate field structure. The argument can and has been extended to arbitrary n-point valence functions in [159].

Applying this argument to all four terms in $\mathcal{L}_{a^2}$ of (5.18) we find the equivalent lagrangian to be

$$\tilde{\mathcal{L}}_{a^2} = -\hat{a}^2 (2N_{\mathrm{s}} W_6' + 2W_8' + 4W_{\mathrm{Mix}}) \langle P_S (\Sigma + \Sigma^\dagger) \rangle \,. \tag{10.4}$$

The W_7' term does not contribute. That the W_{Mix} term does contribute might be surprising at first, since this term contains the projector P_V via the matrix $\tau_3 = P_S - P_V$. However, using $P_V = 1 - P_S$ one finds the trivial identity (up to an irrelevant constant)

$$-\hat{a}^2 W_{\mathrm{Mix}} \langle \tau_3 \Sigma \tau_3 \Sigma^\dagger \rangle = -4\hat{a}^2 W_{\mathrm{Mix}} \langle P_S \Sigma P_S \Sigma^\dagger \rangle \,, \tag{10.5}$$

and the argument given before can be applied to the right hand side.

The lagrangian in (10.4) has the form of a sea quark mass term. Consequently, the $\mathrm{O}(a^2)$ corrections to the vertices can be accounted for by a suitable replacement of m_{s} in the continuum vertices. This can be made even more transparent by expressing the combination of LECs in (10.4) in terms of the two shifts to the sea and mixed pion mass. In terms of Δ_{Sea} and Δ_{Mix} (cf. (5.22) and (5.24)) we can write

$$\tilde{\mathcal{L}}_{a^2} = -\frac{f^2}{4} \hat{a}^2 (\Delta_{\mathrm{Sea}} + 2\Delta_{\mathrm{Mix}}) \langle P_S (\Sigma + \Sigma^\dagger) \rangle \,. \tag{10.6}$$

The Δ_{Sea} contribution can be combined with the quark mass term $2Bm_{\mathrm{s}}$ to give the tree level pion mass $M^2_{0,\mathrm{ss}}$. At this stage we can finally summarize the rule to get the $\mathrm{O}(a^2)$ contributions to the vertices: The vertices are, expressed in terms of tree level pion masses exactly as in continuum PQChPT. In addition, there is one more vertex that has

the form of a sea pion mass vertex but with $M^2_{0,\mathrm{ss}}$ replaced by $2\hat{a}^2\Delta_{\mathrm{Mix}}$. Although we have demonstrated this simple result for Wilson sea quarks the same argument holds for a staggered sea sector. Consequently, a calculation in MAChPT is essentially the same as in continuum PQChPT, and the results for valence pion observables resemble closely the corresponding continuum results.

10.2. Staggered sea quarks

The valence pion mass and decay constant have been computed to one loop in [5]. The calculation has been done for $2+1$ sea quark flavors. For simplicity we quote here the corresponding 2 flavor results with degenerate quark masses in the sea and valence sector. These are easily obtained from the $2+1$ flavor results.[1]

The 1-loop result for the charged valence pion mass (in the LCE regime) reads

$$M^2_{\mathrm{vv,NLO}} = M^2_{0,\mathrm{vv}}\Bigg(1+\frac{1}{32\pi^2 f^2}\Big[(M^2_{0,\mathrm{vv}}-M^2_{0,\pi_I})+(2M^2_{0,\mathrm{vv}}-M^2_{0,\pi_I})\ln\frac{M^2_{0,\mathrm{vv}}}{\mu^2}\Big] - \frac{8}{f^2}\Big[(L_5-2L_8)M^2_{0,\mathrm{vv}}+2(L_4-2L_6)M^2_{0,\pi_5}\Big]+\mathcal{C}a^2\Bigg). \tag{10.7}$$

$\mathcal{C}$ is a combination of unknown LECs associated with the NLO lagrangian of $\mathrm{O}(p^2a^2, ma^2)$. This result is the MAChPT analogue of the continuum PQChPT result given in (5.11), which is correctly reproduced in the limit $a \to 0$. As expected, the sea pion mass in front of the logarithms is the taste singlet pion, since this pion enters the flavor singlet propagator. On the other hand, in the analytic NLO contributions the Goldstone boson mass arises. However, since $M^2_{0,\pi_5} = M^2_{0,\pi_I} - a^2\Delta_I$, one can replace the Goldstone pion mass by the singlet pion mass and absorb the splitting Δ_I in the LEC combination $\mathcal{C}$.

In practice the sea pion masses are known in a mixed action calculation, because these are easily measured in a lattice simulation. Using these measured values the result (10.7) provides the dependence of the valence pion mass on the valence quark mass, hidden in $M^2_{0,\mathrm{vv}} = 2Bm_{\mathrm{v}}$. Monitoring this dependence one obtains estimates for the various LECs in (10.7).[2]

Let us briefly discuss the impact of two matching conditions. If we tune the sea quark mass such that the taste singlet pion mass matches the one of the valence pion, the formula (10.7) simplifies to

$$M^2_{\mathrm{vv,NLO}} = M^2_{0,\mathrm{vv}}\left(1+\frac{M^2_{0,\mathrm{vv}}}{32\pi^2 f^2}\ln\frac{M^2_{0,\mathrm{vv}}}{\mu^2}-\frac{16M^2_{0,\mathrm{vv}}}{f^2}(L_{45}-2L_{68})+\mathcal{C}'a^2\right). \tag{10.8}$$

[1] Consider the degenerate case with all three sea quark masses being the same and essentially replace $N_S = 3$ by $N_S = 2$.

[2] Recall that for GW fermions the quark mass is only multiplicatively renormalized, hence m_{v} is proportional to the bare valence quark mass.

Except for the contribution $\mathcal{C}'a^2$ (with a coefficient $\mathcal{C}'$ different from $\mathcal{C}$) this expression agrees with the continuum result quoted in (2.24). This is expected since the residue for the double pole vanishes for this particular matching. On the other hand, if the tuning is such that the Goldstone pion mass agrees with the valence pion mass some partial quenching effects remain,

$$M^2_{\mathrm{vv,NLO}} = M^2_{0,\mathrm{vv}} \left(1 + \frac{M^2_{0,\mathrm{vv}} - a^2\Delta_I}{32\pi^2 f^2} \ln \frac{M^2_{0,\mathrm{vv}}}{\mu^2} - \frac{16 M^2_{0,\mathrm{vv}}}{f^2}(L_{45} - 2L_{68}) + \mathcal{C}''a^2 \right) . \tag{10.9}$$

With this matching the coefficient of the chiral logarithm is suppressed or enhanced, depending on the sign of Δ_I.[3]

The result for the decay constant reads

$$\frac{f_{\mathrm{vv,NLO}}}{f} = 1 - \frac{M^2_{0,\mathrm{vs}}}{16\pi^2 f^2} \ln \left(\frac{M^2_{0,\mathrm{vs}}}{\mu^2} \right) + \frac{4}{f^2} [L_5 M^2_{0,\mathrm{vv}} + 2L_4 M^2_{0,\pi_5}] + \mathcal{D}a^2 . \tag{10.10}$$

$\mathcal{D}$ is another combination of $\mathrm{O}(p^2a^2, ma^2)$ LECs. Also this result reproduces the one from continuum PQChPT, given in (5.12), in the continuum limit. If we match the valence and Goldstone sea pion masses the analytic NLO contribution simplifies to full unquenched form: $L_5 M^2_{0,\mathrm{vv}} + 2L_4 M^2_{0,\pi_5} \to (2L_4 + L_5) M^2_{0,\mathrm{vv}}$. However, we obtain the same form if we match to the taste singlet pion mass, although the constant $\mathcal{D}$ will be different. The main observation here is that neither matching provides an obvious simplification in the chiral logarithm, since it involves the mixed pion mass. Recall that the mixed pion mass $M^2_{0,\mathrm{vs}}$ in (5.26) contains a shift $a^2\Delta_{\mathrm{Mix}}$ such that it is not the simple average of the valence and a particular sea pion mass. The valence quark mass dependence of the decay constant may therefore differ substantially from the one in continuum PQChPT.

10.3. Wilson sea quarks

Mixed action ChPT with Wilson sea quarks has been studied in [2], although for the GSM regime only. However, according to our general remarks in the beginning of this section, the results for the LCE regime are almost trivially obtained from those for staggered sea quarks. The only difference is the residue of the double pole in the flavor neutral propagator. Comparing the expressions (5.25) and (5.28) we immediately see that we should perform the simple replacement

$$M^2_{0,\pi_I} \to M^2_{0,\mathrm{ss}} + \frac{32 W'_7}{f^2} \hat{a}^2 \tag{10.11}$$

in the flavor singlet contributions of the results in the previous section. From (10.7) we

[3] Recall that for the MILC configurations one finds a positive taste splitting, leading to a suppression of the chiral logarithm.

therefore obtain

$$M^2_{\mathrm{vv,NLO}} = M^2_{0,\mathrm{vv}}\left(1+\frac{1}{32\pi^2 f^2}\left[(M^2_{0,\mathrm{vv}}-M^2_{0,\mathrm{ss}})+\left(2M^2_{0,\mathrm{vv}}-M^2_{0,\mathrm{ss}}-\frac{32W_7'}{f^2}\hat{a}^2\right)\ln\frac{M^2_{0,\mathrm{vv}}}{\mu^2}\right]\right.$$
$$\left.-\frac{8}{f^2}\left[(L_5-2L_8)M^2_{0,\mathrm{vv}}+2(L_4-2L_6)M^2_{0,\mathrm{ss}}\right]+\mathcal{C}a^2\right). \qquad (10.12)$$

for the valence pion mass. We use the same symbol $\mathcal{C}$ here for the analytic correction although numerically it is not the same constant, of course. Almost needless to say that this result reproduces the correct continuum result for vanishing lattice spacing.

If the sea and valence pion masses are matched the expression simplifies to

$$M^2_{\mathrm{vv,NLO}} = M^2_{0,\mathrm{vv}}\left(1+\frac{M^2_{0,\mathrm{vv}}-32\hat{a}^2W_7'/f^2}{32\pi^2 f^2}\ln\frac{M^2_{0,\mathrm{vv}}}{\mu^2}-\frac{16M^2_{0,\mathrm{vv}}}{f^2}(L_{45}-2L_{68})+\mathcal{C}a^2\right). \qquad (10.13)$$

This result resembles closely the one in (10.9) for staggered sea quarks. As discussed in section (5.4), some partial quenching effects remain with this matching since it leaves a remnant residue for the double pole in the flavor neutral propagator.

Finally, the decay constant is given as

$$\frac{f_{\mathrm{vv,NLO}}}{f} = 1-\frac{M^2_{0,\mathrm{vs}}}{16\pi^2 f^2}\ln\left(\frac{M^2_{0,\mathrm{vs}}}{\mu^2}\right)+\frac{4}{f^2}\left[L_5M^2_{0,\mathrm{vv}}+2L_4M^2_{0,\mathrm{ss}}\right]+\mathcal{D}\hat{a}^2\,. \qquad (10.14)$$

Except for the trivial replacement $M^2_{0,\pi_5} \to M^2_{0,\mathrm{ss}}$ in the analytic NLO correction this result is identical to the one for staggered sea quarks. Note, however, that various different $\mathrm{O}(a^2)$ corrections are hidden in the tree level pion masses for the sea and the mixed pion. On the level of these masses the differences between Wilson and staggered sea quarks do play a rôle.

10.4. Comments on other mixed action results

The results for the pion mass and decay constant should be sufficient to demonstrate that a 1-loop calculation in MAChPT is essentially the same as the corresponding one in continuum PQChPT. Once the continuum part of the calculation is done only minor and almost trivial modifications remain to be included. Let us nevertheless point to a few selected references that contain some other MAChPT results. Most MAChPT computations deal with staggered sea quarks, motivated by the freely available gauge configurations of the MILC collaboration.

Scattering of valence pions has been studied in [160], and explicit expressions for the $I = 2$ scattering length for 2 and $2+1$ staggered sea quark flavors can be found in that reference. The analogous results for kaon scattering are given in [161]. These results

have also been used to analyze actual lattice data [162, 163, 109].

The scalar correlator is known to be a sensitive tool to partial quenching effects [96] and therefore also a very useful quantity for partially quenched and mixed action lattice QCD [98, 105]. The calculation of the scalar correlator in MAChPT with staggered sea quarks can be found in [164].

One of the main motivations for mixed action simulations is the computation of weak matrix elements. With respect to this the first computation of the kaon B-parameter B_K in MAChPT is very interesting [165].

The analogous results with Wilson sea quarks are mostly unavailable yet. An exception is the scalar correlator which has recently been studied in [166]. However, according to the universality argument described above many results can be obtained fairly effortlessly by simple 'translation' from the corresponding staggered sea results or directly from the continuum PQChPT calculation.

11. Vector meson ChPT with Wilson fermions

11.1. Beyond pseudoscalar ChPT

So far we exclusively dealt with ChPT for the pions.[1] However, spontaneous chiral symmetry breaking and the Goldstone boson character of the pions largely determine the interactions of other hadrons (e.g. baryons, vector mesons, etc.) as well. Low-energy effective theories can be formulated that describe the interactions of these hadrons with low-momentum ('soft') pions. The symmetry properties of QCD, in particular chiral symmetry and its spontaneous as well as explicit breaking, play again a crucial rôle in the construction of these chiral effective theories, which are therefore called *baryon ChPT* [167], *vector meson ChPT* [168] etc.

Following the principles spelled out in section 3 the extension of these effective theories to describe lattice QCD is straightforward. The link is again the Symanzik effective theory with its higher dimensional operators proportional to powers of the lattice spacing. Just as in pseudo scalar ChPT one can map these additional terms into baryon ChPT or vector meson ChPT. And just as for the pseudo scalars one obtains a chiral effective theory for baryons and vector mesons with explicit dependence on the lattice spacing.

In the following we illustrate this procedure for vector meson ChPT with Wilson fermions. We follow ref. [7] where the 2+1 flavor theory has been constructed. Results for the 2 flavor theory can be found in [169].

11.2. Continuum ChPT for vector mesons

Chiral perturbation theory for vector mesons was first introduced in ref. [168]. There the vector meson mass was calculated to $\mathrm{O}(p^3)$. The computation to one order higher can be found in ref. [170], and pseudo scalar decay constants have been studied in ref. [171].

Let us briefly summarize the formalism of [168]. The vector meson mass does not vanish in the chiral limit but assumes a nonzero value, the so-called *chiral mass* μ_{V}.[2] This mass is of the order of about 1 GeV, which is not small. Also the vector meson four-momenta are not small because of this mass. However, the large part due to the heavy mass can be explicitly 'removed' by introducing a constant vector meson four-velocity

[1] Recall that we collectively refer to all pseudo scalars as 'pions', even if the number of flavors is larger than two and there are kaons as well.

[2] μ_{V} has absolutely nothing to do with any twisted mass.

v_μ with $v^2 = 1$. Vector meson four momenta are then written as $p_\mu = \mu_\mathrm{V} v_\mu + k_\mu$, where k_μ is the *residual momentum*, which we assume to be small compared to $\mu_\mathrm{V} v_\mu$. Vector meson ChPT is essentially an expansion in powers of small pion momenta, small pion masses *and* the small residual vector meson momentum.[3] When a low-momentum pion interacts with the vector meson we typically have $p_\mu \sim k_\mu$, so for simplicity we write $\mathrm{O}(p)$ instead of $\mathrm{O}(p,k)$ when we refer to a particular order in the momentum expansion.

The vector mesons are described by *heavy matter fields*, which are also used in the Heavy Quark Effective Theory (HQET) [172]. We introduce a vector meson octet

$$\mathcal{O}_\mu = \sqrt{2}\rho_\mu^a T^a = \begin{bmatrix} \frac{\rho_\mu^0}{\sqrt{2}} + \frac{\phi_\mu^{(8)}}{\sqrt{6}} & \rho_\mu^+ & K_\mu^{*+} \\ \rho_\mu^- & -\frac{\rho_\mu^0}{\sqrt{2}} + \frac{\phi_\mu^{(8)}}{\sqrt{6}} & K^{*0} \\ K_\mu^{*-} & \bar{K}_\mu^{*0} & -\frac{2\phi_\mu^{(8)}}{\sqrt{6}} \end{bmatrix} \tag{11.1}$$

and a singlet $S_\mu = \phi_\mu^0$. The latter transforms trivially under chiral transformations in $G = \mathrm{SU}(3)_L \times \mathrm{SU}(3)_R$,

$$\mathcal{S}_\mu \xrightarrow{G} \mathcal{S}_\mu \,. \tag{11.2}$$

For the transformation behaviour of the octet we first introduce the square root of the pseudo scalar field Σ,

$$\xi = \sqrt{\Sigma} = \exp(i\pi/f) \,, \tag{11.3}$$

which transforms under chiral transformations according to

$$\xi \to L\xi U^\dagger = U\xi R^{-1} \,, \tag{11.4}$$

with an SU(3) matrix U. In fact, this equation defines U, which is in general a rather complicated function of L, R and π. However, for vector transformations with $L = R$ one finds $U = L = R$. Irrespectively of the particular form of U the octet field transforms under chiral transformations as

$$\mathcal{O}_\mu \xrightarrow{G} U\mathcal{O}_\mu U^\dagger \,. \tag{11.5}$$

For the construction of the chiral Lagrangian we proceed just as in standard ChPT for the pseudo scalars. The chiral lagrangian is simply the most general lagrangian that is compatible with chiral symmetry, parity and charge conjugation. Building blocks for the construction are the vector meson fields $\mathcal{O}_\mu, \mathcal{S}_\mu$ and the velocity v_μ, the pseudo scalar fields Σ and $\xi = \sqrt{\Sigma}$, partial derivatives of the fields and the quark mass matrix M.

Before quoting the lowest order chiral lagrangian we have to make a comment on the power counting. In pseudo scalar ChPT partial derivatives appear in even numbers, simply because a Lorentz scalar cannot be formed with an odd number of partial derivatives. Hence, the expansion in powers of momenta starts with $\mathrm{O}(p^2)$ at LO, followed by $\mathrm{O}(p^4, p^2 m)$ at NLO and so on. This is different in vector meson ChPT. Here other

[3] The true (dimensionless) expansion parameter is k/μ_V.

four-vectors like v_μ and the vector meson fields themselves allow to contract a partial derivative, thus the chiral expansion has orders with odd powers of p as well. Quite generally, the order counting follows the scheme

$$\begin{aligned} \text{LO}: &\quad p \\ \text{NLO}: &\quad m,\, p^2 \\ \text{NNLO}: &\quad mp,\, p^3 \end{aligned} \tag{11.6}$$

Note that we still count $p^2 \sim m$ and recall that p represents both the pion and the residual vector meson momentum.

With these preparations we can write down the lowest terms in the chiral lagrangian. At $\mathrm{O}(p)$ we have[4]

$$\begin{aligned} \mathcal{L}_p = &- iS_\mu^\dagger (v^\nu \partial_\nu) S^\mu - i\langle \mathcal{O}_\mu^\dagger (v^\nu \mathcal{D}_\nu) \mathcal{O}^\mu \rangle \\ &+ ig_1 (S_\mu^\dagger \langle \mathcal{O}_\nu A_\lambda \rangle - S_\mu \langle \mathcal{O}_\nu^\dagger A_\lambda \rangle) v_\sigma \epsilon^{\mu\nu\lambda\sigma} + ig_2 \langle \{\mathcal{O}_\mu^\dagger, \mathcal{O}_\nu\} A_\lambda \rangle v_\sigma \epsilon^{\mu\nu\lambda\sigma} \,, \end{aligned} \tag{11.7}$$

where $\langle \ldots \rangle$ stands again for the trace in flavor space. For convenience we introduced the combinations

$$\mathcal{D}_\nu \mathcal{O}_\mu = \partial_\nu \mathcal{O}_\mu + [V_\nu, \mathcal{O}_\mu] \,, \tag{11.8}$$

$$V_\mu = \frac{1}{2} (\xi \partial_\mu \xi^\dagger + \xi^\dagger \partial_\mu \xi) \,, \tag{11.9}$$

$$A_\mu = \frac{1}{2} (\xi \partial_\mu \xi^\dagger - \xi^\dagger \partial_\mu \xi) \,. \tag{11.10}$$

The first line in (11.7) contains the kinetic terms for the vector mesons. Because of the transformation law (11.5) the octet part requires the covariant derivative $\mathcal{D}_\nu$, which transforms in the same way, $\mathcal{D}_\nu \mathcal{O}_\mu \xrightarrow{G} U \mathcal{D}_\nu \mathcal{O}_\mu U^\dagger$. Note that the derivative $i\partial_\mu$ provides the residual momentum $k_\mu = \mu_\mathrm{S} v_\mu - p_\mu$ ($k_\mu = \mu_\mathrm{O} v_\mu - p_\mu$) for the singlet (octet) meson where μ_S (μ_O) is the singlet (octet) vector meson mass in the chiral limit. The remaining terms describe interactions with the pseudo scalars. The terms proportional to g_1 and g_2 involve the combination A_μ, defined in (11.8). Expanded in terms of the pseudo scalar fields this quantity starts as $A_\mu = \partial_\mu \pi / f + \mathrm{O}(\pi^3)$. The presence of the derivative means that both terms are indeed of $\mathrm{O}(p)$.

The $\mathrm{O}(m)$ term of the NLO lagrangian reads

$$\begin{aligned} \mathcal{L}_m = &\lambda_\mathrm{S} \langle M_+ \rangle S_\mu^\dagger S^\mu + \lambda_\mathrm{OS} (\langle \mathcal{O}_\mu^\dagger M_+ \rangle S^\mu + \langle \mathcal{O}_\mu M_+ \rangle S^{\mu\dagger}) \\ &+ \lambda_\mathrm{O1} \langle M_+ \rangle \langle \mathcal{O}_\mu^\dagger \mathcal{O}^\mu \rangle + \lambda_\mathrm{O2} \langle \{\mathcal{O}_\mu^\dagger, \mathcal{O}^\mu\} M_+ \rangle + \Delta\mu \, S_\mu^\dagger S^\mu \,, \end{aligned} \tag{11.11}$$

[4] Just for convenience we follow ref. [168] and present our results in Minkowski space, which does not make a difference for the computation of the vector meson masses.

element	G	C	P
Σ	$L\Sigma R^\dagger$	Σ^T	$\Sigma^\dagger$
ξ	$L\xi U^\dagger = U\xi R^\dagger$	ξ^T	$\xi^\dagger$
$\mathcal{O}_\mu$	$U\mathcal{O}_\mu U^\dagger$	$-O_\mu^T$	$\mathcal{O}_\mu$
S_μ	S_μ	$-S_\mu$	S_μ
M	$LMR^\dagger$	M^T	$M^\dagger$
M_+	$UM_+U^\dagger$	M_+^T	$\pm M_+$
V_μ	$UV_\mu U^\dagger + U\partial_\mu U^\dagger$	$-V_\mu^T$	V_μ
A_μ	$UA_\mu U^\dagger$	A_μ^T	$-A_\mu$
$\mathcal{D}_\nu\mathcal{O}_\mu$	$U(\mathcal{D}_\nu\mathcal{O}_\mu)U^\dagger$	$-(\mathcal{D}_\nu\mathcal{O}_\mu)^T$	$\mathcal{D}_\nu\mathcal{O}_\mu$

Table 11.1.: Transformation properties under the group $G = \mathrm{SU}(3)_L \times \mathrm{SU}(3)_R$, ($L \in \mathrm{SU}(3)_L$ and $R \in \mathrm{SU}(3)_R$), charge conjugation C and parity P. In the parity transformed expressions it is understood that the argument is $(-\vec{x}, t)$.

with the mass matrix M entering via the combination

$$M_+ = \frac{1}{2}(\xi M^\dagger \xi + \xi^\dagger M \xi^\dagger)\,. \tag{11.12}$$

The last term introduces the mass difference

$$\Delta\mu = \mu_\mathrm{S} - \mu_\mathrm{O} \tag{11.13}$$

between the singlet and octet vector meson mass.[5] Note that the leading order mass terms $\mu_0 S_\mu^\dagger S^\mu$ and $\mu_8\langle\mathcal{O}_\mu^\dagger\mathcal{O}^\mu\rangle$ are absent in the $\mathrm{O}(p)$ lagrangian, because their effect is already included through the definition of the heavy meson fields. The mass difference, however, needs to be introduced explicitly. Since $\Delta\mu$ is small (less than 200 MeV) and of the order of the strange quark mass, it is considered to be of $\mathrm{O}(m)$.

It is easily checked that all terms in $\mathcal{L}_p$ and $\mathcal{L}_m$ are invariant under transformations in G, P and C. For convenience we have collected the transformation properties of the various elements in the chiral lagrangian in table 11.1. Higher order terms can be constructed analogously, but $\mathcal{L}_p$ and $\mathcal{L}_m$ will suffice in the following.[6]

Starting from the chiral lagrangian one can calculate the vector meson propagator. The vector meson masses are then given by the zeros of the inverse propagator. Details can be found [168], here we simply quote the final result. We simplify the results of [168] by setting all quark masses equal, $m_u = m_d = m_s \equiv m$. In this case the masses of the octet vector mesons (and the pseudo scalars) are all the same, which simplifies the final

[5] We assumed the definition $\mu_\mathrm{V} = \mu_\mathrm{O}$. If we had chosen $\mu_\mathrm{V} = \mu_\mathrm{S}$ the last term in eq. (11.11) would be $-\Delta\mu\langle\mathcal{O}_\mu^\dagger\mathcal{O}^\mu\rangle$. Of course, the final results for the vector meson masses are independent of this choice.

[6] Although $\mathcal{L}_{p^2}$ is of the same order as $\mathcal{L}_m$ it does not contribute to the NNLO results for the vector meson masses.

expressions. To NNLO, i.e. to $\mathrm{O}(p^3)$, we find

$$M_{\mathrm{V,NNLO,ct}} = \mu_{\mathrm{O}} + (3\lambda_{\mathrm{O1}} + 2\lambda_{\mathrm{O2}})m - \frac{1}{12\pi f^2}\left[g_1^2 + \frac{10}{3}g_2^2\right](2Bm)^{3/2}\,, \tag{11.14}$$

$$= \mu_{\mathrm{O}} + \tilde{\lambda}M_\pi^2 - \frac{1}{12\pi f^2}\tilde{g}^2 M_\pi^3\,, \tag{11.15}$$

where $\tilde{\lambda} = (3\lambda_{\mathrm{O1}} + 2\lambda_{\mathrm{O2}})/2B$ and $\tilde{g}^2 = g_1^2 + 10g_2^2/3$. In the chiral limit we recover the input that the vector meson mass is equal to μ_{O}. The other two terms proportional to m are the corrections due to the interaction with the pions. The nonanalytic corrections proportional to $m^{3/2} \propto M_\pi^3$ stems from 1-loop self-energy diagrams. In the nondegenerate case one has corrections proportional to M_K^3 and M_η^3 as well [168].

11.3. Including the lattice spacing corrections

It is now a simple matter to extend the results of the previous section to Wilson ChPT. The lattice spacing is introduced using the spurion A that transforms according to (3.6). Recall that A transforms just like the mass spurion M, so it will be convenient to introduce the analogue of M_+,

$$W_+ = \frac{1}{2}(\xi A^\dagger \xi + \xi^\dagger A \xi^\dagger)\,. \tag{11.16}$$

Obviously, W_+ transforms exactly like M_+ under G, P and C. It is thus trivial to write down the lagrangian $\mathcal{L}_a$: Simply take $\mathcal{L}_m$ and replace M_+ by W_+, except for the mass splitting term which has no analogue in $\mathcal{L}_a$. This procedure yields

$$\begin{aligned}\mathcal{L}_a = {}& \alpha_1\langle W_+\rangle S_\mu^\dagger S^\mu + \alpha_2(\langle \mathcal{O}_\mu^\dagger W_+\rangle S^\mu + \langle \mathcal{O}_\mu W_+\rangle S^{\mu\dagger}) \\ & + \alpha_3\langle W_+\rangle\langle \mathcal{O}_\mu^\dagger \mathcal{O}^\mu\rangle + \alpha_4\langle\{\mathcal{O}_\mu^\dagger, \mathcal{O}^\mu\}W_+\rangle\,.\end{aligned} \tag{11.17}$$

The same procedure can be applied to derive the lagrangians $\mathcal{L}_{am}$ and $\mathcal{L}_{a^2}$ from the continuum lagrangian $\mathcal{L}_{m^2}$. We do not need the explicit expressions in the following and do not quote them here, but they can be found in [7]. The main point here is that the additional terms in the chiral lagrangian are very easily constructed from the continuum lagrangian containing the quark mass matrix.

Note that the lagrangian $\mathcal{L}_a$ cannot be absorbed in the continuum lagrangian $\mathcal{L}_m$ by a simple redefinition of the quark masses. We have already used the freedom for the redefinition in the pseudo scalar sector, hence we cannot use it again to simplify the vector meson chiral lagrangian.

Slightly nontrivial is the power counting once we have the chiral symmetry breaking sources m and a. In WChPT for the pseudo scalars we introduced two regimes depending on the relative size of the quark mass and the lattice spacing. This is carried over to vector meson WChPT as well. In the GSM regime we assumed $m \sim a$ (short for $m \sim a\Lambda_{\mathrm{QCD}}^2$). Hence, the generalization of (11.6) reads

GSM regime:

$$\begin{aligned} \text{LO}: &\quad p \\ \text{NLO}: &\quad m,\, p^2,\, a \\ \text{NNLO}: &\quad mp,\, p^3,\, ap\,. \end{aligned} \tag{11.18}$$

In the LCE regime we assumed smaller quark masses such that $m \sim a^2$. Since we also have $m \sim p^2$ we find $p \sim a$, and the scheme (11.18) changes to

LCE regime:

$$\begin{aligned} \text{LO}: &\quad p,\, a \\ \text{NLO}: &\quad m,\, p^2,\, ap,\, a^2 \\ \text{NNLO}: &\quad mp,\, p^3,\, a^2p,\, ma,\, p^2a,\, a^3\,. \end{aligned} \tag{11.19}$$

Technically the calculation of the vector meson masses is as in continuum ChPT, but with additional contributions stemming from the lattice spacing corrections. It is again convenient to perform the computation for the LCE regime; the GSM regime result is then easily obtained by dropping various terms that are higher than the order one works to.

In the LCE regime the $\mathrm{O}(a)$ lagrangian (11.17) is taken at LO. In a one loop calculation it provides additional vertices which give rise to additional loop diagrams proportional to a. Quite generally, these will result in corrections proportional to $aM_\pi^2 \ln M_\pi^2$ to the vector meson masses. The necessary counterterms are provided by the NNLO terms of $\mathrm{O}(am)$. Therefore, working to one loop order in the LCE regime necessarily means working to NNLO, which has been done in [7]. The result for the vector meson mass can be written as

$$M_{\mathrm{V,NNLO,LCE}} = M_{\mathrm{V,NNLO,ct}} + a\Delta M_{\mathrm{V,log}} + a\Delta M_{\mathrm{V,analytic}}\,. \tag{11.20}$$

The leading part is (obviously) the continuum result $M_{\mathrm{V,NNLO,ct}}$. The correction $a\Delta M_{\mathrm{V,log}}$ comprises the nonanalytic (logarithmic) corrections stemming from the 1-loop diagrams proportional to a, as discussed before. The correction $a\Delta M_{\mathrm{V,analytic}}$ contains all the remaining analytic contributions. Most interesting is the nonanalytic correction because it qualitatively changes the quark mass (or pion mass) dependence of the vector meson masses at fixed lattice spacing. It explicitly reads (for the mass degenerate case $m_u = m_d = m_s \equiv m$)

$$\Delta M_{\mathrm{V,log}} = -\frac{1}{6\pi^2 f^2}\left[6\alpha_3 + 5\alpha_4\right] M_\pi^2 \ln \frac{M_\pi^2}{\mu^2}\,. \tag{11.21}$$

Here M_π denotes the LO pion mass in the LCE regime, i.e. including the $\mathrm{O}(a^2)$ corrections. For the nondegenerate case the correction involves logarithms $M_K^2 \ln M_K^2$ and $M_\eta^2 \ln M_\eta^2$ as well [7].

We conclude that at nonzero lattice spacing there are additional chiral logarithms in the results for the vector meson masses. Therefore, together with the continuum result there are two kinds of nonanalytic quark mass dependence. This is qualitatively the same result that we derived for pseudo scalar WChPT in section 6.1. A difference is that the additional chiral logarithms in vector meson WChPT are proportional to one

power of a, while for the pseudo scalars they are associated with a^2 (recall eq. (6.1)).

The analytic correction $\Delta M_{\mathrm{V,analytic}}$ contains the lattice spacing dependence stemming from the remaining parts in the chiral lagrangian. It starts with

$$\Delta M_{\mathrm{V,analytic}} = 3\alpha_3 + 2\alpha_4 + \dots \,. \tag{11.22}$$

The ellipsis stand for the higher $\mathrm{O}(a^2, aM_\pi^2)$ corrections. We do not give them here since they involve the LECs in $\mathcal{L}_{a^2}, \mathcal{L}_{am}$ which we have not listed here. However, the main observation one can make is that $\Delta M_{\mathrm{V,analytic}}$ does not qualitatively change the pion mass dependence of M_{V}. For example, the leading term in the correction (11.22) can be combined with the continuum result, and it amounts to a shift of the vector meson mass in the chiral limit,

$$\mu_{\mathrm{O}} \longrightarrow \mu_{\mathrm{O}} + a(3\alpha_3 + 2\alpha_4)\,. \tag{11.23}$$

Similarly, the $\mathrm{O}(aM_\pi^2)$ correction amounts in an $\mathrm{O}(a)$ shift of the constant $\tilde{\lambda}$ in (11.14). So, except for a-dependent coefficients the pion mass dependence is just as in the continuum result.

As already mentioned, the NNLO result for the GSM regime is easily obtained from the corrections given above: We have to drop all corrections except for the leading term in $\Delta M_{\mathrm{V,analytic}}$. In particular, the chiral logarithm (11.21) needs to be dropped too because it enters at NNNLO in the GSM regime.

The result for the vector meson masses demonstrates once again the nontrivial modifications in WChPT. WChPT is more than making the LECs a-dependent in a continuum result. The truly new and nontrivial effects are the nonanalytic corrections which are not 'guessed' easily. WChPT (as well as its variants for other lattice fermions) provide the framework to systematically work out these corrections.

11.4. Comment on baryon ChPT

The discussion of vector meson WChPT illustrates another aspect: The construction of lattice ChPT is fairly straightforward provided the corresponding continuum version exists. In particular, the $\mathrm{O}(a)$ corrections in the chiral lagrangian are readily obtained from the mass terms of the continuum version.

As an example we mention baryon ChPT. The continuum formulation has been given first in ref. [167]. The baryons are heavy particles and again described by heavy matter fields. The whole approach resembles very closely the construction of vector meson ChPT. The lattice spacing corrections are then included using the spurion field A. This has been done in ref. [173], and a number of nucleon properties (masses and magnetic moments) have been computed in the GSM regime. Electromagnetic properties of baryons like the charge radius have been computed in ref. [174]. The analogous computations in the LCE regime are significantly more involved and have not been done so far. Nevertheless, this demonstrates that the construction of WChPT is not as difficult as one may think. The main work and difficulty lies in the continuum part of the effective theory.

12. Concluding remarks

Chiral perturbation theory is and will remain a useful companion in the analysis of lattice QCD data. Improved algorithms and steady progress in computer technology will result in numerical simulations at smaller quark masses and lattice spacings. The pion masses will be sufficiently small enough to make contact to ChPT in a controlled manner. At the same time, the statistical errors will decrease, leading to reliable results for various physical observables. This, however, requires good control of the systematic uncertainties as well. One source of systematic error is the application of continuum ChPT to lattice data at nonzero lattice spacing. This can lead to uncontrolled uncertainties in the results obtained from lattice simulations.

We have seen here how to formulate ChPT for lattice QCD. The corrections proportional to the nonzero lattice spacing can be systematically included in ChPT by a joint expansion in the quark masses and the lattice spacing. Depending on the particular variant of lattice fermions the details of these corrections differ, but we can conclude with a general lessons: Expectations based on continuum ChPT need not be met.

I cannot resist to illustrate this by quoting from a panel discussion on the chiral extrapolation that took place during the Lattice conference in 2002. S. Hashimoto nicely summarized a common reasoning that was widely accepted in the lattice QCD community at that time. He said (ref. [175], p. 172):

The strategy we have in mind when we do the chiral extrapolation is to use chiral perturbation theory (ChPT) as a theoretical guide to control the quark mass dependence of physical quantities. For this strategy to work one has to push the sea quark mass as light as possible and test whether the lattice data are described by the 1-loop ChPT formula. (The lowest order ChPT prediction usually does not have quark mass dependence.) If so, chiral extrapolation down to the physical pion mass is justified. In full QCD ChPT predicts the chiral logarithm with a definite coefficient depending only on the number of active flavors, which gives a non-trivial test of the unquenched lattice simulations.

He continued by showing lattice results for the pion mass obtained by the JLQCD collaboration, together with the result of an ChPT analysis he just described. He had to conclude:

. . . it is unfortunately clear that the lattice result does not reproduce the characteristic curvature of the chiral logarithm. The same is true for the pseudoscalar meson decay constant, and the ratio test using partially quenched ChPT leads to the same conclusion [14].

One should say that the data he showed were obtained with rather heavy $O(a)$ im-

proved Wilson fermions. The lightest pion mass was still more than half as heavy as the rho meson, so Hashimoto's conclusion that the quark masses are too heavy for a matching with ChPT is most probably correct. Still, even if the quark masses had been smaller one should not expect that the coefficient in front of the chiral logarithm depends on N_f only. According to our result in (6.2) it receives an $\mathrm{O}(a^2)$ correction as well.

Misconceptions are not constrained to the nonanalytic quark mass dependence. Another illustrative example concerns the expected scaling violation in unimproved Wilson fermions. A standard argument, based on the Symanzik effective theory, is that the scaling violations start at $\mathrm{O}(a)$. This argument is invoked in ref. [117] to speculate about the scaling violations in the pion scattering amplitude, calculated with unimproved Wilson fermions. On page 389 of that paper we find the following statements:

Testing relations Eq. (2.2) [results for the pion scattering amplitudes at threshold, O.B.] *is particularly important for Wilson fermions, which we use here. This is because Wilson fermions explicitly break chiral symmetry, the violation only vanishing in the chiral limit. Thus we expect the relativistically normalized amplitude not to vanish in the chiral limit but to have a constant term proportional to the lattice spacing:* $T^R \propto a\Lambda + \mathrm{O}(M_\pi^2)$. *The nonrelativistically normalized amplitude will then behave as* $T^R \propto a\Lambda/M_\pi^2$, *where* Λ *is some nonperturbative scale. This artifact will dominate over the constant term in the chiral limit.*

The nonrelativistically normalized amplitude (at threshold) mentioned in this quote is essentially the ratio of the scattering length and the squared pion mass. The Wilson ChPT result for it is given in (6.10), and we have seen that the residue of the (correctly) expected $1/M_\pi^2$ divergence is not $\mathrm{O}(a)$ but $\mathrm{O}(a^2)$. We also understand the reason for this 'accidental' improvement: The leading $\mathrm{O}(a)$ correction leads to a renormalization of the quark mass, and this is already accounted for in the pion mass. Hence, the anticipated divergence is expected to be much milder and it is perhaps less surprising that the authors of ref. [117] have not seen it. In the conclusions of this paper we can read:

Our results are consistent with the predictions of current algebra; on the other hand, the quarks used in the calculation are not light enough to expose the expected artifacts due to the breaking of chiral symmetry by Wilson fermions. It is important to extend this work to smaller quark masses, where the divergence in T *due to chiral symmetry breaking should show up.*

We could give more examples here, but the main message should already be obvious: Conclusions drawn naively from continuum ChPT or a simple counting of powers of a are easily erroneous. It is much safer to employ the correct low-energy theory with the lattice spacing corrections properly included. This is nowadays fairly easy, since the theoretical foundations are laid and many results have already been obtained. In particular, the chiral lagrangians for the various lattice fermions are available. These will be the starting point for many more calculations and results to come.

Acknowledgements

Throughout the years I have benefited from numerous discussions, among others with S. Aoki, C. Bernard, M. Golterman, S. Sharpe and R. Sommer. Special thanks go to Noam Shoresh who got me interested in the subject during many discussions that took place in a small coffee shop on Boylston Street in Boston. This was in summer 2002.

This work was supported in part by the Deutsche Forschungsgemeinschaft (SFB/TR 09).

Bibliography

[1] O. Bär, G. Rupak, and N. Shoresh. Simulations with different lattice Dirac operators for valence and sea quarks. *Phys. Rev.*, D67:114505, 2003.

[2] Oliver Bär, Gautam Rupak, and Noam Shoresh. Chiral perturbation theory at $O(a^2)$ for lattice QCD. *Phys. Rev.*, D70:034508, 2004.

[3] Oliver Bär. Chiral perturbation theory at non-zero lattice spacing. *Nucl. Phys. Proc. Suppl.*, 140:106–119, 2005.

[4] Sinya Aoki and Oliver Bär. Twisted-mass QCD, $O(a)$ improvement and Wilson chiral perturbation theory. *Phys. Rev.*, D70:116011, 2004.

[5] Oliver Bär, Claude Bernard, Gautam Rupak, and Noam Shoresh. Chiral perturbation theory for staggered sea quarks and Ginsparg-Wilson valence quarks. *Phys. Rev.*, D72:054502, 2005. doi: 10.1103/PhysRevD.72.054502.

[6] S. Aoki, O. Bär, S. Takeda, and T. Ishikawa. Pseudo scalar meson masses in Wilson chiral perturbation theory for 2+1 flavors. *Phys. Rev.*, D73:014511, 2006.

[7] S. Aoki, O. Bär, and S. Takeda. Vector meson masses in 2+1 flavor Wilson chiral perturbation theory. *Phys. Rev.*, D73:094501, 2006. doi: 10.1103/PhysRevD.73.094501.

[8] Sinya Aoki and Oliver Bär. Automatic $O(a)$ improvement for twisted-mass QCD in the presence of spontaneous symmetry breaking. *Phys. Rev.*, D74:034511, 2006.

[9] Sinya Aoki and Oliver Bär. WChPT analysis of twisted mass lattice data. *Eur. Phys. J.*, A31:481, 2007.

[10] Sinya Aoki, Oliver Bär, and Benedikt Biedermann. Pion Scattering in Wilson Chiral Perturbation Theory. *Phys. Rev.*, D78:114501, 2008. doi: 10.1103/PhysRevD.78.114501.

[11] Oliver Bär, Silvia Necco, and Stefan Schaefer. The epsilon regime with Wilson fermions. *JHEP*, 03:006, 2009. doi: 10.1088/1126-6708/2009/03/006.

[12] Sinya Aoki, Oliver Bär, and Stephen R. Sharpe. Vector and Axial Currents in Wilson Chiral Perturbation Theory. *Phys. Rev.*, D80:014506, 2009. doi: 10.1103/PhysRevD.80.014506.

[13] O. Bär, S. Necco, and A. Shindler. The epsilon regime with twisted mass Wilson fermions. *JHEP*, 04:053, 2010.

[14] Stephen R. Sharpe and Robert L. Singleton Jr. Spontaneous flavor and parity breaking with Wilson fermions. *Phys. Rev.*, D58:074501, 1998.

[15] Weon-Jong Lee and Stephen R. Sharpe. Partial flavor symmetry restoration for chiral staggered fermions. *Phys. Rev.*, D60:114503, 1999.

[16] Stephen R. Sharpe. *Applications of chiral perturbation theory to lattice QCD.* Lectures given at the Nara workshop, Oct. 31 – Dec. 11, 2005, Nara, Japan. hep-lat/0607016, 2005.

[17] Maarten Golterman. *Applications of chiral perturbation theory to lattice QCD.* Lectures given at the 2009 Les Houches summer school, Aug. 3 – 28, 2009. arXiv:0912.4042 [hep-lat], 2009.

[18] Gerhard Ecker. *Chiral symmetry.* Lectures given at the 37. Internationale Universitätswochen für Kern- und Teilchenphysik, Schladming, Austria, Feb. 28 – March 7, 1998. hep-ph/9805500, 1998.

[19] Gerhard Ecker. *Strong interactions of light flavours.* Lectures given at the Advanced School on QCD 2000, Benasque, Spain, July 3 – 6, 2000. hep-ph/0011026., 2000.

[20] Stefan Scherer. Introduction to chiral perturbation theory. *Advances in Nuclear Physics.*, Vol. 27:277, 2002.

[21] Jan Smit. *Introduction to quantum fields on a lattice: A robust mate*, volume 15. Cambridge Lect. Notes Phys., 2002.

[22] Thomas DeGrand and Carleton E. Detar. *Lattice methods for quantum chromodynamics.* New Jersey, USA: World Scientific (2006) 345p, 2006.

[23] Christof Gattringer and Christian B. Lang. *Quantum chromodynamics on the lattice*, volume 788. Lect. Notes Phys., 2010. doi: 10.1007/978-3-642-01850-3.

[24] Steven Weinberg. Phenomenological Lagrangians. *Physica*, A96:327, 1979.

[25] J. Gasser and H. Leutwyler. Chiral perturbation theory to one loop. *Ann. Phys.*, 158:142, 1984.

[26] J. Gasser and H. Leutwyler. Chiral perturbation theory: Expansions in the mass of the strange quark. *Nucl. Phys.*, B250:465, 1985.

[27] Johan Bijnens. Status of Strong ChPT, 2009.

[28] H. W. Fearing and S. Scherer. Extension of the chiral perturbation theory meson Lagrangian to order $p(6)$. *Phys. Rev.*, D53:315–348, 1996. doi: 10.1103/PhysRevD.53.315.

[29] Christoph Haefeli, Mikhail A. Ivanov, Martin Schmid, and Gerhard Ecker. On the mesonic Lagrangian of order p^6 in chiral SU(2), 2007.

[30] Silvia Necco. Chiral low-energy constants from lattice QCD. *PoS*, CONFINEMENT8:024, 2008.

[31] K. Symanzik. Continuum limit and improved action in lattice theories. 1. Principles and ϕ^4 theory. *Nucl. Phys.*, B226:187, 1983.

[32] K. Symanzik. Continuum limit and improved action in lattice theories. 2. O(N) non-linear sigma model in perturbation theory. *Nucl. Phys.*, B226:205, 1983.

[33] Kenneth G. Wilson. Confinement of quarks. *Phys. Rev.*, D10:2445–2459, 1974.

[34] B. Sheikholeslami and R. Wohlert. Improved Continuum Limit Lattice Action for QCD with Wilson Fermions. *Nucl. Phys.*, B259:572, 1985. doi: 10.1016/0550-3213(85)90002-1.

[35] Martin Lüscher. Advanced lattice QCD, 2000.

[36] Luuk H. Karsten and Jan Smit. Lattice Fermions: Species Doubling, Chiral Invariance, and the Triangle Anomaly. *Nucl. Phys.*, B183:103, 1981.

[37] Rainer Sommer. Non-perturbative renormalization of QCD. *Lectures given at the 36th Internationale Universitätswochen für Kernphysik und Teilchenphysik, Schladming, Austria*, 1997.

[38] Marco Bochicchio, Luciano Maiani, Guido Martinelli, Gian Carlo Rossi, and Massimo Testa. Chiral Symmetry on the Lattice with Wilson Fermions. *Nucl. Phys.*, B262:331, 1985.

[39] L. Maiani and G. Martinelli. Current Algebra and Quark Masses from a Monte Carlo Simulation with Wilson Fermions. *Phys. Lett.*, B178:265, 1986.

[40] G. Martinelli, Christopher T. Sachrajda, and A. Vladikas. A study of 'improvement' in lattice QCD. *Nucl. Phys.*, B358:212–230, 1991.

[41] G. Martinelli, S. Petrarca, Christopher T. Sachrajda, and A. Vladikas. Nonperturbative renormalization of two quark operators with an improved lattice fermion action. *Phys. Lett.*, B311:241–248, 1993.

[42] D. S. Henty, R. D. Kenway, B. J. Pendleton, and J. I. Skullerud. Current renormalization constants with an O(a) improved fermion action. *Phys. Rev.*, D51:5323–5326, 1995.

[43] G. Rupak and N. Shoresh. Chiral perturbation theory for the Wilson lattice action. *Phys. Rev.*, D66:054503, 2002.

[44] Stephen R. Sharpe and Jackson M. S. Wu. Twisted mass chiral perturbation theory at next-to-leading order. *Phys. Rev.*, D71:074501, 2005.

[45] Sinya Aoki. New phase structure for lattice QCD with Wilson fermions. *Phys. Rev.*, D30:2653, 1984.

[46] Roberto Frezzotti, Pietro Antonio Grassi, Stefan Sint, and Peter Weisz. Lattice QCD with a chirally twisted mass term. *JHEP*, 08:058, 2001.

[47] Roberto Frezzotti, Stefan Sint, and Peter Weisz. O(a) improved twisted mass lattice QCD. *JHEP*, 07:048, 2001.

[48] R. Frezzotti and G. C. Rossi. Chirally improving Wilson fermions. I: O(a) improvement. *JHEP*, 08:007, 2004.

[49] R. Frezzotti and G. C. Rossi. Chirally improving Wilson fermions. II: Four-quark operators. *JHEP*, 10:070, 2004.

[50] Paul H. Ginsparg and Kenneth G. Wilson. A remnant of chiral symmetry on the lattice. *Phys. Rev.*, D25:2649, 1982.

[51] David B. Kaplan. A method for simulating chiral fermions on the lattice. *Phys. Lett.*, B288:342–347, 1992.

[52] Yigal Shamir. Chiral fermions from lattice boundaries. *Nucl. Phys.*, B406:90–106, 1993. doi: 10.1016/0550-3213(93)90162-I.

[53] Herbert Neuberger. Exactly massless quarks on the lattice. *Phys. Lett.*, B417: 141–144, 1998.

[54] Herbert Neuberger. Exactly massless quarks on the lattice. *Phys. Lett.*, B417: 141–144, 1998. doi: 10.1016/S0370-2693(97)01368-3.

[55] Martin Lüscher. Exact chiral symmetry on the lattice and the Ginsparg-Wilson relation. *Phys. Lett.*, B428:342–345, 1998.

[56] Peter Hasenfratz, Victor Laliena, and Ferenc Niedermayer. The index theorem in QCD with a finite cut-off. *Phys. Lett.*, B427:125–131, 1998.

[57] Peter Hasenfratz. Lattice QCD without tuning, mixing and current renormalization. *Nucl. Phys.*, B525:401–409, 1998.

[58] John B. Kogut and Leonard Susskind. Hamiltonian formulation of Wilson's lattice gauge theories. *Phys. Rev.*, D11:395, 1975. doi: 10.1103/PhysRevD.11.395.

[59] Leonard Susskind. Lattice Fermions. *Phys. Rev.*, D16:3031–3039, 1977. doi: 10.1103/PhysRevD.16.3031.

[60] Martin Hasenbusch. Speeding up the Hybrid-Monte-Carlo algorithm for dynamical fermions. *Phys. Lett.*, B519:177–182, 2001. doi: 10.1016/S0370-2693(01)01102-9.

[61] M. Hasenbusch and K. Jansen. Speeding up lattice QCD simulations with clover-improved Wilson fermions. *Nucl. Phys.*, B659:299–320, 2003. doi: 10.1016/S0550-3213(03)00227-X.

[62] Martin Lüscher. Lattice QCD and the Schwarz alternating procedure. *JHEP*, 05: 052, 2003.

[63] Martin Lüscher. Solution of the Dirac equation in lattice QCD using a domain decomposition method. *Comput. Phys. Commun.*, 156:209–220, 2004. doi: 10.1016/S0010-4655(03)00486-7.

[64] Martin Lüscher. Schwarz-preconditioned HMC algorithm for two-flavour lattice QCD. *Comput. Phys. Commun.*, 165:199–220, 2005. doi: 10.1016/j.cpc.2004.10.004.

[65] C. Urbach, K. Jansen, A. Shindler, and U. Wenger. HMC algorithm with multiple time scale integration and mass preconditioning. *Comput. Phys. Commun.*, 174: 87–98, 2006.

[66] Maarten F. L. Golterman and Jan Smit. Selfenergy and flavor interpretation of staggered fermions. *Nucl. Phys.*, B245:61, 1984.

[67] F. Gliozzi. Spinor algebra of the one component lattice fermions. *Nucl. Phys.*, B204:419–428, 1982.

[68] H. Kluberg-Stern, A. Morel, O. Napoly, and B. Petersson. Flavors of lagrangian Susskind fermions. *Nucl. Phys.*, B220:447, 1983.

[69] D. Verstegen. Axial anomaly for lattice fermions. *Nucl. Phys.*, B243:65, 1984.

[70] T. Jolicoeur, A. Morel, and B. Petersson. Continuum symmetries of lattice models with staggered fermions. *Nucl. Phys.*, B274:225, 1986.

[71] Yu-Bing Luo. Improvement of the staggered fermion operators. *Phys. Rev.*, D55: 353–361, 1997.

[72] Yu-Bing Luo. On-shell improved lattice QCD with staggered fermions. *Phys. Rev.*, D57:265–275, 1998.

[73] Stephen R. Sharpe. B_K using staggered fermions: An update. *Nucl. Phys. Proc. Suppl.*, 34:403–406, 1994.

[74] C. Aubin and C. Bernard. Pion and kaon masses in staggered chiral perturbation theory. *Phys. Rev.*, D68:034014, 2003.

[75] Stephen R. Sharpe and Noam Shoresh. Partially quenched chiral perturbation theory without Φ_0. *Phys. Rev.*, D64:114510, 2001. doi: 10.1103/PhysRevD.64.114510.

[76] C. Bernard. Chiral logs in the presence of staggered flavor symmetry breaking. *Phys. Rev.*, D65:054031, 2002.

[77] G. Peter Lepage. Flavor-symmetry restoration and Symanzik improvement for staggered quarks. *Phys. Rev.*, D59:074502, 1999. doi: 10.1103/PhysRevD.59.074502.

[78] Eduardo Follana et al. Further improvements to staggered quarks. *Nucl. Phys. Proc. Suppl.*, 129:447–449, 2004. doi: 10.1016/S0920-5632(03)02610-0.

[79] E. Follana et al. Improvement and taste symmetry breaking for staggered quarks. *Nucl. Phys. Proc. Suppl.*, 129&130:384–386, 2004.

[80] E. Follana et al. Highly Improved Staggered Quarks on the Lattice, with Applications to Charm Physics. *Phys. Rev.*, D75:054502, 2007. doi: 10.1103/PhysRevD.75.054502.

[81] C. Bernard et al. Scaling studies of QCD with the dynamical HISQ action, 2010.

[82] C. Aubin and Qinghai Wang. A possible Aoki phase for staggered fermions. *Phys. Rev.*, D70:114504, 2004.

[83] C. Aubin et al. Light pseudoscalar decay constants, quark masses, and low energy constants from three-flavor lattice QCD. *Phys. Rev.*, D70:114501, 2004.

[84] C. Aubin et al. Light hadrons with improved staggered quarks: Approaching the continuum limit. *Phys. Rev.*, D70:094505, 2004.

[85] A. Bazavov et al. Full nonperturbative QCD simulations with 2+1 flavors of improved staggered quarks, 2009.

[86] A. Bazavov et al. Progress on four flavor QCD with the HISQ action. *PoS*, LAT2009:123, 2009.

[87] Stephen R. Sharpe and Ruth S. Van de Water. Staggered chiral perturbation theory at next-to-leading order, 2004.

[88] C. Aubin and C. Bernard. Pseudoscalar decay constants in staggered chiral perturbation theory. *Phys. Rev.*, D68:074011, 2003.

[89] Claude W. Bernard and Maarten F. L. Golterman. Partially quenched gauge theories and an application to staggered fermions. *Phys. Rev.*, D49:486–494, 1994. doi: 10.1103/PhysRevD.49.486.

[90] Stephen R. Sharpe. Enhanced chiral logarithms in partially quenched QCD. *Phys. Rev.*, D56:7052–7058, 1997. doi: 10.1103/PhysRevD.56.7052.

[91] A. Morel. Chiral logarithms in quenched QCD. *J. Phys. (France)*, 48:1111–1119, 1987.

[92] Stephen R. Sharpe and Noam Shoresh. Physical results from unphysical simulations. *Phys. Rev.*, D62:094503, 2000.

[93] Maarten Golterman, Stephen R. Sharpe, and Robert L. Singleton Jr. Effective theory for quenched lattice QCD and the Aoki phase. *Phys. Rev.*, D71:094503, 2005.

[94] Claude W. Bernard and Maarten F. L. Golterman. Finite volume two pion energies and scattering in the quenched approximation. *Phys. Rev.*, D53:476–484, 1996. doi: 10.1103/PhysRevD.53.476.

[95] Silas R. Beane and Martin J. Savage. Nucleon nucleon interactions on the lattice. *Phys. Lett.*, B535:177–180, 2002. doi: 10.1016/S0370-2693(02)01762-8.

[96] William A. Bardeen, A. Duncan, E. Eichten, Nathan Isgur, and H. Thacker. Chiral loops and ghost states in the quenched scalar propagator. *Phys. Rev.*, D65:014509, 2002.

[97] William A. Bardeen, E. Eichten, and H. Thacker. Chiral Lagrangian parameters for scalar and pseudoscalar mesons. *Phys. Rev.*, D69:054502, 2004. doi: 10.1103/PhysRevD.69.054502.

[98] Sasa Prelovsek, C. Dawson, T. Izubuchi, K. Orginos, and A. Soni. Scalar meson in dynamical and partially quenched two-flavor QCD: Lattice results and chiral loops. *Phys. Rev.*, D70:094503, 2004. doi: 10.1103/PhysRevD.70.094503.

[99] Michael Creutz. The saga of rooted staggered quarks, 2008.

[100] Stephen R. Sharpe. Rooted staggered fermions: Good, bad or ugly? *PoS*, LAT2006:022, 2006.

[101] Andreas S. Kronfeld. Lattice gauge theory with staggered fermions: how, where, and why (not)? *PoS*, LAT2007:016, 2007.

[102] Michael Creutz. Why rooting fails. *PoS*, LAT2007:007, 2007.

[103] Maarten Golterman. QCD with rooted staggered fermions. *PoS*, CONFINEMENT8:014, 2008.

[104] Maarten Golterman, Taku Izubuchi, and Yigal Shamir. The role of the double pole in lattice QCD with mixed actions. *Phys. Rev.*, D71:114508, 2005. doi: 10.1103/PhysRevD.71.114508.

[105] K. C. Bowler, B. Joo, R. D. Kenway, C. M. Maynard, and R. J. Tweedie. Lattice QCD with mixed actions. *JHEP*, 08:003, 2005.

[106] Jiunn-Wei Chen, Maarten Golterman, Donal O'Connell, and Andre Walker-Loud. Mixed Action Effective Field Theory: an Addendum. *Phys. Rev.*, D79:117502, 2009. doi: 10.1103/PhysRevD.79.117502.

[107] R. G. Edwards et al. The nucleon axial charge in full lattice QCD. *Phys. Rev. Lett.*, 96:052001, 2006. doi: 10.1103/PhysRevLett.96.052001.

[108] Ph. Hägler et al. Nucleon Generalized Parton Distributions from Full Lattice QCD. *Phys. Rev.*, D77:094502, 2008. doi: 10.1103/PhysRevD.77.094502.

[109] A. Walker-Loud et al. Light hadron spectroscopy using domain wall valence quarks on an Asqtad sea. *Phys. Rev.*, D79:054502, 2009. doi: 10.1103/PhysRevD.79.054502.

[110] Sinya Aoki. Chiral perturbation theory with Wilson-type fermions including a^2 effects: $N_f = 2$ degenerate case. *Phys. Rev.*, D68:054508, 2003.

[111] Benedikt Biedermann. Pion scattering in WChPT. Master's thesis, Humboldt University Berlin, 2008. http://edoc.hu-berlin.de.

[112] Carsten Urbach. Lattice QCD with two light Wilson quarks and maximally twisted mass. *PoS*, LATTICE2007:022, 2007.

[113] C. Bernard. Order of the chiral and continuum limits in staggered chiral perturbation theory, 2004.

[114] Steven Weinberg. Pion scattering lengths. *Phys. Rev. Lett.*, 17:616–621, 1966. doi: 10.1103/PhysRevLett.17.616.

[115] N. Kawamoto and J. Smit. Effective Lagrangian and Dynamical Symmetry Breaking in Strongly Coupled Lattice QCD. *Nucl. Phys.*, B192:100, 1981. doi: 10.1016/0550-3213(81)90196-6.

[116] Stephen R. Sharpe, Rajan Gupta, and Gregory W. Kilcup. Lattice calculation of $I = 2$ pion scattering length. *Nucl. Phys.*, B383:309–356, 1992. doi: 10.1016/0550-3213(92)90681-Z.

[117] Rajan Gupta, Apoorva Patel, and Stephen R. Sharpe. $I = 2$ pion scattering amplitude with Wilson fermions. *Phys. Rev.*, D48:388–396, 1993. doi: 10.1103/PhysRevD.48.388.

[118] Martin Lüscher, Stefan Sint, Rainer Sommer, and Peter Weisz. Chiral symmetry and O(a) improvement in lattice QCD. *Nucl. Phys.*, B478:365–400, 1996.

[119] G. Martinelli, C. Pittori, Christopher T. Sachrajda, M. Testa, and A. Vladikas. A General method for nonperturbative renormalization of lattice operators. *Nucl. Phys.*, B445:81–108, 1995. doi: 10.1016/0550-3213(95)00126-D.

[120] Gernot Münster and Christian Schmidt. Chiral perturbation theory for lattice QCD with a twisted mass term. *Europhys. Lett.*, 66:652–656, 2004.

[121] S. Hashimoto et al. Chiral extrapolation of light-light and heavy-light decay constants in unquenched QCD. *Nucl. Phys. Proc. Suppl.*, 119:332–334, 2003.

[122] Gernot Münster. On the phase structure of twisted mass lattice QCD. *JHEP*, 09:035, 2004.

[123] Stephen R. Sharpe and Jackson M. S. Wu. The phase diagram of twisted mass lattice QCD. *Phys. Rev.*, D70:094029, 2004.

[124] Luigi Scorzato. Pion mass splitting and phase structure in twisted mass QCD. *Eur. Phys. J.*, C37:445–455, 2004.

[125] Michael I. Buchoff, Jiunn-Wei Chen, and Andre Walker-Loud. $\pi\pi$ Scattering in Twisted Mass Chiral Perturbation Theory. *Phys. Rev.*, D79:074503, 2009. doi: 10.1103/PhysRevD.79.074503.

[126] W. Bietenholz et al. Going chiral: Overlap versus twisted mass fermions. *JHEP*, 12:044, 2004.

[127] Abdou M. Abdel-Rehim, Randy Lewis, and R. M. Woloshyn. Spectrum of quenched twisted mass lattice QCD at maximal twist. *Phys. Rev.*, D71:094505, 2005.

[128] K. Jansen, M. Papinutto, A. Shindler, C. Urbach, and I. Wetzorke. Light quarks with twisted mass fermions. *Phys. Lett.*, B619:184–191, 2005.

[129] K. Jansen, M. Papinutto, A. Shindler, C. Urbach, and I. Wetzorke. Quenched scaling of Wilson twisted mass fermions. *JHEP*, 09:071, 2005.

[130] Stephen R. Sharpe. Observations on discretization errors in twisted-mass lattice QCD. *Phys. Rev.*, D72:074510, 2005.

[131] Karl Jansen, Andrea Shindler, Carsten Urbach, and Ines Wetzorke. Scaling test for Wilson twisted mass QCD. *Phys. Lett.*, B586:432–438, 2004.

[132] K. Jansen et al. Flavour breaking effects of Wilson twisted mass fermions. *Phys. Lett.*, B624:334–341, 2005.

[133] J. Gasser and H. Leutwyler. Light Quarks at Low Temperatures. *Phys. Lett.*, B184:83, 1987. doi: 10.1016/0370-2693(87)90492-8.

[134] J. Gasser and H. Leutwyler. Thermodynamics of Chiral Symmetry. *Phys. Lett.*, B188:477, 1987. doi: 10.1016/0370-2693(87)91652-2.

[135] J. Gasser and H. Leutwyler. Spontaneously Broken Symmetries: Effective Lagrangians at Finite Volume. *Nucl. Phys.*, B307:763, 1988. doi: 10.1016/0550-3213(88)90107-1.

[136] Pilar Hernandez, Karl Jansen, and Laurent Lellouch. Finite-size scaling of the quark condensate in quenched lattice QCD. *Phys. Lett.*, B469:198–204, 1999. doi: 10.1016/S0370-2693(99)01244-7.

[137] Thomas A. DeGrand. Another determination of the quark condensate from an overlap action. *Phys. Rev.*, D64:117501, 2001. doi: 10.1103/PhysRevD.64.117501.

[138] P. Hasenfratz, S. Hauswirth, T. Jorg, F. Niedermayer, and K. Holland. Testing the fixed-point QCD action and the construction of chiral currents. *Nucl. Phys.*, B643:280–320, 2002.

[139] Wolfgang Bietenholz, T. Chiarappa, K. Jansen, K. I. Nagai, and S. Shcheredin. Axial correlation functions in the epsilon-regime: A numerical study with overlap fermions. *JHEP*, 02:023, 2004.

[140] L. Giusti, P. Hernandez, M. Laine, P. Weisz, and H. Wittig. Low-energy couplings of QCD from current correlators near the chiral limit. *JHEP*, 04:013, 2004.

[141] Hidenori Fukaya, Shoji Hashimoto, and Kenji Ogawa. Low-lying mode contribution to the quenched meson correlators in the epsilon-regime. *Prog. Theor. Phys.*, 114:451–476, 2005. doi: 10.1143/PTP.114.451.

[142] Wolfgang Bietenholz and S. Shcheredin. Overlap hypercube fermions in QCD simulations near the chiral limit. *Nucl. Phys.*, B754:17–47, 2006. doi: 10.1016/j.nuclphysb.2006.07.018.

[143] Leonardo Giusti and Silvia Necco. Spontaneous chiral symmetry breaking in QCD: A finite-size scaling study on the lattice. *JHEP*, 04:090, 2007.

[144] L. Giusti et al. Testing chiral effective theory with quenched lattice QCD. *JHEP*, 05:024, 2008. doi: 10.1088/1126-6708/2008/05/024.

[145] H. Fukaya et al. Lattice study of meson correlators in the epsilon-regime of two-flavor QCD. *Phys. Rev.*, D77:074503, 2008. doi: 10.1103/PhysRevD.77.074503.

[146] Anna Hasenfratz, Roland Hoffmann, and Stefan Schaefer. Low energy chiral constants from epsilon-regime simulations with improved Wilson fermions. *Phys. Rev.*, D78:054511, 2008. doi: 10.1103/PhysRevD.78.054511.

[147] Anna Hasenfratz, Roland Hoffmann, and Stefan Schaefer. Reweighting towards the chiral limit. *Phys. Rev.*, D78:014515, 2008. doi: 10.1103/PhysRevD.78.014515.

[148] K. Jansen, A. Nube, A. Shindler, C. Urbach, and U. Wenger. Exploring the epsilon regime with twisted mass fermions. *PoS*, LAT2007:084, 2007.

[149] K. Jansen, A. Nube, and A. Shindler. Wilson twisted mass fermions in the epsilon regime. *PoS*, LAT2008:083, 2008.

[150] P. Hasenfratz and H. Leutwyler. Goldstone boson related finite size effects in field theory and critical phenomena with O(N) symmetry. *Nucl. Phys.*, B343:241–284, 1990. doi: 10.1016/0550-3213(90)90603-B.

[151] F. C. Hansen. Finite size effects in spontaneously broken SU(N)×SU(N) theories. *Nucl. Phys.*, B345:685–708, 1990. doi: 10.1016/0550-3213(90)90405-3.

[152] F. C. Hansen and H. Leutwyler. Charge correlations and topological susceptibility in QCD. *Nucl. Phys.*, B350:201–227, 1991. doi: 10.1016/0550-3213(91)90259-Z.

[153] I.S. Gradshteyn and I.M. Ryzhik. *Table of Integrals, Series and Products*. Academic Press, Inc., Orlando, Florida 32887, fourth edition, 1983.

[154] P. H. Damgaard, M. C. Diamantini, P. Hernandez, and K. Jansen. Finite-size scaling of meson propagators. *Nucl. Phys.*, B629:445–478, 2002. doi: 10.1016/S0550-3213(02)00145-1.

[155] P. H. Damgaard, P. Hernandez, K. Jansen, M. Laine, and L. Lellouch. Finite-size scaling of vector and axial current correlators. *Nucl. Phys.*, B656:226–238, 2003. doi: 10.1016/S0550-3213(03)00117-2.

[156] Anna Hasenfratz, Roland Hoffmann, and Stefan Schaefer. Hypercubic smeared links for dynamical fermions. *JHEP*, 05:029, 2007.

[157] K. Jansen and A. Shindler. The epsilon regime of chiral perturbation theory with Wilson-type fermions, 2009.

[158] A. Shindler. 'private communication', 2009.

[159] Jiunn-Wei Chen, Donal O'Connell, and Andre Walker-Loud. Universality of Mixed Action Extrapolation Formulae. *JHEP*, 04:090, 2009. doi: 10.1088/1126-6708/2009/04/090.

[160] Jiunn-Wei Chen, Donal O'Connell, Ruth S. Van de Water, and Andre Walker-Loud. Ginsparg-Wilson pions scattering on a staggered sea. *Phys. Rev.*, D73:074510, 2006. doi: 10.1103/PhysRevD.73.074510.

[161] Jiunn-Wei Chen, Donal O'Connell, and Andre Walker-Loud. Two meson systems with Ginsparg-Wilson valence quarks. *Phys. Rev.*, D75:054501, 2007. doi: 10.1103/PhysRevD.75.054501.

[162] Silas R. Beane et al. Precise Determination of the $I = 2$ $\pi\pi$ Scattering Length from Mixed-Action Lattice QCD. *Phys. Rev.*, D77:014505, 2008. doi: 10.1103/PhysRevD.77.014505.

[163] Silas R. Beane et al. The K^+K^+ Scattering Length from Lattice QCD. *Phys. Rev.*, D77:094507, 2008. doi: 10.1103/PhysRevD.77.094507.

[164] Sasa Prelovsek. Effects of staggered fermions and mixed actions on the scalar correlator. *Phys. Rev.*, D73:014506, 2006. doi: 10.1103/PhysRevD.73.014506.

[165] C. Aubin, Jack Laiho, and Ruth S. Van de Water. The kaon B-parameter in mixed action chiral perturbation theory. *Phys. Rev.*, D75:034502, 2007. doi: 10.1103/PhysRevD.75.034502.

[166] Andreas Furchner. Unitarity violation in mixed-action lattice QCD. Master's thesis, Humboldt University Berlin, 2010. http://edoc.hu-berlin.de.

[167] Elizabeth Jenkins and Aneesh V. Manohar. Baryon chiral perturbation theory using a heavy fermion Lagrangian. *Phys. Lett.*, B255:558–562, 1991.

[168] Elizabeth Jenkins, Aneesh V. Manohar, and Mark B. Wise. Chiral perturbation theory for vector mesons. *Phys. Rev. Lett.*, 75:2272–2275, 1995.

[169] Hovhannes R. Grigoryan and Anthony W. Thomas. Vector meson mass corrections at $O(a^2)$ in PQChPT with Wilson and Ginsparg-Wilson quarks, 2005.

[170] J. Bijnens, P. Gosdzinsky, and P. Talavera. Vector meson masses in chiral perturbation theory. *Nucl. Phys.*, B501:495–517, 1997.

[171] J. Bijnens, P. Gosdzinsky, and P. Talavera. Chiral corrections to vector meson decay constants. *Phys. Lett.*, B429:111–120, 1998.

[172] Howard Georgi. An effective field theory for heavy quarks at low-energies. *Phys. Lett.*, B240:447–450, 1990. doi: 10.1016/0370-2693(90)91128-X.

[173] Silas R. Beane and Martin J. Savage. Nucleons properties at finite lattice spacing in chiral perturbation theory. *Phys. Rev.*, D68:114502, 2003.

[174] Daniel Arndt and Brian C. Tiburzi. Hadronic electromagnetic properties at finite lattice spacing. *Phys. Rev.*, D69:114503, 2004.

[175] Claude Bernard et al. Panel discussion on chiral extrapolation of physical observables. *Nucl. Phys. Proc. Suppl.*, 119:170–184, 2003. doi: 10.1016/S0920-5632(03)01505-6.

Part III.

Reprints of published papers

PHYSICAL REVIEW D **67**, 114505 (2003)

Simulations with different lattice Dirac operators for valence and sea quarks

Oliver Bär*
Center for Theoretical Physics, Massachusetts Institute of Technology, Cambridge, Massachusetts 02139, USA

Gautam Rupak†
Lawrence Berkeley National Laboratory, Berkeley, California 94720, USA

Noam Shoresh‡
Department of Physics, Boston University, Boston, Massachusetts 02215, USA
(Received 12 November 2002; published 19 June 2003)

We discuss simulations with different lattice Dirac operators for sea and valence quarks. A goal of such a ''mixed'' action approach is to probe deeper the chiral regime of QCD by enabling simulations with light valence quarks. This is achieved by using chiral fermions as valence quarks while computationally inexpensive fermions are used in the sea sector. Specifically, we consider Wilson sea quarks and Ginsparg-Wilson valence quarks. The local Symanzik action for this mixed theory is derived to $\mathcal{O}(a)$, and the appropriate low energy chiral effective Lagrangian is constructed, including the leading $\mathcal{O}(a)$ contributions. Using this Lagrangian one can calculate expressions for physical observables and determine the Gasser-Leutwyler coefficients by fitting them to the lattice data.

DOI: 10.1103/PhysRevD.67.114505 PACS number(s): 11.15.Ha, 12.38.Gc, 12.39.Fe

I. INTRODUCTION

In order to extract predictions of QCD from numerical methods with controlled systematic errors, a lattice formulation is required for which the sources of deviations from QCD are understood and are under control. A significant source of systematic errors for present day lattice simulations are the light quark masses. Even the most powerful computers today do not allow simulations with up- and down-quark masses as light as realized in nature. Instead one simulates with heavier quark masses and fits the analytic predictions obtained in chiral perturbation theory (χPT) to the data. The free parameters in the fit are the low energy constants of χPT [1], and once they are determined an extrapolation to small quark masses is possible [2,3]. Still, to perform the chiral extrapolation the quark masses must be small enough so that χPT is applicable. In practice one would require that next-to-leading order (NLO) χPT describe the data reasonably well.[1]

The present lattice simulations do not meet this requirement [4–6]. The data do not show the characteristic curvature predicted by NLO χPT. In fact the data show a rather linear behavior which either means that higher orders in the chiral expansion are not negligible or worse, one is not in the chiral regime at all (see Bernard's part in [4]). In either case, simulations with lighter quark masses are required in order to apply χPT with confidence.

Lattice simulations with light fermions, especially sea quarks, are computationally demanding and the numerical cost increases substantially with decreasing quark masses. Realistically only the least expensive fermions, Wilson and Kogut-Susskind, can be used on sufficiently large and fine lattices. Lattice fermions with better chiral properties are still too expensive to be used as sea quarks, and this situation is not likely to change in the near future. It is nevertheless expected that the next generation of TFLOP machines will make it possible to generate a few sets of unquenched configurations with sea quarks light enough to be in the chiral regime.

To obtain more information from these configurations they should (and will) be analyzed with various different valence quark masses, i.e. by studying partially quenched (PQ) QCD. By including lattice measurements with lighter valence quarks it is possible to penetrate further the chiral regime of QCD. This leads to more data points and would allow more reliable fits of PQ χPT [7] to the lattice data [2]. The reach of such simulations, however, is limited. The cost of light valence quarks also increases with the decreasing mass, and can become prohibitively high for quark masses that are still not very small. This is particularly true for Wilson fermions because of the explicit chiral symmetry breaking by the Wilson term.

An interesting idea for probing the chiral regime is to use different lattice fermions for the valence and sea quarks. In particular, by choosing lattice fermions with good chiral properties for the valence quarks, the valence quark mass can be made much smaller than in ordinary PQ simulations. A central goal of this strategy is the same as of PQ QCD—to explore a larger portion of the chiral regime by extracting more data points from a given set of unquenched configurations (see Fig. 1). This should result in more reliable estimates for the low-energy constants of χPT at NLO, the Gasser-Leutwyler coefficients. Furthermore, one might expect to reduce the size of explicit chiral symmetry breaking

*Email address: obaer@lns.mit.edu
†Email address: grupak@lbl.gov
‡Email address: shoresh@bu.edu

[1]At next-to-next-to-leading order (NNLO) many new unknown parameters enter the chiral Lagrangian, which greatly reduces the predictive power of χPT.

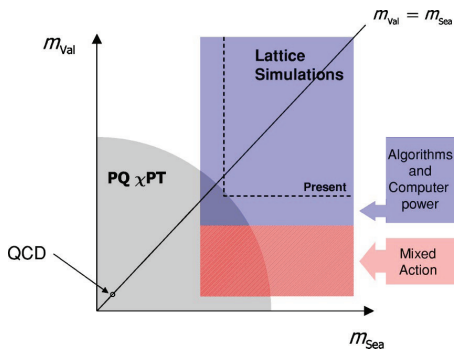

FIG. 1. Qualitative representation of the space of quark masses. The "chiral regime," where PQ χPT can be applied, is the quarter-circular region. The upper right rectangle, limited by the dashed line, describes the part of the space covered by present simulations. As current data suggest, there is very little or no overlap between that rectangle and the chiral regime. It is expected that improvement in algorithms and computer power will allow reducing the sea and valence quark masses in PQ simulations, as is represented by the enlargement of the previous rectangle. It is possible that the chiral region will be penetrated by such simulations, as shown by the small section of overlap between the enlarged rectangle and the chiral region. Finally, using chiral valence fermions in a mixed action simulation would make it possible to extend the reach of simulations significantly in the direction of lighter valence quarks.

by using Ginsparg-Wilson fermions at least for the valence quarks. This is a computationally affordable compromise of the lattice theorist's ideal of using Ginsparg-Wilson fermions for both valence and sea quarks.

In this paper we construct the low-energy chiral effective theory for a "mixed" lattice action, with explicit dependence on powers of the lattice spacing a by first constructing the appropriate local Symanzik action. There are several reasons for taking this approach. First, the defining non-orthodox feature of the mixed action approach—the use of different Dirac operators for the sea and valence sectors—is purely a lattice artifact. This is a consequence of the fact that by construction all proper lattice fermions reproduce the same continuum physics, and therefore all mixed lattice theories reduce to PQ QCD in the continuum limit. An expansion in a is thus a natural tool to investigate potential peculiarities of the mixed action formulation. Second, a theoretical understanding of the a dependence in lattice simulations can guide the continuum limit, or allow the extraction of physical information directly from the lattice data, without taking the continuum limit first. Third, χPT provides a useful framework for studying the chiral symmetry breaking due to the discrete space-time lattice. Effective theories of this type have been studied in several similar contexts [8–11].

What is dubbed here "mixed action methods" refers to a class of lattice theories corresponding to different choices of Dirac operators for the valence and sea quarks. In the next section we use a fairly simple example to illustrate the general framework of mixed lattice theories. We consider Wilson fermions for the sea quarks, together with valence fermions that satisfy the Ginsparg-Wilson relation. To describe the lattice action close to the continuum limit we construct the local Symanzik effective action up to $\mathcal{O}(a)$. The usual arguments used in the formulation of χPT are then applied to this effective action. This leads to a chiral expansion in which the dependence on the lattice spacing is explicit.

II. THE CHIRAL EFFECTIVE ACTION

A. Lattice action

In the following we always consider a hyper-cubic Euclidean space-time lattice with lattice spacing a. We assume either an infinite lattice or a finite lattice large enough that one can safely ignore finite volume effects.

The mixed lattice action that describes N_f Wilson sea and N_V Ginsparg-Wilson valence fermions has the structure

$$S_M = S_{\rm YM}[U] + S_W[\bar{\psi}_S, \psi_S, U] + S_{\rm GW}[\bar{\psi}_V, \psi_V, U]. \quad (1)$$

U denotes the gauge field defined on the links of the lattice, ψ_S ($\bar{\psi}_S$) are the sea quark (anti-quark) fields and ψ_V ($\bar{\psi}_V$) denote vectors with N_V anti-commuting valence quarks (anti-quarks) and N_V c-number-valued ghost quarks (anti-quarks).

The precise choice for the gauge field action $S_{\rm YM}$ is irrelevant in the following, so we leave it unspecified. For the sea quarks we choose the Wilson action [12], given by

$$S_W = a^4 \sum_x \bar{\psi}_S (D_W + m_{\rm Sea}) \psi_S(x), \quad (2)$$

$$D_W = \frac{1}{2}\{\gamma_\mu(\nabla^*_\mu + \nabla_\mu) - a r \nabla^*_\mu \nabla_\mu)\}, \quad (3)$$

where $m_{\rm Sea}$ denotes the $N_f \times N_f$ quark mass matrix in the sea sector and r the Wilson parameter. ∇^*_μ, ∇_μ are the usual covariant, nearest neighbor backward and forward difference operators.

The action for the valence and ghost quarks is given by

$$S_{GW} = a^4 \sum_x \bar{\psi}_V \left\{ D_{GW} + m_{\rm Val}\left(1 - \frac{1}{2} a D_{GW}\right)\right\} \psi_V(x). \quad (4)$$

The valence and ghost quark masses are contained in the $2N_V \times 2N_V$ mass matrix $m_{\rm Val}$ of the form $m_{\rm Val} = {\rm diag}(M_{\rm Val}, M_{\rm Val})$ where $M_{\rm Val}$ is an $N_V \times N_V$ matrix (i.e. each valence quark has a corresponding ghost field with the same mass). The Dirac operator D_{GW} is assumed to be a local operator satisfying the Ginsparg-Wilson relation [13]

$$\gamma_5 D_{GW} + D_{GW}\gamma_5 = a D_{GW}\gamma_5 D_{GW}. \quad (5)$$

Both the fixed-point Dirac operator and the overlap operator satisfy this relation [14–16]. For the following discussion, however, there is no need to specify D_{GW} any further.

B. Flavor symmetry of the lattice action

When $m_{\rm Sea} = 0$, $m_{\rm Val} = 0$, and $r = 0$, the flavor symmetry group of S_M is

$$SU(N_f)_L \otimes SU(N_f)_R \otimes SU(N_V|N_V)_L \otimes SU(N_V|N_V)_R . \tag{6}$$

To see this it is convenient to write S_{GW} and S_W in terms of chiral components. The right- and left-handed sea quark fields are defined with the usual projectors $\frac{1}{2}(1 \pm \gamma_5)$. For the valence and ghost fields, one first defines the Hermitian operator

$$\hat{\gamma}_5 = \gamma_5(1 - aD_{GW}), \tag{7}$$

which is unitary as a consequence of Eq. (5). Valence right- and left-handed fields are now defined by [17]

$$\bar{\psi}_{V,R} = \bar{\psi}_V \frac{1}{2}(1-\gamma_5), \quad \psi_{V,R} = \frac{1}{2}(1+\hat{\gamma}_5)\psi_V , \tag{8}$$

$$\bar{\psi}_{V,L} = \bar{\psi}_V \frac{1}{2}(1+\gamma_5), \quad \psi_{V,L} = \frac{1}{2}(1-\hat{\gamma}_5)\psi_V . \tag{9}$$

The fermionic actions can now be rewritten as

$$\begin{aligned} S_W = a^4 \sum_x \; & \bar{\psi}_{S,L} \frac{1}{2} \gamma_\mu (\nabla_\mu + \nabla^*_\mu) \psi_{S,L}(x) + \bar{\psi}_{S,R} \frac{1}{2} \gamma_\mu (\nabla_\mu \\ & + \nabla^*_\mu) \psi_{S,R}(x) + \bar{\psi}_{S,L} \left(m_{\mathrm{Sea}} - \frac{1}{2} a r \nabla_\mu \nabla^*_\mu \right) \psi_{S,R}(x) \\ & + \bar{\psi}_{S,R} \left(m^\dagger_{\mathrm{Sea}} - \frac{1}{2} a r^\dagger \nabla_\mu \nabla^*_\mu \right) \psi_{S,L}(x), \end{aligned} \tag{10}$$

and

$$\begin{aligned} S_{GW} = a^4 \sum_x \; & \bar{\psi}_{V,L} D_{GW} \psi_{V,L}(x) + \bar{\psi}_{V,R} D_{GW} \psi_{V,R}(x) \\ & + \bar{\psi}_{V,L} m_{\mathrm{Val}} \psi_{V,R}(x) + \bar{\psi}_{V,R} m^\dagger_{\mathrm{Val}} \psi_{V,L}(x). \end{aligned} \tag{11}$$

Here, for reasons that will become clearer shortly, we consider m_{Sea}, m_{Val} and r to be matrices in flavor space, and identify the parameters that appear between right-handed anti-quarks and left-handed quarks as their Hermitian conjugates.

Clearly, when $m_{\mathrm{Sea}} = m_{\mathrm{Val}} = r = 0$, Eqs. (10) and (11) are invariant under independent global rotations of the left-handed and right-handed components of all quark fields:

$$\psi_{X,\chi} \to g_{X,\chi} \psi_{X,\chi}, \quad \bar{\psi}_{X,\chi} \to \bar{\psi}_{X,\chi} g^\dagger_{X,\chi}, \quad X = S,V, \quad \chi = L,R, \tag{12}$$

where $g_{S,L}$ and $g_{S,R}$ are in $SU(N_f)$, while $g_{V,L}$ and $g_{V,R}$ are in $SU(N_V|N_V)$. We conclude that flavor transformations belonging to the group in Eq. (6) are symmetries of the action Eq. (1) broken by the mass terms m_{Val} and m_{Sea} and the Wilson term r.

It is convenient to treat these symmetry breaking parameters as spurion fields, i.e. assuming the transformation rules

$$\begin{aligned} & m_{\mathrm{Val}} \to g_{V,L} m_{\mathrm{Val}} g^\dagger_{V,R}, \quad m^\dagger_{\mathrm{Val}} \to g_{V,R} m^\dagger_{\mathrm{Val}} g^\dagger_{V,L}, \\ & m_{\mathrm{Sea}} \to g_{S,L} m_{\mathrm{Sea}} g^\dagger_{S,R}, \quad m^\dagger_{\mathrm{Sea}} \to g_{S,R} m^\dagger_{\mathrm{Sea}} g^\dagger_{S,L}, \\ & r \to g_{S,L} r g^\dagger_{S,R}, \quad r^\dagger \to g_{S,R} r^\dagger g^\dagger_{S,L}. \end{aligned} \tag{13}$$

The mixed action S_M, even with non-vanishing mass and Wilson terms, is invariant under the combined transformations Eqs. (12),(13).

To complete this part we note that for a transformation to be a symmetry of the theory it must also leave unchanged the integration measure in the functional integral. It is a simple matter to show that the measure for the sea Wilson fermions is invariant under the global rotations in Eq. (12). The situation for the valence quarks is not quite so simple because of the operator $\hat{\gamma}_5$ in the chiral variation. It turns out, however, as has been shown in Ref. [18], that the measure is indeed invariant under the symmetry transformations considered here—the flavor non-singlet transformations. The last statement can be extended to the full valence sector, including the ghost fields.[2]

C. Symanzik action

We construct Symanzik's local effective theory which, close to the continuum, describes the same long-range physics as the discrete lattice action well below the momentum cutoff $1/a$ [21–24].

Since the continuum action S_S is designed to reproduce the same long-range correlation functions as the discrete lattice action S_M, it must have the same symmetries [Eq. (6)] as the underlying theory. Up to $\mathcal{O}(a)$, the quark operators that enter are of mass dimensions 3, 4, and 5, which include only quark bilinears. Moreover, the independent symmetry transformations acting separately on the sea and valence sectors requires that the quark bilinears do not mix the sectors. This implies that up to $\mathcal{O}(a)$, the fermionic operators in S_S (as in S_M) are of two types—one built of sea quarks only and one of valence quarks.

It is straightforward to write down the $\mathcal{O}(a)$ Symanzik action S_S using previous results concerning Wilson fermions [25,26] and Ginsparg-Wilson fermions [17]. The details of the analysis are deferred to Appendix A—here we only quote the result (for the fermionic part of the action):

$$\begin{aligned} S_S = \int d^4x [& \bar{\psi}_V (D + \tilde{m}_{\mathrm{Val}}) \psi_V + \bar{\psi}_S (D + \tilde{m}_{\mathrm{Sea}}) \psi_S \\ & + a c_{SW} \bar{\psi}_S \sigma_{\mu\nu} F_{\mu\nu} \psi_S] + \mathcal{O}(a^2). \end{aligned} \tag{14}$$

[2]The symmetry group that we write here is not the true symmetry group of the quantized theory. As discussed in [19,20], the presence of ghost fields in the functional integral leads to constraints on the allowed symmetry transformations. However, for the derivation of the correct chiral Lagrangian it is possible to use the symmetry group in Eq. (6) [20].

$\tilde{m}_{\rm Val}$ and $\tilde{m}_{\rm Sea}$ are renormalized masses. Two consequences of the exact chiral symmetry of the massless Ginsparg-Wilson fermions are: (a) there is no Pauli term $\bar{\psi}\sigma_{\mu\nu}F_{\mu\nu}\psi$ for the valence sector, and (b) the valence quark mass is only multiplicatively renormalized. No symmetry protects the Wilson sea quarks from getting an additive correction of the order of the cutoff $1/a$.

It is useful at this point to collect the quark fields in a single quark field vector Ψ, and rewrite Eq. (14) as

$$S_S = \int \bar{\Psi}(D+\mathbf{m})\Psi + \bar{\Psi} a\mathbf{c_{SW}}\sigma_{\mu\nu}F_{\mu\nu}\Psi + \mathcal{O}(a^2), \quad (15)$$

$$\Psi = \begin{pmatrix} \psi_S \\ \psi_V \end{pmatrix}, \quad \mathbf{m} = \begin{pmatrix} \tilde{m}_{\rm Sea} & \\ & \tilde{m}_{\rm Val} \end{pmatrix}, \quad a\mathbf{c_{SW}} = \begin{pmatrix} ac_{SW} & \\ & 0 \end{pmatrix}. \quad (16)$$

D. Symmetries of S_S and χPT for the mixed action

We now turn to the construction of a low-energy effective theory for the "underlying" Symanzik action in Eq. (15). The method is completely analogous to the construction of the chiral Lagrangian in QCD [27].[3] The idea is that the spontaneous breaking of the approximate chiral symmetry gives rise to light pseudo Goldstone bosons, the light mesons, which at low energies are the only relevant degrees of freedom. The effective action is written in terms of local interactions of the pseudo-Goldstone fields. Since the pseudo-Goldstone bosons interact weakly at low energies, the action can be organized in a perturbative series.

All observables calculated are expanded in two small parameters,

$$\epsilon \sim \frac{p^2}{\Lambda_\chi^2} \sim \frac{\hat{m}}{\Lambda_\chi^2} \quad \text{and} \quad \delta \sim \frac{\hat{a}}{\Lambda_\chi^2}, \quad (17)$$

where p is the light meson momentum, $\Lambda_\chi \sim 1$ GeV is the chiral symmetry breaking scale, and $\hat{m}$ and $\hat{a}$ stand for matrix elements of[4]

$$\hat{\mathbf{m}} \equiv 2B_0\mathbf{m}, \quad \hat{\mathbf{a}} \equiv 2W_0 a\mathbf{c}_{\rm SW}. \quad (18)$$

[3]It should be noted that as of yet the construction of PQ χPT from PQ QCD is not as well justified as the standard derivation of χPT from QCD. The arguments of the latter cannot be trivially extended to PQ QCD because they rely, in part, on the existence of a Hilbert space of physical states with a positive definite norm, which is absent in the presence of ghost fields. The same is also true for the mixed action. The validity of the χPT for the mixed action is thus on the same footing as that of PQ χPT, which has been discussed in [20].

[4]Though the notation might obscure this fact, $\hat{\mathbf{m}}$ and $\hat{\mathbf{a}}$ both have mass dimension 2—they are the leading contributions to the squared mass of the pseudo Goldstone boson. We nevertheless use this notation as it makes the dependence on the quark masses and the lattice spacing more transparent.

B_0 and W_0 are dimensionful low-energy constants that appear in the effective theory at leading order [see Eq. (B1)]. They depend only on the high-energy scale Λ_χ, and dimensional analysis reveals that the perturbative expansion is in fact in m_q/Λ_χ and $a\Lambda_\chi$. We follow Ref. [9] and choose the $\{\epsilon,\delta\}$ terms as leading order (LO) and the $\{\epsilon^2,\epsilon\delta\}$ terms as NLO in the effective Lagrangian, dropping $\mathcal{O}(a^2)$ contributions. The underlying hierarchy consistent with this ordering is $\{\epsilon,\delta\} \gg \{\epsilon^2,\epsilon\delta\} \gg \delta^2$, and the last inequality also implies $\epsilon \gg \delta$. This ordering is chosen for convenience and is somewhat arbitrary. In practice, the double expansion should be organized according to the actual relative sizes of the quark masses and the lattice spacing.

The effective Lagrangian is constructed from all operators that respect the symmetries of the underlying action S_S. The compact notation of Eq. (15) makes it easy to see that the symmetry group of S_S to $\mathcal{O}(a)$ is

$$SU(N_f+N_V|N_V)_L \otimes SU(N_f+N_V|N_V)_R. \quad (19)$$

This symmetry group (treating $\hat{\mathbf{m}}$ and $\hat{\mathbf{a}}$ as spurion fields) is the same as that of PQ QCD with Wilson fermions. Indeed the effective action S_S in Eq. (15) is the same as the effective Symanzik action for the PQ QCD Wilson action of Ref. [9], with a specific choice of $a\mathbf{c}_{\rm SW}$ that has support only in the sea sector. This fortunate similarity between the mixed action theory and the PQ QCD Wilson theory implies that *the mixed low-energy chiral effective action has the same structure, at* $\mathcal{O}(a)$, *as the action of Wilson* χPT, *introduced in* Ref. [9], *with the restriction that* $a\mathbf{c}_{\rm SW}$ *vanishes in the valence-ghost sector*. The chiral Lagrangian to $\mathcal{O}(a)$, which describes both WχPT and the mixed effective theory, is provided in Appendix B.

E. Application: Meson mass

In this subsection we give an example for the use of the mixed chiral Lagrangian. For simplicity we take all the sea quarks and all the valence quarks to be (separately) degenerate, and the Wilson parameter to be a flavor singlet in the sea sector. This amounts to setting

$$\hat{\mathbf{m}} = \mathrm{diag}(\hat{m}_{\rm Sea}, \hat{m}_{\rm Val}), \quad \hat{\mathbf{a}} = \mathrm{diag}(\hat{a}, 0). \quad (20)$$

The number of sea quark flavors is taken to be $N_f = 3$. We consider the expression for the mass of the flavor charged meson with valence quark flavor indices $AB (A \neq B)$ to NLO. Using the relation between the mixed chiral effective theory and WχPT, one can obtain the result straightforwardly by taking the mass formula from Ref. [9] with the values for $\hat{\mathbf{m}}$ and $\hat{\mathbf{a}}$ given by Eq. (20). We find

$$(M_{\rm AB}^2)_{\rm NLO} = \hat{m}_{\rm Val} + \frac{\hat{m}_{\rm Val}}{48f^2\pi^2}[\hat{m}_{\rm Val} - \hat{m}_{\rm Sea} - \hat{a} + (2\hat{m}_{\rm Val} - \hat{m}_{\rm Sea} - \hat{a})\ln(\hat{m}_{\rm Val})] - \frac{8\hat{m}_{\rm Val}}{f^2}[(L_5 - 2L_8)\hat{m}_{\rm Val} + 3(L_4 - 2L_6)\hat{m}_{\rm Sea} + 3(W_4 - W_6)\hat{a}]. \quad (21)$$

Here, the parameters L_i are the Gasser-Leutwyler coefficients, and W_4 and W_6 are additional low-energy constants that enter the chiral Lagrangian at NLO. Note that for $\hat{a}=0$ the expression for PQ χPT (calculated in [2,28,29]) is recovered.

Equation (21) demonstrates the analytic connection between QCD and the simulated mixed action theory. It shows the latter to be a calculation with controlled systematic errors. From fitting the equation to the appropriate data from numerical simulations one can obtain an estimate for the linear combinations of Gasser-Leutwyler coefficients that appear in it.

Examining Eq. (21) one can also appreciate the potential advantage of using a mixed lattice action. In simulations using Wilson fermions in both sea and valence sectors, an equation similar to Eq. (21) holds [see Eq. (B5)]. In that case, the range of valence quark masses that can be simulated might be too small to convincingly show the curvature coming from the quadratic dependence and the logarithms that enter at NLO. By using Ginsparg-Wilson fermions for the valence quarks one can vary the valence quark masses over a wider range. The expected NLO curvature, on which the extraction of the Gasser-Leutwyler coefficients depends, is consequently much more likely to be seen.

Finally, comparison with the result for WχPT, Eq. (B5), reveals that the latter depends on twice the number of W_i coefficients. This is fortunate for the mixed theory as it makes the predictions of the effective theory less dependent on parameters that have no particular relevance to QCD.

To understand this simplification in the expression for the meson mass, consider the relation between the symmetries of the mixed action and those of PQ Wilson action. On the one hand the massless mixed theory has exact chiral symmetry in the valence sector, which the Wilson action does not. On the other hand, the valence and sea quarks of the Wilson action have the same type of Dirac operator which allows mixing between the sectors—a transformation which is not a symmetry of the mixed action formulation. At $\mathcal{O}(a)$, however, the breaking of the sea-valence symmetry in the mixed theory does not yet show up, and thus the simpler expressions arise due to the larger chiral symmetry.

III. SUMMARY

In this paper we discuss lattice simulations with different fermions for sea and valence quarks. As a particular example we have studied here the case with Wilson sea quarks and Ginsparg-Wilson valence quarks. Using Symanzik's effective action for lattice theories as an intermediate step, we have derived the form of the low-energy chiral Lagrangian for the mixed theory to $\mathcal{O}(a)$. The construction shows that simulations with the mixed action provide as controlled an approximation to QCD as partially quenched simulations. This is to be expected since the mixed action reduces to PQ QCD in the continuum limit.

The goal of the mixed action approach is similar to that of PQ QCD. The use of smaller valence quark masses allows one to probe deeper the chiral regime of QCD and obtain additional information on the low-energy constants, the Gasser-Leutwyler coefficients. Furthermore, the use of chiral lattice fermions in the valence sector, instead of Wilson fermions, makes it possible to simulate much lighter valence quarks. This leads to more data points obtained on the lattice and consequently to more reliable fits of χPT to the data.

Here we have demonstrated the mixed action approach for Wilson sea quarks and Ginsparg-Wilson valence quarks taking into account the leading $\mathcal{O}(a)$ contributions. An important extension of this analysis is the inclusion of $\mathcal{O}(a^2)$ effects. First of all, the lattice spacing determined by the unquenched configurations is possibly not small enough to safely neglect the $\mathcal{O}(a^2)$ corrections. If one wants to fit the lattice data directly to equations like Eq. (21) without taking the continuum limit first, the $\mathcal{O}(a^2)$ corrections should be included to obtain better fits. Second, the $\mathcal{O}(a)$ effects are generated here only by the Wilson sea quarks. Many unquenched simulations are in fact performed with nonperturbatively $\mathcal{O}(a)$-improved Wilson fermions for the sea quarks. The leading corrections for these simulations are of $\mathcal{O}(a^2)$ and need to be computed in order to know how the continuum limit is approached.

While valuable, it should also be noted that the inclusion of $\mathcal{O}(a^2)$ effects in the chiral Lagrangian framework is likely to be a hard task. The main difficulty arises from the many new operators that enter the Symanzik action at this order. Some of these operators break Lorentz invariance, while several others break the chiral symmetry and require the introduction of additional spurion fields.

The approach proposed here should be also studied with other combinations for the lattice fermions. In particular, the case with staggered sea quarks is interesting, since staggered fermions are computationally cheaper. At present the lightest dynamical quark masses are achieved with staggered fermions. It is well known that applying staggered fermions to QCD involves a theoretical uncertainty and is possibly uncontrolled. Consequently, predictions from chiral perturbation theory for staggered fermions would also serve as a test of this discretization method [7].

Finally, the cost of simulations of a mixed action is roughly the sum of the cost of generating a set of unquenched gauge field configurations plus that of analyzing quenched simulations with Ginsparg-Wilson fermions. Thus, we can expect that in the near future simulations with a mixed action will become feasible.

ACKNOWLEDGMENTS

We acknowledge support in part by U.S. DOE grants DF-FC02-94ER40818, DE-AC03-76SF00098, DE-FG03-96ER40956/A006 and DE-FG02-91ER40676. We thank Maarten Golterman and Steve Sharpe for their comments on this manuscript. G.R. would like to thank the Department of Physics, Boston University and the Benasque Center for Science, Benasque, Spain for kind hospitality during part of this work.

APPENDIX A: SYMANZIK ACTION FOR THE WILSON AND GINSPARG-WILSON ACTIONS

In this appendix we derive Eq. (14) for the Symanzik action describing the mixed theory to $\mathcal{O}(a)$. As has been

stated in the text, to this order the Symanzik action is simply the sum of the local effective actions for the valence and the sea sectors.

The local Symanzik action for Wilson fermions has been derived in [25,26]. One first lists all the operators of mass dimension no greater than 5, which respect the symmetries of the Wilson lattice action (the appropriate power of a is inserted to complete the dimensions of terms in the Lagrangian to 4). The operators of dimension 4 (which are a independent) make up, by construction, the continuum action of QCD.

Because the Wilson term explicitly breaks the chiral symmetry, it is expected that the quark mass be additively renormalized, and the size of the correction should be of the order of the cutoff scale $1/a$. Indeed, the only dimension 3 operator is $\bar{\psi}\psi$, which appears in the action with a coefficient proportional to $1/a$ and has precisely this effect.

There are several operators of mass dimension 5 that are allowed by the symmetries. Some of these operators can be eliminated using the leading order equations of motion. Others have the same structure as the mass and kinetic operators that already appear in the QCD action, and have the effect of renormalizing the quark masses and the gauge coupling. Finally, a single term is left—the Pauli term: $\bar{\psi}\sigma_{\mu\nu}F_{\mu\nu}\psi$. Note that the Pauli term breaks the chiral symmetry, and is therefore allowed only because of the Wilson term. Putting it all together, the Symanzik action for the Wilson sea sector is

$$\int d^4x[\bar{\psi}_S(D+\tilde{m}_{\rm Sea})\psi_S + a c_{SW}\bar{\psi}_S\sigma_{\mu\nu}F_{\mu\nu}\psi_S] + \mathcal{O}(a^2), \tag{A1}$$

where $\tilde{m}_{\rm Sea}$ is the renormalized sea quark mass, and c_{SW} is an unknown coefficient.

The analysis for the Ginsparg-Wilson valence quarks is similar. This may seem confusing due to the fact that some of the chiral projectors on the lattice are written in terms of $\hat{\gamma}_5$, and not γ_5 as in the continuum theory. However, it has been shown in Refs. [30,31], that the chiral symmetry of the Ginsparg-Wilson lattice action leads to exactly the same chiral Ward identities which appear in the continuum. Hence, by imposing the usual chiral symmetry on the Symanzik action, the effective theory correctly reproduces the consequences of the lattice chiral symmetry.

Due to the exact chiral symmetry the valence quark mass gets renormalized only multiplicatively and the Pauli term is absent. Consequently, after considering the renormalizations of gauge coupling and quark masses, the Symanzik action for the valence Ginsparg-Wilson quarks contains no $\mathcal{O}(a)$ part [the Ginsparg-Wilson lattice action is automatically $\mathcal{O}(a)$ improved [17]]:

$$\int d^4x[\bar{\psi}_V(D+\tilde{m}_{\rm Val})\psi_V] + \mathcal{O}(a^2). \tag{A2}$$

Equation (14) is the sum of Eq. (A1) and Eq. (A2).

APPENDIX B: WχPT RESULTS

We present the WχPT Lagrangian which also describes the mixed theory to $\mathcal{O}(a)$. Interested readers should consult Ref. [9] for further details on WχPT. We also provide the expression for the mass of a flavor charged meson for comparison with the mixed theory result.

The WχPT Lagrangian is constructed out of operators that respect all the symmetries of the underlying theory in Eq. (15), with explicit flavor axial symmetry breaking terms constructed out of $\hat{m}$ and $\hat{a}$. As described in the text, the LO Lagrangian is linear in ϵ and δ:

$$\mathcal{L}_2 = \frac{f^2}{4}\langle\partial\Sigma\,\partial\Sigma^\dagger\rangle - \frac{f^2}{4}\langle(\hat{m}+\hat{a})\Sigma^\dagger + \Sigma(\hat{m}^\dagger+\hat{a}^\dagger)\rangle. \tag{B1}$$

Here the angled brackets stand for the super-trace over the flavor indices:

$$\langle\Gamma\rangle = \mathrm{str}(\Gamma) = \sum_i \eta_i\Gamma_{ii},$$
$$\eta_i = \begin{cases} 1, & i \text{ is a quark flavor index,} \\ -1, & i \text{ is a ghost flavor index,} \end{cases} \tag{B2}$$

and $\Sigma = \exp(2i\Pi/f)$ is a non-linear representation of the meson fields.

The NLO Lagrangian is[5]

$$\begin{aligned}\mathcal{L}_4 = &-L_1\langle\partial\Sigma\,\partial\Sigma^\dagger\rangle^2 - L_2\langle\partial_\mu\Sigma\,\partial_\nu\Sigma^\dagger\rangle\langle\partial_\mu\Sigma\,\partial_\nu\Sigma^\dagger\rangle - L_3\langle(\partial\Sigma\,\partial\Sigma^\dagger)^2\rangle + L_4\langle\partial\Sigma\,\partial\Sigma^\dagger\rangle\langle\hat{m}\Sigma^\dagger + \Sigma\hat{m}^\dagger\rangle + W_4\langle\partial\Sigma\,\partial\Sigma^\dagger\rangle\langle\hat{a}\Sigma^\dagger + \Sigma\hat{a}^\dagger\rangle \\ &+ L_5\langle\partial\Sigma\,\partial\Sigma^\dagger(\hat{m}\Sigma^\dagger + \Sigma\hat{m}^\dagger)\rangle + W_5\langle\partial\Sigma\,\partial\Sigma^\dagger(\hat{a}\Sigma^\dagger + \Sigma\hat{a}^\dagger)\rangle - L_6\langle\hat{m}\Sigma^\dagger + \Sigma\hat{m}^\dagger\rangle^2 - W_6\langle\hat{m}\Sigma^\dagger + \Sigma\hat{m}^\dagger\rangle\langle\hat{a}\Sigma^\dagger + \Sigma\hat{a}^\dagger\rangle \\ &- L_7\langle\hat{m}\Sigma^\dagger - \Sigma\hat{m}^\dagger\rangle^2 - W_7\langle\hat{m}\Sigma^\dagger - \Sigma\hat{m}^\dagger\rangle\langle\hat{a}\Sigma^\dagger - \Sigma\hat{a}^\dagger\rangle - L_8\langle\hat{m}\Sigma^\dagger\hat{m}\Sigma^\dagger + \Sigma\hat{m}^\dagger\Sigma\hat{m}^\dagger\rangle - W_8\langle\hat{a}\Sigma^\dagger\hat{m}\Sigma^\dagger + \Sigma\hat{a}^\dagger\Sigma\hat{m}^\dagger\rangle. \end{aligned} \tag{B3}$$

These Lagrangians describe both the mixed and the PQ Wilson lattice actions. In the mixed theory $\hat{a}$ has support only in the

[5]There has been an error in Ref. [9] in the sign of some of the terms in $\mathcal{L}_4$. The form that appears here is the correct one.

sea-sea sector. We comment that Eqs. (B1), (B3) contain ordinary χPT. Moreover, since the low-energy constants L_i's and W_i's are independent of $\hat{m}$ and $\hat{a}$ and this theory becomes the familiar χPT in the sea-sea sector when $a \to 0$, the L_i's are exactly the Gasser-Leutwyler coefficients of ordinary χPT.

Next, we provide the WχPT expression for the mass of the flavor charged meson defined in Sec. II E. We consider the case where

$$\hat{\mathbf{m}} = \mathrm{diag}(\hat{m}_{\mathrm{Sea}}, \hat{m}_{\mathrm{Val}}), \quad \hat{\mathbf{a}} = \mathrm{diag}(\hat{a}_{\mathrm{Sea}}, \hat{a}_{\mathrm{Val}}) \tag{B4}$$

[compare with Eq. (20)]. One obtains

$$\begin{aligned}(M_{\mathrm{AB}}^2)_{\mathrm{NLO}} = {} & (\hat{m}_{\mathrm{Val}} + \hat{a}_{\mathrm{Val}}) + \frac{(\hat{m}_{\mathrm{Val}} + \hat{a}_{\mathrm{Val}})}{48 f^2 \pi^2}[(\hat{m}_{\mathrm{Val}} + \hat{a}_{\mathrm{Val}}) - (\hat{m}_{\mathrm{Sea}} + \hat{a}_{\mathrm{Sea}}) + (2(\hat{m}_{\mathrm{Val}} + \hat{a}_{\mathrm{Val}}) - (\hat{m}_{\mathrm{Sea}} + \hat{a}_{\mathrm{Sea}}))\ln(\hat{m}_{\mathrm{Val}} + \hat{a}_{\mathrm{Val}})] \\ & - \frac{8\hat{m}_{\mathrm{Val}}}{f^2}[(L_5 - 2L_8)\hat{m}_{\mathrm{Val}} + 3(L_4 - 2L_6)\hat{m}_{\mathrm{Sea}} + 3(W_4 - W_6)\hat{a}_{\mathrm{Sea}}] - \frac{8\hat{a}_{\mathrm{Val}}}{f^2}[(L_5 + W_5 - 2W_8)\hat{m}_{\mathrm{Val}} + 3(L_4 \\ & - W_6)\hat{m}_{\mathrm{Sea}}]. \end{aligned} \tag{B5}$$

To obtain the expression appropriate for common lattice simulations, in which the Wilson term is the same for all flavors, one sets $\hat{a}_{\mathrm{Val}} = \hat{a}_{\mathrm{Sea}}$ in the last equation. The meson mass for the mixed action [Eq. (21)] can be obtained by setting $\hat{a}_{\mathrm{Val}} = 0$.

[1] J. Gasser and H. Leutwyler, Nucl. Phys. **B250**, 465 (1985).
[2] S.R. Sharpe and N. Shoresh, Phys. Rev. D **62**, 094503 (2000).
[3] A.G. Cohen, D.B. Kaplan, and A.E. Nelson, J. High Energy Phys. **11**, 027 (1999).
[4] C. Bernard *et al.*, hep-lat/0209086.
[5] S. Dürr, hep-ph/0209319.
[6] qq+q, Collaboration, F. Farchioni, C. Gebert, I. Montvay, and L. Scorzato, hep-lat/0209142.
[7] C.W. Bernard and M.F.L. Golterman, Phys. Rev. D **49**, 486 (1994).
[8] S.R. Sharpe and J. Singleton Robert, Phys. Rev. D **58**, 074501 (1998).
[9] G. Rupak and N. Shoresh, Phys. Rev. D **66**, 054503 (2002).
[10] W.-J. Lee and S.R. Sharpe, Phys. Rev. D **60**, 114503 (1999).
[11] C. Aubin *et al.*, hep-lat/0209066.
[12] K.G. Wilson, Phys. Rev. D **10**, 2445 (1974).
[13] P.H. Ginsparg and K.G. Wilson, Phys. Rev. D **25**, 2649 (1982).
[14] P. Hasenfratz, V. Laliena, and F. Niedermayer, Phys. Lett. B **427**, 125 (1998).
[15] H. Neuberger, Phys. Lett. B **417**, 141 (1998).
[16] H. Neuberger, Phys. Lett. B **427**, 353 (1998).
[17] F. Niedermayer, Nucl. Phys. B (Proc. Suppl.) **73**, 105 (1999).
[18] M. Luscher, Phys. Lett. B **428**, 342 (1998).
[19] P.H. Damgaard, J.C. Osborn, D. Toublan, and J.J.M. Verbaarschot, Nucl. Phys. **B547**, 305 (1999).
[20] S.R. Sharpe and N. Shoresh, Phys. Rev. D **64**, 114510 (2001).
[21] K. Symanzik, in *Recent Developments in Gauge Theories*, Proceedings, NATO Advanced Study Institute, Cargese, France, 1979, edited by G. 't Hooft *et al.* (NATO Advanced Study Institute Series, Series B, Physics, Vol. 59) (Plenum, New York, 1980), p. 438.
[22] K. Symanzik, Nucl. Phys. **B226**, 187 (1983).
[23] K. Symanzik, Nucl. Phys. **B226**, 205 (1983).
[24] P. Hernández, K. Jansen, and M. Lüscher, Nucl. Phys. **B552**, 363 (1999).
[25] B. Sheikholeslami and R. Wohlert, Nucl. Phys. **B259**, 572 (1985).
[26] M. Lüscher, S. Sint, R. Sommer, and P. Weisz, Nucl. Phys. **B478**, 365 (1996).
[27] S. Weinberg, Physica A **96**, 327 (1979).
[28] S.R. Sharpe, Phys. Rev. D **56**, 7052 (1997); **62**, 099901(E) (2000).
[29] M.F.L. Golterman and K.-C. Leung, Phys. Rev. D **57**, 5703 (1998).
[30] P. Hasenfratz, Nucl. Phys. **B525**, 401 (1998).
[31] P. Hasenfratz, S. Hauswirth, T. Jorg, F. Niedermayer, and K. Holland, Nucl. Phys. **B643**, 280 (2002).

PHYSICAL REVIEW D **70**, 034508 (2004)

Chiral perturbation theory at $\mathcal{O}(a^2)$ for lattice QCD

Oliver Bär*
Institute of Physics, University of Tsukuba, Tsukuba, Ibaraki 305-8571, Japan

Gautam Rupak†
Lawrence Berkeley National Laboratory, Berkeley, California 94720, USA

Noam Shoresh‡
Department of Physics, Boston University, Boston, Massachusetts 02215, USA
(Received 4 September 2003; revised manuscript received 30 April 2004; published 18 August 2004)

We construct chiral effective Lagrangian for two lattice theories: one with Wilson fermions and the other with Wilson sea fermions and Ginsparg-Wilson valence fermions. For each of these theories we construct the Symanzik action through $\mathcal{O}(a^2)$. The chiral Lagrangian is then derived, including terms of $\mathcal{O}(a^2)$, which have not been calculated before. We find that there are only few new terms at this order. Corrections to existing coefficients in the continuum chiral Lagrangian are proportional to a^2 and appear in the Lagrangian at $\mathcal{O}(a^2p^2)$ or higher. Similarly, $O(4)$ symmetry-breaking terms enter the Symanzik action at $\mathcal{O}(a^2)$, but contribute to the chiral Lagrangian at $\mathcal{O}(a^2p^4)$ or higher. We calculate the light meson masses in chiral perturbation theory for both lattice theories. At next-to-leading order, we find that there are no $\mathcal{O}(a^2)$ corrections to the valence-valence meson mass in the mixed theory due to the enhanced chiral symmetry of the valence sector.

DOI: 10.1103/PhysRevD.70.034508 PACS number(s): 11.15.Ha, 12.38.Gc, 12.39.Fe

I. INTRODUCTION

Chiral perturbation theory (χPT) [1,2] plays an important role in the analysis of current lattice QCD data. Simulations with the quark masses as light as realized in nature are not feasible on present-day computers. Instead one simulates with heavier quark masses and performs a chiral extrapolation to the physical quark masses using the analytic predictions of χPT. To perform the chiral extrapolation one must first take the continuum limit of the lattice data, since χPT describes continuum QCD and is not valid for nonzero lattice spacing. However, it is common practice not to perform the continuum extrapolation and nevertheless fit the lattice data to continuum χPT, assuming that the lattice artifacts are small.

A strategy to reduce this systematic uncertainty was proposed in Refs. [3–7] (a different approach was taken in Refs. [8,9] in the strong coupling limit). There it was shown how the discretization effects stemming from a nonzero lattice spacing can be included in χPT. The basic idea is that lattice QCD is, close to the continuum limit, described by Symanzik's effective theory, which is QCD with additional higher dimensional terms [10–14]. The derivation of χPTfrom QCD can then be extended to this effective theory with additional symmetry-breaking parameters. The result is a chiral expansion in which the leading dependence on the lattice spacing is explicit. This idea was numerically examined in Ref. [15] for a theory with two dynamical sea quarks on a coarse lattice using the results of Ref. [7]. The characteristic chiral log behavior in the pseudo scalar meson mass and decay constant was observed.

A similar approach was taken in Ref. [16] for analyzing lattice theories with two types of lattice fermions—Wilson fermions for the sea quarks and Ginsparg-Wilson fermions for the valence quarks. The latter can be implemented using domain wall [17–19], overlap [20–24], perfect action [25,26], and chirally improved fermions [27,28]. There are several advantages in using different lattice fermions in numerical simulations. Since massless Ginsparg-Wilson fermions exhibit an exact chiral symmetry even at nonzero lattice spacing [29], it is possible to simulate such valence fermions with masses much smaller than the valence quark masses accessible using Wilson fermions [30,31]. This allows a wider numerical sampling of points in the chiral regime of QCD. In addition, the valence sector exhibits all the benefits stemming from the Ginsparg-Wilson relation [32], such as the absence of additive mass renormalization, of operator mixing among different chiral multiplets, and of lattice artifacts linear in the lattice spacing a [23–26,33,34].

In this paper we extend the results of both Refs. [7] and [16] by calculating the chiral Lagrangian including the $\mathcal{O}(a^2)$ lattice effects. There are various reasons for doing this. First, the lattice spacings in current unquenched simulations are not very small, so that neglecting the $\mathcal{O}(a^2)$ contributions might not be justified. Second, the use of nonperturbatively improved Wilson fermions in lattice simulations is becoming more common. The leading corrections for these fermions are of $\mathcal{O}(a^2)$ and hence need to be computed in order to know how the continuum limit is approached.

At $\mathcal{O}(a^2)$ many operators enter the Symanzik action and need to be taken into account for constructing the chiral Lagrangian. Four-fermion operators appear for the first time and operators that explicitly break Euclidean rotational symmetry are encountered. Nevertheless, the number of new op-

*Email address: obaer@het.ph.tsukuba.ac.jp
†Email address: grupak@lbl.gov
‡Email address: shoresh@bu.edu

erators in the chiral Lagrangian is rather small (three for the Wilson action and four for the mixed fermion theory). This is important in practical applications, since every new operator comes with an undetermined low-energy constant. These constants enter the analytic expressions for physical observables and too many free parameters limit the predictability of the chiral extrapolations.

The paper is organized as follows: χPT for the Wilson action is discussed in Sec. II, including the partially quenched case in Sec. II E. The mixed theory with Wilson sea and Ginsparg-Wilson valence quarks is treated in Sec. III. In Sec. IV, we discuss the chiral power counting and compute the pseudoscalar meson mass including the $\mathcal{O}(a^2)$ contributions for both cases. We end with some general comments in Sec. V.

II. WILSON ACTION

In this section we formulate the chiral effective theory for the Wilson lattice action. First, the Wilson action and its symmetries are briefly reviewed, then the local Symanzik action through $\mathcal{O}(a^2)$ is presented. Based on the symmetry properties of the Symanzik action we construct the chiral effective theory. Finally, we consider the extension to the partially quenched case.

A. Lattice action

We consider an infinite hypercubic lattice with lattice spacing a. The quark and antiquark fields are represented by ψ and $\bar{\psi}$, respectively. Wilson's fermion action [35] is given by

$$S_W = a^4 \sum_x \bar{\psi}(D_W + m_0)\psi(x),$$
$$D_W = \frac{1}{2}\{\gamma_\mu(\nabla^*_\mu + \nabla_\mu) - ar\nabla^*_\mu\nabla_\mu)\}, \tag{1}$$

where m_0 denotes the $N_f \times N_f$ bare quark mass matrix and r the Wilson parameter. ∇^*_μ, ∇_μ are the usual covariant, nearest-neighbor backward and forward difference operators.

The Wilson action in Eq. (1) possesses several discrete symmetries—charge conjugation, parity—as well as an $SU(N_c)$ color gauge symmetry. The introduction of a discrete space-time lattice reduces the rotation symmetry group O(4) to the discrete hypercubic group.

Next, we consider the group of chiral flavor transformations,

$$G = SU(N_f)_L \otimes SU(N_f)_R. \tag{2}$$

Introducing the usual projection operators $P_\pm = \frac{1}{2}(1 \pm \gamma_5)$ the left- and right-handed fermion fields are defined by

$$\psi_{L,R} = P_\mp \psi, \quad \bar{\psi}_{L,R} = \bar{\psi} P_\pm. \tag{3}$$

Under a transformation $L \otimes R \in G$ these chiral components transform according to

$$\psi_L \to L\psi_L, \quad \bar{\psi}_L \to \bar{\psi}_L L^\dagger,$$
$$\psi_R \to R\psi_R, \quad \bar{\psi}_R \to \bar{\psi}_R R^\dagger. \tag{4}$$

For small quark masses and lattice spacing, G is an approximate symmetry group of the theory, broken only by the mass and the Wilson terms. If all the quark masses are nonzero but equal the vector subgroup with $L = R$ is a symmetry of the action S_W.

To complete the definition of the lattice theory one should also define a gauge action S_{YM}. However, the precise choice of the gauge action is irrelevant for the purpose of our analysis, so we leave it unspecified.

B. Symanzik action

The Symanzik action for the Wilson lattice action, up to and including $\mathcal{O}(a^2)$, has been calculated first in Ref. [13]. The analysis to $\mathcal{O}(a)$ has been later elaborated on in Ref. [14]. We restate these results in a slightly different form. The explicit breaking of chiral symmetry by the Wilson term leads to an additive renormalization of the quark mass. This causes the pion to become massless along a critical line $m_0 = m_c(a) \sim 1/a$, and a physical quark mass can be defined as the distance from this line, $m_q = m_0 - m_c$. The operators in the Symanzik action are constructed from the quark and gauge fields and their derivatives and powers of m_q. We list all terms in the action through $\mathcal{O}(a^2)$ that are allowed by the symmetries, organized in powers of a (again, we only focus on the fermion action). We use the notation

$$S_S = S_0 + aS_1 + a^2 S_2 \ldots,$$
$$S_k = \sum_i c_i^{(k+4)} O_i^{(k+4)}, \tag{5}$$

where $O_i^{(n)}$ are local operators of dimension n and the constants $c_i^{(n)}$ are unknown coefficients.

Some allowed operators in the Symanzik action are obtained by multiplying lower-dimensional operators with powers of the quark mass m_q. For example, $a\,\mathrm{tr}(m_q)\bar{\psi}\not{D}\psi$, $a\bar{\psi}m_q\not{D}\psi$ and four similar operators at $\mathcal{O}(a^2)$ contribute to the wave function renormalization of the quark fields. Performing a (flavor-dependent) field redefinition one can eliminate these operators while keeping the kinetic term trivial in flavor space. Similarly, the operators $a\,\mathrm{tr}(m_q^2)\bar{\psi}\psi$, $a\,\mathrm{tr}^2(m_q)\bar{\psi}\psi$, $a\,\mathrm{tr}(m_q)\bar{\psi}m_q\psi$, and $a\bar{\psi}m_q^2\psi$ [and seven more operators at $\mathcal{O}(a^2)$] renormalize the mass matrix m_q. These operators can be effectively accounted for by replacing m_q with the renormalized mass m; we do not list them here explicitly. At $\mathcal{O}(a^2)$ in the Symanzik action, differences between inserting m and m_q are at least $\mathcal{O}(a^3)$ and can be neglected. With these caveats we find the following list of operators (we use the same notation as in Ref. [13]):

$$S_0: \quad O_1^{(4)} = \bar{\psi} \not{D} \psi, \qquad O_2^{(4)} = \bar{\psi} m \psi. \tag{6}$$

$$S_1: \quad O_1^{(5)} = \bar{\psi} D_\mu D_\mu \psi, \qquad O_2^{(5)} = \bar{\psi} i \sigma_{\mu\nu} F_{\mu\nu} \psi. \tag{7}$$

S_2, bilinears:

$$\begin{aligned} O_1^{(6)} &= \bar{\psi} \not{D}^3 \psi, & O_5^{(6)} &= \bar{\psi} m D_\mu D_\mu \psi, \\ O_2^{(6)} &= \bar{\psi} (D_\mu D_\mu \not{D} + \not{D} D_\mu D_\mu) \psi, & O_6^{(6)} &= \mathrm{tr}(m) \ \ \bar{\psi} D_\mu D_\mu \psi, \\ O_3^{(6)} &= \bar{\psi} D_\mu \not{D} D_\mu \psi, & O_7^{(6)} &= \bar{\psi} m i \sigma_{\mu\nu} F_{\mu\nu} \psi, \\ O_4^{(6)} &= \bar{\psi} \gamma_\mu D_\mu D_\mu D_\mu \psi, & O_8^{(6)} &= \mathrm{tr}(m) \ \ \bar{\psi} i \sigma_{\mu\nu} F_{\mu\nu} \psi. \end{aligned} \tag{8}$$

S_2, four-quark operators:

$$\begin{aligned} O_9^{(6)} &= (\bar{\psi}\psi)^2, & O_{14}^{(6)} &= (\bar{\psi} t^a \psi)^2, \\ O_{10}^{(6)} &= (\bar{\psi}\gamma_5\psi)^2, & O_{15}^{(6)} &= (\bar{\psi} t^a \gamma_5 \psi)^2, \\ O_{11}^{(6)} &= (\bar{\psi}\gamma_\mu\psi)^2, & O_{16}^{(6)} &= (\bar{\psi} t^a \gamma_\mu \psi)^2, \\ O_{12}^{(6)} &= (\bar{\psi}\gamma_\mu\gamma_5\psi)^2, & O_{17}^{(6)} &= (\bar{\psi} t^a \gamma_\mu \gamma_5 \psi)^2, \\ O_{13}^{(6)} &= (\bar{\psi}\sigma_{\mu\nu}\psi)^2, & O_{18}^{(6)} &= (\bar{\psi} t^a \sigma_{\mu\nu} \psi)^2, \end{aligned} \tag{9}$$

where t^a are the $SU(N_c)$ generators. This list of four-quark operators is slightly different from the one in Ref. [13]. Sheikholeslami and Wohlert's list contains operators with flavor group generators. However, both lists are equivalent and are related by Fierz identities (see Appendix A). Our choice of operators is guided by the fact that for the study of chiral transformation properties, it is more convenient to consider four-quark operators with a trivial flavor structure.

In the context of on-shell improvement, equations of motion have been used to reduce the number of operators at $\mathcal{O}(a)$ in the Symanzik action [13,14]. This involves a redefinition of the effective fields, which are matched to their lattice counterparts [14]. Only the Pauli term $O_2^{(5)}$ is left at this order and can be subsequently canceled by adding the clover term to the lattice action with a properly adjusted coefficient. The generalization of the arguments in Ref. [14] to $\mathcal{O}(a^2)$ has not been carried out yet. We therefore continue with the formulation of the chiral effective theory without making use of equations of motion.

We distinguish two types of operators in the Symanzik action: those that break chiral symmetry and those that do not. At $\mathcal{O}(a)$ all operators break chiral symmetry. At $\mathcal{O}(a^2)$ there are ten symmetry-breaking operators: $O_5^{(6)} - O_{10}^{(6)}$, $O_{13}^{(6)} - O_{15}^{(6)}$, and $O_{18}^{(6)}$. Fermionic operators that do not break the chiral symmetry first appear at $\mathcal{O}(a^2)$. Purely gluonic operators (which we have not listed above) also belong to the second type of operators as they are trivially invariant under chiral transformations. They too enter at $\mathcal{O}(a^2)$.

The operator $O_4^{(6)}$ deserves special attention. While respecting the chiral symmetries it is not invariant under O(4) rotations. This means that it does affect the structure of the chiral Lagrangian by inducing O(4) symmetry breaking terms in it. The analysis leading to the Symanzik action reveals that such terms must be at least of $\mathcal{O}(a^2)$.

C. Spurion analysis

At $\mathcal{O}(a^0)$, the Symanzik action is QCD-like. For small a and m we assume the lattice theory to exhibit the same spontaneous symmetry-breaking pattern $SU(N_f)_L \otimes SU(N_f)_R \to SU(N_f)_V$ as continuum QCD.[1] Consequently, the low-energy physics is dominated by Nambu-Goldstone bosons, which acquire small masses due to the soft explicit symmetry breaking by the small quark masses and discretization effects. The low-energy chiral effective field theory is written in terms of these light bosons.

To construct the chiral Lagrangian we follow the standard procedure of spurion analysis. We write a term in the Symanzik Lagrangian as $C_0 O$ where O contains the fields and their derivatives and C_0 is the remaining constant factor. For symmetry breaking terms, O changes under a chiral transformation of the fermionic fields $O \to O'$. We then promote C_0 to the status of a spurion C, with the transformation $C \to C'$ such that $CO = C'O'$. The chiral effective theory is constructed from the Nambu-Goldstone fields and the spurions with the requirement that the action is invariant under chiral transformations if the spurions are transformed as well. Once the terms in the chiral Lagrangian are obtained, each spurion is set to its original constant value $C = C_0$. This procedure guarantees that the chiral effective theory explicitly breaks chiral symmetry in the same manner as the underlying theory

[1] We assume to be outside of the Aoki phase [36–38].

defined by the Symanzik action and reproduces the same Ward identities.

It might appear that one needs many spurion fields to accommodate all the symmetry-breaking operators in the Symanzik action. However, this is not the case. Two spurions that transform in the same way will lead to the same terms in the chiral Lagrangian; therefore, it is enough to consider only one of them. This is discussed in Appendix B. Since we organize the chiral perturbation theory as an expansion in m and a, we do distinguish between spurions that transform the same way but have different m or a dependence.

In the following we list the representative spurions. Shown are the transformation rules for the different spurions under chiral transformations and the constant values to which the spurions are assigned in the end.

$$\mathcal{O}(a^0):\ M\to LMR^\dagger,\ M^\dagger\to RM^\dagger L^\dagger,\qquad M_0=M_0^\dagger=m=\mathrm{diag}(m_1,\ldots,m_{N_f}). \tag{10}$$

This makes the mass term $\bar\psi_L M\psi_R+\bar\psi_R M^\dagger\psi_L$ invariant under the chiral transformations of Eq. (4).

$$\mathcal{O}(a):\quad A\to LAR^\dagger,\quad A^\dagger\to RA^\dagger L^\dagger,\qquad A_0=A_0^\dagger=aI, \tag{11}$$

where I is the flavor identity matrix. The spurion A renders the operators $O_1^{(5)}$ and $O_2^{(5)}$ in Eq. (7) invariant.

$$\begin{aligned}\mathcal{O}(a^2):\quad & B\equiv B_1\otimes B_2\to LB_1R^\dagger\otimes LB_2R^\dagger,\\ & B^\dagger\equiv B_1^\dagger\otimes B_2^\dagger\to RB_1^\dagger L^\dagger\otimes RB_2^\dagger L^\dagger,\\ & C\equiv C_1\otimes C_2\to RC_1L^\dagger\otimes LC_2R^\dagger,\\ & C^\dagger\equiv C_1^\dagger\otimes C_2^\dagger\to LC_1^\dagger R^\dagger\otimes RC_2^\dagger L^\dagger,\\ & B_0=B_0^\dagger=C_0=C_0^\dagger=a^2I\otimes I.\end{aligned} \tag{12}$$

These spurions are introduced to make the symmetry-breaking four-quark operators invariant and therefore carry four flavor indices (see Ref. [39] and references therein). Consider, for example, the operator

$$(\bar\psi\psi)(\bar\psi\psi)=(\bar\psi_L\psi_R)(\bar\psi_L\psi_R)+(\bar\psi_R\psi_L)(\bar\psi_L\psi_R)+(\bar\psi_R\psi_L)(\bar\psi_R\psi_L)+(\bar\psi_L\psi_R)(\bar\psi_R\psi_L). \tag{13}$$

The first term on the right-hand side can be made invariant with the spurion B as can be seen from

$$B\bar\psi_L\psi_R\bar\psi_L\psi_R=B_{ijkl}(\bar\psi_L)_i(\psi_R)_j(\bar\psi_L)_k(\psi_R)_l=\bar\psi_L B_1\psi_R\bar\psi_L B_2\psi_R. \tag{14}$$

Similarly, all the other symmetry-breaking four-quark operators can be made invariant using the spurions B, C, and their Hermitian conjugates.

No additional spurion fields need to be introduced to make the symmetry-breaking bilinears at $\mathcal{O}(a^2)$ invariant. The combinations $AA^\dagger M$ and $\mathrm{tr}(AM^\dagger)A$ already transform in the right way to make $O_5^{(6)}-O_8^{(6)}$ invariant, and their constant values have the right powers in a and m. Another source of potentially new spurions at $\mathcal{O}(a^2)$ are squares of $\mathcal{O}(a)$ spurions. However, note that A^2, $A^\dagger A$, $(A^\dagger)^2$, and $AA^\dagger$ transform exactly like B, C, $B^\dagger$, and $C^\dagger$, respectively, and therefore need not be treated separately.

D. Chiral Lagrangian

The chiral Lagrangian is expanded in powers of p^2, m, and a. Generalizing the standard chiral power counting, the leading-order Lagrangian contains the terms of $\mathcal{O}(p^2,m,a)$, while the terms of $\mathcal{O}(p^4,p^2m,p^2a,m^2,ma,a^2)$ are of next-to-leading order. In terms of the dimensionless expansion parameters m/Λ_χ and $a\Lambda_\chi$, where $\Lambda_\chi\approx 1$ GeV is the typical chiral symmetry-breaking scale, this power counting assumes that the size of the chiral symmetry breaking due to the mass and the discretization effects are of comparable size.[2]

For the Wilson action, all next-to-leading order terms have already been computed in Ref. [7], except for the $\mathcal{O}(a^2)$ terms. We are now in the position to calculate these contributions, which are the ones associated with the spurions B and C. We find the following three new terms (and their Hermitian conjugates)

$$\langle B_1\Sigma^\dagger\rangle\langle B_2\Sigma^\dagger\rangle\to a^2\langle\Sigma^\dagger\rangle^2, \tag{15}$$

$$\langle B_1\Sigma^\dagger B_2\Sigma^\dagger\rangle\to a^2\langle\Sigma^\dagger\Sigma^\dagger\rangle, \tag{16}$$

$$\langle C_1\Sigma\rangle\langle C_2\Sigma^\dagger\rangle\to a^2\langle\Sigma\rangle\langle\Sigma^\dagger\rangle. \tag{17}$$

Here $\Sigma=\exp(2i\Pi/f)$, with Π being the matrix of Nambu-Goldstone fields. Σ transforms under the chiral transformations in Eq. (4) as $\Sigma\to L\Sigma R^\dagger$. The angled brackets are traces over flavor indices, and the arrows indicate assigning $B=B_0$, $C=C_0$, according to Eq. (12).

So far we only considered the operators in the Symanzik action that explicitly break chiral symmetry. Operators that do not break chiral symmetry also contribute at $\mathcal{O}(a^2)$. These operators do not add any new terms to the chiral Lagrangian, but simply modify the coefficients in front of already existing operators. At leading order, for example, the kinetic term is $f^2/4\langle\partial_\mu\Sigma\partial_\mu\Sigma^\dagger\rangle$. There are corrections to f^2 due to the symmetry-conserving terms in the Symanzik action: $f^2\to f^2+a^2K$ (K is another unknown low-energy constant.) This leads to the correction $a^2K\langle\partial_\mu\Sigma\partial\Sigma_\mu^\dagger\rangle$ for the kinetic term. Thus given a term of $\mathcal{O}(p^2)$ there is another term of $\mathcal{O}(a^2p^2)$. In general, we can rewrite the coefficient of any allowed operator in the chiral Lagrangian to obtain a new allowed operator which is $\mathcal{O}(a^2)$ *higher*. These terms are beyond next-to-leading order and are not included in the present work.

[2]A more detailed discussion of the power-counting scheme is given in Sec. IV.

As already mentioned, the operator $O_4^{(6)}$ breaks the O(4) symmetry in the Symanzik action. However, in order to break the O(4) symmetry, while still preserving the discrete hypercubic symmetry, an operator must carry at least four space-time indices. In the chiral Lagrangian, these are provided by the partial derivative ∂_μ, hence the operator is at least of $\mathcal{O}(p^4)$. Adding the fact that it is also an $\mathcal{O}(a^2)$ effect, we see that the leading O(4) symmetry-breaking terms in the chiral Lagrangian are of $\mathcal{O}(p^4a^2)$ (an example is the operator $a^2\Sigma_\mu\langle\partial_\mu\partial_\mu\Sigma\partial_\mu\partial_\mu\Sigma^\dagger\rangle$). Hence, up to the order considered here, O(4) breaking terms can be excluded from the analysis.

Finally we can write down the terms of $\mathcal{O}(a^2)$ which enter the next-to-leading order chiral Lagrangian. In terms of the two parameters

$$\hat{m}\equiv 2B_0 m = 2B_0\,\mathrm{diag}(m_1,\ldots,m_{N_f}),\quad \hat{a}\equiv 2W_0 a, \tag{18}$$

which have been introduced in Ref. [16],[3] these terms are

$$\mathcal{L}[a^2] = -\hat{a}^2 W_6'\langle\Sigma^\dagger+\Sigma\rangle^2 - \hat{a}^2 W_7'\langle\Sigma^\dagger-\Sigma\rangle^2 - \hat{a}^2 W_8'\langle\Sigma^\dagger\Sigma^\dagger+\Sigma\Sigma\rangle. \tag{19}$$

The coefficients W_i' are new unknown low-energy constants. Putting it all together, also quoting the terms in the Lagrangian of $\mathcal{O}(a)$ from Ref. [7],[4] we find

$$\begin{aligned}\mathcal{L}_\chi = {}& \frac{f^2}{4}\langle\partial_\mu\Sigma\partial_\mu\Sigma^\dagger\rangle - \frac{f^2}{4}\langle\hat{m}\Sigma^\dagger+\Sigma\hat{m}\rangle - \hat{a}\frac{f^2}{4}\langle\Sigma^\dagger+\Sigma\rangle - L_1\langle\partial_\mu\Sigma\partial_\mu\Sigma^\dagger\rangle^2 - L_2\langle\partial_\mu\Sigma\partial_\nu\Sigma^\dagger\rangle\langle\partial_\mu\Sigma\partial_\nu\Sigma^\dagger\rangle - L_3\langle(\partial_\mu\Sigma\partial_\mu\Sigma^\dagger)^2\rangle \\ & + L_4\langle\partial_\mu\Sigma\partial_\mu\Sigma^\dagger\rangle\langle\hat{m}\Sigma^\dagger+\Sigma\hat{m}\rangle + \hat{a}W_4\langle\partial_\mu\Sigma\partial_\mu\Sigma^\dagger\rangle\langle\Sigma^\dagger+\Sigma\rangle + L_5\langle\partial_\mu\Sigma\partial_\mu\Sigma^\dagger(\hat{m}\Sigma^\dagger+\Sigma\hat{m})\rangle + \hat{a}W_5\langle\partial_\mu\Sigma\partial_\mu\Sigma^\dagger(\Sigma^\dagger+\Sigma)\rangle \\ & - L_6\langle\hat{m}\Sigma^\dagger+\Sigma\hat{m}\rangle^2 - \hat{a}W_6\langle\hat{m}\Sigma^\dagger+\Sigma\hat{m}\rangle\langle\Sigma^\dagger+\Sigma\rangle - L_7\langle\hat{m}\Sigma^\dagger-\Sigma\hat{m}\rangle^2 - \hat{a}W_7\langle\hat{m}\Sigma^\dagger-\Sigma\hat{m}\rangle\langle\Sigma^\dagger-\Sigma\rangle \\ & - L_8\langle\hat{m}\Sigma^\dagger\hat{m}\Sigma^\dagger+\Sigma\hat{m}\Sigma\hat{m}\rangle - \hat{a}W_8\langle\hat{m}\Sigma^\dagger\Sigma^\dagger+\Sigma\Sigma\hat{m}\rangle + \mathcal{L}[a^2] + \text{higher order terms}.\end{aligned} \tag{20}$$

Here, the parameters L_i are the usual Gasser-Leutwyler coefficients of continuum χPT.

E. Partially quenched QCD

Partially quenched QCD is formally represented by an action with sea, valence, and ghost quarks [40]. We collect the quark fields in $\Psi=(\psi_S,\psi_V)$, where ψ_S describes the sea quarks, and ψ_V contains both the anticommuting valence quarks and commuting ghost fields. The same is done for the antiquark fields. The mass matrix is given by $m=\mathrm{diag}(m_S,m_V')$, with m_S being the $N_f\times N_f$ mass matrix for the sea quarks and $m_V'=\mathrm{diag}(m_V,m_V)$ is the $2N_V\times 2N_V$ mass matrix for the valence quarks and valence ghosts.

We consider partially quenched lattice QCD with Wilson's fermion action Eq. (1) for all three types of fields. The discrete symmetries and the color-gauge symmetry is as in the unquenched case. The group of chiral flavor transformations, however, is different. If all the masses and the Wilson parameter r are set to zero, the action is invariant under transformations in the graded group[5]

$$G_{PQ}=SU(N_f+N_V|N_V)_L\otimes SU(N_f+N_V|N_V)_R. \tag{21}$$

Based on the symmetries of the lattice theory the Symanzik action for partially quenched lattice QCD is obtained as before. The result is easily quoted: One can simply replace ψ and $\bar{\psi}$ in the Symanzik action for the unquenched theory with the extended fields Ψ and $\bar{\Psi}$ because the only two- and four-quark operators that are invariant under the extended, graded flavor group are still $\bar{\Psi}\Psi$ and its square.

The leading term in the Symanzik action is partially quenched QCD, for which the construction of the chiral Lagrangian (first introduced in Ref. [42]) is essentially the same as for the unquenched case [41]. This remains true when higher dimensional operators in the Symanzik action are included, and the analysis of Sec. II D is readily extended to the partially quenched case. In particular, the form of the chiral Lagrangian for partially quenched lattice QCD with Wilson fermions is *exactly* the same as in Eq. (20). The difference is in the definition of the angled brackets, which now denote supertraces, and the interpretation of Σ and m. These need to be appropriately redefined to reflect the larger flavor content of partially quenched χPT.

III. MIXED ACTION

In this section we consider a lattice theory with Wilson sea quarks and Ginsparg-Wilson valence quarks. As before

[3]Unlike in Ref. [16], here we define $\hat{a}$ without the factor of c_{SW}. The coefficient c_{SW} is not kept explicit as we do not use equations of motion, and S_1 contains $ac_1^{(5)}O_1^{(5)}$ besides the Pauli term $ac_{SW}O_2^{(5)}$. Note that c_{SW} does not refer to the coefficient of the clover-leaf term of improved lattice actions.

[4]There are some typos in the Lagrangian [Eq. (2.10)] in Ref. [7]. The Lagrangian in Eq. (20) is the correct one.

[5]See Ref. [41] for a more honest discussion of the symmetry group of partially quenched QCD.

we first construct Symanzik's effective action through $\mathcal{O}(a^2)$. We then derive the chiral Lagrangian for this theory.

A. Lattice action

The use of different lattice fermions for sea and valence quarks is a generalization of partially quenched lattice QCD. Theoretically it too is formulated by an action with sea and valence quarks and valence ghosts. However, in addition to allowing different quark masses ($m_S \neq m_V$), the Dirac operator in the sea sector is chosen to be different from the one for the valence quarks and ghosts. For this reason we will refer to this type of lattice theory as a "mixed action" theory.

The mixed action theory with Wilson sea quarks and Ginsparg-Wilson valence quarks is defined in Ref. [16]. We refer the reader to this reference for details and notation. Here we just quote that the flavor symmetry group of the mixed lattice action is

$$G_M = G_{Sea} \otimes G_{Val},$$

$$G_{Sea} = SU(N_f)_L \otimes SU(N_f)_R,$$

$$G_{Val} = SU(N_V|N_V)_L \otimes SU(N_V|N_V)_R. \tag{22}$$

The quark mass term in the mixed action breaks both G_{Sea} and G_{Val}. However, in the massless case G_{Val} becomes an exact symmetry [29] while G_{Sea} is still broken by the Wilson term. Because of the different Dirac operators there is no symmetry transformation that mixes the valence and sea sectors, in contrast to the partially quenched case [cf. Eq. (21)].

B. Symanzik action

The Symanzik action for the mixed theory can be derived using the results of the previous section. It is convenient to separately discuss three types of terms—those that contain only sea quark fields, those that contain only valence fields, and those that contain both.

For the first type of terms the analogy with the previous section is evident: the relevant symmetry group is $G_{Sea} = G$, and the explicit symmetry-breaking structure is the same. Thus, all bilinear operators $O_i^{(n)}(\psi)$ and four-quark operators $O_i^{(n)}(\psi,\psi)$, listed in Sec. II B, appear in Symanzik's action, once ψ is replaced by ψ_S.[6]

The construction of the purely valence terms is also analogous to the one for the Wilson action in Sec. II B. However, there are stricter symmetry constraints for Ginsparg-Wilson quarks and ghosts because the Ginsparg-Wilson action possesses an exact chiral symmetry when the quark mass is set to zero. All operators without any insertions of the quark mass must therefore be chirally invariant. Further, operators with insertions of the quark mass m must become chirally invariant when m is transformed like a spurion field. In particular, all dimension-3 and dimension-5 operators are forbidden. Several dimension-6 operators at $\mathcal{O}(a^2)$ are also excluded. Only the bilinears $O_1^{(6)} - O_5^{(6)}$, $O_7^{(6)}$ of Eq. (8) and the four-quark operators $O_i^{(6)}(\psi_V,\psi_V)$, $i = 11$, 12, 16, and 17, of Eq. (9), are G_{Val} invariant and are therefore allowed.

For terms of the third type, note that the symmetry group G_M forbids bilinears that mix valence and sea quarks. Thus, the only terms containing both sea and valence fields are four-quark operators that are products of two bilinears—one from each sector. Again, only the four terms $O_i^{(6)}(\psi_S,\psi_V)$, $i = 11$, 12, 16, and 17, are allowed. All the others break the chiral symmetry in the valence sector when $m_V = 0$.

From these considerations it follows that the Symanzik action for the mixed lattice action up to and including $\mathcal{O}(a^2)$ contains the following terms:

$$S_0: \quad O_i^{(4)}(\psi_S), \quad O_i^{(4)}(\psi_V), \quad i = 1,2. \tag{23}$$

$$S_1: \quad O_i^{(5)}(\psi_S), \quad i = 1,2. \tag{24}$$

$$S_2, \text{ bilinears:} \quad O_i^{(6)}(\psi_S), \quad i = 1-8,$$

$$O_i^{(6)}(\psi_V), \quad i = 1-5,7. \tag{25}$$

$$S_2, \text{ four-quark operators:} \quad O_i^{(6)}(\psi_S,\psi_S), \quad i = 9-18,$$

$$O_i^{(6)}(\psi_V,\psi_V), \quad O_i^{(6)}(\psi_S,\psi_V), \quad i = 11,12,16,17. \tag{26}$$

[6] We make the dependence of bilinear operators on the fields explicit by writing $O(\psi)$. All the four-quark operators that we consider have the structure $O(\psi_1,\psi_2) = \bar{\psi}_1 \Omega^J \psi_1 \bar{\psi}_2 \Omega^J \psi_2$. Here Ω denotes any combination of Clifford algebra elements and color group generators with a combined index J, which is contracted.

C. Spurion analysis

S_0, the leading term in the Symanzik action, is just the continuum action of partially quenched QCD. In the $m\to 0$ limit it is invariant under the flavor symmetry group G_{PQ} inEq. (21), which is larger than G_M [Eq. (22)], the symmetry group of the underlying lattice action. For a sufficiently small a (and m), S_0 determines the spontaneous symmetry-breaking pattern and the symmetry properties of the Nambu-Goldstone particles in the theory. It follows that the mixed theory contains the same set of light particles as partially quenched QCD.

For the construction of the chiral effective theory, we introduce spurion fields that make the entire Symanzik action invariant under G_{PQ}. Notice that all the operators proportional to a and a^2 break G_{PQ}, the flavor symmetry of the leading term. This is obvious for operators that appear with sea quark fields only, such as the dimension 5 operators. However, even if an operator appears "symmetrically" in ψ_S and ψ_V, as in Eq. (25), it still breaks G_{PQ}. To illustrate this point let us consider any of the bilinear terms, suppressing all γ matrices and color-group generators. Any bilinear that is invariant under all rotations of G_{PQ} must have the flavor structure $\bar{\Psi}\Psi=\bar{\psi}_S\psi_S+\bar{\psi}_V\psi_V$. In general, though, $\bar{\psi}_S\psi_S$ and $\bar{\psi}_V\psi_V$ will not appear in the Symanzik action with equal coefficients, and therefore will not be invariant under transformations in G_{PQ} that mix the sea and valence sectors.

As before we begin the construction of the chiral Lagrangian by listing the representative spurions required at each order in a to make the Symanzik action invariant. Shown are the transformation properties of the spurions under chiral transformations in G_{PQ} and the constant structures to which the spurion fields are assigned in the end. Since different operators appear in the sea and valence sector, it is convenient to introduce the projection operators

$$P_S=\mathrm{diag}(I_S,0),\quad P_V=\mathrm{diag}(0,I_V), \tag{27}$$

where I_S denotes the $N_f\times N_f$ identity matrix in the sea sector, and I_V the $2N_V\times 2N_V$ identity matrix in the space of valence quarks and ghosts (recall that ψ_V includes both valence quarks and ghosts).

$$\mathcal{O}(a^0):\quad M\to LMR^\dagger,\quad M^\dagger\to RM^\dagger L^\dagger,$$
$$M_0=M_0^\dagger=m=\mathrm{diag}(m_S,m_V'). \tag{28}$$
$$\mathcal{O}(a):\quad A\to LAR^\dagger,\quad A^\dagger\to RA^\dagger L^\dagger,$$
$$A_0=A_0^\dagger=aP_S. \tag{29}$$

The last spurion arises from the sea sector symmetry breaking terms at $\mathcal{O}(a)$.

The quark bilinears $O_1^{(6)}-O_4^{(6)}$ at $\mathcal{O}(a^2)$ couple fields with the same chirality. Since there are bilinears for both sea and valence fields we obtain the following spurions:

$$\mathcal{O}(a^2),\ \text{bilinears:}\quad B\to LBL^\dagger,\quad C\to RCR^\dagger,$$
$$B_0,\ C_0\in\{a^2P_S,a^2P_V\}. \tag{30}$$

No *additional* spurion fields need to be introduced to make the remaining bilinears $O_5^{(6)}-O_8^{(6)}$ invariant. Appropriate combinations of the spurion fields M and A (and their complex conjugates) have already the required transformation behavior and the correct constant structure.

We can distinguish two types of four-quark operators. The first type is made of bilinears that only couple fields of the same chirality. These operators appear with only sea or valence fields as well as in the "mixed" form $O(\psi_S,\psi_V)$. The remaining four-quark operators, which couple fields with opposite chirality, appear only with sea quarks. We therefore introduce the following spurions:

$$\mathcal{O}(a^2),\ \text{four-quark operators:}$$
$$D\equiv D_1\otimes D_2\to LD_1L^\dagger\otimes LD_2L^\dagger,$$
$$E\equiv E_1\otimes E_2\to RE_1R^\dagger\otimes RE_2R^\dagger,$$
$$F\equiv F_1\otimes F_2\to LF_1L^\dagger\otimes RF_2R^\dagger,$$
$$G\equiv G_1\otimes G_2\to RG_1R^\dagger\otimes LG_2L^\dagger,$$
$$D_0,E_0,F_0,G_0\in\{a^2P_S\otimes P_S,a^2P_S\otimes P_V,a^2P_V\otimes P_V\}, \tag{31}$$
$$H\equiv H_1\otimes H_2\to LH_1R^\dagger\otimes LH_2R^\dagger,$$
$$H^\dagger\equiv H_1^\dagger\otimes H_2^\dagger\to RH_1^\dagger L^\dagger\otimes RH_2^\dagger L^\dagger,$$
$$J\equiv J_1\otimes J_2^\dagger\to LJ_1R^\dagger\otimes RJ_2^\dagger L^\dagger,$$
$$J^\dagger\equiv J_1^\dagger\otimes J_2\to RJ_1^\dagger L^\dagger\otimes LJ_2R^\dagger,$$
$$H_0=H_0^\dagger=J_0=J_0^\dagger=a^2P_S\otimes P_S. \tag{32}$$

Squaring the spurions of $\mathcal{O}(a)$ does not lead to any new spurions.

D. Chiral Lagrangian

The chiral Lagrangian for the mixed action theory including the cutoff effects linear in a is derived in Ref. [16]. Terms of $\mathcal{O}(a^2)$ are constructed from the spurions in Eqs. (30)–(32). It is easily checked that the spurions B, C, D, and E lead necessarily to operators higher than $\mathcal{O}(a^2)$ [at least $\mathcal{O}(p^2a^2,ma^2)$], so we can ignore them. From the other spurions we obtain the following independent operators (and their Hermitian conjugates):

$$\langle F_1\Sigma F_2\Sigma^\dagger\rangle\to a^2\langle\tau_3\Sigma\tau_3\Sigma^\dagger\rangle, \tag{33}$$
$$\langle H_1\Sigma^\dagger H_2\Sigma^\dagger\rangle\to a^2\langle P_S\Sigma^\dagger P_S\Sigma^\dagger\rangle, \tag{34}$$
$$\langle H_1\Sigma^\dagger\rangle\langle H_2\Sigma^\dagger\rangle\to a^2\langle P_S\Sigma^\dagger\rangle\langle P_S\Sigma^\dagger\rangle, \tag{35}$$

$$\langle J_1\Sigma^\dagger\rangle\langle J_2^\dagger\Sigma\rangle \to a^2\langle P_S\Sigma^\dagger\rangle\langle P_S\Sigma\rangle. \tag{36}$$

For Eq. (33) we use the fact that $P_S=\frac{1}{2}(I+\tau_3)$ and $P_V=\frac{1}{2}(I-\tau_3)$, with $\tau_3=\mathrm{diag}(I_S,-I_V)$. When assigning $F_{1,2}=(I\pm\tau_3)$ and expanding, the fields Σ and $\Sigma^\dagger$ are next to each other and cancel whenever the identity matrix is inserted, so the only nontrivial operator is the one shown in Eq. (33).

We conclude that for the mixed action theory with Wilson sea and Ginsparg-Wilson valence quarks the terms of $\mathcal{O}(a^2)$ in the chiral Lagrangian are

$$\begin{aligned}\mathcal{L}[a^2]=&-\hat{a}^2W_M\langle\tau_3\Sigma\tau_3\Sigma^\dagger\rangle-\hat{a}^2W_6'\langle P_S\Sigma^\dagger+\Sigma P_S\rangle^2\\&-\hat{a}^2W_7'\langle P_S\Sigma^\dagger-\Sigma P_S\rangle^2\\&-\hat{a}^2W_8'\langle P_S\Sigma^\dagger P_S\Sigma^\dagger+\Sigma P_S\Sigma P_S\rangle.\end{aligned} \tag{37}$$

The parameters $\hat{m}$ and $\hat{a}$ are defined as in the unquenched case in Eq. (18). Note that the projector P_S in the last three terms implies that these operators involve only the sea-sea block of Σ.

The final result, including the terms from Ref. [16], reads

$$\begin{aligned}\mathcal{L}_\chi=&\frac{f^2}{4}\langle\partial_\mu\Sigma\partial_\mu\Sigma^\dagger\rangle-\frac{f^2}{4}\langle\hat{m}\Sigma^\dagger+\Sigma\hat{m}\rangle-\hat{a}\frac{f^2}{4}\langle P_S\Sigma^\dagger+P_S\Sigma\rangle-L_1\langle\partial_\mu\Sigma\partial_\mu\Sigma^\dagger\rangle^2-L_2\langle\partial_\mu\Sigma\partial_\nu\Sigma^\dagger\rangle\langle\partial_\mu\Sigma\partial_\nu\Sigma^\dagger\rangle\\&-L_3\langle(\partial_\mu\Sigma\partial_\mu\Sigma^\dagger)^2\rangle+L_4\langle\partial_\mu\Sigma\partial_\mu\Sigma^\dagger\rangle\langle\hat{m}\Sigma^\dagger+\Sigma\hat{m}\rangle+\hat{a}W_4\langle\partial_\mu\Sigma\partial_\mu\Sigma^\dagger\rangle\langle P_S\Sigma^\dagger+\Sigma P_S\rangle+L_5\langle\partial_\mu\Sigma\partial_\mu\Sigma^\dagger(\hat{m}\Sigma^\dagger+\Sigma\hat{m})\rangle\\&+\hat{a}W_5\langle\partial_\mu\Sigma\partial_\mu\Sigma^\dagger(P_S\Sigma^\dagger+\Sigma P_S)\rangle-L_6\langle\hat{m}\Sigma^\dagger+\Sigma\hat{m}\rangle^2-\hat{a}W_6\langle\hat{m}\Sigma^\dagger+\Sigma\hat{m}\rangle\langle P_S\Sigma^\dagger+\Sigma P_S\rangle-L_7\langle\hat{m}\Sigma^\dagger-\Sigma\hat{m}\rangle^2\\&-\hat{a}W_7\langle\hat{m}\Sigma^\dagger-\Sigma\hat{m}\rangle\langle P_S\Sigma^\dagger-\Sigma P_S\rangle-L_8\langle\hat{m}\Sigma^\dagger\hat{m}\Sigma^\dagger+\Sigma\hat{m}\Sigma\hat{m}\rangle-\hat{a}W_8\langle\hat{m}\Sigma^\dagger P_S\Sigma^\dagger+\Sigma P_S\Sigma\hat{m}\rangle\\&+\mathcal{L}[a^2]+\text{higher order terms}.\end{aligned} \tag{38}$$

The chiral Lagrangian for the mixed action theory at $\mathcal{O}(a^2)$ has four terms while there are only three terms at this order in the chiral Lagrangian for the Wilson action. The reason that the mixed theory has an additional operator (and consequently an additional unknown low-energy constant multiplying it) is its reduced symmetry group, G_M in Eq. (22), compared to G_{PQ} in Eq. (21). The use of different Dirac operators for sea and valence quarks forbids transformations between the sea and valence sectors and allows the additional term $\langle\tau_3\Sigma\tau_3\Sigma^\dagger\rangle$ in Eq. (37).

The presence of more terms in the Lagrangian does not entail that chiral expressions for all observables in the mixed theory depend on more free parameters than in χPT for the Wilson action. By definition, the correlation functions measured in numerical simulations involve operators that are made of valence quarks only, and the enhanced chiral symmetry of the Ginsparg-Wilson fields plays an important role in that sector. The chiral symmetry leads to constraints on operators in the Symanzik action that contain valence fields, and ultimately it restricts and simplifies the form of chiral expressions for valence quark observables. This can already be seen by considering the terms in $\mathcal{L}[a^2]$ with coefficients W_6', W_7', and W_8' [see Eq. (37)]. These terms depend only on the sea-sea block of Σ. This entails that all the multi-pion interaction vertices obtained from these terms necessarily contain some mesons with at least a single sea quark in them. Consequently, these terms cannot contribute at tree level to any expectation value of operators made entirely out of valence fields. This is easily understood: the W' terms arise from the breaking of chiral symmetry in the sea sector by the Wilson term, and this breaking is communicated to the valence sector only through loop effects. A more concrete demonstration of this point is provided by the calculation of the pseudo scalar valence-valence meson mass in the next section.

IV. APPLICATION

We conclude our analysis of the chiral effective theories for the Wilson action and the mixed action theory with an explicit calculation of the light meson masses. Before presenting the calculations, however, a discussion of the chiral power counting is appropriate.

A. Power counting

χPT reproduces low-momentum correlation functions of the underlying theory, provided that the typical momentum p and the mass of the Nambu-Goldstone boson M_{NGB} are sufficiently small, $p\ll\Lambda_\chi$ and $M_{NGB}\ll\Lambda_\chi$. The standard convention is to consider p and M_{NGB} as formally of the same order, and take a single expansion parameter $\epsilon\sim M_{NGB}^2/\Lambda_\chi^2\sim p^2/\Lambda_\chi^2$. Thus, a typical next-to-leading order (one-loop) expression for a correlation function in χPT has the structure

$$\begin{aligned}C&=C_{\mathrm{LO}}+C_{\mathrm{NLO}}+\cdots,\\C_{\mathrm{LO}}&=\mathcal{O}(\epsilon)=\mathcal{O}\left(\frac{M_{NGB}^2}{\Lambda_\chi^2},\ \frac{p^2}{\Lambda_\chi^2}\right),\\C_{\mathrm{NLO}}&=\mathcal{O}(\epsilon^2)=\mathcal{O}\left(\frac{M_{NGB}^4}{\Lambda_\chi^4},\ \frac{p^4}{\Lambda_\chi^4},\ \frac{M_{NGB}^2p^2}{\Lambda_\chi^4}\right).\end{aligned} \tag{39}$$

In some cases of interest the momentum scale and the Nambu-Goldstone boson mass are significantly different, $p \ll M_{NGB}$ for instance. In such a case one could treat the two dimensionless parameters separately and introduce another expansion parameter p/M_{NGB}. However, as long as both M_{NGB}^2/Λ_χ^2 and p^2/Λ_χ^2 are sufficiently small, Eq. (39) still holds. Consequently, a reasonable approach in the case that p and M_{NGB} are very different is to take Eq. (39) and to ignore (or not calculate) terms that are smaller than the error associated with the larger expansion parameter.

In the case of χPT for lattice theories there are two possible sources of explicit chiral symmetry breaking: the quark masses and the lattice spacing. Consequently, the mass of the pseudo-Nambu-Goldstone boson is given by $M_{NGB}^2/\Lambda_\chi^2 \sim m/\Lambda_\chi + a\Lambda_\chi$. The discussion of the previous paragraph applies here as well: we can take $\varepsilon \sim p^2/\Lambda_\chi^2 \sim m/\Lambda_\chi \sim a\Lambda_\chi$ and Eq. (39) (properly extended) still holds. As long as the largest of these parameters is sufficiently small, this is a consistent power-counting scheme, and Eq. (39) is applicable even when some of the dimensionless parameters are significantly smaller than the others. This is the power-counting that is used in organizing the terms in the Lagrangians in Eqs. (20) and (38).

A different power-counting scheme does need to be employed in some cases. To illustrate this we consider a realistic example: for some fermion actions there are no discretization effects at $\mathcal{O}(a)$. This is the case, for example, for nonperturbatively $\mathcal{O}(a)$ improved Wilson fermions. If, in addition, the lattice spacing in a simulation is large such that $a^2\Lambda_\chi^2 \sim m/\Lambda_\chi$, an expansion in two parameters may be required, and the leading-order contributions are $\mathcal{O}(p^2/\Lambda_\chi^2, m/\Lambda_\chi, a^2\Lambda_\chi^2)$.

B. Pseudoscalar-meson masses

We now turn to the calculation of the pseudoscalar-meson masses. As in Refs. [7] and [16], we only consider mesons with different valence flavor indices ($A \neq B$). In addition, we also take the sea quark masses and the valence quark masses to be separately degenerate. For the partially quenched Wilson action we find

$$\begin{aligned} M_{AB}^2 = {} & (\hat{m}_{\mathrm{Val}} + \hat{a}) + \frac{1}{16 N_f f^2 \pi^2} (\hat{m}_{\mathrm{Val}} + \hat{a}) [\hat{m}_{\mathrm{Val}} - \hat{m}_{\mathrm{Sea}} \\ & + (2\hat{m}_{\mathrm{Val}} - \hat{m}_{\mathrm{Sea}} + \hat{a}) \ln(\hat{m}_{\mathrm{Val}} + \hat{a})] - \frac{8}{f^2} (\hat{m}_{\mathrm{Val}} + \hat{a}) \\ & \times [N_f (L_4 \hat{m}_{\mathrm{Sea}} + W_4 \hat{a}) + L_5 \hat{m}_{\mathrm{Val}} + W_5 \hat{a}] \\ & + \frac{8 N_f}{f^2} [2 L_6 \hat{m}_{\mathrm{Val}} \hat{m}_{\mathrm{Sea}} + W_6 (\hat{m}_{\mathrm{Val}} + \hat{m}_{\mathrm{Sea}}) \hat{a} + 2 W_6' \hat{a}^2] \\ & + \frac{16}{f^2} [L_8 \hat{m}_{\mathrm{Val}}^2 + W_8 \hat{m}_{\mathrm{Val}} \hat{a} + W_8' \hat{a}^2] + \mathcal{O}(\epsilon^3), \end{aligned} \tag{40}$$

where N_f is the number of sea quark flavors.

Next, we consider the mixed action theory. A direct calculation shows that *there are no $\mathcal{O}(a^2)$ corrections to the pseudoscalar-meson mass*. The expression for M_{AB} is, therefore, the same as in Ref. [16], which we quote here for completeness:[7]

$$\begin{aligned} M_{AB}^2 = {} & \hat{m}_{\mathrm{Val}} + \frac{1}{16 N_f f^2 \pi^2} \hat{m}_{\mathrm{Val}} [\hat{m}_{\mathrm{Val}} - \hat{m}_{\mathrm{Sea}} \\ & - \hat{a} + (2\hat{m}_{\mathrm{Val}} - \hat{m}_{\mathrm{Sea}} - \hat{a}) \ln(\hat{m}_{\mathrm{Val}})] \\ & - \frac{8}{f^2} \hat{m}_{\mathrm{Val}} [(L_5 - 2L_8) \hat{m}_{\mathrm{Val}} \\ & + N_f (L_4 - 2L_6) \hat{m}_{\mathrm{Sea}} + N_f (W_4 - W_6) \hat{a}] + \mathcal{O}(\epsilon^3). \end{aligned} \tag{41}$$

The fact that there are no $\mathcal{O}(a^2)$ contributions at next-to-leading order is not as surprising as one might think at first. Only the valence quark mass term breaks the chiral symmetry for Ginsparg-Wilson fermions. Hence the pseudoscalar-meson mass is proportional to the quark mass and vanishes in the limit $m_{Val} \to 0$. It follows that any lattice contribution to M_{AB}^2 is suppressed by at least one factor of m_{Val}, and the largest lattice correction quadratic in the lattice spacing is of $\mathcal{O}(m_{Val} a^2)$. Note that this higher order term becomes the leading discretization effect in the meson mass if an $\mathcal{O}(a)$ improved Wilson action is used for the sea quarks. This example illustrates the beneficial properties of Ginsparg-Wilson fermions, which are preserved even in the presence of a "non-Ginsparg-Wilson" sea sector.

V. SUMMARY

In the previous sections we presented chiral Lagrangian for two lattice theories: one with Wilson fermions and the other with Wilson sea fermions and Ginsparg-Wilson valence fermions. One consequence of the analysis is that corrections to the low-energy constants of continuum χPT (coming from symmetry-conserving discretization effects) are of $\mathcal{O}(a^2)$. Since the coefficients in the chiral Lagrangian themselves multiply terms of $\mathcal{O}(p^2)$ (B_0 and f) and $\mathcal{O}(p^4)$ (Gasser-Leutwyler coefficients), such effects can only be detected by measuring observables at the accuracy of $\mathcal{O}(a^2 p^2)$ and $\mathcal{O}(a^2 p^4)$, respectively. Another important discretization effect that enters the Symanzik action at $\mathcal{O}(a^2)$ is the breaking of O(4) rotational invariance. An O(4) breaking term in the chiral Lagrangian, however, must contain at least four derivatives, so it is a higher-order term as well [at least $\mathcal{O}(a^2 p^4)$].

The main purpose of constructing chiral effective theories for lattice actions is to capture discretization effects analytically and to guide the chiral extrapolations of numerical lattice data. This is achieved by the explicit a dependence of observables that can be calculated in these effective theories.

[7] In Ref. [16] the number of flavors N_f was set to 3.

In particular, the chiral Lagrangian is sufficient for the determination of the pseudoscalar-meson masses. For the calculation of matrix elements, such as f_π, an additional a dependence coming from the effective continuum operators needs to be taken into account, but no conceptual difficulties are expected to arise in this step.

There is a more subtle cutoff dependence that is not explicit in the Symanzik action. All the unknown coefficients in the Symanzik action, including c_{SW}, implicitly include short-distance effects that make them a dependent. For the chiral Lagrangian this results in an implicit a dependence of the low-energy constants [7]. The existence of a well-defined continuum limit implies that all the parameters of continuum χPT, such as the Gasser-Leutwyler coefficients, have a leading a-independent part. The other coefficients in the Lagrangian, loosely referred to as the W's, are expected to show a weak, logarithmic a dependence.

From a practical point of view there are several ways to approach this issue. One option is not to vary a. For a given lattice spacing a, one fits the chiral forms by only varying the quark masses. Note that even if a is not varied, the inclusion of the discretization effects in the chiral expressions, particularly in the chiral logarithms, is more accurate than simply using the continuum expressions. From the fits, one extracts values for the coefficients in the Lagrangian, including the W's. Applying this procedure again, independently and for lattice data with different lattice spacings, these parameters are allowed to vary with a. It should be verified that the values obtained in this way for the continuum low-energy constants do not exhibit an a dependence beyond the error expected at the order of the calculation. It might be the case that the a dependence of the W's is so slow that they do not change much over the range of lattice spacings simulated. In that case a simultaneous fit in a and m might be appropriate. More generally, a simultaneous fit can be used when the a dependence of the W's is known. In particular, provided that the equations of motion can be consistently applied through $\mathcal{O}(a^2)$ to eliminate all but the Pauli term in the Symanzik action at $\mathcal{O}(a)$, one can treat the W's that enter the chiral Lagrangian at $\mathcal{O}(a)$ as being proportional to a single parameter c_{SW}. If the a dependence of this parameter is numerically known, one has control over all the a dependence in the chiral Lagrangian at $\mathcal{O}(a)$, pushing the unknown a dependence to $\mathcal{O}(a^2)$. This is "automatically" done in $\mathcal{O}(a)$-improved lattice simulations.

All the qualifications of the previous paragraphs notwithstanding, chiral perturbation theory for lattice actions provides a better understanding of the relation between lattice observables and their continuum counterparts. It is encouraging that at $\mathcal{O}(a^2)$ only a few new low-energy constants are needed. Thus χPT is still predictive at this order and it is likely to play an important role in the extraction of quantitative predictions of QCD from numerical simulations.

ACKNOWLEDGMENTS

We acknowledge support in part by U.S. DOE Grants No. DF-FC02-94ER40818, No. DE-AC03-76SF00098, No. DE-FG03-96ER40956/A006, and No. DE-FG02-91ER40676. G.R. would like to thank the Center for Theoretical Physics at MIT, and N.S. would like to thank the Nuclear Theory Group at LBNL for kind hospitality and financial support during parts of this work.

APPENDIX A: FLAVOR, COLOR, AND DIRAC STRUCTURE OF FOUR-QUARK OPERATORS IN THE SYMANZIK ACTION

In this section we discuss four-quark operators in the Symanzik action that are invariant under the vector flavor symmetry group $SU(N_f)_V$, the color-gauge group $SU(N_c)$, the hypercubic transformations, parity, and charge conjugation.

It is convenient to label the quark fields $\bar{\psi}^{(1)}$, $\psi^{(2)}$, $\bar{\psi}^{(3)}$, $\psi^{(4)}$. Considering first the flavor group, we write the most general term (summation over repeated indices is assumed)

$$C_{i_1 i_2 i_3 i_4} \bar{\psi}^{(1)}_{i_1} \psi^{(2)}_{i_2} \bar{\psi}^{(3)}_{i_3} \psi^{(4)}_{i_4}. \tag{A1}$$

There are only two possibilities for C (up to a multiplicative constant), which make this term invariant:

$$C_{i_1 i_2 i_3 i_4} = \delta_{i_1 i_2} \delta_{i_3 i_4}, \quad \text{and} \quad C_{i_1 i_2 i_3 i_4} = \delta_{i_1 i_4} \delta_{i_3 i_2}. \tag{A2}$$

These correspond (up to a sign from the interchange of the Grassman fields) to

$$\bar{\psi}^{(1)}_i \psi^{(2)}_i \;\; \bar{\psi}^{(3)}_j \psi^{(4)}_j \quad \text{and} \quad \bar{\psi}^{(1)}_i \psi^{(4)}_i \;\; \bar{\psi}^{(3)}_j \psi^{(2)}_j. \tag{A3}$$

At this point we are free to redefine the labels on the quark fields in the second term by exchanging the second and fourth indices. In this way we only need to consider the first invariant in the last equation. From this point on, the order of the fields will remain fixed, so the labels of the fields can be dropped, and the trivial flavor contractions will be suppressed.

The same analysis holds for the color structure. The difference is that now we have already exhausted the freedom to reshuffle and relabel the fields—they are distinguishable by their flavor indices—and so there are two genuinely different invariant operators:

$$\bar{\psi}_a \psi_a \;\; \bar{\psi}_b \psi_b, \quad \text{and} \quad \bar{\psi}_a \psi_b \;\; \bar{\psi}_b \psi_a. \tag{A4}$$

We find it convenient to "untwist" the color indices in the second term using the Fierz rule

$$\delta_{ac}\delta_{bd} = \frac{1}{N_c}\delta_{ab}\delta_{cd} + 2t^e_{ab}t^e_{cd}, \tag{A5}$$

where the t^e are the generators of the color group in the fundamental representation. The possible terms can now be written as

$$\bar{\psi}\psi \;\; \bar{\psi}\psi, \quad \text{and} \quad \bar{\psi}t^a\psi \;\; \bar{\psi}t^a\psi, \tag{A6}$$

where the contraction of color indices is straightforward and can also be suppressed.[8]

Finally, we take into account the Dirac structure. To maintain the hypercubic symmetry and parity invariance, the space-time indices must be contracted in pairs and γ_5 matrices must appear in pairs. One set of invariant terms can be obtained by adding a Dirac structure to the terms in Eq. (A6) in the following way:

$$\bar{\psi}\Gamma^A\psi \;\; \bar{\psi}\Gamma^A\psi \quad \text{and} \quad \bar{\psi}\Gamma^A t^a\psi \;\; \bar{\psi}\Gamma^A t^a\psi, \tag{A7}$$

where $\bar{\psi}\Gamma^A\psi$ can be a scalar, pseudoscalar, vector, pseudovector, or a tensor, with A denoting the appropriate space-time indices. In addition, as in the cases of color and flavor, it is also possible to have the Dirac matrices connect the first and fourth fields, and the second and the third. These operators, however, are linearly dependent on the previous terms, because of the identity

$$\Gamma^A_{\alpha\delta}\Gamma^B_{\gamma\beta} = \sum_{C,D} K^{AB}_{CD}\Gamma^C_{\alpha\beta}\Gamma^D_{\gamma\delta},$$

$$K^{AB}_{CD} = \frac{1}{16}\mathrm{Tr}[\Gamma^A\Gamma^D\Gamma^B\Gamma^C]. \tag{A8}$$

This identity holds for any pair of Clifford algebra elements and not only for the case $A=B$ in which we are interested.

This completes the derivation of the list of four-quark operators in Eq. (9). There are several equivalent sets of operators. A different path leads to the list of operators that appear in Ref. [13]: starting with the color structure, one considers the invariants of Eq. (A3), but with color indices instead of the flavor ones. Fierz rules can be used to replace the identity matrices with color generators that are either "straight" (connecting the first and second fields, and the third and fourth) or "crossed." As was done above with respect to flavor, it is possible to choose a convention in which all the color generators are straight (reorder the fields). Thus the only invariant is $\bar{\psi}t^a\psi\bar{\psi}t^a\psi$. Once that convention is fixed, one again faces the possibility of crossed Dirac and flavor indices. The Dirac matrices are straightened in the same manner as above. Finally, using Fierz rules for the flavor group, one can also eliminate the crossed Kronecker deltas at the price of introducing terms with flavor group generators β^i. The final set of invariants is $\bar{\psi}\Gamma^A t^a\psi\bar{\psi}\Gamma^A t^a\psi$ and $\bar{\psi}\Gamma^A t^a\beta^i\psi\bar{\psi}\Gamma^A t^a\beta^i\psi$.

[8]In fact, the color structure is completely inconsequential in the construction of the chiral Lagrangian.

APPENDIX B: REDUNDANCY OF SPURIONS

We note the following fact: If A and B are two spurions, which are of the same order in the (m,a) power counting, transform in the same manner, and have a similar "original" structure, $B_0 = kA_0$ where k carries no indices, then one can use only one of them to construct the chiral action. The reason is the following. If $f(A)$ is an operator in the chiral Lagrangian, which contains A, then $f(B)$ is also an allowed term because of the assumption that both spurions transform in the same way. Since the spurions transform linearly, the relation between the constants A_0 and B_0 also holds for the spurions. Assuming a power expansion in the spurions, this leads to $f(B) = k^n f(A)$. Recalling that each operator in the chiral Lagrangian appears with an unknown coefficient, we have in the Lagrangian

$$K_1 f(A) + K_2 f(B) = (K_1 + K_2 k^n) f(A). \tag{B1}$$

Since neither K_1 nor K_2 are known (and in most cases neither is k), this is equivalent to considering only a single term in the Lagrangian, $Kf(A)$, which we would have written anyway if we had considered only the first spurion.

Example: At $\mathcal{O}(a)$ the Symanzik Lagrangian contains the terms

$$ac_1\bar{\psi}_L D_\mu D_\mu \psi_R + ac_2\bar{\psi}_L i\sigma_{\mu\nu}F_{\mu\nu}\psi_R. \tag{B2}$$

To make these terms invariant one can introduce two spurions A and B, which are flavor matrices that transform as $A \to LAR^\dagger$, $B \to LBR^\dagger$. Both are $\mathcal{O}(a)$, and their constant values are $A_0 = ac_1 I$, $B_0 = ac_2 I$ (here I is the flavor identity matrix). With these spurions it is possible to construct the following invariant terms in the chiral Lagrangian [at $\mathcal{O}(a)$]:

$$K_1\langle A\Sigma^\dagger\rangle + K_2\langle B\Sigma^\dagger\rangle \tag{B3}$$

but after setting the spurions to their constant values we obtain only a single term

$$K_1 ac_1\langle\Sigma^\dagger\rangle + K_2 ac_2\langle\Sigma^\dagger\rangle = aK'\langle\Sigma^\dagger\rangle, \tag{B4}$$

which we would have writing down even if we had kept only A in the analysis.

[1] S. Weinberg, Physica A **96**, 327 (1979).
[2] J. Gasser and H. Leutwyler, Nucl. Phys. **B250**, 465 (1985).
[3] W.-J. Lee and S.R. Sharpe, Phys. Rev. D **60**, 114503 (1999).
[4] MILC Collaboration, C. Bernard, Phys. Rev. D **65**, 054031 (2002).
[5] C. Aubin and C. Bernard, Phys. Rev. D **68**, 034014 (2003).
[6] S.R. Sharpe and R.J. Singleton, Jr., Phys. Rev. D **58**, 074501 (1998).
[7] G. Rupak and N. Shoresh, Phys. Rev. D **66**, 054503 (2002).
[8] S. Myint and C. Rebbi, Nucl. Phys. **B421**, 241 (1994).
[9] A.R. Levi, V. Lubicz, and C. Rebbi, Phys. Rev. D **56**, 1101 (1997).
[10] K. Symanzik, NATO Advanced Study Institutes Series: Series B, Physics, Vol. 59 (Plenum, New York, 1980).
[11] K. Symanzik, Nucl. Phys. **B226**, 187 (1983).
[12] K. Symanzik, Nucl. Phys. **B226**, 205 (1983).
[13] B. Sheikholeslami and R. Wohlert, Nucl. Phys. **B259**, 572 (1985).

[14] M. Lüscher, S. Sint, R. Sommer, and P. Weisz, Nucl. Phys. **B478**, 365 (1996).
[15] qq+q Collaboration, F. Farchioni, C. Gebert, I. Montvay, E. Scholz, and L. Scorzato, Phys. Lett. B **561**, 102 (2003).
[16] O. Bär, G. Rupak, and N. Shoresh, Phys. Rev. D **67**, 114505 (2003).
[17] D.B. Kaplan, Phys. Lett. B **288**, 342 (1992).
[18] Y. Shamir, Nucl. Phys. **B406**, 90 (1993).
[19] V. Furman and Y. Shamir, Nucl. Phys. **B439**, 54 (1995).
[20] R. Narayanan and H. Neuberger, Phys. Lett. B **302**, 62 (1993).
[21] R. Narayanan and H. Neuberger, Nucl. Phys. **B412**, 574 (1994).
[22] R. Narayanan and H. Neuberger, Nucl. Phys. **B443**, 305 (1995).
[23] H. Neuberger, Phys. Lett. B **417**, 141 (1998).
[24] H. Neuberger, Phys. Lett. B **427**, 353 (1998).
[25] P. Hasenfratz, V. Laliena, and F. Niedermayer, Phys. Lett. B **427**, 125 (1998).
[26] P. Hasenfratz, Nucl. Phys. **B525**, 401 (1998).
[27] C. Gattringer, Phys. Rev. D **63**, 114501 (2001).
[28] C. Gattringer, I. Hip, and C.B. Lang, Nucl. Phys. **B597**, 451 (2001).
[29] M. Lüscher, Phys. Lett. B **428**, 342 (1998).
[30] H. Neuberger, Phys. Rev. D **57**, 5417 (1998).
[31] H. Neuberger, hep-lat/9910040.
[32] P.H. Ginsparg and K.G. Wilson, Phys. Rev. D **25**, 2649 (1982).
[33] F. Niedermayer, Nucl. Phys. B (Proc. Suppl.) **73**, 105 (1999).
[34] H. Neuberger, Annu. Rev. Nucl. Part. Sci. **51**, 23 (2001).
[35] K.G. Wilson, Phys. Rev. D **10**, 2445 (1974).
[36] S. Aoki, Phys. Rev. D **30**, 2653 (1984).
[37] S. Aoki, Phys. Rev. Lett. **57**, 3136 (1986).
[38] S. Aoki, Prog. Theor. Phys. Suppl. **122**, 179 (1996).
[39] C. W. Bernard, Lectures given at TASI '89, Boulder, CO, Jun, 1989.
[40] A. Morel, J. Phys. (Paris) **48**, 1111 (1987).
[41] S.R. Sharpe and N. Shoresh, Phys. Rev. D **64**, 114510 (2001).
[42] C.W. Bernard and M.F.L. Golterman, Phys. Rev. D **49**, 486 (1994).

Chiral perturbation theory at non-zero lattice spacing

Oliver Bär[a]

[a]Graduate School of Pure and Applied Sciences, University of Tsukuba, Tsukuba 305-8571, Japan

A review of chiral perturbation theory for lattice QCD at non-zero lattice spacing is given.

1. Introduction

In spite of constant progress in computer technology, numerical lattice simulations with quark masses as light as realized in nature are out of reach. The smallest values for the ratio M_π/M_ρ reported by various collaborations during this conference [1] range from 0.35 to 0.66 for Wilson fermions with 2 flavors to 0.62 for those with 2+1 flavors. Simulations with staggered fermions reached a value of 0.3, and 2 flavor domain-wall fermions were performed at a value of 0.53. All these numbers are still far away from the physical value 0.18. Consequently, numerical lattice simulations still require a rather long extrapolation in the light quark masses to their physical values.

The necessary guidance to perform the extrapolation is usually provided by chiral perturbation theory (χPT) [2,3]. This low-energy effective theory for QCD predicts the quark mass dependence of various physical quantities. A well-known example is the one-loop expression for the pion mass ($N_f = 2$ and $m_u = m_d = m$),

$$\frac{M_\pi^2}{2Bm} = 1 + \frac{2Bm}{32\pi^2 f^2} \ln \frac{2Bm}{\Lambda^2} + \text{analytic}. \qquad (1)$$

In order to use this expression one must make sure that one is in the chiral regime where χPT holds. It is widely believed that a non-trivial check for this is provided by the logarithmic quark mass dependence in eq. (1): Once the lattice data shows the characteristic curvature of the chiral logarithm one can apply eq. (1) with confidence for the chiral extrapolation [4].

There is a potential problem with this argument. The derivation of χPT is essentially based on symmetry properties of *continuum* QCD. Hence the continuum limit has to be taken first before χPT can be employed to perform the chiral extrapolation.

There are various reasons why one may like to reverse this order. Obviously, as long as data for only one lattice spacing is available the continuum limit cannot be taken. Performing the chiral extrapolation first is also simpler in practice.

Whatever the reasons might be, performing the chiral extrapolation before taking the continuum limit raises the question whether it is legitimate to use expressions derived in continuum χPT. Optimistically one may hope to commit just a small error, assuming the lattice spacing is small. However, it is a priori not clear whether the functional form in eq. (1) is valid at all at non-zero lattice spacing. This concern is even more justified taking into account that each of the traditional lattice fermions (Wilson and staggered) compromises chiral symmetry in some respects. In case eq. (1) is not appropriate at non-zero a, the question is which expression should be used instead.

χPT can be formulated for lattice QCD at non-zero lattice spacing. The main idea goes back to two papers [5, 6] published about five years ago. Since then we have learned a lot about the chiral limit at non-zero lattice spacing. Moreover, formulae for masses, decay constants etc. were derived that include explicitly the contributions due to a non-vanishing lattice spacing. These formulae are the proper expressions one should use when the chiral extrapolation is performed before the continuum limit is taken.

In this review I give an overview of χPT at non-zero lattice spacing. I focus on the methodology, point out important differences compared to continuum χPT and cover the main theoretical

results.

Some of these results entered already the analysis of numerical lattice data. I briefly comment on these analyses with the question in mind whether the simulations are carried out in the chiral regime so that χPT can be applied. I do not discuss the physical results of these simulations for the hadron spectrum, quark masses and heavy quark physics. For these I refer to the plenary talks given by K-I. Ishikawa, P. Rakow and M. Wingate at this conference [7].

2. χPT for lattice theories

The basic strategy for constructing χPT for lattice theories at non-zero lattice spacing is a two-step matching to effective theories [5, 6]. We first write down Symanzik's effective theory [8,9], an effective continuum theory which describes the lattice theory close to the continuum limit. The cut-off effects appear in terms of higher dimensional operators in the effective action and the effective operators, multiplied by powers of the lattice spacing a. In the second step one derives the chiral Lagrangian for this effective theory using the standard arguments of χPT. This results in a chiral expansion in which the dependence on the lattice spacing is made explicit.

The main rôle of Symanzik's effective theory in this two-step procedure is that it provides a systematic expansion of the lattice theory around continuum limit. It organizes the non-zero lattice spacing effects in powers of a and therefore according to their importance when the continuum limit is approached. The structure of the higher dimensional operators in the Symanzik action determines if and how the cut-off effects break the symmetries of the corresponding continuum theory. In particular, the way chiral symmetry is broken by the lattice spacing effects is made transparent, which is crucial for constructing the chiral Lagrangian. Finally, Symanzik's effective theory is a continuum theory, and the well-established derivation of χPT from continuum QCD can be readily extended to this effective theory with additional symmetry breaking parameters.

2.1. χPT for Wilson fermions

Consider lattice QCD with Wilson fermions. Based on locality and the symmetries of the lattice theory, Symanzik's effective action is of the form [10, 11]

$$S_{\rm Sym} = S_0 + aS_1 + a^2 S_2 + \ldots, \quad (2)$$

$$S_k = \sum_i c_i^{(k+4)} O_i^{(k+4)}, \quad (3)$$

where the $O_i^{(n)}$ are local operators of dimension n constructed from the gauge and quark fields and their derivatives. The constants $c_i^{(n)}$ are unknown coefficients. The first term S_0 is the usual continuum QCD action. Note that the quark mass in the fermion part of S_0 includes the additive mass renormalization proportional to $1/a$, otherwise a term S_{-1} would be present in eq. (2).

Using equations of motion there is essentially only the Pauli term in S_1,

$$S_1 = c_1 \int d^4x\, \overline{\psi} i\sigma_{\mu\nu} G_{\mu\nu} \psi. \quad (4)$$

This term breaks chiral symmetry, and its presence is a consequence of the explicit chiral symmetry breaking by the Wilson term in Wilson's fermion action. The complete list of dimension six operators in S_2 can be found in Ref. [10]. Among the terms with fermions (bilinears and 4-quark-operators) are operators which break chiral symmetry and ones which preserve it. It is also at this order in the Symanzik action that the lattice structure of the underlying theory shows up in form of quark bilinears that break O(4) rotation symmetry.

It should be mentioned that not all a dependence is explicit in eq. (2). The coefficients $c_i^{(n)}$ are functions of the gauge coupling g^2 and are therefore expected to show a presumably weak, logarithmic a dependence.

Since the leading term in eq. (2) is the continuum QCD action we expect the lattice theory to exhibit the same spontaneous symmetry breaking pattern as in the continuum, provided both m and a are small. In that case the low-energy physics is dominated by pseudo Goldstone bosons, which acquire a non-zero mass due to the explicit chiral symmetry breaking by the quark mass and by the

additional chiral symmetry breaking terms in S_1 and S_2.

The low-energy chiral effective theory for these bosons, often called Wilson χPT, is defined by a chiral effective Lagrangian. In order to construct this Lagrangian one writes down the most general Lagrangian that is invariant under the symmetries of the underlying Symanzik theory. Symmetry breaking terms are consistently included performing a spurion analysis. This procedure is analogous to the way the quark mass is included in continuum χPT. Here, however, one has to perform a spurion analysis for each symmetry breaking term in eq. (2), also those stemming from the discretization effects.

The Pauli term (4) is a particularly simple example for this procedure because it breaks chiral symmetry exactly like a mass term. As usual, the chiral Lagrangian is parameterized in terms of $\Sigma = \exp(2i\Pi/f)$ with Π being the matrix of Goldstone boson fields, which transforms under chiral transformations as $\Sigma \to L\Sigma R^\dagger$. The $\mathcal{L}_2$-Lagrangian, containing the terms of $\mathrm{O}(p^2, m, a)$, is found to be given by [12]

$$\mathcal{L}_2 = \frac{f^2}{4}\left\langle \partial_\mu \Sigma \partial_\mu \Sigma^\dagger \right\rangle - \frac{f^2 B}{2}\left\langle m\Sigma^\dagger + \Sigma m^\dagger \right\rangle - \frac{f^2 \tilde{W}_0}{2} c_1 a \left\langle \Sigma^\dagger + \Sigma \right\rangle . \quad (5)$$

The angled brackets denote traces over the flavor indices. The first line contains the familiar terms from continuum χPT, the kinetic and the mass term (here m stands for the quark mass *matrix*), multiplied by unknown low-energy constants f and B. These two terms stem from the leading part S_0 in eq. (2). The third term has its origin in the Pauli term, and it has, as expected, the structure of a degenerate mass term (degenerate because the Pauli term is diagonal in flavor space). The coefficient $\tilde{W}_0$ is another low-energy constant not determined by symmetries. In contrast to B the mass dimension of $\tilde{W}_0$ is three instead of one.

Since both $\tilde{W}_0$ and c_1 are unknown parameters it is customary to combine them in form of one coefficient W_0. In this parameterization, however, the coefficient W_0 inherits the weak a dependence of c_1 and is no longer a true constant. Furthermore, W_0 vanishes if the underlying lattice theory is non-perturbatively $\mathrm{O}(a)$ improved, because c_1 is zero in this case.

The $\mathcal{L}_4$-Lagrangian comprises all terms of $\mathrm{O}(p^4, p^2m, m^2, p^2a, ma, a^2)$ and it is of the form

$$\mathcal{L}_4 = \mathcal{L}_4^{\mathrm{GL}}(p^4, p^2m, m^2) + \mathcal{L}_4^a(p^2a, ma, a^2). \quad (6)$$

The first term on the r.h.s. is the well-known Gasser-Leutwyler Lagrangian [2, 3] stemming from the continuum part in Symanzik's effective action. The second term parameterizes the additional chiral symmetry breaking effects coming from S_1 and S_2 [12, 13]. It turns out that the operators in $\mathcal{L}_4^a$ are easily obtained from the Gasser-Leutwyler Lagrangian: Take any operator containing the mass matrix m and replace it by a, this gives all terms in $\mathcal{L}_4^a$. This simple final result is not obvious. Some 4-quark operators in S_2 break chiral symmetry in a different way than a mass term and rotational O(4) symmetry is broken at $\mathrm{O}(a^2)$. However, the spurion analysis shows that all these effects do not enter the $\mathcal{L}_4$-Lagrangian, but only appear at higher orders in the chiral expansion [13].

The total number of unknown low-energy constants in $\mathcal{L}_4$ is eighteen. Ten of those are Gasser-Leutwyler coefficients in the Gasser-Leutwyler Lagrangian, while the lattice spacing effects contribute eight additional unknown coefficients. This number is reduced to three for fully $\mathrm{O}(a)$ improved Wilson fermions, since all am terms in $\mathcal{L}_4^a$ vanish in this case.

The main motivation for constructing a chiral effective Lagrangian for lattice QCD is to compute the explicit a dependence of observables and to guide the chiral extrapolation of numerical lattice data. Obviously, too many unknown low-energy constants limit the predictability of the chiral extrapolation. However, the situation is not as bad as the number eighteen may suggest. The number of free parameters in the chiral expressions for m_π and f_π is much smaller because many low-energy constants appear in particular linear combinations and can therefore be combined in form of a few unknown parameters. Still, an increased number of free parameters is the price one has to pay when one wants to perform

the chiral extrapolation before taking the continuum limit.

Having constructed the chiral effective Lagrangian we can compute expressions for the pseudo scalar masses, decay constants, scattering lengths etc. However, in order to correctly describe the underlying lattice theory we need to properly match the parameters in both theories, which is not entirely straightforward.

Starting from eq. (5) one easily derives the tree-level expression ($m_u = m_d = m$ for simplicity)

$$M_\pi^2 \quad = \quad 2Bm + 2W_0 a \tag{7}$$

for the pion mass. Hence, the leading $\mathrm{O}(a)$ effect is a shift in the pion mass. Consequently, the pion mass does not vanish for $m = 0$.

The mass m, however, is not the one that is usually used in the lattice theory [5, 14]. Due to the explicit chiral symmetry breaking, the quark mass receives an additive mass renormalization proportional to $1/a$. A common definition for the renormalized quark mass is in terms of a vanishing pion mass. By definition, $M_\pi^2 = 0$ for $m' = Z_m(m_0 - m_{\mathrm{cr}})/a = 0$, where m_0 is the bare lattice mass. So defined, the critical quark mass m_{cr} accounts not only for the divergent additive mass shift, but also for finite shifts proportional to powers of a. Therefore, at leading order in the effective theory, the appropriate mass parameter is given by

$$m' \quad = \quad m + aW_0/B. \tag{8}$$

Eq. (7) now reads $M_\pi^2 = 2Bm'$ and the pion mass vanishes for $m' = 0$, as required. Note that the proper parameter matching needs to be adjusted when we work beyond LO: The terms of $\mathrm{O}(a^2)$ in $\mathcal{L}_4^a$ cause an additional shift in the critical mass and the r.h.s. of eq. (8) receives an additional contribution of $\mathrm{O}(a^2)$.

Having found the proper parameter matching (8), one can replace m by m' in the effective Lagrangian. After the replacement the $\mathrm{O}(a)$ term in $\mathcal{L}_2$ has disappeared, but the terms linear in a in $\mathcal{L}_4^a$ are still present.

There are other definitions for the renormalized quark mass on the lattice. For example, one can define it in terms of the quark mass that enters the PCAC relation. All these definitions differ by $\mathrm{O}(a^n)$ terms in the critical quark mass. Depending on the definition in the lattice theory the parameter matching might be different from eq. (8) and needs to be done accordingly.

Another subtlety in Wilson χPT has its origin in the presence of two expansion parameters, m and a, or, to be more precise

$$\frac{2Bm'}{(4\pi f)^2}, \qquad \frac{2W_0 a}{(4\pi f)^2}. \tag{9}$$

Both parameters must be smaller than one for the chiral expansion to make sense. But even if this requirement is satisfied, the *relative* size of these parameters is crucial for the proper power counting. In order to discuss this let us consider the following two terms which appear in the chiral Lagrangian:

$$O_1 \quad = \quad c_1 m' \langle \Sigma + \Sigma^\dagger \rangle, \tag{10}$$

$$O_2 \quad = \quad c_2 a^2 \langle \Sigma + \Sigma^\dagger \rangle^2. \tag{11}$$

O_1 is just the mass term in $\mathcal{L}_2$, parameterized in terms of m' and using the short-hand notation $c_1 = f^2 B/4$. O_2 appears in $\mathcal{L}_4^a$ and the coefficient c_2 denotes a particular combination of low-energy constants in $\mathcal{L}_4^a$.

As long as $c_1 m' \gg c_2 a^2$ the term O_2 is much smaller than O_1 and can safely be considered a next-to-leading order (NLO) contribution. However, decreasing the quark mass at fixed lattice spacing (this is approximately done in numerical lattice simulations at fixed β) one will eventually enter a regime where both terms are of comparable size. In this regime both contributions should be taken to be of leading order (LO).

The regime $c_1 m' \gg c_2 a^2$ is considered in Ref. [13], and the pseudo-scalar mass was calculated to one loop as an example. The resulting expression is essentially the one-loop continuum expression, containing the non-analytic continuum chiral logarithms, plus additional analytic terms proportional to am' and a^2.

Qualitative changes start to occur in the regime $c_1 m' \approx c_2 a^2$. To be more concrete let us consider the leading terms in the potential energy for two degenerate flavors [5],

$$V = -\frac{c_1}{4} m' \langle \Sigma + \Sigma^\dagger \rangle + \frac{c_2}{16} a^2 \langle \Sigma + \Sigma^\dagger \rangle^2, \tag{12}$$

which is essentially the sum of the terms in eqs. (10) and (11) (the relative sign is convention).[1] For $c_1 m' \approx c_2 a^2$ the two terms in the potential are of comparable size, and the competition between them can result in a non-trivial ground state.

It turns out that there are only two different scenarios possible, and the sign of c_2 determines which of those is realized [5]. If c_2 is positive, the ground state configuration Σ_0 is no longer proportional to the identity for $m' < 2c_2 a^2/c_1$. Parity and flavor are spontaneously broken and massless pions exist even at non-zero lattice spacing. In other words, the effective theory predicts the properties of the Aoki phase, which was proposed a long time ago [15]. The alternative scenario with negative c_2 exhibits a first order phase transition where $\Sigma_0 = 1$ changes sign. Parity and flavor are unbroken irrespective of the size of m' and no massless pions exist at non-zero a.

The same analysis for quenched Lattice QCD is more subtle due to the ghost fields and the graded symmetry group. Nevertheless, the conclusion is that the phase structure is the same as in the unquenched theory [16].

The chiral effective theory cannot predict whether c_2 is positive or negative. After all, c_2 is a combination of unknown low-energy constants whose values are essentially determined by the action of the underlying lattice theory. In particular, magnitude and sign of c_2 can be different for improved Wilson fermions.

Numerical data to date support the existence of an Aoki phase for quenched simulations [17, 18]. Recent unquenched 2-flavor simulations using the plaquette gauge action and unimproved Wilson fermions at $\beta = 5.2$ show evidence for a first-order phase transition [19, 20] (see also Ref. [21]). The results suggest that the scenario with negative c_2 is realized for this particular lattice action, but more data is needed to draw a definite conclusion. In the scenario with negative c_2 the minimal pion mass is determined by $|c_2|$. Hence, from the point of view of numerical simulations, $|c_2|$ should be as small as possible, and it is an open question which lattice action is most suitable in this respect.

[1] Note that the definitions for c_1 and c_2 differ from Ref. [5]. I have pulled out the factors m' and a^2.

A second feature of the regime $c_1 m' \approx c_2 a^2$ is that additional chiral log contributions appear in the one-loop expressions for observables. This has been shown for the two flavor case in Ref. [14]. The $\mathrm{O}(a^2)$ term in (11) and also the $\mathrm{O}(am')$ contributions are kept at LO in the chiral Lagrangian. These terms give rise to additional vertices proportional to a^2 and am' and therefore to additional loop diagrams. Explicitly, the one-loop expression for the pion mass is given by

$$\frac{M_\pi^2}{2Bm'} = 1 + \frac{m'(2B + w_1 a)}{32\pi^2 f^2} \ln \frac{2Bm'}{\Lambda^2} + \frac{w_0 a^2}{32\pi^2 f^2} \ln \frac{2Bm'}{\Lambda^2} + \text{analytic.} \quad (13)$$

Here w_0 and w_1 denote some combinations of unknown low-energy constants and m' includes the $\mathrm{O}(a^2)$ shift coming from the $c_2 a^2$ term in the potential (12).

Eq. (13) coincides with the continuum one-loop expression in eq. (1) in the limit $a \to 0$. However, the coefficient of the $m' \ln m'$ term receives a correction of $\mathrm{O}(a)$. Furthermore, the lattice spacing effects generate an additional $a^2 \ln m'$ contribution.

This $a^2 \ln m'$ contribution will eventually become dominant when we decrease m' further. In fact, the r.h.s. of eq. (13) diverges in the $m' \to 0$ limit (M_π^2 itself, however, remains finite). Toward the chiral limit terms proportional to $a^2 (\ln 2Bm')^n$, $n = 2, 3, \ldots$ become more and more important. Aoki performed a resummation of these terms and derived a resummed one-loop formulae for the pion mass:

$$\frac{M_\pi^2}{2\tilde{B}m'} = \left[1 + \frac{(2B + w_1 a)m'}{32\pi^2 f^2} \ln \frac{2Bm'}{\Lambda^2}\right] \times \left\{ \ln \frac{2Bm'}{\tilde{\Lambda}^2} \right\}^{\tilde{w}_0 a^2 / 32\pi^2 f^2} + \text{analytic.} \quad (14)$$

Expanding $\{\ldots\}^{a^2 \cdots}$ and dropping higher powers of $a^2 (\ln 2Bm')^n$ one recovers eq. (13).

The derivation of eq. (14) assumes the Aoki scenario for the phase diagram (positive c_2) where the pion becomes massless at a second order phase transition point. Approaching this point the correlation length (or the inverse pion mass)

diverges with the critical exponent of a four dimensional scalar theory. Comparing the general form for the diverging correlation length with eq. (13) one can match the parameters and obtains formula (14). Note that the parameters with a tilde in eq. (14) may be different from those in eq. (13). The matching at this order does not determine the parameters unambiguously [14].

Analogous one-loop calculations for the pseudo-scalar decay constant and the PCAC quark mass $m_{\rm AWI}$ were also carried out [14]. The results exhibit the same qualitative features as in eqs. (13) and (14). Additional logarithmic contributions proportional to $am' \ln m'$ and $a^2 \ln m'$ are present and modify the familiar results obtained in continuum χPT.

These results show that the chiral limit at non-zero lattice spacing is quite different from the one in continuum χPT. The differences become more pronounced the smaller the mass m' is. This is a warning that expectations concerning the quark mass dependence of M_π^2, f_π and other quantities based on continuum χPT might be misleading when naively applied to lattice QCD. Performing the chiral extrapolation of lattice data using the chiral forms of continuum χPT, as is often done, might not be justified.

From a practical point of view the crucial question is what $c_1 m' \approx c_2 a^2$ precisely means. This question is not easily answered, since nothing is known about the size of the low-energy constants that go into c_2. A simple dimensional analysis tells us that c_1 and c_2 are of mass dimension three and six, respectively. Hence $c_1 m' \approx c_2 a^2$ can be translated into $m' \approx a^2 \Lambda_{\rm QCD}^3$, assuming that the size of any dimensionful quantity is determined by the typical QCD scale. This argument should be taken with care, since factors of 2 or 3 are easily amplified by taking powers.

Nevertheless, assuming $\Lambda_{\rm QCD} \approx 300$MeV and a lattice spacing $a \approx 0.15$fm we find $a^2 \Lambda_{\rm QCD}^3 \approx 15$MeV. Even though the physical quark masses simulated in present day numerical simulations are larger than this value, they are probably not large enough to conclude $m' \gg a^2 \Lambda_{\rm QCD}^3$ and to neglect the effects due to a non-zero a. Ultimately the fits of the chiral forms to the numerical lattice data have to decide which power counting is more appropriate in explaining the data at hand.

2.2. Partially quenched and mixed fermion theories

The construction of a chiral effective Lagrangian is readily extended to partially quenched lattice QCD with different masses for the sea and valence Wilson fermions. The partially quenched lattice theory is described by a lattice action with sea, valence and ghost quarks. The Symanzik action through $O(a^2)$ is obtained as in the unquenched case, based on locality and the symmetries of the lattice theory [13]. The chiral effective Lagrangian through $O(a^2)$ has the same form as in the unquenched case, with the angled brackets (cf. eq. (7)) now representing super-traces and the field Σ reflecting the larger flavor content of partially quenched χPT.

Mixed fermion (or hybrid) theories are a generalization of partially quenched lattice theories. In addition to choosing different quark masses, the lattice Dirac operator is different in the sea and valence sector. Particularly interesting combinations contain a Dirac operator for the sea quarks that is fast to simulate, i.e. staggered or (twisted mass) Wilson fermions, and Ginsparg-Wilson fermions for the valence quarks, realized by domain-wall [22] or overlap fermions [23, 24]. This type of mixed fermion simulations offers an efficient compromise towards full unquenched simulations with Ginsparg-Wilson fermions. Some new results using configurations generated with staggered sea quarks and domain wall or overlap valence quarks have been reported at this conference [25].

The naive argument why mixed fermion theories are expected to give meaningful physical results is that the two Dirac operators differ by terms of $O(a)$ and these should vanish in the continuum limit. However, there are potential dangers. Unitarity is lost and it is restored in the continuum limit only. This is in contrast to partially quenched theories with the same Dirac operator, which become unitary when the valence and sea quarks are chosen equal. Moreover, it is not at all obvious that a "better" Dirac operator for the valence quarks (one that has exact chiral symmetry at non-zero a) automatically implies

better results for physical quantities. Analytic control of the expected $O(a)$ difference is clearly desirable.

The chiral effective Lagrangian for lattice QCD with Wilson sea quarks and Ginsparg-Wilson valence quarks was constructed in [13, 26]. It turns out that the effective Lagrangian contains one more operator at $O(a^2)$ and consequently one more unknown low-energy constant than the Lagrangian for Wilson sea and Wilson valence quarks. Nevertheless, an explicit calculation shows that this additional unknown constant does not enter the one-loop result for the pion mass of a pion made of two valence quarks. In fact, compared to the case with Wilson sea and Wilson valence quarks one finds a reduced a dependence.

This example demonstrates that the cut-off dependence of mixed fermion theories can be studied analytically using the chiral effective field theory. Work on the mixed theory with staggered sea and Ginsparg-Wilson valence quarks is in progress [27].

2.3. Twisted mass Lattice QCD

The advantages of the twisted mass formulation of lattice QCD [tmLQCD] [28–30] with Wilson fermions have been reviewed by R. Frezzotti at this conference [31]. A twisted mass term

$$m_{\rm tm} \;=\; m + i\mu\gamma_5\sigma_3 \qquad (15)$$

protects the Wilson-Dirac operator against very small eigenvalues and solves the problem of exceptional configurations. Recent results indicate that unquenched simulations also benefit from a twisted mass, and their "numerical cost" is comparable with staggered fermions [32]. Hence, simulations with smaller physical quark masses seem possible in tmLQCD and the chiral regime is probably easier reached than with an untwisted mass term. In addition, certain physical quantities like hadron masses are automatically $O(a)$ improved [33, 34].

The construction of the chiral effective theory for tmLQCD follows the same two-step procedure that was described before [35, 36]. The form of Symanzik's effective action is as in eq. (2), with the leading term S_0 now being the continuum twisted mass QCD action. Since a twisted mass term breaks parity and flavor, there are more terms present in S_1 and S_2 compared to the untwisted case. Nevertheless, after performing the spurion analysis one finds the same $\mathcal{L}_2$- and $\mathcal{L}_4$-Lagrangian as in eq. (5) and (6), with m replaced by the twisted mass $m_{\rm tm}$.

The effective Lagrangian was used to analyze the phase diagram of tmLQCD, generalizing the analysis for the untwisted theory [35–39]. As before, there exist two scenarios, depending on the sign of (the same) coefficient c_2, and for a vanishing mass μ one recovers the results in the untwisted case.

One-loop calculations for M_π^2 and f_π have been performed for the regime $\mu \gg a^2\Lambda_{\rm QCD}^3$, but only the terms linear in a were kept [40, 41]. It is desirable to repeat these calculations including the $O(a^2)$ terms and with a power counting appropriate for $\mu \approx a^2\Lambda_{\rm QCD}^3$, since numerical simulations with small twisted mass may well be in this regime.

The masses of the neutral and charged pions differ due to explicit flavor breaking by a twisted mass term. The mass splitting is found to be of $O(a^2)$ and proportional to c_2 [35, 36, 39],

$$M_{\pi_3}^2 - M_{\pi_\pm}^2 \;=\; \frac{2c_2}{f^2}a^2(1-\cos^2\phi), \qquad (16)$$

where the angle ϕ parameterizes the vacuum state $\Sigma_0 = \exp i\phi\tau_3$ of the effective theory. Hence, as pointed out in [39], the sign of c_2 can be determined, at least in principle, by measuring the mass difference of the charged and neutral pions.

A proof for automatic $O(a)$ improvement at maximal twist was presented in Ref. [33]. It was subsequently shown [42] that a crucial assumption about the critical quark mass does not hold if c_2 is positive. Consequently, $O(a)$ improvement is lost unless $m \gg a^2\Lambda_{\rm QCD}^3$. This restriction on the quark mass, however, can be avoided with a different definition for maximal twist, and $O(a)$ improvement can be guaranteed irrespective of the size of the quark mass.

The differences between different definitions for maximal twist was illustrated using the framework of the chiral effective theory. The absence or presence of the leading $O(a)$ effect in the pion mass, depending on the definition for maximal

twist and the size of the quark mass, is explicitly shown in Ref. [42].

2.4. Nucleon properties

Starting from the Symanzik action in eq. (2), continuum Baryon χPT has been extended to accommodate the leading linear a dependence due to the Pauli term S_1 [43]. This extension is rather straightforward. Since the Pauli term breaks chiral symmetry like a mass term, the construction of the chiral effective Lagrangian involves one additional spurion field proportional to a, but is otherwise analogous to the construction based on continuum QCD [44].

Assuming a power counting with $m \approx a\Lambda_{\rm QCD}^2$, a variety of nucleon properties (masses, magnetic moments, matrix elements of the axial vector current etc.) have been computed in the one-loop approximation. At this order the main effect of the non-zero lattice spacing is the shift of the pseudo scalar masses in eq. (7). As discussed before, this shift might already be absorbed in the definition of the critical mass. Non-trivial effects, however, can be expected at $\mathrm{O}(a^2)$.

Electromagnetic properties of baryons and mesons (charge radii, magnetic moments etc.) including the linear lattice spacing contribution have also been discussed in Ref. [45]. Again, the main a effect is implicit in the pseudo-scalar masses, for example for the charge radius of the ϕ meson. It would be interesting to extend these results by including the $\mathrm{O}(a^2)$ corrections.

2.5. χPT for staggered fermions

Staggered fermions are numerically very fast to simulate compared with other lattice fermions. They possess an exact axial U(1) symmetry at non-zero lattice spacing, which protects the quark mass from an additive renormalization. As a result, lattice QCD simulations with staggered fermions reach significantly smaller values for M_π/M_ρ than those using Wilson fermions. The numerical performance of the known lattice fermions in unquenched simulations was reviewed by A. Kennedy at this conference [32]. The major disadvantage of staggered fermions is that they do not solve the fermion doubling problem completely: Each flavor comes in four different tastes.

In order to reduce the number of tastes one usually employs the so-called "fourth root trick": The fermion determinant of the staggered Dirac operator is replaced by $\sqrt[4]{\det D}$ in numerical lattice simulations. This trick legitimately raises the question whether the fourth root theory correctly describes QCD in the continuum limit. By taking the fourth root one sacrifices the locality of the theory and all known universality arguments no longer hold. This and additional problems are reviewed in Ref. [46].

Using the fourth root trick also poses a problem for constructing a chiral effective theory. Since the lattice theory is no longer local, it is not described by a local Symanzik theory close to the continuum limit. Hence the previously described two-step procedure cannot be applied directly.

To circumvent this problem the following strategy has been proposed [47]. One first considers lattice QCD with N_f staggered flavors without using the fourth root trick. This theory is local and one can indeed construct Symanzik's effective theory. The leading term S_0 is the continuum QCD action with $4N_f$ fermions (4 tastes for each flavor). Assuming spontaneous chiral symmetry breaking one constructs the chiral Lagrangian for this lattice theory with $(4N_f)^2 - 1$ pseudo Goldstone bosons. Starting from this Lagrangian one calculates pseudo scalar masses, decay constants etc. to the desired order (one loop in practice). These results are finally corrected for taking the fourth root of the determinant. This adjustment amounts to properly placing factors of $1/4$ for each sea quark loop contribution. This step requires, besides performing a partially quenched calculation in order to distinguish between sea and valence quarks, that the meson diagrams in the effective theory are correctly interpreted in terms of the underlying quark diagrams [48].

This procedure, staggered χPT for short, is field theoretically not absolutely rigorous. Potential non-local contributions due to taking the fourth root of the fermion determinant would not be captured by it. Consequently, the validity of the fourth root trick would be seriously questioned if staggered lattice data cannot be described by staggered χPT. Turning this numerical argument around is not so simple. Even if

no problems are found numerically, some doubts may still remain. More analytic studies are certainly desired (see Ref. [49] for a recent example).

Putting these issues aside, the construction of staggered χPT follows the two-step procedure outlined before. In one respect staggered χPT is simpler than Wilson χPT because the quark mass is not additively renormalized.

The form of Symanzik's effective action is as in eq. (2), but the symmetries of the staggered lattice action exclude any terms of dimension 3 and 5, so S_1 vanishes [6,50,51]. The leading term S_0 is the continuum QCD action with N_f flavors, each coming in four different tastes. S_0 possesses an exact SU(4) taste symmetry for each flavor, but this symmetry is broken at $\mathrm{O}(a^2)$ by dimension six operators in S_2. In addition, SO(4) rotation invariance is broken at this order.

The chiral Lagrangian is constructed in the same way as described for Wilson fermions. The symmetry breaking terms are consistently included by performing a spurion analysis. The generic form of the $\mathcal{L}_2$-Lagrangian is given by [6]

$$\mathcal{L}_2 \quad = \quad \mathcal{L}_{\mathrm{kin}} + \mathcal{L}_{\mathrm{mass}} + a^2\mathcal{V}. \tag{17}$$

The kinetic and the mass term are as in eq. (5), however, the field Σ and the mass matrix are $4N_f \times 4N_f$ matrices, reflecting the larger particle content due to the taste degree of freedom.

The potential $\mathcal{V} = \sum_i c_i \mathcal{O}_i$ comprises eight taste symmetry breaking operators $\mathcal{O}_i$, each of which is multiplied by an unknown low-energy constant c_i [6, 47, 52] (two of the operators are redundant in the one flavor case). However, the taste symmetry is not completely broken and $\mathcal{V}$ retains an accidental SO(4) taste symmetry. Moreover, $\mathcal{V}$ is SO(4) rotationally invariant, even though rotation invariance is broken in the Symanzik action at $\mathrm{O}(a^2)$.

Expanding eq. (17) to quadratic order in the pion fields one obtains ($m = m_u = m_d$)

$$M_{\pi_i}^2 \quad = \quad 2Bm + a^2\Delta(\xi_i) \tag{18}$$

for the leading order pion mass where the index $i = 5, \mu 5, \mu\nu, \mu, I$ labels the different tastes and the ξ_i denote the SU(4) taste generators [6, 52]. The accidental SO(4) taste symmetry of $\mathcal{L}_2$ implies that the mass shift $\Delta(\xi_i)$ is the same for all ξ_μ, all $\xi_{5\mu}$, and all $\xi_{\mu\nu}$. The shift $\Delta(\xi_5)$ for the Goldstone pion π_5 is of course zero because of the exact axial U(1) symmetry.

The mass degeneracy is not exact since it is a consequence of the SO(4) taste symmetry of $\mathcal{L}_2$, and this symmetry is broken by higher order terms in the effective Lagrangian. Nevertheless, the approximate degeneracy is clearly observed in numerical lattice data, both in quenched [53, 54] and unquenched simulations [55, 56]. In fact, it was observed long before the analysis in the chiral effective theory offered a theoretical understanding for it.

The chiral effective theory does not say anything about the mass shifts $\Delta(\xi_i)$, neither the sign nor the size. A negative shift would imply a vanishing meson mass before the chiral limit and the existence of non-trivial phases, similar to the Aoki phase for Wilson fermions. However, the mass shifts observed in numerical simulations are all positive. Moreover, the shifts are fairly large. The most recent simulations by the MILC collaboration [56] still show significant mass shifts, even though the lattice spacing is fairly small ($a_{\mathrm{min}} \approx 0.09$fm) and the highly improved Asqtad quark action is used. In fact, the lattice spacing contribution $a^2\Delta(\xi_i)$ to the pion masses is of the same order as the quark mass contribution $2Bm$. This justifies, even requires, to consider the contribution $a^2\mathcal{V}$ in the leading order Lagrangian, while all the terms of $\mathrm{O}(p^2a^2, ma^2, a^4)$ enter the next-to-leading order Lagrangian $\mathcal{L}_4$.

The full next-to-leading order Lagrangian has been constructed just recently [57,58]. The number of terms is fairly large, more than 200 operators enter $\mathcal{L}_4$. At this order in the chiral expansion the accidental SO(4) taste symmetry of $\mathcal{L}_2$ is broken by terms of $\mathrm{O}(p^2a^2)$, and the symmetry group of the effective theory coincides with the one of the underlying lattice theory.

Despite the fact that there are so many operators at NLO, some non-trivial predictions have been found [57,58]. At NLO the SO(4) taste symmetry is essentially only broken by the $\mathrm{O}(p^2a^2)$ terms, and these terms contribute to both the pseudo-scalar masses and the matrix elements of the pseudo scalar density, $\langle 0|P^a|\pi_b\rangle = \delta^{ab} f_{\pi_a}^P$. It turns out that there are sufficiently many inde-

pendent relations in order to predict relationships that do not contain any unknown low-energy constants. For example, one finds ($k = 1, 2, 3$)

$$\frac{f^P_{\pi_k} - f^P_{\pi_4}}{f^P_{\pi_k} + f^P_{\pi_4}} = \frac{1}{2}\frac{M^2_{\pi_k} - M^2_{\pi_4}}{M^2_{\pi_k} + M^2_{\pi_4}}, \tag{19}$$

and the same relations involving the taste pairs π_{k5}, π_{45} and $\pi_{lm}, \pi_{k5}, (k, l, m = 1, 2, 3)$. These expressions show that the degeneracies among the tastes with $\xi_\mu, \xi_{\mu 5}$ and $\xi_{\mu\nu}$ are removed.

Non-trivial predictions for the pion dispersion relations have also been established [57, 58], but eq. (19) seems to be the simplest prediction to test in numerical simulations. To this end it is extremely beneficial that the renormalization factors entering eq. (19) are SO(4) taste invariant. They are therefore identical for both tastes and cancel in the ratio, hence permitting eq. (19) to be tested using bare lattice operators. This is not true in general. In particular it would not hold if the l.h.s. in eq. (19) involved the matrix element $\langle 0|A^a_\mu|\pi_a\rangle$ of the axial vector current A^a_μ.

Checking these relationships in numerical simulations may serve as an additional test for the fourth root trick. Most of these relations are unaffected by the necessary modifications due to taking the fourth root of the determinant. The trick is certainly not justified if the simulations cannot reproduce these predictions.

Taking the $a^2\mathcal{V}$ term in $\mathcal{L}_2$ to be of leading order gives rise to additional interaction vertices and consequently to logarithmic contributions proportional to a^2 in loop calculations for physical quantities. The masses and decay constants of the pseudo-Goldstone bosons have been computed to one loop in Refs. [52, 59]. For three degenerate flavors the mass of the charged Goldstone pion reads [52]

$$\begin{aligned}\frac{M^2_{\pi^+_5}}{2Bm} &= 1 + \frac{1}{48\pi^2 f^2} M^2_{\pi_I} \ln\frac{M^2_{\pi_I}}{\Lambda^2} \\ &+ \frac{1}{12\pi^2 f^2}\left[M^2_{\eta'_V} \ln\frac{M^2_{\eta'_V}}{\Lambda^2} - M^2_{\pi_V} \ln\frac{M^2_{\pi_V}}{\Lambda^2})\right] \\ &+ \frac{1}{12\pi^2 f^2}\left[M^2_{\eta'_A} \ln\frac{M^2_{\eta'_A}}{\Lambda^2} - M^2_{\pi_A} \ln\frac{M^2_{\pi_A}}{\Lambda^2})\right] \\ &+ \text{analytic terms.}\end{aligned} \tag{20}$$

The dependence on the lattice spacing is implicit and enters in form of the leading order pseudoscalar masses given in eq. (18). The first line reproduces the familiar continuum χPT result for $a \to 0$, while the second and third line vanish in this limit (note that all masses $M^2_{\pi_i}$ become degenerate in the continuum limit). At non-zero a, however, this result may differ significantly from the result in the continuum limit, depending on the size of the mass shifts for the various pseudoscalar mesons. Note that the perhaps naively expected term proportional to $M^2_{\pi^+_5} \ln(M^2_{\pi^+_5}/\Lambda^2)$ does not appear on the r.h.s. of eq. (20).

The one-loop expressions for the decay constants $f_{\pi^+_5}$ and $f_{K^+_5}$ show similar qualitative modifications compared to the continuum χPT results for these quantities [59]. It should be mentioned that the expressions for 2+1 partially quenched flavors, which is the relevant case for the simulations carried out by the MILC collaboration, are much lengthier than the special example for 3 unquenched flavors in eq. (20).

2.6. Staggered χPT for heavy-light mesons

Staggered χPT has been extended to describe heavy-light mesons [60]. The starting point is Symanzik's effective action for staggered light quarks given in (17). No Symanzik analysis was done for the heavy quark lattice action. Instead, the leading order HQET action is assumed to give a proper description of the heavy quark. This assumption neglects the discretization effects due to the heavy quark and is only justified for either a highly improved heavy quark lattice action or when lattice HQET [61] is used.

Starting from this effective continuum theory it is straightforward to generalize the arguments of continuum heavy-light χPT [62] and construct the chiral Lagrangian. One difference is that we now have three expansion parameters: the quark mass m, the lattice spacing a and the residual momentum k of the heavy-light meson.

Based on the chiral Lagrangian the decay constant f_B was calculated to one loop. The additional vertices proportional to a^2 generate extra chiral logarithms. These terms can again significantly change the quark mass dependence that the continuum expressions predict. An illustra-

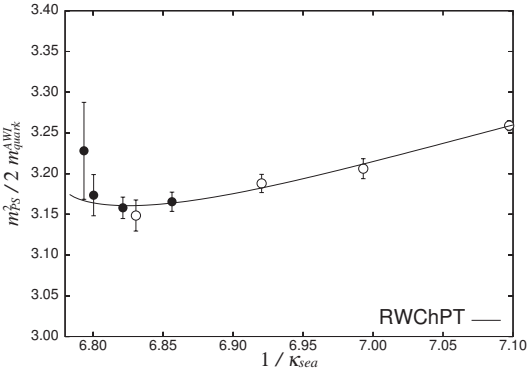

Figure 1. Fit result for $M_\pi^2/2m_{\rm AWI}$ using resummed Wilson χPT. From Ref. [63].

tive plot showing this can be found in [60].

3. Comparison with numerical data

The main motivation for constructing chiral effective Lagrangians for lattice theories is to capture the discretization effects analytically and to guide the chiral extrapolation of numerical lattice data without taking the continuum limit first. Of course, one has to be in the regime where the chiral effective theory provides a valid description of the lattice data. This can only be checked by trying to fit the chiral fit forms to the lattice data. In case one obtains fits with a good χ^2 and reasonable values for the unknown coefficients one gains confidence that the chiral effective theory describes the data.

Both the CP-PACS collaboration [63, 64] and the qq+q collaboration [65–67] used Wilson χPT to analyze their unquenched lattice data which were obtained with Wilson fermions.

The CP-PACS collaboration generated their data with an RG-improved gauge action and a meanfield improved clover quark action with 2 flavors. The simulations were performed at one lattice spacing $a \approx 0.2$fm and for eight different quark masses corresponding to the range $M_\pi/M_\rho = 0.35 - 0.8$. Data for four mass values were generated some time ago [68] and were combined with new data [63].

Chiral fits for M_π^2 and $m_{\rm AWI}$ were performed using the results of continuum χPT as well as the Wilson χPT expressions in eqn. (13) and (14) for M_π^2 and the corresponding expressions for $m_{\rm AWI}$. The power counting underlying these formulae seems appropriate since the bare quark mass am' is of $\mathrm{O}(a^3\Lambda_{\rm QCD}^3)$ in the CP-PACS simulations.

Fig. 1 shows the fit result for $M_\pi^2/2m_{\rm AWI}$ using the resummed formulae for both quantities. A good fit is obtained including all data points. Using the unresummed formulae (cf. eq. (13) for M_π^2) gives similar results. A reasonable fit is also possible with the 1-loop continuum expression when the three heaviest data points are excluded from the fit. However, the lowest five data points can also be fitted by a straight line within errors. Hence, even though fits to continuum χPT are possible there is no clear evidence for the curvature due to the chiral logarithms.

The good fit result over the whole range of quark masses is quite unexpected since the chiral expansion is not expected to work at such high values for M_π/M_ρ. The reason why the formulae of Wilson χPT work so well in figure 1 can be traced back to the coefficient of the $m' \ln m'$ term. The result for this coefficient is roughly 80% smaller than the value expected from continuum χPT. Hence the curvature due to the chiral logarithm is highly suppressed and the fairly linear data is fitted well.

This strong suppression is slightly surprising. The coefficient of the $m' \ln m'$ term is proportional to $(2B - \tilde{\omega}_1 a)$ where $\tilde{\omega}_1$ is the difference of the ω_1 coefficients in the chiral expressions for M_π^2 and $m_{\rm AWI}$. Large linear lattice spacing effects with $\tilde{\omega}_1 a = \mathrm{O}(2B)$ are required in order to achieve the 80% suppression. Since a mean-field improved quark action was used one would have expected smaller values for $\tilde{\omega}_1$.[2] More data at various lattice spacings is required in order to confirm these results. In particular, one needs to check that $\tilde{\omega}_1 a$ goes indeed linearly to zero for $a \to 0$.

The qq+q collaboration employed the plaquette gauge action and the 2-flavor unimproved Wilson quark action. Data was generated at $\beta =$

[2] $\tilde{\omega}_1$ would be zero for non-perturbatively O(a) improved Wilson fermions.

5.1 ($a \approx 0.195$fm) with four different sea quark masses corresponding to the range $M_\pi/M_\rho = 0.47 - 0.76$. Partially quenched data has been accumulated with various valence quark masses for one sea quark mass. For the smallest two sea quark masses, however, $m_{\rm Val}$ had to be chosen equal or larger than $m_{\rm Sea}$ in order to avoid problems with exceptional configurations.

Figure 2 shows the result for the ratio $M_\pi^2/2m_{\rm AWI}$, normalized by its value at the heaviest quark mass and denoted by Rn, as a function of $\sigma = m_{\rm AWI}/m_{\rm AWI,heaviest}$. Note that the normalization by the values at heaviest quark mass disguises the fact that there is a fourth data point at $\sigma = 1$. The solid line is the fit result using one-loop continuum χPT. Similarly to the CP-PACS data the qq+q data can be fitted by continuum χPT, but the data for the pion mass shows no indication for a curvature due to the chiral logarithms. Even though the data for the pion decay constant shows some curvature [66] more data is needed to corroborate the interpretation in terms of chiral logarithms.

The qq+q collaboration also performed fits using the Wilson χPT expressions including the linear a dependence which were derived in Ref. [12]. The values for the fit parameters associated with the a contributions turn out to be very small. It was therefore concluded that the lattice artifacts are small.

This conclusion seems premature. The lattice spacing $a \approx 0.195$fm and the range of M_π/M_ρ is comparable with the values of the CP-PACS collaboration. As mentioned before, the naive dimensional analysis suggests $m' \approx a^2\Lambda_{\rm QCD}^3$ for these parameter values. The appropriate fit forms for M_π^2 are therefore eqn. (13) or (14). The fit forms in Ref. [12] were derived under the assumption $m' \gg a^2\Lambda_{\rm QCD}^3$ and are most probably not applicable here. Moreover, $m_{\rm AWI}$ was identified with m' (the vector Ward identity mass) in the chiral fit forms. The relation between $m_{\rm AWI}$ and m' is highly non-linear in Wilson χPT with the power counting $m' \approx a^2\Lambda_{\rm QCD}^3$ and involves chiral logarithms proportional to am' and a^2. The simple identification of $m_{\rm AWI}$ with m' is therefore not always justified. It would be interesting to re-

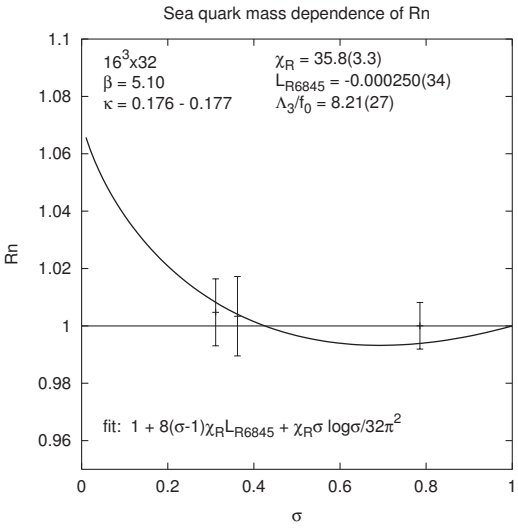

Figure 2. Data for $M_\pi^2/2m_{\rm AWI}$ as a function of $m_{\rm AWI}$, normalized by the values at the heaviest quark mass (see text). From Ref. [66].

analyze the qq+q data using the proper fit forms for the $m' \approx a^2\Lambda_{\rm QCD}^3$ regime. This needs to be done before one can draw final conclusions about the size of the lattice artifacts.

The MILC collaboration has been carrying out 2+1 flavor simulations with staggered fermions, employing a Symanzik improved gauge action and the Asqtad quark action [56, 69]. Computations have been done for two lattice spacings ($a \approx 0.125$fm and $a \approx 0.09$fm), and fairly small meson masses with $M_\pi/M_\rho \approx 0.3$ have been reached. Very precise partially quenched data for the Goldstone boson masses and decay constants have been accumulated with errors of typically $0.1\% - 0.7\%$, and 416 data points are available in total, 208 each for the masses and the decay constants.

Fits of the NLO staggered χPT expressions (the partially quenched analogue of eq. (20) for 2+1 flavors) to the data give poor results, even if only a subset of 94 data points corresponding to the lightest masses is taken into account. This is not unexpected since the statistical error of the data is much smaller than the estimated uncertainty in the chiral expressions due to neglecting NNLO terms.

A full NNLO calculation in staggered χPT has not been done yet. Meanwhile, only the analytic NNLO contributions are added to the full NLO chiral fit forms. The total number of unknown parameters in these expressions is 40, which is fairly large. However, only 4 of them are associated with the non-zero lattice spacing effects. 36 parameters still remain if one sets a to zero in these expressions.

The details of the fits are rather involved, but the bottom line is that good fits are possible with these fit forms (although 176 data points for heavy masses still need to be excluded). One might be tempted to attribute the good fit results to the large number of free parameters. However, good fits are not possible using the fit forms of continuum χPT, even though the number of free parameters is 36. Similarly, no good fits are possible without the chiral logarithms (38 free parameters).

The good fits are therefore not a simple consequence of a large number of free parameters. The very precise data is able to discriminate between various fit forms, and the results strongly suggest the presence and importance of the taste violating effects of $O(a^2)$. Nevertheless, in order to perform correct fits it seems mandatory to use the complete NNLO expressions including the NNLO chiral logarithms. Recent results in partially quenched continuum χPT at NNLO [70] should help to perform the necessary 2-loop calculations.

4. Concluding remarks

The two-step matching procedure to effective field theories (Lattice $\rightarrow$ Symanzik $\rightarrow$ χPT) has proven to be an appropriate tool for systematically constructing χPT at non-zero lattice spacing. The resulting expressions for physical quantities can differ significantly from the corresponding expressions derived in continuum χPT, depending on the relative size of the quark mass and the lattice spacing contributions. Expectations from continuum χPT, in particular with respect to a curvature in lattice data caused by chiral logarithms, might be misleading.

Many quantities have been computed to one loop, both in Wilson and in staggered χPT. Many more calculations remain to be done. Some calculations need to be extended by using a different power counting or by working in the partially quenched approximation. Including the lattice spacing effects in χPT for vector mesons [71] has not been done at all yet. All these calculations need to be done in order to obtain appropriate expressions for the chiral extrapolation at non-zero lattice spacing.

With the formulation of χPT at non-zero lattice spacing we are able analytically to capture particular lattice artifacts which otherwise would be an uncontrolled uncertainty. The more uncertainties we control analytically, the better will be our numerical results for physical quantities.

Acknowledgements

I would like to thank S. Aoki, C. Aubin, C. Bernard, J. Bijnens, C. DeTar, M. Golterman, K. Jansen, I. Montvay, G. Münster, Y. Namekawa, G. Schierholz, S. Sharpe, N. Shoresh, R. Sommer, R. Van de Water and C. Urbach for providing me with material and for helpful discussions.

REFERENCES

1. Talks by C. Bernard, T. Ishikawa, T. Izubuchi, Y. Namekawa, E. Scholz and C. Tarantino, this conference.
2. J. Gasser and H. Leutwyler, Ann. Phys. **158** (1984) 142.
3. J. Gasser and H. Leutwyler, Nucl. Phys. **B250** (1985) 465.
4. C. Bernard *et al.*, Nucl. Phys. Proc. Suppl. **106** (2002) 199.
5. S. R. Sharpe and J. Singleton, Robert, Phys. Rev. **D58** (1998) 074501.
6. W.-J. Lee and S. R. Sharpe, Phys. Rev. **D60** (1999) 114503.
7. Plenary talks by K.-I. Ishikawa, P. Rakow and M. Wingate, this conference.
8. K. Symanzik, Nucl. Phys. **B226** (1983) 187.
9. K. Symanzik, Nucl. Phys. **B226** (1983) 205.
10. B. Sheikholeslami and R. Wohlert, Nucl. Phys. **B259** (1985) 572.
11. M. Lüscher, S. Sint, R. Sommer and P. Weisz, Nucl. Phys. **B478** (1996) 365.

12. G. Rupak and N. Shoresh, Phys. Rev. **D66** (2002) 054503.
13. O. Bär, G. Rupak and N. Shoresh, Phys. Rev. **D70** (2004) 034508.
14. S. Aoki, Phys. Rev. **D68** (2003) 054508.
15. S. Aoki, Phys. Rev. **D30** (1984) 2653.
16. Talk by S. R. Sharpe, this conference.
17. S. Aoki, Prog. Theor. Phys. Suppl. **122** (1996) 179.
18. S. Aoki, Nucl. Phys. Proc. Suppl. **60A** (1998) 206.
19. Talks by F. Farchioni and C. Urbach, this conference.
20. F. Farchioni *et al.*, hep-lat/0406039.
21. E.-M. Ilgenfritz *et al.*, Phys. Rev. **D69** (2004) 074511.
22. D. B. Kaplan, Phys. Lett. **B288** (1992) 342.
23. R. Narayanan and H. Neuberger, Phys. Lett. **B302** (1993) 62.
24. R. Narayanan and H. Neuberger, Nucl. Phys. **B412** (1994) 574.
25. Talks by G. Fleming, D. Renner, W. Schroers and R. J. Tweedie, this conference.
26. O. Bär, G. Rupak and N. Shoresh, Phys. Rev. **D67** (2003) 114505.
27. O. Bär, C. Bernard, G. Rupak and N. Shoresh, work in progress.
28. R. Frezzotti, S. Sint and P. Weisz, JHEP **07** (2001) 048.
29. R. Frezzotti, P. A. Grassi, S. Sint and P. Weisz, JHEP **08** (2001) 058.
30. R. Frezzotti, Nucl. Phys. Proc. Suppl. **119** (2003) 140.
31. Plenary talk by R. Frezzotti, this conference.
32. Plenary talk by A. Kennedy, this conference.
33. R. Frezzotti and G. C. Rossi, JHEP **08** (2004) 007.
34. R. Frezzotti and G. C. Rossi, hep-lat/0407002.
35. Talk by J. M. S. Wu, this conference.
36. S. R. Sharpe and J. M. S. Wu, hep-lat/0407025.
37. G. Münster, hep-lat/0407006.
38. Talk by G. Münster, this conference.
39. L. Scorzato, hep-lat/0407023.
40. G. Münster and C. Schmidt, Europhys. Lett. **66** (2004) 652.
41. G. Münster, C. Schmidt and E. E. Scholz, hep-lat/0402003.
42. S. Aoki and O. Bär, hep-lat/0409006.
43. S. R. Beane and M. J. Savage, Phys. Rev. **D68** (2003) 114502.
44. E. Jenkins and A. V. Manohar, Phys. Lett. **B255** (1991) 558.
45. D. Arndt and B. C. Tiburzi, Phys. Rev. **D69** (2004) 114503.
46. K. Jansen, Nucl. Phys. Proc. Suppl. **129** (2004) 3.
47. C. Bernard, Phys. Rev. **D65** (2002) 054031.
48. S. R. Sharpe, Phys. Rev. **D46** (1992) 3146.
49. plenary talk D. H. Adams, this conference.
50. S. R. Sharpe, Nucl. Phys. Proc. Suppl. **34** (1994) 403.
51. Y.-B. Luo, Phys. Rev. **D57** (1998) 265.
52. C. Aubin and C. Bernard, Phys. Rev. **D68** (2003) 034014.
53. N. Ishizuka *et al.*, Nucl. Phys. **B411** (1994) 875.
54. S. Aoki *et al.*, Phys. Rev. **D62** (2000) 094501.
55. K. Orginos and D. Toussaint, Phys. Rev. **D59** (1999) 014501.
56. C. Aubin *et al.*, hep-lat/0407028.
57. Talk by R. S. Van de Water, this conference.
58. S. R. Sharpe and R. S. Van de Water, hep-lat/0409018.
59. C. Aubin and C. Bernard, Phys. Rev. **D68** (2003) 074011.
60. Talk by C. Aubin, this conference.
61. E. Eichten and B. Hill, Phys. Lett. **B234** (1990) 511.
62. M. B. Wise, Phys. Rev. **D45** (1992) 2188.
63. Y. Namekawa *et al.*, hep-lat/0404014.
64. Talk by Y. Namekawa, this conference.
65. F. Farchioni, I. Montvay, E. Scholz and L. Scorzato, Eur. Phys. J. **C31** (2003) 227.
66. F. Farchioni, I. Montvay and E. Scholz, hep-lat/0403014.
67. Talk by E. Scholz, this conference.
68. A. Ali Khan *et al.*, Phys. Rev. **D65** (2002) 054505.
69. Talk by C. Bernard, this conference.
70. J. Bijnens, N. Danielsson and T. A. Lahde, hep-lat/0406017.
71. E. Jenkins, A. V. Manohar and M. B. Wise, Phys. Rev. Lett. **75** (1995) 2272.

PHYSICAL REVIEW D **70,** 116011 (2004)

Twisted mass QCD, O(a) improvement, and Wilson chiral perturbation theory

Sinya Aoki[1,2] and Oliver Bär[1]

[1]*Graduate School of Pure and Applied Sciences, University of Tsukuba, Tsukuba 305-8571, Japan*
[2]*Riken BNL Research Center, Brookhaven National Laboratory, Upton, New York 11973, USA*
(Received 18 October 2004; published 23 December 2004)

We point out a caveat in the proof for automatic O(a) improvement in twisted mass lattice QCD at maximal twist angle. With the definition for the twist angle previously given by Frezzotti and Rossi, automatic O(a) improvement can fail unless the quark mass satisfies $m_q \gg a^2\Lambda_{\rm QCD}^3$. We propose a different definition for the twist angle which does not require a restriction on the quark mass for automatic O(a) improvement. In order to illustrate explicitly automatic O(a) improvement we compute the pion mass in the corresponding chiral effective theory. We consider different definitions for maximal twist and show explicitly the absence or presence of the leading O(a) effect, depending on the size of the quark mass.

DOI: 10.1103/PhysRevD.70.116011 PACS numbers: 11.30.Hv, 11.30.Rd, 12.38.Gc, 12.39.Fe

I. INTRODUCTION

Recently more and more evidence has been accumulated that the twisted mass formulation of lattice QCD (tmLQCD) [1,2] with Wilson fermions has significant advantages compared to its untwisted counterpart (for reviews on the subject see Refs. [3,4]). The presence of a nonzero twisted mass term protects the Dirac operator against very small eigenvalues and consequently solves the problem of "exceptional configurations" in the quenched approximation [5,6]. The absence of these small eigenvalues is also very beneficial in unquenched simulations [7]. Recent results indicate that unquenched simulations with twisted mass Wilson fermions are comparable in numerical cost to unquenched simulations with staggered fermions [8]. Moreover, a twisted mass term simplifies the renormalization of matrix elements of certain local operators such as the isotriplet axial current and the isosinglet scalar density. Finally, it has been shown in Refs. [9,10] that hadronic masses and certain matrix elements are automatically O(a) improved at maximal twist.

The automatic O(a) improvement is quite remarkable since it does not require the computation of any improvement coefficients in the standard improvement program proposed by Symanzik [11–13]. This is a significant advantage taking into account that a nonperturbative determination of all improvement coefficients can be quite demanding.

In this paper we point out a caveat in the proof of automatic O(a) improvement given in Ref. [9]. This caveat has its origin in the way the twist angle is defined. With the definition in Ref. [9] one can show that, under certain conditions, automatic O(a) improvement is only guaranteed if the quark mass satisfies the condition $m_q \gg a^2\Lambda_{\rm QCD}^3$. Many current lattice simulations, in particular, unquenched simulations, probably do not satisfy this inequality well enough and automatic O(a) improvement might be lost.

The restriction $m_q \gg a^2\Lambda_{\rm QCD}^3$, however, is not a fundamental limitation. In fact, the restriction is entirely due to the way the twist angle is defined. In this paper we propose an alternative definition for the twist angle, and with this definition automatic O(a) improvement at maximal twist holds without any restriction on m_q.

The differences between the different definitions for the twist angle and its consequences for automatic O(a) improvement can be explicitly demonstrated using Wilson chiral perturbation theory (WChPT), i.e., the chiral effective theory for lattice QCD with Wilson fermions [14–17] (for a review see Ref. [18]). As an example we compute the pion mass including the leading lattice spacing contributions in this effective theory. We explicitly show that the pion mass is O(a) improved as long as the inequality $m_q \gg a^2\Lambda_{\rm QCD}^3$ holds. However, uncanceled O(a) cutoff effects are present if this bound is violated and the definition in Ref. [9] for maximal twist is used. On the other hand, if we define maximal twist employing our alternative definition, this O(a) contribution is absent for any value of the quark mass.

This paper is organized as follows. In Sec. II we briefly repeat the argument in Ref. [9] for automatic O(a) improvement at maximal twist angle and we point out where it can fail. We also propose an alternative definition for the twist angle, which guarantees automatic O(a) improvement irrespective of the size of m_q. In Sec. III we set up WChPT for tmLQCD and use it in Sec. IV to discuss O(a) improvement of the pion mass for different definitions of maximal twist. Some final remarks are made in Sec. V.

II. CRITICAL QUARK MASS AND TWIST ANGLE

A. Automatic O(a) improvement at maximal twist

First we briefly repeat the argument given in Ref. [9] for automatic O(a) improvement at maximal twist angle. For convenience we follow the notation introduced in this reference.

The fermion mass term of tmLQCD with Wilson fermions is defined as

$$\bar{\psi}_{\rm ph}(x)\left\{\left[-a\frac{r}{2}\sum_\mu \nabla^\star_\mu\nabla_\mu + M_{\rm cr}(r)\right]\exp(-i\omega\gamma_5\tau_3) + m_q\right\}\psi_{\rm ph}(x) \tag{1}$$

in the so-called physical basis, while it becomes

$$\bar{\psi}(x)\left\{\left[-a\frac{r}{2}\sum_\mu \nabla^\star_\mu\nabla_\mu + M_{\rm cr}(r)\right] + m_q\exp(i\omega\gamma_5\tau_3)\right\}\psi(x) \tag{2}$$

in the so-called twisted mass basis when one performs the field redefinition

$$\psi_{\rm ph} = \exp\left(i\frac{\omega}{2}\gamma_5\tau_3\right)\psi, \qquad \bar{\psi}_{\rm ph} = \bar{\psi}\exp\left(i\frac{\omega}{2}\gamma_5\tau_3\right). \tag{3}$$

Here $M_{\rm cr}(r)$ denotes the critical quark mass and m_q is the subtracted quark mass defined by $m_q = m_0 - M_{\rm cr}(r)$ with the bare quark mass m_0. Setting the twist angle ω to zero the critical mass cancels and the standard Wilson mass term remains. This is no longer true for nonzero twist. For $\omega \neq 0$ Eq. (2) corresponds to a Wilson mass term with a mass $m + i\mu\gamma_5\tau_3$ where m and μ are given by

$$m = m_q\cos\omega + M_{\rm cr}(r), \tag{4}$$

$$\mu = m_q\sin\omega. \tag{5}$$

A particular definition for $M_{\rm cr}(r)$ is not relevant for the following argument. However, a crucial assumption is that the critical mass $M_{\rm cr}(r)$ is an odd function of the Wilson parameter r,

$$M_{\rm cr}(-r) = -M_{\rm cr}(r). \tag{6}$$

Provided that this is true, one can show that any observable $\langle O\rangle(r, m_q, \omega)$[1] can be O($a$) improved by either taking the Wilson average (WA), defined as

$$\langle O\rangle^{\rm WA}(r, m_q, \omega) \equiv \frac{1}{2}[\langle O\rangle(r, m_q, \omega) + \langle O\rangle(-r, m_q, \omega)], \tag{7}$$

or by taking the mass average (MA)

$$\langle O\rangle^{\rm MA}(r, m_q, \omega) \equiv \frac{1}{2}[\langle O\rangle(r, m_q, \omega) + (-1)^{P_{\mathcal{R}_5}[O]}\langle O\rangle(r, -m_q, \omega)]. \tag{8}$$

The factor $(-1)^{P_{\mathcal{R}_5}[O]}$ is called the $\mathcal{R}_5$ parity of the operator O [9]. O(a) improvement means that

$$\langle O\rangle^{\rm WA}(r, m_q, \omega) = \langle O\rangle^{\rm cont}(m_q) + {\rm O}(a^2), \tag{9}$$

$$\langle O\rangle^{\rm MA}(r, m_q, \omega) = \langle O\rangle^{\rm cont}(m_q) + {\rm O}(a^2). \tag{10}$$

Using this one can show that any observable even in ω is automatically O(a) improved at $\omega = \pm\pi/2$ as follows. Consider the twist average (TA) at $\omega = \pm\pi/2$:

$$\langle O\rangle^{\rm TA}\left(r, m_q, \omega = \frac{\pi}{2}\right) \equiv \frac{1}{2}\left[\langle O\rangle\left(r, m_q, \omega = \frac{\pi}{2}\right) + \langle O\rangle\left(r, m_q, \omega = -\frac{\pi}{2}\right)\right]. \tag{11}$$

The expectation value at $\omega = -\pi/2$ on the right-hand side is equal to the expectation value at $\omega = 2\pi - \pi/2 = \pi + \pi/2$, and the mass term in the action, Eq. (1), becomes

$$\bar{\psi}_{\rm ph}(x)\left\{\left[-a\frac{r}{2}\sum_\mu \nabla^\star_\mu\nabla_\mu + M_{\rm cr}(r)\right]\exp\left[-i\left(\pi + \frac{\pi}{2}\right)\gamma_5\tau_3\right] + m_q\right\}\psi_{\rm ph}(x) = \bar{\psi}_{\rm ph}(x)\left\{\left[-a\frac{-r}{2}\sum_\mu \nabla^\star_\mu\nabla_\mu + M_{\rm cr}(-r)\right] \times \exp\left(-i\frac{\pi}{2}\gamma_5\tau_3\right) + m_q\right\}\psi_{\rm ph}(x), \tag{12}$$

provided that $-M_{\rm cr}(r) = M_{\rm cr}(-r)$. Hence the twist average at $\omega = \pi/2$ is given by

$$\langle O\rangle^{\rm TA}\left(r, m_q, \omega = \frac{\pi}{2}\right) = \frac{1}{2}\left[\langle O\rangle\left(r, m_q, \omega = \frac{\pi}{2}\right) + \langle O\rangle\left(-r, m_q, \omega = \frac{\pi}{2}\right)\right], \tag{13}$$

which is nothing but the Wilson average and therefore is O(a) improved. If, in addition, the observable O is even in

[1] $\langle O\rangle(r, m_q, \omega)$ denotes the expectation value of a local and gauge invariant operator, where the dependence on r, m_q, and ω is made explicit.

ω,

$$\langle O\rangle\left(r, m_q, \omega = \pm\frac{\pi}{2}\right) = \langle O\rangle^{\mathrm{TA}}\left(r, m_q, \omega = \frac{\pi}{2}\right), \quad (14)$$

the observable O is automatically O(a) improved without taking an average. Important examples of ω-even quantities are hadronic masses and some matrix elements [9].

B. The critical mass

A crucial assumption for the results of the previous subsection is that the critical mass is odd under $r \to -r$. This transformation property, however, is not at all obvious. It can be proven in perturbation theory if one defines the critical mass in terms of the pole of the lattice quark propagator [19], but it is likely not to be true nonperturbatively. For example, even if the symmetry properties of the lattice theory imply that the pion mass satisfies [9]

$$m_\pi[r, m_0] = m_\pi[-r, -m_0] \quad (15)$$

as a function of r and the bare quark mass m_0, one cannot conclude that the critical mass, implicitly defined by

$$m_\pi[r, M_{\mathrm{cr}}(r)] = 0, \quad (16)$$

is an odd function of r. Of course, property (15) implies

$$0 = m_\pi[-r, M_{\mathrm{cr}}(-r)] = m_\pi[r, -M_{\mathrm{cr}}(-r)], \quad (17)$$

hence both $M_{\mathrm{cr}}(r)$ and $-M_{\mathrm{cr}}(-r)$ are solutions of (16). If Eq. (16) has exactly one solution this implies that $M_{\mathrm{cr}}(r)$ is indeed an odd function of r. However, as soon as Eq. (16) has two or more solutions, this is no longer guaranteed.

We emphasize that the existence of a massless pion at nonzero lattice spacing is not trivial since chiral symmetry is explicitly broken by the Wilson term even if the bare mass is set to zero. A scenario for how a massless pion is realized at nonzero lattice spacing has been proposed a long time ago in Ref. [19]. The expected phase diagram for Wilson fermions is sketched in Fig. 1. The solid line represents a second order phase transition line where parity and flavor are spontaneously broken. As a consequence of this spontaneous parity-flavor symmetry breaking the pion mass vanishes along this line. This phase diagram implies the existence of multiple solutions (two for large g^2 and ten for small g^2) to the defining equation (16) for the critical mass.

Figure 1 is also naturally predicted by WChPT as one of two possible scenarios for the phase diagram for Wilson fermions [20].[2] Moreover, the presence of an r-even contribution in $M_{\mathrm{cr}}(r)$ at O(a^2) has been explicitly shown. This contribution manifests itself as the width of the "fingers" in the phase diagram where parity and flavor are spontaneously broken.

[2]In the second scenario no massless pion appears for nonzero lattice spacing. We briefly come back to this scenario in Sec. V.

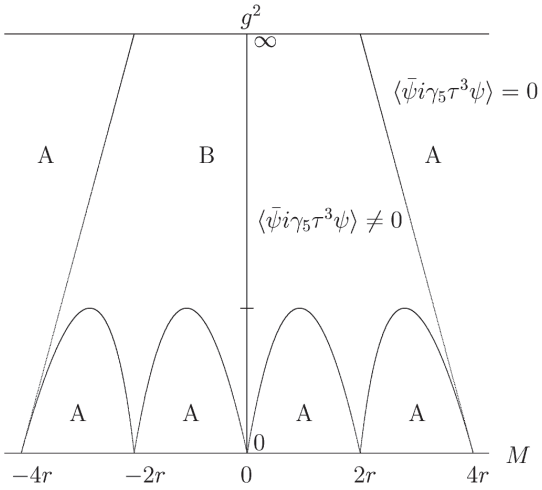

FIG. 1. Phase diagram for $N_f = 2$ lattice QCD with Wilson fermions, where $M \equiv m_0 a + 4r$. The parity and flavor symmetries are spontaneously broken in phase B.

In view of these results we assume $M_{\mathrm{cr}}(r)$ to have the structure

$$M_{\mathrm{cr}}(r) = M_{\mathrm{odd}}(r) + a^2 c M_{\mathrm{even}}(r) \equiv M_{\mathrm{cr}}^{(1)}(r) \quad (18)$$

where $M_{\mathrm{odd}}(r)$ is odd and $M_{\mathrm{even}}(r)$ is even under $r \to -r$. The unknown coefficient c is of mass dimension two and its size is of O(Λ_{QCD}^2). Performing the transformation $r \to -r$ we obtain a second independent solution

$$-M_{\mathrm{cr}}(-r) = M_{\mathrm{odd}}(r) - a^2 c M_{\mathrm{even}}(r) \equiv M_{\mathrm{cr}}^{(2)}(r) \quad (19)$$

to Eq. (16). These two solutions correspond to the two critical lines near the physical continuum limit, defined at $m_0 = 0$ (or $M = 4r$) and $g^2 = 0$ in Fig. 1, and their distance is of O(a^2).

There exist other definitions for the critical mass than Eq. (16). For example, one can define it in terms of the quark mass entering the partially conserved axial vector (PCAC) relation. All these definitions differ by terms of O(a), and it is again not obvious that a particular definition is odd in r. As long as one has not proven this it seems more appropriate to assume the form in Eq. (18) as the general structure for the critical mass. Of course, the details of the functions $M_{\mathrm{odd}}(r)$ and $M_{\mathrm{even}}(r)$ will differ for each definition of M_{cr}.

C. Subtleties at $\omega = \pm\pi/2$

Let us assume expression (18) for the critical mass and let us see what the consequences are for automatic O(a) improvement at maximal twist. Since the additional contribution in M_{cr} is of O(a^2), Eqs. (9) and (10) still hold in the presence of the M_{even} term. However, Eq. (12) is

modified and now reads

$$\bar{\psi}_{\rm ph}(x)\Big\{\Big[-a\frac{r}{2}\sum_\mu \nabla^\star_\mu\nabla_\mu + M_{\rm cr}(r)\Big]\exp\Big[-i\Big(\pi+\frac{\pi}{2}\Big)\gamma_5\tau_3\Big] + m_q\Big\}\psi_{\rm ph}(x) = \bar{\psi}_{\rm ph}(x)\Big\{\Big[-a\frac{-r}{2}\sum_\mu \nabla^\star_\mu\nabla_\mu + M_{\rm cr}(-r)\Big] \times \exp\Big(-i\frac{\pi}{2}\gamma_5\tau_3\Big) - 2a^2cM_{\rm even} \times \exp\Big(-i\frac{\pi}{2}\gamma_5\tau_3\Big) + m_q\Big\}\psi_{\rm ph}(x) = \bar{\psi}_{\rm ph}(x)\Big\{\Big[-a\frac{-r}{2}\sum_\mu \nabla^\star_\mu\nabla_\mu + M_{\rm cr}(-r)\Big] \times \exp\Big(-i\frac{\pi}{2}\gamma_5\tau_3\Big) + \hat{m}_q\exp(i\hat{\omega}\gamma_5\tau_3)\Big\}\psi_{\rm ph}(x), \tag{20}$$

where we have defined

$$\hat{m}_q = \sqrt{m_q^2 + [2a^2cM_{\rm even}(r)]^2}, \qquad \tan\hat{\omega} = \frac{2a^2cM_{\rm even}(r)}{m_q}. \tag{21}$$

Performing a basis change similar to (3) with the angle $\hat{\omega}$, Eq. (13) for the twist average also gets modified and is now given by

$$\langle O\rangle^{\rm TA}\Big(r, m_q, \omega=\frac{\pi}{2}\Big) = \frac{1}{2}\Big[\langle O\rangle\Big(r, m_q, \omega=\frac{\pi}{2}\Big) + \langle O\rangle\Big(-r, \hat{m}_q, \omega=\frac{\pi}{2}+\hat{\omega}\Big)\Big]. \tag{22}$$

The twist average is therefore no longer equal to the Wilson average and one cannot straightforwardly argue that the twist average is automatically O(a) improved. In order to still prove

$$\langle O\rangle^{\rm TA}\Big(r, m_q, \omega=\frac{\pi}{2}\Big) = \langle O\rangle^{\rm cont}(m_q) + {\rm O}(a^2), \tag{23}$$

the new mass parameter $\hat{m}_q$ and the angle $\hat{\omega}$ must satisfy the conditions

$$\hat{m}_q = m_q + {\rm O}(a^2), \qquad \hat{\omega} = {\rm O}(a^2). \tag{24}$$

These conditions are met if the quark mass satisfies the bound $m_q \gg 2a^2cM_{\rm even}(r)$. Assuming that the size of all dimensionful quantities on the right-hand side of this bound is determined by the typical QCD scale $\Lambda_{\rm QCD}$, this bound can be translated into the inequality

$$m_q \gg a^2\Lambda^3_{\rm QCD}. \tag{25}$$

Only when the quark mass satisfies this inequality is automatic O(a) improvement at $\omega = \pm\pi/2$ guaranteed.

D. Alternative definition for maximal twist

In this subsection we propose an alternative definition for the twist angle ω. Setting this angle to the values $\pm\pi/2$ results in automatic O(a) improvement for ω-even quantities without any restriction on the size of m_q.

We first define $M_{\rm cr}(r)$ as the point where the pion mass vanishes in the infinite volume limit of lattice QCD at zero twisted mass. This definition of $M_{\rm cr}(r)$ is unambiguous, contrary to other definitions such as a vanishing quark mass in the axial-vector Ward-Takahashi (WT) identity, since $M_{\rm cr}(r)$ is equivalent to a second order phase transition point of the spontaneous parity-flavor breaking [19–22]. Secondly, as we already discussed, there exist (at least) two independent values of $M_{\rm cr}(r)$, given in (18) and (19), which are related to each other by

$$M^{(1)}_{\rm cr}(r) = M_{\rm cr}(r), \qquad M^{(2)}_{\rm cr}(r) = -M_{\rm cr}(-r). \tag{26}$$

Neither of these solutions is odd in r. However, we can define

$$\overline{M}_{\rm cr}(r) = \frac{M^{(1)}_{\rm cr}(r) + M^{(2)}_{\rm cr}(r)}{2} = -\overline{M}_{\rm cr}(-r), \tag{27}$$

$$\Delta M_{\rm cr}(r) = \frac{M^{(1)}_{\rm cr}(r) - M^{(2)}_{\rm cr}(r)}{2} = \Delta M_{\rm cr}(-r), \tag{28}$$

and $\overline{M}_{\rm cr}(r)$ is, by construction, odd in r. In terms of $\overline{M}_{\rm cr}$ and $\Delta M_{\rm cr}$ we now propose an alternative definition for the twist angle, which in the physical basis reads

$$\bar{\psi}_{\rm ph}(x)\Big\{\Big[-a\frac{r}{2}\sum_\mu \nabla^\star_\mu\nabla_\mu + \overline{M}_{\rm cr}(r)\Big]\exp(-i\omega'\gamma_5\tau_3) + m_q + \Delta M_{\rm cr}(r)\Big\}\psi_{\rm ph}(x). \tag{29}$$

Performing a field transformation analogous to Eq. (3) it can be rewritten in the twisted mass basis,

$$\bar{\psi}(x)\Big[-a\frac{r}{2}\sum_{\mu}\nabla^{\star}_{\mu}\nabla_{\mu}+\overline{M}_{\rm cr}(r) + (m_q+\Delta M_{\rm cr}(r))\exp(i\omega'\gamma_5\tau_3)\Big]\psi(x). \tag{30}$$

Setting $\omega'=0$ the critical mass cancels out in these expressions and we are left with the standard Wilson mass term. However, choosing $\omega'\neq 0$ corresponds to a Wilson mass term with a mass $m+i\mu\gamma_5\tau_3$, where m and μ are given by

$$m=[m_q+\Delta M_{\rm cr}(r)]\cos\omega'+\overline{M}_{\rm cr}(r), \tag{31}$$

$$\mu=[m_q+\Delta M_{\rm cr}(r)]\sin\omega', \tag{32}$$

in contrast to the definition of ω, which leads to Eqs. (4) and (5).

With this definition the Wilson average is the average over $[m_0=M^{(1)}_{\rm cr}(r)+m_q, r]$ and $[m_0=-M^{(2)}_{\rm cr}(r)+m_q,-r]$, which seems to be the natural choice in the presence of two values for $M_{\rm cr}$. Similarly, the mass average is the average over $m_0=M^{(1)}_{\rm cr}(r)+m_q$ and $m_0=M^{(2)}_{\rm cr}(r)-m_q$ with r fixed. Both averages are O(a) improved, since $\overline{M}_{\rm cr}(r)$ is odd under a sign flip in r, which is the crucial property for showing O(a) improvement.

At $\omega'=-\pi/2=\pi+\pi/2$ one can show

$$\bar{\psi}_{\rm ph}(x)\Big\{-\Big[-a\frac{r}{2}\sum_{\mu}\nabla^{\star}_{\mu}\nabla_{\mu}+\overline{M}_{\rm cr}(r)\Big]\exp\Big[-i\Big(\pi+\frac{\pi}{2}\Big)\gamma_5\tau_3\Big]+m_q+\Delta M_{\rm cr}(r)\Big\}\psi_{\rm ph}(x)$$
$$=\bar{\psi}_{\rm ph}(x)\Big\{\Big[-a\frac{-r}{2}\sum_{\mu}\nabla^{\star}_{\mu}\nabla_{\mu}+\overline{M}_{\rm cr}(-r)\Big]\exp\Big(-i\frac{\pi}{2}\gamma_5\tau_3\Big)+m_q+\Delta M_{\rm cr}(-r)\Big\}\psi_{\rm ph}(x).$$

This proves that the twist average at $\omega'=\pm\pi/2$ is indeed equal to the Wilson average without any restrictions on the size of m_q.

Let us discuss the meaning of the definition in Eqs. (29) and (30). For $\omega'=0$ and bare mass values $M^{(2)}_{\rm cr}(r)<m_0<M^{(1)}_{\rm cr}(r)$ parity and flavor are spontaneously broken and the condensate $\langle\bar{\psi}i\gamma_5\tau_3\psi\rangle$ is nonzero. There is a second order phase transition at the critical values $M^{(1)}_{\rm cr}(r)$ and $M^{(2)}_{\rm cr}(r)$ where the pion mass vanishes. If one turns on a twisted mass by choosing $\omega'\neq 0$, this phase transition becomes a crossover and no massless pion appears. The point $m_0=\overline{M}_{\rm cr}(r)$ is the center of the parity-flavor broken phase, where the parity-flavor breaking is maximal, i.e., $|\langle\bar{\psi}i\gamma_5\tau_3\psi\rangle|$ assumes its largest value for a given fixed μ. In this sense maximal twist corresponds to $m_0=\overline{M}_{\rm cr}(r)$, which, according to Eq. (31), coincides with the definition of maximal twist in terms of the twist angle, i.e., $\omega'=\pm\pi/2$.

With the definition of $\omega=\pm\pi/2$ in Ref. [9] via $M^{(1)}_{\rm cr}(r)$, the massless limit of a maximally twisted quark mass coincides with the massless limit of an untwisted quark mass for conventional Wilson fermions. There exists no argument that massless Wilson fermions are O(a) improved, and it is therefore not surprising that an uncanceled O(a) contribution remains when the maximally twisted mass, defined in Ref. [9], is made smaller and smaller.

The apparent contradiction between O(a) improvement and the massless limit has already been realized in Ref. [9]. The authors argued that the spontaneous breaking of chiral symmetry must be dominated by the mass term and not by lattice artifacts if one wants to extract physical information from Green's functions. Consequently they imposed the bound $m_q\gg a^2\Lambda^3_{\rm QCD}$ and argued that the chiral limit should only be approached under this condition. As we have shown here, no such bound needs to be imposed as long as one defines the twist angle appropriately. Automatic O(a) improvement at maximal twist can be achieved without any restriction on the quark mass, and it is irrelevant whether the vacuum state is determined by the mass term or by the lattice artifacts.

The two different definitions of the twist angle are sketched in Fig. 2. The angles are approximately equal as long as either m or μ is much larger than $\Delta M_{\rm cr}(r)$. Note that for constant $\omega=\pi/2$ the angle ω' goes to zero with $\mu\to 0$.

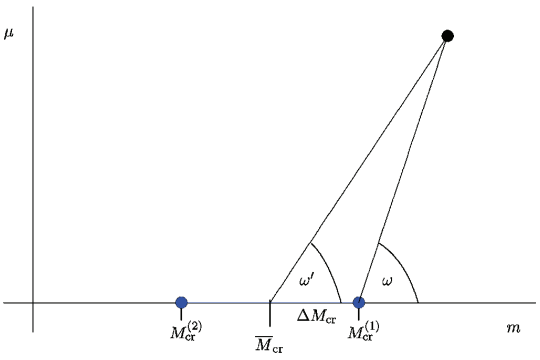

FIG. 2 (color online). Sketch of two different definitions for the twist angle in the m–μ plane. The angle ω is defined in Eqs. (4) and (5), while the angle ω' corresponds to the definition in Eqs. (31) and (32).

We finally note that the $m_q \to 0$ limit should be taken after the infinite volume limit. This is the usual requirement in the case that a global symmetry is (expected to be) spontaneously broken. In practice one should extrapolate the results calculated at nonzero m_q to the massless point in sufficiently large volume.

III. WILSON CHIRAL PERTURBATION THEORY

In this section we study the question of automatic O(a) improvement in the chiral effective theory of tmLQCD, i.e., Wilson chiral perturbation theory. As an example we compute the tree-level pion mass including the lattice spacing effects through O(a^2) for various definitions of the twist angle, and we explicitly show under what conditions the leading lattice spacing effects of O(a) cancel at maximal twist.

A. Chiral effective Lagrangian

The chiral effective Lagrangian for low-energy tmLQCD has been constructed in Refs. [23,24], where it has been used to analyze the phase diagram of tmLQCD as a function of the quark mass and the lattice spacing (see also Refs. [25–27] for similar results on the phase diagram). In terms of the SU(2) matrix-valued field Σ, which transforms under chiral transformations as $\Sigma \to L\Sigma R^\dagger$, the chiral Lagrangian in Ref. [23] reads

$$\begin{aligned}\mathcal{L}_\chi = {} & \frac{f^2}{4}\langle\partial_\mu\Sigma\partial_\mu\Sigma^\dagger\rangle - \frac{f^2}{4}\langle\hat{m}^\dagger\Sigma + \Sigma^\dagger\hat{m}\rangle - \frac{f^2}{4}\langle\hat{a}^\dagger\Sigma + \Sigma^\dagger\hat{a}\rangle - L_1\langle\partial_\mu\Sigma\partial_\mu\Sigma^\dagger\rangle^2 - L_2\langle\partial_\mu\Sigma\partial_\nu\Sigma^\dagger\rangle\langle\partial_\mu\Sigma\partial_\nu\Sigma^\dagger\rangle \\ & + (L_4 + L_5/2)\langle\partial_\mu\Sigma^\dagger\partial_\mu\Sigma\rangle\langle\hat{m}^\dagger\Sigma + \Sigma^\dagger\hat{m}\rangle + (W_4 + W_5/2)\langle\partial_\mu\Sigma^\dagger\partial_\mu\Sigma\rangle\langle\hat{a}^\dagger\Sigma + \Sigma^\dagger\hat{a}\rangle \\ & - (L_6 + L_8/2)\langle\hat{m}^\dagger\Sigma + \Sigma^\dagger\hat{m}\rangle^2 - (W_6 + W_8/2)\langle\hat{m}^\dagger\Sigma + \Sigma^\dagger\hat{m}\rangle\langle\hat{a}^\dagger\Sigma + \Sigma^\dagger\hat{a}\rangle - (W_6' + W_8'/2)\langle\hat{a}^\dagger\Sigma + \Sigma^\dagger\hat{a}\rangle^2. \quad (33)\end{aligned}$$

The angled brackets denote traces over the flavor indices and the short-hand notation

$$\hat{m} = 2Bm_R e^{i\omega_L\tau_3} \equiv 2B(m + i\mu\tau_3), \qquad \hat{a} = 2W_0 a, \quad (34)$$

is used [28]. Here m_R, ω_L, and a denote the (renormalized) quark mass, twist angle, and lattice spacing. We have chosen to attach a subscript "L" to the twist angle in order to highlight that ω_L is the twist angle that enters the chiral Lagrangian. As we will see later this angle neither corresponds to the twist angle defined in Ref. [9] nor to the angle ω' in Eq. (29). The coefficients B and W_0 are unknown low-energy parameters of dimension one and three, respectively, and f is the pion decay constant in the chiral limit. The L_i's are the usual Gasser-Leutwyler coefficients of continuum chiral perturbation theory [29,30], while the W_i's and W_i''s are additional low-energy parameters associated with the nonzero lattice spacing contributions [14,16].

The chiral Lagrangian in Ref. [23] contains some more terms than in Eq. (33) since it includes external sources for vector and axial-vector currents as well as for scalar and pseudoscalar densities. We do not need these terms in the following and have set them to zero.

In the Lagrangian (33) the twist angle is associated with the mass term. Performing the transformation

$$\Sigma \to e^{-i(\omega_L/2)\tau_3}\Sigma e^{-i(\omega_L/2)\tau_3}, \quad (35)$$

the twist angle can be shuffled to the lattice spacing. The Lagrangian is the same as in Eq. (33), but now parametrized in terms of

$$\hat{m} = 2Bm_R, \qquad \hat{a} = 2W_0 a e^{-i\omega_L\tau_3}. \quad (36)$$

B. Gap equation

In this section we derive a gap equation for the ground state of the chiral effective theory. For our purposes it will be enough to only consider the terms of O(m, a, a^2) in the potential energy, which are given by

$$\begin{aligned}V_\chi = {} & \frac{f^2}{4}\langle\hat{m}^\dagger\Sigma + \Sigma^\dagger\hat{m}\rangle + \frac{f^2}{4}\langle\hat{a}^\dagger\Sigma + \Sigma^\dagger\hat{a}\rangle \\ & + (W_6' + W_8'/2)\langle\hat{a}^\dagger\Sigma + \Sigma^\dagger\hat{a}\rangle^2. \quad (37)\end{aligned}$$

We assume the ansatz

$$\Sigma_0 = e^{i\phi\tau_3} \quad (38)$$

for the vacuum expectation value (VEV) of the field Σ. In general, the ground state configuration could have a contribution pointing in a direction orthogonal to τ_3. However, as has already been shown in Refs. [23,27], this is not realized for the potential in Eq. (37). With this ansatz the potential energy becomes

$$\begin{aligned}V_\chi = {} & f^2 2Bm_R\cos(\phi - \omega_L) + f^2 2W_0 a\cos\phi \\ & - f^2 c_2 a^2\cos^2\phi, \quad (39)\end{aligned}$$

where we introduced the short-hand notation[3]

$$c_2 = -32(2W_6' + W_8')\frac{W_0^2}{f^2}. \quad (40)$$

In the following we always assume this parameter to be positive, since this sign corresponds to the scenario with spontaneous parity-flavor breaking [20].

[3]Note that our definition for c_2 differs by a factor of f^2a^2 from the one in Ref. [23]. Furthermore, we have dropped the terms proportional to the quark mass.

The ground state is determined by the *gap equation*,

$$\frac{dV_\chi}{d\phi} = -f^2 2Bm_R \sin(\phi - \omega_L) - f^2 2W_0 a \sin\phi + 2f^2 c_2 a^2 \sin\phi\cos\phi = 0, \quad (41)$$

which can be rewritten in terms of m and μ (defined in Eq. (34)) as

$$2B\mu\cos\phi = \sin\phi(2Bm + 2W_0 a - 2c_2 a^2\cos\phi). \quad (42)$$

This equation is invariant under the sign reversal $\mu \to -\mu$, $\phi \to -\phi$. This implies that once we have found a solution for positive values of μ we have also found the solution for negative twisted mass values. Hence, without loss of generality we can assume μ to be positive and we can take the square of Eq. (42). Setting

$$t = \cos\phi \quad (43)$$

the squared gap equation can be brought into the form

$$\alpha^2 t^2 = (\chi - t)^2(1 - t^2), \quad (44)$$

where we introduced

$$\alpha = \frac{2B\mu}{2c_2 a^2}, \qquad \chi = \frac{2Bm + 2W_0 a}{2c_2 a^2}. \quad (45)$$

We give some approximate solutions to the gap equation in Sec. III D, but some general statements about the solutions can be made just from the structure of Eq. (44). As long as χ is larger than 1 the gap equation always has two solutions, one positive and one negative one. Only for $|\chi| < 1$ can it have up to four solutions. If $\alpha \neq 0$ the modulus of the solution is strictly smaller than 1 and t goes to zero for $\alpha \to \infty$. Finally, $t = 0$ is a solution only if $\chi = 0$.

C. Pion mass formulas

In order to calculate the pion masses we expand Σ around the vacuum configuration Σ_0. As usual we parametrize the field Σ in terms of the pion fields according to

$$\Sigma(x) = \Sigma_0 \exp\Big[\sum_{i=1}^{3} i\pi_i(x)\tau_i/f\Big]. \quad (46)$$

Using this form in expression (37) for the potential energy we expand in powers of the pion fields. The contribution quadratic in π reads

$$V_{\chi,\mathrm{quad}} = \frac{1}{2}\{[2Bm_R\cos(\phi - \omega_L) + 2W_0 a\cos\phi - 2c_2 a^2\cos^2\phi]\pi\cdot\pi + 2c_2 a^2\sin^2\phi\,\pi_3^2\}, \quad (47)$$

and the pion masses are therefore given by

$$m_{\pi_a}^2 = 2Bm_R\cos(\phi - \omega_L) + 2W_0 a\cos\phi - 2c_2 a^2\cos^2\phi, \quad a = 1, 2, \quad (48)$$

$$m_{\pi_3}^2 = m_{\pi_a}^2 + 2c_2 a^2\sin^2\phi. \quad (49)$$

Multiplying the gap equation (42) by $\sin\phi$ one easily finds

$$2Bm_R\cos(\phi - \omega_L) + 2W_0 a\cos\phi - 2c_2 a^2\cos^2\phi = \frac{2Bm + 2W_0 a}{t} - 2c_2 a^2, \quad (50)$$

which can be used to rewrite the pion mass formulas as

$$m_{\pi_a}^2 = \frac{2Bm + 2W_0 a}{t} - 2c_2 a^2, \qquad a = 1, 2, \quad (51)$$

$$\Delta m_\pi^2 \equiv m_{\pi_3}^2 - m_{\pi_a}^2 = 2c_2 a^2(1 - t^2). \quad (52)$$

As expected, the pions are degenerate only for $t = 1$, i.e., when Σ_0 is proportional to the identity and the flavor symmetry is unbroken. The appearance of t in the denominator in Eq. (51) does not imply a divergence in the pion mass, since $t = 0$ is a solution to the gap equation only if $2Bm + 2W_0 a = 0$. This is evident from the alternative expression[4]

$$m_{\pi_a}^2 = \frac{2B\mu}{\sqrt{1 - t^2}}, \qquad a = 1, 2, \quad (53)$$

for the pion mass, which is easily obtained by rewriting Eq. (44) as

$$\frac{\alpha^2}{1 - t^2} = \left(\frac{\chi}{t} - 1\right)^2. \quad (54)$$

This form is valid as long as $t^2 \neq 1$.

Note that the pion mass in the untwisted case does not vanish for $m = 0$, but is rather given by ($m = m_R$ for $\omega_L = 0$)

$$m_{\pi_a}^2 = m_{\pi_3}^2 = 2Bm_R + 2W_0 a - 2c_2 a^2. \quad (55)$$

Even though the definition of the quark mass m_R includes the subtraction of the additive renormalization proportional to $1/a$, it does not include the full subtraction of the critical quark mass [20]. If we define a renormalized mass $\tilde{m}_R = Z_m(m_0 - M_{\mathrm{cr}})$ such that the pion mass vanishes for $m_0 = M_{\mathrm{cr}}$, the renormalized mass parameters $\tilde{m}_R$ and m_R are related by

$$\tilde{m}_R = m_R + \frac{W_0}{B}a - \frac{c_2}{B}a^2. \quad (56)$$

Equation (55), by definition, now reads $m_{\pi_a}^2 = m_{\pi_3}^2 = 2B\tilde{m}_R$ and the pion mass vanishes for $\tilde{m}_R = 0$. The terms

[4]This relation shows that the charged pions are massless Nambu-Goldstone bosons in the parity-flavor broken phase ($t^2 < 1$) at $\mu = 0$. At nonzero μ an exact lattice vector Ward-Takahashi identity leads to this PCVC (Partially Conserved Vector Current) relation [21,22]. We would like to thank Y. Shamir for reminding us of this point.

proportional to a and a^2 on the right-hand side of (56) are contributions to the critical quark mass stemming from the Pauli term and chiral symmetry breaking four-quark operators in Symanzik's effective action, which is used in an intermediate step in order to derive the chiral effective Lagrangian [20]. Note, in particular, the contribution c_2a^2/B to the critical quark mass, which corresponds to the r-even contribution in the ansatz equation (18).

D. VEV and pion masses

In this section we present some approximate solutions to the gap equation (44). Approximate solutions will be sufficient for our purposes, since we are mainly interested in generic cases where the quark mass m and/or the twisted mass μ is either much larger or much smaller than the lattice artifacts. In these cases the gap equation usually simplifies and an approximate solution is easily found.

Consider, for example, the case where both $2Bm + 2W_0a$ and $2B\mu$ are much larger than $2c_2a^2$, i.e., $\chi \gg 1$ and $\alpha \gg 1$. In this case we can approximate the gap equation by

$$\alpha^2 t_0^2 = \chi^2(1 - t_0^2), \tag{57}$$

and the approximate solution $t_0 \approx t$ is readily found to be

$$t_0 = \frac{\chi}{\sqrt{\chi^2 + \alpha^2}}. \tag{58}$$

Once we have found the dominant part t_0 of the solution, we write $t = t_0 - \delta$ and substitute this into the gap equation. Since the correction satisfies $\delta \ll t_0$ we only keep the terms linear in δ, and the resulting equation is easily inverted to give δ. The result for t can then be used in Eqs. (51) and (52) in order to obtain approximate expressions for the pion masses. Using this procedure we find the following approximate solutions for the gap equation:

(1) $\chi \gg 1$ and $\alpha \gg 1$ (i.e., $2Bm + 2W_0a \geq \mathrm{O}(a)$ and $2B\mu \geq \mathrm{O}(a)$). We set $t = t_0 - \delta$ and find

$$t_0 = \frac{\chi}{\sqrt{\chi^2 + \alpha^2}}, \qquad \delta = \frac{\alpha^2\chi}{(\chi^2 + \alpha^2)^2}. \tag{59}$$

In this case the pion masses become

$$m_{\pi_a}^2 = 2c_2a^2\left[\sqrt{\chi^2 + \alpha^2} - \frac{\chi^2}{\chi^2 + \alpha^2}\right], \tag{60}$$

$$\Delta m_\pi^2 = 2c_2a^2\frac{\alpha^2}{\chi^2 + \alpha^2}. \tag{61}$$

(2) $\chi \approx 1$ and $\alpha \gg 1$ (i.e., $2Bm + 2W_0a = \mathrm{O}(a^2)$ and $2B\mu \geq \mathrm{O}(a)$). Again, $t = t_0 - \delta$,

$$t_0 = \frac{\chi}{\alpha}, \qquad \delta = \frac{\chi}{\alpha^2}, \tag{62}$$

$$m_{\pi_a}^2 = 2c_2a^2\left[\frac{\alpha}{1 - 1/\alpha} - 1\right] \simeq 2c_2a^2\alpha + \mathrm{O}\left(\frac{a^2}{\alpha}\right), \tag{63}$$

$$\Delta m_\pi^2 = 2c_2a^2\left[1 - \frac{\chi^2}{\alpha^2}\right] \simeq 2c_2a^2. \tag{64}$$

(3) $\chi > 1$ and $\chi \gg \alpha$ (i.e., $2Bm + 2W_0a \gg 2B\mu$). The solution of the gap equation is close to 1 in this case. We define $t = 1 - \delta$ and find

$$2\delta = \frac{\alpha^2}{(\chi - 1)^2 + \alpha^2}, \tag{65}$$

$$m_{\pi_a}^2 = 2c_2a^2[\chi - 1 + \chi\delta], \tag{66}$$

$$\Delta m_\pi^2 = 4c_2a^2\delta. \tag{67}$$

(4) $\chi < 1$ and $\chi \gg \alpha$ (i.e., $2Bm + 2W_0a \gg 2B\mu$). In this case we define $t = \chi - \delta$,

$$\delta = \frac{\alpha\chi}{\sqrt{1 - \chi^2}}, \tag{68}$$

$$m_{\pi_a}^2 = 2c_2a^2\frac{\delta}{\chi - \delta} \simeq 2c_2a^2\frac{\delta}{\chi} = 2c_2a^2\frac{\alpha}{\sqrt{1 - \chi^2}}, \tag{69}$$

$$\Delta m_\pi^2 = 2c_2a^2[1 - \chi^2 + 2\chi\delta]. \tag{70}$$

(5) $\chi = 1$ and $\chi \gg \alpha$ (i.e., $2Bm + 2W_0a = 2c_2a^2$ and $2Bm + 2W_0a \gg 2B\mu$). We define $t = 1 - \delta$ and find

$$2\delta = (2\alpha)^{2/3}, \tag{71}$$

$$m_{\pi_a}^2 = c_2a^2(2\alpha)^{2/3}, \tag{72}$$

$$\Delta m_\pi^2 = 2c_2a^2(2\alpha)^{2/3}. \tag{73}$$

E. Twist angle from the Ward-Takahashi identities

In the continuum formulation of twisted mass QCD one can derive the vector and axial-vector WT identities [1]

$$\partial_\mu V_\mu^a = -2\mu\epsilon^{3ab}P^b, \qquad \partial_\mu A_\mu^a = 2mP^a + 2i\mu S^0\delta^{a3}, \tag{74}$$

where the currents and densities are given as

$$V_\mu^a = \bar\psi\gamma_\mu t^a\psi, \qquad A_\mu^a = \bar\psi\gamma_\mu\gamma_5 t^a\psi, \qquad S^0 = \bar\psi\psi, \qquad P^a = \bar\psi\gamma_5 t^a\psi. \tag{75}$$

A twist angle $\omega_{\rm WT}$ can be defined by

$$\tan\omega_{\rm WT} = \frac{\langle \partial_\mu V^2_\mu P^1\rangle}{\langle \partial_\mu A^1_\mu P^1\rangle}. \tag{76}$$

Using the WT identities (74) one can easily establish $\tan\omega_{\rm WT} = \mu/m$, i.e., the twist angle defined by the WT identities coincides with the one in the action.

Similarly, a twist angle $\omega_{\rm WT}$ can be defined in tmLQCD. Because of the explicit breaking of chiral symmetry, however, the WT identity for the axial vector receives additional contributions proportional to powers of the lattice spacing. These contributions can be made explicit by deriving the WT identities on the basis of the Symanzik action for lattice tm-QCD: The Pauli term at O(a), for example, will give rise to contributions linear in a on the right-hand side of the axial-vector WT identity in (74).

The ratio on the right-hand side of (76) can also be computed in the chiral effective theory. To do this we first derive the vector and axial-vector WT identities in the effective theory. Vector and axial-vector transformations of the field are defined by

$$\Sigma \rightarrow L\Sigma R^\dagger, \tag{77}$$

where

$$R = e^{i(\theta^a_V+\theta^a_A)\tau_a}, \qquad L = e^{i(\theta^a_V-\theta^a_A)\tau_a}. \tag{78}$$

For a vector transformation ($\theta^a_A = 0$) we have $L = R$, while a pure axial-vector transformation is defined by $\theta^a_V = 0$ and satisfies $L = R^\dagger$. Under an infinitesimal local variation the field transforms as

$$\delta\Sigma = i\theta^a_V[\tau_a, \Sigma] + i\theta^a_A\{\tau_a, \Sigma\}, \tag{79}$$

$$\delta\Sigma^\dagger = i\theta^a_V[\tau_a, \Sigma^\dagger] - i\theta^a_A\{\tau_a, \Sigma^\dagger\}, \tag{80}$$

and the variation of the kinetic term plus the potential energy (37) in the Lagrangian is given by

$$\delta L = i\theta^a_V[-\partial_\mu V^a_\mu + X^a_V] + i\theta^a_A[-\partial_\mu A^a_\mu + X^a_A], \tag{81}$$

where

$$V^a_\mu = \frac{f^2}{2}\langle\tau_a(\Sigma^\dagger\partial_\mu\Sigma + \Sigma\partial_\mu\Sigma^\dagger)\rangle, \tag{82}$$

$$A^a_\mu = \frac{f^2}{2}\langle\tau_a(\Sigma^\dagger\partial_\mu\Sigma - \Sigma\partial_\mu\Sigma^\dagger)\rangle, \tag{83}$$

$$X^a_V = -f^2 2\frac{2B\mu}{4}\epsilon^{3ab}P^b, \tag{84}$$

$$X^a_A = f^2\frac{2(2Bm + 2W_0a) - c_2a^2S^0}{4}P^b - if^2 2\frac{2B\mu}{4}S^0\delta^{a3}. \tag{85}$$

In the last two lines we introduced $P^a = \langle\tau_a(\Sigma - \Sigma^\dagger)\rangle$ and $S^0 = \langle\Sigma + \Sigma^\dagger\rangle$. The variation δL implies the WT identities

$$\partial_\mu V^a_\mu = X^a_V, \qquad \partial_\mu A^a_\mu = X^a_A, \tag{86}$$

which are the analogue of Eq. (74) in the effective theory. Using Eqs. (84) and (85) we find

$$\tan\omega_{\rm WT} = \frac{\langle X^2_V P^1\rangle}{\langle X^1_A P^1\rangle} = \frac{2B\mu}{2Bm + 2W_0a - 2c_2a^2\cos\phi} = \frac{\alpha}{\chi - t}, \tag{87}$$

where we used the expansion

$$\langle S^0P^1P^1\rangle = 4\cos\phi\langle P^1P^1\rangle + \langle {\rm O}(\pi^3)\rangle \tag{88}$$

and dropped the cubic terms in the pion fields. Note that $\omega_{\rm WT} \neq \omega_L$ since the twist angle in the chiral Lagrangian satisfies $\tan\omega_L = \mu/m$, according to Eq. (34). Instead, using Eq. (54), we find $\omega_{\rm WT} = \pm\phi$.

IV. MAXIMAL TWIST AND O(a) IMPROVEMENT

In this section we study the question of automatic O(a) improvement at maximal twist in the case of the pion mass. We emphasize again that setting the angle ω_L in the chiral Lagrangian to $\pi/2$ neither corresponds to maximal twist in the sense of Ref. [9] nor in the sense of definition (29). The reason is the parametrization of the chiral Lagrangian in terms of the renormalized mass m_R which does not include the O(a) and O(a^2) contributions to the critical mass. It is, however, not difficult to define the previously discussed twist angles in terms of the parameters in the chiral Lagrangian.

A. $\omega_L = \pi/2$

In order to illustrate the possible subtleties of O(a) improvement we first consider the case where the twist angle in the chiral Lagrangian is taken to be $\pi/2$. With this choice we have $\mu = m_R$, and we need to discuss the following two cases:

(1) $2B\mu = 2Bm_R \geq 2W_0a$. This corresponds to case 1 in Sec. III D and the pion mass is given by

$$m^2_{\pi_a} = \sqrt{(2B\mu)^2 + (2W_0a)^2}, \tag{89}$$

$$\Delta m^2_\pi = 2c_2a^2\frac{(2B\mu)^2}{(2B\mu)^2 + (2W_0a)^2}. \tag{90}$$

For $2B\mu \gg 2W_0a$ we can expand the square root and find $m^2_{\pi_a} \approx 2B\mu + {\rm O}(a^2)$, hence the pion mass is O(a) improved. On the other hand, this simple

$O(a^2)$ scaling behavior no longer holds for $2B\mu \approx 2W_0 a$.

(2) $2B\mu = 2Bm_R \ll 2W_0 a$. In this case we find

$$m_{\pi_a}^2 = 2W_0 a - 2c_2 a^2 + \frac{(2B\mu)^2}{2W_0 a}, \tag{91}$$

$$\Delta m_\pi^2 = 2c_2 a^2 \frac{(2B\mu)^2}{(2W_0 a)^2} \ll O(a^2), \tag{92}$$

and the $O(a)$ term is present in the pion mass. In the massless limit the pion mass does not vanish and is instead given by $m_{\pi_a}^2 = 2W_0 a - 2c_2 a^2 \neq 0$.

If we define maximal twist as $\omega_L = \pi/2$, automatic $O(a)$ improvement is guaranteed only for $2B\mu \gg 2W_0$, which can be translated into $\mu \gg O(a\Lambda_{\rm QCD}^2)$.

Note that the twist angle defined through the WT identities is given by

$$\tan\omega_{\rm WT} \simeq \frac{2B\mu}{2W_0 a} \neq \infty. \tag{93}$$

Therefore $\omega_{\rm WT} = \pi/2 + O(a)$ for $2B\mu \gg 2W_0$ and $\omega_{\rm WT} \approx 2B\mu/2W_0 a \approx 0$ for $2B\mu \ll 2W_0 a$. This result is consistent with the observation that the pion mass is $O(a)$ improved only for $\mu \gg O(a\Lambda_{\rm QCD}^2)$.

B. Maximal twist of Frezzotti and Rossi

In Ref. [9] the twist angle is defined by

$$[m_0 - M_{\rm cr}(r)]e^{i\omega\tau_3\gamma_5} \tag{94}$$

in lattice QCD. In other words, the phase factor $\exp i\omega\tau_3\gamma_5$ multiplies the mass $\tilde{m}_R$ introduced in Eq. (56). Consequently, this definition translates into

$$\tilde{m}_R e^{i\omega\tau_3} \tag{95}$$

in the effective theory. Simple trigonometry (see Fig. 3) relates a given pair $(\tilde{m}_R, \omega)$ to the corresponding parameters (m_R, ω_L) in the chiral Lagrangian and we find

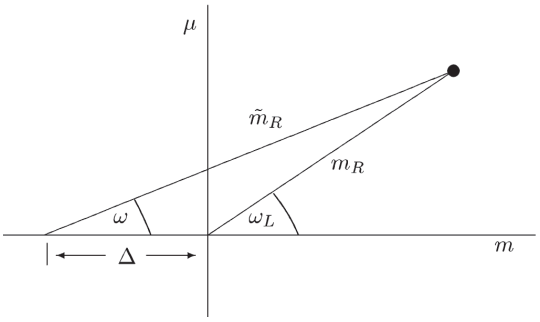

FIG. 3. A sketch showing the relation between the twist angles ω and ω_L. The masses m_R and $\tilde{m}_R$ differ by $\Delta = W_0 a/B - c_2 a^2/B$ in the case of zero twist (cf. Eq. (56)).

$$\tan\omega = \frac{2B\mu}{2Bm + 2W_0 a - 2c_2 a^2} = \frac{2Bm_R \sin\omega_L}{2Bm_R \cos\omega_L + 2W_0 a - 2c_2 a^2}. \tag{96}$$

A maximal twist angle $\omega = \pi/2$ therefore corresponds to $2Bm + 2W_0 a = 2c_2 a^2$.

As before we consider two cases, which correspond to cases 2 and 5 of Sec. III D:

(1) $2B\mu \geq O(a)$.

$$m_{\pi_a}^2 = 2B\mu, \tag{97}$$

$$\Delta m_\pi^2 = 2c_2 a^2. \tag{98}$$

The result is $O(a)$ improved in this case. The twist angle from the WT identities is given by

$$\tan\omega_{\rm WT} \simeq \frac{2B\mu}{2c_2 a^2}, \tag{99}$$

so that $\omega_{\rm WT} = \pi/2 + O(a^2)$ for $2B\mu \gg 2c_2 a^2$.

(2) $2B\mu \ll 2c_2 a^2$.

$$m_{\pi_a}^2 = (c_2 a^2)^{1/3}(2B\mu)^{2/3}, \tag{100}$$

$$\Delta m_\pi^2 = 2(c_2 a^2)^{1/3}(2B\mu)^{2/3}. \tag{101}$$

Although all pion masses vanish in the $\mu \to 0$ limit, the power $\mu^{2/3}$ is different from the behavior in the continuum limit, where the pion masses vanish linearly with μ. The fractional power 2/3 is the mean-field critical exponent for the second order phase transition: As the external field μ decreases, the correlation length diverges as $\mu^{-1/3}$ at $T = T_c$.

The twist angle from the WT identities becomes

$$\tan\omega_{\rm WT} \simeq \left(\frac{2B\mu}{2c_2 a^2}\right)^{1/3}. \tag{102}$$

Therefore $\omega_{\rm WT} \neq \pi/2$. In particular $\omega_{\rm WT} = 0$ at $\mu = 0$.

It seems that automatic $O(a)$ improvement holds only for $2B\mu \geq O(a^2\Lambda_{\rm QCD}^4)$ if we define maximal twist by the condition $2Bm + 2W_0 a - 2c_2 a^2 = 0$.

C. New proposal for maximal twist

Finally we consider the alternative definition for the twist angle proposed in Sec. II D. In tmLQCD it is defined by

$$\left(m_0 - \frac{M_{\rm cr}(r) - M_{\rm cr}(-r)}{2}\right)e^{i\omega'\tau_3\gamma_5}, \tag{103}$$

where $M_{\rm cr}(r) = M_{\rm cr}^{(1)}(r)$ is the critical quark mass as a function of r given in Sec. II D. Since the $c_2 a^2/B$ contribution to the critical quark mass is even in r, it cancels in the difference $M_{\rm cr}(r) - M_{\rm cr}(-r)$ in Eq. (103). The

definition (103) therefore corresponds in the effective theory to

$$\left(m_R + \frac{W_0}{B}a\right)e^{i\omega'\tau_3}, \tag{104}$$

and the twist angle ω' relates to the parameters in the chiral Lagrangian according to

$$\tan\omega' = \frac{2B\mu}{2Bm + 2W_0 a} = \frac{2Bm_R \sin\omega_L}{2Bm_R \cos\omega_L + 2W_0 a}. \tag{105}$$

This formula together with Eq. (96) yields the simple relation

$$\frac{2c_2 a^2}{2B\mu} = \cot\omega' - \cot\omega \tag{106}$$

between the two angles ω and ω'. As already illustrated in Fig. 2, the two angles are approximately equal if $2B\mu \gg 2c_2 a^2$.

According to Eq. (105), maximal twist $\omega' = \pi/2$ means $2Bm + 2W_0 a = 0$. In this case $t = \cos\phi = 0$ is the solution of the gap equation. Since the expression (51) for the pion mass is ill-defined in this case, we have to calculate the ratio $(2Bm + 2W_0 a)/t$ in the $2Bm + 2W_0 a \to 0^+$ limit.

Since $t \ll 1$ is the solution for $\chi \ll 1$, we can solve the approximate gap equation

$$\alpha^2 t^2 = (\chi - t)^2. \tag{107}$$

The solution is given by

$$t = \frac{\chi}{\alpha + 1} = \frac{2Bm + 2W_0 a}{2B\mu + 2c_2 a^2}, \tag{108}$$

and we therefore obtain

$$m_{\pi_a}^2 = 2B\mu, \tag{109}$$

$$\Delta m_\pi^2 = 2c_2 a^2, \tag{110}$$

for the pion masses. This result can also be derived from the expression (53) which is valid for all $t^2 \neq 1$. In this case, O(a) improvement is automatically satisfied, irrespective of the value of $2B\mu$.[5]

In addition to the result for the pion masses, the twist angle from the WT identities is calculated as

$$\tan\omega_{\mathrm{WT}} = \frac{2B\mu + 2c_2 a^2}{2Bm + 2W_0 a}. \tag{111}$$

In the limit $2Bm + 2W_0 a \to 0^+$ we consistently obtain $\omega' = \omega_{\mathrm{WT}} = \pi/2$.

[5]This result is only true for the *squared* pion masses. The mass itself of the neutral pion, m_{π_3}, is of O(a) for $2B\mu \ll 2c_2 a^2$. This has similarities to staggered fermions. Even though the staggered fermion action is automatically O(a) improved, the masses of the non-Goldstone pions are of O(a) for small quark masses [31,32].

We want to emphasize that our analysis only shows that the leading term linear in the lattice spacing a is absent in the result for the pion mass. There are, of course, subleading terms proportional to am^k which must be absent too. In order to show this explicitly one has to consistently include higher-order terms in the expression for the potential energy (37) and the gap equation. This is possible in principle. In practice, however, even the discussion of the O(am) contribution becomes much more involved and goes beyond the scope of this paper.

V. FINAL REMARKS

We pointed out a caveat in the proof for automatic O(a) improvement in tmLQCD at maximal twist if the twist angle is defined as in Ref. [9]. The proof hinges on the assumption that the critical quark mass is an odd function of the Wilson parameter r. This property, however, does not hold for the critical quark mass defined as the value where the pion becomes massless. As a result one has to impose the bound $m_q \gg a^2\Lambda_{\mathrm{QCD}}^3$ in order to guarantee automatic O(a) improvement at maximal twist. In this paper we gave an alternative definition for the twist angle which does not require such a restriction on the quark mass. Automatic O(a) improvement can be achieved even if the bound $m_q \gg a^2\Lambda_{\mathrm{QCD}}^3$ is not satisfied, provided the twist angle is properly defined.

The symmetry property for the critical quark mass probably does not hold for other definitions of the critical mass, for example, for the quark mass which enters the PCAC relation. The symmetry property needs to be established separately for each definition of the critical quark mass. This seems a formidable task taking into account the nonperturbative character of low-energy QCD. However, this difficulty does not rule out the existence of an r-odd critical mass. In fact, the average $\overline{M}_{\mathrm{cr}} = (M_{\mathrm{cr}}^{(1)} + M_{\mathrm{cr}}^{(2)})/2$ that enters our alternative definition for the twist angle is nothing but such an r-odd critical mass. Instead of saying we have defined a proper twist angle we could equally well summarize our results by saying we have defined a proper r-odd critical quark mass. Once this has been achieved the proof for automatic O(a) improvement in Ref. [9] goes through without any bound for the quark mass.

Having O(a) improvement without a restriction on the quark mass is quite relevant for numerical lattice simulations. Keeping the quark mass large enough such that the inequality $m_q \gg a^2\Lambda_{\mathrm{QCD}}^3$ is satisfied would imply fairly large quark and consequently pion masses. To be more explicit let us assume approximately 300 MeV for the scale Λ_{QCD}. In order to satisfy the bound for a lattice spacing of about 0.1 fm (which is already rather small) we need to keep the quark mass larger than half the strange quark mass. This would compromise one of the main motivations for using twisted mass lattice QCD, namely,

that one can perform numerical simulations with fairly small quark masses.

Our alternative definition for the twist angle involves the average $\overline{M}_{\rm cr} = (M_{\rm cr}^{(1)} + M_{\rm cr}^{(2)})/2$ over two values for the critical mass. In practice, however, it might be unnecessary to determine these two values independently in a numerical simulation. The analysis in the chiral effective theory has shown that our definition for the twist angle coincides with the twist angle defined by the WT identities in the case of maximal twist. Maximal twist is therefore realized when we tune the bare untwisted mass parameter in a simulation such that the denominator in Eq. (76) vanishes.

The crucial assumption for automatic O(a) improvement is the symmetry property of the critical mass. This property cannot be guaranteed if the defining equation (16) for the critical mass has more than one solution. This is the case if the massless pion is realized by the spontaneous breakdown of parity and flavor [19,21,22]. As we already mentioned, it is also possible that Eq. (16) has no solution at all and that the pion is never massless at nonzero lattice spacing. This scenario also emerges quite naturally in WChPT as the alternative to the case where parity and flavor are spontaneously broken [20]. Recent numerical results suggest that this scenario might be realized when the Wilson plaquette action and the unimproved Wilson fermion action is employed [33–35].

Although further confirmation for the existence of this scenario is needed, let us briefly consider this case here. Without a solution for the defining equation (16) we have to look for a different definition of $M_{\rm cr}$. A natural choice might be that the pion masses assume their minimal value for $m_0 = M_{\rm cr}$ (in infinite volume). This is an unambiguous definition since this point corresponds to a first order phase transition, at least in the framework of the chiral effective theory [20,23]. Furthermore, the analysis in the chiral effective theory shows that this minimum is unique. Consequently, this $M_{\rm cr}$ is odd under a sign flip in r and the arguments for automatic O(a) improvement in Ref. [9] can be applied. Our analysis of O(a) improvement for the pion mass in the chiral effective theory can also be performed for this scenario, and the relevant steps are presented in Appendix A.

The numerical results in Ref. [35] have been obtained with the standard Wilson plaquette action and the unimproved Wilson fermion action. It is unknown how a change in the lattice action, for example by adding a clover term, influences the results. A different lattice action can, at least in principle, affect the size and/or sign of the coefficient c_2 in the chiral Lagrangian of the effective theory, which eventually determines the phase diagram of tmLQCD close to the continuum limit.

Lattice actions with good scaling properties are important for numerical simulations. Automatic O(a) improvement at maximal twist may give us an extra handle to achieve this. We no longer need to fix the coefficient of the clover term in order to cancel the linear cutoff artifacts. It is an interesting question whether one can tune this coefficient in order to make c_2 substantially smaller, i.e., to reduce cutoff artifacts at O(a^2).

ACKNOWLEDGMENTS

We would like to thank S. Sharpe and K. Jansen for useful discussions. O. B. would also like to thank M. Golterman, Y. Shamir, and S. Sint for discussions during the workshop "Matching light quarks to hadrons" in Benasque, where this work was completed. Support of the Benasque Center of Science is gratefully acknowledged. We also thank M. Golterman, Y. Shamir, and A. Shindler for their helpful comments concerning the first draft of this paper. Finally we would like to thank G. C. Rossi for clarifying comments about the critical quark mass. This work is supported in part by the Grants-in-Aid for Scientific Research from the Ministry of Education, Culture, Sports, Science and Technology (No. 13135204, No. 15204015, No. 15540251, No. 16028201). O. B. is supported in part by the University of Tsukuba Research Project.

APPENDIX A: THE $c_2 < 0$ CASE

It has been pointed out recently that tmLQCD undergoes a first order phase transition at small μ for $\beta = 5.2$ [35]. The authors interpret the existence of this first order phase transition as the alternative scenario in WChPT where $c_2 < 0$ [20]. Motivated by these results we extend our analysis to this case. (A similar analysis has already been made in Refs. [23,25,27].)

At $\mu = 0$, the vacuum expectation value has a gap at $\tilde{c}_1 = 2Bm_R + 2W_0 a = 0$:

$$\Sigma_0 = \begin{cases} 1 & \text{for } \tilde{c}_1 > 0, \\ -1 & \text{for } \tilde{c}_1 < 0. \end{cases} \tag{A1}$$

Accordingly the pion masses become

$$m_{\pi_a}^2 = m_{\pi_3}^2 = |\tilde{c}_1| - 2c_2 a^2 \tag{A2}$$

and remain massive for $\tilde{c}_1 = 0$,

$$m_{\pi_a}^2 = m_{\pi_3}^2 = -2c_2 a^2 > 0. \tag{A3}$$

We now consider how this result changes for nonzero μ by solving approximately the gap equation (44).

(1) Small μ ($2B\mu \ll |\tilde{c}_1| - 2c_2 a^2$)

The first order phase transition persists in this case:

$$t = \begin{cases} 1 - \delta & \text{for } \tilde{c}_1 > 0, \\ -1 + \delta & \text{for } \tilde{c}_1 < 0, \end{cases} \tag{A4}$$

where

$$\delta = \frac{1}{2}\left(\frac{2B\mu}{|\tilde{c}_1| - 2c_2 a^2}\right)^2 = \mathrm{O}(\mu^2). \tag{A5}$$

The pion masses are given by

$$m^2_{\pi_a} = |\tilde{c}_1|(1+\delta) - 2c_2a^2 \tag{A6}$$

$$\Delta m^2_\pi = 4c_2a^2\delta < 0. \tag{A7}$$

The point where the first order phase transition occurs ($\tilde{c}_1 = 0$) corresponds to maximal twist according to our new proposal, $\omega' = \pm\pi/2$.
As before we can define the twist angle $\omega_{\rm WT}$ using the WT identities, and Eq. (87) reads

$$\tan\omega_{\rm WT} = \frac{2B\mu}{\tilde{c}_1 - 2c_2a^2 t} \tag{A8}$$

in terms of $\tilde{c}_1$. According to the solution (A4) this angle is discontinuous at the phase transition line. In particular, for vanishing $\tilde{c}_1$ we find the approximate values

$$\tan\omega_{\rm WT} = \begin{cases} \frac{2B\mu}{-2c_2a^2} > 0 & \text{for } \tilde{c}_1 \to 0^+, \\ -\frac{2B\mu}{-2c_2a^2} < 0 & \text{for } \tilde{c}_1 \to 0^-. \end{cases} \tag{A9}$$

Notice that $\omega_{\rm WT} \neq \pm\pi/2$, even though the twist angle $\omega' = \pm\pi/2$.

(2) Large μ ($2B\mu \gg |\tilde{c}_1| - 2c_2a^2$)
For large μ we can neglect the term proportional to c_2 in Eq. (41) and the first order phase transition disappears:

$$t = \frac{\tilde{c}_1}{\sqrt{\tilde{c}_1^2 + (2B\mu)^2}}. \tag{A10}$$

Therefore $|t| < 1$ and no gap exists at $\tilde{c}_1 = 0$. The pion masses are given by

$$m^2_{\pi_a} = \sqrt{(2B\mu)^2 + \tilde{c}_1^2} - 2c_2a^2 \tag{A11}$$

$$\Delta m^2_\pi = 2c_2a^2\frac{(2B\mu)^2}{(2B\mu + \tilde{c}_1^2)^2} < 0. \tag{A12}$$

The solution (A10) and consequently the denominator of the right-hand side in (A8) go to zero for $\tilde{c}_1 \to 0$. Hence, setting $\omega' = \pm\pi/2$ coincides with $\omega_{\rm WT} = \pm\pi/2$.

(3) General μ for $\tilde{c}_1 = 0$
In order to estimate the value of μ at which the first order phase transition disappears, we consider the case $\tilde{c}_1 = 0$ for arbitrary values of μ. In this case, the solution to the gap equation is given by

$$t = \begin{cases} \sqrt{1 - \frac{(2B\mu)^2}{(2c_2a^2)^2}}, & |2B\mu| < -2c_2a^2, \quad \tilde{c}_1 \to 0^+, \\ -\sqrt{1 - \frac{(2B\mu)^2}{(2c_2a^2)^2}}, & |2B\mu| < -2c_2a^2, \quad \tilde{c}_1 \to 0^-, \\ 0, & |2B\mu| \geq -2c_2a^2, \quad \tilde{c}_1 \to 0. \end{cases} \tag{A13}$$

Therefore there is no first order phase transition for $|2B\mu| > -2c_2a^2$, and $2B\mu = \mp 2c_2a^2$ are the two endpoints of the first order phase transition line. It is easy to verify that the solution, expanded in terms of small μ,

$$t = \begin{cases} 1 - \frac{1}{2}\frac{(2B\mu)^2}{(2c_2a^2)^2}, & |2B\mu| < -2c_2a^2, \quad \tilde{c}_1 \to 0^+, \\ -1 + \frac{1}{2}\frac{(2B\mu)^2}{(2c_2a^2)^2}, & |2B\mu| < -2c_2a^2, \quad \tilde{c}_1 \to 0^-, \end{cases} \tag{A14}$$

agrees with the one in Eq. (A4) for $\tilde{c}_1 = 0$. The corresponding pion masses are given by

$$m^2_{\pi_a} = \begin{cases} -2a^2c_2, & |2B\mu| < -2c_2a^2, \\ |2B\mu|, & |2B\mu| \geq -2c_2a^2, \end{cases} \tag{A15}$$

$$\Delta m^2_\pi = \begin{cases} 2c_2a^2(\frac{2B\mu}{2c_2a^2})^2 < 0, & |2B\mu| < -2c_2a^2, \\ 2c_2a^2 < 0, & |2B\mu| \geq -2c_2a^2. \end{cases} \tag{A16}$$

Therefore $m^2_{\pi_3} = 0$ vanishes at the two endpoints of the first order phase transition line, defined by $|2B\mu| = -2c_2a^2$. According to Eq. (105), $\tilde{c}_1 = 0$ corresponds to $\omega' = \pi/2$ ($-\pi/2$) for positive (negative) values of μ.
Using the solution for the gap equation in (A13) one easily finds

$$\tan\omega_{\rm WT} = \begin{cases} \frac{2B\mu}{-2c_2a^2}/\sqrt{1 - (\frac{2B\mu}{-2c_2a^2})^2} > 0, & |2B\mu| < -2c_2a^2, \quad \tilde{c}_1 \to 0^+, \\ -\frac{2B\mu}{-2c_2a^2}/\sqrt{1 - (\frac{2B\mu}{-2c_2a^2})^2} < 0, & |2B\mu| < -2c_2a^2, \quad \tilde{c}_1 \to 0^-, \\ \infty, & |2B\mu| \geq -2c_2a^2, \quad \tilde{c}_1 \to 0. \end{cases} \tag{A17}$$

For $|2B\mu| \ll -2c_2a^2$ one recovers the approximate solution in Eq. (A9). As noted before, the angle ω_{WT} never assumes the maximal value $\pm\pi/2$ as long as $|2B\mu| \leq -2c_2a^2$. Instead, the angle changes its sign when crossing the phase transition line. Similarly, the PCAC quark mass changes sign since the denominator in (A8) is proportional to this quark mass.

We emphasize that the difference Δm_π^2 is negative for $c_2 < 0$, i.e., the charged pions are heavier than the neutral one. Hence, as has already been pointed out in Ref. [27], the sign of the coefficient c_2 can be determined, at least in principle, by measuring the masses of the charged and neutral pions.

[1] ALPHA Collaboration, R. Frezzotti, P. A. Grassi, S. Sint, and P. Weisz, J. High Energy Phys. 08 (2001) 058.
[2] ALPHA Collaboration R. Frezzotti, S. Sint, and P. Weisz, J. High Energy Phys. 07 (2001) 048.
[3] R. Frezzotti, Nucl. Phys. B, Proc. Suppl. **119**, 140 (2003).
[4] R. Frezzotti, hep-lat/0409138.
[5] S. Aoki and A. Gocksch, Phys. Lett. B **231**, 449 (1989).
[6] S. Aoki and A. Gocksch, Phys. Lett. B **243**, 409 (1990).
[7] S. Aoki and A. Gocksch, Phys. Rev. D **45**, 3845 (1992).
[8] A. D. Kennedy, hep-lat/0409167.
[9] R. Frezzotti and G. C. Rossi, J. High Energy Phys. 08 (2004) 007.
[10] R. Frezzotti and G. C. Rossi, J. High Energy Phys. 10 (2004) 070.
[11] K. Symanzik, *Recent Developments in Gauge Theories*, NATO Advanced Study Institutes, Ser. B, Vol. 59, edited by G. 't Hooft *et al.* (Plenum Press, New York, 1980).
[12] K. Symanzik, Nucl. Phys. **B226**, 187 (1983).
[13] K. Symanzik, Nucl. Phys. **B226**, 205 (1983).
[14] G. Rupak and N. Shoresh, Phys. Rev. D **66**, 054503 (2002).
[15] S. Aoki, Phys. Rev. D **68**, 054508 (2003).
[16] O. Bär, G. Rupak, and N. Shoresh, Phys. Rev. D **70**, 034508 (2004).
[17] O. Bär, G. Rupak, and N. Shoresh, Nucl. Phys. B, Proc. Suppl. **129**, 185 (2004).
[18] O. Bär, hep-lat/0409123.
[19] S. Aoki, Phys. Rev. D **30**, 2653 (1984).
[20] S. R. Sharpe and R. J. Singleton, Phys. Rev. D **58**, 074501 (1998).
[21] S. Aoki, Phys. Rev. Lett. **57**, 3136 (1986).
[22] S. Aoki, Nucl. Phys. **B314**, 79 (1989).
[23] S. R. Sharpe and J. M. S. Wu, Phys. Rev. D **70**, 094029 (2004).
[24] S. R. Sharpe and J. M. S. Wu, hep-lat/0407035.
[25] G. Münster and C. Schmidt, Europhys. Lett. **66**, 652 (2004).
[26] G. Münster, J. High Energy Phys. 09 (2004) 035.
[27] L. Scorzato, Eur. Phys. J. C **37**, 445 (2004).
[28] O. Bär, G. Rupak, and N. Shoresh, Phys. Rev. D **67**, 114505 (2003).
[29] J. Gasser and H. Leutwyler, Ann. Phys. (N.Y.) **158**, 142 (1984).
[30] J. Gasser and H. Leutwyler, Nucl. Phys. **B250**, 465 (1985).
[31] W. J. Lee and S. R. Sharpe, Phys. Rev. D **60**, 114503 (1999).
[32] C. Aubin and C. Bernard, Phys. Rev. D **68**, 034014 (2003).
[33] A. Sternbeck, E. M. Ilgenfritz, W. Kerler, M. Müller-Preussker, and H. Stüben, Nucl. Phys. B, Proc. Suppl. **129**, 898 (2004).
[34] E. M. Ilgenfritz, W. Kerler, M. Müller-Preussker, A. Sternbeck, and H. Stüben, Phys. Rev. D **69**, 074511 (2004).
[35] F. Farchioni *et al.*, hep-lat/0406039.

PHYSICAL REVIEW D **72,** 054502 (2005)

Chiral perturbation theory for staggered sea quarks and Ginsparg-Wilson valence quarks

Oliver Bär,[1,*] Claude Bernard,[2,†] Gautam Rupak,[3,‡] and Noam Shoresh[4,§]

[1]*Institute of Physics, University of Tsukuba, Tsukuba, Ibaraki 305-8571, Japan*
[2]*Department of Physics, Washington University, St. Louis, Missouri 63130, USA*
[3]*Los Alamos National Laboratory, Theoretical Division T-16, Los Alamos, New Mexico 87545, USA*
[4]*Department of Physics, Boston University, Boston, Massachusetts 02215, USA*

(Received 30 March 2005; published 2 September 2005)

We study lattice QCD with staggered sea and Ginsparg-Wilson valence quarks. The Symanzik effective action for this mixed lattice theory, including the lattice spacing contributions of $\mathcal{O}(a^2)$, is derived. Using this effective theory we construct the leading-order chiral Lagrangian. The masses and decay constants of pseudoscalars containing two Ginsparg-Wilson valence quarks are computed at one-loop order.

DOI: 10.1103/PhysRevD.72.054502 PACS numbers: 11.15.Ha, 12.38.Gc, 12.39.Fe

I. INTRODUCTION

Unquenched simulations with fermions that satisfy the Ginsparg-Wilson relation [1] are computationally much more demanding than those with staggered or Wilson fermions. A precise comparison between the numerical cost depends on many details of the simulation, for example, the lattice spacing, the quark masses and also the practical implementation of the Ginsparg-Wilson (GW) fermion, i.e., how well the overlap [2–4] or the domain-wall fermion [5,6] is approximated. A recent review [7], however, suggests that dynamical Ginsparg-Wilson fermions may be about ten to one hundred times more expensive than corresponding simulations at comparable masses with either improved staggered fermions using the Asqtad action [8–10] or twisted-mass Wilson fermions [11]. For that reason most dynamical GW simulations so far have been carried out on small volumes together with rather heavy quark masses (see Ref. [7] and references therein). Simulating volumes and quark masses comparable to those in present day staggered simulations [10], for example, is out of reach in the near future.

A computationally affordable compromise for certain applications may be the so-called mixed fermion simulations. This type of simulation employs GW fermions only for the valence quarks, while the sea quarks are either staggered or Wilson fermions. In such an approach at least the valence sector exhibits all the benefits stemming from the exact chiral symmetry at nonzero lattice spacing [12]. Moreover, provided one can use already existing unquenched configurations generated with either staggered or Wilson fermions, mixed simulations only require the computation of correlators in the background of these configurations. The additional numerical cost is therefore comparable to quenched GW fermion simulations. Such mixed actions in two dimensions were studied in the Schwinger model in Ref. [13]. In four dimensions, preliminary results using the publicly available MILC configurations together with domain-wall or overlap valence fermions have been reported recently [14–16].

In this paper we construct the low-energy chiral effective Lagrangian for a mixed lattice theory with staggered sea and GW valence quarks. Based on this effective Lagrangian we compute the pseudoscalar meson masses and decay constants to one loop. Our results provide the leading quark mass and lattice spacing dependence of these quantities. The formulas are needed in order to analyze numerical data of mixed simulations.

This paper parallels Refs. [17,18], where the chiral Lagrangian for the mixed lattice theory with Wilson sea quarks and GW valence quarks was constructed. We first find all the relevant operators of $\mathcal{O}(a^2)$ in the Symanzik effective action [19,20] for the mixed lattice theory. A spurion analysis similar to that in ordinary χPT [21–23] is applied to the Symanzik effective action [24,25]. The result is a chiral effective theory that exhibits explicit quark mass and lattice spacing dependence of the underlying lattice theory. A recent review of this method can be found in Ref. [26].

The leading-order chiral Lagrangian presented here includes the lattice spacing effects proportional to a^2. Compared to the leading-order Lagrangian of staggered χPT [27–30], which is the appropriate low-energy effective theory for ''unmixed'' lattice QCD with staggered sea and valence quarks, it contains only one additional operator together with an undetermined low-energy constant. This new operator contributes to the masses of ''mixed'' mesons (one valence and one sea quark) at tree level in the chiral expansion. The decay constant of valence-valence mesons then receives contributions from the new operator through the mixed meson masses at one loop. However, the masses of valence-valence mesons themselves get no one-loop contribution from the new operator. Besides an analytic contribution of $\mathcal{O}(m_{\text{quark}}a^2)$, the one-loop pseudoscalar masses depend only on the leading-order low-energy constants of staggered χPT and the next-to-leading-

*Electronic address: obaer@het.ph.tsukuba.ac.jp
†Electronic address: cb@lump.wustl.edu
‡Electronic address: grupak@lanl.gov
§Electronic address: shoresh@cgr.harvard.edu

order (NLO) low-energy constants of continuum χPT, the Gasser-Leutwyler coefficients. To the extent that these low-energy constants are known from previously performed staggered simulations [10], the quark mass and lattice spacing dependence of the valence-valence pseudoscalar mesons in the mixed theory are highly restricted and depend on only one free parameter.

The paper is organized as follows: In Sec. II we discuss the Symanzik effective action for the mixed lattice theory and list all those operators that are relevant in the subsequent analysis. We then perform the necessary spurion analysis and derive the $\mathcal{O}(a^2)$ terms in the chiral effective Lagrangian. The tree-level meson masses are written down in Sec. III A. In Sec. III B we calculate the valence-valence meson masses at one loop; while the corresponding calculation of the pseudoscalar decay constants is given in Sec. III C. We conclude with a discussion of the results in Sec. IV. The appendix is devoted to some technical details of our calculation.

II. THE CHIRAL EFFECTIVE LAGRANGIAN

A. Lattice theory

Mixed fermion theories are a generalization of partially quenched theories. Theoretically they can be formulated by an action with anticommuting sea and valence quarks and commuting valence ghosts [31], where the quark masses and the Dirac operators are chosen differently in the sea and in the valence sector.[1] In the following we consider a mixed theory with N_f staggered sea and N_V valence fermions.

The sea sector is described by the standard staggered fermion action,

$$S_{\text{Sea}} = a^4 \sum_{x,\mu} \overline{\chi}_S(x)[\eta_\mu \nabla_\mu + m_{\text{Sea}}]\chi_S(x), \tag{1}$$

where ∇_μ denotes the gauge covariant central difference operator and m_{Sea} is the $N_f \times N_f$ mass matrix in the sea sector. For brevity we have suppressed the flavor and color indices. This action is invariant under lattice rotations, axis reversal, and translations by one lattice spacing (the so-called shift symmetry). In addition, the single-flavor staggered theory possesses vector and (in the massless case) axial-vector $U(1)$ symmetries. The explicit expressions for the field transformations that correspond to these symmetries can be found in Ref. [33]. For N_f flavors, these symmetries extend to a $U(N_f)_\ell \times U(N_f)_r$ symmetry [29] that corresponds to flavor transformations on the odd and even sites separately.[2]

[1]Instead of this "ghost" formulation one could also employ the "replica method" with valence quarks only [32].

[2]The subscripts ℓ and r are used instead of L and R because the chiral rotations in $U(N_f)_\ell \times U(N_f)_r$ act on the spin *and* taste degrees of freedom (see Ref. [29]).

The action for the valence and ghost quarks is given by

$$S_{\text{Val}} = a^4 \sum_x \overline{\psi}_V(x)\{D_{\text{GW}} + m_{\text{Val}}(1 - \tfrac{1}{2}aD_{\text{GW}})\}\psi_V(x). \tag{2}$$

The valence and ghost quark masses are contained in the $2N_V \times 2N_V$ mass matrix m_{Val}. The Dirac operator D_{GW} is assumed to be a local operator that satisfies the Ginsparg-Wilson relation [1], realized by either overlap [2–4] or domain-wall fermions [5]. Crucial is that the valence action has an exact chiral symmetry if the valence mass is set to zero [12]. In addition it is invariant under the lattice symmetries (translations, rotations, and reflections).

B. Symanzik action

At momenta p much below the lattice cutoff momentum $1/a$, the long distance physics of the lattice theory can be described by the continuum Symanzik effective theory [19,20]. The effects due to a nonzero lattice spacing appear in the form of higher dimensional operators in the effective action, multiplied by appropriate powers of a. These operators are constrained by the symmetries of the underlying lattice theory. The Symanzik effective action for the mixed lattice theory has the generic form

$$S_{\text{Sym}} = S_4 + a^2 S_6 + \cdots. \tag{3}$$

The first term is the known continuum partially quenched QCD action [31,34] containing $4N_f$ sea quark fields $\overline{\psi}_{\text{S}}$, ψ_{S}, and N_V valence quark and ghost fields $\overline{\psi}_{\text{V}}$, ψ_{V}.[3] Each staggered flavor field comes in four different tastes, hence the four-fold degeneracy in the sea quark sector. The mass matrix consists of the renormalized quark masses proportional to the bare lattice quark masses. The symmetries of the lattice action forbid any dimension three operator that would lead to an additive mass renormalization.

There are no terms linear in a in Eq. (3), because no dimension five operator is compatible with the symmetries of the underlying lattice theory. Dimension five quark bilinears with two valence fields are ruled out by the chiral symmetry in the valence sector [35], and staggered quark bilinears are forbidden by the axial U(1) and the shift symmetry [36,37]. Mixed bilinears with one sea and one valence field are not compatible with the separate flavor symmetries in the sea and valence sector.

In order to find the terms in S_6 it will be convenient to distinguish three types of operators: Operators that involve only sea quark fields, operators that contain only valence

[3]We collect a valence quark field ψ_V^{q} and the associated ghost field $\tilde{\psi}_V^{\text{gh}}$ in one valence field $\psi_V = (\psi_V^{\text{q}}, \tilde{\psi}_V^{\text{gh}})$ and similarly for the antivalence fields.

quark fields, and those that contain both.[4] The terms of the first two types have been constructed previously and can be found in the literature. The operators involving only sea quark fields are listed in Refs. [27,38] for the $N_f = 1$ case, and the results were generalized to the arbitrary N_f case in Refs. [29,39]. Similarly, the operators containing only valence fields are listed in Ref. [18], where the Symanzik action for the mixed lattice theory with Wilson sea and GW valence quarks was constructed.

What remains to be done here is the construction of the mixed operators containing sea and valence fields. Bilinears of dimension six with one sea and one valence field are ruled out by the separate flavor symmetries in the sea and valence sector, analogously to the dimension five bilinears. The mixed operators are therefore four-fermion operators that are products of two bilinears, one from the sea and one from the valence sector.

We construct these four-fermion operators by closely following the procedure described in Ref. [27]. We first construct all relevant lattice operators that are compatible with the symmetries of the lattice theory and correspond to dimension six four-fermion operators in the continuum limit. Sending then a to zero gives the desired terms in the Symanzik action. This procedure was used in Ref. [27] to construct all four-fermion operators made of two staggered quark bilinears. The method is easily adapted to the mixed operators. We present the details of the construction in the appendix and quote here the final result.

The allowed mixed four-fermion operators are of the form

$$O^{(6)}_{\mathrm{Mix}} = \overline{\psi}_{\mathrm{S}}(\gamma_{\mathrm{Spin}} \otimes t^a_{\mathrm{Color}})\psi_{\mathrm{S}}\overline{\psi}_{\mathrm{V}}(\gamma_{\mathrm{Spin}} \otimes t^a_{\mathrm{Color}})\psi_{\mathrm{V}}. \quad (4)$$

The matrix γ_{Spin} represents one of the 16 Clifford algebra elements and t^a_{Color} denotes a color gauge group generator.[5] The Dirac and color indices are contracted in such a way that the four-fermion operator is a singlet under $O(4)$ rotation and $SU(3)$ color symmetry. Furthermore, in writing Eq. (4) it is understood that the bilinear $\overline{\psi}_{\mathrm{V}}(\gamma_{\mathrm{Spin}} \otimes t^a_{\mathrm{Color}})\psi_{\mathrm{V}}$ is a $SU(N_V|N_V)$ flavor singlet and that the bilinear $\overline{\psi}_{\mathrm{S}}(\gamma_{\mathrm{Spin}} \otimes t^a_{\mathrm{Color}})\psi_{\mathrm{S}}$ is a $SU(4N_f)$ taste singlet. It is worth emphasizing that the mixed four-fermion operators do not break the taste symmetry in the sea quark sector.

The separate axial symmetries in the sea and valence sector imply that the bilinears in Eq. (4) transform either as a vector or an axial vector. Writing $\gamma_{\mathrm{Spin}} \otimes t^a_{\mathrm{Color}}$ more compactly as $\gamma_S t^a$ we therefore find only four mixed four-fermion operators that are allowed by the symmetries:

$$\begin{aligned} o^{(6)}_{\mathrm{Mix},1} &= (\bar{\psi}_S\gamma_\mu\psi_S)(\bar{\psi}_V\gamma_\mu\psi_V), \\ o^{(6)}_{\mathrm{Mix},2} &= (\bar{\psi}_S\gamma_\mu\gamma_5\psi_S)(\bar{\psi}_V\gamma_\mu\gamma_5\psi_V), \\ o^{(6)}_{\mathrm{Mix},3} &= (\bar{\psi}_S\gamma_\mu t^a\psi_S)(\bar{\psi}_V\gamma_\mu t^a\psi_V), \\ o^{(6)}_{\mathrm{Mix},4} &= (\bar{\psi}_S\gamma_\mu\gamma_5 t^a\psi_S)(\bar{\psi}_V\gamma_\mu\gamma_5 t^a\psi_V), \end{aligned} \quad (5)$$

where we have explicitly separated out bilinears containing the color identity matrix and now restrict t^a to be traceless, summing over a.

C. Spurion analysis

The leading term in the Symanzik action, S_4, is just the continuum action of partially quenched QCD. In the massless limit it is invariant under the flavor symmetry group[6]

$$G_{\mathrm{PQ\ QCD}} = SU(4N_f + N_V|N_V)_L \otimes SU(4N_f + N_V|N_V)_R, \quad (6)$$

which is expected to be spontaneously broken to its vector part $SU(4N_f + N_V|N_V)_V$. The low-energy physics is therefore dominated by Nambu-Goldstone bosons. These pseudoscalar bosons acquire small masses due to nonvanishing quark masses and a nonzero lattice spacing. The latter contribution has its origin in chiral symmetry breaking terms in S_6.

To construct the chiral Lagrangian that describes these pseudoscalar bosons we follow the standard procedure of a spurion analysis. The coefficient c_i of each term O_i in the Symanzik effective action is promoted to a spurion field that transforms under flavor transformations in Eq. (6) in such a way that the product c_iO_i is invariant. The chiral effective Lagrangian is constructed from the pseudoscalar fields and the spurion fields with the requirement that it is invariant under flavor rotations. Once the chiral Lagrangian is constructed the spurion field is set to its original constant value. This guarantees that the chiral Lagrangian explicitly breaks the chiral symmetries in the same manner as the underlying Symanzik effective action, and reproduces the same Ward identities.

In order to perform the spurion analysis for the mixed theory it is convenient to introduce the following notation. We collect the quark and antiquark fields in single fields,

$$\Psi = (\psi_S, \psi_V), \qquad \overline{\Psi} = (\overline{\psi}_S, \overline{\psi}_V), \quad (7)$$

where ψ_V contains both the anticommuting valence quarks and the commuting ghost fields. The mass matrix is given by $m = \mathrm{diag}(m_S, m_V)$, with m_S being the $4N_f \times 4N_f$ mass matrix for the sea quarks and m_V is the $2N_V \times 2N_V$ mass matrix for the valence quarks and valence ghosts. We also

[4] We do not need to discuss purely gluonic operators, which also appear at $\mathcal{O}(a^2)$, since they transform trivially under chiral transformations and therefore will not affect the form of the chiral effective Lagrangian.

[5] The identity in color space, for which we use the notation t^0_{Color}, also is allowed here.

[6] The true symmetry group of partially quenched QCD differs slightly from $G_{\mathrm{PQ\ QCD}}$ in Eq. (6). Nevertheless, this $G_{\mathrm{PQ\ QCD}}$ is sufficient to derive the chiral Lagrangian under the assumption that the theory is in the phase that reproduces QCD in the continuum, unquenched limit [40].

introduce the projection operators

$$P_S = \mathrm{diag}(I_S, 0), \qquad P_V = \mathrm{diag}(0, I_V), \tag{8}$$

where I_S denotes the $4N_f \times 4N_f$ identity matrix in the sea sector, and I_V the $2N_V \times 2N_V$ identity matrix in the space of valence fields.

For our purposes it will not be necessary to construct all spurion fields that make the Symanzik action in Eq. (3) invariant. Most of the analysis has already been done and we can rely on previously published results. The results of the spurion analysis to $\mathcal{O}(a^2)$ for the case with staggered sea and valence quarks were written down in Ref. [29]; the analysis can be found in detail in Ref. [39], which also works to higher order. Since now only the sea sector contains staggered quarks all we need to do is to include the projector P_S appropriately in all spurion fields associated with sea quarks in this reference. These spurion fields render invariant all terms in the Symanzik effective action that are built only of sea quarks. To illustrate this point consider the mass term for the sea quarks, $\overline{\psi}_S m_S \psi_S$. In Ref. [39] this term is made invariant by promoting the mass to a spurion field that transforms as $m_S \to L m_S R^\dagger$ under left and right transformations L and R. In order to make use of this spurion field in the mixed theory we write $\overline{\psi}_S m_S \psi_S = \overline{\Psi} P_S m P_S \Psi$ and assume the same transformation property as before, i.e., $m \to L m R^\dagger$. The constant value to which the spurion is assigned in the end, however, is now $P_S m P_S$. One can proceed analogously with all the other spurion fields in Ref. [39]. From the results in Ref. [18] for the mixed theory with Wilson sea quarks and GW valence quarks we can directly determine the spurion fields that are necessary to make the valence field operators invariant. What we need in addition are the new spurion fields that make the mixed four-fermion operators in Eq. (5) invariant.

We want to emphasize that the mixed four-fermion operators do break the symmetry group $G_{\mathrm{PQ\ QCD}}$, even though each bilinear in them couples fields of the same chirality only. The reason is that any four-fermion operator that is invariant under all transformations in $G_{\mathrm{PQ\ QCD}}$ must be of the form

$$(\overline{\Psi}\Gamma\Psi)^2 = (\psi_S\Gamma\psi_S)^2 + (\psi_V\Gamma\psi_V)^2 + 2(\psi_S\Gamma\psi_S)(\psi_V\Gamma\psi_V), \tag{9}$$

where Γ represents one of the four combinations $\gamma_S t^a$ in Eq. (5). All three types of four-fermion operators on the right-hand side of Eq. (9) appear in the Symanzik effective action. However, because the lattice theory does not posses any symmetries relating the staggered sea and the GW valence fermions, they do not enter with the same coefficient in front in order to sum up to the square on the left-hand side. Consequently, although an arbitrary linear combination of the three operator types is invariant under the subgroup $SU(4N_f)_L \otimes SU(4N_f)_R \otimes SU(N_V|N_V)_L \otimes SU(N_V|N_V)_R$ of $G_{\mathrm{PQ\ QCD}}$, it is not invariant under the larger symmetry transformations of $G_{\mathrm{PQ\ QCD}}$ that mix the sea and valence sector.

Following the notation in Ref. [18], the mixed four-fermion operators can be made invariant under arbitrary chiral flavor transformations $L \in SU(4N_f + N_V|N_V)_L$ and $R \in SU(4N_f + N_V|N_V)_R$ by introducing the spurion fields

$$\begin{aligned} D &\equiv D_1 \otimes D_2 \to L D_1 L^\dagger \otimes L D_2 L^\dagger, \\ E &\equiv E_1 \otimes E_2 \to R E_1 R^\dagger \otimes R E_2 R^\dagger, \\ F &\equiv F_1 \otimes F_2 \to L F_1 L^\dagger \otimes R F_2 R^\dagger, \\ G &\equiv G_1 \otimes G_2 \to R G_1 R^\dagger \otimes L G_2 L^\dagger, \\ D_0 &= E_0 = F_0 = G_0 = a^2 P_S \otimes P_V. \end{aligned} \tag{10}$$

The constant values to which the spurion fields are assigned to in the end carry the subscript "0." The spurion fields transform as 4-tensors under chiral flavor transformations and therefore carry four indices, which need to be properly contracted with the indices of the fermion fields in order to form invariants.[7] For example, decomposing $O^{(6)}_{\mathrm{Mix},1} = (\overline{\psi}_S \gamma_\mu \psi_S)(\overline{\psi}_V \gamma_\mu \psi_V) \equiv (\overline{\psi}\gamma_\mu\psi)_S (\overline{\psi}\gamma_\mu\psi)_V$ in chiral components we obtain

$$\begin{aligned} (\overline{\psi}\gamma_\mu\psi)_S (\overline{\psi}\gamma_\mu\psi)_V = {} & (\overline{\psi}_L\gamma_\mu\psi_L)_S (\overline{\psi}_L\gamma_\mu\psi_L)_V \\ & + (\overline{\psi}_L\gamma_\mu\psi_L)_S (\overline{\psi}_R\gamma_\mu\psi_R)_V \\ & + (\overline{\psi}_R\gamma_\mu\psi_R)_S (\overline{\psi}_L\gamma_\mu\psi_L)_V \\ & + (\overline{\psi}_R\gamma_\mu\psi_R)_S (\overline{\psi}_R\gamma_\mu\psi_R)_V. \end{aligned} \tag{11}$$

Both bilinears in the first term on the right-hand side couple left-handed fields only. It is made invariant with the spurion field D, where the indices are contracted according to

$$\begin{aligned} D(\psi_L\gamma_\mu\psi_L)_S (\overline{\psi}_L\gamma_\mu\psi_L)_V = {} & (\psi_L D_1 \gamma_\mu \psi_L)_S \\ & \times (\overline{\psi}_L D_2 \gamma_\mu \psi_L)_V. \end{aligned} \tag{12}$$

The other three terms in Eq. (11) are analogously made invariant using the spurion fields E, F, and G.

We remark that the spurion fields in Eq. (10) transform in the same way as the ones for the valence-valence four-fermion operators; they differ only in their constant final values: $a^2 P_S \otimes P_V$ is replaced by $a^2 P_V \otimes P_V$ in the valence-valence case [18].

D. Chiral Lagrangian

Assuming that the symmetry in Eq. (6) is spontaneously broken down to its vector part, the particle spectrum contains light pseudoscalar bosons. These bosons are described by the field

[7] Spurion fields with the same transformation properties appear also in weak matrix element studies. See Ref. [41] and references therein.

$$\Sigma = \exp(2i\Phi/f), \tag{13}$$

which is an element of $U(4N_f + N_V|N_V)$. Φ is a matrix that collects the pseudoscalar fields in the usual way [34]. For example, for three sea quark flavors (u, d, and s) and two valence flavors (x, y for the valence quarks and $\tilde{x}$, $\tilde{y}$ for the valence ghosts) we arrange the fields as follows:

$$\Phi = \begin{pmatrix} U & \pi^+ & K^+ & Q_{ux} & Q_{uy} & \cdots & \cdots \\ \pi^- & D & K^0 & Q_{dx} & Q_{dy} & \cdots & \cdots \\ K^- & \bar{K}^0 & S & Q_{sx} & Q_{sy} & \cdots & \cdots \\ Q^\dagger_{ux} & Q^\dagger_{dx} & Q^\dagger_{sx} & X & P^+ & R^\dagger_{\tilde{x}x} & R^\dagger_{\tilde{y}x} \\ Q^\dagger_{uy} & Q^\dagger_{dy} & Q^\dagger_{sy} & P^- & Y & R^\dagger_{\tilde{x}y} & R^\dagger_{\tilde{y}y} \\ \cdots & \cdots & \cdots & R_{\tilde{x}x} & R_{\tilde{x}y} & \tilde{X} & \tilde{P}^+ \\ \cdots & \cdots & \cdots & R_{\tilde{y}x} & R_{\tilde{y}y} & \tilde{P}^- & \tilde{Y} \end{pmatrix}. \tag{14}$$

Here P^+, X, and Y are the $x\bar{y}$, $x\bar{x}$, and $y\bar{y}$ valence bound states, respectively; $\tilde{P}^+$, $\tilde{X}$, and $\tilde{Y}$ are the analogous combinations of valence ghost quarks. $R_{\tilde{x}x}$ is the (fermionic) bound state $\tilde{x}\bar{x}$, and similarly for $R_{\tilde{x}y}$, $R_{\tilde{y}x}$, and $R_{\tilde{y}y}$. Likewise, Q_{Fv} represents the mixed bound state $F\bar{v}$, where F is a sea quark, $F \in \{u, d, s\}$, and v is a valence quark, $v \in \{x, y\}$.[8] Q_{Fv} is a 4×1 matrix in taste space; while $Q^\dagger_{Fv} \equiv Q_{vF}$ is a 1×4 matrix. The sea quark bound state fields are U, π^+, K^+, etc. These are 4×4 matrices when we take into account the taste degree of freedom. We write

$$U = \sum_{b=1}^{16} U_b \frac{T_b}{2}, \tag{15}$$

(and similarly for $\pi^+, K^+, \ldots$) where

$$T_b = \{\xi_5, i\xi_\mu\xi_5, i\xi_\mu\xi_\nu, \xi_\mu, \xi_I\} \tag{16}$$

are the 16 taste matrices in the form of Euclidean gamma matrices (ξ_I denotes the 4×4 identity matrix). Unlike Ref. [29], we include a factor of 2 in Eq. (13) and divide T_b by 2 in Eq. (15) in order to keep a consistent normalization of all fields in Eq. (14).

Under chiral symmetry transformations in Eq. (6), the field Σ transforms as

$$\Sigma \to L\Sigma R^\dagger, \tag{17}$$

where $L \in SU(4N_f + N_V|N_V)_L$ and $R \in SU(4N_f + N_V|N_V)_R$.

The chiral Lagrangian is expanded in powers of p^2, m_q, and a^2, where m_q stands generically for either a sea or a valence quark mass. We adopt a power counting that assumes that the size of the chiral symmetry breaking due to the quark masses and the discretization effects are of comparable size, i.e.,

$$m_q/\Lambda_{\rm QCD} \approx a^2\Lambda^2_{\rm QCD}, \tag{18}$$

where $\Lambda_{\rm QCD}$ denotes the typical QCD scale, of the order of 300 MeV. A different power counting is necessary if one of the two parameters $m_q/\Lambda_{\rm QCD}$ and $a^2\Lambda^2_{\rm QCD}$ is much larger than the other one. However, the approximate equality in Eq. (18) is realized in current lattice simulations using improved staggered fermions [10].

Assuming Eq. (18), the leading-order chiral Lagrangian contains the terms of $\mathcal{O}(p^2, m_q, a^2)$ and is of the form

$$\mathcal{L}_\chi = \frac{f^2}{8}\langle\partial_\mu\Sigma\partial_\mu\Sigma^\dagger\rangle - \frac{f^2B}{4}\langle\Sigma M^\dagger + M\Sigma^\dagger\rangle + \frac{m_0^2}{6}\langle\Phi\rangle^2 + a^2\mathcal{V}. \tag{19}$$

Here $\langle\ldots\rangle$ denotes a supertrace in flavor space and the parameters f and B are undetermined low-energy constants.[9] For our concrete example of three sea quark flavors and two valence flavors the diagonal mass matrix M is given by $M = \mathrm{diag}(m_u\xi_I, m_d\xi_I, m_s\xi_I, m_x, m_y, m_x, m_y)$.

As in Refs. [28–30], for convenience we leave explicit the m_0^2 term, which is allowed because of the anomaly, and we take $m_0^2 \to \infty$ at the end. Note that

$$\langle\Phi\rangle = 2U_I + 2D_I + 2S_I + X + Y - \tilde{X} - \tilde{Y}, \tag{20}$$

where U_I is the taste-singlet component of U [Eq. (15)] and similarly for D_I and S_I.

The potential $\mathcal{V}$ in the leading-order Lagrangian comprises all terms proportional to a^2. For our mixed theory it can be written as a sum of three terms,

$$\mathcal{V} = \mathcal{U}_{\rm S} + \mathcal{U}'_{\rm S} + \mathcal{U}_{\rm V}. \tag{21}$$

The first two terms are just the known taste breaking potentials for the sea sector [27,29]:

$$\begin{aligned} -\mathcal{U}_S = {} & C_1\langle\hat{\xi}_5 P_S\Sigma\hat{\xi}_5 P_S\Sigma^\dagger\rangle \\ & + C_3\frac{1}{2}\sum_\nu[\langle\hat{\xi}_\nu P_S\Sigma\hat{\xi}_\nu P_S\Sigma\rangle + \text{h.c.}] \\ & + C_4\frac{1}{2}\sum_\nu[\langle\hat{\xi}_{\nu 5} P_S\Sigma\hat{\xi}_{5\nu} P_S\Sigma\rangle + \text{h.c.}] \\ & + C_6\sum_{\mu<\nu}\langle\hat{\xi}_{\mu\nu} P_S\Sigma\hat{\xi}_{\nu\mu} P_S\Sigma^\dagger\rangle, \end{aligned} \tag{22}$$

and

[8] We have not bothered to name the mixed bound states of sea quarks with ghost valence quarks in Eq. (14) because such states will not enter into the calculations below.

[9] We adopt a normalization that corresponds to a tree-level pion decay constant $f \approx 131$ MeV.

$$
\begin{aligned}
-\mathcal{U}'_S = {} & C_{2V}\frac{1}{4}\sum_\nu[\langle\hat{\xi}_\nu P_S\Sigma\rangle\langle\hat{\xi}_\nu P_S\Sigma\rangle + \text{h.c.}] \\
& + C_{2A}\frac{1}{4}\sum_\nu[\langle\hat{\xi}_{\nu 5} P_S\Sigma\rangle\langle\hat{\xi}_{5\nu} P_S\Sigma\rangle + \text{h.c.}] \\
& + C_{5V}\frac{1}{2}\sum_\nu\langle\hat{\xi}_\nu P_S\Sigma\rangle\langle\hat{\xi}_\nu P_S\Sigma^\dagger\rangle \\
& + C_{5A}\frac{1}{2}\sum_\nu\langle\hat{\xi}_{\nu 5} P_S\Sigma\rangle\langle\hat{\xi}_{5\nu} P_S\Sigma^\dagger\rangle. \qquad (23)
\end{aligned}
$$

Here we introduced the shorthand notation $\hat{\xi}_5 = (\xi_{5,\text{taste}} \otimes 1_{\text{flavor}}) \oplus 1_V$, etc., for the multiflavor generalizations of the taste matrices T_b. For instance, in our concrete example we have $\hat{\xi}_5 = \text{diag}(\xi_5, \xi_5, \xi_5, 1, 1, 1)$. The coefficients C_i are low-energy constants.

Note that all terms in the two potentials $\mathcal{U}_S$ and $\mathcal{U}'_S$ only involve the fields in the upper left sea-sea block of Σ. This is easily seen by first noting that the matrices $\hat{T}_b$ commute with the projector P_S. Consequently, the structure $\langle T_b P_S\Sigma T_b P_S\Sigma^\dagger\rangle$, for instance, also can be written as $\langle T_b P_S\Sigma P_S T_b P_S\Sigma^\dagger P_S\rangle$. This is not surprising. The taste matrices $\hat{T}_b$ played the role of spurion fields in the derivation of the potential $\mathcal{U}_S + \mathcal{U}'_S$ in Refs. [29,39]. As explained in Sec. II C, the spurion fields need to be sandwiched by the projector P_S in the mixed theory, i.e., $\hat{T}_b \to P_S\hat{T}_b P_S$. In fact, that was the way we obtained the potential $\mathcal{U}_S + \mathcal{U}'_S$ without repeating the details of the spurion analysis in Refs. [29,39].

The remaining potential $\mathcal{U}_V$ comprises all terms that stem from the operators in the Symanzik effective action that involve valence fields. Some of these arise from the mixed 4-fermion operators in Eq. (5). The corresponding chiral operators are constructed by forming invariants involving one of the spurion fields in Eq. (10) together with arbitrarily many Σ and $\Sigma^\dagger$. Insertions of the mass matrix and derivatives are excluded since they lead to terms that are necessarily of higher order in the chiral expansion, at least $\mathcal{O}(p^2a^2, m_q a^2)$.

We can only form nontrivial invariants with the fields F and G, which collapse to the same term once the spurion fields are set to their final value:

$$
\begin{aligned}
\langle F_1\Sigma F_2\Sigma^\dagger\rangle &\to a^2\langle\tau_3\Sigma\tau_3\Sigma^\dagger\rangle, \\
\langle G_1\Sigma^\dagger G_2\Sigma\rangle &\to a^2\langle\tau_3\Sigma^\dagger\tau_3\Sigma\rangle.
\end{aligned} \qquad (24)
$$

Here we used $P_S = \frac{1}{2}(I + \tau_3)$ and $P_V = \frac{1}{2}(I - \tau_3)$, with $\tau_3 = \text{diag}(I_S, -I_V)$ and dropped an irrelevant factor of $1/4$. When we write $(I \pm \tau_3)$ for $F_{1,2}$ and $G_{1,2}$, the fields Σ and $\Sigma^\dagger$ cancel whenever they sandwich the identity matrix. The only nontrivial operator is the one involving two τ_3 matrices.

The last terms in $\mathcal{U}_V$ stem from the four-fermion operators involving only valence fields.[10] As we remarked at the end of the last section, the corresponding spurion fields transform exactly as the ones for the mixed four-fermion operators. The only difference is the final constant value; $a^2P_S \otimes P_V$ is replaced by $a^2P_V \otimes P_V$. This change only involves a sign flip in the first projection operator and therefore leads to the same term $a^2\langle\tau_3\Sigma\tau_3\Sigma^\dagger\rangle$ for the chiral Lagrangian.[11]

We conclude that the leading-order chiral Lagrangian for the mixed action theory with staggered sea and GW valence quarks contains only one more operator compared to the chiral Lagrangian of SχPT:

$$
\mathcal{U}_V = -C_{\text{Mix}}\langle\tau_3\Sigma\tau_3\Sigma^\dagger\rangle. \qquad (25)
$$

The potential $\mathcal{V}$ for the mixed action theory involves nine unknown low-energy constants compared to eight in SχPT. We want to emphasize that the eight constants in $\mathcal{U}_S + \mathcal{U}'_S$ are the *same* constants as those in SχPT. Some combinations of them have already been determined by fits to staggered lattice data [10].

The potential $\mathcal{U}_S + \mathcal{U}'_S$ breaks the $SU(4)$ taste symmetry in the sea sector but not entirely—an accidental $SO(4)$ subgroup remains unbroken [27]. The part $\mathcal{U}_V$, on the other hand, preserves the full $SU(4)$ taste symmetry. This is expected because the four-fermion operators in Eq. (5) which give rise to $\mathcal{U}_V$ are trivial in taste space. Interaction vertices involving pseudoscalars with one or more valence quark constituents stem from $\mathcal{U}_V$ only. The $SU(4)$ taste symmetry implies that correlation functions that include such external pseudoscalars respect the $SU(4)$ taste symmetry in one-loop NLO diagrams. Analytic, taste symmetry violating contributions do appear at NLO: $\mathcal{O}(a^4, a^2p^2, a^2m_q)$; while nonanalytic symmetry violating contributions start beyond NLO.

III. PSEUDOSCALAR MASSES AND DECAY CONSTANTS

In this section we compute the one-loop expressions for the (valence-valence) pseudoscalar masses and decay constants. For concreteness we now restrict ourselves to the case with three sea quark flavors and two valence quark flavors. This is the most relevant case phenomenologically.

[10]The allowed valence bilinears either have the same symmetries as the lowest order terms, in which case they merely give $\mathcal{O}(a^2)$ corrections to lowest order parameters, or they have different symmetries (violate $O(4)$ rotation invariance) and contribute only at higher order in the chiral expansion [18].

[11]This also explains that this term is present independently of a change of basis in the Symanzik effective action. Using Eq. (9) one could replace either the mixed or the pure valence four-fermion operators at the expense of $(\bar{\Psi}\Gamma\Psi)^2$, which is invariant under transformations in $G_{\text{PQ QCD}}$. Nevertheless, one can remove only one type of four-fermion operators, the other type still gives rise to the term $a^2\langle\tau_3\Sigma\tau_3\Sigma^\dagger\rangle$ in the chiral Lagrangian.

Further, the resulting one-loop expressions can be readily used in the analysis of unquenched configurations generated with the Asqtad action by the MILC Collaboration (see Refs. [9,10] and references therein).

In the following we also adjust for the so-called "fourth-root trick," which is commonly employed in staggered simulations in order to reduce the taste degree of freedom from four to one. In the context of the chiral effective theory this adjustment requires proper insertions of factors of $1/4$ in the sea quark loop contributions in our expressions [28], depending on the quark flow [42] that corresponds to the meson loop diagram in the chiral effective theory.

The fourth-root trick raises legitimate locality questions and its validity is controversial. Recently various studies have addressed this issue using either numerical or analytical methods [13,43–49]. In the following we assume that the fourth-root trick can be given a field theoretically sound underpinning, so that we can follow the procedure described in Ref. [28].

A. Leading-order masses and propagators

At tree level, the new operator of the mixed theory, $\mathcal{U}_V$, contributes only to the masses of valence-sea mesons, represented in Eq. (14) by Q_{Fv} ($F \in \{u, d, s\}$; $v \in \{x, y, \tilde{x}, \tilde{y}\}$). Sea-sea and valence-valence mesons get no such contributions because a block-diagonal Φ commutes with τ_3, and $\Sigma\Sigma^\dagger = I$. Similarly, the potentials in the sea sector, $\mathcal{U}_S$ and $\mathcal{U}'_S$, Eqs. (22) and (23), give no contribution to the valence-valence mesons. Thus the valence-valence mesons obey the continuumlike mass relations exemplified by

$$m_P^2 = B(m_x + m_y). \tag{26}$$

Of course such relations follow immediately from the exact chiral symmetry (for massless quarks) in the valence sector.

In the sea-sea sector, $\mathcal{U}_S$ and $\mathcal{U}'_S$ contribute, and the tree-level results are identical to those in Ref. [29]. For a meson of taste b made up of sea quarks F and F' ($F = F'$), we have

$$m_{FF',b}^2 = B(m_F + m'_F) + a^2\Delta(\xi_b), \tag{27}$$

with

$$\begin{aligned}
\Delta(\xi_5) &\equiv \Delta_P = 0, \\
\Delta(\xi_{\mu 5}) &\equiv \Delta_A = \frac{16}{f^2}(C_1 + 3C_3 + C_4 + 3C_6), \\
\Delta(\xi_{\mu\nu}) &\equiv \Delta_T = \frac{16}{f^2}(2C_3 + 2C_4 + 4C_6), \\
\Delta(\xi_\mu) &\equiv \Delta_V = \frac{16}{f^2}(C_1 + C_3 + 3C_4 + 3C_6), \\
\Delta(\xi_I) &\equiv \Delta_I = \frac{16}{f^2}(4C_3 + 4C_4).
\end{aligned} \tag{28}$$

As mentioned above, $\mathcal{U}_V$ contributes to the masses of the valence-sea mesons. For the $F\bar{x}$ meson, with field Q_{Fx}, the mass is

$$m_{Fx}^2 = B(m_F + m_x) + a^2\Delta_{\text{Mix}}, \tag{29}$$

where

$$\Delta_{\text{Mix}} \equiv \frac{16C_{\text{Mix}}}{f^2}. \tag{30}$$

The violation of the Goldstone theorem in Eq. (29) clearly arises because there is no lattice axial symmetry that mixes valence and sea quarks.

In a simulation using staggered sea quark configurations, Δ_{Mix} could be directly determined from the propagator of a mixed meson with one GW valence quark and one staggered valence quark.[12] Such a direct determination of Δ_{Mix} would be useful because it would reduce the number of free parameters in chiral-log fits. For example, Δ_{Mix} enters (through m_{fx}^2) into the NLO expression for the decay constant of a meson with two GW valence quarks (see Sec. III C).

Since we have no *a priori* reason to expect a particular sign for C_{Mix} (or equivalently Δ_{Mix}), Eq. (29) shows there is a possibility of a lattice "Aoki phase" [50] if $\Delta_{\text{Mix}} < 0$. This would be similar to the type of lattice phases for staggered quarks discussed in Refs. [27,29,51]. The direct measurement of Δ_{Mix} discussed in the previous paragraph would determine if this possibility can be realized in practice.

We emphasize that we have expanded the chiral Lagrangian around $\Sigma = 1$, assuming that the theory is in the right phase which reproduces QCD in the continuum, unquenched limit. Even though the phase structure of the lattice theory can be studied in the effective theory [24,27], the presence of a ghost sector in partially quenched theories makes such an analysis nontrivial. It has recently been pointed out [52] that one has to properly take into account the constraints for a convergent ghost sector path integral in order to perform nonperturbative phase diagram studies. These constraints are not easily implemented for Wilson fermions, and the analysis of the phase structure in the quenched theory [52] is significantly more difficult than the one in the unquenched theory [24]. Although most of these subtleties do not apply for Ginsparg-Wilson ghosts, which are employed here, it seems advisable to confirm directly that the mixed theory is indeed in the right phase, for example, by comparing our theoretical predictions with simulation results.

[12] At least within the context of staggered chiral perturbation theory, taking the fourth root of the staggered sea quark determinant will not change the standard equivalence between masses of particles on internal and external lines. The fourth-root procedure only changes the weighting, not the mass, of an internal meson made from one valence and one sea quark.

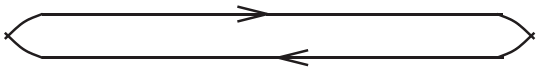

FIG. 1. Quark flow diagram for a connected meson propagator.

The flavor-charged (nondiagonal) fields in Eq. (14) have only connected propagators in the quark flow sense, Fig. 1; while flavor-neutral (diagonal, e.g., U or X) mesons also have disconnected contributions, Fig. 2. The only complication in the connected case is getting the sign of the propagator right for mesons with one or more ghost valence quarks. Using $[AB](p^2)$ to denote the Euclidean space propagator of field A and B with momentum p, examples of connected propagators are

$$[P^+P^-](p^2) = \frac{1}{p^2 + m_P^2}, \qquad [\pi_a^+\pi_b^-](p^2) = \frac{\delta_{ab}}{p^2 + m_{\pi_a}^2}, \qquad [XX]_{\text{conn}}(p^2) = \frac{1}{p^2 + m_X^2},$$
$$[\tilde{X}\,\tilde{X}]_{\text{conn}}(p^2) = \frac{-1}{p^2 + m_{\tilde{X}}^2}, \qquad [Q_{u_i x}Q_{u_j x}^\dagger](p^2) = \frac{\delta_{ij}}{p^2 + m_{ux}^2}, \qquad [R_{\tilde{x}y}R_{\tilde{x}y}^\dagger](p^2) = -[R_{\tilde{x}y}^\dagger R_{\tilde{x}y}](p^2) = \frac{1}{p^2 + m_{\tilde{x}y}^2}. \quad (31)$$

Here $a, b = \{1, 2, \ldots, 16\}$ are meson taste indices as in Eq. (15); while $i, j = \{1, 2, 3, 4\}$ are quark taste indices.

Disconnected propagators for flavor-neutral mesons can be generated by the anomaly (m_0^2) term in Eq. (19), which gives a ''hairpin'' interaction (two-meson vertex with disconnected quark flow). Summing such graphs as in Refs. [29,53] gives, for the disconnected X-Y propagator

$$[XY]_{\text{disc}}(p^2) = -\frac{m_0^2}{3}\frac{(p^2 + m_{U_I}^2)(p^2 + m_{D_I}^2)(p^2 + m_{S_I}^2)}{(p^2 + m_X^2)(p^2 + m_Y^2)(p^2 + m_{\pi_I^0}^2)(p^2 + m_{\eta_I}^2)(p^2 + m_{\eta_I'}^2)}, \quad (32)$$

where, for concreteness, we have again assumed three sea quark flavors. The π_I^0, η_I, and η_I' are the mass eigenstates in the flavor-neutral, taste-singlet channel, found by diagonalizing the mass matrix including the m_0^2 term. The subscript ''disc'' is included for clarity, but of course the XY propagator has no connected contribution. In the sea-sea sector, only the taste-singlet, flavor-neutral mesons feel the anomaly hairpin vertex. In addition, sea-sea flavor-neutral mesons of vector or axial taste get hairpin contributions from $\mathcal{U}_S'$ [29]. Since the corresponding disconnected propagators do not enter into the quantities calculated in Secs III B and III C , we do not write them explicitly here.

It is convenient to take $m_0^2 \to \infty$ at this point to decouple the η_I'. In the case of most current interest, with three staggered flavors and the fourth root of the determinant taken to eliminate the extraneous taste degree of freedom, $m_{\eta_I'}^2 \cong m_0^2$ for large m_0^2 [29]. Equation (32) then becomes

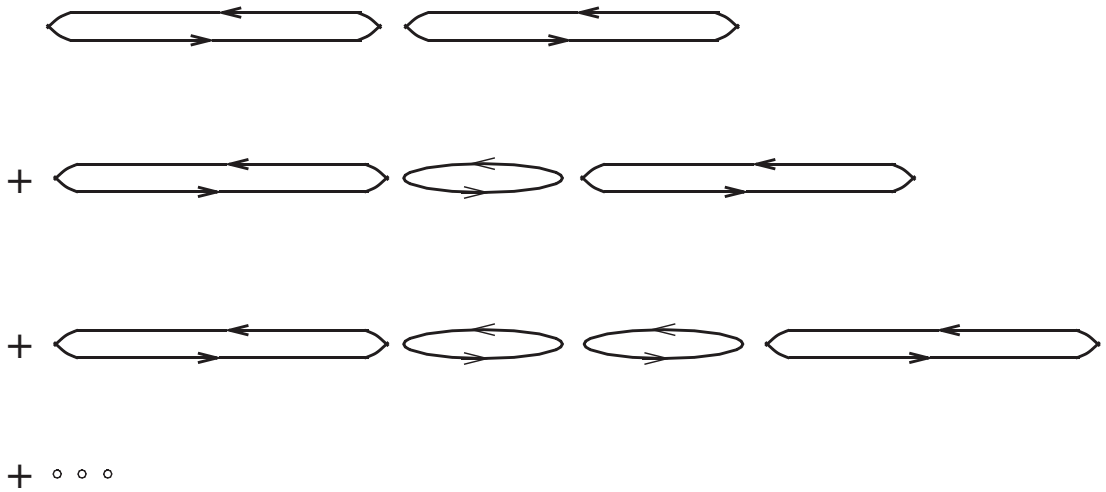

FIG. 2. Quark flow diagrams for the disconnected meson propagator.

$$[XY]_{\rm disc}(p^2) = -\frac{1}{3}\frac{(p^2+m_{U_I}^2)(p^2+m_{D_I}^2)(p^2+m_{S_I}^2)}{(p^2+m_X^2)(p^2+m_Y^2)(p^2+m_{\pi_I^0}^2)(p^2+m_{\eta_I}^2)}. \quad (33)$$

Other disconnected valence-valence propagators are found from Eq. (33) by substitution: Let $Y \to X$ for $[XX]_{\rm disc}$, $X \to Y$ for $[YY]_{\rm disc}$. If $m_u = m_d$, as in the MILC simulations [9,10], then

$$m_{\pi_I^0}^2 = m_{U_I}^2 = m_{D_I}^2, \qquad m_{\eta_I}^2 = \frac{m_{U_I}^2}{3} + \frac{2m_{S_I}^2}{3}. \quad (34)$$

If we take the fourth root but keep the number N_f of flavors arbitrary, then $m_{\eta_I'}^2 \cong N_f m_0^2/3$, and the more general version of Eq. (33) is

$$[XY]_{\rm disc}(p^2) = -\frac{1}{N_f} \times \frac{\prod_{L=1}^{N_f}(p^2+m_{L_I}^2)}{(p^2+m_X^2)(p^2+m_Y^2)\prod_{L'=1}^{N_f-1}(p^2+m_{L_I'}^2)}, \quad (35)$$

where L runs over diagonal flavor-neutral states (U, D, S, ...), and L' runs over the neutral mass eigenstates (π_0, η, ...), excluding the η'.

B. NLO valence-valence mass

We are interested in computing the one-loop correction to the meson made from valence quark x and $\bar{y}$, i.e., a P^+. The P^+ self energy comes from the meson graphs in Fig. 3. We thus need the four-meson vertices generated by the kinetic energy, by the mass term, and by $\mathcal{U}_V$, with at least one P^+ and one P^- field.

Expanding the kinetic energy, and including the minus sign for a vertex, gives the following terms with derivatives acting on both P^+ and P^-:

$$V_{\rm KE}^{(1)} = \frac{1}{3f^2}\partial_\mu P^+ \partial_\mu P^- [2P^+P^- + X^2 + Y^2 + R_{\tilde{x}x}^\dagger R_{\tilde{x}x} + R_{\tilde{y}x}^\dagger R_{\tilde{y}x} + R_{\tilde{x}y}^\dagger R_{\tilde{x}y} + R_{\tilde{y}y}^\dagger R_{\tilde{y}y} + \sum_F (Q_{Fx}^\dagger Q_{Fx} + Q_{Fy}^\dagger Q_{Fy}) - 2XY]. \quad (36)$$

The fields in this expression are defined in Eq. (14). The summation index F runs over sea quarks, typically u, d, and s. There is also an implied sum over the taste index in the product $Q^\dagger Q$. As usual, terms with a derivative on P^+ or P^-, but not both, are not needed since the corresponding diagrams in Fig. 3 will vanish by symmetric momentum integration. The kinetic energy terms with no derivatives on the P^+, P^- fields are

$$V_{\rm KE}^{(2)} = \frac{1}{3f^2}P^+P^-[(\partial_\mu X)^2 + (\partial_\mu Y)^2 + \partial_\mu R_{\tilde{x}x}^\dagger \partial_\mu R_{\tilde{x}x} + \partial_\mu R_{\tilde{y}x}^\dagger \partial_\mu R_{\tilde{y}x} + \partial_\mu R_{\tilde{x}y}^\dagger \partial_\mu R_{\tilde{x}y} + \partial_\mu R_{\tilde{y}y}^\dagger \partial_\mu R_{\tilde{y}y} + \sum_F (\partial_\mu Q_{Fx}^\dagger \partial_\mu Q_{Fx} + \partial_\mu Q_{Fy}^\dagger \partial_\mu Q_{Fy}) - 2\partial_\mu X \partial_\mu Y]. \quad (37)$$

Similarly, the mass term and the "mixed potential" $\mathcal{U}_V$ give, respectively,

$$V_{\rm mass} = \frac{B}{3f^2}P^+P^-\Big[(m_x+m_y)P^+P^- + (3m_x+m_y)X^2 + (m_x+3m_y)Y^2 + (3m_x+m_y)R_{\tilde{x}x}^\dagger R_{\tilde{x}x} + 2(m_x+m_y)(R_{\tilde{y}x}^\dagger R_{\tilde{y}x} + R_{\tilde{x}y}^\dagger R_{\tilde{x}y}) + (m_x+3m_y)R_{\tilde{y}y}^\dagger R_{\tilde{y}y} + \sum_F\{(2m_x+m_y+m_F)Q_{Fx}^\dagger Q_{Fx} + (m_x+2m_y+m_F)Q_{Fy}^\dagger Q_{Fy}\} + 2(m_x+m_y)XY\Big] \quad (38)$$

and

$$V_{\rm Mix} = \frac{a^2\Delta_{\rm Mix}}{3f^2}P^+P^-\sum_F(Q_{Fx}^\dagger Q_{Fx} + Q_{Fy}^\dagger Q_{Fx}), \quad (39)$$

where we have used Eq. (30).

By including the ghost quark contributions we have guaranteed that quark loop terms from the valence quarks will be canceled automatically, thereby accomplishing the partial quenching. However, we still must understand the meson diagrams at the quark flow level [42] in order to adjust for the effects of the fourth-root procedure on the staggered quarks. If we assume three flavors of sea quarks

(a) (b)

FIG. 3. Meson graphs for the P^+ self energy. Graph (a) has a connected internal propagator (Fig. 1 in the quark flow picture); while graph (b) has a disconnected internal propagator (Fig. 2).

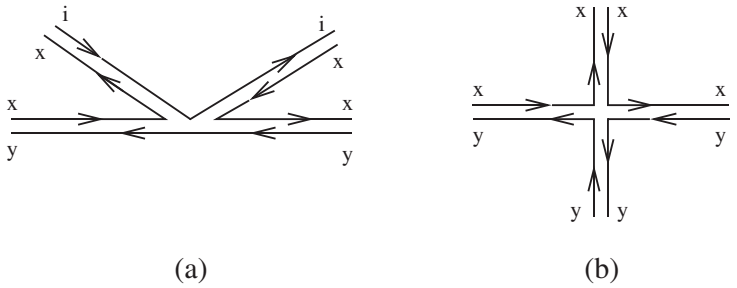

FIG. 4. Quark flow graphs corresponding to the four meson vertices in the P^+ self energy, Eqs. (36)–(39). The horizontal x, y lines produce the external $P^{\pm}$ fields. Graph (a) represents terms where the P^+ and P^- are next to each other in the supertrace; an almost identical graph with $x \leftrightarrow y$ is not shown. The free index i represents any quark type, but the numerical coefficient of the graph may depend on i. Graph (b) represents terms where P^+ and P^- are not next to each other in the supertrace.

for definiteness, the fields P^+ and P^- correspond to Φ_{45} and Φ_{54}, respectively [cf. Eq. (14)]. The vertices, Eqs. (36)–(39), then come generically from two types of terms in the supertrace of four Φ fields: terms where P^+ and P^- are next to each other: $\sim\sum_i \Phi_{45}\Phi_{54}\Phi_{4i}\Phi_{i4}$ (or $\sim\sum_i \Phi_{54}\Phi_{45}\Phi_{5i}\Phi_{i5}$), and terms where P^+ and P^- are separated: $\sim\Phi_{45}\Phi_{55}\Phi_{54}\Phi_{44}$. These can be represented by the vertices (a) and (b) in Fig. 4, respectively. The index i in Fig. 4(a) should be summed over all valence, ghost valence, and sea quarks. The last contributions (proportional to XY) in Eqs. (36)–(38) correspond to vertex Fig. 4(b); while all other terms come from the sum over i in Fig. 4(a).

Note that the graphs in Fig. 4 represent quark flow only; the numerical value of each graph depends on the term in the Lagrangian that generates it, and may also depend on the free index i. In particular the mixed potential $\mathcal{U}_V$ generates only vertex Fig. 4(a) terms, and only gives nonzero coefficients of terms where i is a sea quark flavor. This follows from the fact that τ_3 in Eq. (25) is proportional to the identity in the pure valence sector, and therefore $\mathcal{U}_V$ reduces to a field-independent constant in that sector.

When two meson lines at the vertices are contracted, as in Fig. 3, the quark flow diagrams in Fig. 5 result. The connected contraction of Fig. 4(a) gives Fig. 5(a), which clearly involves an internal sea quark loop. This means that terms from Fig. 4(a) where i is a valence or ghost valence quark must cancel in the connected contractions. This arises algebraically from Eqs. (36)–(38) using Eq. (31): Contractions of $R^\dagger R$ terms cancel connected contractions of XX and YY and P^+P^- terms. This leaves just connected $Q^\dagger Q$ contractions [Fig. 5(a)], disconnected XX and YY contractions [Fig. 5(b)], and disconnected XY contractions [Fig. 5(c)].

At this point it is easy to make the "by-hand" adjustment necessary to correspond with the fourth-root procedure. The only explicit sea quark loop in Fig. 5 is in diagram (a), so we just divide those terms by 4. We already know such terms come only from $Q^\dagger Q$ contractions; dividing them by 4 is equivalent to ignoring the implicit sum over the 4 tastes in the $Q^\dagger Q$ terms. There are also sea quark loop insertions in the disconnected meson propagators in Figs. 5(b) and 5(c). Such insertions have already been corrected for the fourth root in Eq. (33) or Eq. (35).

Let Σ_{P^+} be the P^+ self energy, defined to be the negative of the sum of self energy diagrams. At NLO, we have

$$\Sigma_{P^+}(p^2) = \frac{1}{16\pi^2 f^2}(\sigma_0 m_P^2 + \sigma_1 p^2) + \text{ analytic terms}, \tag{40}$$

where σ_0 and σ_1 come from the one-loop diagrams and are independent of momentum p. Since we have not determined the NLO chiral Lagrangian, we cannot express the analytic contributions in terms of chiral parameters. For the quantities of interest, however, it will be sufficient for our purposes to write down the most general contributions consistent with the symmetries. Putting together the one-loop contributions from the vertices Eqs. (36)–(39), we get

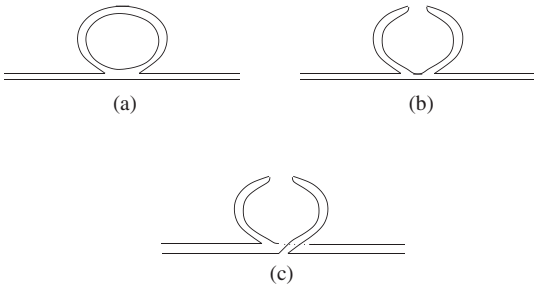

FIG. 5. Quark flow graphs corresponding to the P^+ self energy, Fig. 3. Graphs (a) and (b) come from connected and disconnected contractions, respectively, of the internal meson lines in vertex Fig. 4(a); graph (c), from the disconnected contraction in vertex Fig. 4(b). Iterations of sea quark loops in the disconnected propagators, as in Fig. 2, is implied in graphs (b) and (c).

$$\sigma_0 = -\frac{1}{3}\int\Bigg[\sum_F\Big(\frac{1}{q^2+m_{Fx}^2}+\frac{1}{q^2+m_{Fy}^2}\Big)+[XX]_{\rm disc}(q^2) + [YY]_{\rm disc}(q^2)+4[XY]_{\rm disc}(q^2)\Bigg], \tag{41}$$

$$\sigma_1 = -\frac{1}{3}\int\Bigg[\sum_F\Big(\frac{1}{q^2+m_{Fx}^2}+\frac{1}{q^2+m_{Fy}^2}\Big)+[XX]_{\rm disc}(q^2) + [YY]_{\rm disc}(q^2)-2[XY]_{\rm disc}(q^2)\Bigg], \tag{42}$$

where, as usual, F runs over sea quark flavor (e.g., u, d, s), and

$$\int \equiv 16\pi^2\int\frac{d^4q}{(2\pi)^4}, \tag{43}$$

suitably regulated. The disconnected propagator is given in Eq. (33) or Eq. (35). In Eq. (42), we have dropped (constant) quartic divergences and have used Eqs. (26), (29), and (27) to replace factors of quark masses with the corresponding meson masses. The simple identity

$$\frac{q^2+m_X^2}{q^2+m_Y^2}[XX]_{\rm disc}(q^2) = \frac{q^2+m_Y^2}{q^2+m_X^2}[YY]_{\rm disc}(q^2) = [XY]_{\rm disc}(q^2) \tag{44}$$

has allowed us to remove all explicit factors of q^2 in the integrands involving disconnected propagators.

We now focus explicitly on computing the $P^\pm$ mass. The chiral symmetry in the valence sector implies that the analytic contributions to $(m_P^{\rm NLO})^2$ must be proportional to the tree-level $m_P^2 \propto (m_x + m_y)$. In the continuum limit, these contributions just go over to the standard form in terms of the Gasser-Leutwyler parameters L_i [22]. At finite lattice spacing, the only possible new NLO analytic term is $Ca^2m_P^2$, where C is an unknown constant that depends on the details of the lattice action in both the valence and the sea sectors. Indeed it is easy to write down terms that will appear in the NLO Lagrangian and will contribute to C, for example,

$$a^2\langle P_V\partial_\mu\Sigma P_V\partial_\mu\Sigma^\dagger\rangle,\qquad a^2\mathcal{U}_S\langle\partial_\mu\Sigma\partial_\mu\Sigma^\dagger\rangle,\qquad a^2\mathcal{U}_S\langle\Sigma M^\dagger + M\Sigma^\dagger\rangle, \tag{45}$$

with $\mathcal{U}_S$ given in Eq. (22). The one-loop corrections to the $P^\pm$ mass squared are then found by evaluating $\Sigma_{P^+}(p^2)$ at $p^2 = -m_P^2$, giving

$$\frac{(m_P^{\rm NLO})^2}{B(m_x+m_y)} = 1+\frac{1}{16\pi^2f^2}(\sigma_0-\sigma_1) + \frac{16B}{f^2}(2L_8-L_5)(m_x+m_y) + \frac{32B}{f^2}(2L_6-L_4)\sum_f m_f + a^2C, \tag{46}$$

where, from Eqs. (42) and (43),

$$\sigma_0-\sigma_1 = -2\int[XY]_{\rm disc}(q^2). \tag{47}$$

The integral in Eq. (47) can be evaluated in terms of the chiral logarithm and residue functions defined in Refs. [29,30]. For completeness we include the definitions here. The chiral logarithm functions, coming from integration over a single and double pole, respectively, are

$$\ell(m^2) \equiv m^2\Big(\ln\frac{m^2}{\Lambda_\chi^2}+\delta_1(mL)\Big),\qquad \tilde\ell(m^2) \equiv -\Big(\ln\frac{m^2}{\Lambda_\chi^2}+1\Big)+\delta_3(mL), \tag{48}$$

where Λ_χ is the chiral scale, L is the spatial dimension, and the finite volume correction terms are [28]

$$\delta_1(mL) \equiv 4\sum_{\vec r\neq 0}\frac{K_1(|\vec r|mL)}{mL|\vec r|},\qquad \delta_3(mL) \equiv 2\sum_{\vec r\neq 0}K_0(|\vec r|mL). \tag{49}$$

K_0 and K_1 are Bessel functions of imaginary argument, and $\vec r$, which labels the various periodic images, is a three-dimensional vector with integer components.

The residue functions $R_j^{[n,k]}$ allow one to write integrals over ratios of products of (q^2+m^2) terms, such as $[XY]_{\rm disc}(q^2)$, as integrals over single poles. They are defined by

$$R_j^{[n,k]}(\{\mathcal{M}\};\{\mu\}) \equiv \frac{\prod_{a=1}^k(\mu_a^2-m_j^2)}{\prod_{i=1}^{\prime n}(m_i^2-m_j^2)}. \tag{50}$$

The residues are a function of two sets of masses, the "denominator" set $\{\mathcal{M}\} = \{m_1, m_2, \ldots, m_n\}$ and the "numerator" set $\{\mu\} = \{\mu_1, \mu_2, \ldots, \mu_k\}$. The indices j and i, $1 \le j, i \le n$, refer to particular denominator masses; the prime on the product in the denominator of Eq. (50) means that $i = j$ is omitted. In cases of degeneracy, we also need the double-pole residue functions, $D_{j,\ell}^{[n,k]}$:

$$D_{j,\ell}^{[n,k]}(\{\mathcal{M}\};\{\mu\}) \equiv -\frac{d}{dm_\ell^2}R_j^{[n,k]}(\{\mathcal{M}\};\{\mu\}). \tag{51}$$

We can now write out Eq. (46) explicitly in various useful cases. In the $N_f = 3$ partially quenched case, with no mass degeneracies, we have

$$\frac{(m_{P^+}^{\mathrm{NLO}})^2}{B(m_x+m_y)} = 1 + \frac{1}{16\pi^2 f^2} \times \left(\frac{2}{3}\sum_{j=1}^{4} R_j^{[4,3]}(\{\mathcal{M}_{XY,I}^{[4]}\};\{\mu_I^{[3]}\})\ell(m_j^2)\right) + \frac{16B}{f^2}(2L_8 - L_5)(m_x+m_y) + \frac{32B}{f^2}(2L_6 - L_4)(m_u+m_d+m_s) + a^2C. \tag{52}$$

The index j is summed over the denominator masses, as it will be also in subsequent cases; the mass-set arguments are

$$\{\mathcal{M}_{XY,I}^{[4]}\} \equiv \{m_X, m_Y, m_{\pi_I^0}, m_{\eta_I}\}, \quad \{\mu_I^{[3]}\} \equiv \{m_{U_I}, m_{D_I}, m_{S_I}\}. \tag{53}$$

Equation (52) is identical to the corresponding continuum partially quenched result with no degeneracies [53], except for the explicit discretization term a^2C and the fact that the neutral sea-sea mesons are specified to be taste singlets. For us, "no degeneracies" means that none of the seven meson masses in Eq. (53) are equal. We have chosen the normalization of quark masses in the chiral Lagrangian, Eq. (19), so that the same constant B appears in the relation between quark and meson masses in both sea and valences cases. However, degeneracies between sea-sea and valence-valence mesons in Eq. (53) would *not* imply equal valence and sea quark masses, because of the splitting of the taste-singlet sea-sea mesons, Eq. (27).

Taking $m_u = m_d \equiv \hat{m} \Rightarrow m_{U_I} = m_{D_I} = m_{\pi_I^0}$, but with no other degeneracies, then gives

$$\frac{(m_{P^+}^{\mathrm{NLO}})^2}{B(m_x+m_y)} = 1 + \frac{1}{16\pi^2 f^2} \times \left(\frac{2}{3}\sum_{j=1}^{3} R_j^{[3,2]}(\{\mathcal{M}_{XY,I}^{[3]}\};\{\mu_I^{[2]}\})\ell(m_j^2)\right) + \frac{16B}{f^2}(2L_8 - L_5)(m_x+m_y) + \frac{32B}{f^2}(2L_6 - L_4)(2\hat{m}+m_s) + a^2C, \tag{54}$$

with

$$\{\mathcal{M}_{XY,I}^{[3]}\} \equiv \{m_X, m_Y, m_{\eta_I}\}, \qquad \{\mu_I^{[2]}\} \equiv \{m_{U_I}, m_{S_I}\}. \tag{55}$$

When $m_u = m_d \equiv \hat{m}$ and $m_x = m_y \Rightarrow m_X = m_Y$, but no degeneracies between sea-sea and valence-valence mesons, we have a "partially quenched pion" with

$$\frac{(m_{P^+}^{\mathrm{NLO}})^2}{2Bm_x} = 1 + \frac{1}{16\pi^2 f^2}\frac{2}{3}\left(R_1^{[2,2]}(\{\mathcal{M}_{X,I}^{[2]}\};\{\mu_I^{[2]}\})\tilde{\ell}(m_X^2) \times \sum_{j=1}^{2} D_{j,1}^{[2,2]}(\{\mathcal{M}_{X,I}^{[2]}\};\{\mu_I^{[2]}\})\ell(m_j^2)\right) + \frac{16B}{f^2}(2L_8 - L_5)(2m_x) + \frac{32B}{f^2}(2L_6 - L_4)(2\hat{m}+m_s) + a^2C, \tag{56}$$

where

$$\{\mathcal{M}_{X,I}^{[2]}\} \equiv \{m_X, m_{\eta_I}\}, \tag{57}$$

and $\{\mu_I^{[2]}\}$ is given by Eq. (55).

At finite lattice spacing, the cases that most resemble the full (unquenched) theory are ones with degeneracies among the valence-valence and sea-sea mesons in Eq. (53). For current purposes, we might call a "full pion" one with $m_X = m_Y = m_{U_I} = m_{D_I} = m_{\pi_I^0}$, which requires $m_x = m_y$ and $m_u = m_d = \hat{m}$, but $m_x > \hat{m}$, since the taste splitting $\Delta_{\pi_I^0}$ in Eq. (27) is positive.[13] In this case, we have

$$\frac{(m_{\pi^+}^{\mathrm{NLO}})^2}{2Bm_x} = 1 + \frac{1}{16\pi^2 f^2}\left(\ell(m_{\pi_I^0}^2) - \frac{1}{3}\ell(m_{\eta_I}^2)\right) + \frac{16B}{f^2}(2L_8 - L_5)(2m_x) + \frac{32B}{f^2}(2L_6 - L_4)(2\hat{m}+m_s) + a^2C, \tag{58}$$

where we have used Eq. (34) to simplify the residues. Similarly, calling a "full kaon" a meson with $m_X = m_{U_I} = m_{D_I}$ and $m_Y = m_{S_I}$, results in

$$\frac{(m_K^{\mathrm{NLO}})^2}{B(m_x+m_y)} = 1 + \frac{1}{16\pi^2 f^2}\frac{2}{3}\ell(m_{\eta_I}^2) + \frac{16B}{f^2}(2L_8 - L_5)(m_x+m_y) + \frac{32B}{f^2}(2L_6 - L_4)(2\hat{m}+m_s) + a^2C. \tag{59}$$

Equations (58) and (59) clearly approach the standard results [22] as $a \to 0$.

C. NLO valence-valence pseudoscalar decay constant

The decay constant f_P of the $P^{\pm}$ meson is defined by the matrix element of the corresponding axial current, $j_{\mu 5}^P$,

$$\langle 0|j_{\mu 5}^P|P(p)\rangle = -if_P p_\mu. \tag{60}$$

[13] This is at least true for the simulations carried out by the MILC Collaboration.

In the LO chiral theory of Eq. (19), the axial current is given by[14]

$$j^P_{\mu 5} = \frac{-if^2}{4}\langle \lambda(\partial_\mu \Sigma \Sigma^\dagger + \Sigma^\dagger \partial_\mu \Sigma)\rangle. \tag{61}$$

Here λ projects out the appropriate flavors: With three sea quark flavors as in Eq. (14), the valence quarks x and y correspond to indices 4 and 5 of Φ, and then $\lambda_{ij} = \delta_{i5}\delta_{j4}$.

At NLO, the decay constant has the form

$$\frac{f_P^{\rm NLO}}{f} = 1 + \frac{1}{16\pi^2 f^2}\,\delta f_P + \text{ analytic terms.} \tag{62}$$

The term δf_P comes from the one-loop diagrams, and the analytic contributions are generated at tree-level by NLO terms in the chiral Lagrangian and corresponding corrections to the current in Eq. (61). There are two contributions to δf_P,

$$\delta f_P = \delta f_P^{\rm current} + \frac{1}{2}\delta Z_P, \tag{63}$$

where $\delta f_P^{\rm current}$ comes from diagrams generated directly by expanding the current in Eq. (61) to cubic order in Φ, and δZ_P is the one-loop wave function renormalization. From Eq. (40) we have

$$\delta Z_P \equiv -16\pi^2 f^2 \frac{d\Sigma_{P^+}(p^2)}{dp^2} = -\sigma_1. \tag{64}$$

As in Ref. [30], a straightforward calculation shows that $\delta f_P^{\rm current} = -2\delta Z_P$. From Eq. (42), we then have

$$\delta f_P = \frac{3}{2}\sigma_1 = -\frac{1}{2}\int\Bigg[\sum_F\Big(\frac{1}{q^2+m_{Fx}^2}+\frac{1}{q^2+m_{Fy}^2}\Big) + [XX]_{\rm disc}(q^2) + [YY]_{\rm disc}(q^2) - 2[XY]_{\rm disc}(q^2)\Bigg], \tag{65}$$

with F summed over sea quark flavors.

The analytic terms in Eq. (62) come only from NLO terms in the chiral Lagrangian with derivatives, which affect the decay constant either directly, through wave function renormalization, or indirectly, by leading to higher corrections to the axial current. Thus, $\mathcal{O}(a^4)$ corrections to the chiral Lagrangian have no effect on Eq. (62). There will however be analytic terms from $\mathcal{O}(p^4)$, $\mathcal{O}(mp^2)$, and $\mathcal{O}(a^2p^2)$ Lagrangian corrections. The former two are identical to those in the continuum and produce terms proportional to quark masses. The effects of the latter corrections on f_P can be absorbed into a single term proportional to a^2. We thus have,

$$\frac{f_P^{\rm NLO}}{f} = 1 + \frac{1}{16\pi^2 f^2}\,\delta f_P + \frac{8B}{f^2}L_5(m_x+m_y) + \frac{16B}{f^2}L_4\sum_F m_F + a^2\mathcal{F}, \tag{66}$$

where L_4 and L_5 are standard [22], $\mathcal{F}$ is a new constant, and δf_P is given by Eq. (65). Because Lagrangian terms of $O(ma^2)$ do not affect $\mathcal{F}$, it is easy to see from the discussion surrounding Eq. (45) that $\mathcal{F}$ is independent of the corresponding constant C occurring in the expression for the meson mass, Eq. (46). Like C, $\mathcal{F}$ depends on the details of the lattice action in both the sea and valence sectors.

We can now write out the NLO expression for the decay constant in various special cases. In the $N_f = 3$ partially quenched case, with no mass degeneracies, we have

$$\frac{f_P^{\rm NLO}}{f} = 1 + \frac{1}{16\pi^2 f^2}\Bigg[-\frac{1}{2}\sum_F[\ell(m_{Fx}^2)+\ell(m_{Fy}^2)] + \frac{1}{6}\Bigg(R_1^{[3,3]}(\{\mathcal{M}_{X,I}^{[3]}\};\{\mu_I^{(3)}\})\tilde{\ell}(m_X^2) + R_1^{[3,3]}(\{\mathcal{M}_{Y,I}^{[3]}\};\{\mu_I^{(3)}\})\tilde{\ell}(m_Y^2) + \sum_{j=1}^{3} D_{j,1}^{[3,3]}(\{\mathcal{M}_{X,I}^{[3]}\};\{\mu_I^{(3)}\})\ell(m_j^2) + \sum_{j=1}^{3} D_{j,1}^{[3,3]}(\{\mathcal{M}_{Y_l}^{[3]}\};\{\mu_I^{(3)}\})\ell(m_j^2) - 2\sum_{j=1}^{4} R_j^{[4,3]}(\{\mathcal{M}_{XY,I}^{[4]}\};\{\mu_I^{(3)}\})\ell(m_j^2)\Bigg)\Bigg] + \frac{8B}{f^2}L_5(m_x+m_y) + \frac{16B}{f^2}L_4\sum_F m_F + a^2\mathcal{F}, \tag{67}$$

where F runs over u, d, and s. The mass sets $\{\mathcal{M}_{XY,I}^{[4]}\}$ and $\{\mu_I^{(3)}\}$ are given by Eq. (53), and

$$\{\mathcal{M}_{X,I}^{[3]}\} \equiv \{m_X, m_{\pi_I^0}, m_{\eta_I}\}, \qquad \{\mathcal{M}_{Y,I}^{[3]}\} \equiv \{m_Y, m_{\pi_I^0}, m_{\eta_I}\}. \tag{68}$$

[14] We use the Noether current corresponding to axial-vector rotations as our partially conserved axial-vector current. This is justified if the analogous current is used in the underlying lattice theory. A convenient method to construct this current in numerical simulations is described in Ref. [54]. Alternatively, one may employ the corresponding covariant pseudoscalar density to define the decay constant [54]. On the other hand, using a conserved but not covariant axial-vector current would result in extra terms proportional to am_x and am_y, which are not captured in the following results.

With $m_u = m_d \equiv \hat{m} \Rightarrow m_{U_I} = m_{D_I} = m_{\pi_I^0}$, but no other degeneracies, the result is

$$\frac{f_P^{\rm NLO}}{f} = 1 + \frac{1}{16\pi^2 f^2}\Bigg[-\frac{1}{2}[2\ell(m_{ux}^2) + \ell(m_{sx}^2) + 2\ell(m_{uy}^2) + \ell(m_{sy}^2)] + \frac{1}{6}\Bigg(R_1^{[2,2]}(\{\mathcal{M}_{X,I}^{[2]}\};\{\mu_I^{(2)}\})\tilde{\ell}(m_X^2) + R_1^{[2,2]}(\{\mathcal{M}_{Y,I}^{[2]}\};\{\mu_I^{(2)}\})\tilde{\ell}(m_Y^2) + \sum_{j=1}^{2} D_{j,1}^{[2,2]}(\{\mathcal{M}_{X,I}^{[2]}\};\{\mu_I^{(2)}\})\ell(m_j^2) + \sum_{j=1}^{2} D_{j,1}^{[2,2]}(\{\mathcal{M}_{Y_I}^{[2]}\};\{\mu_I^{(2)}\})\ell(m_j^2) - 2\sum_{j=1}^{3} R_j^{[3,2]}(\{\mathcal{M}_{XY,I}^{[3]}\};\{\mu_I^{(2)}\})\ell(m_j^2)\Bigg)\Bigg] + \frac{8B}{f^2}L_5(m_x + m_y) + \frac{16B}{f^2}L_4(2\hat{m} + m_s) + a^2\mathcal{F}. \tag{69}$$

Here, $\{\mathcal{M}_{XY,I}^{[3]}\}$ and $\{\mu_I^{(2)}\}$ are given in Eq. (55); while $\{\mathcal{M}_{X,I}^{[2]}\}$ is defined in Eq. (57) (for $\{\mathcal{M}_{Y,I}^{[2]}\}$ take $X \to Y$).

For a "partially quenched pion" with $m_x = m_y$, there is considerable simplification because the disconnected contributions in Eq. (65) will cancel. Taking in addition $m_u = m_d \equiv \hat{m}$ for simplicity, we have

$$\frac{f_P^{\rm NLO}}{f} = 1 + \frac{1}{16\pi^2 f^2}[-2\ell(m_{ux}^2) - \ell(m_{sx}^2)] + \frac{8B}{f^2}L_5(2m_x) + \frac{16B}{f^2}L_4(2\hat{m} + m_s) + a^2\mathcal{F}. \tag{70}$$

There is no obviously preferred way here to define a "full pion" to make the NLO corrections take on a continuumlike form. In the $a \to 0$ limit, the splitting $a^2\Delta_{\rm Mix}$ in Eq. (29) will vanish, and the logarithm terms will clearly approach the standard form [22]: $-2\ell(m_\pi^2) - \ell(m_K^2)$. At finite lattice spacing, we can choose m_x so that m_{ux}^2 and m_{sx}^2 have the masses of the sea-sea pion and sea-sea kaon of any one taste, but there seems to be no advantage in doing that. In particular, the value of m_x so chosen will *not* be the same in general as the value needed to give the logarithms in the meson mass their continuumlike form, Eq. (58).

For the kaon, it makes some sense to define a full kaon as we did in Sec. III B: $m_X = m_{U_I} = m_{D_I} = m_{\pi_I^0}$ and $m_Y = m_{S_I}$. This at least gives the disconnected contributions the form they would have in the continuum. We then have

$$\frac{f_K^{\rm NLO}}{f} = 1 + \frac{1}{16\pi^2 f^2}\Bigg[-\ell(m_{ux}^2) - \frac{1}{2}\ell(m_{sx}^2) - \ell(m_{uy}^2) - \frac{1}{2}\ell(m_{sy}^2) + \frac{1}{4}\ell(m_{\pi_I^0}^2) + \frac{1}{2}\ell(m_{S_I}^2) - \frac{3}{4}\ell(m_{\eta_I}^2)\Bigg] + \frac{8B}{f^2}L_5(m_x + m_y) + \frac{16B}{f^2}L_4(2\hat{m} + m_s) + a^2\mathcal{F}. \tag{71}$$

In the continuum limit, $m_{ux} = m_{\pi_I^0} \equiv m_\pi$, $m_{sx} = m_{uy} \equiv m_K$, $m_{\eta_I} \equiv m_\eta$, and $m_{sy} = m_{S_I}$, thereby reproducing the known result [22].

IV. DISCUSSION

Our results for 2 + 1 sea quark flavors are currently the most relevant ones, since they can be applied to simulations using the existing configurations generated by the MILC Collaboration. Equations (56) and (70) describe the quark mass and lattice spacing dependence of the pion masses and decay constants, and these expressions can be directly fitted to lattice data obtained with Ginsparg-Wilson valence fermions.

The number of unknown fit parameters in these expressions is fairly small. For instance, the pion mass depends on the usual low-energy constants of continuum χPT (f, B and two familiar combinations of Gasser-Leutwyler coefficients), the sea-sea meson masses $m_{\pi_I^0}^2$, $m_{\eta_I}^2$, the sea quark masses $\hat{m}$, m_s, and the constant C. At one-loop order we can express the sea quark mass combination $2\hat{m} + m_s$ through leading-order sea-sea meson masses [cf. Eq. (27)]:

$$B(2\hat{m} + m_s) = \frac{1}{2}m_{\pi_5^+}^2 + m_{K_5^+}^2. \tag{72}$$

These masses as well as $m_{\pi_I^0}^2$ and $m_{\eta_I}^2$ already have been measured by the MILC Collaboration and are therefore not unknown parameters.[15] The only true unknown parameter

[15]The measurement of the singlet meson masses is difficult because disconnected diagrams contribute to the correlator. For $m_u = m_d$, however, there are no disconnected contributions to the π_I^0 propagator, and its mass is degenerate with the π_I^+ mass. The η_I mass is also not affected by disconnected diagrams if $m_u = m_d \neq m_s$ and the limit $m_0 \to \infty$ is taken. In that case it is consistent to employ Eq. (34) where the m_{S_I} and m_{U_I} masses are from connected diagrams only. In reality m_0^2 is not infinity, and there can be $\eta - \eta'$ mixing, which would be proportional to $(m_s - m_u)/m_0^2$. Such corrections are not taken into account in the MILC determination of m_{η_I}.

in addition to the ones from continuum χPT is thus the constant C.

Similar statements apply to the pion decay constant in Eq. (70). Even though the masses m_{ux}^2, m_{sx}^2 of the valence-sea mesons have not been measured yet, they can be straightforwardly determined from the propagator of the mixed meson and a linear fit to the leading-order mass formula in Eq. (29). Using this information leaves one additional parameter, the constant $\mathcal{F}$, besides the familiar parameters of continuum χPT.

Let us compare our results for Ginsparg-Wilson valence quarks with the corresponding expressions for staggered valence quarks. The one loop expression for the Goldstone pion π_5^+ in the 2 + 1 flavor case reads (see Eq. (75) in Ref. [29])

$$\begin{aligned}\frac{(m_{\pi_5^+}^{\mathrm{NLO}})^2}{2B\hat{m}} &= 1 + \frac{1}{16\pi^2 f^2}\left(\ell(m_{\pi_I^0}^2) - \frac{1}{3}\ell(m_{\eta_I}^2)\right) \\ &\quad + \frac{16B}{f^2}(2L_8 - L_5)(2\hat{m}) + \frac{32B}{f^2}(2L_6 - L_4)(2\hat{m} + m_s) + a^2\tilde{C} \\ &\quad - \frac{1}{16\pi^2 f^2}\left(4\ell(m_{\pi_V^0}^2) + \frac{2a^2\delta_V'}{m_{\eta_V'}^2 - m_{\eta_V}^2}\left[\frac{m_{S_V}^2 - m_{\eta_V}^2}{m_{\pi_V^0}^2 - m_{\eta_V}^2}\ell(m_{\eta_V}^2) - \frac{m_{S_V}^2 - m_{\eta_V'}^2}{m_{\pi_V^0}^2 - m_{\eta_V'}^2}\ell(m_{\eta_V'}^2)\right]\right. \\ &\quad \left. + 4\ell(m_{\pi_A^0}^2) + \frac{2a^2\delta_A'}{m_{\eta_A'}^2 - m_{\eta_A}^2}\left[\frac{m_{S_A}^2 - m_{\eta_A}^2}{m_{\pi_A^0}^2 - m_{\eta_A}^2}\ell(m_{\eta_A}^2) - \frac{m_{S_A}^2 - m_{\eta_A'}^2}{m_{\pi_A^0}^2 - m_{\eta_A'}^2}\ell(m_{\eta_A'}^2)\right]\right). \end{aligned} \tag{73}$$

The first two rows of this expression give the corresponding result in Eq. (58) for Ginsparg-Wilson valence quarks. The remaining contributions involve many more sea-sea meson masses as well as the two hairpin parameters δ_V' and δ_A'.[16] These parameters cannot be expressed in terms of leading-order charged meson masses and are therefore true unconstrained fit parameters.

The one-loop result for the pion decay constant—given in Eq. (27) in Ref. [30]—also has contributions proportional to δ_V' and δ_A':

$$\begin{aligned}\frac{f_{\pi_5^+}^{\mathrm{NLO}}}{f} &= 1 + \frac{1}{16\pi^2 f^2}\sum_b \frac{-2\ell(m_{\pi_b^0}^2) - \ell(m_{K_b^+}^2)}{16} + \frac{16B}{f^2}(2\hat{m} + m_s)L_4 + \frac{16B}{f^2}\hat{m}L_5 + a^2\tilde{\mathcal{F}} \\ &\quad + \frac{1}{16\pi^2 f^2}\left(2a^2\delta_V'\left[\frac{m_{S_V}^2 - m_{\eta_V}^2}{(m_{\pi_V^0}^2 - m_{\eta_V}^2)(m_{\eta_V'}^2 - m_{\eta_V}^2)}\ell(m_{\eta_V}^2) + \frac{m_{S_V}^2 - m_{\eta_V'}^2}{(m_{\pi_V^0}^2 - m_{\eta_V'}^2)(m_{\eta_V}^2 - m_{\eta_V'}^2)}\ell(m_{\eta_V'}^2)\right.\right. \\ &\quad \left. + \frac{m_{S_V}^2 - m_{\pi_V^0}^2}{(m_{\eta_V}^2 - m_{\pi_V^0}^2)(m_{\eta_V'}^2 - m_{\pi_V^0}^2)}\ell(m_{\pi_V^0}^2)\right] + 2a^2\delta_A'\left[\frac{m_{S_A}^2 - m_{\eta_A}^2}{(m_{\pi_A^0}^2 - m_{\eta_A}^2)(m_{\eta_A'}^2 - m_{\eta_A}^2)}\ell(m_{\eta_A}^2)\right. \\ &\quad \left.\left. + \frac{m_{S_A}^2 - m_{\eta_A'}^2}{(m_{\pi_A^0}^2 - m_{\eta_A'}^2)(m_{\eta_A}^2 - m_{\eta_A'}^2)}\ell(m_{\eta_A'}^2) + \frac{m_{S_A}^2 - m_{\pi_A^0}^2}{(m_{\eta_A}^2 - m_{\pi_A^0}^2)(m_{\eta_A'}^2 - m_{\pi_A^0}^2)}\ell(m_{\pi_A^0}^2)\right]\right). \end{aligned} \tag{74}$$

The factor of $1/16$ in the first line is canceled in the continuum limit by the sum over b, which runs over all 16 different meson tastes. As was the case for the pseudoscalar masses, the corresponding expression for the mixed theory, Eq. (70), is much simpler and does not involve the contributions proportional to the hairpin parameters δ_V' and δ_A'. Note that the constants $\tilde{C}$, $\tilde{\mathcal{F}}$ in Eqs. (73) and (74) are different from C and $\mathcal{F}$ in Eqs. (58) and (70).

[16]These two parameters are combinations of the low-energy constants in the potential $\mathcal{U}'$: $\delta_V' = C_{2V} - C_{5V}$, and analogously for δ_A' [29].

Obviously the functional dependence in the expressions for staggered valence quarks is much more complicated and involves more undetermined parameters than in the corresponding results for the mixed theory. However, the physical low-energy constants, the Gasser-Leutwyler coefficients, enter the expressions in the same way. Therefore, as already pointed out in Ref. [17], mixed simulations may be used to extract these phenomenologically relevant parameters from numerical lattice simulations.

The NLO formulas computed in Secs. III B and III C also make concrete a rather obvious fact about mixed action theories: At nonzero lattice spacing there is no

way to define equality of valence and sea quark masses in order to have all properties that might be desired of a ''full'' (unquenched) theory. The lattice theory will always have some features of partial quenching, and it is only in the continuum limit that the full theory is obtained. Depending on the purpose one may wish to choose various definitions to match the sea and valence quark masses. Since the scalar correlator is very sensitive to the effects of partial quenching [55], it has been proposed to choose the valence quark mass such that the scalar correlator does not have a negative contribution [16]. For the results reported in Ref. [14] the masses were chosen so that the valence-valence pion mass coincides with the Goldstone pion mass made of staggered quarks, i.e., $m^2_{\pi^+} = m^2_{\pi^+_5}$. The NLO results have suggested yet another definition with $m^2_{\pi^+} = m^2_{\pi^+_I}$. In this case, as we have seen in Sec. III B, some chiral logarithms resemble their continuum form and one might expect smaller partial quenching effects than with other definitions.[17] From a theoretical point of view all these definitions are equally good since they guarantee that full unquenched QCD is reached in the continuum limit. Practically, they differ with respect to the size of the partial quenching effects at nonzero lattice spacing, and the quark mass tuning can be rather difficult to achieve, depending on, for example, the statistical errors in the observables used for the matching.

Nevertheless, at least in the context of chiral perturbation theory, there is no fundamental difficulty with using mixed action theories to simulate QCD. The effects of finite lattice spacing can be controlled by first fitting to the chiral forms of the type derived here and then extrapolating to the continuum limit. Furthermore, as in the pure staggered case [57], we expect the chiral and continuum limits to commute in the mixed theory for any quantity that has a well-defined chiral limit in the continuum.

ACKNOWLEDGMENTS

We thank M. Golterman and S. Sharpe for helpful discussions. O. B. and C. B. gratefully acknowledge support of the Benasque Center of Science, where part of this work was done during the workshop ''Matching Light Quarks to Hadrons.'' This work is supported in part by the Grants-in-Aid for Scientific Research from the Japanese Ministry of Education, Culture, Sports, Science and Technology (Nos. 13135204, 15204015, 15540251, 16028201), the University of Tsukuba Research Project, and by the U.S. Department of Energy under Grants Nos. DE-FG02-91ER40628, W-7405-ENG-36, DE-FG03-96ER40956/A006, and DE-FG02-91ER40676.

[17]With the definition in Ref. [14] the scalar correlator becomes negative [56], a clear signal for partial quenching.

APPENDIX: CONSTRUCTION OF MIXED FOUR-FERMION OPERATORS

In this appendix we construct the mixed four-fermion operators in Eq. (5) that enter the Symanzik effective theory at $\mathcal{O}(a^2)$. We closely follow the procedure and notation in Ref. [27] where the four-fermion operators made of sea quarks only were constructed. The method determines first all lattice four-fermion operators without derivatives and mass insertions that are singlets under the symmetries of the lattice theory. Taking the continuum limit of these terms results in the allowed continuum operators that appear in the Symanzik effective action.

First we convert the staggered fields into hypercube fields, since these fields yield the proper continuum fields when the lattice spacing is sent to zero. Following Refs. [58–60] the lattice is divided into hypercubes containing 16 sites whose coordinates are written as[18]

$$x_\mu = 2y_\mu + \eta_\mu. \tag{A1}$$

The hypercube vector η labels the sites within the hypercube and its components η_μ are either 0 or 1. In terms of the site variables $\chi, \overline{\chi}$ and the gauge links U the hypercube fields are defined by

$$\begin{aligned}\psi_{S,\alpha a}(y) &= \frac{1}{2}\sum_\eta \Gamma^{\alpha a}_\eta U(2y, 2y+\eta)\chi_S(2y+\eta),\\ \overline{\psi}_{S,\alpha a}(y) &= \frac{1}{2}\sum_\eta \overline{\chi}_S(2y+\eta)U^\dagger(2y, 2y+\eta)\Gamma^{*\alpha a}_\eta,\end{aligned} \tag{A2}$$

where $U(2y, 2y+\eta)$ denotes a product of link variables along a path going from $2y$ to $2y+\eta$, and

$$\Gamma_\eta = \gamma_1^{\eta_1}\gamma_2^{\eta_2}\gamma_3^{\eta_3}\gamma_4^{\eta_4}. \tag{A3}$$

The indices α and a represent the Dirac and taste index, respectively (we suppress the flavor and the color index).

Using the hypercube fields we now construct all mixed four-fermion operators O_{4f} that are allowed by the symmetries and that correspond to dimension six operators in the continuum limit. Four-fermion operators that contain derivatives and/or quark masses are higher than $\mathcal{O}(a^2)$ in the Symanzik action and can be ignored here. Since no quark mass appears the operators must be invariant under the full chiral symmetries of the massless lattice theory.

The construction proceeds in five steps [27]:

(1) Multiply a sea quark bilinear on a hypercube by a valence bilinear at the same lattice point and sum over all hypercubes,

[18]We use lattice units and set $a = 1$ in this appendix.

$$O_{4f}(\Gamma_S, \Gamma_V) = \sum_y (\overline{\psi}_S(y)\Gamma_S\psi_S(y))(\overline{\psi}_V(y)\Gamma_V\psi_V(y)). \tag{A4}$$

The flavor symmetries dictate that the sea quark bilinear is an $SU(N_f)$ singlet while the valence bilinear is a singlet under $SU(N_V|N_V)$. Γ_S represents an arbitrary tensor product $\gamma_A \otimes t^a \otimes \xi_\alpha$ of a gamma matrix acting in Dirac space, a color generator t^a, and an $SU(4)$ taste group generator ξ_α. Similarly, Γ_V denotes an arbitrary combination $\gamma_B \otimes t^b$ acting on the valence fields. It does not include a slot for a taste matrix since the valence fields do not have the taste degree of freedom.

In Eq. (A4) all the sea quark indices are contracted with Γ_S while all the valence indices are contracted with Γ_V, so the operator truly is a product of two bilinears. One can write down other operators that do not have this simple structure. For example, one could contract the color indices of ψ_S and $\overline{\psi}_V$ and the indices of ψ_V and $\overline{\psi}_S$. Similarly one can contract the Dirac indices in such a ''twisted'' manner. However, all these operators are redundant [18]. Making use of Fierz identities one can always ''untwist'' these operators and bring them into the form in Eq. (A4).

On each hypercube there are 16^2 possibilities to form a valence field bilinear. The one chosen in Eq. (A1) involves only the fields at the lattice point y where the staggered hypercube field lives. Close to the continuum, all other valence bilinears can be written as the one in Eq. (A4), plus terms involving derivatives, which we can drop.

(2) The sum over all hypercubes in Eq. (A4) makes the operator O_{4f} invariant under lattice translations by one hypercube, i.e., $y \to y + 1$. In order to obtain the part that is invariant under single site translations we apply the projection operator

$$\mathcal{P} = \prod_\mu \frac{1}{2}(1 + T_S^\mu \otimes T_V^\mu), \tag{A5}$$

with $T_S^\mu \otimes T_V^\mu$ being the translation operator in the μ direction. The translation operator acts differently in the sea and valence sector. In the valence sector it is a trivial shift of the fields,

$$\begin{aligned} T_V^\mu \psi_V(x) &= \psi_V(x + \hat{\mu}), \\ T_V^\mu \overline{\psi}_V(x) &= \overline{\psi}_V(x + \hat{\mu}), \end{aligned} \tag{A6}$$

where $\hat{\mu}$ denotes the unit vector in the μ direction. In the sea sector it involves transformations of the spin and taste degrees of freedom. Explicitly [61]

$$\begin{aligned} T_S^\mu \psi_S(y) &= \frac{1}{2}[(I \otimes \xi_\mu - \gamma_{\mu 5} \otimes \xi_5)\psi_S(y) \\ &\quad + (I \otimes \xi_\mu + \gamma_{\mu 5} \otimes \xi_5)\psi_S(y + 2\mu)], \\ T_S^\mu \overline{\psi}_S(y) &= \frac{1}{2}[\overline{\psi}_S(y)(I \otimes \xi_\mu + \gamma_{\mu 5} \otimes \xi_5) \\ &\quad + \overline{\psi}_S(y + 2\mu)(I \otimes \xi_\mu - \gamma_{\mu 5} \otimes \xi_5)]. \end{aligned} \tag{A7}$$

Note that the translation operators for different directions commute when acting on staggered bilinears, so the order of them is irrelevant in the product in Eq. (A5).

Applying the projection operator Eq. (A5) results in many terms with derivatives, which we can neglect. Acting with T_V^μ on the valence bilinear gives

$$\begin{aligned} \overline{\psi}_V(y)\Gamma_V\psi_V(y) \to (\overline{\psi}_V(y) + \nabla_\mu^f \overline{\psi}_V(y))\Gamma_V(\psi_V(y) \\ + \nabla_\mu^f \psi_V(y)), \end{aligned} \tag{A8}$$

where we have introduced the usual nearest-neighbor forward difference operator in μ direction, ∇_μ^f. Similarly, acting with T_S^μ on sea quark bilinear produces many derivative terms. Using Eqs. (A7) and (A8) one straightforwardly establishes

$$\begin{aligned} \sum_y \overline{\psi}_S(y)\Gamma_S\psi_S(y) \to \sum_y \overline{\psi}_S(y)(I \otimes \xi_\mu)\Gamma_S(I \otimes \xi_\mu) \\ \times \psi_S(y) + \text{ derivative terms.} \end{aligned} \tag{A9}$$

Using these two results we find

$$\begin{aligned} \mathcal{P}[O_{4f}(\Gamma_S, \Gamma_V)] = O_{4f}(\tilde{\Gamma}_S, \Gamma_V) \\ + \text{ derivative terms.} \end{aligned} \tag{A10}$$

The matrix $\tilde{\Gamma}_S$ differs from Γ_S only in the taste matrix: ξ_α is replaced by the average

$$\tilde{\xi}_\alpha = \frac{1}{16}\sum_{i=1}^{16} \xi_i^\dagger \xi_\alpha \xi_i, \tag{A11}$$

where the sum runs over all 16 elements of the Clifford algebra. Only the identity $\xi_\alpha = I$ survives this average; for the other 15 taste matrices the average is zero. Thus we conclude that we only

need to consider sea quark bilinears in Eq. (A4) that are taste singlets.

(3) Next we impose the constraint that the operators must be color singlets. There are only two ways to form such singlets. Either the color group generators in Γ_S and Γ_V are equal and a summation over the generator index is performed, or the identity matrix is inserted instead

(4) Now we form linear combinations of $O_{4f}(\Gamma_S, \Gamma_V)$ that are singlets under the hypercubic symmetry group of the lattice ($\pi/2$ rotations and reflections) and also charge conjugation. The transformation properties of the staggered fields in the hypercube notation are listed in Refs. [37,62]. Since the matrix Γ_S is trivial in taste space these transformations act in spin space only and their form is the same as for continuum Dirac spinors. We therefore find that the gamma matrices in Γ_S and Γ_V must be equal with their open indices being properly contracted in order to form scalars under rotations and reflections.

(5) Finally we select the operators that are invariant under the chiral symmetries. Each bilinear must be separately invariant under the full chiral symmetry group. This excludes all gamma matrices but the vector and axial vector.

This procedure produces all mixed four-fermion operators without derivatives that are singlets under all lattice symmetries. Taking the continuum limit one finds the four invariant operators listed in Eq. (5).

[1] P. H. Ginsparg and K. G. Wilson, Phys. Rev. D **25**, 2649 (1982).
[2] R. Narayanan and H. Neuberger, Phys. Lett. B **302**, 62 (1993).
[3] R. Narayanan and H. Neuberger, Nucl. Phys. **B412**, 574 (1994).
[4] R. Narayanan and H. Neuberger, Nucl. Phys. **B443**, 305 (1995).
[5] D. B. Kaplan, Phys. Lett. B **288**, 342 (1992).
[6] V. Furman and Y. Shamir, Nucl. Phys. **B439**, 54 (1995).
[7] A. D. Kennedy, Nucl. Phys. B Proc. Suppl. **140**, 190 (2005).
[8] C. W. Bernard *et al.*, Phys. Rev. D **64**, 054506 (2001).
[9] C. Aubin *et al.*, Phys. Rev. D **70**, 094505 (2004).
[10] C. Aubin *et al.*, Phys. Rev. D **70**, 114501 (2004).
[11] R. Frezzotti, P. A. Grassi, S. Sint, and P. Weisz, J. High Energy Phys. 08 (2001) 058.
[12] M. Lüscher, Phys. Lett. B **428**, 342 (1998).
[13] S. Dürr and C. Hoelbling, Phys. Rev. D **69**, 034503 (2004).
[14] D. B. Renner *et al.*, Nucl. Phys. B Proc. Suppl. **140**, 255 (2005).
[15] K. C. Bowler, B. Joo, R. D. Kenway, C. M. Maynard, and R. J. Tweedie, Nucl. Phys. B Proc. Suppl. **140**, 252 (2005).
[16] K. C. Bowler, B. Joo, R. D. Kenway, C. M. Maynard, and R. J. Tweedie, hep-lat/0411005.
[17] O. Bär, G. Rupak, and N. Shoresh, Phys. Rev. D **67**, 114505 (2003).
[18] O. Bär, G. Rupak, and N. Shoresh, Phys. Rev. D **70**, 034508 (2004).
[19] K. Symanzik, Nucl. Phys. **B226**, 187 (1983).
[20] K. Symanzik, Nucl. Phys. **B226**, 205 (1983).
[21] S. Weinberg, Phys. Rev. D **19**, 1277 (1979).
[22] J. Gasser and H. Leutwyler, Nucl. Phys. **B250**, 465 (1985).
[23] J. Gasser and H. Leutwyler, Ann. Phys. (N.Y.) **158**, 142 (1984).
[24] S. R. Sharpe and R. Singleton, Jr., Phys. Rev. D **58**, 074501 (1998).
[25] G. Rupak and N. Shoresh, Phys. Rev. D **66**, 054503 (2002).
[26] O. Bär, Nucl. Phys. B Proc. Suppl.. **140**, 106 (2005).
[27] W.-J. Lee and S. R. Sharpe, Phys. Rev. D **60**, 114503 (1999).
[28] C. Bernard, Phys. Rev. D **65**, 054031 (2002).
[29] C. Aubin and C. Bernard, Phys. Rev. D **68**, 034014 (2003).
[30] C. Aubin and C. Bernard, Phys. Rev. D **68**, 074011 (2003).
[31] A. Morel, J. Phys. (France) **48**, 1111 (1987).
[32] P. H. Damgaard and K. Splittorff, Phys. Rev. D **62**, 054509 (2000).
[33] M. F. L. Golterman and J. Smit, Nucl. Phys. **B245**, 61 (1984).
[34] C. W. Bernard and M. F. L. Golterman, Phys. Rev. D **49**, 486 (1994).
[35] F. Niedermayer, Nucl. Phys. B Proc. Suppl. **73**, 105 (1999).
[36] S. R. Sharpe, Nucl. Phys. B Proc. Suppl. **34**, 403 (1994).
[37] Y.-b. Luo, Phys. Rev. D **55**, 353 (1997).
[38] Y.-b. Luo, Phys. Rev. D **57**, 265 (1998).
[39] S. R. Sharpe and R. S. Van de Water, Phys. Rev. D **71**, 114505 (2005).
[40] S. R. Sharpe and N. Shoresh, Phys. Rev. D **64**, 114510 (2001).
[41] C. W. Bernard, "Proceedings of TASI '89, Boulder, Colorado," 1989.
[42] S. R. Sharpe, Phys. Rev. D **46**, 3146 (1992).
[43] S. Dürr, C. Hoelbling, and U. Wenger, Phys. Rev. D **70**, 094502 (2004).
[44] S. Dürr, C. Hoelbling, and U. Wenger, hep-lat/0409108.
[45] S. Dürr and C. Hoelbling, Phys. Rev. D **71**, 054501 (2005).
[46] E. Follana, A. Hart, and C. T. H. Davies, Phys. Rev. Lett. **93**, 241 601 (2004).
[47] F. Maresca and M. Peardon, hep-lat/0411029.
[48] D. H. Adams, hep-lat/0411030.
[49] Y. Shamir, Phys. Rev. D **71**, 034509 (2005).
[50] S. Aoki, Phys. Rev. D **30**, 2653 (1984).
[51] C. Aubin and Q. Wang, Phys. Rev. D **70**, 114504 (2004).
[52] M. Golterman, S. Sharpe, and R. L. Singleton, Phys. Rev. D **71**, 094503 (2005).

[53] S. R. Sharpe and N. Shoresh, Phys. Rev. D **62**, 094503 (2000).
[54] P. Hasenfratz, S. Hauswirth, T. Jörg, F. Niedermayer, and K. Holland, Nucl. Phys. **B643**, 280 (2002).
[55] W. A. Bardeen, A. Duncan, E. Eichten, N. Isgur, and H. Thacker, Phys. Rev. D **65**, 014509 (2002).
[56] W. Schroers (private communication).
[57] C. Bernard, Phys. Rev. D **71** 094020 (2005).
[58] F. Gliozzi, Nucl. Phys. **B204**, 419 (1982).
[59] A. Duncan, R. Roskies, and H. Vaidya, Phys. Lett. **114B**, 439 (1982).
[60] H. Kluberg-Stern, A. Morel, O. Napoly, and B. Petersson, Nucl. Phys. **B220**, 447 (1983).
[61] T. Jolicoeur, A. Morel, and B. Petersson, Nucl. Phys. **B274**, 225 (1986).
[62] D. Verstegen, Nucl. Phys. **B249**, 685 (1985).

PHYSICAL REVIEW D **73,** 014511 (2006)

Pseudoscalar meson masses in Wilson chiral perturbation theory for 2 + 1 flavors

S. Aoki,[1,2] O. Bär,[1] T. Ishikawa,[3] and S. Takeda[1]

[1]*Graduate School of Pure and Applied Sciences, University of Tsukuba, Tsukuba, Ibaraki 305-8571, Japan*
[2]*Riken BNL Research Center, Brookhaven National Laboratory, Upton, New York 11973, USA*
[3]*Center for Computational Physics, University of Tsukuba, Tsukuba 305-8577, Japan*

(Received 19 September 2005; published 18 January 2006)

We consider 2 + 1 flavor Wilson chiral perturbation theory including the lattice spacing contributions of $O(a^2)$. We adopt a power counting appropriate for the unquenched lattice simulations carried out by the CP-PACS/JLQCD Collaboration and compute the pseudoscalar meson masses to one loop. These expression are required to perform the chiral extrapolation of the CP-PACS/JLQCD lattice data.

DOI: 10.1103/PhysRevD.73.014511 PACS numbers: 12.38.Gc, 11.30.Hv, 11.30.Rd, 12.39.Fe

I. INTRODUCTION

The limitations of the quenched approximation in numerical lattice QCD simulations is by now well established. For example, the light hadron mass spectrum calculated by the CP-PACS Collaboration [1] deviates from the experimentally measured values by about 10%. Even though the quenching error is different for different observables, one must assume the quenching error to be of the same order for other quantities as well. Once the effect of dynamical up and down quarks is included, the quenching error is significantly reduced and the discrepancy between the numerically calculated and the experimentally measured values is much smaller compared with the quenched results [2]. Still, ignoring the effect of a dynamical strange quark in these unquenched 2 flavor simulations leads to an uncertainty, which is expected to be non-negligible. Only simulations with a dynamical strange quark will provide numerical results, which can be compared with experiment with confidence.

In order to eliminate the remaining source of quenching error the CP-PACS and JLQCD Collaborations have been carrying out unquenched 2 + 1 flavor simulations. A RG-improved gauge action and an $O(a)$ improved Wilson quark action have been adopted. The size of the lattice is modest ($L \simeq 2$ fm) and simulations at three different lattice spacings ($a \simeq 0.7$ fm, 1.0 fm, 1.22 fm) are planned so that the continuum limit can be taken. Five different masses for the degenerate up and down type quarks are simulated leading to pseudoscalar meson masses in the range $m_{PS}/m_V \simeq 0.62 - 0.78$. The physical strange quark mass lies between the two simulated strange quark masses and can therefore be reached by an interpolation. More details and the status of these simulations have been recently summarized in Ref. [3].

The masses for the up and down quarks are rather heavy and an extrapolation to their physical values is required. The functional forms for the extrapolation are usually given by Chiral Perturbation Theory (ChPT). In its standard form [4,5] the expressions derived in ChPT can be used after the continuum limit of the lattice data has been taken. However, for various reasons it is advantageous to perform the chiral extrapolation before the continuum limit. In this case ChPT needs to be formulated for lattice QCD at nonzero lattice spacing a. The main idea how this can be done was proposed in Ref. [6,7]. Since then many observables have been calculated at one loop order (for an overview see Ref. [8]). For lattice theories with Wilson fermions, however, all results were derived for unquenched 2 flavor Wilson ChPT (WChPT) and the chiral expressions are therefore not applicable for the CP-PACS/JLQCD simulations.

This is the first paper in a series where we provide the one loop expressions of 2 + 1 flavor WChPT for a variety of observables, which will be measured by the CP-PACS/JLQCD Collaboration. Here we present the results for the simplest observables, the pseudoscalar meson masses. The second paper is devoted to the vector meson masses and the third to the pseudoscalar decay constants and axial vector Ward identity quark mass [9,10]. In our calculations we include the lattice spacing contributions through $O(a^2)$ and adopt various power countings. Even though we have primarily the CP-PACS/JLQCD simulations in mind, our expressions are equally useful for other unquenched 2 + 1 flavor simulations employing Wilson fermions.

There is no fundamental difficulty in applying the framework of WChPT to 2 + 1 flavors, the main difference to the 2 flavor results is just the increased complexity of the final results. Since we follow the standard strategy of WChPT we will be brief in presenting our results. In Sec. II we explain the power counting which we assume and present the chiral Lagrangian up to next-to-leading order. The calculation of the pseudoscalar masses from this Lagrangian is straightforward and we summarize our final results in Sec. III. Many technical details and some intermediate results are collected in Appendices A and B.

II. THE CHIRAL EFFECTIVE LAGRANGIAN

A. The order counting

In continuum chiral perturbation theory (ChPT), $M = m$ or p^2 is the expansion parameter, where m is the quark mass and p is the momentum of the pseudoscalar meson. Since chiral symmetry is explicitly broken in lattice QCD with Wilson-type quarks, corrections due to the nonzero lattice spacing a are non-negligible. The construction of the chiral effective theory for Lattice QCD with Wilson fermions, so-called Wilson ChPT (WChPT), has become standard by now. From a conceptional point of view there is nothing new in applying the familiar techniques [6,11–13] to 2 + 1 flavor lattice QCD. The only nontrivial choice one has to make is the order counting one adopts in the chiral expansion, which we are going to explain in this section.[1]

The leading order (LO) chiral Lagrangian of the WChPT is constructed from $O(M)$ terms and the $O(a)$ term. Since the $O(a)$ term has the same chiral structure as the mass term, the LO Lagrangian of the WChPT assumes the same form as the one of continuum ChPT, provided one performs the replacement $m \to \tilde{m} = m + c_1 a$ with c_1 being a combination of two low-energy constants [6,11]. Based on this LO Lagrangian, however, the pion becomes a tachyon for $\tilde{m} = m + c_1 a < 0$ since the pion mass squared m_π is given by $m_\pi^2 = 2B(m + c_1 a)$ at tree level. This is in contrast to continuum ChPT where chiral symmetry dictates that the pion mass is given by $m_\pi^2 = B|m|$. This already indicates that the first nontrivial modification to continuum ChPT starts at $O(a^2)$. Indeed, including the $O(a^2)$ term in the LO chiral Lagrangian removes the unphysical tachyon from the theory, as has been shown in Ref. [12] for the 2 flavor theory. We therefore conclude that, for the consistency of the theory, the $O(a^2)$ term should be included in the LO Lagrangian in the WChPT.

Although the $O(a)$ term is superficially larger than the $O(a^2)$ term, the former term is irrelevant since it is absorbed in the definition of the shifted mass $\tilde{m}$. The $O(a^2)$ correction, on the other hand, becomes important in the regime where $\tilde{m}/\Lambda_{\rm QCD} \simeq \Lambda_{\rm QCD}^2 a^2$, even though the $\Lambda_{\rm QCD}^2 a^2$ correction is much smaller than 1 in general.

Suppose we consider the $O(\tilde{M}) = O(\tilde{m}, p^2)$ and the $O(a^2)$ term as LO terms. Then the terms of $O(\tilde{M}^2, \tilde{M}a^2, a^4)$ can be regarded as next-to-leading order (NLO), since the loop expansion in WChPT increases in units of $\tilde{M}$. We remark that the $O(a^4)$ term is not as relevant as the $O(\tilde{M}^2, \tilde{M}a^2)$ terms for our final results for the pseudoscalar masses. We will need the tree level contribution of the $O(a^4)$ term only to satisfy $m_{\rm PS,NLO}^2 = 0$ at $m_{\rm PS,LO}^2 = 0$, where $m_{\rm PS,NLO}$ is the pseudoscalar meson mass at NLO. This means that there is essentially no unknown low-energy constant associated with the $O(a^4)$ correction.[2]

The proper order counting of the $O(\tilde{M}a)$ term is more subtle than for the previously discussed terms.[3] Depending on the size of the $O(\tilde{M}a)$ contributions we may include it at leading order where it subsequently enters the chiral logs, or we treat it as a NLO term and include it at tree level only. The size of this term is indeed expected to vary significantly, depending on details of the action of the underlying lattice theory. The $O(\tilde{M}a)$ term contains one power of a and stems from the Pauli term in the Symanzik's effective action [15–17], which is used in an intermediate step to match the lattice to the chiral effective theory. Consequently, the $O(\tilde{M}a)$ contribution in the chiral Lagrangian is directly proportional to the coefficient of the Pauli term [11], and the size of this coefficient is much smaller for improved theories with a clover term in the action than for standard Wilson fermions. For fully nonperturbatively improved theories the coefficient is equal to zero and no $O(\tilde{M}a)$ term appears in the chiral Lagrangian.[4]

Since we have no *a priori* knowledge about the size of the $O(\tilde{M}a)$ term we will be as general as possible and present our results for three different order countings of this term. We first keep the $O(\tilde{M}a)$ term at LO where it gives a contribution to the chiral log corrections. If the $O(\tilde{M}a)$ term is assumed to be much smaller than the other LO terms we can easily expand our results. Performing this expansion is equivalent to doing the calculation with keeping the $O(\tilde{M}a)$ term at NLO. Finally we can set this term to zero in order to obtain the results for nonperturbatively improved theories.

B. Leading order Lagrangian

According to the discussion in the previous section, we use the following LO Lagrangian, which consists of terms of $O(\tilde{M}, a^2, \tilde{M}a)$:

[1] For notational simplicity we assume N degenerate quark masses in the following discussion.

[2] This may seem odd within WChPT, but it is a simple consequence of the fact that the pseudoscalar meson becomes massless in lattice QCD at the critical quark mass. In other words, the $O(a^4)$ term merely results in an additional shift in the critical quark mass. An implicit assumption we make here is the presence of a phase where flavor and parity is spontaneously broken [14].

[3] The $O(a^3)$ term is unproblematic since the arguments we gave for the $O(a^4)$ contribution also apply for the $O(a^3)$ term.

[4] Strictly speaking this only holds if the chiral Lagrangian is parameterized in terms of renormalized quark masses which absorb some of the $O(a)$ cutoff effects. Particular terms linear in a will appear if other choices are used (see Sec. III C).

$$L_{\mathrm{LO}} = \frac{f^2}{4}\langle \partial_\mu \Sigma \partial_\mu \Sigma^\dagger \rangle - \frac{f^2 B}{2}\langle M_q \Sigma + \Sigma^\dagger M_q \rangle + \frac{f^2}{16}[c_2 \langle \Sigma + \Sigma^\dagger \rangle^2 + \tilde{c}_2 \langle (\Sigma + \Sigma^\dagger)^2 \rangle + c_4 \langle \Sigma - \Sigma^\dagger \rangle^2]$$
$$+ \frac{f^2}{4}[c_0 \langle \Sigma + \Sigma^\dagger - 2 \rangle \langle \partial_\mu \Sigma \partial_\mu \Sigma^\dagger \rangle + \tilde{c}_0 \langle (\Sigma + \Sigma^\dagger - 2)\partial_\mu \Sigma \partial_\mu \Sigma^\dagger \rangle] + \frac{f^2 B}{8}[2c_3 \langle \Sigma + \Sigma^\dagger \rangle \langle M_q \Sigma + \Sigma^\dagger M_q \rangle$$
$$+ \tilde{c}_3 \langle (\Sigma + \Sigma^\dagger)(M_q \Sigma + \Sigma^\dagger M_q) \rangle] + \frac{f^2 B}{8}[2c_5 \langle \Sigma - \Sigma^\dagger \rangle \langle M_q \Sigma - \Sigma^\dagger M_q \rangle + \tilde{c}_5 \langle (\Sigma - \Sigma^\dagger)(M_q \Sigma - \Sigma^\dagger M_q) \rangle], \quad (1)$$

where $\langle X \rangle = \mathrm{tr} X$, f is the pseudoscalar meson decay constant,

$$\Sigma = \exp\left[i \frac{1}{f} \sum_a \pi_a T^a \right], \quad (2)$$

is an element of SU(3) with π_a being the pseudoscalar meson fields. The SU(3) generators T^a are normalized according to $\mathrm{tr} T^a T^b = \frac{1}{2}\delta_{ab}$. The first and the second term in the first line are the standard $\mathrm{O}(p^2)$ and $\mathrm{O}(\tilde{m})$ terms [5], respectively. The second line comprises the $\mathrm{O}(a^2)$ terms [12,13]. The last three lines contain the $\mathrm{O}(p^2 a)$ and $\mathrm{O}(\tilde{m}a)$ contributions [11].

For notational simplicity only we use a different notation for the low-energy constants associated with the nonzero lattice spacing (the c and $\tilde{c}$'s) compared to the notation in Refs. [11–13]. In particular, we have chosen to absorb the explicit powers of the lattice spacing a into the coefficients $c, \tilde{c}$. Consequently, as a function of a these coefficients scale according to

$$c_0, \tilde{c}_0, c_3, \tilde{c}_3, c_5, \tilde{c}_5 = \mathrm{O}(a), \qquad c_2, \tilde{c}_2, c_4 = \mathrm{O}(a^2). \quad (3)$$

The quark mass matrix is given by

$$M_q = \begin{pmatrix} m & 0 & 0 \\ 0 & m & 0 \\ 0 & 0 & m_s \end{pmatrix} = M_0 \mathbf{1} + M_8 T^8,$$
$$M_0 = \frac{2m + m_s}{3}, \qquad M_8 = \frac{2(m - m_s)}{\sqrt{3}}, \quad (4)$$

where isospin symmetry ($m_u = m_d = m$) is assumed. Note that $\mathrm{O}(a)$ contribution is already absorbed in the definition of M_q, so there is no $\mathrm{O}(a)$ term in the chiral Lagrangian. In the $a \longrightarrow 0$ limit, the pseudoscalar meson masses are related to m and m_s according to

$$m_a^2 = \begin{cases} m_\pi^2 = 2Bm, & a = 1, 2, 3, \\ m_K^2 = B(m + m_s), & a = 4, 5, 6, 7, \\ m_\eta^2 = \frac{2B}{3}(m + 2m_s), & a = 8, \end{cases} \quad (5)$$

which, of course, agree with the continuum ChPT result. We also define the average mass

$$m_{\mathrm{av}}^2 = \frac{1}{N^2 - 1} \sum_a m_a^2 = 2B \frac{2m + m_s}{3}, \quad (6)$$

which will be a useful short hand notation in the following.

Note that, except for a π_a independent constant, the term proportional to $\tilde{c}_5$ is identical to the term with $\tilde{c}_3$. Therefore we can set $\tilde{c}_5 = 0$ without loss of generality.

C. Shifted quark mass at leading order

By expanding the LO Lagrangian to second order in π_a, we obtain

$$L^{(2)} = \frac{1}{2} \sum_a [(\partial_\mu \pi_a)^2 + \tilde{m}_a^2 \pi_a^2]. \quad (7)$$

The pseudoscalar meson masses at LO are therefore given by

$$\tilde{m}_a^2 = m_a^2(1 - Nc_3 - \tilde{c}_3) - m_{\mathrm{av}}^2 N c_3 - N c_2 - \tilde{c}_2. \quad (8)$$

In the following we keep the number of flavors N arbitrary, but put $N = 3$ in the final expressions.

We now define *shifted quark masses*, which satisfy

$$\tilde{m}_a^2 = \begin{cases} \tilde{m}_\pi^2 = 2B\tilde{m}, & a = 1, 2, 3, \\ \tilde{m}_K^2 = B(\tilde{m} + \tilde{m}_s), & a = 4, 5, 6, 7, \\ \tilde{m}_\eta^2 = \frac{2B}{3}(\tilde{m} + 2\tilde{m}_s), & a = 8. \end{cases} \quad (9)$$

Explicitly they are given by

$$\tilde{m} = m(1 - Nc_3 - \tilde{c}_3) - \frac{2m + m_s}{3} N c_3 - \frac{N c_2 + \tilde{c}_2}{2B}, \quad (10)$$

$$\tilde{m}_s = m_s(1 - Nc_3 - \tilde{c}_3) - \frac{2m + m_s}{3} N c_3 - \frac{N c_2 + \tilde{c}_2}{2B}. \quad (11)$$

From these expressions the LO critical mass for $N = 3$ is defined by the condition

$$\tilde{m}_{\mathrm{av}}^2 = m_{\mathrm{av}}^2(1 - 6c_3 - \tilde{c}_3) - 3c_2 - \tilde{c}_2 = 0, \quad (12)$$

leading to

$$2Bm_{\mathrm{critical}} = \frac{3c_2 + \tilde{c}_2}{1 - 6c_3 - \tilde{c}_3} \equiv -\delta m_{\mathrm{av}}^2. \quad (13)$$

This definition for the critical quark mass assumes that all three quark masses are extrapolated to the massless point, including the strange quark mass. In numerical spectroscopy calculations, however, a different definition is sometimes employed where the strange quark mass is kept fixed at (approximately) its physical value. For this procedure the condition for the critical quark mass reads

$$\tilde{m}_\pi^2 = m_\pi^2(1 - 3c_3 - \tilde{c}_3) - m_{\rm av}^2 3c_3 - 3c_2 - \tilde{c}_2 = 0, \tag{14}$$

which results in

$$2Bm_{\rm critical}(m_s) = \frac{2Bm_s c_3 + 3c_2 + \tilde{c}_2}{1 - 5c_3 - \tilde{c}_3}. \tag{15}$$

The difference between these two values is therefore

$$m_{\rm critical} - m_{\rm critical}(m_s) = \frac{c_3}{1 - 5c_3 - \tilde{c}_3}\left[\frac{3c_2 + \tilde{c}_2}{1 - 6c_3 - \tilde{c}_3} - 2Bm_s\right]. \tag{16}$$

Indeed, numerical 2 + 1 flavor simulations [18] suggest a nonvanishing value for this difference with

$$m_{\rm critical} - m_{\rm critical}(m_s) > 0. \tag{17}$$

D. NLO Lagrangian

The NLO Lagrangian provides the necessary counter terms in order to remove the UV divergences in the 1-loop integrals. The contribution of $O(\tilde{M}^2)$ is given by

$$\begin{aligned} L_{{\rm NLO},\tilde{M}^2} = {} & L_4\langle\Sigma_{\mu\mu}\rangle\langle\hat{M}_q\Sigma + \Sigma^\dagger\hat{M}_q\rangle \\ & + L_5\langle\Sigma_{\mu\mu}(\hat{M}_q\Sigma + \Sigma^\dagger\hat{M}_q)\rangle \\ & + L_6\langle\hat{M}_q\Sigma + \Sigma^\dagger\hat{M}_q\rangle^2 + L_7\langle\hat{M}_q\Sigma - \Sigma^\dagger\hat{M}_q\rangle^2 \\ & + L_8\langle\hat{M}_q\Sigma\hat{M}_q\Sigma + \Sigma^\dagger\hat{M}_q\Sigma^\dagger\hat{M}_q\rangle, \end{aligned} \tag{18}$$

where we introduced $\Sigma_{\mu\mu} = \partial_\mu\Sigma\partial_\mu\Sigma^\dagger$ and $\hat{M}_q = B\tilde{M}_q$, where $\tilde{M}_q$ is the shifted quark mass matrix constructed from $\tilde{m}$ and $\tilde{m}_s$ (cf. previous section). The NLO constants L_i are related with standard Gasser-Leutwyler coefficients L_i^{GL} [5] as $L_{4,5} = 2L_{4,5}^{GL}$ and $L_{6,7,8} = -4L_{6,7,8}^{GL}$.

The complete Lagrangian at $O(a^2\tilde{M})$ and $O(a\tilde{M}^2)$ is cumbersome and has not been computed so far. Here we only list the terms that contribute to the meson propagators, which we need for the calculation of the pseudoscalar masses. These terms are straightforwardly found by a spurion analysis with spurion fields proportional to the lattice spacing [6,11,13]. Our result for the $O(a^2\tilde{M})$ Lagrangian reads

$$\begin{aligned} L_{{\rm NLO},a^2\tilde{M}} = {} & \langle\Sigma_{\mu\mu}\rangle\left(W_0 + \frac{W_1}{4N^2}\langle\Sigma + \Sigma^\dagger\rangle^2 + \frac{W_2}{2N}\langle\Sigma^2 + (\Sigma^\dagger)^2\rangle\right) + \frac{W_3}{4N}\langle\Sigma_{\mu\mu}(\Sigma + \Sigma^\dagger)\rangle\langle\Sigma + \Sigma^\dagger\rangle \\ & + \frac{W_4}{2}\langle\Sigma_{\mu\mu}(\Sigma^2 + (\Sigma^\dagger)^2)\rangle + W_5\langle\hat{M}_q\Sigma + \Sigma^\dagger\hat{M}_q\rangle + W_6\langle\Sigma + \Sigma^\dagger\rangle^2\langle\hat{M}_q\Sigma + \Sigma^\dagger\hat{M}_q\rangle + W_7\langle\Sigma^2 + (\Sigma^\dagger)^2\rangle \\ & \times\langle\hat{M}_q\Sigma + \Sigma^\dagger\hat{M}_q\rangle + W_8\langle\Sigma + \Sigma^\dagger\rangle\langle\hat{M}_q\Sigma^2 + (\Sigma^\dagger)^2\hat{M}_q\rangle + W_9\langle\hat{M}_q\Sigma^3 + (\Sigma^\dagger)^3\hat{M}_q\rangle + W_{10}\langle\Sigma + \Sigma^\dagger\rangle\langle\hat{M}_q\rangle \\ & + W_{11}\langle(\partial_\mu\Sigma)^2 + (\partial_\mu\Sigma^\dagger)^2\rangle + W_{12}\langle(\partial_\mu\Sigma)^2(\Sigma^\dagger)^2 + \Sigma^2(\partial_\mu\Sigma^\dagger)^2\rangle. \end{aligned} \tag{19}$$

while the terms of $O(a\tilde{M}^2)$ are given by

$$\begin{aligned} L_{{\rm NLO},a\tilde{M}^2} = {} & \langle\Sigma_{\mu\mu}\rangle\left[2V_0\langle\hat{M}_q\rangle + \frac{V_1}{2N}\langle\Sigma + \Sigma^\dagger\rangle\langle\hat{M}_q\Sigma + \Sigma^\dagger\hat{M}_q\rangle + V_2\langle\hat{M}_q\Sigma^2 + (\Sigma^\dagger)^2\hat{M}_q\rangle\right] + \frac{V_3}{2}\langle\Sigma_{\mu\mu}(\Sigma + \Sigma^\dagger)\rangle \\ & \times\langle\hat{M}_q\Sigma + \Sigma^\dagger\hat{M}_q\rangle + \frac{V_4}{2N}\langle\Sigma_{\mu\mu}(\hat{M}_q\Sigma + \Sigma^\dagger\hat{M}_q)\rangle\langle\Sigma + \Sigma^\dagger\rangle + V_5\langle\Sigma_{\mu\mu}(\hat{M}_q\Sigma^2 + (\Sigma^\dagger)^2\hat{M}_q)\rangle \\ & + 2V_6\langle\Sigma_{\mu\mu}\hat{M}_q\rangle + V_{16}\langle(\partial_\mu\Sigma)^2\hat{M}_q + \hat{M}_q(\partial_\mu\Sigma^\dagger)^2\rangle + V_{17}\langle(\partial_\mu\Sigma)^2\Sigma^\dagger\hat{M}_q\Sigma^\dagger + \Sigma\hat{M}_q\Sigma(\partial_\mu\Sigma^\dagger)^2\rangle \\ & + \langle\Sigma + \Sigma^\dagger\rangle[V_7\langle\hat{M}_q^2\rangle + V_8\langle\hat{M}_q\Sigma + \Sigma^\dagger\hat{M}_q\rangle^2 + V_9\langle\hat{M}_q\Sigma\hat{M}_q\Sigma + \Sigma^\dagger\hat{M}_q\Sigma^\dagger\hat{M}_q\rangle] + \langle\hat{M}_q\Sigma + \Sigma^\dagger\hat{M}_q\rangle \\ & \times[V_{10}\langle\hat{M}_q\rangle + V_{11}\langle\hat{M}_q\Sigma^2 + (\Sigma^\dagger)^2\hat{M}_q\rangle] + V_{12}\langle\hat{M}_q^2\Sigma + \Sigma^\dagger\hat{M}_q^2\rangle + V_{13}\langle\hat{M}_q\Sigma\hat{M}_q\Sigma^2 + (\Sigma^\dagger)^2\hat{M}_q\Sigma^\dagger\hat{M}_q\rangle \\ & + V_{14}\langle\Sigma + \Sigma^\dagger\rangle\langle\hat{M}_q\Sigma - \Sigma^\dagger\hat{M}_q\rangle^2 + V_{15}\langle\hat{M}_q\Sigma^2 - (\Sigma^\dagger)^2\hat{M}_q\rangle\langle\hat{M}_q\Sigma - \Sigma^\dagger\hat{M}_q\rangle. \end{aligned} \tag{20}$$

As in the leading order Lagrangian we have absorbed the explicit powers of the lattice spacing in the low-energy constants, and their scaling behavior is therefore

$$W_i = O(a^2), \qquad i = 0\ldots12, \tag{21}$$

$$V_i = O(a), \qquad i = 0\ldots17. \tag{22}$$

III. RESULTS

A. Quark mass dependence of meson masses

The calculation of the pseudoscalar masses from the chiral Lagrangian in the previous section is straightforward. We collect some details and intermediate results of our calculation in the appendix. Here we simply quote the final result for the quark mass and lattice spacing depen-

dence of the pseudoscalar meson masses. The total contribution from LO tree, LO 1-loop plus NLO tree for m_π and m_K and m_η are given as follows:

$$\begin{aligned} m^2_{\pi,\text{total}} &= x + 2y + \frac{1}{f^2}[L^r_\pi\{A^\pi_\pi x + B^\pi_\pi y + 5C\} \\ &+ L^r_K\{A^\pi_K x + B^\pi_K y + 4C\} + L^r_\eta\{A^\pi_\eta x + B^\pi_\eta y + C\} \\ &- \{(C_0 + D_0)x + 2C_0 y + (C_{\text{av}} + D_{\text{av}})x^2 \\ &+ D^\pi_{yy} y^2 + 2Dxy\}], \end{aligned} \tag{23}$$

$$\begin{aligned} m^2_{K,\text{total}} &= x - y + \frac{1}{f^2}[L^r_K\{A^K_K x + B^K_K y + 6C\} \\ &+ L^r_\pi\{A^K_\pi x + B^K_\pi y + 3C\} \\ &+ L^r_\eta\{A^K_\eta x + B^K_\eta y + C\} - \{(C_0 + D_0)x - C_0 y \\ &+ (C_{\text{av}} + D_{\text{av}})x^2 + D^K_{yy} y^2 - Dxy\}], \end{aligned} \tag{24}$$

$$\begin{aligned} m^2_{\eta,\text{total}} &= x - 2y + \frac{1}{f^2}[L^r_\eta\{A^\eta_\eta x + B^\eta_\eta y + 3C\} \\ &+ L^r_\pi\{A^\eta_\pi x + B^\eta_\pi y + 3C\} \\ &+ L^r_K\{A^\eta_K x + B^\eta_K y + 4C\} - \{(C_0 + D_0)x - 2C_0 y \\ &+ (C_{\text{av}} + D_{\text{av}})x^2 + D^\eta_{yy} y^2 - 2Dxy\}]. \end{aligned} \tag{25}$$

The parameters

$$\begin{aligned} x &= \tilde{m}^2_{\text{av}} = \frac{2B}{3}(2\tilde{m} + \tilde{m}_s), \\ y &= \frac{1}{4\sqrt{3}} 2B\tilde{M}_8 = \frac{2B}{6}(\tilde{m} - \tilde{m}_s), \end{aligned} \tag{26}$$

represent the quark mass dependence. The chiral log is denoted by

$$L^r_a = \frac{\tilde{m}^2_a}{16\pi^2} \log(\tilde{m}^2_a), \tag{27}$$

whose coefficients contain

$$C = \frac{1}{6}Z, \qquad A^\pi_\pi = \frac{1}{3}\left(2C^\pi_\pi - \frac{5}{2}X\right), \qquad A^\pi_K = \frac{1}{3}(2C^\pi_K - 2X), \qquad A^\pi_\eta = \frac{1}{3}\left(2C^\pi_\eta - \frac{1}{2}X\right), \qquad B^\pi_\pi = \frac{1}{3}(4C^\pi_\pi - 5Y),$$
$$B^\pi_K = \frac{1}{3}(C^\pi_K - Y), \quad B^\pi_\eta = \frac{1}{3}(12c_5 - Y), \qquad A^K_K = \frac{1}{3}(2C^K_K - 3X), \qquad A^K_\pi = \frac{1}{3}\left(2C^K_\pi - \frac{3}{2}X\right),$$
$$A^K_\eta = \frac{1}{3}\left(2C^K_\eta - \frac{1}{2}X\right), \qquad B^K_K = \frac{1}{3}(-2C^K_K + 3Y), \qquad B^K_\pi = \frac{1}{3}\left(C^K_\pi - \frac{3}{4}Y\right), \qquad B^K_\eta = \frac{1}{3}\left(-3C^K_\eta + \frac{5}{4}Y - 6c_5\right),$$
$$A^\eta_\eta = \frac{1}{3}\left(2C^\eta_\eta - \frac{3}{2}X\right), \qquad A^\eta_\pi = \frac{1}{3}(2C^\eta_\pi - \frac{3}{2}X), \qquad A^\eta_K = \frac{1}{3}(2C^\eta_K - 2X), \qquad B^\eta_\eta = \frac{1}{3}(-4C^\eta_\eta + 5Y - 24c_5),$$
$$B^\eta_\pi = \frac{1}{3}(-3Y + 36c_5), \qquad B^\eta_K = \frac{1}{3}(-3C^\eta_K + 5Y - 24c_5).$$

These terms are parametrized by

$$\begin{aligned} X &= \tilde{A}[1 - 6c_3 - 4\tilde{c}_3 - 36c^2_3\tilde{B}], \\ Y &= (1 - 3c_3 - 4\tilde{c}_3)\tilde{B}, \\ Z &= [9c_2 + 4\tilde{c}_2 + \delta m^2_{\text{av}}(1 - 18c_3 - 4\tilde{c}_3)], \end{aligned} \tag{28}$$

$$\begin{aligned} C^\pi_\pi &= 2 + 18c_0 + 9\tilde{c}_0 + 15c_3\tilde{B}, \\ C^\pi_K &= 1 + 24c_0 + 6\tilde{c}_0 + 12c_3\tilde{B}, \\ C^\pi_\eta &= 6c_0 + \tilde{c}_0 + 3c_3\tilde{B}, \end{aligned} \tag{29}$$

$$\begin{aligned} C^K_K &= \frac{3}{2} + 24c_0 + 9\tilde{c}_0 + 18c_3\tilde{B}, \\ C^K_\pi &= \frac{3}{4} + 18c_0 + \frac{9}{2}\tilde{c}_0 + 9c_3\tilde{B}, \\ C^K_\eta &= \frac{3}{4} + 6c_0 + \frac{5}{2}\tilde{c}_0 + 3c_3\tilde{B}, \end{aligned} \tag{30}$$

$$\begin{aligned} C^\eta_\eta &= 6c_0 + 3\tilde{c}_0 + 9c_3\tilde{B}, \\ C^\eta_\pi &= 18c_0 + 3\tilde{c}_0 + 9c_3\tilde{B}, \\ C^\eta_K &= 3 + 24c_0 + 10\tilde{c}_0 + 12c_3\tilde{B}, \end{aligned} \tag{31}$$

with

$$\begin{aligned} \tilde{A} &= \frac{1}{1 - 2Nc_3 - \tilde{c}_3}, \\ \tilde{B} &= \frac{1}{1 - Nc_3 - \tilde{c}_3}, \\ \delta m^2_{\text{av}} &= -\frac{Nc_2 + \tilde{c}_2}{1 - 2Nc_3 - \tilde{c}_3}. \end{aligned}$$

The polynomial (nonlogarithmic) terms contain

$$
\begin{aligned}
D^{\pi}_{yy} &= 16\tilde{L}_5 + 8(\tilde{L}_8 + \tilde{L}'_8) + 48V_\Delta,\\
D^{K}_{yy} &= 4\tilde{L}_5 + 20\tilde{L}_8 - 16\tilde{L}'_8 + 48V_\Delta,\\
D^{\eta}_{yy} &= 16\tilde{L}_5 + 24\tilde{L}_8 + 24\tilde{L}'_8 + 96\tilde{L}_7 + 48V_\Delta,\\
D &= C_{\rm av} + 4\tilde{L}_5 + 4(\tilde{L}_8 + \tilde{L}'_8),\\
C_{\rm av} &= 4(N\tilde{L}_6 + N\tilde{L}_4 + \tilde{L}_5),\\
D_{\rm av} &= 2(\tilde{L}_8 + \tilde{L}'_8) + V_{\rm av},\\
C_0 &= 4(W_0 + W_1 + W_2 + W_3 + W_4) + 2W_5 + 8N^2W_6\\
&\quad + 4NW_7 + 16NW_8 + 18W_9 - 8(W_{11} + W_{12})\\
&= a^2W_C,\\
D_0 &= N[16(NW_6 + W_7) + 4W_8 + 2W_{10}] = a^2W_D,
\end{aligned}
$$

where

$$
\begin{aligned}
\tilde{L}_4 &= L_4 + V_0 + V_1 + V_2 + V_3 = L_4 + aL^1_4,\\
\tilde{L}_5 &= L_5 + V_4 + V_5 + V_6 - V_{16} - V_{17} = L_5 + aL^1_5,\\
\tilde{L}_6 &= L_6 + 2NV_8 + \frac{1}{4}V_{10} + \frac{5}{2}V_{11} = L_6 + aL^1_6,\\
\tilde{L}_7 &= L_7 + 2NV_{14} + 2V_{15} = L_7 + aL^1_7,\\
\tilde{L}_8 &= L_8 + 2NV_9 + \frac{1}{2}V_{12} + \frac{5}{2}V_{13} = L_8 + aL^{1a}_8,\\
\tilde{L}'_8 &= L_8 + 2NV_9 + 2V_{13} = L_8 + aL^{1b}_8,\\
V_{\rm av} &= N(V_7 + 2V_9 + 4NV_8),\\
V_\Delta &= \frac{1}{2}(V_7 + 2V_9).
\end{aligned}
$$

Even though the NLO parameters have been used to remove the divergent terms from the loop integrals we use the same notation for these coefficients. We finally note that there exists the following constraint among some of the coefficients:

$$
\sum_b A^a_b = \frac{1}{3}[6 + 96c_0 + 32\tilde{c}_0 + 60c_3B - 5X]. \tag{32}
$$

Consequently, in the limit $y \to 0$ we obtain identical results for m_π, m_K or m_η, as it should be for three degenerate quark masses.

Obviously the final results for the pseudoscalar masses are fairly lengthy. From a practical point of view the number of independent unknown parameters in these expressions is crucial for their usefulness. Unknown parameters are the critical quark mass $m_{\rm critical}$, the constant $2B$ and the decay constant f. The coefficients of the chiral log terms, given in Eq. (29)–(32), are defined through five independent O(a) parameters, c_0, $\tilde{c}_0$, c_3, $\tilde{c}_3$, and c_5, and the coefficient C, which is an independent O(a^2) parameter. In the analytic NLO correction we find the independent combinations $C_{\rm av} + D_{\rm av}$, D^{π}_{yy}, D^{K}_{yy}, D^{η}_{yy}, and D, which start at O(1), and the two coefficients C_0, D_0 are of O(a^2). Therefore, the total number of independent parameters is 13 besides $m_{\rm critical}$, $2B$, and f.

B. O($\tilde{M}a$) term at NLO

In Eqs. (24)–(26), O($\tilde{M}a$) terms are considered at LO. In this subsection we present the results for the case that these terms are treated as NLO corrections. First of all, the expressions for the shifted quark masses simplify to

$$
\tilde{m} = m - \frac{Nc_2 + \tilde{c}_2}{2B} = m - m_{\rm critical}, \tag{33}
$$

$$
\tilde{m}_s = m_s - \frac{Nc_2 + \tilde{c}_2}{2B} = m_s - m_{\rm critical}. \tag{34}
$$

The quark mass dependence of the pseudoscalar meson masses becomes

$$
\begin{aligned}
m^2_{\pi,\rm total} &= (x + 2y)[1 - Nc_3 - \tilde{c}_3] - xNc_3\\
&\quad + \frac{1}{f^2}\Big[L^r_\pi\Big\{\frac{1}{2}x + y + 5C\Big\} + L^r_K 4C\\
&\quad + L^r_\eta\Big\{\frac{1}{2}x - \frac{1}{3}y + C\Big\} - \{(C_0 + D_0)x + 2C_0y\\
&\quad + (C_{\rm av} + D_{\rm av})x^2 + D^{\pi}_{yy}y^2 + 2Dxy\}\Big],
\end{aligned} \tag{35}
$$

$$
\begin{aligned}
m^2_{K,\rm total} &= (x - y)[1 - Nc_3 - \tilde{c}_3] - xNc_3\\
&\quad + \frac{1}{f^2}\Big[L^r_K 6C + L^r_\pi\Big\{-\frac{1}{4}x + 3C\Big\}\\
&\quad + L^r_\eta\Big\{\frac{1}{3}(x - y) + C\Big\} - \Big\{(C_0 + D_0)x - C_0y\\
&\quad + (C_{\rm av} + D_{\rm av})x^2 + D^{K}_{yy}y^2 - Dxy\Big\}\Big],
\end{aligned} \tag{36}
$$

$$
\begin{aligned}
m^2_{\eta,\rm total} &= (x - 2y)[1 - Nc_3 - \tilde{c}_3] - xNc_3\\
&\quad + \frac{1}{f^2}\Big[L^r_\eta\Big\{-\frac{1}{2}x + \frac{5}{3}y + 3C\Big\}\\
&\quad + L^r_\pi\Big\{-\frac{1}{2}x - y + 3C\Big\} + L^r_K\Big\{\frac{4}{3}(x - y) + 4C\Big\}\\
&\quad - \{(C_0 + D_0)x - 2C_0y + (C_{\rm av} + D_{\rm av})x^2\\
&\quad + D^{\eta}_{yy}y^2 - 2Dxy\}\Big],
\end{aligned} \tag{37}
$$

where

$$C = \frac{Z}{6} = \frac{(9-N)c_2 + 3\tilde{c}_2}{6},$$
$$D^{\pi}_{yy} = 16L_5 + 16L_8 = 4D^{K}_{yy},$$
$$D^{\eta}_{yy} = 16L_5 + 48L_8 + 96L_7,$$
$$D = C_{\rm av} + 4L_5 + 8L_8,$$
$$C_{\rm av} = 4(NL_6 + NL_4 + L_5),$$
$$D_{\rm av} = 4L_8,$$
$$C_0 = 4(W_0 + W_1 + W_2 + W_3 + W_4) + 2W_5 + 8N^2W_6 + 4NW_7 + 16NW_8 + 18W_9 - 8(W_{11} + W_{12}) = a^2 W_C,$$
$$D_0 = N[16(NW_6 + W_7) + 4W_8 + 2W_{10}] = a^2 W_D.$$

The number of independent parameters is reduced compared to the result given in the previous section. Besides $m_{\rm critical}$, $2B$ and f there are c_3, $\tilde{c}_3$, C, $L_4 + L_6$, $L_5 + L_8$ (note that $C_{\rm av} + D_{\rm av}$, D^{π}_{yy}, D^{K}_{yy}, and D can be expressed by $L_4 + L_6$ and $L_5 + L_8$.) and D^{η}_{yy}. The total number of independent parameters besides $m_{\rm critical}$, $2B$, and f is reduced from 13 to 6.

However, for improved theories there is some lattice spacing dependence implicit in the definition of the renormalized quark mass. This results in 3 parameters ($b_B + b^{(2)}_m$, $b^{(1)}_m$, $b^{(3)}_m$), as we will show in the next subsection, where we discuss O(a) improved theories.

C. Formula in O(a) improved theories

We finally consider the case that a nonperturbatively O(a) improved quark action (i.e. the clover quark action) is used in the lattice simulations [15–17,19,20]. In this case there are no on-shell O(a) terms in the Symanzik's effective theory provided that the relevant improvement coefficients are tuned nonperturbatively to an appropriate value. In particular, O(a) improvement requires that some a dependence is absorbed in the definition of renormalized masses and the gauge coupling:

$$m \to m + b^{(1)}_m m^2 a + b^{(2)}_m (2m + m_s) m a + b^{(3)}_m (2m^2 + m_s^2) a, \tag{38}$$

$$m_s \to m_s + b^{(1)}_m m_s^2 a + b^{(2)}_m (2m + m_s) m_s a + b^{(3)}_m (2m^2 + m_s^2) a, \tag{39}$$

$$g_0^2 \to g_0^2 \left(1 + b_g \frac{(2m + m_s)a}{3}\right), \tag{40}$$

where b_g and $b_m = b^{(1)}_m + 3(b^{(2)}_m + b^{(3)}_m)$ are improvement coefficients defined in Ref. [19,20]. Therefore, as long as on-shell quantities are considered, there are no terms of O(a), O($\tilde{M}a$), O($\tilde{M}^2 a$) etc. in the WChPT Lagrangian, if we replace

$$\tilde{m} \to \bar{m} = \tilde{m} + b^{(1)}_m \tilde{m}^2 a + b^{(2)}_m (2\tilde{m} + \tilde{m}_s)\tilde{m} a + b^{(3)}_m (2\tilde{m}^2 + \tilde{m}_s^2) a, \tag{41}$$

$$\tilde{m}_s \to \bar{m}_s = \tilde{m}_s + b^{(1)}_m \tilde{m}_s^2 a + b^{(2)}_m (2\tilde{m} + \tilde{m}_s)\tilde{m}_s a + b^{(3)}_m (2\tilde{m}^2 + \tilde{m}_s^2) a, \tag{42}$$

$$B \to \bar{B} = B[1 + b_B(2\tilde{m} + \tilde{m}_s)a]. \tag{43}$$

Here the last modification comes from the mass dependence of g_0^2 in the Symanzik's effective theory.

We emphasize that there are no terms linear in a in the chiral Lagrangian and in the results for the pseudoscalar masses as long as one parameterizes it in terms of $\bar{m}$, which absorbs some O(a) dependence through proper renormalization. Using $\bar{m}$ instead, which is simpler in practice since this mass is directly proportional to the difference between the bare and the critical quark mass, there is some O(a) dependence left explicit.

Having made these remarks we can write down the WChPT expressions for nonperturbatively O(a) improved theories:

$$m^2_{\pi,\rm total} = \bar{x} + 2\bar{y} + \frac{1}{f^2}\Big[L^r_\pi \Big\{\frac{1}{2}x + y + 5C\Big\} + L^r_K 4C + L^r_\eta \Big\{\frac{1}{2}x - \frac{1}{3}y + C\Big\} - \Big\{(C_0 + D_0)x + 2C_0 y + (C_{\rm av} + D_{\rm av})x^2 + D^{\pi}_{yy} y^2 + 2Dxy\Big\}\Big], \tag{44}$$

$$m^2_{K,\rm total} = \bar{x} - \bar{y} + \frac{1}{f^2}\Big[L^r_K 6C + L^r_\pi \Big\{-\frac{1}{4}x + 3C\Big\} + L^r_\eta \Big\{\frac{1}{3}(x - y) + C\Big\} - \{(C_0 + D_0)x - C_0 y + (C_{\rm av} + D_{\rm av})x^2 + D^{K}_{yy} y^2 - Dxy\}\Big], \tag{45}$$

$$m^2_{\eta,\rm total} = \bar{x} - 2\bar{y} + \frac{1}{f^2}\Big[L^r_\eta \Big\{-\frac{1}{2}x + \frac{5}{3}y + 3C\Big\} + L^r_\pi \Big\{-\frac{1}{2}x - y + 3C\Big\} + L^r_K \Big\{\frac{4}{3}(x - y) + 4C\Big\} - \Big\{(C_0 + D_0)x - 2C_0 y + (C_{\rm av} + D_{\rm av})x^2 + D^{\eta}_{yy} y^2 - 2Dxy\Big\}\Big], \tag{46}$$

where

$$\bar{x} = \frac{2\bar{B}}{3}(2\bar{m} + \bar{m}_s) = x[1 + (b_B + b^{(2)}_m)(2\tilde{m} + \tilde{m}_s)a] + (b^{(1)}_m + 3b^{(3)}_m)(2\tilde{m}^2 + \tilde{m}_s^2)a, \tag{47}$$

$$\bar{y} = \frac{2\bar{B}}{6}(\bar{m} - \bar{m}_s) = y[1 + (b_B + b_m^{(2)})(2\tilde{m} + \tilde{m}_s)a + b_m^{(1)}(\tilde{m} + \tilde{m}_s)a], \quad (48)$$

and

$$C = \frac{Z}{6} = \frac{(9-N)c_2 + 3\tilde{c}_2}{6},$$
$$D_{yy}^{\pi} = 16L_5 + 16L_8 = 4D_{yy}^{K},$$
$$D_{yy}^{\eta} = 16L_5 + 48L_8 + 96L_7,$$
$$D = C_{\mathrm{av}} + 4L_5 + 8L_8,$$
$$C_{\mathrm{av}} = 4(NL_6 + NL_4 + L_5),$$
$$D_{\mathrm{av}} = 4L_8,$$
$$C_0 = 4(W_0 + W_1 + W_2 + W_3 + W_4) + 2W_5 + 8N^2W_6 + 4NW_7 + 16NW_8 + 18W_9 - 8(W_{11} + W_{12}) = a^2W_C,$$
$$D_0 = N[16(NW_6 + W_7) + 4W_8 + 2W_{10}] = a^2W_D.$$

Independent parameters (besides m_{critical}, $2B$, and f) are $b_B + b_m^{(2)}$, $b_m^{(1)}$, $b_m^{(3)}$, C, $L_4 + L_6$, $L_5 + L_8$, and D_{yy}^{η}. The number of independent parameters besides m_{critical}, $2B$ and f is therefore 7, reduced from previously found 13.

IV. CONCLUDING REMARKS

In this paper we computed the pseudoscalar masses in 2 + 1 flavor WChPT. We presented results for three different order countings, appropriate for various sizes of the $\mathrm{O}(a\tilde{M})$ term in the chiral Lagrangian. Depending on the lattice action used in the numerical simulation (unimproved, perturbatively improved, nonperturbatively improved) one has to choose one result for the chiral extrapolation. Since we have no prior knowledge about the size of the $\mathrm{O}(a\tilde{M})$ contribution we suggest to perform fits to the data with all three forms and let the data decide which form is most appropriate.

The number of unknown fit parameters is significantly larger than in 2 flavor WChPT. Using our results requires sufficiently enough data points in order to perform the chiral fits. The CP-PACS/JLQCD Collaboration is currently performing 2 + 1 flavor simulations at three lattice spacings with five values for the light up and down quark mass and two different strange quark masses. At least for these simulations the number of data points exceeds the number of unknown fit parameters. Performing the chiral extrapolation of the CP-PACS/JLQCD data using our results is work in progress.

ACKNOWLEDGMENTS

This work is supported in part by the Grants-in-Aid for Scientific Research from the Ministry of Education, Culture, Sports, Science, and Technology (Nos. 13135204, 15204015, 15540251, 16028201, 16.11968). O. B. is supported in part by the University of Tsukuba Research Project. S. T. is supported by research grants of the Japan Society for the Promotion of Science for Young Scientists.

APPENDIX A: USEFUL FORMULAE

1. Expansions in terms of π

In this subsection we collect some useful formulae necessary for the expansion of the chiral Lagrangian in terms of the π fields.

a. LO terms

At LO we have to expand terms at $\mathrm{O}(\pi^4)$.

$$\langle \partial_\mu \Sigma \partial_\mu \Sigma^\dagger \rangle = \frac{4}{f^2}\langle \partial_\mu \pi \partial_\mu \pi \rangle + \frac{8}{3f^4}\langle \partial_\mu \pi [\pi, \partial_\mu \pi]\pi \rangle, \qquad \langle M\Sigma + \Sigma^\dagger M \rangle = \langle 2M \rangle - \frac{4}{f^2}\langle M\pi^2 \rangle + \frac{4}{3f^4}\langle M\pi^4 \rangle,$$
$$\langle \Sigma + \Sigma^\dagger \rangle = \langle 2 \rangle - \frac{4}{f^2}\langle \pi^2 \rangle + \frac{4}{3f^4}\langle \pi^4 \rangle, \qquad \langle \Sigma + \Sigma^\dagger \rangle^2 = \langle 2 \rangle^2 - \frac{8}{f^2}\langle 2 \rangle\langle \pi^2 \rangle + \frac{8}{3f^4}\langle 2 \rangle\langle \pi^4 \rangle + \frac{16}{f^4}\langle \pi^2 \rangle^2,$$
$$\langle (\Sigma + \Sigma^\dagger)^2 \rangle = \langle 4 \rangle - \frac{16}{f^2}\langle \pi^2 \rangle + \frac{64}{3f^4}\langle \pi^4 \rangle, \qquad \langle \Sigma + \Sigma^\dagger - 2 \rangle\langle \partial_\mu \Sigma \partial_\mu \Sigma^\dagger \rangle = -\frac{16}{f^4}\langle \pi^2 \rangle\langle \partial_\mu \pi \partial_\mu \pi \rangle,$$
$$\langle (\Sigma + \Sigma^\dagger - 2)\partial_\mu \Sigma \partial_\mu \Sigma^\dagger \rangle = -\frac{16}{f^4}\langle \pi^2 \partial_\mu \pi \partial_\mu \pi \rangle,$$
$$\langle \Sigma + \Sigma^\dagger \rangle\langle M\Sigma + \Sigma^\dagger M \rangle = \langle 2 \rangle\langle 2M \rangle - \frac{8}{f^2}\langle M \rangle\langle \pi^2 \rangle - \frac{8}{f^2}\langle 1 \rangle\langle M\pi^2 \rangle + \frac{16}{f^4}\langle \pi^2 \rangle\langle M\pi^2 \rangle + \frac{8}{3f^4}\langle M \rangle\langle \pi^4 \rangle + \frac{8}{3f^4}\langle 1 \rangle\langle M\pi^4 \rangle,$$
$$\langle (\Sigma + \Sigma^\dagger)(M\Sigma + \Sigma^\dagger M) \rangle = \langle 4M \rangle - \frac{16}{f^2}\langle M\pi^2 \rangle + \frac{64}{3f^4}\langle M\pi^4 \rangle, \qquad \langle \Sigma - \Sigma^\dagger \rangle^2 = 0,$$
$$\langle (\Sigma - \Sigma^\dagger)^2 \rangle = -\frac{16}{f^2}\langle \pi^2 \rangle + \frac{64}{3f^4}\langle \pi^4 \rangle, \qquad \langle \Sigma - \Sigma^\dagger \rangle\langle M\Sigma - \Sigma^\dagger M \rangle = \frac{32}{3f^4}\langle \pi^3 \rangle\langle M\pi \rangle,$$
$$\langle (\Sigma - \Sigma^\dagger)(M\Sigma - \Sigma^\dagger M) \rangle = -\frac{16}{f^2}\langle M\pi^2 \rangle + \frac{64}{3f^4}\langle M\pi^4 \rangle.$$

b. NLO terms

We have to expand the NLO terms to $O(\pi^2)$.

$$\langle \Sigma_{\mu\mu}\rangle\langle M\Sigma + \Sigma^\dagger M\rangle = \frac{4}{f^2}\langle \partial_\mu \pi \partial_\mu \pi\rangle\langle 2M\rangle, \quad \langle \Sigma_{\mu\mu}(M\Sigma + \Sigma^\dagger M)\rangle = \frac{4}{f^2}\langle \partial_\mu \pi \partial_\mu \pi 2M\rangle,$$

$$\langle M\Sigma + \Sigma^\dagger M\rangle^2 = \langle 2M\rangle^2 - \frac{8}{f^2}\langle 2M\rangle\langle M\pi^2\rangle, \quad \langle M\Sigma - \Sigma^\dagger M\rangle^2 = -\frac{16}{f^2}\langle M\pi\rangle^2,$$

$$\langle M\Sigma M\Sigma + \Sigma^\dagger M\Sigma^\dagger M\rangle = -\frac{8}{f^2}\langle M\pi M\pi + M^2\pi^2\rangle, \quad \langle \Sigma^2 + (\Sigma^\dagger)^2\rangle = \langle 2\rangle - \frac{16}{f^2}\langle \pi^2\rangle,$$

$$\langle M\Sigma^2 + (\Sigma^\dagger)^2 M\rangle = \langle 2M\rangle - \frac{16}{f^2}\langle M\pi^2\rangle, \quad \langle M\Sigma^3 + (\Sigma^\dagger)^3 M\rangle = \langle 2M\rangle - \frac{36}{f^2}\langle M\pi^2\rangle,$$

$$\langle M^2\Sigma + \Sigma^\dagger M^2\rangle = \langle 2M^2\rangle - \frac{4}{f^2}\langle M^2\pi^2\rangle, \quad \langle M\Sigma M\Sigma^2 + (\Sigma^\dagger)^2 M\Sigma^\dagger M\rangle = \langle 2M^2\rangle - \frac{4}{f^2}\langle 4M\pi M\pi + 5M^2\pi^2\rangle,$$

$$\langle M\Sigma - \Sigma^\dagger M\rangle = \frac{4i}{f}\langle M\pi\rangle, \quad \langle M\Sigma^2 - (\Sigma^\dagger)^2 M\rangle = \frac{8i}{f}\langle M\pi\rangle,$$

$$\langle (\partial_\mu \Sigma)^2 + (\partial_\mu \Sigma^\dagger)^2\rangle = \langle (\partial_\mu \Sigma)^2(\Sigma^\dagger)^2 + \Sigma^2(\partial_\mu \Sigma^\dagger)^2\rangle = -\frac{8}{f^2}\langle \partial_\mu \pi \partial_\mu \pi\rangle.$$

2. Formula for traces

After expanding the Lagrangian in terms of the π fields, we have to take the trace in the flavor space.

a. LO terms

$$\langle 1\rangle = N, \quad \langle M_q\rangle = NM_0, \quad \langle \pi^2\rangle = \frac{1}{2}\sum_a \pi_a^2, \quad 2B\langle M_q\pi^2\rangle = \frac{1}{2}\sum_a m_a^2\pi_a^2,$$

$$m_a^2 = \begin{cases} m_\pi^2 = 2Bm, & a = 1,2,3, \\ m_K^2 = B(m+m_s), & a = 4,5,6,7, \\ m_\eta^2 = \frac{2B}{3}(m+2m_s), & a = 8, \end{cases} \qquad 2B\langle M_q\pi^4\rangle = \sum_{a,b,c,d} F^{abcd}\pi_a\pi_b\pi_c\pi_d,$$

$$\langle \pi^4\rangle = \frac{1}{4N}\sum_{a,b}\pi_a^2\pi_b^2 + \frac{1}{8}\sum_{a\sim e} d^{abe}d^{cde}\pi_a\pi_b\pi_c\pi_d,$$

$$4F^{abcd} = \frac{2BM_0}{2}\left\{\frac{2}{N}\delta^{ab}\delta^{cd} + \sum_e d^{abe}d^{cde}\right\} + \frac{2BM_8}{4}\left\{\frac{2}{N}(\delta^{ab}d^{cd8} + d^{ab8}\delta^{cd}) + \sum_e d^{ee8}d^{abe}d^{cde}\right\},$$

$$\langle \partial_\mu \pi \partial_\mu \pi\rangle = \frac{1}{2}\sum_a \partial_\mu \pi_a \partial_\mu \pi_a, \quad \langle \pi^2 \partial_\mu \pi \partial_\mu \pi\rangle = \frac{1}{4N}\sum_{a,b}\pi_a^2 \partial_\mu \pi_b \partial_\mu \pi_b + \frac{1}{8}\sum_{a\sim e} d^{abe}d^{cde}\pi_a\pi_b\partial_\mu \pi_c \partial_\mu \pi_d,$$

$$\langle \partial_\mu \pi[\pi, \partial_\mu \pi]\pi\rangle = -\frac{1}{4}\sum_{a\sim e} f^{abe}f^{cde}\partial_\mu \pi_a\pi_b\partial_\mu \pi_c\pi_d, \quad \langle \pi^3\rangle = \frac{1}{4}\sum_{a,b,c} d^{abc}\pi_a\pi_b\pi_c, \quad 2B\langle M_q\pi\rangle = \frac{1}{2}2BM_8\pi_8.$$

b. NLO terms

$$\langle 2B\tilde{M}_q\rangle = N\tilde{m}_{\rm av}^2, \qquad \langle \pi^2\rangle = \frac{1}{2}\sum_a \pi_a^2, \qquad \langle 2B\tilde{M}_q\rangle^2 = N^2(\tilde{m}_{\rm av}^2)^2,$$

$$\langle (\partial_\mu \pi)^2 2B\tilde{M}_q\rangle = \tilde{m}_{\rm av}^2 \frac{1}{2}\sum_a (\partial_\mu \pi_a)^2 + \Delta\tilde{m}^2 \frac{1}{4}\sum_a d^{aa8}(\partial_\mu \pi_a)^2, \qquad \langle (2B\tilde{M}_q)^2\rangle = N(\tilde{m}_{\rm av}^2)^2 + \frac{1}{2}(\Delta\tilde{m}^2)^2,$$

$$\langle 2B\tilde{M}_q \pi^2\rangle = \frac{1}{2}\sum_a \tilde{m}_a^2 \pi_a^2, \qquad \langle 2B\tilde{M}_q \pi\rangle^2 = \frac{1}{4}(\Delta\tilde{m}^2)^2 \pi_8^2,$$

$$2\langle (2B\tilde{M}_q \pi)^2\rangle = (\tilde{m}_{\rm av}^2)^2 \sum_a \pi_a^2 + \tilde{m}_{\rm av}^2 \Delta\tilde{m}^2 \sum_a d^{aa8}\pi_a^2 + \frac{(\Delta\tilde{m}^2)^2}{4}\left[\frac{2}{N}\pi_8^2 + \sum_a \left\{(d^{aa8})^2 - \sum_b (f^{ab8})^2\right\}\pi_a^2\right],$$

$$\langle (2B\tilde{M}_q)^2 \pi^2\rangle = \frac{1}{2}(\tilde{m}_{\rm av}^2)^2 \sum_a \pi_a^2 + \frac{1}{2}\tilde{m}_{\rm av}^2 \Delta\tilde{m}^2 \sum_a d^{aa8}\pi_a^2 + (\Delta\tilde{m}^2)^2 \sum_a \left\{\frac{1}{4N} - \frac{1}{8\sqrt{3}} d^{aa8}\right\}\pi_a^2.$$

3. Group factors

We have to calculate some Lie group factors.

$$C^{ab} \equiv \sum_c f^{abc} f^{abc} = (1-\delta^{ab})C^{AB} = C^{ba}, \qquad C^{\pi\pi} = C^{K_1K_1} = C^{K_2K_2} = 1,$$
$$C^{\pi K} = C^{K_1K_2} = 1/4, \qquad C^{\pi\eta} = 0, \qquad C^{K\eta} = 3/4,$$

where π represents $a = 1, 2, 3$, K represents $a = 4, 5$ (K_1) and $a = 6, 7$ (K_2) and η represents $a = 8$.

$$D^{ab} \equiv \sum_c d^{aac} d^{bbc} = d^{aa3} d^{bb3} + d^{aa8} d^{bb8} = D^{ba}, \qquad D^{\pi\pi} = D^{K_1K_1} = D^{K_2K_2} = D^{\eta\eta} = 1/3,$$
$$D^{\pi K} = D^{K_1K_2} = -1/6, \qquad D^{\pi\eta} = -1/3, \qquad D^{K\eta} = 1/6.$$

$$E^{ab} \equiv \sum_c d^{cc8} d^{aac} d^{bbc} = \frac{1}{\sqrt{3}}[d^{aa3} d^{bb3} - d^{aa8} d^{bb8}] = E^{ba}, \qquad E^{\pi\pi} = E^{K_1K_2} = E^{\eta\eta} = -\frac{1}{3\sqrt{3}},$$
$$E^{\pi K} = E^{K_1K_1} = E^{K_2K_2} = \frac{1}{6\sqrt{3}}, \qquad E^{\pi\eta} = \frac{1}{3\sqrt{3}}, \qquad E^{K\eta} = -\frac{1}{6\sqrt{3}}.$$

$$\tilde{E}^{ab} \equiv \sum_c d^{cc8} d^{abc} d^{abc} = \tilde{E}^{ba}, \qquad \tilde{E}^{aa} = \frac{1}{\sqrt{3}}\begin{cases} -1/3 & \text{for } \pi, \\ 1/6 & \text{for } K, \\ -1/3 & \text{for } \eta, \end{cases} \qquad \tilde{E}^{\pi K} = -\frac{1}{8\sqrt{3}}, \qquad \tilde{E}^{\pi\eta} = \frac{1}{3\sqrt{3}},$$
$$\tilde{E}^{K_1K_2} = \frac{1}{4\sqrt{3}}, \qquad \tilde{E}^{K\eta} = -\frac{1}{24\sqrt{3}}, \qquad \text{others} = 0.$$

With these definition we have

$$4F^{aabb} = 2BM_0\left\{\frac{1}{N} + \frac{1}{2}D^{ab}\right\} + 2BM_8\left\{\frac{1}{2N}(d^{aa8} + d^{bb8}) + \frac{1}{4}E^{ab}\right\},$$
$$4F^{abab} = 2BM_0\left\{\frac{1}{N}\delta^{ab} + \frac{1}{2}\tilde{D}^{ab}\right\} + 2BM_8\left\{\frac{1}{N}\delta^{ab} d^{aa8} + \frac{1}{4}\tilde{E}^{ab}\right\}.$$

The following formulae for $N = 3$ are useful.

$$\frac{1}{N}+\frac{1}{2}D^{ab}+\tilde{D}^{ab}=\begin{pmatrix}5/6 & 1/2 & 1/2 & 1/2 & 1/2 & 1/2 & 1/2 & 1/2\\ 1/2 & 1/2 & 1/2 & 5/6 & 1/2 & 1/2 & 1/2 & 1/2\\ 1/2 & 1/2 & 1/2 & 1/2 & 1/2 & 1/2 & 1/2 & 5/6\end{pmatrix},$$

$$\frac{1}{2N}(d^{aa8}+d^{bb8})+\frac{1}{4}E^{ab}+\frac{1}{2}\tilde{E}^{ab}=\frac{1}{4\sqrt{3}}\begin{pmatrix}1/3 & 1 & 1 & 1/4 & 1/4 & 1/4 & 1/4 & 1\\ 1/4 & 1/4 & 1/4 & -1/6 & -1/2 & -1/2 & -1/2 & -5/4\\ 1 & 1 & 1 & -5/4 & -5/4 & -5/4 & -5/4 & -7/3\end{pmatrix},$$

where $a=1,4,8$.

4. 1-loop contractions

The following contraction formula is useful for the calculation of the meson propagators at 1-loop.

$$\langle\partial_\mu\pi[\pi,\partial_\mu\pi]\pi\rangle\to-\frac{1}{4}\sum_{a,b}C^{ab}[(\partial_\mu\pi_a)^2I_0(\tilde{m}_b^2)+\pi_a^2I_1(\tilde{m}_b^2)],\qquad C^{ab}=\sum_c f^{abc}f^{abc},$$

$$I_0(m^2)=-\frac{m^2}{16\pi^2}[\Delta+1-\log m^2],\qquad \Delta=\frac{2}{\epsilon}-\gamma+\log(4\pi),\qquad I_1(m^2)=-m^2I_0(m^2),$$

$$\langle 2BM\pi^4\rangle\to\sum_{a,b}\pi_a^2 2I_0(\tilde{m}_b^2)[F^{aabb}+2F^{abab}],\qquad \langle\pi^4\rangle\to\sum_{a,b}\pi_a^2I_0(\tilde{m}_b^2)\left[\frac{1}{2N}(1+2\delta_{ab})+\frac{1}{4}\sum_e(d^{aae}d^{bbe}+2d^{abe}d^{abe})\right],$$

$$\langle\pi^2\rangle^2\to\frac{1}{2}\sum_{a,b}\pi_a^2I_0(\tilde{m}_b^2)(1+2\delta_{ab}),\qquad \langle\pi^2\rangle\langle 2BM\pi^2\rangle\to\frac{1}{4}\sum_{a,b}\pi_a^2I_0(\tilde{m}_b^2)(m_a^2+m_b^2)(1+2\delta_{ab}),$$

$$\langle\pi^2\rangle\langle(\partial_\mu\pi)^2\rangle\to\frac{1}{4}\sum_{a,b}[(\partial_\mu\pi_a)^2I_0(\tilde{m}_b^2)+\pi_a^2I_1(\tilde{m}_b^2)],$$

$$\langle\pi^2(\partial_\mu\pi)^2\rangle\to\sum_{a,b}[(\partial_\mu\pi_a)^2I_0(\tilde{m}_b^2)+\pi_a^2I_1(\tilde{m}_b^2)]\left(\frac{1}{4N}+\frac{1}{8}\sum_e d^{aac}d^{bbc}\right),$$

$$\langle\pi^3\rangle\langle 2BM\pi\rangle\to\frac{3}{8}2BM_8d^{aa8}[I_0(\tilde{m}_a^2)\pi_8^2+I_0(\tilde{m}_8^2)\pi_a^2].$$

APPENDIX B: CALCULATION OF THE PSEUDOSCALAR MESON PROPAGATOR AT 1-LOOP

In this appendix we give some details of the calculation of the pseudoscalar meson propagator at 1-loop in the WChPT.

1. Effective action for BG fields

In order to calculate meson masses at 1-loop, we use the background (BG) field method. We first split the π field as

$$\pi=\pi_Q+\pi_G, \tag{B1}$$

where π_Q represents quantum field while π_G is a BG field which satisfies the equation of motion. Inserting this into the chiral effective Lagrangian, we have

$$L_{\rm LO}(\pi)=L_{\rm LO}(\pi_G)+L^{(2)}(\pi_Q)+L^{(4)}(\pi_Q+\pi_G)-L^{(4)}(\pi_G). \tag{B2}$$

Integrating out π_Q we obtain the following formula

$$\begin{aligned}e^{-S_{\rm eff}(\pi_G)}&=\int\mathcal{D}\pi_Q e^{-\int d^4xL_{\rm LO}(\pi)}\\&=e^{-\int d^4xL_{\rm LO}(\pi_G)}\int\mathcal{D}\pi_Q e^{-\int d^4xL^{(2)}(\pi_Q)}\\&\quad\times e^{-\int d^4x(L^{(4)}(\pi_Q+\pi_G)-L^{(4)}(\pi_G))}.\end{aligned} \tag{B3}$$

This leads to

$$\begin{aligned}S_{\rm eff}(\pi_G)&=\int d^4xL_{\rm LO}(\pi_G)\\&\quad-\log\langle e^{-\int d^4x(L^{(4)}(\pi_Q+\pi_G)-L^{(4)}(\pi_G))}\rangle,\end{aligned} \tag{B4}$$

where

$$\langle f(\pi_Q,\pi_G)\rangle=\int\mathcal{D}\pi_Q e^{-\int d^4xL^{(2)}(\pi_Q)}f(\pi_Q,\pi_G). \tag{B5}$$

Expanding $S_{\rm eff}$ in terms of π_G, we obtain

$$S_{\rm eff}(\pi_G) = \text{const.} + S^{(2)}_{\rm eff}(\pi_G) + \sum_{n=3}^{\infty} S^{(n)}_{\rm eff}(\pi_G), \qquad \text{(B6)}$$

where $S^{(n)}_{\rm eff}(\pi_G)$ contains the n-th power of the field π_G. In the calculation of the pseudoscalar masses we are interested in the $n = 2$ case. We write

$$S^{(2)}_{\rm eff}(\pi_G) = \int d^4x L_{\rm LO}(\pi_G) + S^{(2)}_{1-\rm loop}(\pi_G) + \cdots, \qquad \text{(B7)}$$

where $\cdots$ represent the higher loop contributions. We call $S^{(2)}_{1-\rm loop}$ the 1-loop contribution to the meson propagator and write

$$S^{(2)}_{1-\rm loop}(\pi_G) = \int d^4x L^{(2)}_{1-\rm loop}(\pi_G). \qquad \text{(B8)}$$

2. Expansion of the LO Lagrangian

We now expand the LO Lagrangian (1) in terms of the pseudoscalar field π_a. Using the expansion and trace formulae given in Appendix A, we obtain

$$\begin{aligned} L^{(2)} &= \langle(\partial_\mu \pi)^2\rangle + 2B\langle M_q \pi^2\rangle - \frac{c_2}{2}\langle 2\rangle\langle\pi^2\rangle - \tilde{c}_2\langle\pi^2\rangle \\ &\quad - c_3\langle 2BM_q\rangle\langle\pi^2\rangle - c_3\langle 1\rangle 2B\langle M_q\pi^2\rangle - \tilde{c}_3 2B\langle M_q\pi^2\rangle \\ &= \frac{1}{2}\sum_a [(\partial_\mu \pi_a)^2 + \tilde{m}_a^2 \pi_a^2], \end{aligned} \qquad \text{(B9)}$$

at second order in π_a, where the pseudoscalar meson masses at LO are given by

$$\tilde{m}_a^{\,2} = m_a^2(1 - Nc_3 - \tilde{c}_3) - m_{\rm av}^2 Nc_3 - Nc_2 - \tilde{c}_2, \qquad \text{(B10)}$$

$$m_{\rm av}^2 = \frac{1}{N^2-1}\sum_a m_a^2. \qquad \text{(B11)}$$

For $N = 3$ flavors we have

$$m_a^2 = \begin{cases} m_\pi^2 = 2Bm, & a = 1, 2, 3, \\ m_K^2 = B(m + m_s), & a = 4, 5, 6, 7, \\ m_\eta^2 = \frac{2B}{3}(m + 2m_s), & a = 8. \end{cases} \qquad \text{(B12)}$$

$$m_{\rm av}^2 = 2B\frac{2m + m_s}{3},$$

Equation (B9) gives the pseudoscalar meson propagator at LO.

The 4-th order terms in the LO Lagrangian become

$$\begin{aligned} L^{(4)} &= \frac{2}{3f^2}\langle\partial_\mu\pi[\pi, \partial_\mu\pi]\pi\rangle - \frac{1 - Nc_3 - 4\tilde{c}_3}{3f^2} 2B\langle M\pi^4\rangle \\ &\quad + \frac{Nc_2 + 4\tilde{c}_2 + Nc_3 m_{\rm av}^2}{3f^2}\langle\pi^4\rangle + \frac{c_2}{f^2}\langle\pi^2\rangle^2 \\ &\quad + \frac{2c_3}{f^2}\langle\pi^2\rangle\langle 2BM\pi^2\rangle - \frac{4c_0}{f^2}\langle\pi^2\rangle\langle(\partial_\mu\pi)^2\rangle \\ &\quad - \frac{4\tilde{c}_0}{f^2}\langle\pi^2(\partial_\mu\pi)^2\rangle + \frac{4c_5}{3f^2}\langle\pi^3\rangle\langle 2BM\pi\rangle. \end{aligned} \qquad \text{(B13)}$$

There terms give the 4-point interaction vertices of the pseudoscalar mesons.

3. 1-loop contribution to the propagator

Using the formulae in Appendix A, it is now easy to calculate $L^{(2)}_{1-\rm loop}$. Including the tree level contribution we obtain

$$S^{(2)}_{\rm eff}(\pi) = \int d^4x \frac{1}{2}\sum_a Z_a[(\partial_\mu\pi_a)^2 + m_{a,R}^2\pi_a^2]. \qquad \text{(B14)}$$

For the π ($a = 1, 2, 3$), K ($a = 4, 5, 6, 7$), and η ($a = 8$) we find the wave function renormalization as

$$\begin{aligned} Z_\pi &= 1 - \frac{1}{3f^2}[L_\pi\{2 + 9(2c_0 + \tilde{c}_0)\} \\ &\quad + L_K\{1 + 6(4c_0 + \tilde{c}_0)\} + L_\eta(6c_0 + \tilde{c}_0)], \\ Z_K &= 1 - \frac{1}{3f^2}[L_\pi\{3/4 + 9(2c_0 + \tilde{c}_0/2)\} \\ &\quad + L_K\{3/2 + 3(8c_0 + 3\tilde{c}_0)\} \\ &\quad + L_\eta(3/4 + 6c_0 + 5\tilde{c}_0/2)], \\ Z_\eta &= 1 - \frac{1}{3f^2}[L_\pi 3(6c_0 + \tilde{c}_0) + L_K\{3 + 2(12c_0 + 5\tilde{c}_0)\} \\ &\quad + L_\eta 3(2c_0 + \tilde{c}_0)], \end{aligned} \qquad \text{(B15)}$$

where

$$L_\pi = I_0(\tilde{m}_\pi^2), \qquad L_K = I_0(\tilde{m}_K^2), \qquad L_\eta = I_0(\tilde{m}_\eta^2). \qquad \text{(B16)}$$

Similarly we have

$$\begin{aligned} m_{\pi,R}^2 &= \tilde{m}_\pi^2 + \frac{1}{3f^2}\Big[L_\pi\Big\{C_\pi^\pi 2\tilde{m}_\pi^2 - \frac{5}{2}X\tilde{m}_{\rm av}^2 - 5Y\frac{\Delta\tilde{m}^2}{4\sqrt{3}} + \frac{5}{2}Z\Big\} + L_K\Big\{C_K^\pi(\tilde{m}_K^2 + \tilde{m}_\pi^2) - 2X\tilde{m}_{\rm av}^2 - Y\frac{\Delta\tilde{m}^2}{4\sqrt{3}} + 2Z\Big\} \\ &\quad + L_\eta\Big\{C_\eta^\pi(\tilde{m}_\eta^2 + \tilde{m}_\pi^2) - \frac{1}{2}X\tilde{m}_{\rm av}^2 - (Y - 12c_5)\frac{\Delta\tilde{m}^2}{4\sqrt{3}} + \frac{1}{2}Z\Big\}\Big], \end{aligned} \qquad \text{(B17)}$$

$$m^2_{K,R} = \tilde{m}^2_K + \frac{1}{3f^2}\Big[L_K\Big\{C^K_K 2\tilde{m}^2_K - 3X\tilde{m}^2_{\rm av} + 3Y\frac{\Delta\tilde{m}^2}{4\sqrt{3}} + 3Z\Big\} + L_\pi\Big\{C^K_\pi(\tilde{m}^2_\pi + \tilde{m}^2_K) - \frac{3}{2}X\tilde{m}^2_{\rm av} - \frac{3}{4}Y\frac{\Delta\tilde{m}^2}{4\sqrt{3}} + \frac{3}{2}Z\Big\}$$
$$+ L_\eta\Big\{C^K_\eta(\tilde{m}^2_\eta + \tilde{m}^2_K) - \frac{1}{2}X\tilde{m}^2_{\rm av} + \frac{5}{4}\Big(Y - \frac{24}{5}c_5\Big)\frac{\Delta\tilde{m}^2}{4\sqrt{3}} + \frac{1}{2}Z\Big\}\Big], \tag{B18}$$

$$m^2_{\eta,R} = \tilde{m}^2_\eta + \frac{1}{3f^2}\Big[L_\eta\Big\{C^\eta_\eta 2\tilde{m}^2_\eta - \frac{3}{2}X\tilde{m}^2_{\rm av} + 5\Big(Y - \frac{24}{5}c_5\Big)\frac{\Delta\tilde{m}^2}{4\sqrt{3}} + \frac{3}{2}Z\Big\}$$
$$+ L_\pi\Big\{C^\eta_\pi(\tilde{m}^2_\pi + \tilde{m}^2_\eta) - \frac{3}{2}X\tilde{m}^2_{\rm av} - 3(Y - 12c_5)\frac{\Delta\tilde{m}^2}{4\sqrt{3}} + \frac{3}{2}Z\Big\}$$
$$+ L_K\Big\{C^\eta_K(\tilde{m}^2_K + \tilde{m}^2_\eta) - 2X\tilde{m}^2_{\rm av} + 5\Big(Y - \frac{24}{5}c_5\Big)\frac{\Delta\tilde{m}^2}{4\sqrt{3}} + 2Z\Big\}\Big]. \tag{B19}$$

for the pseudoscalar meson mass. The parameters in these expressions have already been given in subsection III A.

4. NLO contribution to meson propagators

Using the formulae for the expansion in powers of the pion field and the trace formulae in the Appendix A, we have

$$L_{\rm NLO} = \frac{1}{2}Z^{\rm NLO}_a[(\partial_\mu\pi_a)^2 + m^2_{a,\rm NLO}\pi^2_a], \tag{B20}$$

where the wave function renormalization factor is given by

$$Z^{\rm NLO}_a = \frac{1}{f^2}[\tilde{m}^2_{\rm av}z_{\rm av} + \Delta\tilde{m}^2 z^a_\Delta + z_0],$$
$$z_{\rm av} = 4(N\tilde{L}_4 + \tilde{L}_5), \qquad z^a_\Delta = 2d^{aa8}\tilde{L}_5,$$
$$z_0 = 4(W_0 + W_1 + W_2 + W_3 + W_4) - 8(W_{11} + W_{12}),$$

and the mass term is defined as

$$m^2_{a,\rm NLO} = -\frac{1}{f^2}[\tilde{m}^2_a\{\tilde{m}^2_{\rm av}C_{\rm av} + \Delta\tilde{m}^2 C^a_\Delta + C_0\}$$
$$+ \tilde{m}^2_{\rm av}\{\tilde{m}^2_{\rm av}D_{\rm av} + \Delta\tilde{m}^2 D^a_\Delta + D_0\} + (\Delta\tilde{m}^2)^2 E^a_\Delta],$$
$$C_{\rm av} = 4(N\tilde{L}_6 + N\tilde{L}_4 + \tilde{L}_5),$$
$$D_{\rm av} = 2(\tilde{L}_8 + \tilde{L}'_8) + V_{\rm av}, \qquad C^a_\Delta = 2d^{aa8}\tilde{L}_5,$$
$$D^a_\Delta = 2d^{aa8}(\tilde{L}_8 + \tilde{L}'_8),$$
$$E^a_\Delta = e_a\tilde{L}_8 + e'_a\tilde{L}'_8 + V_\Delta + \delta_{a8}\Big(2\tilde{L}_7 + \frac{1}{N}\tilde{L}'_8\Big),$$
$$C_0 = 4(W_0 + W_1 + W_2 + W_3 + W_4) + 2W_5$$
$$+ 8N^2W_6 + 4NW_7 + 16NW_8 + 18W_9$$
$$- 8(W_{11} + W_{12}) = a^2W_C,$$
$$D_0 = N[16(NW_6 + W_7) + 4W_8 + 2W_{10}] = a^2W_D. \tag{B21}$$

The constants here are given by

$$\tilde{L}_4 = L_4 + V_0 + V_1 + V_2 + V_3 = L_4 + aL^1_4, \tag{B22}$$

$$\tilde{L}_5 = L_5 + V_4 + V_5 + V_6 - V_{16} - V_{17} = L_5 + aL^1_5, \tag{B23}$$

$$\tilde{L}_6 = L_6 + 2NV_8 + \frac{1}{4}V_{10} + \frac{5}{2}V_{11} = L_6 + aL^1_6, \tag{B24}$$

$$\tilde{L}_7 = L_7 + 2NV_{14} + 2V_{15} = L_7 + aL^1_7, \tag{B25}$$

$$\tilde{L}_8 = L_8 + 2NV_9 + \frac{1}{2}V_{12} + \frac{5}{2}V_{13} = L_8 + aL^{1a}_8, \tag{B26}$$

$$\tilde{L}'_8 = L_8 + 2NV_9 + 2V_{13} = L_8 + aL^{1b}_8, \tag{B27}$$

and

$$V_{\rm av} = N(V_7 + 2V_9 + 4NV_8), \qquad V_\Delta = \frac{1}{2}(V_7 + 2V_9), \tag{B28}$$

$$e_a = \frac{1}{N} - \frac{1}{2\sqrt{3}}d^{aa8}, \qquad (e_\pi, e_K, e_\eta) = \Big(\frac{1}{6}, \frac{5}{12}, \frac{1}{2}\Big), \tag{B29}$$

$$e'_a = \frac{1}{2}[(d^{aa8})^2 - \sum_b (f^{ab8})^2],$$
$$(e'_\pi, e'_K, e'_\eta) = \Big(\frac{1}{6}, -\frac{1}{3}, \frac{1}{6}\Big). \tag{B30}$$

5. Cancellation of UV divergence

In order to perform the renormalization, we consider divergent parts of meson masses in Eq. (B17)–(B19), which are given by

$$[m^2_a]_{\rm div.} = -\frac{\Delta}{48\pi^2 f^2}[C^a_x x + C^a_y y + C^a_{xx}x^2 + C^a_{yy}y^2$$
$$+ C^a_{xy}xy], \tag{B31}$$

where $x = \tilde{m}^2_{\rm av}$ and $y = \frac{1}{4\sqrt{3}}\Delta\tilde{m}^2$, in terms of which, $\tilde{m}^2_\pi = x + 2y$, $\tilde{m}^2_K = x - y$, and $\tilde{m}^2_\eta = x - 2y$. Constants are

given by

$$
\begin{aligned}
&C_x^\pi = C_x^K = C_x^\eta = 5Z, \qquad C_y^\pi = 2Z, \qquad C_y^K = -Z, \qquad C_y^\eta = -2Z,\\
&C_{xx}^a = 2\sum_b C_{ba}^a - 5X = 2(3 + 48c_0 + 16\tilde{c}_0 + 30c_3 B) - 5X,\\
&C_{yy}^\pi = 8C_\pi^\pi - C_K^\pi - 7Y - 24c_5\tilde{B} = 15 + 120c_0 + 66\tilde{c}_0 + \tilde{B}[-7 + 129c_3 + 28\tilde{c}_3 - 24c_5],\\
&C_{yy}^K = 2C_K^K + 2C_\pi^K + 6C_\eta^K - 7Y + 12c_5\tilde{B} = 9 + 120c_0 + 42\tilde{c}_0 + \tilde{B}[-7 + 93c_3 + 28\tilde{c}_3 + 12c_5],\\
&C_{yy}^\eta = 8C_\eta^\eta + 3C_K^\eta - 21Y + 144c_5\tilde{B} = 9 + 120c_0 + 54\tilde{c}_0 + \tilde{B}[-21 + 171c_3 + 84\tilde{c}_3 + 144c_5],\\
&C_{xy}^\pi = 8C_\pi^\pi - C_K^\pi - 4C_\eta^\pi - 2X - 7Y + 12c_5\tilde{B} = 15 + 96c_0 + 62\tilde{c}_0 + 96c_3\tilde{B} - 2X - 7Y + 12c_5\tilde{B},\\
&C_{xy}^K = -4C_K^K + 5C_\pi^K - 7C_\eta^K + X + \frac{7}{2}Y - 6c_5\tilde{B} = -\frac{1}{2}C_{xy}^\pi,\\
&C_{xy}^\eta = -8C_\eta^\eta + 4C_\pi^\eta - 5C_K^\eta + 2X + 7Y - 12c_5\tilde{B} = -C_{xy}^\pi.
\end{aligned}
$$

On the other hand, the NLO contributions lead to

$$
[m_a^2]_{\mathrm{NLO}} = -\frac{1}{f^2}[D_x^a x + D_y^a y + D_{xx}^a x^2 + D_{yy}^a y^2 + D_{xy}^a xy],
$$

where

$$
\begin{aligned}
&D_x^a = C_0 + D_0, \qquad D_y^\pi = 2C_0, \qquad D_y^K = -C_0, \qquad D_y^\eta = -2C_0, \qquad D_{xx}^a = C_{\mathrm{av}} + D_{\mathrm{av}},\\
&D_{yy}^\pi = 16\tilde{L}_5 + 8(\tilde{L}_8 + \tilde{L}_8') + 48V_\Delta, \qquad D_{yy}^K = 4\tilde{L}_5 + 20\tilde{L}_8 - 16\tilde{L}_8' + 48V_\Delta,\\
&D_{yy}^\eta = 16\tilde{L}_5 + 24\tilde{L}_8 + 24\tilde{L}_8' + 96\tilde{L}_7 + 48V_\Delta, \qquad D_{xy}^\pi = 2C_{\mathrm{av}} + 8\tilde{L}_5 + 8(\tilde{L}_8 + \tilde{L}_8') = -2D_{xy}^K = -D_{xy}^\eta.
\end{aligned}
$$

In order to cancel the UV divergences, the divergent part in the NLO terms must be chosen according to

$$
\begin{aligned}
[C_0]_{\mathrm{div.}} &= -\frac{\Delta}{48\pi^2}Z, \qquad [D_0]_{\mathrm{div.}} = -\frac{\Delta}{48\pi^2}4Z,\\
[C_{\mathrm{av}} + D_{\mathrm{av}}]_{\mathrm{div.}} &= -\frac{\Delta}{48\pi^2}[2(3 + 48c_0 + 16\tilde{c}_0 + 30c_3\tilde{B}) - 5X],\\
[16\tilde{L}_5 + 8(\tilde{L}_8 + \tilde{L}_8') + 48V_\Delta]_{\mathrm{div}} &= -\frac{\tilde{\Delta}}{48\pi^2}[15 + 120c_0 + 66\tilde{c}_0 + \tilde{B}(-7 + 129c_3 + 28\tilde{c}_3 - 24c_5)],\\
[4\tilde{L}_5 + 20\tilde{L}_8 - 16\tilde{L}_8' + 48V_\Delta]_{\mathrm{div}} &= -\frac{\tilde{\Delta}}{48\pi^2}[9 + 120c_0 + 42\tilde{c}_0 + \tilde{B}(-7 + 93c_3 + 28\tilde{c}_3 + 12c_5)],\\
[16\tilde{L}_5 + 96\tilde{L}_7 + 24(\tilde{L}_8 + \tilde{L}_8') + 48V_\Delta]_{\mathrm{div}} &= -\frac{\tilde{\Delta}}{48\pi^2}[9 + 120c_0 + 54\tilde{c}_0 + \tilde{B}(-21 + 171c_3 + 84\tilde{c}_3 + 144c_5)],\\
[2C_{\mathrm{av}} + 8\tilde{L}_5 + 8\tilde{L}_8 + 8\tilde{L}_8']_{\mathrm{div.}} &= -\frac{\Delta}{48\pi^2}[15 + 96c_0 + 62\tilde{c}_0 + 96c_3\tilde{B} - 2X - 7Y + 12c_5\tilde{B}].
\end{aligned}
$$

Notice that we can remove all divergences $[m_a^2]_{\mathrm{div.}}$ consistently by these parameters, as it should be.

[1] S. Aoki *et al.*, Phys. Rev. D **67**, 034503 (2003).
[2] A. Ali Khan *et al.*, Phys. Rev. D **65**, 054505 (2002).
[3] T. Ishikawa *et al.*, Nucl. Phys. B, Proc. Suppl. **140**, 225 (2005).
[4] J. Gasser and H. Leutwyler, Ann. Phys. (N.Y.) **158**, 142 (1984).
[5] J. Gasser and H. Leutwyler, Nucl. Phys. **B250**, 465 (1985).
[6] S. R. Sharpe and R. Singleton, Jr., Phys. Rev. D **58**, 074501 (1998).
[7] W.-J. Lee and S. R. Sharpe, Phys. Rev. D **60**, 114503 (1999).
[8] O. Bär, Nucl. Phys. B, Proc. Suppl. **140**, 106 (2005).
[9] S. Aoki, O. Bär, T. Ishikawa, and S. Takeda (to be published).

[10] S. Aoki, O. Bär, T. Ishikawa, and S. Takeda(work in progress).
[11] G. Rupak and N. Shoresh, Phys. Rev. D **66**, 054503 (2002).
[12] S. Aoki, Phys. Rev. D **68**, 054508 (2003).
[13] O. Bär, G. Rupak, and N. Shoresh, Phys. Rev. D **70**, 034508 (2004).
[14] S. Aoki, Phys. Rev. D **30**, 2653 (1984).
[15] K. Symanzik, Nucl. Phys. **B226**, 187 (1983).
[16] K. Symanzik, Nucl. Phys. **B226**, 205 (1983).
[17] B. Sheikholeslami and R. Wohlert, Nucl. Phys. **B259**, 572 (1985).
[18] T. Kaneko *et al.*, Nucl. Phys. B, Proc. Suppl. **129**, 188 (2004).
[19] M. Lüscher, S. Sint, R. Sommer, and P. Weisz, Nucl. Phys. **B478**, 365 (1996).
[20] M. Lüscher *et al.*, Nucl. Phys. **B491**, 323 (1997).

PHYSICAL REVIEW D **73,** 094501 (2006)

Vector meson masses in 2 + 1 flavor Wilson chiral perturbation theory

S. Aoki

Graduate School of Pure and Applied Sciences, University of Tsukuba, Tsukuba, Ibaraki 305-8571, Japan and Riken BNL Research Center, Brookhaven National Laboratory, Upton, New York 11973, USA

O. Bär* and S. Takeda*

Graduate School of Pure and Applied Sciences, University of Tsukuba, Tsukuba, Ibaraki 305-8571, Japan
(Received 17 January 2006; published 8 May 2006)

We calculate the vector meson masses in $N_f = 2 + 1$ Wilson chiral perturbation theory at next-to-leading order. Generalizing the framework of heavy vector meson chiral perturbation theory, the quark mass and the lattice cutoff dependence of the vector meson masses is derived. Our chiral order counting assumes that the lattice cutoff artifacts are of the order of the typical pion momenta, $p \sim a\Lambda_{\mathrm{QCD}}^2$. This counting scheme is consistent with the one in the pseudoscalar meson sector where the $\mathrm{O}(a^2)$ terms are included in the leading order chiral Lagrangian.

DOI: 10.1103/PhysRevD.73.094501 PACS numbers: 12.38.Gc, 11.30.Hv, 11.30.Rd, 12.39.Fe

I. INTRODUCTION

This is the second in a series of papers where we compute a variety of mesonic quantities in 2 + 1 flavor Wilson Chiral Perturbation Theory (Wilson χPT). After having computed the pseudoscalar mesons masses [1] we present here the results for the vector meson masses. The calculation of the pseudoscalar decay constants and the axial vector Ward identity quark mass is in progress [2]. The main goal of this series of papers is to provide the necessary chiral fit forms for unquenched 2 + 1 flavor Lattice QCD simulations with improved Wilson fermions, as they have been currently performed by the CP-PACS/JLQCD collaboration [3].

The quark masses in the CP-PACS/JLQCD simulations are heavier than their physical values. The ratio of the pseudoscalar to vector meson mass is in the range $m_{\mathrm{PS}}/m_V \simeq 0.62$–$0.78$. A chiral extrapolation in the light up and down quark masses is thus required. In order to perform the chiral extrapolation before taking the continuum limit we formulate χPT at nonzero lattice spacing, as originally proposed in Refs. [4,5]. A variety of pseudoscalar quantities has been already computed, mainly for 2 flavor Wilson χPT (see Ref. [6] and references therein). Although the vector meson masses were calculated recently in 2 flavor partially quenched Wilson χPT [7], the result for 2 + 1 flavors was missing.

In this paper we follow the heavy vector meson formalism first introduced by Jenkins *et al.* in Ref. [8]. The generalization to Lattice QCD at nonzero lattice spacing a is straightforward and mirrors the strategy spelled out in Refs. [4,5]. However, since the lattice spacing is an additional expansion parameter the power counting requires some care. Here we adopt a power counting which assumes that lattice cut-off artifacts are of the order of the typical pion momenta, $a\Lambda_{\mathrm{QCD}}^2 \sim p$, as it was assumed in Ref. [9]. Previous results in unquenched 2-flavor simulations [10] seem to indicate that this is the appropriate power counting for describing the lattice results of the CP-PACS/JLQCD collaboration.

There is a price to pay if one wants to perform the chiral extrapolation before taking the continuum limit. The chiral fit forms contain terms proportional to powers of the lattice spacing accompanied by additional unknown low-energy constants. These constants are essentially unconstrained and serve as additional fit parameters. Obviously, the presence of too many of these additional parameters would limit or even spoil the chiral extrapolation. Our one-loop results for the ρ and K^* meson masses contain seven unknown fit parameters compared to three in the corresponding continuum χPT result of Ref. [8]. This number is still small enough for the results to be useful for the chiral extrapolation of the CP-PACS/JLQCD collaboration data.

This paper is organized as follows. In Sec. II, we briefly review the heavy meson formalism, as it was introduced in Ref. [8]. In Sec. III we first summarize the meson and spurion fields which are necessary in our calculation. After discussing the power counting we derive the chiral effective Lagrangian and compute the vector meson masses to one loop. Concluding remarks are given in Sec. IV.

II. HEAVY VECTOR MESON EFFECTIVE THEORY

We adopt the heavy vector meson effective theory to derive the quark mass and lattice spacing dependence of the vector meson masses.[1] This effective theory can deal with vector number conserving decay processes like $V \to V'X$, where V and V' are vector mesons, and X represents a state with one or more low momentum pseudoscalar mesons. On the other hand, it cannot be applied to the process

*Present address: Institut für Physik, Humboldt Universität zu Berlin, Newtonstr. 15, 12489 Berlin, Germany.

[1]This formalism is very similar to heavy baryon chiral perturbation theory [11].

$\rho \to \pi\pi$, for example, since this decay includes hard pions in the final state.

Some physical quantities have been calculated within the continuum formulation of the heavy vector meson effective theory. The first result for the vector meson masses up to $O(p^3)$ can be found in Ref. [8]. The effects of isospin breaking and electromagnetic corrections are included in Ref. [12]. The calculation of the vector meson masses to $O(p^4)$ was done in Ref. [13], while the results for the decay constants are given in Ref. [14]. For results in quenched and partially quenched χPT, see Ref. [15,16], respectively.

Let us briefly review the main idea behind the heavy vector meson formalism. The following argument can be found in Ref. [14]. The vector meson sector introduces a typical energy scale, the vector meson mass m_V. This mass does not vanish in the chiral limit, and it is of about the same size as the chiral symmetry breaking scale, $4\pi f_\pi \sim 1$ GeV. The vector mesons are described by heavy matter fields. In order to obtain the Lagrangian of the effective theory one expands the relativistic Lagrangian in powers of $1/m_V$. The starting point is the free relativistic vector meson Lagrangian,

$$\mathcal{L}_R = -\tfrac{1}{4}V^{\mu\nu}V_{\mu\nu} + \tfrac{1}{2}m_V^2 V^\mu V_\mu, \tag{1}$$

with $V_{\mu\nu} = \partial_\mu V_\nu - \partial_\nu V_\mu$. The relativistic field V_μ is decomposed into two parts, a parallel and a perpendicular component with respect to the 4-velocity v_μ ($v^2 = 1$) of the vector meson,

$$V_\mu = P_{\mu\nu}V^\nu + v_\mu(v \cdot V) = V_{\perp\mu} + v_\mu V_\parallel, \tag{2}$$

where

$$P_{\mu\nu} = g_{\mu\nu} - v_\mu v_\nu, \tag{3}$$

is the projector which selects the perpendicular component of the vector field ($P^2 = P$, $v^\mu P_{\mu\nu} = 0$). $V_{\perp\mu}$ and $V_\parallel$ can further be written as

$$V_{\perp\mu} = \frac{1}{\sqrt{2m_V}}[e^{-im_V v\cdot x}W_\mu + e^{im_V v\cdot x}W_\mu^\dagger], \tag{4}$$

$$V_\parallel = \frac{1}{\sqrt{2m_V}}[e^{-im_V v\cdot x}W_\parallel + e^{im_V v\cdot x}W_\parallel^\dagger], \tag{5}$$

where W_μ and $W_\mu^\dagger$ are effective vector meson fields, and $P_{\mu\nu}W^\nu = W_\mu$ and $P_{\mu\nu}W^{\nu\dagger} = W_\mu^\dagger$ are understood. By neglecting terms proportional to $\exp(\pm 2im_V v \cdot x)$, which oscillate rapidly if one takes m_V to infinity, the Lagrangian $\mathcal{L}_R$ in terms of the W fields is given by

$$\begin{aligned}\mathcal{L}_R \to{}& \frac{1}{2m_V}[-\partial_\mu W_\parallel^\dagger \partial^\mu W_\parallel + (v\cdot\partial W_\parallel^\dagger)(v\cdot\partial W_\parallel)] \\ &+ \frac{m_V}{2}W_\parallel^\dagger W_\parallel + \frac{1}{2}[-i\partial_\mu W_\parallel^\dagger W^\mu + iW_\mu^\dagger \partial^\mu W_\parallel] \\ &+ \frac{1}{2m_V}[\partial_\mu W_\parallel^\dagger (v\cdot\partial W^\mu) + (v\cdot\partial W_\mu^\dagger)\partial^\mu W_\parallel] \\ &- iW_\mu^\dagger (v\cdot\partial)W^\mu.\end{aligned} \tag{6}$$

In the infinite mass limit, $m_V \to \infty$, the $W_\parallel$ field decouples because of the presence of the mass term $m_V W_\parallel^\dagger W_\parallel/2$. In order to remove the parallel component, one can impose the constraint $v \cdot V = 0$ or $v \cdot W = 0$. Alternatively, we can remove $W_\parallel$ by making use of the equation of motion,

$$W_\parallel = \frac{-i}{m_V}\partial_\mu W^\mu + O(1/m_V^2), \tag{7}$$

which also shows that $W_\parallel$ is suppressed by powers of $1/m_V$ relative to the perpendicular component W_μ. Having removed the parallel component the resulting effective Lagrangian simplifies to

$$\mathcal{L}_R = -iW_\mu^\dagger (v\cdot\partial)W^\mu + O(1/m_V). \tag{8}$$

The first term is the kinetic term for the vector meson in the heavy effective theory. Vector meson fields which appear in the following are the effective fields W_μ and $W_\mu^\dagger$. The partial derivative $i\partial_\mu$ acting on these effective fields produces a small residual momentum r_μ, defined as

$$k_\mu = m_V v_\mu + r_\mu, \tag{9}$$

where k_μ is the usual four-momentum of the vector meson. We assume here that the residual momentum is of the size of the low momentum of the pseudoscalar meson. This assumption holds in interaction processes with soft pions.

III. WILSON CHIRAL PERTURBATION THEORY FOR VECTOR MESONS

The chiral effective Lagrangian for heavy vector mesons is expanded in powers of the small pseudoscalar momenta and masses, and the residual momentum r_μ of the vector mesons. The symmetries of QCD, in particular, chiral symmetry, dictate the form of the terms in the chiral Lagrangian. Even though the quark masses explicitly break chiral symmetry, their effect is properly taken into account by a spurion analysis, where the quark mass matrix is assumed to transform nontrivially under chiral transformations in an intermediate step.

The same principles apply to Wilson χPT, the low-energy effective theory for Lattice QCD with Wilson fermions. The main difference is the presence of an additional expansion parameter, the lattice spacing a [4,17]. The nonzero lattice spacing is also taken into account by the spurion analysis, and the transformation behavior of the corresponding spurion field is exactly the same as for the quark masses. Constructing the terms in the chiral Lagrangian of Wilson χPT for vector mesons is therefore straightforward. Apart from the presence of two instead of one spurion field there is essentially no difference to Ref. [8]. The order counting, however, is not entirely obvious, since both the quark masses and the lattice spacing are expansion parameters and their relative size is important for a consistent power counting, as we will discuss in section III B.

A. Matter and spurion fields

The pseudoscalar meson field is introduced as usual as an $SU(3)$ unitary matrix

$$\Sigma = \exp\left(\frac{2i\Pi}{f}\right), \tag{10}$$

where

$$\Pi = \sqrt{2}\pi^a T^a = \begin{bmatrix} \frac{\pi^0}{\sqrt{2}} + \frac{\eta}{\sqrt{6}} & \pi^+ & K^+ \\ \pi^- & -\frac{\pi^0}{\sqrt{2}} + \frac{\eta}{\sqrt{6}} & K^0 \\ K^- & \bar{K}^0 & -\frac{2\eta}{\sqrt{6}} \end{bmatrix}. \tag{11}$$

The $SU(3)$ generators T^a $(a = 1, \ldots, 8)$ are normalized such that

$$\mathrm{tr}[T^a T^b] = \tfrac{1}{2}\delta^{ab}, \tag{12}$$

and f is the leading order pseudoscalar decay constant in the chiral limit.[2] The field Σ transforms according to $\Sigma \to L\Sigma R^{-1}$ under chiral rotations with $L \in SU(3)_L$ and $R \in SU(3)_R$. The square root of Σ,

$$\xi = \exp\left(\frac{i\Pi}{f}\right) = \sqrt{\Sigma}, \tag{13}$$

is needed to describe the interaction of the pseudo scalars with the vector mesons. It transforms under chiral transformations according to

$$\xi \to L\xi U^\dagger = U\xi R^{-1}, \tag{14}$$

with an $SU(3)$ matrix U. In fact, Eq. (14) defines U, which is a function of L, R, and Π. For vector transformations with $L = R$ one finds $U = L = R$.

The vector meson fields are introduced as an octet

$$\mathcal{O}_\mu = \sqrt{2}\rho_\mu^a T^a = \begin{bmatrix} \frac{\rho_\mu^0}{\sqrt{2}} + \frac{\phi_\mu^{(8)}}{\sqrt{6}} & \rho_\mu^+ & K_\mu^{*+} \\ \rho_\mu^- & -\frac{\rho_\mu^0}{\sqrt{2}} + \frac{\phi_\mu^{(8)}}{\sqrt{6}} & K^{*0} \\ K_\mu^{*-} & \bar{K}_\mu^{*0} & -\frac{2\phi_\mu^{(8)}}{\sqrt{6}} \end{bmatrix}, \tag{15}$$

and a singlet $S_\mu = \phi_\mu^0$. These fields are required to satisfy the constraints

$$v \cdot S = v \cdot \mathcal{O} = 0, \tag{16}$$

in order to describe spin 1 particles with three polarization states. As stated in the previous section, this constraint can be enforced by applying the projector $P_{\mu\nu}$ on the vector meson fields. In the following we assume that this projector has been applied, i.e. we implicitly assume $S_\mu = P_{\mu\nu}S^\nu$ and $\mathcal{O}_\mu = P_{\mu\nu}\mathcal{O}^\nu$.

For the construction of the chiral Lagrangian the quark masses and the lattice spacing are treated as spurion fields. For the quark mass matrix we use

$$\tilde{M}_q = \mathrm{diag}(\tilde{m}, \tilde{m}, \tilde{m}_s) = \tilde{M}_0 I + \tilde{M}_8 T^8, \tag{17}$$

where $\tilde{M}_0$ and $\tilde{M}_8$ are expressed in terms of $\tilde{m}$ and $\tilde{m}_s$

$$\tilde{M}_0 = \frac{2\tilde{m} + \tilde{m}_s}{3}, \qquad \tilde{M}_8 = \frac{2(\tilde{m} - \tilde{m}_s)}{\sqrt{3}}. \tag{18}$$

We use the tilde in order to highlight that the quark masses $\tilde{m}$ and $\tilde{m}_s$ denote shifted quark masses, which are defined such that the tree level pseudoscalar meson masses become zero if $\tilde{m} = \tilde{m}_s = 0$. See Ref. [1] and also Appendix A for details.

We introduce a spurion field A to include the effect of a nonzero lattice spacing a. This field transforms under chiral transformations just as the quark mass field M ($M = \tilde{M}_q$ after the spurion analysis), i.e.

$$A \to LAR^{-1}. \tag{19}$$

Once the chiral Lagrangian is derived, the spurion is set to aI where I denotes the unit matrix in flavor space.

For the construction of the chiral Lagrangian it will also be useful to introduce the following quantities:

$$M_\pm = \frac{1}{2}(\xi M^\dagger \xi \pm \xi^\dagger M \xi^\dagger), \tag{20}$$

$$W_\pm = \frac{1}{2}(\xi A^\dagger \xi \pm \xi^\dagger A \xi^\dagger), \tag{21}$$

$$V_\mu = \frac{1}{2}(\xi \partial_\mu \xi^\dagger + \xi^\dagger \partial_\mu \xi), \tag{22}$$

$$A_\mu = \frac{i}{2}(\xi \partial_\mu \xi^\dagger - \xi^\dagger \partial_\mu \xi), \tag{23}$$

$$\mathcal{D}_\nu \mathcal{O}_\mu = \partial_\nu \mathcal{O}_\mu + [V_\nu, \mathcal{O}_\mu]. \tag{24}$$

The transformation behavior of these quantities as well as of the meson and spurion fields under chiral rotations in $G = SU(3)_L \times SU(3)_R$, charge conjugation C and parity P are summarized in Table I.

TABLE I. Transformation properties under the group $G = SU(3)_L \times SU(3)_R$, ($L \in SU(3)_L$ and $R \in SU(3)_R$), charge conjugation C and parity P. In the parity transformed expressions it is understood that the argument is $(-\vec{x}, t)$.

element	G	C	P
Σ	$L\Sigma R^\dagger$	Σ^T	$\Sigma^\dagger$
ξ	$L\xi U^\dagger = U\xi R^\dagger$	ξ^T	$\xi^\dagger$
$\mathcal{O}_\mu$	$U\mathcal{O}_\mu U^\dagger$	$-O_\mu^T$	$\mathcal{O}_\mu$
S_μ	S_μ	$-S_\mu$	S_μ
M	$LMR^\dagger$	M^T	$M^\dagger$
$M_\pm$	$UM_\pm U^\dagger$	$M_\pm^T$	$\pm M_\pm$
A	$LAR^\dagger$	A^T	$A^\dagger$
$W_\pm$	$UW_\pm U^\dagger$	$W_\pm^T$	$\pm W_\pm$
V_μ	$UV_\mu U^\dagger + U\partial_\mu U^\dagger$	$-V_\mu^T$	V_μ
A_μ	$UA_\mu U^\dagger$	A_μ^T	$-A_\mu$
$\mathcal{D}_\nu \mathcal{O}_\mu$	$U(\mathcal{D}_\nu \mathcal{O}_\mu)U^\dagger$	$-(\mathcal{D}_\nu \mathcal{O}_\mu)^T$	$\mathcal{D}_\nu \mathcal{O}_\mu$

[2] Our normalization corresponds to $f \approx 132$ MeV.

B. Power counting

Having defined the meson and spurion fields it is straightforward to write down the most general chiral Lagrangian which is compatible with chiral symmetry, charge conjugation and parity. However, since we have two sources for explicit chiral symmetry breaking, the quark masses and the lattice spacing, their relative size matters for an appropriate power counting. Moreover, the power counting one wants to employ for the vector meson chiral Lagrangian should be consistent with the one adopted for the pure pseudoscalar chiral Lagrangian.

In Ref. [1] the $O(a^2)$ terms are included in the leading order chiral Lagrangian. To be consistent we adopt here the following power counting scheme:

$$\begin{aligned} \text{LO: } & O(p), \quad O(a), \\ \text{NLO: } & O(m), \quad O(a^2), \quad O(ap), \quad O(p^2), \\ \text{NNLO: } & O(mp), \quad O(p^3), \quad O(am), \quad O(a^3), \\ & O(ap^2), \quad O(a^2p). \end{aligned} \tag{25}$$

Here p represents both the residual momentum of the vector meson and the momentum of the pseudoscalar meson, and m denotes the quark mass. This counting scheme assumes $p \sim a$. This implies $p^2 \sim a^2$, and therefore maintains consistency with the power counting of Ref. [1] for the pure pseudoscalar sector.

We have listed the NNLO contributions in Eq. (25), because some NNLO terms enter already the one-loop calculation of the vector meson masses. To discuss this point, let us define a generic power counting scale E of order $p \sim a$, so that the LO terms or of $O(E)$, the NLO terms are $O(E^2)$ and so on. Just from a dimensional analysis one finds that a one-loop integral involving a vertex from the LO Lagrangian gives an $O(E^3)$ contribution to the vector meson mass. Therefore, some of the coefficients in the NNLO Lagrangian are needed as counterterms for the cancellation of the one-loop divergences. The coefficients of the NLO Lagrangian, on the other hand, are not needed as counterterms, since there are no one-loop corrections with dimension E^2. This situation is different from the pure pseudoscalar sector where the divergences in the one-loop contribution from the LO Lagrangian are canceled by the tree level terms coming from the NLO Lagrangian.

The structure of the correction to the vector meson masses can be summarized as follows:

$$\begin{aligned} m_V = \mu_c + \underbrace{[\text{tree level contribution from the LO Lagrangian}]}_{O(E)} + \underbrace{[\text{tree level contribution from the NLO Lagrangian}]}_{O(E^2)} \\ + \underbrace{[\text{one-loop contribution from the LO Lagrangian}]}_{O(E^3)} + \underbrace{[\text{tree level contribution from the NNLO Lagrangian}]}_{O(E^3)} + O(E^4), \end{aligned} \tag{26}$$

where μ_c is the vector meson mass in the chiral limit. In fact, the second term on the right hand side of Eq. (26) comes from the $O(a)$ Lagrangian only. As has been shown in Ref. [8], the $O(p)$ term does not contribute at tree level and the chiral correction to the vector meson mass starts at $O(E^2)$.

In this paper we are only interested in deriving the vector meson masses through $O(E^3)$. In that case we neither need the NLO terms of $O(ap, p^2)$ nor the NNLO terms of $O(mp, p^3, ap^2, a^2p)$. The reason is as follows. All these terms contain at least one momentum factor p which have two origins, the pseudoscalar meson momentum p_π and the residual vector meson momentum p_V. For the former, $p_\pi \sim \partial_\mu \pi$ implies that the term always contains at least one pseudoscalar field together with a derivative ∂_μ. This kind of term results in a three-point vertex (vector-vector-pseudoscalar) as a nonvanishing leading term when expanded in pseudoscalar fields and does not give a tree level contribution to the vector meson mass. For the latter, $p_V \sim \partial_\mu V$ (where V is the vector meson field) implies that we can replace p_V with p_π and a contribution proportional to a. One can see this by using the lowest order equation of motion,

$$-iv \cdot \partial V_\mu + (\partial \pi X)_\mu + aY_\mu = 0, \tag{27}$$

where X and Y are functions of low-energy constants and the pseudoscalar field (the flavor structure is suppressed in Eq. (27)). The equation is derived from the leading order Lagrangian $\mathcal{L}_p + \mathcal{L}_a$ which we derive in the next subsection. After the replacement, the resulting term has a part with at least one p_π and a part of $O(a^2, am, a^3)$. For the former part, we repeat the argument given above. The latter part is absorbed into the original terms in Eq. (25). Hence the terms of $O(ap, p^2, mp, p^3, ap^2, a^2p)$ are not needed for our calculation and we do not list these terms in the next subsection. The terms which do contribute to the vector meson mass to the order we are working to are

$$\begin{aligned} \text{LO: } & O(p), \quad O(a), \\ \text{NLO: } & O(m), \quad O(a^2), \\ \text{NNLO: } & O(am), \quad O(a^3), \end{aligned} \tag{28}$$

and we will consider them in the next subsection.

C. Effective Lagrangian

In this section, we show our results for the terms in the chiral Lagrangian which contribute to the vector meson mass through order E^3. By construction it involves the

meson fields and is invariant under Lorentz and chiral transformations, charge conjugation and parity.[3]

O(p):

$$\begin{aligned}\mathcal{L}_p = &-iS_\mu^\dagger(v\cdot\partial)S^\mu - i\langle\mathcal{O}_\mu^\dagger(v\cdot\mathcal{D})\mathcal{O}^\mu\rangle \\ &+ ig_1(S_\mu^\dagger\langle\mathcal{O}_\nu A_\lambda\rangle - S_\mu\langle\mathcal{O}_\nu^\dagger A_\lambda\rangle)v_\sigma\epsilon^{\mu\nu\lambda\sigma} \\ &+ ig_2\langle\{\mathcal{O}_\mu^\dagger,\mathcal{O}_\nu\}A_\lambda\rangle v_\sigma\epsilon^{\mu\nu\lambda\sigma},\end{aligned} \tag{29}$$

with $\langle X\rangle = \mathrm{tr}(X)$ for flavor indices. The derivative $i\partial_\mu$ acting on the vector mesons provides the residual momentum $r_\mu = k_\mu - \mu_V v_\mu$. We therefore consider the kinetic terms for the vector mesons as O(p). The terms proportional to g_1 and g_2 involve A_λ, defined in Eq. (23). Expanding in terms of the pseudoscalar fields this quantity starts as $A_\lambda = \partial_\lambda\Pi/f + \mathrm{O}(\Pi^3)$. The presence of the derivative means that both the g_1 and g_2 term are of O(p).

As is well known, the vector mesons are not stable. This effect can be taken into account by including an anti-Hermitian term in the Lagrangian whose coefficient is proportional to the decay width. However, the decay width is rather small and this contribution is usually ignored [8]. We also neglect this term in this paper.

O(a):

$$\begin{aligned}\mathcal{L}_a = &\alpha_1\langle W_+\rangle S_\mu^\dagger S^\mu + \alpha_2(\langle\mathcal{O}_\mu^\dagger W_+\rangle S^\mu + \langle\mathcal{O}_\mu W_+\rangle S^{\mu\dagger}) \\ &+ \alpha_3\langle\{\mathcal{O}_\mu^\dagger,\mathcal{O}^\mu\}W_+\rangle + \alpha_4\langle W_+\rangle\langle\mathcal{O}_\mu^\dagger\mathcal{O}^\mu\rangle\end{aligned} \tag{30}$$

This O(a) Lagrangian is a new element of this study. Since the spurion field A associated with the lattice spacing transforms exactly like the quark mass spurion field (cf. Eq. (19)), this part of the Lagrangian has the same structure as the following O(m) Lagrangian.

O(m):

$$\begin{aligned}\mathcal{L}_m = &\lambda_s\langle M_+\rangle S_\mu^\dagger S^\mu + \lambda_{os}(\langle\mathcal{O}_\mu^\dagger M_+\rangle S^\mu + \langle\mathcal{O}_\mu M_+\rangle S^{\mu\dagger}) \\ &+ \lambda_{o1}\langle M_+\rangle\langle\mathcal{O}_\mu^\dagger\mathcal{O}^\mu\rangle + \lambda_{o2}\langle\{\mathcal{O}_\mu^\dagger,\mathcal{O}^\mu\}M_+\rangle + \Delta\mu S_\mu^\dagger S^\mu\end{aligned} \tag{31}$$

Note that the leading order mass terms $\mu_s S_\mu^\dagger S^\mu$ and $\mu_o\langle\mathcal{O}_\mu^\dagger\mathcal{O}^\mu\rangle$, where μ_s and μ_o are the masses for the singlet and octet vector meson in the chiral limit, respectively, are absent in the O(p) Lagrangian. Their effect is already included through the phase factor $\exp(-im_V v\cdot x)$ in the definition of the heavy meson fields. The mass difference

$$\Delta\mu \equiv \mu_s - \mu_o \tag{32}$$

between the singlet and octet vector meson mass, however, needs to be introduced explicitly. This term, which is the last term in Eq. (31), is considered to be of O(m), since $\Delta\mu < 200\ \mathrm{MeV} \sim m_s$ [8].[4]

O(a^2):

$$\begin{aligned}\mathcal{L}_{a^2} = &\beta_1\langle W_+W_+\rangle S_\mu^\dagger S^\mu + \beta_2\langle W_+\rangle^2 S_\mu^\dagger S^\mu + \beta_3(\langle\mathcal{O}_\mu^\dagger W_+W_+\rangle S^\mu + \langle\mathcal{O}_\mu W_+W_+\rangle S^{\mu\dagger}) + \beta_4\langle W_+\rangle(\langle\mathcal{O}_\mu^\dagger W_+\rangle S^\mu \\ &+ \langle\mathcal{O}_\mu W_+\rangle S^{\mu\dagger}) + \beta_5\langle\{\mathcal{O}_\mu^\dagger,\mathcal{O}^\mu\}W_+W_+\rangle + \beta_6\langle\mathcal{O}_\mu^\dagger W_+\mathcal{O}^\mu W_+\rangle + \beta_7\langle W_+\rangle\langle\{\mathcal{O}_\mu^\dagger,\mathcal{O}^\mu\}W_+\rangle \\ &+ \beta_8\langle W_+W_+\rangle\langle\mathcal{O}_\mu^\dagger\mathcal{O}^\mu\rangle + \beta_9\langle W_+\rangle^2\langle\mathcal{O}_\mu^\dagger\mathcal{O}^\mu\rangle + \beta_{10}\langle\mathcal{O}_\mu^\dagger W_+\rangle\langle\mathcal{O}^\mu W_+\rangle + (W_+\to W_-).\end{aligned} \tag{33}$$

In total we find 20 terms, however, the parts involving W_- are not needed. By expanding in powers of the pseudoscalar field one finds $W_- = (2ia/f)\Pi$ at leading order. Hence, all these terms have at least two pseudoscalar fields and therefore do not contribute to the vector meson masses at tree level.

O(am):

$$\begin{aligned}\mathcal{L}_{am} = &\gamma_1\langle W_+M_+\rangle S_\mu^\dagger S^\mu + \gamma_2\langle W_+\rangle\langle M_+\rangle S_\mu^\dagger S^\mu + \gamma_3\langle M_+\rangle(\langle\mathcal{O}_\mu^\dagger W_+\rangle S^\mu + \langle\mathcal{O}_\mu W_+\rangle S^{\mu\dagger}) + \gamma_4(S_\mu^\dagger\langle\mathcal{O}^\mu\{M_+,W_+\}\rangle \\ &+ S_\mu\langle\mathcal{O}^{\mu\dagger}\{M_+,W_+\}\rangle) + \gamma_5\langle W_+\rangle(\langle\mathcal{O}_\mu^\dagger M_+\rangle S^\mu + \langle\mathcal{O}_\mu M_+\rangle S^{\mu\dagger}) + \gamma_6\langle M_+\rangle\langle\{\mathcal{O}_\mu^\dagger,\mathcal{O}^\mu\}W_+\rangle + \gamma_7\langle\mathcal{O}_\mu^\dagger\mathcal{O}^\mu\rangle\langle M_+W_+\rangle \\ &+ \gamma_8\langle W_+\rangle\langle M_+\rangle\langle\mathcal{O}_\mu^\dagger\mathcal{O}^\mu\rangle + \gamma_9\langle\{\mathcal{O}_\mu^\dagger,\mathcal{O}^\mu\}\{M_+,W_+\}\rangle + \gamma_{10}(\langle\mathcal{O}_\mu^\dagger M_+\mathcal{O}^\mu W_+\rangle + \langle\mathcal{O}_\mu^\dagger W_+\mathcal{O}^\mu M_+\rangle) \\ &+ \gamma_{11}\langle W_+\rangle\langle\{\mathcal{O}_\mu^\dagger,\mathcal{O}^\mu\}M_+\rangle + \gamma_{12}(\langle\mathcal{O}_\mu^\dagger M_+\rangle\langle\mathcal{O}^\mu W_+\rangle + \langle\mathcal{O}_\mu^\dagger W_+\rangle\langle\mathcal{O}^\mu M_+\rangle) + (M_+,W_+\to M_-,W_-).\end{aligned} \tag{34}$$

One can easily check that $M_- \sim \Pi$ at leading order. Therefore, the terms involving M_- and W_- do not contribute to the vector meson mass at the order we are working.

For our purposes it is not necessary to list the full O(a^3) Lagrangian, which is quite cumbersome. Since we will not encounter any divergences proportional to a^3 in our calculation, we do not need the coefficients in the O(a^3)

[3]Just for convenience we present our results in Minkowski space, which does not make a difference for the computation of the vector meson masses. The underlying lattice theory, however, is usually formulated for Euclidean space time.

[4]We assumed the definition $m_V = \mu_o$. If we had chosen $m_V = \mu_s$ the last term in Eq. (31) would be $-\Delta\mu\langle\mathcal{O}_\mu^\dagger\mathcal{O}^\mu\rangle$. Our final results for the vector meson masses are, of course, independent of this particular choice.

Lagrangian as counterterms. The tree level contribution of the $O(a^3)$ Lagrangian merely gives an analytic a^3 term to the singlet and octet vector meson mass, which we can simply add to our final one-loop result. Note, however, that the $O(a^3)$ Lagrangian does not give an off-diagonal contribution to the singlet-octet two point function at $O(E^3)$. All possible ways to take the trace in terms like

$$S_\mu^\dagger \mathcal{O}^\mu W_+ W_+ W_+ + \text{H.c.} \quad \text{or} \quad S_\mu^\dagger \mathcal{O}^\mu W_+ W_- W_- + \text{H.c.} \tag{35}$$

yield at least two pseudoscalar fields in the nonvanishing leading term when one expands $W_\pm$ in powers of the Π field. By noting $\langle \mathcal{O}^\mu \rangle = 0$, $W_+ = 1 + O(\pi)$ and $W_- = O(\pi)$, one can easily check this statement.

Having determined the chiral effective Lagrangian we can set the spurion fields to their constant values, i.e. we take $A \to aI$ in Eqs. (29)–(31), (33), and (34). This replacement simplifies the fields $W_\pm$ to

$$W_\pm \to \frac{a}{2}(\Sigma \pm \Sigma^\dagger). \tag{36}$$

The Lagrangian in terms of the component fields π^a, ρ_μ^a for the pseudoscalar and vector mesons is presented in appendix A, together with the Feynman rules relevant for the calculation of the vector meson masses.

D. Vector meson masses

The full propagator for the ρ and the K^* is given by

$$\begin{aligned} i\Delta_{\mu\nu}^{ab}(k) &= \frac{-iP_{\mu\nu}}{v\cdot r - a\alpha_{o1}}\delta^{ab} + \frac{-iP_{\mu\alpha}}{v\cdot r - a\alpha_{o1}} \\ &\quad \times [-iP^{\alpha\beta}\Sigma_O^{ab}(k)]\frac{-iP_{\beta\nu}}{v\cdot r - a\alpha_{o1}} + \cdots \\ &= -iP_{\mu\nu}[v\cdot k - \mu_o - a\alpha_{o1} + \Sigma_O(k)]_{ab}^{-1}, \end{aligned} \tag{37}$$

where a, b runs from 1 to 7. Recall that the external four-momentum for the octet vector meson is written as $k_\nu = \mu_o v_\nu + r_\nu$ where μ_o is the octet mass in the chiral limit. Using the Feynman rules summarized in appendix A we obtain for the octet-to-octet self energy through $O(E^3)$

$$\begin{aligned} \Sigma_O^{ab}(k) = &-[(N\tilde{M}_0\lambda_{o1} + a^2\beta_o + Na\tilde{M}_0\gamma_{o1})\delta^{ab} \\ &+ (\lambda_{o2} + a\gamma_{o2})(2\tilde{M}_0\delta_{aa} + \tilde{M}_8 d^{ab8})] \\ &+ \frac{g_1^2}{f^2}\delta^{ab}2C_{21}(w_s, \tilde{m}_a) \\ &+ \frac{2g_2^2}{f^2}\sum_{c,e} d^{ace}d^{bce}2C_{21}(w_o, \tilde{m}_c) \\ &+ a\frac{2\alpha_{o1}}{Nf^2}\delta^{ab}\sum_c I_0(\tilde{m}_c) + a\frac{2\alpha_{o2}}{Nf^2}\sum_{c,e} d^{abe}d^{cce}I_0(\tilde{m}_c), \end{aligned} \tag{38}$$

where

$$w_{o,s} = v\cdot r - a\alpha_{o1,s}, \tag{39}$$

and d^{abc} is the totally symmetric d-symbol of $su(N)$.[5] The coefficients α_{oi} are particular combinations of the low-energy constants $\alpha_1, \ldots, \alpha_4$ which enter Eq. (30). Similarly, the coefficients β_o and γ_{oi} are combinations of the low-energy constants $\beta_1, \ldots, \beta_{10}$ and $\gamma_1, \ldots, \gamma_{12}$, respectively. The full expressions for these combinations can be found in appendix A, even though it will not be necessary to keep track of the original constants in the following. The functions $C_{21}(\omega, M)$ and $I_0(M)$ stem from the loop integral and are defined as

$$\begin{aligned} C_{21}(w, M) = &\frac{1}{3}[(M^2 - w^2)J(w, M) + wI_0(M)] \\ &- \frac{w}{12\pi^2}\left(\frac{M^2}{2} - \frac{w^2}{3}\right), \end{aligned} \tag{40}$$

$$\begin{aligned} J(w, M) = &\frac{w}{8\pi^2}\left[R + \ln\frac{M^2}{\mu^2} - 1\right] \\ &+ \frac{1}{8\pi^2}\left[2\sqrt{M^2 - w^2}\arccos\left(-\frac{w}{M}\right)\right], \\ &\text{for } w^2 < M^2, \end{aligned} \tag{41}$$

$$I_0(M) = \frac{M^2}{16\pi^2}\left[R + \ln\frac{M^2}{\mu^2}\right], \tag{42}$$

$$R = \frac{2}{n-4} - [\ln(4\pi) + \Gamma'(1) + 1], \tag{43}$$

with the dimension n. The one-loop integrals encountered here are essentially the same as those in baryon chiral perturbation theory, and a detailed derivation of the formulas (40)–(43) can be found in Ref. [18].

In order to cancel the divergence in R, defined in Eq. (43), the $O(am)$ coefficients γ_i ($i = o1, o2$) need to be properly renormalized,

$$\gamma_i = \gamma_i^r(\mu) + \frac{2BC_i}{8\pi^2 f^2}R, \tag{44}$$

where the coefficient B is a low-energy parameter in the LO chiral Lagrangian for the pseudo scalars (see Ref. [1] and Appendix A). The coefficients $\gamma_i^r(\mu)$ denote renormalized parameters, μ is the renormalization scale[6], and the coefficients C_i are given by

[5] We keep the number of flavors N undetermined at intermediate stages since N provides some useful checks for our equations. In the final results we will set N equal to 3. Note, however, that intermediate results like eq. ((38)) do not hold for arbitrary N unless all masses are degenerate.

[6] In the following we will simply write γ_i^r for the renormalized parameters and suppress the dependence on μ.

$$C_{\mathrm{o}1} = \alpha_{\mathrm{o}1}\frac{N^2-1}{N} - \alpha_{\mathrm{o}2}\frac{5}{3N}, \tag{45}$$

$$C_{\mathrm{o}2} = \alpha_{\mathrm{o}2}\frac{5}{6N}. \tag{46}$$

The on-shell condition for the ρ and K^* meson ($a = 1, \cdots, 7$) is given by (no sum over a)

$$\begin{aligned} 0 &= v\cdot k - \mu_{\mathrm{o}} - a\alpha_{\mathrm{o}1} + \Sigma_{\mathrm{O}}^{aa}(k), \\ k_\mu &= m_a v_\mu, \qquad k^2 = m_a^2, \end{aligned} \tag{47}$$

where m_a is the physical mass. So far we have chosen to express the self energy as a function of the four-momentum k_μ. $\Sigma_{\mathrm{O}}^{aa}(k)$ may also be parametrized by the scalar variables w_{o} and w_{s}, defined in Eq. (39), and we can write $\Sigma_{\mathrm{O}}^{aa}(k) = \Sigma_{\mathrm{O}}^{aa}(w_{\mathrm{o}}, w_{\mathrm{s}})$. It is easy to see that the definition of w_{o} together with the on-shell condition (47) yields,

$$w_{\mathrm{o}} = m_a - \mu_{\mathrm{o}} - a\alpha_{\mathrm{o}1} = -\Sigma_{\mathrm{O}}^{aa}(k = m_a v). \tag{48}$$

w_{o} is considered to be of $\mathrm{O}(E^2)$ since the self energy Σ_{O}^{aa} is of $\mathrm{O}(E^2)$. For w_{s} we find the similar result

$$w_{\mathrm{s}} = m_a - \mu_{\mathrm{o}} - a\alpha_{\mathrm{s}} = -\Sigma_{\mathrm{O}}^{aa}(k = m_a v) - a(\alpha_{\mathrm{s}} - \alpha_{\mathrm{o}1}). \tag{49}$$

Here we assume that the difference between the leading lattice artifacts for the octet and the singlet mass is of order E^2 and therefore small[7],

$$a(\alpha_{\mathrm{s}} - \alpha_{\mathrm{o}1}) = a\Delta\alpha = O(E^2). \tag{50}$$

This is supported by a strong coupling analysis performed in Ref. [19]. Expanding the effective potential through second order in terms of the vector meson fields, it has been shown that there exists no difference between the singlet and octet vector meson to all orders in the strong coupling expansion. Whether w_{s} and w_{o} is small away from the strong coupling limit can and should be checked in the actual lattice simulation.

Provided the assumption (50), both w_{s} and w_{o} are of $\mathrm{O}(E^2)$ and we can set $w_{\mathrm{o,s}} = 0$ in Σ_{O}^{aa}, since the difference is beyond the order we are working to. We therefore conclude that

$$m_a = \mu_{\mathrm{o}} + a\alpha_{\mathrm{o}1} - \Sigma_{\mathrm{O}}^{aa}(w_{\mathrm{o}} = 0, w_{\mathrm{s}} = 0). \tag{51}$$

Note that the function C_{21} becomes much simpler when the first argument is set to zero,

$$C_{21}(w = 0, M) = \frac{1}{24\pi}M^3. \tag{52}$$

Let us now consider the sector of the ρ^8 and the ϕ^0 mesons. Because of mixing, the propagator for this sector is written as a 2×2 matrix,

$$i\Delta_{\mu\nu}(k) = -iP_{\mu\nu}\begin{bmatrix} v\cdot r - a\alpha_{\mathrm{o}1} + \Sigma_{\mathrm{O}}(k) & \Sigma_{\mathrm{OS}}(k) \\ \Sigma_{\mathrm{OS}}(k) & v\cdot r - a\alpha_{\mathrm{s}} + \Sigma_{\mathrm{S}}(k) \end{bmatrix}^{-1}, \tag{53}$$

where the self energies for octet-to-octet ($a = 8$), singlet-to-singlet and octet-to-singlet are given by

$$\Sigma_{\mathrm{O}}(k) = \Sigma_{\mathrm{O}}^{a=8,b=8}(k), \tag{54}$$

$$\begin{aligned} \Sigma_{\mathrm{S}}(k) = &-(N\tilde{M}_0\lambda_{\mathrm{s}} + a^2\beta_{\mathrm{s}} + Na\tilde{M}_0\gamma_{\mathrm{s}} + \Delta\mu) \\ &+ \frac{g_1^2}{f^2}\sum_c 2C_{21}(w_{\mathrm{o}}, \tilde{m}_c) + a\frac{2\alpha_{\mathrm{s}}}{Nf^2}\sum_c I_0(\tilde{m}_c), \end{aligned} \tag{55}$$

$$\begin{aligned} \Sigma_{\mathrm{OS}}(k) = &-\frac{\tilde{M}_8}{\sqrt{2}}(\lambda_{\mathrm{os}} + a\gamma_{\mathrm{os}}) \\ &+ \frac{\sqrt{2}g_1g_2}{f^2}\sum_c d^{cc8}2C_{21}(w_{\mathrm{o}}, \tilde{m}_c) \\ &+ a\frac{\alpha_{\mathrm{os}}\sqrt{2}}{Nf^2}\sum_c d^{cc8}I_0(\tilde{m}_c). \end{aligned} \tag{56}$$

For the cancellation of R, in a similar way to the case of ρ-K^* sector, $\mathrm{O}(am)$ coefficients γ_i ($i = \mathrm{s}, \mathrm{os}$) should be renormalized as in Eq. (44) with

$$C_{\mathrm{s}} = \alpha_{\mathrm{s}}\frac{N^2-1}{N^2}, \tag{57}$$

$$C_{\mathrm{os}} = \alpha_{\mathrm{os}}\frac{5}{6N}. \tag{58}$$

The physical masses m_i, $i = 1, 2$, for this sector are determined by the on-shell condition

$$\det\begin{bmatrix} v\cdot r - a\alpha_{\mathrm{o}1} + \Sigma_{\mathrm{O}}(k) & \Sigma_{\mathrm{OS}}(k) \\ \Sigma_{\mathrm{OS}}(k) & v\cdot r - a\alpha_{\mathrm{s}} + \Sigma_{\mathrm{S}}(k) \end{bmatrix} = 0, \tag{59}$$

at $k_\mu = m_i v_\mu$. The task is to solve the equation

[7] If this assumption is not valid, then w_{s} is of $\mathrm{O}(a) \sim \mathrm{O}(E)$. In this case, the function $C_{21}(w_s, \tilde{m}_a)$ in Eq. (38) contains divergences whose coefficients are of order am and a^3. Such divergences would alter the renormalization conditions for $\gamma_{\mathrm{o}1,\mathrm{o}2}$ in Eq. (44). Also the $\mathrm{O}(a^3)$ counterterms may receive a divergent renormalization in order to cancel additional divergences. Furthermore, if w_{s} is of $\mathrm{O}(a)$, the condition $w^2 < M^2$ in Eq. (41) may not be valid. Hence the functional form of $J(w, M)$ might be changed according to the relation between w and M as in Ref. [18] eq. (C.27).

$$\det\begin{bmatrix} m-\mu_{\rm o}-a\alpha_{\rm o1}+\Sigma_{\rm O}(k=m\upsilon) & \Sigma_{\rm OS}(k=m\upsilon) \\ \Sigma_{\rm OS}(k=m\upsilon) & m-\mu_{\rm s}-a\alpha_{\rm s}+\Sigma'_{\rm S}(k=m\upsilon) \end{bmatrix}=0, \tag{60}$$

with respect to the mass m_i, where we have defined $\Sigma'_{\rm S}$ as $\Sigma_{\rm S}=\Sigma'_{\rm S}-\Delta\mu$. The solutions of the equation are given by

$$m_\pm=\frac{1}{2}\Big[\mu_{\rm s}+\mu_{\rm o}+a(\alpha_{\rm s}+\alpha_{\rm o1})-(\Sigma'_{\rm S}+\Sigma_{\rm O})\pm\sqrt{\{\Delta\mu+a\Delta\alpha-(\Sigma'_{\rm S}-\Sigma_{\rm O})\}^2+4(\Sigma_{\rm OS})^2}\,\Big]. \tag{61}$$

Assuming that the $SU(3)$ breaking $(\tilde{m}-\tilde{m}_s)/3$ is smaller than the average $(2\tilde{m}+\tilde{m}_s)/3$ of the quark masses[8] together with $\{\Delta\mu+a\Delta\alpha-(\Sigma'_{\rm S}-\Sigma_{\rm O})\}>0$, the physical masses are given by

$$m_+=\mu_{\rm s}+a\alpha_{\rm s}-\Sigma'_{\rm S}+\frac{(\Sigma_{\rm OS})^2}{\Delta\mu+a\Delta\alpha-(\Sigma'_{\rm S}-\Sigma_{\rm O})}, \tag{62}$$

$$m_-=\mu_{\rm o}+a\alpha_{\rm o1}-\Sigma_{\rm O}-\frac{(\Sigma_{\rm OS})^2}{\Delta\mu+a\Delta\alpha-(\Sigma'_{\rm S}-\Sigma_{\rm O})}. \tag{63}$$

As in the case of the ρ and K^* sector, we consider the self energies $\Sigma_{\rm O,OS}$ and $\Sigma'_{\rm S}$ as functions of $w_{\rm o,s}$ when we impose the on-shell condition. Setting the physical masses equal to $m_\pm$, the parameters $w_{\rm o,s}$ are given as

$$w_{\rm o}=m-\mu_{\rm o}-a\alpha_{\rm o1}=\begin{cases}\Delta\mu+a\Delta\alpha-\Sigma'_{\rm S}-\frac{(\Sigma_{\rm OS})^2}{\Delta\mu+a\Delta\alpha-(\Sigma'_{\rm S}-\Sigma_{\rm O})}, & \text{for } m=m_+,\\ -\Sigma_{\rm O}-\frac{(\Sigma_{\rm OS})^2}{\Delta\mu+a\Delta\alpha-(\Sigma'_{\rm S}-\Sigma_{\rm O})}, & \text{for } m=m_-,\end{cases} \tag{64}$$

$$w_{\rm s}=m-\mu_{\rm o}-a\alpha_{\rm s}=\begin{cases}\Delta\mu-\Sigma'_{\rm S}-\frac{(\Sigma_{\rm OS})^2}{\Delta\mu+a\Delta\alpha-(\Sigma'_{\rm S}-\Sigma_{\rm O})}, & \text{for } m=m_+,\\ -a\Delta\alpha-\Sigma_{\rm O}-\frac{(\Sigma_{\rm OS})^2}{\Delta\mu+a\Delta\alpha-(\Sigma'_{\rm S}-\Sigma_{\rm O})}, & \text{for } m=m_-,\end{cases} \tag{65}$$

Hence it turns out that both $w_{\rm o}$ and $w_{\rm s}$ are of $O(E^2)$, since $\Delta\mu$, $a\Delta\alpha$, $\Sigma_{\rm O,S}$ and $\Sigma_{\rm OS}$ are of $O(E^2)$. Therefore, we can set $w_{\rm o,s}=0$ in the self energies, as we did in the ρ-K^* sector.

With these preparations our one-loop results for the vector meson masses are as follows:

$$\begin{aligned} m_\rho=m_{\rm O}(a)+\lambda_x(a)x+2\lambda_y(a)y-\frac{1}{12\pi f^2}\Big[&\Big(g_1^2+\frac{2}{3}g_2^2\Big)\\ &\times(x+2y)^{3/2}+2g_2^2(x-y)^{3/2}+\frac{2}{3}g_2^2(x-2y)^{3/2}\Big]\\ -\frac{2a}{3f^2}\Big[&(3\alpha_{\rm o1}+\alpha_{\rm o2})L_\pi+\Big(4\alpha_{\rm o1}-\frac{2}{3}\alpha_{\rm o2}\Big)L_K\\ &+\Big(\alpha_{\rm o1}-\frac{1}{3}\alpha_{\rm o2}\Big)L_\eta\Big], \end{aligned} \tag{66}$$

$$\begin{aligned} m_{K^*}=m_{\rm O}(a)+\lambda_x(a)x-\lambda_y(a)y-\frac{1}{12\pi f^2}\Big[&\frac{3}{2}g_2^2(x+2y)^{3/2}\\ &+\Big(g_1^2+\frac{5}{3}g_2^2\Big)(x-y)^{3/2}+\frac{1}{6}g_2^2(x-2y)^{3/2}\Big]\\ -\frac{2a}{3f^2}\Big[&\Big(3\alpha_{\rm o1}-\frac{1}{2}\alpha_{\rm o2}\Big)L_\pi+\Big(4\alpha_{\rm o1}+\frac{1}{3}\alpha_{\rm o2}\Big)L_K\\ &+\Big(\alpha_{\rm o1}+\frac{1}{6}\alpha_{\rm o2}\Big)L_\eta\Big], \end{aligned} \tag{67}$$

$$m_+=m_{(00)}+\frac{m_{(08)}^2}{m_{(00)}-m_{(88)}}, \tag{68}$$

$$m_-=m_{(88)}-\frac{m_{(08)}^2}{m_{(00)}-m_{(88)}}, \tag{69}$$

$$\begin{aligned} m_{(88)}=m_{\rm O}(a)+\lambda_x(a)x-2\lambda_y(a)y-\frac{1}{12\pi f^2}\Big[&2g_2^2(x+2y)^{3/2}\\ &+\frac{2}{3}g_2^2(x-y)^{3/2}+\Big(g_1^2+\frac{2}{3}g_2^2\Big)(x-2y)^{3/2}\Big]\\ -\frac{2a}{3f^2}\Big[&\Big(3\alpha_{\rm o1}-\alpha_{\rm o2}\Big)L_\pi+\Big(4\alpha_{\rm o1}+\frac{2}{3}\alpha_{\rm o2}\Big)L_K\\ &+\Big(\alpha_{\rm o1}+\frac{1}{3}\alpha_{\rm o2}\Big)L_\eta\Big], \end{aligned} \tag{70}$$

$$\begin{aligned} m_{(00)}=m_{\rm S}(a)+\sigma_x(a)x-\frac{1}{12\pi f^2}g_1^2[&3(x+2y)^{3/2}\\ &+4(x-y)^{3/2}+(x-2y)^{3/2}]\\ -\frac{2a}{3f^2}\alpha_{\rm s}[&3L_\pi+4L_K+L_\eta], \end{aligned} \tag{71}$$

[8]This assumption means that the diagonal part is dominant compared to the off-diagonal element, $\{\Delta\mu+a\Delta\alpha-(\Sigma'_{\rm S}-\Sigma_{\rm O})\}^2>4(\Sigma_{\rm OS})^2$

$$m_{(08)} = \sigma_y(a)y - \frac{1}{12\pi f^2} g_1 g_2 \sqrt{\frac{2}{3}}[3(x+2y)^{3/2} - 2(x-y)^{3/2} - (x-2y)^{3/2}] - \frac{a}{3f^2}\alpha_{\rm os}\sqrt{\frac{2}{3}}[3L_\pi - 2L_K - L_\eta], \quad (72)$$

$$\tan 2\theta = \frac{2m_{(08)}}{m_{(00)} - m_{(88)}}, \quad (73)$$

where θ denotes the mixing angle in the ρ^8-ϕ^0 sector. We introduced the two parameters

$$x = \frac{2B}{3}(2\tilde{m} + \tilde{m}_{\rm s}), \quad (74)$$

$$y = \frac{B}{3}(\tilde{m} - \tilde{m}_{\rm s}), \quad (75)$$

as a short hand notation for convenient combinations of quark masses [1]. The leading order pseudoscalar masses assume a very simple form in terms of x and y,

$$\tilde{m}_\pi^2 = x + 2y, \qquad \tilde{m}_K^2 = x - y, \qquad \tilde{m}_\eta^2 = x - 2y. \quad (76)$$

For the chiral logarithms stemming from the loop integration we have introduced

$$L_\pi = \frac{\tilde{m}_\pi^2}{16\pi^2}\ln\left(\frac{\tilde{m}_\pi^2}{\mu^2}\right), \qquad L_K = \frac{\tilde{m}_K^2}{16\pi^2}\ln\left(\frac{\tilde{m}_K^2}{\mu^2}\right), \qquad L_\eta = \frac{\tilde{m}_\eta^2}{16\pi^2}\ln\left(\frac{\tilde{m}_\eta^2}{\mu^2}\right). \quad (77)$$

The functions

$$m_{\rm O}(a) = V_0 + V_1 a + V_2 a^2 + V_3 a^3, \quad (78)$$

$$m_{\rm S}(a) = S_0 + S_1 a + S_2 a^2 + S_3 a^3, \quad (79)$$

$$\lambda_x(a) = \lambda_x^{(0)} + \lambda_x^{(1)} a, \qquad \lambda_y(a) = \lambda_y^{(0)} + \lambda_y^{(1)} a, \quad (80)$$

$$\sigma_x(a) = \sigma_x^{(0)} + \sigma_x^{(1)} a, \qquad \sigma_y(a) = \sigma_y^{(0)} + \sigma_y^{(1)} a, \quad (81)$$

parametrize the analytic lattice spacing dependence. We have, for convenience and for the sake of transparency, introduced new constants V_i, S_i, $i = 1, \ldots 4$ and $\lambda_{x,y}^{(j)}$, $\sigma_{x,y}^{(j)}$, $j = 1, 2$. These new constants are combinations of the low-energy constants in the chiral Lagrangian. They are explicitly given

$$V_0 = \mu_{\rm o}, \qquad V_1 = \alpha_{\rm o1}, \qquad V_2 = \beta_{\rm o}, \quad (82)$$

$$S_0 = \mu_{\rm s}, \qquad S_1 = \alpha_{\rm s}, \qquad S_2 = \beta_{\rm s}, \quad (83)$$

$$\lambda_x^{(0)} = \frac{N\lambda_{\rm o1} + 2\lambda_{\rm o2}}{2B}, \qquad \lambda_x^{(1)} = \frac{N\gamma_{\rm o1}^r + 2\gamma_{\rm o2}^r}{2B}, \quad (84)$$

$$\lambda_y^{(0)} = \frac{\lambda_{\rm o2}}{B}, \qquad \lambda_y^{(1)} = \frac{\gamma_{\rm o2}^r}{B}, \quad (85)$$

$$\sigma_x^{(0)} = \frac{N\lambda_{\rm s}}{2B}, \qquad \sigma_x^{(1)} = \frac{N\gamma_{\rm s}^r}{2B}, \quad (86)$$

$$\sigma_y^{(0)} = \frac{\sqrt{6}\lambda_{\rm os}}{B}, \qquad \sigma_y^{(1)} = \frac{\sqrt{6}\gamma_{\rm os}^r}{B}. \quad (87)$$

However, from a practical point of view there is no need to keep track of the original low-energy constants. Note that we have added an $O(a^3)$ term for the octet and singlet vector meson mass, but not for the singlet-octet mixed contribution $m_{(08)}$, as discussed in sect. III C.

Note that there are chiral logarithms present in the results for the vector meson masses. These chiral corrections are a lattice artifact, as can be seen from the presence of the a in front of the logarithms. This chiral log contribution vanishes in the continuum limit and the mass formulas converge to the results given in Ref. [8]. However, as long as the lattice spacing is nonzero, there are two kinds of nonanalytical quark mass dependence, proportional to $m_q^{3/2}$ and $m_q \log m_q$. It will be very interesting to study the competition of these two contributions in actual lattice simulations.

Let us count the number of unknown parameters. In the case of the ρ and K^* meson, we find 12 unknown combinations of low-energy constants: V_i, $\lambda_x^{(j)}$, $\lambda_y^{(j)}$, g_1, g_2, $\alpha_{\rm o1}$, $\alpha_{\rm o2}$. However, as long as we are interested in performing fits to lattice data at a given and fixed lattice spacing a, this number essentially reduces to seven independent constants: $m_{\rm O}$, λ_x, λ_y, g_1, g_2, $\alpha_{\rm o1}$, $\alpha_{\rm o2}$. For the $m_\pm$ sector, we have additional ten low-energy constants: S_i, $\sigma_x^{(j)}$, $\sigma_y^{(j)}$, $\alpha_{\rm os}$, $\alpha_{\rm s}$. When we consider at a fixed lattice spacing, there are essentially five independent constants: $m_{\rm S}$, σ_x, σ_y, $\alpha_{\rm os}$, $\alpha_{\rm s}$.

IV. CONCLUDING REMARKS

We have derived the one-loop expressions for vector meson masses using an effective theory based on the heavy vector meson formalism of Ref. [8]. The effects due to a nonvanishing lattice spacing introduce a fair number of new unknown low-energy constants in the chiral Lagrangian. However, the actual number of fit parameters in the mass formulas seems small enough for the expressions to be useful for the chiral extrapolation of actual lattice data. In the case of the ρ and K^* meson mass, the number of unknown fit parameters is seven. The numerical simulations of the CP-PACS/JLQCD collaboration are carried out with five different (degenerate) up and down quark masses and two different values for the strange quark mass. The total number of independent data points is 18 without data for the ϕ and ω mesons. If one measures these masses including noisy disconnected contributions, the number of

data points increases to 36. In both cases the number of data points is well above 7.

Here we have calculated the expressions for the vector meson masses only. In the calculation of the vector meson decay constants some additional low-energy constants enter, depending on the choice for the vector current. Apart from this, the calculation is straightforward and currently under way [20].

Our main motivation for the calculation presented here was to derive fit forms for the chiral extrapolation of the vector meson masses. Whether ratios $m_{\rm PS}/m_V \simeq 0.62$–$0.78$ are light enough to be in the regime where our results are applicable is *a priori* not known. The values are still fairly heavy and one may have doubts, but careful fits will eventually answer this question.

However, provided our formulas describe the lattice QCD data well, we obtain, as a byproduct, estimates for the low-energy constants of the chiral effective theory for vector mesons. Particularly promising are the leading order parameters g_1 and g_2. These couplings are not corrected by lattice artifacts through $\mathrm{O}(E^3)$. Provided that the corrections of $\mathrm{O}(E^4)$ and higher are negligible, we have a good chance to determine g_1 and g_2 in a fit, even if lattice data is available for one lattice spacing only.[9] The chiral quark model [21] predicts $g_2 = 0.75$ in the large N_c limit where $g_1 = \frac{2}{\sqrt{3}} g_2$. On the other hand, the estimate $g_2 \sim 0.6$ is given in Ref. [22], where vector meson χPT is applied to τ decay processes together with a comparison of the results with experimental data. If we are able to extract g_1 and g_2 in a fit to lattice QCD data, we obtain results based on first principles QCD without relying on model dependent assumptions or the large N_c limit.

The heavy vector meson formalism of Ref. [8] is not the only way to derive an effective theory for vector mesons. Another approach employs the so-called hidden local symmetry [23]. Also this approach has a definite counting scheme, and in principle one can formulate it for nonzero lattice spacing too. The two effective theories are, however, not equivalent at any given order in the expansion. It might therefore be interesting to perform the calculation of the vector meson masses based on this hidden local symmetry approach and compare the two effective theories.

ACKNOWLEDGMENTS

This work is supported in part by the Grants-in-Aid for Scientific Research from the Ministry of Education, Culture, Sports, Science and Technology (Nos. 13135204, 15204015, 15540251, 16028201, 16.11968). O. B. is supported in part by the University of Tsukuba Research Project. S. T. is supported by the Japan Society for the Promotion of Science for Young Scientists.

[9]Even though fits of lattice data at one lattice spacing are possible it seems mandatory to fit data for various lattice spacings in order to check that one is indeed in the chiral regime where our formulas can be applied.

APPENDIX: FEYNMAN RULES

In this appendix, we present the Feynman rules needed in the calculation for the vector meson masses. The lattice spacing a shown in the following equations stems from the spurion field $W_\pm$ once the replacement $A \to aI$ has been made.

1. Expanding the Lagrangian

In terms of the component fields, the LO Lagrangian which includes up to two pseudoscalar meson fields is expressed as

$$\mathcal{L}_{\rm LO} = \mathcal{L}_p + \mathcal{L}_a = (\mathcal{L}_p^{0\pi} + \mathcal{L}_a^{0\pi}) + \mathcal{L}_p^{1\pi} + (\mathcal{L}_p^{2\pi} + \mathcal{L}_a^{2\pi}) + O(\pi^3), \tag{A1}$$

$$\mathcal{L}_p^{0\pi} + \mathcal{L}_a^{0\pi} = S_\mu^\dagger(-iv\cdot\partial + a\alpha_{\rm s})S^\mu + \sum_a \rho_\mu^{a\dagger}(-iv\cdot\partial + a\alpha_{\rm o1})\rho^{a\mu}, \tag{A2}$$

$$\mathcal{L}_p^{1\pi} = \frac{ig_1}{f}\sum_a (S_\mu^\dagger \rho_\nu^a - S_\mu \rho_\nu^{a\dagger})\partial_\lambda \pi_a v_\sigma \epsilon^{\mu\nu\lambda\sigma} + \frac{ig_2\sqrt{2}}{f}\sum_{a,b,c} d_{abc}\rho_\mu^{a\dagger}\rho_\nu^b \partial_\lambda \pi_c v_\sigma \epsilon^{\mu\nu\lambda\sigma}, \tag{A3}$$

$$\begin{aligned}\mathcal{L}_p^{2\pi} + \mathcal{L}_a^{2\pi} = &-\frac{i}{f^2}\sum_{a,b,c,d,e} f_{ade}f_{bce}\rho_\mu^{a\dagger}\pi^b(v\cdot\partial\pi^c)\rho^{d\mu} \\ &- a\frac{\sqrt{2}\alpha_{\rm os}}{Nf^2}\sum_{a,b,c} d_{abc}(S^\mu \rho_\mu^{a\dagger}\pi^b\pi^c \\ &+ S^{\mu\dagger}\rho_\mu^a\pi^b\pi^c) - a\frac{2}{Nf^2}\sum_{a,b,c,d}\Big(\alpha_{\rm o1}\delta_{ab}\delta_{cd} \\ &+ \alpha_{\rm o2}\sum_e d_{abe}d_{cde}\Big)\rho_\mu^{a\dagger}\rho^{\mu b}\pi^c\pi^d \\ &- a\frac{2\alpha_{\rm s}}{Nf^2}\sum_{a,b}\delta_{ab}S_\mu^\dagger S^\mu \pi^a\pi^b,\end{aligned} \tag{A4}$$

where the newly introduced coefficients relate to the ones defined in Eq. (30) according to

$$\alpha_{\rm s} = N\alpha_1, \tag{A5}$$

$$\alpha_{\rm os} = N\alpha_2, \tag{A6}$$

$$\alpha_{\rm o1} = 2\alpha_3 + N\alpha_4, \tag{A7}$$

$$\alpha_{o2} = N\alpha_3. \tag{A8}$$

The summation over roman indices is understood to range from 1 to 8. f_{abc} and d_{abc} are the structure constants and the totally symmetric d-symbol of $su(N)$ respectively. Obviously, we are most interested in the case $N = 3$.

The NLO and NNLO Lagrangian results in the following tree level contribution to the vector meson masses:

$$\begin{aligned}\mathcal{L}_{\mathrm{NLO}} + \mathcal{L}_{\mathrm{NNLO}} &= (\mathcal{L}_m + \mathcal{L}_{a^2}) + \mathcal{L}_{am} \\ &= \mathcal{L}_m^{0\pi} + \mathcal{L}_{a^2}^{0\pi} + \mathcal{L}_{am}^{0\pi} + O(\pi),\end{aligned} \tag{A9}$$

$$\begin{aligned}\mathcal{L}_m^{0\pi} + \mathcal{L}_{a^2}^{0\pi} + \mathcal{L}_{am}^{0\pi} &= (N\tilde{M}_0\lambda_s + a^2\beta_s + N\tilde{M}_0 a\gamma_s + \Delta\mu)S_\mu^\dagger S^\mu + (\lambda_{os} + a\gamma_{os})\frac{\tilde{M}_8}{\sqrt{2}}\sum_a \delta_{a8}(\rho_\mu^{a\dagger} S^\mu + \rho_\mu^a S^{\mu\dagger}) \\ &\quad + (N\tilde{M}_0\lambda_{o1} + a^2\beta_o + N\tilde{M}_0 a\gamma_{o1})\sum_a \rho_\mu^{a\dagger}\rho^{\mu a} + (\lambda_{o2} + a\gamma_{o2})\sum_{a,b}(2\tilde{M}_0\delta_{ab} + \tilde{M}_8 d_{ab8})\rho_\mu^{a\dagger}\rho^{\mu b},\end{aligned} \tag{A10}$$

where

$$\beta_s = N\beta_1 + N^2\beta_2, \tag{A11}$$

$$\beta_o = 2\beta_5 + \beta_6 + 2N\beta_7 + N\beta_8 + N^2\beta_9, \tag{A12}$$

$$\gamma_s = \gamma_1 + N\gamma_2, \tag{A13}$$

$$\gamma_{os} = 2\gamma_4 + N\gamma_5, \tag{A14}$$

$$\gamma_{o1} = 2\gamma_6 + \gamma_7 + N\gamma_8, \tag{A15}$$

$$\gamma_{o2} = 2\gamma_9 + \gamma_{10} + N\gamma_{11}. \tag{A16}$$

2. Propagators

The propagator for the singlet and octet vector meson is given by

$$G^S_{\mu\nu}(r) = \frac{-iP_{\mu\nu}}{v\cdot r - a\alpha_s}, \tag{A17}$$

$$G^{O,ab}_{\mu\nu}(r) = \frac{-iP_{\mu\nu}\delta^{ab}}{v\cdot r - a\alpha_{o1}}, \tag{A18}$$

where r_μ is the residual momentum.

For the pseudoscalar meson, the propagator is

$$G^{ab}_{PS}(p) = \frac{i\delta^{ab}}{p^2 - \tilde{m}_a^2}, \tag{A19}$$

where the leading order pseudoscalar mass $\tilde{m}_a^2$ of Ref. [1] is used. The explicit form of the mass is

$$\tilde{m}_a^{\,2} = m_a^2(1 - Nc_3 - \tilde{c}_3) - m_{av}^2 Nc_3 - Nc_2 - \tilde{c}_2, \tag{A20}$$

with

$$m_{av}^2 = \frac{1}{N^2-1}\sum_a m_a^2, \tag{A21}$$

where m_a^2 is the meson mass in the continuum limit (i.e. $m_1^2 = m_2^2 = m_3^2 = m_\pi^2$, $m_4^2 = m_5^2 = m_6^2 = m_7^2 = m_K^2$, $m_8^2 = m_\eta^2$). c_1, c_3, $\tilde{c}_3$ are O(a) terms [17], and c_2, $\tilde{c}_2$ are O(a^2) terms [9,24]. They are low-energy constants in the pure pseudoscalar meson sector. The mass $\tilde{m}_a^2$ is expressed in terms of the shifted quark masses,

$$\tilde{m}_a^{\,2} = \begin{cases} \tilde{m}_\pi^2 = 2B\tilde{m}, & a = 1, 2, 3, \\ \tilde{m}_K^2 = B(\tilde{m} + \tilde{m}_s), & a = 4, 5, 6, 7, \\ \tilde{m}_\eta^2 = \frac{2B}{3}(\tilde{m} + 2\tilde{m}_s), & a = 8. \end{cases} \tag{A22}$$

3. Vertices

(i) NLO vector-vector 2-point vertex from $\mathcal{L}_m^{0\pi} + \mathcal{L}_{a^2}^{0\pi} + \mathcal{L}_{am}^{0\pi}$

$\nu,\ b$ $\qquad$ $\mu,\ a$

$$\begin{aligned}&= iP_{\mu\nu}[\delta_{ab}(N\tilde{M}_0\lambda_{o1} + a^2\beta_o + N_a\tilde{M}_0\gamma_{o1} \\ &\quad + (2\tilde{M}_0\delta_{ab} + \tilde{M}_8 d_{ab8}(\lambda_{o2} + a\gamma_{o2})],\end{aligned}$$

$\nu,\ a$ $\qquad$ μ

$$= iP_{\mu\nu}\delta_{a8}\frac{\tilde{M}_8}{\sqrt{2}}(\lambda_{os} + a\gamma_{os}),$$

ν $\qquad$ μ

$$= iP_{\mu\nu}(N\tilde{M}_0\lambda_s + a^2\beta_s + Na\tilde{M}_0\gamma_s + \Delta\mu).$$

The oriented narrow line represents the singlet vector meson and the oriented wide line represents the octet vector meson.

(ii) LO vector-vector-pseudo-scalar 3-point vertex from $\mathcal{L}_p^{1\pi}$

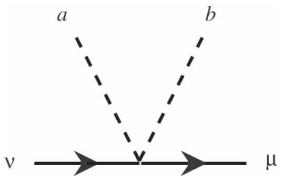

$$= \frac{ig_1}{f} p_\lambda v_\sigma \epsilon^{\mu\nu\lambda\sigma} \delta_{ab},$$

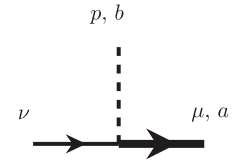

$$= \frac{ig_1}{f} p_\lambda v_\sigma \epsilon^{\mu\nu\lambda\sigma} \delta_{ab},$$

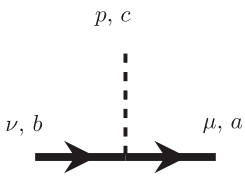

$$= \frac{ig_2\sqrt{2}}{f} p_\lambda u_\sigma \epsilon^{\mu\nu\lambda\sigma} d_{abc}.$$

The dotted line represents the incoming pseudoscalar meson.

(iii) LO vector-vector-pseudoscalar-pseudoscalar 4-point vertex from $\mathcal{L}_a^{2\pi}$

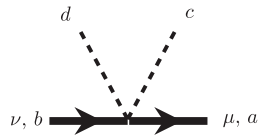

$$= iP_{\mu\nu}\left[-a\frac{4}{Nf^2}(\alpha_{o1}\delta_{ab}\delta_{cd} + \alpha_{o2}\Sigma_e d_{abe}d_{cde}) \right],$$

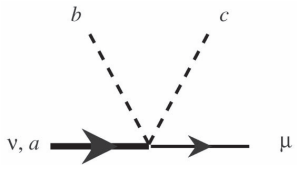

$$= iP_{\mu\nu}\left[-a\frac{2\sqrt{2}}{Nf^2}\alpha_{os} d_{abc} \right],$$

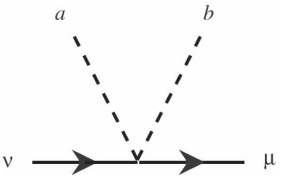

$$= iP_{\mu\nu}\left[-a\frac{4}{Nf^2}\alpha_s \delta_{ab} \right].$$

[1] S. Aoki, O. Bär, T. Ishikawa, and S. Takeda, Phys. Rev. D **73**, 014511 (2006).
[2] S. Aoki, O. Bär, T. Ishikawa, and S. Takeda, to be published.
[3] T. Ishikawa *et al.*, Nucl. Phys. B, Proc. Suppl. **140**, 225 (2005).
[4] S. R. Sharpe and Robert J. Singleton, Phys. Rev. D **58**, 074501 (1998).
[5] W.-J. Lee and S. R. Sharpe, Phys. Rev. D **60**, 114503 (1999).
[6] O. Bär, Nucl. Phys. B, Proc. Suppl. **140**, 106 (2005).
[7] H. R. Grigoryan and A. W. Thomas, Phys. Lett. B **632**, 657 (2006).
[8] E. Jenkins, A. V. Manohar, and M. B. Wise, Phys. Rev. Lett. **75**, 2272 (1995).
[9] S. Aoki, Phys. Rev. D **68**, 054508 (2003).
[10] Y. Namekawa *et al.*, Phys. Rev. D **70**, 074503 (2004).
[11] E. Jenkins and A. V. Manohar, Phys. Lett. B **255**, 558 (1991).
[12] J. Bijnens and P. Gosdzinsky, Phys. Lett. B **388**, 203 (1996).
[13] J. Bijnens, P. Gosdzinsky, and P. Talavera, Phys. Lett. B **429**, 111 (1998).
[14] J. Bijnens, P. Gosdzinsky, and P. Talavera, Nucl. Phys. **B501**, 495 (1997).
[15] M. Booth, G. Chiladze, and A. F. Falk, Phys. Rev. D **55**, 3092 (1997).
[16] C.-K. Chow and S.-J. Rey, Nucl. Phys. **B528**, 303 (1998).
[17] G. Rupak and N. Shoresh, Phys. Rev. D **66**, 054503 (2002).
[18] S. Scherer, Adv. Nucl. Phys. **27**, 277 (2003).
[19] S. Aoki, Phys. Rev. D **34**, 3170 (1986).
[20] S. Aoki and S. Takeda (work in progress).
[21] A. Manohar and H. Georgi, Nucl. Phys. **B234**, 189 (1984).
[22] H. Davoudiasl and M. B. Wise, Phys. Rev. D **53**, 2523 (1996).
[23] M. Harada and K. Yamawaki, Phys. Rep. **381**, 1 (2003).
[24] O. Bär, G. Rupak, and N. Shoresh, Phys. Rev. D **70**, 034508 (2004).

PHYSICAL REVIEW D **74,** 034511 (2006)

Automatic $O(a)$ improvement for twisted mass QCD in the presence of spontaneous symmetry breaking

Sinya Aoki[1,2] and Oliver Bär[1,3]

[1]*Graduate School of Pure and Applied Sciences, University of Tsukuba, Tsukuba 305-8571, Ibaraki Japan*
[2]*Riken BNL Research Center, Brookhaven National Laboratory, Upton, New York 11973, USA*
[3]*Institute of Physics, Humboldt University Berlin, Newtonstrasse 15, 12489 Berlin, Germany*

(Received 29 May 2006; published 23 August 2006)

In this paper we present a proof for automatic $O(a)$ improvement in twisted mass lattice QCD at maximal twist, which uses only the symmetries of the leading part in the Symanzik effective action. In the process of the proof we clarify that the twist angle is dynamically determined by vacuum expectation values in the Symanzik theory. For maximal twist according to this definition, we show that scaling violations of all quantities which have nonzero values in the continuum limit are even in a. In addition, using Wilson chiral perturbation theory, we investigate this definition for maximal twist and compare it to other definitions which were already employed in actual simulations.

DOI: 10.1103/PhysRevD.74.034511 PACS numbers: 11.15.Ha

I. INTRODUCTION

It becomes more and more apparent that twisted mass lattice QCD (tmLQCD) [1,2] is a promising formulation to approach the chiral limit of QCD, despite the fact that the flavor symmetry is explicitly broken. A twisted mass protects the Wilson-Dirac operator against small eigenvalues and therefore solves the problem of exceptional configurations, thus making numerical simulations with small quark masses feasible. Recent studies [3–6] in the quenched simulation were performed with m_π/m_ρ values as small as 0.3 without running into problems due to exceptional configurations. Even though it will be challenging to reach such small pion masses in dynamical simulations, $m_\pi/m_\rho < 0.5$ seems fairly possible [7]. This numerical advantage of tmLQCD is supplemented by the property of automatic $O(a)$ improvement at maximal twist [8–10]. For a recent review of these and some more results in twisted mass LQCD see Ref. [11].

Some issues, however, remain to be fully understood. The proof of automatic $O(a)$ improvement in Ref. [8] makes use of the symmetries $m_q \equiv m_0 - m_{\rm cr} \to -m_q$ and $r \to -r$, where m_0 is the bare (untwisted) quark mass, r is the parameter in the Wilson term and $m_{\rm cr}(r)$ is the critical quark mass. Maximal twist is defined by setting the bare mass to a critical value, $m_0 = m_{\rm cr}(r)$. A concrete definition of $m_{\rm cr}(r)$ is not required in the proof as long as the symmetry property $m_{\rm cr}(-r) = -m_{\rm cr}(r)$ is satisfied, and tuning to the bare quark mass where the pion mass vanishes has been suggested as one particular choice for $m_{\rm cr}(r)$ (we call this definition ''the pion mass definition'' in the following). However, it was pointed out in Ref. [12] that the condition $m_{\rm cr}(-r) = -m_{\rm cr}(r)$ is violated for the pion mass definition by nonperturbative effects. Consequently, the $O(a^2)$ scaling violation, expected from an $O(a)$ improved theory, is lost unless the twisted quark mass satisfies the bound $\mu > a^2\Lambda_{\rm QCD}^3$. Instead, terms linear in a and with fractional powers of a are predicted by Wilson chiral perturbation theory (WChPT) for very small twisted quark masses. On the other hand, automatic $O(a)$ improvement is expected to hold if the critical mass is defined through the partially conserved axial vector Ward identity quark mass (PCAC mass definition).

A recent paper [13] comes to a different conclusion. It is claimed that both the pion and the PCAC mass definition guarantee automatic $O(a)$ improvement, but the remaining $O(a^2)$ effects differ significantly. In particular, the pion mass definition for $m_{\rm cr}$ exhibits cutoff artifacts of $O(a^2/m_\pi^2)$ which are enhanced for small pion masses. These enhanced lattice artifacts are shown to be absent for the PCAC mass definition.

Closely related to the issue of automatic $O(a)$ improvement is the so-called ''bending phenomenon,'' observed in quenched simulations [3–6]. The pion mass, the pion decay constant, and the vector meson mass show an unexpected strong nonlinear quark mass dependence for small quark masses if the pion mass definition for the critical quark mass is used. This curvature is significantly reduced and consistent with an $O(a^2)$ scaling violation [14] when the untwisted quark mass is tuned according to the optimal choice proposed in Ref. [13]. That this bending is indeed a lattice artifact of the twisted mass formulation is also supported by calculations using the overlap operator on the same gauge field configurations with similarly small pion masses. Here the bending is absent [3].

In this paper we revisit the property of automatic $O(a)$ improvement in twisted mass QCD. We first give an alternative proof for automatic $O(a)$ improvement at maximal twist which uses only the symmetries of the leading term in the Symanzik effective action. Our proof follows closely the one given in [13], even though we generalize it and also consider lattice operators which are not multiplicatively renormalizable but involve the subtraction of power divergencies. We also do not make use of equations of motions in our proof. However, the main point is that we can clarify the meaning of ''maximal twist'' in the process of our

proof. We will argue that, in presence of spontaneous symmetry breaking, the twist angle θ is determined dynamically by the ratio of two vacuum expectation values in the Symanzik theory, namely,

$$\cot\theta = \frac{\langle\bar{\psi}\psi\rangle}{\langle\bar{\psi}i\gamma_5\tau^3\psi\rangle}. \tag{1}$$

Provided that the mass parameters of the theory are tuned such that $\theta = \pm\pi/2$, we can show that the scaling violations of observables start with a^2, i.e. the theory is $O(a)$ improved.[1] This definition of maximal twist is not afflicted with infrared enhanced cutoff effects of $O(a^2/m_\pi^2)$ discussed in Ref. [13].

We also investigate this new definition for maximal twist using WChPT [16,17] (for a review see Ref. [18]). We explicitly show the absence of $O(a, a\mu)$ contributions in the expressions for the pion mass and decay constant.

We finally compare our new criterion with other definitions of maximal twist, the pion mass and the PCAC mass definition, which were previously employed in numerical simulations. We find that, although these two definitions show asymptotic a^2 scaling violations, they do not exhibit the expected a^2 scaling until a becomes small such that the bound $\mu > a^2\Lambda_{\rm QCD}^3$ is satisfied.

II. ALTERNATIVE PROOF OF $O(a)$ IMPROVEMENT

A. Main idea for $O(a)$ improvement

The twisted mass lattice QCD action for the 2-flavor theory is given by

$$S_{\rm tmQCD} = S_G + S_{\rm tm}. \tag{2}$$

The details of the gauge action S_G are irrelevant in the following, so we leave it unspecified. $S_{\rm tm}$ denotes the 2-flavor Wilson fermion action with a twisted mass term, which is defined as

$$S_{\rm tm} = \sum_{x,\mu}\bar{\psi}_L(x)\frac{1}{2}[\gamma_\mu(\nabla_\mu^+ + \nabla_\mu^-)\psi_L - ar\nabla_\mu^+\nabla_\mu^-\psi_L](x) + \sum_x \bar{\psi}_L(x)M_0 e^{i\theta_0\gamma_5\tau^3}\psi_L(x) \tag{3}$$

with

$$[\nabla_\mu^+\psi_L](x) = \frac{1}{a}(U_\mu(x)\psi_L(x+\mu) - \psi_L(x)), \tag{4}$$

$$[\nabla_\mu^-\psi_L](x) = \frac{1}{a}(\psi_L(x) - U_\mu^\dagger(x-\mu)\psi_L(x-\mu)) \tag{5}$$

being the standard forward and backward difference operators. We supplemented the fields with the subscript "L" in order to highlight the fact that these fields are lattice fields. The parameters M_0 and θ_0 denote the bare mass and bare twist angle. Instead of using this exponential notation, it is also customary to write

$$M_0 e^{i\theta_0\gamma_5\tau^3} = m_0 + i\mu_0\gamma_5\tau^3, \tag{6}$$

where the bare untwisted mass m_0 and the bare twisted mass μ_0 are given by

$$m_0 = M_0\cos\theta_0, \qquad \mu_0 = M_0\sin\theta_0. \tag{7}$$

The lattice action (2) is invariant under the following global symmetry transformations [2,19]:

(1) U(1) ⊗ U(1) vector symmetry

$$\psi_L \to e^{i(\alpha_0+\alpha_3\tau^3)}\psi_L, \qquad \bar{\psi}_L \to \bar{\psi}_L e^{-i(\alpha_0+\alpha_3\tau^3)}.$$

This transformation is part of the U(2) flavor symmetry of the untwisted theory.

(2) Extended parity symmetry

$$P_F^{1,2}\colon \psi_L \to \tau^{1,2}P\psi_L, \qquad \bar{\psi}_L \to P\bar{\psi}_L\tau^{1,2}, \tag{8}$$

where P is the parity transformation, given by

$$P\psi_L(\vec{x},t) = i\gamma_0\psi_L(-\vec{x},t),$$
$$P\bar{\psi}_L(\vec{x},t) = -i\bar{\psi}_L(-\vec{x},t)\gamma_0.$$

For the gauge fields P_F is equal to the standard parity transformation. Note that ordinary parity P is not a symmetry unless it is combined with a flavor rotation in the 1 or 2 direction. Alternatively, one can also augment P with a sign change of the twisted mass term μ_0,

$$\tilde{P} = P\times[\mu_0 \to -\mu_0], \tag{9}$$

which is also a symmetry of the action.

(3) Charge conjugation symmetry

$$C\colon \psi_L(x) \to i\gamma_0\gamma_2\bar{\psi}_L(x)^T,$$
$$\bar{\psi}_L(x) \to -\psi_L(x)^T i\gamma_0\gamma_2,$$

together with the charge conjugation transformation for the gauge fields, $U(x,\mu) \to U(x,\mu)^*$.

Besides these symmetries the lattice action is also invariant under hypercubic lattice rotations and local gauge transformations.

According to Symanzik [20,21], the lattice theory can be described by an effective continuum theory. The form of the effective action of this theory is restricted by locality and the symmetries of the underlying lattice theory. Taking into account the symmetries listed above one finds [19]

$$S_{\rm eff} = S_0 + aS_1 + a^2S_2 + \cdots, \tag{10}$$

where the first two terms are given as

[1] Automatic $O(a)$ improvement in a theory without spontaneous symmetry breaking has been studied in the two-dimensional Schwinger model in Ref. [15].

$$S_0 = S_{0,\text{gauge}} + \int d^4x \bar{\psi}(x)[\gamma_\mu D_\mu + M_R e^{i\theta\gamma_5\tau^3}]\psi(x), \tag{11}$$

$$S_1 = C_1 \int d^4x \bar{\psi}(x)\sigma_{\mu\nu}F_{\mu\nu}(x)\psi(x). \tag{12}$$

$S_{0,\text{gauge}}$ denotes the standard continuum gauge field action in terms of the gauge field tensor $F_{\mu\nu}$. The second term in S_0 is the continuum twisted mass fermion action. The mass parameters are renormalized masses, and we assume the renormalization scheme in [1].[2] It is worth mentioning that there is no "twisted" Pauli term $\bar{\psi}\gamma_5\tau^3\sigma_{\mu\nu}F_{\mu\nu}\psi$ present in S_1, since such a term violates the symmetry in Eq. (9).[3]

In addition to the effective action, we have to specify the direction of the chiral condensate, since chiral symmetry is spontaneously broken. From the fact that the direction of the chiral condensate is completely controlled by the direction of the symmetry breaking external field (i.e. the quark mass) in the continuum theory, we can take

$$\langle \bar{\psi}^i_\alpha \psi^j_\beta \rangle_{S_0} = \frac{v(M_R)}{8}[e^{-i\theta\gamma_5\tau^3}]^{ji}_{\beta\alpha}, \tag{13}$$

where $\lim_{M_R\to 0}\lim_{V\to\infty} v(M_R) \neq 0$.[4] Here the vacuum expectation value (VEV) is defined with respect to the continuum action S_0. To say it differently, the VEV (13) defines the twist angle θ in the Symanzik theory. The above condensate is equivalent to

$$\langle \bar{\psi}\psi \rangle_{S_0} = v(M_R)\cos\theta, \tag{14}$$

$$\langle \bar{\psi} i\gamma_5\tau^3\psi \rangle_{S_0} = v(M_R)\sin\theta. \tag{15}$$

We now want to argue that the choice $\theta = \pi/2$ (or $-\pi/2$) corresponds to maximal twist. In terms of the mass parameters this is equivalent to $M_R = \mu_R$ and $m_R = 0$. In this case the action and the VEVs become

$$S_0 = S_{0,\text{gauge}} + \int d^4x \bar{\psi}[\gamma_\mu D_\mu + iM_R\gamma_5\tau^3]\psi(x), \tag{16}$$

$$S_1 = C_1 \int d^4x \bar{\psi}(x)\sigma_{\mu\nu}F_{\mu\nu}(x)\psi(x), \tag{17}$$

$$\langle \bar{\psi}\psi \rangle_{S_0} = 0, \tag{18}$$

$$\langle \bar{\psi} i\gamma_5\tau^3\psi \rangle_{S_0} = v(M_R). \tag{19}$$

It is easy to check that S_0, the continuum part of the effective action, is invariant under

$$\psi \to e^{iw\gamma_5\tau^{1,2}}\psi, \qquad \bar{\psi} \to \bar{\psi}e^{iw\gamma_5\tau^{1,2}}, \tag{20}$$

and therefore also under the Z_2 subgroup T_1 of this continuous transformation, defined by[5]

$$T_1\psi = i\gamma_5\tau^1\psi, \qquad T_1\bar{\psi} = \bar{\psi}i\gamma_5\tau^1. \tag{21}$$

Since $T_1^2 = 1$ in the space of fermion number conserving operators, which contain equal numbers of ψ and $\bar{\psi}$, the eigenvalues of T_1 are 1 (T_1 even) or -1 (T_1 odd). The crucial observation is that the VEVs (18) and (19) are also invariant under this transformation. The symmetry (20) (and its discrete subgroup T_1) is *not* spontaneously broken, hence it is an exact symmetry of the continuum theory. The $O(a)$ term

$$aS_1 = aC_1 \int d^4x \bar{\psi}(x)\sigma_{\mu\nu}F_{\mu\nu}(x)\psi(x), \tag{22}$$

on the other hand, is odd under T_1. Therefore, nonvanishing physical observables, which must be even under T_1, cannot have an $O(a)$ contribution, since the $O(a)$ term is odd under T_1 and therefore must vanish identically. This is automatic $O(a)$ improvement at maximal twist.[6] Note that noninvariant, i.e. T_1-odd quantities, which vanish in the continuum limit, can have $O(a)$ contributions.

The above argument gives just the main idea of our proof for automatic $O(a)$ improvement, and we will give a detailed proof in the next subsection. However, one of the most important points of our analysis is that the condition for maximal twist and for automatic $O(a)$ improvement is determined dynamically by the VEV $\langle \bar{\psi}^i_\alpha \psi^j_\beta \rangle$ in the Symanzik theory. More explicitly, the symmetry (20) or (21) of the continuum theory must keep the VEV intact, so that the symmetry is not spontaneously broken. This condition seems natural, since the symmetry (20) corresponds

[2]Other choices for the renormalized parameters are of course possible but at the expense of additional terms in S_1 of the effective action [19]. We also assume that use of the leading-order equations of motion has been made in order to drop some $O(a)$ terms in S_1. Without using the renormalization scheme in [1] and equations of motion there would be seven terms present in S_1 instead of only one [19]. However, this larger number of terms would not alter the conclusion of this section.

[3]This property can also be derived from a different point of view. Since parity is conserved at $\mu_0 = 0$ in the lattice theory, $\bar{\psi}\gamma_5\tau^3\sigma_{\mu\nu}F_{\mu\nu}\psi$ does not appear without μ_0. This argument can be extended to the case where the parity-flavor symmetry is spontaneously broken for a certain range of the untwisted mass $M_0\cos\theta_0$ [22–26] in the lattice theory. In this case, the charged pions become massless Nambu-Goldstone bosons in the lattice theory, associated with this spontaneous symmetry breaking in the zero twisted mass limit. Therefore, it must also become massless in the Symanzik theory in the same limit. This fact also tells us that explicit parity-flavor breaking terms such as $\bar{\psi}i\gamma_5\tau^3\sigma_{\mu\nu}F_{\mu\nu}\psi$ must be absent in the Symanzik theory without μ_0.

[4]The computation of this condensate follows standard arguments where one first considers the theory in a finite box with 4-volume V. See, for example, the appendix of Ref. [16].

[5]A similar argument using this symmetry has been given independently by S. Sint [27].

[6]This argument does not rely on our particular renormalization scheme and the use of the equations of motion. All possible terms in S_1 are T_1 odd once the continuum part is invariant under the transformation (21).

to a part of the exact vector symmetry in the continuum QCD at maximal twist. Note that this symmetry refers to the vector symmetry in the so-called twisted basis [2,8]. After rotating to the physical basis the theory is invariant under ordinary vector rotations in the 1 or 2 direction. However, for the proof of $O(a)$ improvement in the next subsection we prefer to stay in the twisted basis.

B. Proof of $O(a)$ improvement

Let us consider an arbitrary multilocal lattice operator $\mathcal{O}^{tp,d}_{\rm lat}(\{x\})$, where $\{x\}$ represents $x_1, x_2, \cdots, x_n$, d is the canonical dimension of the operator, $t = 0, 1$ and $p = 0, 1$ denote transformation properties under T_1 and parity P:

$$T_1\colon \mathcal{O}^{tp,d}_{\rm lat}(\{x\}) \to (-1)^t \mathcal{O}^{tp,d}_{\rm lat}(\{x\}), \tag{23}$$

$$P\colon \mathcal{O}^{tp,d}_{\rm lat}(\{\vec{x}, t\}) \to (-1)^p \mathcal{O}^{tp,d}_{\rm lat}(\{-\vec{x}, t\}). \tag{24}$$

Here we do not include the dimension coming from powers of the quark mass in the canonical dimension d of operators. For example,

$$\begin{aligned}
\mathcal{O}^{01,3}_{\rm lat}(x) &= \bar{\psi}_L i\gamma_5\tau^3\psi_L(x),\\
\mathcal{O}^{10,3}_{\rm lat}(x) &= \bar{\psi}_L\psi_L(x),\\
\mathcal{O}^{00,4}_{\rm lat}(x) &= \sum_\mu \bar{\psi}_L \frac{1}{2}\gamma_\mu(\nabla^+_\mu + \nabla^-_\mu)\psi_L(x),\\
\mathcal{O}^{10,5}_{\rm lat}(x) &= \sum_\mu \bar{\psi}_L \frac{1}{2}\nabla^+_\mu\nabla^-_\mu\psi_L(x),
\end{aligned} \tag{25}$$

and in terms of these operators the lattice action is given by

$$\begin{aligned}
S_{\rm tm} = \sum_x [&\mathcal{O}^{00,4}_{\rm lat}(x) - ar\mathcal{O}^{10,5}_{\rm lat}(x) + m_0\mathcal{O}^{10,3}_{\rm lat}(x)\\
&+ \mu_0\mathcal{O}^{01,3}_{\rm lat}(x)],
\end{aligned} \tag{26}$$

with untwisted quark mass $m_0 = M_0\cos\theta_0$ and twisted quark mass $\mu_0 = M_0\sin\theta_0$.

The lattice operator $\mathcal{O}^{tp,d}_{\rm lat}$ corresponds to a sum of continuum operators $\mathcal{O}^{t_n p_n,n}_{i_n}$ (n: nonnegative integer) in the Symanzik theory as

$$\mathcal{O}^{tp,d}_{\rm lat} \Leftrightarrow \mathcal{O}^{tp,d}_{\rm eff} = \sum_{n=0}^{\infty} a^{n-d} \sum_{t_n,p_n} \sum_{i_n} c^{tp,d}_{t_n p_n,n,i_n} \mathcal{O}^{t_n p_n,n}_{i_n}, \tag{27}$$

where n is the canonical dimension of the continuum operator $\mathcal{O}^{t_n p_n,n}_{i_n}$ which consists of $\bar{\psi}$, ψ, A_μ, and D_μ only without any mass parameters, and

$$T_1\colon \mathcal{O}^{t_n p_n,n}_{i_n}(\{x\}) \to (-1)^{t_n} \mathcal{O}^{t_n p_n,n}_{i_n}(\{x\}), \tag{28}$$

$$P\colon \mathcal{O}^{t_n p_n,n}_{i_n}(\{\vec{x}, t\}) \to (-1)^{p_n} \mathcal{O}^{t_n p_n,n}_{i_n}(\{-\vec{x}, t\}), \tag{29}$$

with $t_n, p_n = 0, 1$. Here we distinguish different operators with the same $(t_n p_n, n)$ by an index i_n. To have a total dimension d in the expansion in Eq. (27), the coefficients $c^{tp,d}_{t_n p_n,n,i_n}$ must be dimensionless: $c^{tp,d}_{t_n p_n,n,i_n} = c^{tp,d}_{t_n p_n,n,i_n}(g^2, \log(\Lambda a), m_q a, \mu_0 a)$, where g^2 is the bare gauge coupling constant, $\log(\Lambda a)$ represents log-divergences of the lattice theory with some scale parameter Λ introduced in the Symanzik theory, and $m_q = m_0 - m_{\rm cr}$ is a subtracted quark mass with an additive mass counterterm $m_{\rm cr}$, which will be specified later. Note that we consider possible power divergences of lattice operators by including operators with $n = 0, 1, \cdots, d-1$ in the expansion.

The following selection rules among these operators are crucial for our proof of automatic $O(a)$ improvement:

$$t + p + d = t_n + p_n + n \ \mathrm{mod}(2), \tag{30}$$

$$p + \#\mu_0 = p_n + (\#\mu_0)_n \ \mathrm{mod}(2), \tag{31}$$

where $\#\mu_0$ and $(\#\mu_0)_n$ denote the numbers of μ_0's in $\mathcal{O}^{tp,d}_{\rm lat}$ and $c^{tp,d}_{t_n p_n,n,i_n}$, respectively. The second equality can be easily proven by the invariance of the lattice action (3) under the $\tilde{P} = P \times [\mu_0 \to -\mu_0]$ transformation, Eq. (9). To prove the first equality (30), we introduce the following transformation:

$$\mathcal{D}^1_d\colon \begin{cases} U_\mu(x) \to U^\dagger_\mu(-x - a\mu)\\ (A_\mu(x) \to -A_\mu(-x))\\ \psi(x) \to (e^{i\pi\tau_1})^{3/2}\psi(-x)\\ \bar{\psi}(x) \to \bar{\psi}(-x)(e^{i\pi\tau_1})^{3/2} \end{cases}, \tag{32}$$

which is a modified version of the transformation $\mathcal{D}_d$ introduced in Ref. [8]. Since it is easy to show that the lattice action (3) is invariant under $T_1 \times \mathcal{D}^1_d$, in addition to the invariance under P^1_F, the lattice action is invariant under $T_1 \times \mathcal{D}^1_d \times P^1_F$. On the other hand, combining the transformation property

$$\mathcal{D}^1_d\colon \begin{cases} (\nabla^+_\mu + \nabla^-_\mu)\cdot f(x) \to -(\nabla^+_\mu + \nabla^-_\mu)\cdot f(-x)\\ (D_\mu \cdot f(x) \to -D_\mu \cdot f(-x)) \end{cases} \tag{33}$$

for an arbitrary function $f(x)$ with Eqs. (8) and (32), we can see easily that $\mathcal{D}^1_d \times P^1_F$ counts the canonical dimension times the parity of the operator as

$$\mathcal{D}^1_d \times P^1_F\colon \mathcal{O}^{tp,d}_{\rm lat}(\{\vec{x}, t\}) \to (-1)^{d+p} \mathcal{O}^{tp,d}_{\rm lat}(\{\vec{x}, -t\}), \tag{34}$$

$$\mathcal{D}^1_d \times P^1_F\colon \mathcal{O}^{t_n p_n,n}_{i_n}(\{\vec{x}, t\}) \to (-1)^{n+p_n} \mathcal{O}^{t_n p_n,n}_{i_n}(\{\vec{x}, -t\}). \tag{35}$$

Therefore, the invariance of the action under $T_1 \times \mathcal{D}^1_d \times P^1_F$ implies the first equality (30).

Let us show how these selection rules are used to determine the structure of operators in the Symanzik theory. As an example, we consider the operator $\mathcal{O}^{01,3}_{\rm lat}(x)$ in Eq. (25). Since $t + p + d = 4$, the first selection rule gives $t_n + d_n + n = 0$ mod(2), which leads to

$$\mathcal{O}^{01,3}_{\rm eff} = \frac{c^{01,3}_{00,0}}{a^3}\mathcal{O}^{00,0} + c^{01,3}_{10,3}\mathcal{O}^{10,3} + c^{01,3}_{01,3}\mathcal{O}^{01,3} + ac^{01,3}_{00,4,A}\mathcal{O}^{00,4}_A + ac^{01,3}_{00,4,B}\mathcal{O}^{00,4}_B + ac^{01,3}_{11,4}\mathcal{O}^{11,4} + a^2c^{01,3}_{01,5,A}\mathcal{O}^{01,5}_A + a^2c^{01,3}_{01,5,B}\mathcal{O}^{01,5}_B + a^2c^{01,3}_{10,5,A}\mathcal{O}^{10,5}_A + a^2c^{01,3}_{10,5,B}\mathcal{O}^{10,5}_B + \cdots, \tag{36}$$

where

$$\begin{aligned} &\mathcal{O}^{00,0} = \mathbf{1}, \qquad \mathcal{O}^{01,3} = \bar\psi i\gamma_5\tau^3\psi, \qquad \mathcal{O}^{10,3} = \bar\psi\psi, \\ &\mathcal{O}^{00,4}_A = \bar\psi\gamma_\mu D_\mu\psi, \qquad \mathcal{O}^{00,4}_B = -\frac{1}{4}\,\mathrm{tr}F_{\mu\nu}F_{\mu\nu}, \\ &\mathcal{O}^{11,4} = \bar\psi\gamma_\mu D_\mu i\gamma_5\tau^3\psi, \qquad \mathcal{O}^{01,5}_A = \bar\psi i\gamma_5\tau^3 D^2\psi, \\ &\mathcal{O}^{01,5}_B = \bar\psi i\gamma_5\tau^3\sigma_{\mu\nu}F_{\mu\nu}\psi, \qquad \mathcal{O}^{10,5}_A = \bar\psi D^2\psi, \\ &\mathcal{O}^{10,5}_B = \bar\psi\sigma_{\mu\nu}F_{\mu\nu}\psi. \end{aligned} \tag{37}$$

Applying the second selection rule that $p + \#\mu_0 = 1 = p_n + (\#\mu_0)_n \bmod(2)$, we obtain

$$\begin{aligned} c^{01,3}_{00,0}(\mu_0 a) &= \mu_0 a\tilde c^{01,3}_{00,0}(\mu_0^2a^2), \\ c^{01,3}_{10,3}(\mu_0 a) &= \mu_0 a\tilde c^{01,3}_{10,3}(\mu_0^2a^2), \\ c^{01,3}_{00,4,A(B)}(\mu_0 a) &= \mu_0 a\tilde c^{01,3}_{00,4,A(B)}(\mu_0^2a^2), \\ c^{01,3}_{10,5,A(B)}(\mu_0 a) &= \mu_0 a\tilde c^{01,3}_{10,5,A(B)}(\mu_0^2a^2), \end{aligned} \tag{38}$$

where only the $\mu_0 a$ dependence is explicitly written, and the other $c^{01,3}_{t_np_n,n,i_n}$'s are even functions of $\mu_0 a$. We then finally have

$$\mathcal{O}^{01,3}_{\rm eff} = a^{-2}\mu_0\tilde c^{01,3}_{00,0}\mathcal{O}^{00,0} + c^{01,3}_{01,3}\mathcal{O}^{01,3} + a^2\mu_0\tilde c^{01,3}_{00,4,A}\mathcal{O}^{00,4}_A + a^2\mu_0\tilde c^{01,3}_{00,4,B}\mathcal{O}^{00,4}_B + a^2c^{01,3}_{01,5,A}\mathcal{O}^{01,5}_A + a^2c^{01,3}_{01,5,B}\mathcal{O}^{01,5}_B + a\mu_0\tilde c^{01,3}_{10,3}\mathcal{O}^{10,3} + ac^{01,3}_{11,4}\mathcal{O}^{11,4} + a^3\mu_0\tilde c^{01,3}_{10,5,A}\mathcal{O}^{10,5}_A + a^3\mu_0\tilde c^{01,3}_{10,5,B}\mathcal{O}^{10,5}_B + \cdots, \tag{39}$$

where all dimensionless functions are even in $\mu_0 a$. It is important to observe that all operators with $t = 0$ contain only even powers of a, while those with $t = 1$ have only odd powers of a.

Repeating the analysis given above for all operators which appear in the lattice action (26) and introducing renormalized quantities (see Appendix A for more details), we obtain

$$S_{\rm tmQCD} \Leftrightarrow S_{\rm eff} = S_0 + m_qS_m + \sum_{n=1}^{\infty}[a^{2n}S^0_{2n} + a^{2n-1}S^1_{2n-1}], \tag{40}$$

where

$$S_0 = \int d^4x\Big\{\bar\psi_R(\gamma_\mu D_\mu + i\mu_R\gamma_5\tau^3)\psi_R(x) - \frac{1}{4}F^2_{\mu\nu,R}(x)\Big\}, \tag{41}$$

$$m_qS_m = m_RS_{m_R} \equiv m_R\int d^4x\bar\psi_R\psi_R(x), \tag{42}$$

$$S^0_{2n} = \int d^4x\Big[\sum_i Z^i_{00,2n+4}\cdot\mathcal{O}^{00,2n+4}_{R,i}(x) + \sum_i Z^i_{01,2n+3}\cdot\mu_R\cdot\mathcal{O}^{01,2n+3}_{R,i}(x)\Big], \tag{43}$$

$$S^1_{2n-1} = \int d^4x\Big[\sum_i Z^i_{10,2n+3}\cdot\mathcal{O}^{10,2n+3}_{R,i}(x) + \sum_i Z^i_{11,2n+2}\cdot\mu_R\cdot\mathcal{O}^{11,2n+2}_{R,i}(x)\Big]. \tag{44}$$

Renormalized parameters are introduced as[7]

$$\begin{aligned} \mu_0 &= Z^{-1}_\mu(g_R, \log(\Lambda a), m_Ra, \mu_R^2a^2)\mu_R, \\ m_q &= Z^{-1}_m(g_R, \log(\Lambda a), m_Ra, \mu_R^2a^2)m_R, \\ g &= Z^{1/2}_G(g_R, \log(\Lambda a), m_Ra, \mu_R^2a^2)g_R, \end{aligned} \tag{45}$$

where g_R, m_R, μ_R are kept constant and finite as $a \to 0$. We also define renormalized fields as

$$\begin{aligned} \psi_R &= Z^{1/2}_F(g_R^2, \log(\Lambda a), m_Ra, \mu_R^2a^2)\psi, \\ A_{\mu,R} &= Z^{1/2}_G(g_R^2, \log(\Lambda a), m_Ra, \mu_R^2a^2)A_\mu. \end{aligned} \tag{46}$$

A subscript R in $\mathcal{O}^{t_np_n,n}_{R,i}$ means that the operators are expressed in terms of renormalized fields, and therefore $Z^i_{t_np_n,n} = Z^i_{t_np_n,n}(g_R^2, \log(\Lambda a), m_Ra, \mu_R^2a^2)$.

Similarly, applying the selection rules to an arbitrary operator $\mathcal{O}^{tp,d}_{\rm lat}$ (again we give more details in Appendix A), we obtain

$$\mathcal{O}^{tp,d}_{\rm lat} \Leftrightarrow \mathcal{O}^{tp,d}_{\rm eff} = \sum_{l=-d}^{\infty} a^l\Big[\sum_i c^{tp,d}_{[t+l]p,d+l,i}\mathcal{O}^{[t+l]p,d+l}_{R,i} + \mu_R\sum_i\tilde c^{tp,d}_{[t+l]\bar p,d+l-1,i}\mathcal{O}^{[t+l]\bar p,d+l-1}_{R,i}\Big], \tag{47}$$

where $[t + l] = t + l \bmod(2)$, $\bar p = 1 - p$, and coefficients $c^{tp,d}_{t_np,n,i}$ and $\tilde c^{tp,d}_{t_np,n.i}$ are even functions of $\mu_R a$. Note here that, even though we use the same notations as in Eq. (27), these coefficients are functions of g_R^2, $\log(\Lambda a)$, m_Ra, and $\mu_R^2a^2$; therefore, the functional forms are different from the original ones. Formula (47) tells us that, if the lattice operator has $t = 0$, operators with $t_n = 0$ in the

[7]Note that the renormalization differs from the one usually employed in the Symanzik improvement program.

Symanzik expansion appear with even powers of a while those with $t_n = 1$ are associated with odd powers of a. This is reversed in the case that the lattice operator has $t = 1$: operators with $t_n = 0$ are multiplied by odd powers of a in the Symanzik expansion and those with $t_n = 1$ by even powers of a.

In order to obtain a finite result in the continuum limit, we have to remove possible power divergences in the expansion (47) by subtracting lower-dimensional lattice operators from the original operator $\mathcal{O}_{\rm lat}$, in addition to subtractions of $\log(\Lambda a)$ divergences including a possible mixing among operators whose canonical dimension is the same as the original operator. We denote such a renormalized and subtracted operator as $\mathcal{O}_{\rm lat,sub}$, which corresponds to

$$\mathcal{O}^{tp,d}_{\rm lat,R,sub} \Leftrightarrow \mathcal{O}^{tp,d}_{\rm eff,R,sub} = \mathcal{O}^{tp,d}_{R} + \sum_{l=1}^{\infty} a^l \mathcal{O}^{[t+l],d+l}_{R;tpd}, \quad (48)$$

$$\mathcal{O}^{[t+l],d+l}_{R;tpd} = \sum_i c^{tp,d}_{[t+l]p,d+l,i} \mathcal{O}^{[t+l]p,d+l}_{R,i} + \mu_R \sum_i \tilde{c}^{tp,d}_{[t+l]\bar{p},d+l-1,i} \mathcal{O}^{[t+l]\bar{p},d+l-1}_{R,i}, \quad (49)$$

where $d + l$ in the shorthand notation $\mathcal{O}^{[t+l],d+l}_{R;tpd}$ represents a canonical dimension of the operator and $[t + l]$ labels the transformation property under T_1:

$$T_1\colon \mathcal{O}^{[t+l],d+l}_{R;tpd} \to (-1)^{t+l} \mathcal{O}^{[t+l],d+l}_{R;tpd}. \quad (50)$$

We conclude that, in terms of this general description in the Symanzik theory, the maximal twist condition corresponds to the property that the continuum theory is invariant under the T_1 transformation. This condition then entails $m_R = 0$, which we call exact invariance condition. However, it can be relaxed to $m_R = O(a)$, which we call weak invariance condition. Imposing either of these we find

$$\langle \mathcal{O}^{1p,d}_R \rangle_{S_0 + m_R S_{m_R}} = \frac{1}{Z} \int \mathcal{D}\psi_R \mathcal{D}\bar{\psi}_R \mathcal{D}A_{\mu,R} e^{S_0 + m_R S_{m_R}} \mathcal{O}^{1p,d}_R = \begin{cases} 0 & \text{exact} \\ O(a) & \text{weak} \end{cases} \quad (51)$$

for an arbitrary continuum operator $\mathcal{O}^{1p,d}_R$ which is odd under T_1. [In the operator formalism, this condition expresses the fact that the vacuum $|0\rangle$ of $S_0 + m_R S_{m_R}$ is invariant under T_1: $\mathcal{T}_1|0\rangle = 0$ or $O(a)$.]

Assuming the maximal twist condition is satisfied, i.e. $m_R = O(a)$ at least, we now consider the following correlation function:

$$\langle \mathcal{O}^{tp,d}_{\rm lat,R,sub}(\{x\}) \rangle \equiv \frac{1}{Z_{\rm lat}} \int \mathcal{D}\psi_L \mathcal{D}\bar{\psi}_L \mathcal{D}U e^{S_{\rm tmQCD}} \mathcal{O}^{tp,d}_{\rm lat,R,sub}(\{x\}), \quad (52)$$

where $Z_{\rm lat}$ is the partition function defined by $\langle 1 \rangle = 1$. In terms of the Symanzik effective theory, this correlation function corresponds to

$$\langle \mathcal{O}^{tp,d}_{\rm lat,R,sub}(\{x\}) \rangle = \langle \mathcal{O}^{tp,d}_{\rm eff,R,sub}(\{x\}) \rangle_{S_{\rm eff}}, \quad (53)$$

where we define

$$\langle \mathcal{O} \rangle_S = \frac{1}{Z} \int \mathcal{D}\psi_R \mathcal{D}\bar{\psi}_R \mathcal{D}A_{\mu,R} e^S \mathcal{O}. \quad (54)$$

For simplicity, we first consider the $m_R = 0$ case. In this case we have

$$e^{S_{\rm eff}} = e^{S_0} \exp\left\{ \sum_{n=1}^{\infty} [a^{2n} S^0_{2n} + a^{2n-1} S^1_{2n-1}] \right\} \equiv e^{S_0} \sum_{n=0}^{\infty} a^n S^{(n)}, \quad (55)$$

where we define $a^n S^{(n)}$ to be the sum of the a^n terms in Eq. (55). For example, the first few terms are given as

$$S^{(0)} = 1, \qquad S^{(1)} = S^1_1, \qquad S^{(2)} = S^0_2 + \frac{(S^1_1)^2}{2!}. \quad (56)$$

Under the T_1 transformation, they behave as

$$T_1\colon S^{(n)} \to (-1)^n S^{(n)}. \quad (57)$$

By expanding both action and operator, we have

$$\langle \mathcal{O}^{tp,d}_{\rm eff,R,sub}(\{x\}) \rangle_{S_{\rm eff}} = \left\langle \left[\mathcal{O}^{tp,d}_R(\{x\}) + \sum_{l=1}^{\infty} a^l \mathcal{O}^{[t+l],d+l}_{R;tpd}(\{x\}) \right] \sum_{n=0}^{\infty} a^n S^{(n)} \right\rangle_{S_0} = \left\langle \mathcal{O}^{tp,d}_R(\{x\}) \rangle_{S_0} + \sum_{l,n=0, l+n\neq 0}^{\infty} a^{l+n} \langle \mathcal{O}^{[l+t],d+l}_{R;tpd}(\{x\}) S^{(n)} \right\rangle_{S_0}. \quad (58)$$

Since terms with $t + l + n =$ odd in the above expansion vanish from the maximal twist condition (51), terms with $t + l + n = 2s$ remain as

$$\langle \mathcal{O}^{tp,d}_{\mathrm{eff,R,sub}}(\{x\})\rangle_{S_{\mathrm{eff}}} = \delta_{t,0}\langle \mathcal{O}^{tp,d}_{R}(\{x\})\rangle_{S_0} + \sum_{s=1}^{\infty} a^{2s-t} \sum_{l=0}^{2s-t} \langle \mathcal{O}^{[l+t],d+l}_{R;tpd}(\{x\}) S^{(2s-t-l)}\rangle_{S_0}$$
$$= \delta_{t,0}\langle \mathcal{O}^{tp,d}_{R}(\{x\})\rangle_{S_0} + \sum_{s=1}^{\infty} a^{2s-t} F_d^{2s-t}(\{x\}, g_R^2, \log(\Lambda a), \mu_R; \mu_R^2 a^2) \tag{59}$$

where we define

$$F_d^{2s-t}(\{x\}, g_R^2, \log(\Lambda a), \mu_R; \mu_R^2 a^2) = \sum_{l=0}^{2s-t} \langle \mathcal{O}^{[l+t],d+l}_{R;tpd}(\{x\}) S^{(2s-t-l)}\rangle_{S_0}, \tag{60}$$

which is an analytic function for small $\mu_R^2 a^2$ (the last argument). This expression tells us that

$$\langle \mathcal{O}^{tp,d}_{\mathrm{eff,R,sub}}(\{x\})\rangle_{S_{\mathrm{eff}}} = \begin{cases} \langle \mathcal{O}^{tp,d}_{R}(\{x\})\rangle_{S_0} + a^2 F_d^2 + a^4 F_d^4 + \cdots, & t=0 \\ a F_d^1 + a^3 F_d^3 + \cdots, & t=1 \end{cases}. \tag{61}$$

This proves automatic $O(a)$ improvement at maximal twist that scaling violations of T_1 invariant quantities are even functions of a: a^{2n+1} contributions are completely absent, while T_1 noninvariant quantities have only contributions odd in a and vanish in the continuum limit. This completes our proof of automatic $O(a)$ improvement at maximal twist. (Here $O(a^n)$ $(n \geq 1)$ represents contributions of the form $a^{n+s}[\log(\Lambda a)]^k$ with $s, k = 0, 1, 2, \cdots$).

Notice that this proof for automatic $O(a)$ improvement is not restricted to on-shell quantities, and the equation of motion is not required at all for the proof. It is also noted that the proof does not require $\mu_R = 0$: Automatic $O(a)$ improvement is realized also for the massive theory.

If $m_R = O(a)$ (weak invariance), the proof goes through with just a little modification (see Appendix A). In the special case that m_R is odd in a [$m_R = af(a^2)$], we obtain Eq. (61) with a little modification in F_d^n, while in more general cases with $m_R = O(a)$ the result becomes

$$\langle \mathcal{O}^{tp,d}_{\mathrm{eff,R,sub}}(\{x\})\rangle_{S_{\mathrm{eff}}} = \begin{cases} \langle \mathcal{O}^{tp,d}_{R}(\{x\})\rangle_{S_0} + O(a^2), & t=0 \\ O(a), & t=1 \end{cases}. \tag{62}$$

C. Ambiguity of the maximal twist condition in the lattice theory

In this subsection we consider the maximal twist condition in the lattice theory and discuss the possible ambiguities of it.

In the Symanzik theory, maximal twist is uniquely defined by the condition that an arbitrary T_1 noninvariant operator $\mathcal{O}^{t=1\,p,d}$ has a vanishing expectation value,

$$\langle \mathcal{O}^{1\,p,d}\rangle_{S_0} = 0. \tag{63}$$

Provided this condition is fulfilled, the expectation values of all T_1-odd operators vanish. Hence the particular choice for $\mathcal{O}^{1\,p,d}$ is irrelevant, and in that sense the condition (63) is unique. In the lattice theory, however, the maximal twist condition, which may be defined by

$$\langle \mathcal{O}^{1\,p,d}_{\mathrm{lat,R,sub}}\rangle = 0, \tag{64}$$

depends on the choice of the operator $\mathcal{O}^{1\,p,d}_{\mathrm{lat,R,sub}}$, and is therefore not unique. In order to discuss this we make the Symanzik expansion of (64), which gives (see Appendix A for unexplained notation and the derivation)

$$0 = \langle \mathcal{O}^{1\,p,d}_{\mathrm{eff,R,sub}}\rangle$$
$$= a H_d^0(\mu_R; a^2, m_R^2, m_R a, \mu_R^2 a^2)$$
$$+ m_R H_d^1(\mu_R; a^2, m_R^2, m_R a, \mu_R^2 a^2). \tag{65}$$

The solution m_R^{maximal} to Eq. (65), provided it is unique,[8] is of the form $m_R^{\mathrm{maximal}} = af(a^2)$, due to the symmetry of Eq. (65) under the transformation $m_R \to -m_R$ and $a \to -a$. Therefore, according to the analysis in the previous subsection, scaling violations in T_1-invariant quantities are even in a.

A different choice for the lattice operator in (64) leads to a different solution $\tilde{m}_R^{\mathrm{maximal}} = a\tilde{f}(a^2)$, so that the difference between the two definitions is of $O(a)$: $\Delta m_R^{\mathrm{maximal}} = a\{f(a^2) - \tilde{f}(a^2)\}$. Note that a solution m_R^{maximal} in general depends on μ_R, inherited from the μ_R dependence of H_d^δ.

Let us consider some examples for maximal twist in the lattice theory. A simple one is given by

$$\langle (\bar{\psi}\psi)_{\mathrm{lat,R,sub}}\rangle = 0. \tag{66}$$

Unfortunately, this definition is not very useful in practice, since the subtraction of power divergences necessary for $\langle\bar{\psi}\psi\rangle$ prevents a reliable determination of this VEV in the lattice theory. Instead one may take $\mathcal{O}_{\mathrm{lat}}(x, y) = A_\mu^a(x)P^a(y)$ or $\mathcal{O}_{\mathrm{lat}}(x, y) = \partial_\mu A_\mu^a(x)P^a(y)$ $(a = 1, 2)$, as was done in Refs. [3,4,14]:

$$\langle A_\mu^a(x)P^a(y)\rangle = 0 \quad \text{or} \quad \langle \partial_\mu A_\mu^a(x)P^a(y)\rangle = 0, \tag{67}$$

where A_μ^a and P^a denote the axial vector current and

[8] This seems plausible at small enough a and μ_R, since the solution is unique in the Symanzik theory.

pseudoscalar density, respectively. Yet another choice is [28]

$$\langle A_\mu^3(x)P^3(y)\rangle = 0. \tag{68}$$

Depending on the choice for the axial vector current, either the local or the conserved one, the conditions (67) lead to a different definition of maximal twist. However, the difference will be again of $O(a)$.

We close this subsection with a final comment. Any maximal twist condition in the lattice theory determines a value for the bare mass m_0 as a function of the bare twisted mass μ_0. It has been suggested to tune the bare mass to its critical value $m_0 = m_{\rm cr}$ where the pion mass vanishes in the untwisted theory. However, this condition is not related to T_1 invariance. For example, contributions from excited states violate Eq. (67) even at $m_\pi = 0$. Consequently, the pion mass definition does not correspond to maximal twist according to the T_1 invariance condition.

III. WCHPT ANALYSIS FOR $O(a)$ IMPROVEMENT IN TMQCD

According to our analysis in the Symanzik effective theory, maximal twist is determined by requiring T_1 invariance of expectation values. For example, for maximal twist we could impose

$$\langle\bar\psi\psi\rangle = 0, \qquad \langle\bar\psi i\gamma_5\tau_3\psi\rangle = v(M_R) \neq 0. \tag{69}$$

In this section we study this condition in Wilson chiral perturbation theory [16,17,29,30], and check explicitly whether $O(a)$ improvement is indeed realized. We also compare to some other definitions of maximal twist, which have been used already in numerical simulations.

Automatic $O(a)$ improvement has been studied before in WChPT for various definitions of the twist angle and also for different power countings, which are determined by the relative size between the quark masses and the lattice spacing [12,28,31,32]. Our analysis follows closely the one in Ref. [12]. We work mainly in the regime where m and μ are of $O(a^2)$ unless stated otherwise.[9] It is in this regime where the phase structure of the theory is determined by the competition between the mass term and lattice spacing artifacts [19,33], and where the differences of the various maximal twist definitions start to become relevant [12]. In contrast to Ref. [12], we work at higher order and include the terms of $O(ma, \mu a, a^3)$ in our analysis. These terms, which were also included in Refs. [32,34], provide a nontrivial check for automatic $O(a)$ improvement, since they are odd in the lattice spacing and, according to our Symanzik analysis, should not contribute to observables.

A. Chiral Lagrangian and power counting

In terms of the $SU(2)$ matrix-valued field Σ, which transforms under chiral transformations as $\Sigma \to L\Sigma R^\dagger$, the chiral effective Lagrangian reads

$$\begin{aligned}\mathcal{L}_\chi = {}& \frac{f^2}{4}\langle\partial_\mu\Sigma\partial_\mu\Sigma^\dagger\rangle - \frac{f^2}{4}\langle\hat m^\dagger\Sigma + \Sigma^\dagger\hat m\rangle - \frac{f^2}{4}\langle\hat a^\dagger\Sigma + \Sigma^\dagger\hat a\rangle + (W_4 + W_5/2)\langle\partial_\mu\Sigma^\dagger\partial_\mu\Sigma\rangle\langle\hat a^\dagger\Sigma + \Sigma^\dagger\hat a\rangle \\ & - (W_6 + W_8/2)\langle\hat m^\dagger\Sigma + \Sigma^\dagger\hat m\rangle\langle\hat a^\dagger\Sigma + \Sigma^\dagger\hat a\rangle - (W_6' + W_8'/2)\langle\hat a^\dagger\Sigma + \Sigma^\dagger\hat a\rangle^2 - W_{c1}\langle\hat a^\dagger\Sigma + \Sigma^\dagger\hat a\rangle^3 \\ & - W_{c2}\langle\hat a^\dagger\hat a\rangle\langle\hat a^\dagger\Sigma + \Sigma^\dagger\hat a\rangle - W_X\langle\hat a^\dagger\hat m + \hat m^\dagger\hat a\rangle.\end{aligned} \tag{70}$$

The terms through $O(a^2)$ have been constructed previously [19,35]. Two terms of $O(a^3)$ in the last line, which were included also in Refs. [32,34] are derived easily with the spurion fields in Ref. [36]. Note that the $O(ma)$ term proportional to W_X does not depend on Σ. This term is usually neglected since it does not contribute to the pseudoscalar masses and decay constant. Here, however, we will need it since it gives a contribution to the condensates. The coefficients f, B are familiar low-energy coefficients of continuum chiral perturbation theory [37,38], while all the W's are additional low-energy parameters associated with the nonzero lattice spacing contributions [17,36]. As usual, angled brackets denote traces over the flavor indices and the shorthand notation

$$\hat m = 2B(m + i\mu\tau_3) \equiv 2Bm' e^{i\omega_L\tau_3}, \qquad \hat a = 2W_0 a, \tag{71}$$

is used [39]. The mass parameters m and μ denote the renormalized untwisted and twisted mass [2], which are defined according to[10]

$$m = Z_m(m_0 - m_{\rm cr}), \qquad \mu = Z_\mu\mu_0. \tag{72}$$

Even though the critical mass $m_{\rm cr}$ includes the additive shift proportional to $1/a$, it does not include certain contributions coming from the $O(a, a^2)$ terms in the chiral

[9] Since the parameters m and μ in WChPT are renormalized parameters we drop the subscript "R" in this section.

[10] The renormalization constants Z_m, Z_μ are related to the renormalization constant Z_A of the axial vector, $Z_A = Z_m/Z_\mu$, which follows from the vector and axial vector Ward identities [2].

Lagrangian [16]. For example, the third term in the first line of (70) gives rise to an $O(a)$ shift in the critical mass.[11]

Our power counting is based on the assumption that $m \approx a^2$ [12,30,40], where m stands for both the untwisted and the twisted mass and for p^2 (proper powers of $\Lambda_{\rm QCD}$ are, as usual in this type of argument, understood). Since m and a are smaller than 1, we have the inequalities

$$m \approx a^2 > ma \approx a^3 > m^2 \approx ma^2 \approx a^4. \tag{73}$$

According to this power counting, the terms of $O(m, a^2)$ in the chiral Lagrangian are of leading order (LO), while the $O(ma, a^3)$ contributions are of next-to-leading order (NLO). Note that the size of the $O(a)$ term does not matter for the power counting, since it only contributes to the critical quark mass.

B. Gap equation

Starting from the chiral Lagrangian, a gap equation for the ground state of the chiral effective theory can be derived. From the NLO expression of the chiral Lagrangian we find the potential

$$\begin{aligned} V_\chi = & \frac{f^2}{4} 2Bm' \langle P^\dagger \Sigma + \Sigma^\dagger P \rangle \\ & + \frac{f^2}{4} 2W_0 a (1 + \tilde{c}_3 a^2) \langle \Sigma + \Sigma^\dagger \rangle \\ & - \frac{f^2}{16} c_2 a^2 \langle \Sigma + \Sigma^\dagger \rangle^2 + \frac{f^2}{16} \tilde{c}_2 a m' \langle \Sigma + \Sigma^\dagger \rangle \\ & \times \langle P^\dagger \Sigma + \Sigma^\dagger P \rangle + \frac{f^2}{64} c_3 a^3 \langle \Sigma + \Sigma^\dagger \rangle^3 \\ & + \frac{2Bf^2 m'}{4} c_X a \langle P^\dagger + P \rangle. \end{aligned} \tag{74}$$

Here we introduced $P = \exp i\omega_L \tau_3$ with $\tan\omega_L = \mu/m$, and the following combinations of low-energy parameters:

$$\begin{aligned} c_2 &= -32(2W_6' + W_8') \frac{W_0^2}{f^2}, \\ \tilde{c}_2 &= 32(2W_6 + W_8) \frac{W_0 B}{f^2}, \qquad c_3 = 64 W_{c1} \frac{(2W_0)^3}{f^2}, \\ \tilde{c}_3 &= 32 W_{c2} \frac{W_0^2}{f^2}, \qquad c_X = 8 W_X \frac{W_0}{f^2}. \end{aligned} \tag{75}$$

These parameters are dimensionful and have $[c_2] = 4$, $[\tilde{c}_2] = [\tilde{c}_3] = 2$, $[c_3] = 5$, and $[c_X] = 1$.

Since a twisted mass term breaks flavor symmetry, we make the ansatz

$$\Sigma_0 = e^{i\phi\tau_3} \tag{76}$$

for the ground state, and this ground state is determined by $dV_\chi/d\phi = 0$ with

$$\begin{aligned} V_\chi = & 2Bf^2(mt + \mu\sqrt{1-t^2}) + 2f^2 W_0 a (1 + \tilde{c}_3 a^2) t \\ & - f^2 c_2 a^2 t^2 + f^2 \tilde{c}_2 a (mt + \mu\sqrt{1-t^2}) t + f^2 c_3 a^3 t^3 \\ & + 2Bf^2 c_X m a. \end{aligned} \tag{77}$$

Taking the derivative with respect to ϕ in (77), we obtain a *gap equation* for

$$t = \cos\phi, \tag{78}$$

which can be brought into the form

$$\sqrt{1-t^2}[\chi - t + 2\beta_m t + \gamma t^2] = \alpha[t - \beta_\mu(1 - 2t^2)], \tag{79}$$

where we introduced the dimensionless parameters

$$\begin{aligned} \alpha &= \frac{2B\mu}{2c_2 a^2}, \qquad \chi = \frac{2Bm + 2W_0 a(1 + \tilde{c}_3 a^2)}{2c_2 a^2}, \\ \beta_m &= \frac{\tilde{c}_2 a m}{2c_2 a^2}, \qquad \beta_\mu = \frac{\tilde{c}_2 a}{2B}, \qquad \gamma = \frac{3c_3 a^3}{2c_2 a^2}. \end{aligned} \tag{80}$$

In the following we will assume

$$|\beta_\mu| < 1, \qquad |\beta_m| < 1, \qquad |\gamma| < 1, \tag{81}$$

which can be justified by a naïve dimensional analysis when all dimensionfull constants are assumed to be of $O(\Lambda_{\rm QCD})$ together with the conditions $a\Lambda_{\rm QCD} < 1$ and $m/\Lambda_{\rm QCD} < 1$.

Note the sign convention for the coefficient c_2. A positive sign corresponds to the scenario with spontaneous parity-flavor breaking [16], which guarantees the existence of a massless pion [22]. A negative coefficient c_2 results in a scenario with a first-order phase transition [19,33].[12] The details of the discussion of $O(a)$ improvement differ depending on the scenario for the phase diagram. In the rest of this section we are mainly interested in the scenario with $c_2 > 0$, where spontaneous parity-flavor breaking causes some subtleties for automatic $O(a)$ improvement. These subtleties are absent for $c_2 < 0$, and we come back to this scenario at the end of this section.

C. Condition for $O(a)$ improvement in WChPT

Taking derivatives of V_χ with respect to m and μ, the two VEVs $\langle\bar{\psi}\psi\rangle$ and $\langle\bar{\psi} i\gamma_5\tau_3\psi\rangle$ are easily computed with the result

$$\begin{aligned} \langle\bar{\psi}\psi\rangle &\equiv \frac{dV_\chi}{dm} = 2f^2 B[(1 + \beta_\mu t)t + c_X a], \\ \langle\bar{\psi} i\gamma_5\tau_3\psi\rangle &\equiv \frac{dV_\chi}{d\mu} = 2f^2 B(1 + \beta_\mu t)\sqrt{1-t^2}. \end{aligned} \tag{82}$$

[11] This term is often absorbed in the untwisted mass, giving rise to the so-called shifted mass [16,28,32].

[12] See also Ref. [32] where it has been shown that the NLO terms in the chiral Lagrangian do not change the existence of two qualitatively different scenarios for the phase diagram.

Therefore, the T_1 invariance condition (69) corresponds to $t = -c_X a + O(a^3)$ in WChPT. If general scalar and pseudoscalar operators are employed for $\bar{\psi}\psi$ and $\bar{\psi} i\gamma_5 \tau^3 \psi$, these results are modified by $O(a)$ stemming from the effective operators in the Symanzik effective theory [41]. This leads to

$$\begin{aligned} \langle \bar{\psi}\psi \rangle &= \frac{2f^2 B}{Z_S}[(1 + c_S a t)t + \tilde{c}_S a], \\ \langle \bar{\psi} i\gamma_5 \tau_3 \psi \rangle &= \frac{2f^2 B}{Z_P}(1 + c_P a t)\sqrt{1 - t^2}. \end{aligned} \tag{83}$$

Nevertheless, even in this case the condition (69) leads to a similar result: $t = -\tilde{c}_S a + O(a^3)$.

We would find a similar result using the alternative condition $\langle A_\mu^2 P^2 \rangle = 0$, which is equivalent to $\cot\omega_{\rm WT} = 0$ with

$$\cot\omega_{\rm WT} \equiv \frac{\langle A_\mu^2 P^2 \rangle}{\langle V_\mu^1 P^2 \rangle}. \tag{84}$$

Note that A_μ^2 is T_1 odd while V_μ^1 and P^2 are T_1 even. Provided Noether currents are used for A_μ^2 and V_μ^1, one finds (see also Appendix B)

$$\begin{aligned} \langle 0|A_{\mu=0}^2|\pi_2\rangle &= f m_\pi t(1 + c_0 a t), \\ \langle 0|V_{\mu=0}^1|\pi_2\rangle &= f m_\pi \sqrt{1 - t^2}(1 + c_0 a t), \end{aligned} \tag{85}$$

where we defined the coefficient

$$c_0 = 16(2W_4 + W_5)\frac{W_0}{f^2} \tag{86}$$

in analogy to the definitions in Eq. (75). This leads to $\cot\omega_{\rm WT} = \cot\phi$, hence the condition $\langle A_\mu^2 P^2 \rangle = 0$ implies $t = 0$. The result differs if one uses general non-Noether currents. Additional contributions of $O(a)$ appear in the effective operators in the Symanzik expansion, which carry over to the chiral effective theory as well:

$$\begin{aligned} \langle 0|A_{\mu=0}^2|\pi_2\rangle &= \frac{f m_\pi}{Z_A}[t(1 + c_A a t) - \tilde{c}_A a], \\ \langle 0|V_{\mu=0}^1|\pi_2\rangle &= \frac{f m_\pi}{Z_V}\sqrt{1 - t^2}[1 + c_V a t]. \end{aligned} \tag{87}$$

Note that here the currents on the left-hand side are bare currents, as one can infer from the explicit appearance of the renormalization constants Z_A, Z_V. The way we have written the expectation values correspond to what can be directly measured in a lattice simulation without the knowledge of Z_A, Z_V. For $\cot\omega_{\rm WT}$ we find

$$\cot\omega_{\rm WT} = \frac{t(1 + c_A a t) - \tilde{c}_A a}{\sqrt{1 - t^2}} \times \frac{Z_V}{Z_A} \times \frac{1}{1 + c_V a t}, \tag{88}$$

and the maximal twist condition $\cot\omega_{\rm WT} = 0$ gives $t = \tilde{c}_A a + O(a^3)$, which has the same form as in the case of the VEVs. Note here that imposing a nonvanishing value for $\cot\omega_{\rm WT}$ is sensitive to the ratio Z_V/Z_A as well as to c_A, $\tilde{c}_A$, and c_V. As a final example we consider the condition $\langle A_\mu^3 P^3 \rangle = 0$ introduced in [28]. Since

$$\langle 0|P^3|\pi^3\rangle = \frac{fB}{Z_P}[t - (1 - 2t^2)c_P a], \tag{89}$$

we again find $t = c_P a + O(a^3)$.

To summarize, imposing T_1 invariance we find the condition $t = Xa + O(a^3)$ with some constant X. This constant depends on the specific choice for the operator in the matrix element. Nevertheless, all definitions guarantee automatic $O(a)$ improvement, as we want to show next.

It is instructive to first consider the simpler condition $t = 0$ (which is equivalent to a vacuum angle $\phi = \pm\pi/2$). In this case, the pseudoscalar mass and decay constant of charged pions, m_π^2 and f_π, are given by (see also Appendix B)

$$m_\pi^2 = \frac{2B\mu}{\sqrt{1 - t^2}} \frac{1 + \beta_\mu t}{1 + c_0 a t}, \tag{90}$$

$$f_\pi = f\sqrt{1 - t^2}[1 + c_0 a t]. \tag{91}$$

The result for the decay constant assumes that the so-called indirect method [1,42] is used,

$$f_\pi = \frac{2\mu}{m_\pi^2}\langle 0|P^\pm|\pi_\mp\rangle. \tag{92}$$

The results (90) and (91) are valid for arbitrary t, but for $t = 0$ they turn into the results familiar from leading-order continuum ChPT,

$$m_\pi^2 = 2B\mu, \qquad f_\pi = f. \tag{93}$$

Apparently there are no $O(a, a^3)$ corrections in these results. In addition, the $O(a^2)$ corrections are absent too, but this is not as surprising as one might first think. The charged pions are the Goldstone bosons associated with the spontaneous breaking of flavor and parity in the theory without a twisted mass term. Hence they must become massless when one enters the broken phase, i.e. when μ goes to zero. With the same argument one would also conclude that no terms of order $O(a, a^3)$ terms are present. The same argument, however, does not apply to the $O(\mu a)$ terms, and their absence is indeed a nontrivial demonstration of automatic $O(a)$ improvement once T_1 invariance is imposed.

It is now simple to show that we can relax $t = 0$ to the weaker condition $t = O(a)$ without loosing automatic $O(a)$ improvement.[13] Suppose that $t = Xa$ with some constant X. If we insert this into (90) and (91) we find (after expanding the denominator)

[13]A similar argument that the theory is $O(a)$ improved for $t = O(a)$ has also been given independently by S. Sharpe [43].

$$m_\pi^2 = 2B\mu\left(1 + \left[\frac{\tilde{c}_2}{2B} - c_0 + \frac{X}{2}\right]Xa^2\right) + O(\mu a^4), \quad (94)$$

$$f_\pi = f(1 + [c_0 - X/2]Xa^2) + O(a^4). \quad (95)$$

Again no $O(a, \mu a)$ corrections appear. This demonstrates, within WChPT and at least for the two observables we have chosen, that $t = O(a)$, which follows from imposing T_1 invariance, is a sufficient condition for automatic $O(a)$ improvement.

D. Other conditions for maximal twist and $O(a)$ improvement

In the following we want to compare the condition of T_1 invariance to some other conditions for maximal twist which are proposed in the literature. In particular we are interested in definitions where the untwisted mass m_0 is set to a particular value and kept fixed as one varies the twisted mass μ_0. Such definitions obviously have a practical advantage for numerical simulations. Finding the μ_0 dependent value m_0 such that a matrix element like the ones in (66) or (67) vanishes is computationally quite demanding, in particular, in dynamical simulations. One can save a substantial amount of computer time if one does not need to do this tuning for each twisted mass one wants to simulate, but rather stay at one fixed value of m_0. However, such definitions do violate T_1 invariance for most μ_0 values, and it is therefore not obvious how this affects automatic $O(a)$ improvement. This is the issue we want to study in this section.

The following two definitions keep the untwisted mass constant and both have been employed already in quenched numerical simulations [3–6]:

(1) *PCAC mass definition.*—For a given (bare) twisted mass μ_0, the untwisted mass $m_0(\mu_0)$ is first tuned such that the PCAC quark mass, defined by

$$2m_{\mathrm{PCAC}} = \frac{\langle \partial_\mu A_\mu^2 P^2\rangle}{\langle P^2 P^2\rangle}, \quad (96)$$

vanishes. Then $m_0(0) = \lim_{\mu_0\to 0} m_0(\mu_0)$ is used as the choice for m_0 of the PCAC mass definition for all μ_0. Therefore, this definition is independent of μ_0.[14]

(2) *Pion mass definition.*—The bare untwisted quark mass is set to its critical quark mass where the pion mass vanishes at $\mu_0 = 0$. In practice, this value is usually obtained in the untwisted theory by performing an extrapolation of m_π^2 data to the massless point.

In order to study these two definitions we have to translate ("match") them to the corresponding ones in WChPT:

(1) *PCAC definition.*—The denominator in Eq. (96) is found to be given by

$$\langle 0|P^2|\pi_2\rangle = \frac{Bf}{Z_P}(1 + \beta_\mu t) \quad (97)$$

so that the PCAC condition reads

$$m_{\mathrm{PCAC}} = \mu\frac{Z_P}{Z_A}\frac{t(1 + c_A a t) - \tilde{c}_A a}{\sqrt{1 - t^2}(1 + c_0 a t)} = 0. \quad (98)$$

This leads to $t = \tilde{c}_A a + O(a^3)$ for any nonzero μ. Keeping, for simplicity, only the leading term and setting $t = \tilde{c}_A a$ into the gap equation, one finds

$$\chi = \tilde{c}_A a[1 - 2\beta_m - \gamma\tilde{c}_A a] \quad (99)$$

in WChPT. In the following we will assume this χ to be smaller than 1. This is in accordance with our previously made assumption that all dimensionful coefficients are of order Λ_{QCD} and $a\Lambda_{\mathrm{QCD}} < 1$.

(2) *Pion definition.*—We need the expression for the pion mass in the untwisted theory. We cannot simply take the $\mu \to 0$ limit of Eq. (90), since t is equal to 1 in this limit and the whole expression is ill defined. Instead, we first use the gap equation and rewrite the pion mass as

$$m_\pi^2 = \frac{2c_2 a^2}{1 + c_0 a t}\left[\frac{\chi}{t} - 1 + 2\beta_m + \gamma t + 2\beta_\mu\alpha\frac{\sqrt{1 - t^2}}{t}\right]. \quad (100)$$

Here the limit $\mu \to 0$ is well defined and the condition $m_\pi^2 = 0$ reads

$$\chi = 1 - 2\beta_m - \gamma. \quad (101)$$

In order to check whether $O(a)$ improvement is realized, we have to verify that t is at least of $O(a)$. To do so we have to solve the gap Eq. (79) with the χ values in (99) and (101), respectively. It is not necessary to solve the gap equation exactly; approximate solutions will be sufficient for our purposes.

Let us assume $t \ll 1$, since we are interested in the small t case. In this case we can neglect the t^2 terms in (79) and obtain the approximate solution

$$t \simeq \frac{\alpha\beta_\mu + \chi}{\alpha + 1 - 2\beta_m}. \quad (102)$$

For the PCAC mass condition we set χ to the value in (99) and find

[14]Note that one can choose $m_0(\mu_0)$ at a fixed nonvanishing value μ_0 as a (different) PCAC mass definition. Employing such a definition requires the determination of $m_0(\mu_0)$ at only one μ_0 value. Taking the $\mu_0 \to 0$ limit, on the other hand, requires the determination of $m_0(\mu_0)$ for various twisted mass values and a subsequent extrapolation. Hence the latter is numerically more demanding.

$$t \simeq a\frac{\tilde{c}_2\mu + 2\tilde{c}_A(c_2 + \tilde{c}_2 W_0/B)a^2}{2B\mu + 2(c_2 + \tilde{c}_2 W_0/B)a^2}. \quad (103)$$

Here we rewrote (99) as

$$am = -\frac{W_0}{B}a^2 + O(a^4), \quad (104)$$

and dropped all but the leading term proportional to a^2. Taking into account that the denominator in Eq. (103) is always of $O(a^2)$ or larger for $c_2 + \tilde{c}_2 W_0/B > 0$, together with our convention that $B > 0$ and $\mu > 0$, t is always of $O(a)$ and our assumption that $t \ll 1$ is consistently satisfied.[15] The solution in Eq. (103) is of the form $t = aX$ which we used at the end of the previous section [cf. Eqs. (94) and (95)], with X representing the fraction in (103). However, here the value of X does depend on the relative size between a and μ. For small a and fixed μ such that $2B\mu \gg 2(c_2 + \tilde{c}_2 W_0/B)a^2$, we can expand the denominator and find

$$t \approx a\frac{\tilde{c}_2}{2B}, \quad (105)$$

so $X = \tilde{c}_2/2B$ and $t = O(a)$. Hence our discussion in the last section can be applied and we find $O(a^2)$ scaling violations in physical observables. On the other hand, for larger a such that $\mu = O(a^2)$, we expect a modification of the simple linear a dependence of t, and this leads to distortions of the expected $O(a^2)$ scaling violations. In the extreme case of small fixed μ and large a such that $2B\mu \ll 2(c_2 + \tilde{c}_2 W_0/B)a^2$, we find

$$t \approx a\tilde{c}_A, \quad (106)$$

as expected from the definition according to the PCAC definition. Even though we recover a constant X, it is different from (105). Since the sign of the low-energy constants are *a priori* not known, it is even possible that the slope of t changes sign, depending on the size of a. This is of potential danger when one analyzes numerical data assuming a simple $O(a^2)$ scaling violation. The nontrivial a dependence of the right-hand side in Eq. (103) is likely to obscure automatic $O(a)$ improvement in the region where μ is of $O(a^2)$.[16]

Let us now turn to the pion mass definition. Inserting (101) into the approximate solution (102) we obtain

$$t \simeq a\frac{\tilde{c}_2\mu + 2(c_2 + \tilde{c}_2 W_0/B)a}{2B\mu + 2(c_2 + \tilde{c}_2 W_0/B)a^2}. \quad (107)$$

In order to derive this result we rewrote (101) as in Eq. (104) and used, for simplicity, only the leading term proportional to a^2. As before we find $t \approx a\tilde{c}_2/2B = O(a)$ for small values of a, and, since the denominator is the same as for the PCAC definition, we expect the modifications to become visible once the lattice spacing is such that μ is of $O(a^2)$. The details of the modification will be different because the numerator differs compared to the PCAC mass definition.

However, the crucial difference between the PCAC and the pion mass definition is that the approximation (102) will eventually break down for the pion mass definition, since t goes to 1 for a vanishing μ. In that case the t^2 terms can no longer be ignored. Interestingly, the approximate solution (107) gives the correct value $t = 1$ at $\mu = 0$ even though this approximation cannot be justified. A more careful analysis finds [12]

$$t \simeq 1 - \delta,$$
$$\delta = \frac{1}{2}\left[\frac{\mu(2B + \tilde{c}_2 a)}{(c_2 + \tilde{c}_2 W_0/B)a^2}\right]^{2/3} = O\left(\left[\frac{\mu}{a^2}\right]^{2/3}\right). \quad (108)$$

Therefore, the condition $t = O(a)$ for automatic $O(a)$ improvement is satisfied only for small lattice spacings where $2B\mu \gg 2(c_2 + \tilde{c}_2 W_0/B)a^2$. Even though this bound is asymptotically satisfied as $a \to 0$, at a given nonvanishing lattice spacing the scaling violation becomes sizable for small twisted quark masses. In particular in the region $2B\mu \ll 2(c_2 + \tilde{c}_2 W_0/B)a^2$, where $t \to 1$ in the $\mu \to 0$ limit, automatic $O(a)$ improvement fails.

This failure is seen when one inserts (108) into expression (91) for the decay constant, for example. Ignoring the small correction coming δ^2 and higher powers we find

$$f_\pi = f\sqrt{2\delta}(1 + c_0 a - c_0 a\delta), \quad (109)$$

which obviously has a term linear in a. We emphasize that the reason for the presence of terms linear in a is the leading 1 in $t = 1 - \delta$, and not the correction δ with the peculiar dependence on fractional powers of a, even though the overall factor $\sqrt{2\delta}$ complicates the whole a dependence.[17] The leading constant term is the crucial difference to the PCAC mass definition, where $t = O(a)$, and this constant term spoils automatic $O(a)$ improvement for lattice spacings where $2B\mu \ll 2(c_2 + \tilde{c}_2 W_0/B)a^2$.

We summarize the results in this section as follows. Although the PCAC mass and pion mass definitions lead to $O(a)$ improvement for small enough lattice spacings, the asymptotic $O(a^2)$ behavior can be seen only at lattice spacings where the bound $\mu \gg a^2\Lambda_{\mathrm{QCD}}^3$ is realized for a given μ. If this bound is not satisfied, the naïvely expected scaling violation is compromised, in particular, for the pion mass definition, but also for the PCAC mass definition, even though to a much lesser extent. Note that the bound

[15] Recall that we here consider the case with $c_2 > 0$. If $c_2 + \tilde{c}_2 W_0/B < 0$, the assumption $t \ll 1$ could be violated at some value of μ. Therefore, in the latter case, we exclude such values of μ in the following consideration.

[16] We emphasize that the nontrivial behavior in $t = aX(a^2)$ does not mean that there are terms linear in a in physical observables.

[17] The expression (109) goes to zero in the $\mu \to 0$ limit, because f_π was computed with the indirect method [cf. Eq. (92)]. The true decay constant defined by the usual matrix element involving the axial vector current goes to a nonvanishing constant.

$2B\mu \gg 2(c_2 + \tilde{c}_2 W_0/B)a^2$ excludes automatic $O(a)$ improvement for the massless theory in the case of the pion mass definition, which is not unexpected since it is identical to the massless (untwisted) Wilson theory.

E. Automatic $O(a)$ improvement for the $c_2 < 0$ case

Since the condition for automatic $O(a)$ improvement discussed in the previous section does not depend on the details of the lattice QCD dynamics, it seems applicable quite generally. However, there are circumstances when conditions like $\langle A_\mu^2 P^2 \rangle = 0$ or $\cot\omega_{\rm WT} = 0$ cannot be satisfied. This is the case when the first-order phase transition scenario of Refs. [16,44] is realized.

Let us consider this case in WChPT. For simplicity we work at LO only and set $\tilde{c}_2 = c_3 = 0$ in the following argument. In this case, if $c_2 < 0$, a first-order phase transition appears at $\chi = 0$ [16,33] and t is given by [12]

$$t = \begin{cases} \sqrt{1-\alpha^2}, & \alpha^2 < 1, \quad \chi \to 0^+ \\ -\sqrt{1-\alpha^2}, & \alpha^2 < 1, \quad \chi \to 0^- \\ 0, & \alpha^2 \geq 1, \quad \chi \to 0 \end{cases}, \qquad \alpha = \frac{\mu}{\mu_{\rm min}}. \tag{110}$$

Although the condition $t = 0$ can be realized for $\chi = 0$, the twisted mass μ must satisfy the bound $\mu^2 \geq \mu_{\rm min}^2$, where

$$\mu_{\rm min}^2 = \left(\frac{2c_2 a^2}{2B}\right)^2. \tag{111}$$

Therefore, automatic $O(a)$ improvement can only be realized for $\mu^2 \geq \mu_{\rm min}^2$, in contrast to the parity conservation definition for the $c_2 > 0$ case, where no restriction on μ needs to be imposed. Note, however, that the same restriction on μ (at LO) is required for the pion mass definition in the $c_2 > 0$ case.

This argument does not change qualitatively when one includes the NLO terms, as has been done in Ref. [32]. The phase transition line is no longer a straight line in the $m_0 - \mu_0$ parameter plane. If the term with $\tilde{c}_2$ is included, the maximal twist condition which gives $t = 0$ becomes μ dependent and reads $\chi = -\mu\tilde{c}_2 a/(2c_2 a^2)$. Nevertheless, the conclusion that one has to stay above the phase transition line in order to be able to satisfy the maximal twist condition remains unchanged.

IV. CONCLUSION

In this paper we gave an alternative proof for automatic $O(a)$ improvement in twisted mass lattice QCD at maximal twist. The most important observation is that a precise definition for the twist angle, and therefore a condition for maximal twist, is determined dynamically by the ratio of two vacuum expectation values in the Symanzik theory:

$$\cot\theta = \frac{\langle i\bar{\psi}\psi\rangle}{\langle \bar{\psi} i\gamma_5 \tau^3 \psi\rangle}. \tag{112}$$

At $\theta = \pm\pi/2$, which is equivalent to T_1 invariance of the vacuum in the continuum theory, scaling violations for all quantities are shown to be even powers in a, as long as they are invariant under the T_1 transformation. Noninvariant quantities, on the other hand, vanish as odd powers in a. It is also shown that the ambiguity for the maximal twist condition in the lattice theory does not spoil automatic $O(a)$ improvement.

We also studied the T_1 invariance condition in WChPT. As expected, for the pseudoscalar mass and the decay constant we find automatic $O(a)$ improvement.

We finally compared the T_1 invariance condition to two other definitions for maximal twist, the PCAC mass and the pion mass definition. Both definitions have been used already in numerical simulations. Although both definitions give asymptotic a^2 scaling violations for $\mu \gg a^2\Lambda_{\rm QCD}^3$, we have shown that the expected a^2 scaling can be obscured once this bound is violated. Hence naïve continuum extrapolations can be deceiving and may lead to wrong results for these definitions of maximal twist. Here a WChPT analysis can be a powerful tool for a controlled continuum extrapolation.

The PCAC mass and the pion mass definition do have the practical advantage that the untwisted mass is tuned to a fixed value independent of the twisted mass μ. This advantage is particularly beneficial in unquenched simulations where the tuning of the critical mass is extremely time consuming. Here one may have to find a compromise between the theoretically desirable and the practically feasible, depending on the available computer resources. Introducing a clover term to the fermion action, as one does in the standard improvement program, helps in this context [45], even though this option seems somewhat against the spirit of automatic $O(a)$ improvement.

ACKNOWLEDGMENTS

We acknowledge useful discussions with R. Frezzotti, M. Golterman, K. Jansen, G. Rossi, S. Sharpe, S. Sint, and P. Weisz. We would like to thank M. Golterman and S. Sharpe for a careful reading of the manuscript. We also thank the Institute for Nuclear Theory at the University of Washington for its hospitality and the Department of Energy for partial support during the completion of this work. This work is supported in part by the Grants-in-Aid for Scientific Research from the Ministry of Education, Culture, Sports, Science and Technology. (No. 13135204, No. 15204015, No. 15540251, No. 16028201). O. B. is supported in part by the University of Tsukuba Research Project.

APPENDIX A: SOME DETAILS FOR THE PROOF OF $O(a)$ IMPROVEMENT

1. Derivation of Symanzik action

We apply the Symanzik expansion to all operators which appear in the lattice action, as was done to $\mathcal{O}^{01,3}_{\rm lat}$ in the main text, After a little algebra we obtain the following expression for the effective action:

$$S_{\rm tmQCD} \Leftrightarrow S_{\rm eff} = S_0 + m_q S_m + \sum_{n=1}^{\infty}[a^{2n} S^0_{2n} + a^{2n-1} S^1_{2n-1}], \tag{A1}$$

where

$$S_0 = \int d^4x [Z_F \mathcal{O}^{00,4}_A(x) + Z_F Z_\mu \mu \mathcal{O}^{01,3}(x) + Z_G \mathcal{O}^{00,4}_B], \tag{A2}$$

$$S_m = \int d^4x Z_F \cdot Z_m \mathcal{O}^{10,3}(x), \tag{A3}$$

and

$$S^0_{2n} = \int d^4x \sum_i C^i_{00,2n+4} \mathcal{O}^{00,2n+4}_i(x) + \sum_i C^i_{01,2n+3} \mu \mathcal{O}^{01,2n+3}_i(x), \tag{A4}$$

$$S^1_{2n-1} = \int d^4x \sum_i C^i_{10,2n+3} \mathcal{O}^{10,2n+3}_i(x) + \sum_i C^i_{11,2n+2} \mu \mathcal{O}^{11,2n+2}_i(x). \tag{A5}$$

In the definitions of $S^{t_n}_n$, the superscripts $t_n = 0, 1$ represent the transformation property under T_1:

$$T_1 \colon S^{t_n}_n \to (-1)^{t_n} S^{t_n}_n. \tag{A6}$$

All coefficients which appear in the expressions above, such as $Z_{\{F,\mu,m,G\}}$ and $C^i_{tp,d}$, are dimensionless functions of g^2, $\log(\Lambda a)$, $m_q a$ and $\mu_0^2 a^2$. They are given in terms of $c^{tp,d}_{t_n p_n, n, i}$, but their explicit forms are unimportant except for $m_{\rm cr}$, which is given by

$$Z_F Z_m m_{\rm cr} a = c^{10,5}_{10,3} - c^{00,4}_{10,3} - \mu_0^2 a^2 \tilde{c}^{01,3}_{10,3}, \tag{A7}$$

where $\mu a \tilde{c}^{01,3}_{10,3} \equiv c^{01,3}_{10,3}$. Using the selection rule (31), it is easy to show that $c^{10,5}_{10,3}$, $c^{00,4}_{10,3}$, and $\tilde{c}^{01,3}_{10,3}$ are even functions of $\mu_0 a$.

Using renormalized fields (46) and parameters (45), we finally obtain (40)–(44) in the main text.

2. Symanzik expansion of operators

Using the selection rules Eqs. (30) and (31), we here determine the structure of the Symanzik expansion for the lattice operator, given by

$$\mathcal{O}^{tp,d}_{\rm lat} \Leftrightarrow \mathcal{O}^{tp,d}_{\rm eff} = \sum_{n=0}^{\infty} a^{n-d} \sum_{t_n, p_n} \sum_i c^{tp,d}_{t_n p_n, n, i_n} \mathcal{O}^{t_n p_n, n}_{i_n}. \tag{A8}$$

In the case with $d = 2s$, the selection rule (30) gives

$$\mathcal{O}^{tp,2s}_{\rm eff} = \sum_{l=0}^{\infty} \sum_i [a^{2(l-s)} \{c^{tp,2s}_{tp,2l,i} \mathcal{O}^{tp,2l}_i + c^{\bar{t}\bar{p},2s}_{\bar{t}\bar{p},2l,i} \mathcal{O}^{\bar{t}\bar{p},2l}_i\} + a^{2(l-s)+1} \{c^{tp,2s}_{\bar{t}\bar{p},2l+1,i} \mathcal{O}^{\bar{t}\bar{p},2l+1}_i + c^{tp,2s}_{\bar{t}\bar{p},2l+1,i} \mathcal{O}^{t\bar{p},2l+1}_i\}] \tag{A9}$$

where $\bar{t} = 1 - t$ and $\bar{p} = 1 - p$. Furthermore, using the second selection rule (31), we have

$$\begin{aligned} \mathcal{O}^{tp,2s}_{\rm eff} = \sum_{l=0}^{\infty} \sum_i [& a^{2(l-s)} \{c^{tp,2s}_{tp,2l,i} \mathcal{O}^{tp,2l}_i \\ & + \mu_R \tilde{c}^{tp,2s}_{t\bar{p},2l-1,i} \mathcal{O}^{t\bar{p},2l-1}_i\} \\ & + a^{2(l-s)+1} \{c^{tp,2s}_{\bar{t}p,2l+1,i} \mathcal{O}^{\bar{t}p,2l+1}_i \\ & + \mu_R c^{tp,2s}_{\bar{t}\bar{p},2l,i} \mathcal{O}^{\bar{t}\bar{p},2l}_i\}]. \end{aligned} \tag{A10}$$

Similarly, for $d = 2s + 1$ we obtain

$$\begin{aligned} \mathcal{O}^{tp,2s+1}_{\rm eff} = \sum_{l=0}^{\infty} \sum_i [& a^{2(l-s)} \{c^{tp,2s+1}_{tp,2l+1,i} \mathcal{O}^{tp,2l+1}_i \\ & + \mu_R \tilde{c}^{tp,2s+1}_{t\bar{p},2l,i} \mathcal{O}^{t\bar{p},2l}_i\} + a^{2(l-s)+1} \{c^{tp,2s+1}_{\bar{t}p,2l,i} \mathcal{O}^{\bar{t}p,2l}_i \\ & + \mu_R c^{tp,2s+1}_{\bar{t}\bar{p},2l-1,i} \mathcal{O}^{\bar{t}\bar{p},2l-1}_i\}]. \end{aligned} \tag{A11}$$

Combining the results and rewriting the operators in terms of renormalized fields we finally obtain Eq. (47).

3. Expressions for $m_q = O(a)$ case

In the case of $m_R = O(a)$, the expansion of $e^{S_{\rm eff}}$ becomes

$$\begin{aligned} e^{S_{\rm eff}} &= e^{S_0} \exp\left\{ m_R S_{m_R} + \sum_{n=1}^{\infty} [a^{2n} S^0_{2n} + a^{2n-1} S^1_{2n-1}] \right\} \\ &\equiv e^{S_0} \sum_{k,n=0}^{\infty} \frac{m_R^k}{k!} S^k_{m_R} a^n S^{(n)}. \end{aligned} \tag{A12}$$

Under the T_1 transformation, it is easy to see that

$$T_1 \colon S^k_{m_R} \to (-1)^k S^k_{m_R}, \qquad S^{(n)} \to (-1)^n S^{(n)}. \tag{A13}$$

Expanding both the action and the operator, and using the fact that terms with $t + l + k + n =$ odd in the above expansion vanish by the maximal twist condition (51), we obtain

$$\langle \mathcal{O}^{pt,d}_{\mathrm{eff,R,sub}}(\{x\})\rangle_{S_{\mathrm{eff}}} = \delta_{t,0}\langle \mathcal{O}^{tp,d}_{R}\rangle_{S_0} + \sum_{s=1}^{\infty}\sum_{k=0}^{2s-t} a^{2s-k-t} m_R^k F_d^{2s-t,k}(\{x\}, g_R^2, \log(\Lambda a), \mu_R; m_R a, \mu_R^2 a^2), \tag{A14}$$

where

$$F_d^{2s-t,k}(\{x\}, g_R^2, \log(\Lambda a), \mu_R; m_R a, \mu_R^2 a^2) = \sum_{l=0}^{2s-t-k}\left\langle \mathcal{O}^{[l+t],d+l}_{R;tpd}(\{x\})\frac{S^k_{m_R}}{k!}S^{(2s-t-k-l)}\right\rangle_{S_0} \tag{A15}$$

is an analytic function for small $m_R a$ and $\mu_R^2 a^2$. This expression tells us that

$$\langle \mathcal{O}^{tp,d}_{\mathrm{eff,R,sub}}(\{x\})\rangle_{S_{\mathrm{eff}}} = \begin{cases} \langle \mathcal{O}^{tp,d}_{R}\rangle_{S_0} + O(a^2), & t=0 \\ O(a), & t=1 \end{cases} \tag{A16}$$

for $m_R = O(a)$.

If we take m_R odd in a such that $m_R = a f(a^2)$, we have

$$\begin{aligned}\langle \mathcal{O}^{tp,d}_{\mathrm{eff,R,sub}}(\{x\})\rangle_{S_{\mathrm{eff}}} &= \delta_{t,0}\langle \mathcal{O}^{tp,d}_{R}\rangle_{S_0} + \sum_{s=1}^{\infty} a^{2s-t} F_d^{2s-t}(\{x\}, g_R^2, \log(\Lambda a), \mu_R; a^2, \mu_R^2 a^2) \\ &= \begin{cases} \langle \mathcal{O}^{tp,d}_{R}\rangle_{S_0} + a^2 F_d^2 + a^4 F_d^4 + \cdots, & t=0 \\ a F_d^1 + a^3 F_d^3 + \cdots, & t=1 \end{cases}\end{aligned} \tag{A17}$$

where

$$F_d^{2s-t}(\{x\}, g_R^2, \log(\Lambda a), \mu_R; a^2, \mu_R^2 a^2) = \sum_{k=0}^{2s-t}(f(a^2))^k F_d^{2s-t,k}(\{x\}, g_R^2, \log(\Lambda a), \mu_R; a^2 f^2, \mu_R^2 a^2).$$

4. Maximal twist condition on the lattice

The maximal twist condition on the lattice leads to

$$\begin{aligned} 0 = \langle \mathcal{O}^{1p,d}_{\mathrm{lat,R,sub}}\rangle &= \langle \mathcal{O}^{1p,d}_{\mathrm{eff,R,sub}}\rangle = \sum_{s=1}^{\infty}\sum_{k}^{2s-1} a^{2s-k-1} m_R^k F_d^{2s-1,k} \\ &= \sum_{k=0}^{\infty}\sum_{s=k+1}^{\infty}[m_R^{2k} a^{2(s-k)-1} F_d^{2s-1,2k} + m_R^{2k+1} a^{2(s-k-1)} F_d^{2s-1,2k+1}] \\ &= a H_d^0(\mu_R; a^2, m_R^2, m_R a, \mu_R^2 a^2) + m_R H_d^0(\mu_R; a^2, m_R^2, m_R a, \mu_R^2 a^2), \end{aligned} \tag{A18}$$

where

$$H_d^{\delta}(\mu_R; a^2, m_R^2, m_R a, \mu_R^2 a^2) \equiv \sum_{k=0}^{\infty} m_R^{2k}\sum_{s=k+1}^{\infty} a^{2(s-k-1)} F_d^{2s-1,2k+\delta}(g_R^2, \log(\Lambda a), \mu_R; m_R a, \mu_R^2 a^2)$$

for $\delta = 0$, 1, and we keep the dependency on g_R^2 and $\log(\Lambda a)$ implicit in H_d^{δ}.

APPENDIX B: WARD-TAKAHASHI ANGLE, PION MASS, AND DECAY CONSTANT IN WCHPT

In this appendix we provide some details about the calculation of $\cot\omega_{\mathrm{WT}}$ and the pseudoscalar masses and decay constant. At leading order in our power counting scheme this has been done already in Ref. [12], and we refer also to this reference.

Our first observable is the twist angle ω_{WT} defined in Eq. (84). Instead of Eq. (84) the twist angle can be expressed also as

$$\cot\omega_{\mathrm{WT}} = \frac{\langle \partial_\mu A^2_\mu P^2\rangle}{\langle \partial_\mu V^1_\mu P^2\rangle}. \tag{B1}$$

The extra derivative gives rise to an additional factor of the pion mass in both the numerator and the denominator, which consequently cancels.

The Noether's currents appearing in the correlators on the right-hand side of Eq. (B1) are given by ($a = 1, 2$)

$$\begin{aligned} V^a_\mu &= V^a_{0,\mu}\left[1 + \frac{c_0 a}{4}\langle\Sigma + \Sigma^\dagger\rangle\right], \\ V^a_{0,\mu} &= \frac{if^2B}{4}\langle\tau_a(\Sigma\partial_\mu\Sigma^\dagger + \Sigma^\dagger\partial_\mu\Sigma)\rangle, \end{aligned} \tag{B2}$$

$$\begin{aligned} A^a_\mu &= A^a_{0,\mu}\left[1 + \frac{c_0 a}{4}\langle\Sigma + \Sigma^\dagger\rangle\right], \\ A^a_{0,\mu} &= \frac{if^2B}{4}\langle\tau_a(\Sigma\partial_\mu\Sigma^\dagger - \Sigma^\dagger\partial_\mu\Sigma)\rangle. \end{aligned} \tag{B3}$$

The factor involving $c_0 a$ stems from the wave function renormalization due to the $O(p^2 a)$ contribution in the chiral Lagrangian, cf. (70). In Ref. [12] $\cot\omega_{\rm WT}$ was computed without the $O(a\mu, a^3)$ contributions. Repeating the calculation including these terms we find

$$\cot\omega_{\rm WT} = \frac{t}{\sqrt{1-t^2}} = \cot\phi. \tag{B4}$$

This is the same result as in Ref. [12]. The functional dependence of $\cot\omega_{\rm WT}$ is unchanged, and the $O(a\mu, a^3)$ corrections contribute only indirectly through the gap equation.

Result Eq. (B4) assumes that the currents in the correlators are Noether currents stemming from the vector and axial vector Ward-Takahashi identities [1]. This means that the point split currents must be used in the lattice simulation. However, local currents are often used instead of there point split counter parts. This introduces additional contributions proportional to a. Taking into account the leading corrections of $O(a)$ only, we obtain

$$Z_V V^{a,\rm local}_\mu = V^a_{0,\mu}\left[1 + \frac{c_{\rm V}}{4} a\langle\Sigma + \Sigma^\dagger\rangle\right], \tag{B5}$$

$$\begin{aligned} Z_A A^{a,\rm local}_\mu = A^a_{0,\mu}&\left[1 + \frac{c_{\rm A}}{4} a\langle\Sigma + \Sigma^\dagger\rangle\right] \\ &+ \frac{if^2B}{4}\tilde{c}_A\partial_\mu\langle\Sigma - \Sigma^\dagger\rangle, \end{aligned} \tag{B6}$$

where $c_{\rm V,A}$ and $\tilde{c}_A$ are additional coefficients parametrizing the lattice artifacts stemming from the currents. Using these currents, the expression (B4) changes to

$$\cot\omega_{\rm WT} = \frac{Z_V}{Z_A}\frac{1}{1 + ac_{\rm V}t}\frac{(1 + ac_{\rm A}t)t - \tilde{c}_A a}{\sqrt{1-t^2}}, \tag{B7}$$

which is the result in Eq. (88).

In order to calculate the pion masses, we expand Σ around the vacuum configuration Σ_0 defined in (76). We parametrize the field Σ in terms of the pion fields according to[18]

$$\Sigma(x) = \Sigma_0^{1/2}\exp\left(\sum_{i=1}^{3} i\pi_i(x)\tau_i/f\right)\Sigma_0^{1/2}. \tag{B8}$$

Using this form in expression (74) for the potential energy, we expand in powers of the field π. The contribution quadratic in π leads to the pion mass formulas

$$\begin{aligned} m^2_{\pi_\pm} = {}& 2Bm'\cos(\phi - \omega_L) + 2W_0 a\cos\phi - 2c_2a^2\cos^2\phi \\ &+ 3c_3a^3\cos^3\phi + 2\tilde{c}_2 am'\cos\phi\cos(\phi - \omega_L), \end{aligned} \tag{B9}$$

$$\begin{aligned} m^2_{\pi_3} = {}& m^2_{\pi_a} + 2c_2a^2\sin^2\phi - 6c_3a^3\sin^2\phi\cos\phi \\ &- 2\tilde{c}_2 am'\sin\phi\sin(\phi - \omega_L). \end{aligned} \tag{B10}$$

Expressing this in terms of m and μ and taking into account the gap equation we can express the mass for the charged pion alternatively as

$$m^2_{\pi_\pm} = \frac{2B\mu}{\sqrt{1-t^2}}\frac{1 + \beta_\mu t}{1 + c_0 at}. \tag{B11}$$

Note that the expression (B11) is not singular for $t = 1$. From the gap equation one can infer that $t = 1$ can be a solution only if $\mu = 0$, and in that case the result (B11) is not well defined. For $t \neq 0$ one can, using the gap equation, rewrite the pion mass formula as in (100), which is well behaved for $t = 1$.

The decay constant is conveniently computed with the so-called indirect method [1,42], which is based on an exact partially conserved vector current relation and does not require the computation of any renormalization constants:

$$f_\pi = \frac{2\mu}{m^2_\pi}\langle 0|P^\pm|\pi_\mp\rangle. \tag{B12}$$

In order to calculate the decay constant according to Eq. (B12), we need the matrix element of the pseudoscalar between the vacuum and the one pion state, where the pseudoscalar in the effective theory is defined by ($\tau_\pm = \frac{\tau_1 \pm i\tau_2}{\sqrt{2}}$)

[18]This parametrization differs slightly from the one used in Ref. [12]. This difference does not affect any of the results in this reference.

$$P^{\pm} = \frac{f^2 B}{4i}\left[1 + \frac{\beta_\mu}{4}\langle \Sigma + \Sigma^\dagger\rangle\right]\langle \tau_\pm(\Sigma - \Sigma^\dagger)\rangle,$$
$$\pi_\pm = \frac{\pi_1 \pm i\pi_2}{\sqrt{2}}. \tag{B13}$$

The matrix element in Eq. (B12) is readily calculated at tree level with the result

$$\langle 0|P^\pm|\pi_\mp\rangle = fB(1 + \beta_\mu t). \tag{B14}$$

With the expression for the charged pion mass we obtain

$$f_\pi = f(1 + c_0 at)\sqrt{1 - t^2} \tag{B15}$$

for the decay constant.

[1] R. Frezzotti, S. Sint, and P. Weisz, J. High Energy Phys. 07 (2001) 048.
[2] R. Frezzotti, P. A. Grassi, S. Sint, and P. Weisz, J. High Energy Phys. 08 (2001) 058.
[3] W. Bietenholz *et al.*, J. High Energy Phys. 12 (2004) 044.
[4] A. M. Abdel-Rehim, R. Lewis, and R. M. Woloshyn, Phys. Rev. D **71**, 094505 (2005).
[5] K. Jansen *et al.*, Phys. Lett. B **619**, 184 (2005).
[6] K. Jansen *et al.*, J. High Energy Phys. 08 (2005) 071.
[7] C. Urbach, K. Jansen, A. Shindler, and U. Wenger, Comput. Phys. Commun. **174**, 87 (2006).
[8] R. Frezzotti and G. C. Rossi, J. High Energy Phys. 08 (2004) 007.
[9] R. Frezzotti and G. C. Rossi, J. High Energy Phys. 10 (2004) 070.
[10] R. Frezzotti and G. Rossi, hep-lat/0507030.
[11] A. Shindler, PoS, LAT2005 (2005) 014.
[12] S. Aoki and O. Bär, Phys. Rev. D **70**, 116011 (2004).
[13] R. Frezzotti, G. Martinelli, M. Papinutto, and G. C. Rossi, J. High Energy Phys. 04 (2006) 038.
[14] K. Jansen *et al.*, PoS, LAT2005 (2005) 231.
[15] M. Della Morte and M. Luz, Phys. Lett. B **632**, 663 (2006).
[16] S. R. Sharpe and Robert Singleton, Jr., Phys. Rev. D **58**, 074501 (1998).
[17] G. Rupak and N. Shoresh, Phys. Rev. D **66**, 054503 (2002).
[18] O. Bär, Nucl. Phys. B, Proc. Suppl. **140**, 106 (2005).
[19] S. R. Sharpe and J. M. S. Wu, Phys. Rev. D **70**, 094029 (2004).
[20] K. Symanzik, Nucl. Phys. **B226**, 187 (1983).
[21] K. Symanzik, Nucl. Phys. **B226**, 205 (1983).
[22] S. Aoki, Phys. Rev. D **30**, 2653 (1984).
[23] S. Aoki, Phys. Rev. D **33**, 2399 (1986).
[24] S. Aoki, Phys. Rev. D **34**, 3170 (1986).
[25] S. Aoki, Phys. Rev. Lett. **57**, 3136 (1986).
[26] S. Aoki, Nucl. Phys. **B314**, 79 (1989).
[27] S. Sint, Proceedings of the Nara Workshop, 2005, Nara, Japan.
[28] S. R. Sharpe and J. M. S. Wu, Phys. Rev. D **71**, 074501 (2005).
[29] O. Bär, G. Rupak, and N. Shoresh, Nucl. Phys. B, Proc. Suppl. **129**, 185 (2004).
[30] S. Aoki, Phys. Rev. D **68**, 054508 (2003).
[31] G. Münster and C. Schmidt, Europhys. Lett. **66**, 652 (2004).
[32] S. R. Sharpe, Phys. Rev. D **72**, 074510 (2005).
[33] G. Münster, J. High Energy Phys. 09 (2004) 035.
[34] S. Aoki and O. Bär, PoS, LAT2005 (2005) 046.
[35] S. R. Sharpe and J. M. S. Wu, Nucl. Phys. B, Proc. Suppl. **140**, 323 (2005).
[36] O. Bär, G. Rupak, and N. Shoresh, Phys. Rev. D **70**, 034508 (2004).
[37] J. Gasser and H. Leutwyler, Ann. Phys. (N.Y.) **158**, 142 (1984).
[38] J. Gasser and H. Leutwyler, Nucl. Phys. **B250**, 465 (1985).
[39] O. Bär, G. Rupak, and N. Shoresh, Phys. Rev. D **67**, 114505 (2003).
[40] S. Aoki, O. Bär, S. Takeda, and T. Ishikawa, Phys. Rev. D **73**, 014511 (2006).
[41] S. Aoki, O. Bär, and S. Takeda, "Currents and Densities in Wilson Chiral Perturbation Theory" (unpublished).
[42] K. Jansen, A. Shindler, C. Urbach, and I. Wetzorke, Phys. Lett. B **586**, 432 (2004).
[43] S. R. Sharpe, Proceedings of the Nara Workshop, 2005, Nara, Japan.
[44] F. Farchioni *et al.*, Eur. Phys. J. C **39**, 421 (2005).
[45] D. Becirevic, P. Boucaud, V. Lubicz, G. Martinelli, F. Mescia, S. Simula, and C. Tarantino, hep-lat/0605006.

Eur. Phys. J. A **31**, 781–783 (2007)
DOI 10.1140/epja/i2006-10202-x

THE EUROPEAN PHYSICAL JOURNAL A

Special Article – QNP 2006

WChPT analysis of twisted mass lattice data

S. Aoki[1,2] and O. Bär[3,a]

[1] Graduate School of Pure and Applied Sciences, University of Tsukuba, Tsukuba 305-8571, Japan
[2] Riken BNL Research Center, Brookhaven National Laboratory, Upton, NY 11973, USA
[3] Institute of Physics, Humboldt University Berlin, Newtonstrasse 15, 12489 Berlin, Germany

Received: 25 October 2006
Published online: 28 February 2007 –

Abstract. We perform a Wilson Chiral Perturbation Theory (WChPT) analysis of quenched twisted mass lattice data. The data were generated by two independent groups with three different choices for the critical mass. For one choice, the so-called pion mass definition, one observes a strong curvature for small quark masses in various mesonic observables ("bending phenomenon"). Performing a combined fit to the next-to-leading (NLO) expressions, we find that WChPT describes the data very well and the fits provide very reasonable values for the low-energy parameters.

PACS. 12.38.Gc Lattice QCD calculations – 11.15.Ha Lattice gauge theory

1 Introduction

Twisted mass lattice QCD [1,2] has many advantages for numerical lattice simulations, with automatic O(a) improvement at maximal twist [3–5] being probably the most striking one (for a recent review see ref. [6]). Maximal twist is achieved by tuning the bare untwisted mass m_0 to a particular (critical) value such that some matrix element vanishes. The condition for maximal twist is not unique and various choices have been employed in quenched simulations [7–11].

A puzzle observed in early quenched simulations is the so-called "bending phenomenon" [7]. Employing the pion mass definition for maximal twist (*i.e.* tuning m_0 to the value where the pion mass would vanish without a twisted mass term), one observed a strong curvature in the quark mass dependence of many observables (m_π, f_π, m_ρ) for small twisted quark masses μ. This unexpected observation spurred further numerical simulations with other definitions for maximal twist [8–10] as well as theoretical studies. Nowadays the bending phenomenon seems well understood both in terms of the Symanzik effective theory [12] as well as in Wilson Chiral Perturbation theory (WChPT) [13–15] (for introductions to lattice ChPT see also refs. [16,17]).

It is a pleasant side effect of this effort to understand the bending phenomenon that there are lots of data available for five different lattice spacings and three definitions of maximal twist. Moreover, light quark masses could be reached with values for m_π/m_ρ down to ~ 0.3, where one might expect WChPT to provide an effective description of the data. In particular, the characteristic curvature of the bending phenomenon provides a distinctive test for WChPT to pass if it is the correct low-energy effective theory for twisted mass lattice QCD. Provided WChPT describes the data very well we may also obtain estimates for some combinations of low-energy constants of the effective theory. This was sufficient motivation for us to carry out a WChPT analysis of the existing lattice data. Preliminary results involving data for two definitions of maximal twist only can be found in ref. [18].

[a] Spokesperson; e-mail: obaer@physik.hu-berlin.de

2 Fitting the data

We analyzed quenched lattice data generated by two different groups [7–10] with the Wilson plaquette action at $\beta = 5.85$ ($a \approx 0.123\,\mathrm{fm}$) and $\beta = 6.0$ ($a \approx 0.093\,\mathrm{fm}$). The standard Wilson fermion action with a twisted mass term was employed to calculate a variety of mesonic observables. The twisted quark mass covers the range $m_\pi \approx$ 270–1200 MeV, or, alternatively, $m_\pi/m_\rho \approx 0.3$–0.8. Besides the pion mass there is data available for the pseudoscalar decay constant, the angle $\cot\omega_{\mathrm{WT}}$, as well as some more observables which we did not analyze. The untwisted bare quark mass was tuned according to three different definitions of maximal twist: the pion mass definition, the PCAC mass definition and the parity conservation definition. In total there are at most 52 data points available for each lattice spacing.

There exists a vast literature on WChPT for twisted mass lattice QCD [19,20,13,21,14], which contains expres-

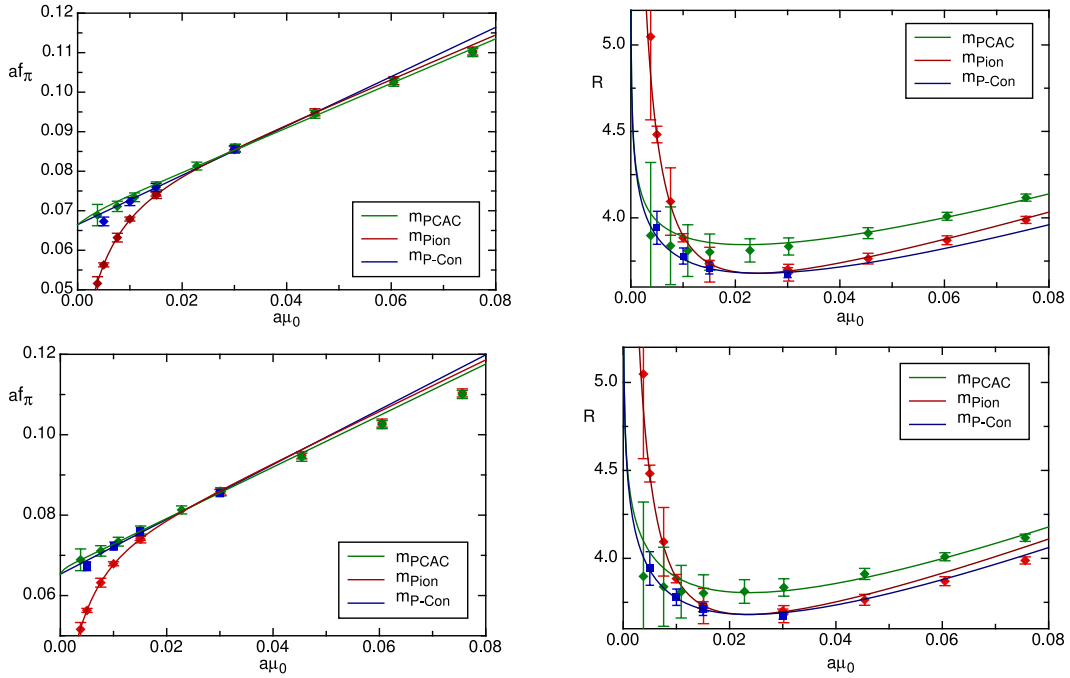

Fig. 1. (Colour on-line) Results of a combined fit for f_π and R at $\beta = 6.0$ (χ^2/d.o.f. = 0.23 with d.o.f. = 26). The upper plots show the results where all data points are included in the fit, while data points with $a\mu_0 \leq 0.0302$ only are included in the fits shown in the lower plots.

sions for various mesonic observables up to next-to-leading order (NLO). The lattice artifacts are included through order $O(a^2)$ for different power countings and definitions of maximal twist. Here we use the NLO formulae given in ref. [15], which include all NLO terms consistently for the two regimes where either $\mu \sim a$ or $\mu \sim a^2$. The quenched chiral logarithm [22,23] is also included in the formulae.

We performed combined fits of the WChPT formulae at NLO to the data for three observables: f_π,

$$R = \frac{(a\, m_\pi)^2}{a\mu}, \tag{1}$$

$$\cot \omega_{\mathrm{WT}} = \frac{\langle \partial_\mu A^1_\mu P^1 \rangle}{\langle \partial_\mu V^2_\mu P^1 \rangle}, \tag{2}$$

where V^a_μ and A^a_μ denote the (nonsinglet) vector and axial vector current, respectively. At NLO we have in total thirteen free fit parameters. Even though this is a fairly large number it is still small compared to the number of data points.

We performed various fits, starting with all data points included and then successively remove the data points at high quark masses. In all cases we obtain good fit results with χ^2/d.o.f. $\approx$ 0.2–0.5, even if all data points up to $m_\pi/m_\rho \approx 0.8$ are included[1]. Since we do not trust ChPT to work at such high masses we prefer to drop the data for the highest three masses. The fit results for f_π and R at $\beta = 6.0$ are shown in fig. 1. Even in this fit the heaviest point corresponds to $m_\pi/m_\rho \approx 0.63$, which is still heavy. Dropping more data points, however, makes the fit more and more unstable, so we cannot reduce the number of data points much further.

Apparently, WChPT describes the data very well. In particular, the bending for small masses in case of the pion mass definition is very well reproduced. This feature is independent of the number of data points included in the fit, even though the values for the fit parameters are different (see below). Note that the curvature in the data for R with $a\mu_0 \geq 0.3$ is also well described even though the heavier data points are excluded from the fit.

The fits give reasonable values for the fit parameters. For the quenched chiral log parameter δ_0, for example, we find

$$\delta_0 = \begin{cases} 0.10 \pm 0.03, & \beta = 6.0, \\ 0.054 \pm 0.011, & \beta = 5.85, \end{cases} \tag{3}$$

which is in very good agreement with the results obtained by other groups (for a summary, see ref. [24]).

We also obtain an estimate for the low-energy constant c_2. This parameter was first introduced in ref. [25] and

[1] Note that the χ^2 value is underestimated since the data is highly correlated.

enters the chiral Lagrangian according to[2]

$$L_\chi = \ldots + \frac{c_2}{16}\left\{\mathrm{tr}(\Sigma + \Sigma^\dagger)\right\}^2 \ldots . \tag{4}$$

The sign of c_2 determines the phase diagram of the lattice theory and the pion mass splitting $\Delta m_\pi^2 = m_{\pi^0}^2 - m_{\pi^\pm}^2$ in the chiral limit is given by c_2/f_π^2 [25].

From our fits we obtain for c_2 the value

$$c_2 = \left[291\,\mathrm{MeV}^{+4\%}_{-5\%}\right]^4, \quad \beta = 5.85. \tag{5}$$

This is the first determination of this low-energy constant, so we cannot compare with other results. However, the value seems reasonable based on dimensional analysis arguments. The fit for the smaller lattice spacing with $\beta = 6.0$ does not determine c_2 very well; for the mean value we obtain approximately $[170\,\mathrm{MeV}]^4$, but the error is of the same size.

The physical parameters, on the other hand, are very well determined by the fit. For the pseudoscalar decay constant in the chiral limit we find

$$f_0 = \begin{cases} 141.2\,\mathrm{MeV} \pm 1\%, & \beta = 6.0, \\ 141.4\,\mathrm{MeV} \pm 1\%, & \beta = 5.85, \end{cases} \tag{6}$$

which is in very good agreement with earlier determinations. For the low-energy constant α_5^{q} [26], entering the NLO expression for the decay constant, we obtain

$$\alpha_5^{\mathrm{q}} = \begin{cases} 1.03(5), & \beta = 6.0, \\ 0.97(4), & \beta = 5.85. \end{cases} \tag{7}$$

Also these values agree very well with previous results in ref. [26]. Note that the results for f_0 and α_5^{q} do not show any significant dependence on the lattice spacing. This is expected if WChPT works, since the main dependence on a is captured by other terms in the chiral expansion, being directly proportional to powers of a.

We emphasize that the errors we quoted so far are only the statistical errors given by MINUIT which we used to perform the fits. These errors are underestimated due to the highly correlated data and the true statistical error can be substantially larger. A second error source are systematic uncertainties, induced, for example, by the number of data points included in the fit. It is not simple to give a precise estimate for this error but we observed that the central value for f_0 changes by roughly 3 percent for the different fits we performed, while α_5^{q} varies by about 7 percent.

3 Conclusions

We performed fits of WChPT to quenched twisted mass data for m_π^2, f_π and the Ward-Takahashi angle $\cot\omega_{\mathrm{WT}}$. We find that the NLO expressions describe the data very well with small χ^2 values and reasonable values for the low-energy parameters. In particular, the bending phenomenon in case of the pion mass definition is very well reproduced.

The bending phenomenon is a very characteristic feature of twisted mass lattice QCD. It is encouraging that WChPT describes this distinct curvature very well. This indicates that WChPT, *i.e.* ChPT for lattice QCD, seems to work. Previous studies [27–29], using untwisted Wilson fermions, came to contradicting results and were not conclusive at all.

So far we performed separate fits for each lattice spacing. In a next step it would be very interesting to perform a combined fit to the entire data set and take the continuum limit. These results should be compared to the results one obtains after a standard continuum extrapolation where one assumes a polynomial lattice spacing dependence. This would partly answer the question whether WChPT is not only able to describe the lattice data but also necessary to extract the correct continuum physics from the data.

[2] The definition of c_2 is not unique and it is sometimes defined differently, for example in ref. [13].

References

1. R. Frezzotti, S. Sint, P. Weisz, JHEP **07**, 048 (2001).
2. R. Frezzotti, P.A. Grassi, S. Sint, P. Weisz, JHEP **08**, 058 (2001).
3. R. Frezzotti, G.C. Rossi, JHEP **08**, 007 (2004).
4. R. Frezzotti, G.C. Rossi, JHEP **10**, 070 (2004).
5. R. Frezzotti, G. Rossi, hep-lat/0507030.
6. A. Shindler, PoS (LAT2005) 014 (2005).
7. W. Bietenholz *et al.*, JHEP **12**, 044 (2004).
8. A.M. Abdel-Rehim, R. Lewis, R.M. Woloshyn, Phys. Rev. D **71**, 094505 (2005).
9. K. Jansen *et al.*, Phys. Lett. B **619**, 184 (2005).
10. K. Jansen *et al.*, JHEP **09**, 071 (2005).
11. A.M. Abdel-Rehim, R. Lewis, R.M. Woloshyn, J.M.S. Wu, Phys. Rev. D **74**, 014507 (2006).
12. R. Frezzotti, G. Martinelli, M. Papinutto, G.C. Rossi, JHEP **04**, 038 (2006).
13. S. Aoki, O. Bär, Phys. Rev. D **70**, 116011 (2004).
14. S.R. Sharpe, Phys. Rev. D **72**, 074510 (2005).
15. S. Aoki, O. Bär, hep-lat/0604018.
16. O. Bär, Nucl. Phys. Proc. Suppl. **140**, 106 (2005).
17. S.R. Sharpe, hep-lat/0607016.
18. S. Aoki, O. Bär, PoS (LAT2005) 046 (2005).
19. G. Münster, C. Schmidt, Europhys. Lett. **66**, 652 (2004).
20. L. Scorzato, Eur. Phys. J. C **37**, 445 (2004).
21. S.R. Sharpe, J.M.S. Wu, Phys. Rev. D **71**, 074501 (2005).
22. C.W. Bernard, M.F.L. Golterman, Phys. Rev. D **46**, 853 (1992).
23. S.R. Sharpe, Phys. Rev. D **46**, 3146 (1992).
24. H. Wittig, Nucl. Phys. Proc. Suppl. **119**, 59 (2003).
25. S.R. Sharpe, J. Singleton, Robert, Phys. Rev. D **58**, 074501 (1998).
26. J. Heitger, R. Sommer, H. Wittig, Nucl. Phys. B **588**, 377 (2000).
27. F. Farchioni, I. Montvay, E. Scholz, Eur. Phys. J. C **37**, 197 (2004).
28. S. Aoki, Phys. Rev. D **68**, 054508 (2003).
29. Y. Namekawa *et al.*, Phys. Rev. D **70**, 074503 (2004).

PHYSICAL REVIEW D **78,** 114501 (2008)

Pion scattering in Wilson chiral perturbation theory

Sinya Aoki,[1,2] Oliver Bär,[3] and Benedikt Biedermann[3]

[1]*Graduate School of Pure and Applied Sciences, University of Tsukuba, Tsukuba 305-8571, Ibaraki, Japan*
[2]*Riken BNL Research Center, Brookhaven National Laboratory, Upton, New York 11973, USA*
[3]*Institute of Physics, Humboldt University Berlin, Newtonstrasse 15, 12489 Berlin, Germany*

(Received 7 July 2008; published 3 December 2008)

We compute the scattering amplitude for pion scattering in Wilson chiral perturbation theory for two degenerate quark flavors. We consider two different regimes where the quark mass m is of order (i) $a\Lambda_{\rm QCD}^2$ and (ii) $a^2\Lambda_{\rm QCD}^3$. Analytic expressions for the scattering lengths in all three isospin channels are given. As a result of the $O(a^2)$ terms the $I=0$ and $I=2$ scattering lengths do not vanish in the chiral limit. Moreover, additional chiral logarithms proportional to $a^2 \ln M_\pi^2$ are present in the one-loop results for regime (ii). These contributions significantly modify the familiar results from continuum chiral perturbation theory.

DOI: 10.1103/PhysRevD.78.114501 PACS numbers: 11.15.Ha, 12.39.Fe, 12.38.Gc

I. INTRODUCTION

The scattering of low-energy pions is an important process in QCD. Since the pions are the pseudo Goldstone bosons associated with the spontaneous breaking of chiral symmetry, one can use chiral perturbation theory (ChPT) to compute the scattering amplitude and the associated scattering lengths to high precision. These theoretical predictions are in excellent agreement with the experiment [1,2].

Since a few years ago lattice QCD has started to impact ChPT and the study of pion scattering. Increase in computer power and algorithmic advances nowadays allow unquenched simulations with light pion masses so that contact with ChPT can be made. Monitoring the quark mass dependence of the pion mass and the pion decay constant various lattice groups have obtained estimates for the low-energy constants $\bar{l}_3$ and $\bar{l}_4$ that enter the one-loop ChPT results of these two observables [3–5]. These two constants play an important role for pion scattering, in particular $\bar{l}_3$, since it dominates the uncertainties in the isospin zero and isospin two scattering lengths [6] (see also [2]).

The scattering lengths can also be computed directly on the lattice, and two unquenched calculations for the $I=2$ scattering length a_0^2 have been performed so far. The CP-PACS collaboration simulated two dynamical Wilson quarks at three lattice spacings between 0.1 and 0.2 fm [7]. The pion masses, however, were rather heavy, spanning the range 0.5 to 1.1 GeV. Thus, contact to ChPT is not expected. The NPLQCD collaboration [8,9] performed a mixed action simulation with domain-wall valence quarks and staggered sea quarks.[1] The four pion masses were in the range 290 to 490 MeV and the lattice spacing $a \approx 0.125$ fm.[2] Since data at one lattice spacing only was generated and due to the use of different actions in the sea and valence sector mixed action ChPT [11–13] was used to extrapolate simultaneously to the continuum and chiral limit. The obtained result for a_0^2 agrees very well with the experimentally measured one.

In this paper we study pion scattering in Wilson ChPT (WChPT) [14,15], the low-energy effective theory for lattice QCD with Wilson quarks. We compute the scattering amplitude to one loop including the leading corrections due to the nonzero lattice spacing. From the scattering amplitude we derive expressions for the scattering lengths in all three isospin channels which can be used to analyze lattice data before the continuum limit has been taken. We work in two different quark mass regimes: (i) $m \sim a\Lambda_{\rm QCD}^2$ and (ii) $m \sim a^2\Lambda_{\rm QCD}^3$. These are most likely applicable to today's and future simulations with light Wilson quarks. The $I=2$ scattering length in regime (i) has already been calculated before in Ref. [16], and we agree with this result.

The lattice spacing is, just as the quark mass, a source of explicit chiral symmetry breaking. Therefore, the lattice artifacts modify the results from continuum ChPT. For example, the scattering lengths a_0^I for $I=0$, 2 do not vanish in the chiral limit but assume nonzero values. This is not unexpected [17–19]. However, the value in the chiral limit is of order a^2 and not of order a, as one might naively think based on the (broken) symmetries of the Wilson fermion action.

[1]The unquenched configurations were generated by the MILC collaboration [10] and are publicly available.

[2]The pion masses refer to the staggered Goldstone pion. The masses of the other pions are significantly heavier. The taste singlet pion, which is the heaviest, is about 450 MeV heavier than the Goldstone pion at this lattice spacing [3].

In addition, at sufficiently small quark masses there appear additional chiral logarithms proportional to $a^2 \ln M_\pi^2$ in the chiral expansion. These additional contributions may obscure the continuum chiral logarithms. Consequently, fits of the continuum ChPT expressions to the lattice data may easily result in erroneous determinations of the Gasser-Leutwyler coefficients associated with pion scattering.

II. PION SCATTERING AT TREE LEVEL

A. Setup

The chiral effective Lagrangian of WChPT is expanded in powers of (small) pion momenta p^2, quark masses m, and the lattice spacing a. Based on the symmetries of the underlying Symanzik action [20,21] the chiral Lagrangian including all terms of $O(p^4, p^2m, m^2, p^2a, ma)$ is given in Ref. [15]. The $O(a^2)$ contributions are constructed in Ref. [22] and, independently, in Ref. [23] for the two-flavor case.

In the following we will restrict ourselves to $N_f = 2$ with degenerate quark mass m. In this case the chiral Lagrangian (in Euclidean space-time) including the p^2, m, and a^2 terms is found to be [22,23]

$$\mathcal{L}_2 = \frac{f^2}{4}\langle \partial_\mu \Sigma \partial_\mu \Sigma^\dagger \rangle - \frac{f^2}{4}\hat{m}\langle \Sigma + \Sigma^\dagger \rangle - \frac{1}{2}(2W_6' + W_8')\hat{a}^2 \langle \Sigma + \Sigma^\dagger \rangle^2, \quad (1)$$

where the angled brackets denote traces over the flavor indices. The field Σ containing the pion fields is defined as usual,

$$\Sigma(x) = \exp\left(\frac{2i}{f}\pi(x)\right), \qquad \pi(x) = \pi^a(x)\frac{\sigma^a}{2}, \quad (2)$$

with the standard Pauli matrices σ^a. The quark mass and the lattice spacing enter through the combinations

$$\hat{m} = 2Bm, \qquad \hat{a} = 2W_0 a. \quad (3)$$

The coefficients B and f are the familiar leading order (LO) low-energy coefficients (LECs) from continuum ChPT [24,25], while W_0, W_6', W_8' are LECs associated with the nonzero lattice spacing artifacts [15,22].

Note that the mass parameter m in Eq. (3) is the so-called *shifted mass* [14]. Besides the dominant additive mass renormalization proportional to $1/a$ it also contains the correction of $O(a)$. Consequently, there is no term linear in the lattice spacing present in the chiral Lagrangian in Eq. (1).

Note also that we keep the $O(a^2)$ correction in $\mathcal{L}_2$ and promote it to a LO term in the chiral expansion. This is justified (and necessary) for small enough quark masses such that the $O(m)$ and the $O(a^2)$ terms are of the same order of magnitude, i.e. for $m \sim a^2\Lambda_{\mathrm{QCD}}^3$. We call this scenario the *large cutoff effects* (LCE) regime, in contrast to the so-called *generic small quark mass* (GSM) regime [26,27], which assumes $m \sim a\Lambda_{\mathrm{QCD}}^2$. Nevertheless, even though we almost exclusively work in the LCE regime we will be able to obtain the corresponding results for the GSM regime as well by appropriately expanding our final results (see Sec. III D).

It will be useful to introduce [28]

$$c_2 = -32(2W_6' + W_8')\frac{W_0^2}{f^2} \quad (4)$$

for the combination of LECs in front of the $O(a^2)$ term in the chiral Lagrangian. The sign of c_2 determines the phase diagram of the theory [14].[3] For $c_2 > 0$ there exists a second-order phase transition separating a phase where parity and flavor are spontaneously broken [29]. The charged pions are massless in this phase due to the spontaneous breaking of the flavor symmetry. Outside this phase the pion mass is given by

$$M_0^2 = 2Bm - 2c_2a^2, \quad (5)$$

and it vanishes at $m = c_2a^2/B$. For even smaller values of m the charged pions remain massless, while the neutral pion becomes massive again [14].

Negative values of c_2, on the other hand, imply a first order phase transition with a minimal nonvanishing pion mass. All three pions are massive for all quark masses, and the pion mass assumes its minimal value at $m = 0$, resulting in

$$M_{0,\mathrm{min}}^2 = 2|c_2|a^2. \quad (6)$$

The magnitude and the sign of c_2 depend on the details of the underlying lattice theory, i.e. what particular lattice action has been chosen. However, it is not a simple task to measure c_2 numerically. Adding a twisted mass term [30] to the theory the pion mass splitting between the neutral and the charged pion is equal to $2c_2a^2$ at LO in the chiral expansion [28,31]. This has been exploited by the ETM collaboration [32,33] and an estimate for c_2 has been obtained. Within errors c_2 is negative if the standard Wilson fermion action and the tree-level Symanzik improved gauge action is used. However, the statistical uncertainties for c_2 were rather large due to the presence of disconnected diagrams in the calculation of the neutral pion mass.

B. Scattering amplitude and scattering lengths

We are interested in the two-pion scattering process

$$\pi^\alpha(p) + \pi^\beta(k) \to \pi^\gamma(p') + \pi^\delta(k'). \quad (7)$$

This process is described by the scattering amplitude A. It is convenient to use the three Mandelstam variables as

[3]Note that our definition for c_2 differs by a factor f^2a^2 from the one in Ref. [14].

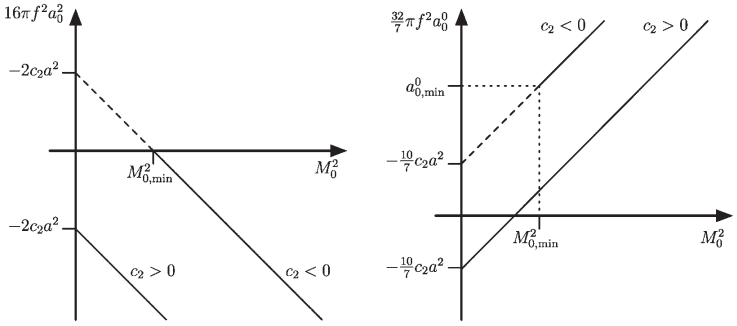

FIG. 1. Sketch of the scattering lengths as a function of the pion mass at nonzero lattice spacing. The left panel shows $16\pi f^2 a_0^2$ as a function of the tree-level pion mass M_0^2. For $c_2 < 0$ the pion mass cannot be smaller than $M_{0,\min}^2$ in Eq. (6). Nevertheless, extrapolating to the massless point the scattering length assumes the value $-2c_2a^2$, as indicated by the dashed line. For $c_2 > 0$ the pion mass can be taken as zero. At this mass the scattering length also assumes the value $-2c_2a^2$, now with the opposite sign. The right panel shows the analogous sketch for the $I = 0$ scattering length.

arguments for it, $A = A(s, t, u)$. The scattering amplitude is straightforwardly calculated as the residue of the four pion pole in the four-point function. Starting from Eq. (1) we obtain the tree-level result[4]

$$A(s, t, u) = \frac{1}{f^2}(s - M_0^2 - 2c_2a^2). \tag{8}$$

Setting the lattice spacing to zero we recover, as expected, the familiar result of continuum ChPT [24].

Having calculated the scattering amplitude we perform the standard partial wave expansion and obtain the scattering lengths [24]. Most interesting are the scattering lengths a_0^I for definite isospin $I = 0$ and $I = 2$:

$$a_0^0 = \frac{7}{32\pi f^2}\left(M_0^2 - \frac{5}{7}2c_2a^2\right), \tag{9}$$

$$a_0^2 = -\frac{1}{16\pi f^2}(M_0^2 + 2c_2a^2). \tag{10}$$

Again, for $a = 0$ we recover the tree-level continuum results, first obtained by Weinberg [34]. For a nonzero lattice spacing, however, the continuum results are modified in such a way that the scattering lengths no longer vanish in the chiral limit. Instead, they assume nonzero values of $O(a^2)$. In other words, the ratio a_0^I/M_π^2 is no longer a constant but has the functional form

$$\frac{a_0^I}{M_\pi^2} = \frac{A_{00}^I}{M_\pi^2} + A_{10}^I, \tag{11}$$

with A_{10}^I being a constant and A_{00}^I being of order a^2. Hence, the ratio a_0^I/M_π^2 diverges in the chiral limit. This divergence has been anticipated first by Kawamoto and Smit [17]. However, note that the coefficient A_{00}^I is of order a^2 rather than of order a. This holds even for unimproved Wilson fermions, in contrast to earlier expectations [18,19].

On the other hand, the divergence in the chiral limit will only be present if $c_2 > 0$, because only in this case can the pion indeed become massless. For the opposite sign the pion mass cannot be smaller than the minimal value quoted in Eq. (6), resulting in the following minimal values for the scattering lengths:

$$a_{0,\min}^0 = \frac{12}{32\pi f^2}2|c_2|a^2, \qquad a_{0,\min}^2 = 0. \tag{12}$$

Figure 1 sketches the pion mass dependence of the scattering lengths for the two possible signs of c_2. It seems feasible that measurements of the scattering lengths will allow more precise determinations of c_2. Extrapolating the data for a_0^2 to the chiral limit one may directly read off c_2 as the value at vanishing pion mass, even for the $c_2 < 0$ case. A practical advantage is that the calculation of a_0^2 does not involve disconnected diagrams which introduce large statistical uncertainties.

The $I = 1$ channel is somewhat special. The scattering amplitude for this isospin channel is given by $A(t, s, u) - A(u, t, s)$. The c_2 contribution drops out in this difference and the scattering length a_1^1 is given by

$$a_1^1 = \frac{1}{24\pi f^2}M_0^2. \tag{13}$$

This is exactly the tree-level result of continuum ChPT [24] and it suggests that the scaling violations in a_1^1 are very small.[5]

[4]Recall that the Lagrangian in Eq. (1) is given in Euclidean space-time, so one has to Wick-rotate back to Minkowski space in order to get the physical scattering amplitude.

[5]Note that our definition of the scattering length a_1^1 differs by a factor of M_0^2 from the one in Ref. [24].

III. PION SCATTERING AT ONE LOOP

A. Power counting and higher order terms

Having promoted the $O(a^2)$ correction to the LO Lagrangian, it will contribute to the one-loop results of various quantities in a nontrivial way. Expanding the $O(a^2)$ term in terms of pion fields we obtain vertices proportional to $2c_2a^2$. As part of one-loop diagrams these lead to nonanalytic corrections proportional to $2c_2a^2\ln M_0^2$, for example, in the expression of the pion mass (see Fig. 2).

The presence of additional chiral logarithms of order $a^2\ln M_0^2$ is well known in staggered ChPT (SChPT) [35–37], and has been pointed out first in Ref. [23] for WChPT. They are considered to be one reason why the chiral logarithms known from continuum ChPT are not reproduced in the lattice data: The additional chiral logs obscure the nonanalytic quark mass dependence due to the continuum chiral logs, and the naively expected behavior is lost.

The power counting in WChPT is slightly nontrivial if we take the $O(a^2)$ term at LO. The LO Lagrangian consists of the terms of $O(p^2, m, a^2)$. In order to renormalize the divergencies of the loop diagrams we need higher order counterterms in the chiral Lagrangian. These are, besides the standard ones in $\mathcal{L}_4$ of continuum ChPT [24,25], the terms of order p^2a^2, ma^2, a^4. However, terms of order p^2a, ma, a^3 are also present and formally of lower order. Hence these should also be included, even though their LECs do not get renormalized at one loop. To conclude, one-loop calculations in the LCE regime require the following terms in the chiral Lagrangian:

LCE regime:

$$\begin{aligned}&\text{LO}: p^2, m, a^2, \qquad \text{NLO}: p^2a, ma, a^3,\\ &\text{NNLO}: p^4, p^2m, m^2, p^2a^2, ma^2, a^4.\end{aligned} \tag{14}$$

The standard next-to-leading-order (NLO) terms of continuum ChPT appear here at next-to-next-to-leading-order (NNLO), a consequence of the fact that $m \sim a^2\Lambda_{\text{QCD}}^3$ in the LCE regime.[6] In the GSM regime, however, we recover the standard ordering. Since $m \sim a\Lambda_{\text{QCD}}^2 > a^2\Lambda_{\text{QCD}}^3$ in this regime, a one-loop calculation requires the following terms:

GSM regime:

$$\text{LO}: p^2, m, \qquad \text{NLO}: p^4, p^2m, m^2, p^2a, ma, a^2. \tag{15}$$

Note that all terms in (15) are also present in (14), even though reshuffled. This already indicates that a result obtained in the LCE regime yields the corresponding result in the GSM regime if appropriately expanded.

Most of the necessary terms in (14) have already been constructed. So far unknown are the contributions of order p^2a^2, ma^2, a^3, a^4. Performing a standard spurion analysis with the spurion fields in Ref. [22] it is straightforward to construct these missing terms, at least the ones we need as counterterms for the observables we are interested in here, the pion mass and the scattering amplitude. Some details concerning the construction of these terms are collected in Appendix A.

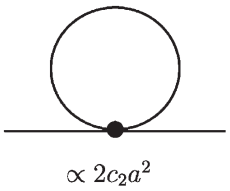

FIG. 2. Additional one-loop diagram contributing to the self-energy. The vertex is proportional to c_2a^2, leading to a chiral logarithm $c_2a^2\ln M_0^2$.

Finally, if the underlying lattice theory is nonperturbatively $O(a)$ improved according to the Symanzik improvement program [20,21], the terms of order p^2a, ma are absent in (14) and (15). In the following we will always keep these contributions in our calculation; the $O(a)$ improved result is simply obtained by dropping the appropriate terms linear in the lattice spacing.

B. Pion mass to one loop

The modification due to the additional chiral logarithms is illustrated best in the one-loop result for the pion mass, which we will also need in the next section. In terms of the tree-level pion mass M_0^2, cf. Eq. (5), we find

$$M_\pi^2 = M_0^2\Big[1 + \frac{1}{32\pi^2}\frac{M_0^2}{f^2}\ln\Big(\frac{M_0^2}{\Lambda_3^2}\Big) + \frac{5}{32\pi^2}\frac{2c_2a^2}{f^2}\ln\Big(\frac{M_0^2}{\Xi_3^2}\Big) + k_1\frac{W_0a}{f^2}\Big] + k_3\frac{2c_2W_0a^3}{f^2} + k_4\frac{(2c_2a^2)}{f^2}. \tag{16}$$

The coefficients Λ_3^2, Ξ_3^2 and k_1, k_3, k_4 are (combinations of) unknown LECs. Λ_3^2 is the familiar scale independent LEC present in the continuum result [24], and in complete analogy we introduced the new LEC Ξ_3. Note that we have chosen the coefficients k_i to be dimensionless.[7] In the $O(a)$ improved theory the k_1 term is absent.

A few comments concerning (16) are in order. First, setting the lattice spacing to zero we recover the familiar result from continuum ChPT [24], as expected. This result gets modified at nonzero lattice spacing. In particular, there exists the anticipated chiral logarithm proportional to $c_2a^2\ln M_0^2$. Note that the coefficient in front of it is 10 times larger than the coefficient in front of the continuum chiral log proportional to $M_0^2\ln M_0^2$. Hence, even small

[6]The terms of $O(p^2a, ma, a^3)$ are not present in SChPT due to the axial U(1) symmetry. Consequently, the terms of the third row in (14) are the NLO terms.

[7]Details about how the LECs in (16) are related to the ones in the chiral Lagrangian can be found in [38].

$O(a^2)$ contributions may dilute the continuum chiral logarithm completely. This is better seen if we rewrite the square bracket in (16) as

$$\left[1+\frac{1}{32\pi^2}\{M_2^0+10c_2a^2\}\ln\left(\frac{M_2^0}{\Lambda_3^2}\right)+\frac{10}{32\pi^2 f^2}c_2a^2\ln\left(\frac{\Lambda_3^2}{\Xi_3^2}\right)+k_1\frac{W_0a}{f^2}\right], \tag{17}$$

so that the quark mass dependence comes entirely from the $\ln M_0^2/\Lambda_3^2$ term. Negative values of c_2 can render the factor $M_0^2+10c_2a^2$ exceptionally small such that the chiral logarithm is effectively not active.

This scenario is not as unlikely as one may think. We remark that the ETM collaboration has found a negative value for c_2 in their twisted mass simulations, and the calculation of the pion mass splitting provides a rough estimate for $-2c_2a^2=M_{\pi^\pm}^2-M_{\pi^0}^2$. The data [33] for $a\approx 0.086$ fm and $M_{\pi^\pm}\approx 300$ MeV results in $-2c_2a^2\approx(185\ \text{MeV})^2$. Such a value completely suppresses the chiral log for pion masses around 400 MeV, a value not unusual in lattice simulations performed these days.

Finally, note that the pion mass (16) does not vanish in the limit $M_0^2=0$ because of the corrections proportional to k_3, k_4. However, these are contributions of $O(a^3, a^4)$ to the additive mass renormalization (the critical quark mass) and can be absorbed by an appropriate finite renormalization. To be specific, define $\tilde{m}$ and $\tilde{M}_0^2$ by

$$\begin{aligned}\tilde{M}_0^2&=2B\tilde{m}\\&\equiv 2Bm-2c_2a^2+k_3\frac{2c_2W_0a^3}{f^2}\\&\quad+\left(k_4\frac{(2c_2a^2)^2}{f^2}-k_1\frac{W_0a}{f^2}k_3\frac{2c_2W_0a^3}{f^2}\right),\end{aligned} \tag{18}$$

such that the quark masses $\tilde{m}$ and m differ by order a^2 and higher. In terms of $\tilde{m}$ the result (16) reads (up to the order we are working here)

$$M_\pi^2=\tilde{M}_0^2\left[1+\frac{1}{32\pi^2}\frac{\tilde{M}_0^2}{f^2}\ln\left(\frac{\tilde{M}_0^2}{\Lambda_3^2}\right)+\frac{5}{32\pi^2}\frac{2c_2a^2}{f^2}\ln\left(\frac{\tilde{M}_0^2}{\Xi_3^2}\right)+k_1\frac{W_0a}{f^2}\right]. \tag{19}$$

The k_3, k_4 contributions no longer appear explicitly but are absorbed in the definition of the quark mass $\tilde{m}$. With this parametrization the pion mass vanishes in the chiral limit for $\tilde{m}=0$. Therefore, $\tilde{m}$ is proportional to the subtracted bare lattice quark mass (m_0-m_{cr}) if the critical quark mass m_{cr} is defined by a vanishing pion mass for $m_0=m_{\text{cr}}$. In other words, doing the definition (18) we have appropriately matched the chiral effective theory to the underlying lattice theory for this particular renormalization condition. Obviously, the matching differs for other definitions of the lattice quark mass, for example, through the partially conserved axial vector current (PCAC) relation.

In the following we are not interested in the quark mass dependence of scattering observables, but rather in the dependence on the pion mass. For this the parametrization in terms of m is sufficient, since at the end we will replace m by M_π^2 using Eq. (16).

C. Scattering at one loop

At one loop there contribute the four diagrams in Fig. 3 to the four-point function. The vertices in these diagrams can be either a vertex also present in continuum ChPT or the vertex proportional to c_2a^2 stemming from the $O(a^2)$ term in Eq. (1). Hence, we expect additional chiral logarithms $c_2a^2M_0^2\ln M_0^2$ and $(c_2a^2)^2\ln M_0^2$ in the scattering amplitude and the scattering lengths.

The one-loop result for the scattering amplitude can be written as

$$A(s,t,u)=\frac{1}{f^2}(s-M_0^2-2c_2a^2)+B(s,t,u)+C(s,t,u), \tag{20}$$

where the functions B and C contain the one-loop corrections. The general structure of these functions is

$$B(s,t,u)=B_{\text{cont}}(s,t,u)+2c_2a^2B_{a^2}(s,t,u), \tag{21}$$

$$C(s,t,u)=C_{\text{cont}}(s,t,u)+2c_2a^2C_{a^2}(s,t,u). \tag{22}$$

The first parts B_{cont}, C_{cont} are the contributions from continuum ChPT and can be found in Refs. [24,39]. The contributions B_{a^2}, C_{a^2} come from the $O(a^2)$ correction. Since these expressions are cumbersome and not very illuminating we present them in Appendix B. Here we just mention that these functions are finite in the limit $a\to 0$, so in the continuum limit we recover the continuum result for the scattering amplitude.

With the amplitude at hand we can compute the scattering lengths as before. As a shorthand notation we introduce

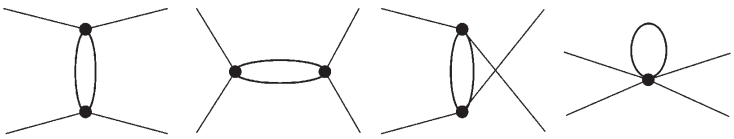

FIG. 3. One-loop diagrams contributing to the four-point function. The diagrams with one or two vertices stemming from the $O(a^2)$ term in the chiral Lagrangian will give rise to chiral logs proportional to $c_2a^2M_0^2\ln M_0^2$ and $(c_2a^2)^2\ln M_0^2$.

$$\bar{l}_i(M_0^2) = -\ln\left(\frac{M_0^2}{\Lambda_i^2}\right), \qquad i = 1, 2, 3, \tag{23}$$

$$\bar{\xi}_i(M_0^2) = -\ln\left(\frac{M_0^2}{\Xi_i^2}\right), \qquad i = 3, \ldots, 6 \tag{24}$$

for the chiral logarithms in the following expressions. The $\bar{l}_i$ are the standard scale invariant LECs of continuum ChPT [24], and the parameters $\bar{\xi}_i$ are defined in complete analogy to them. However, we have made the dependence on M_0^2 explicit. This seems appropriate since the pion mass is varied in lattice simulations and the $\bar{l}_i$, $\bar{\xi}_i$ are indeed functions of the pion mass.

With these definitions the one-loop results for the isospin zero and isospin two scattering lengths read

$$\begin{aligned} a_0^0 = {} & \frac{7}{32\pi}\frac{M_0^2}{f^2}\left(1 + \frac{5}{84\pi^2}\frac{M_0^2}{f^2}\left\{\bar{l}_1(M_0^2) + 2\bar{l}_2(M_0^2) + \frac{21}{8}\right\}\right. \\ & \left. - \frac{5}{84\pi^2}\frac{2c_2a^2}{f^2}\left\{9\bar{\xi}_4(M_0^2) - \frac{33}{8}\bar{\xi}_5(M_0^2) + \frac{15}{4}\right\}\right) \\ & - \frac{5}{32\pi}\frac{2c_2a^2}{f^2}\left(1 - \frac{W_0a}{f^2}k_5 - \frac{2c_2a^2}{32\pi^2f^2}\right. \\ & \left. \times\{11\bar{\xi}_6(M_0^2) - 1\}\right) + \frac{3}{8\pi f^2}(M_\pi^2 - M_0^2), \end{aligned} \tag{25}$$

$$\begin{aligned} a_0^2 = {} & -\frac{M_0^2}{16\pi f^2}\left(1 - \frac{M_0^2}{12\pi^2f^2}\left\{\bar{l}_1(M_0^2) + 2\bar{l}_2(M_0^2) + \frac{3}{8}\right\}\right. \\ & \left. - \frac{2c_2a^2}{32\pi^2f^2}\{11\bar{\xi}_5(M_0^2) + 2\}\right) - \frac{2c_2a^2}{16\pi f^2} \\ & \times\left(1 - \frac{W_0a}{f^2}k_5 - \frac{2c_2a^2}{32\pi^2f^2}\{11\bar{\xi}_6(M_0^2) - 7\}\right). \end{aligned} \tag{26}$$

Here k_5 is another LEC associated with the $O(a^3)$ terms in the chiral Lagrangian. As anticipated, we find additional chiral logarithms $a^2M_0^2\ln M_0^2$ (the terms involving $\bar{\xi}_4$, $\bar{\xi}_5$) and $a^4\ln M_0^2$ (the $\bar{\xi}_6$ term).

The results (25) and (26) are given as a function of the quark mass m via the tree-level pion mass M_0^2, except for the last line in a_0^0, where the one-loop expression M_π^2 enters.[8] As already mentioned at the end of Sec. III B, these results have to be properly matched to the lattice theory. Depending on the particular renormalization condition for the quark mass the final results differ by terms of order a. For this reason it is advantageous to express the scattering lengths as a function of the pion mass and not of the quark mass. Using the one-loop result (16) in order to replace M_0^2 by M_π^2 we obtain the scattering lengths as a function of M_π^2:

$$\begin{aligned} a_0^0 = {} & \frac{7}{32\pi}\frac{M_\pi^2}{f^2}\left(1 + \frac{5}{84\pi^2}\frac{M_\pi^2}{f^2}\left\{\bar{l}_1(M_\pi^2) + 2\bar{l}_2(M_\pi^2)\right.\right. \\ & \left. - \frac{3}{8}\bar{l}_3(M_\pi^2) + \frac{21}{8}\right\} + \frac{5}{7}k_1\frac{W_0a}{f^2} - \frac{5}{84\pi^2}\frac{2c_2a^2}{f^2} \\ & \left.\times\left\{\frac{15}{8}\bar{\xi}_3(M_\pi^2) + 9\bar{\xi}_4(M_\pi^2) - \frac{33}{8}\bar{\xi}_5(M_\pi^2) + \frac{15}{4}\right\}\right) \\ & - \frac{5}{32\pi}\frac{2c_2a^2}{f^2}\left(1 - \{k_3 + k_5\}\frac{W_0a}{f^2} - k_4\frac{2c_2a^2}{f^2}\right. \\ & \left. - \frac{2c_2a^2}{32\pi^2f^2}\{11\bar{\xi}_6(M_\pi^2) - 1\}\right), \end{aligned} \tag{27}$$

$$\begin{aligned} a_0^2 = {} & -\frac{M_\pi^2}{16\pi f^2}\left(1 - \frac{M_\pi^2}{12\pi^2f^2}\left\{\bar{l}_1(M_\pi^2) + 2\bar{l}_2(M_\pi^2)\right.\right. \\ & \left. - \frac{3}{8}\bar{l}_3(M_\pi^2) + \frac{3}{8}\right\} - k_1\frac{W_0a}{f^2} - \frac{2c_2a^2}{32\pi^2f^2}\{-5\bar{\xi}_3(M_\pi^2) \\ & \left. + 11\bar{\xi}_5(M_\pi^2) + 2\}\right) - \frac{2c_2a^2}{16\pi f^2}\left(1 - \{k_3 + k_5\}\frac{W_0a}{f^2}\right. \\ & \left. - k_4\frac{2c_2a^2}{f^2} - \frac{2c_2a^2}{32\pi^2f^2}\{11\bar{\xi}_6(M_\pi^2) - 7\}\right). \end{aligned} \tag{28}$$

Here the coefficients $\bar{l}_i$ and $\bar{\xi}_i$ are as in (23) and (24) but with the tree-level pion mass replaced by M_π^2.

Note that we have still expressed the scattering lengths as a function of f, the decay constant in the chiral and continuum limit, and not in terms of f_π. The reason is that f_π has not been computed yet to one loop in the LCE regime.[9] This is not an impediment to our results, but it means that f is a free fit parameter when our results are used to fit them to numerical lattice data.[10] We briefly come back to this in Sec. III E.

Our final results for the scattering lengths differ significantly from the corresponding ones in continuum ChPT. The scattering lengths do not vanish in the chiral limit, but rather diverge as $a^4\ln M_\pi^2$. However, if $c_2 < 0$ there is no divergence since the pion mass cannot become smaller than the minimal value in Eq. (6). For the opposite sign massless pions are in principle possible, but for small pion masses the chiral expansion eventually breaks down when $c_2a^2\ln M_\pi^2$ becomes of order unity. In that case higher order terms leading to powers $(c_2a^2\ln M_\pi^2)^n$, $n = 2, 3, \ldots$, become relevant too and a summation of all these terms is necessary. This can presumably be done along the lines in Ref. [23], where a resummed pion mass formula has been derived. Here, however, we assume that the pion masses are heavy enough such that the chiral logarithm $c_2a^2\ln M_\pi^2$

[8]The definition of a_0^0 involves the physical pion mass when one goes on shell and uses $s + t + u = 4M_\pi^2$.

[9]The calculation of the decay constant poses additional complications: The axial vector current in the effective theory needs to be constructed to the appropriate order and the proper renormalization condition has to be taken into account [40].

[10]Note that the replacement of f by f_π does not reduce the number of unknown LECs since the latter contains new LECs that are not present in the expressions parametrized by f [40].

is a reasonably small correction to the leading order contribution. This is most likely the relevant case for actual numerical simulations.

In any case, the pion mass dependence of the scattering lengths on the lattice can be very different in contrast to what one may expect from continuum ChPT. Consequently, attempts to fit lattice data using expressions from continuum ChPT may easily fail.

D. Results for the GSM regime

In this section we summarize the results for the GSM regime where $m \sim a\Lambda_{\rm QCD}^2 > a^2\Lambda_{\rm QCD}^3$. These are easily obtained from the expressions in the last section by expanding the logarithms according to $\ln(M_0^2) \approx \ln(2Bm) - 2c_2a^2/2Bm$ and dropping consistently all higher order terms.

For example, the one-loop expression (16) for the pion mass reduces to

$$M_\pi^2 = 2Bm\left[1 + \frac{2Bm}{32\pi^2 f^2}\ln\left(\frac{2Bm}{\Lambda_3^2}\right) + k_1\frac{W_0 a}{f^2}\right] - 2c_2a^2. \tag{29}$$

This result is easily understood. The LO Lagrangian consists only of the kinetic and the mass term. Hence, the tree-level pion mass is equal to $2Bm$ and the chiral logarithm in the one-loop result is just the one from continuum ChPT. The $O(ma, a^2)$ terms enter at NLO and give analytic corrections only.

Similarly we obtain the results for the scattering lengths:

$$a_0^0 = \frac{7}{32\pi}\frac{M_\pi^2}{f^2}\left(1 + \frac{5}{84\pi^2}\frac{M_\pi^2}{f^2}\left\{\bar{l}_1(M_\pi^2) + 2\bar{l}_2(M_\pi^2) - \frac{3}{8}\bar{l}_3(M_\pi^2) + \frac{21}{8}\right\} + \frac{5}{7}k_1\frac{W_0 a}{f^2}\right) - \frac{5}{32\pi}\frac{2c_2a^2}{f^2}, \tag{30}$$

$$a_0^2 = -\frac{M_\pi^2}{16\pi f^2}\left(1 - \frac{M_\pi^2}{12\pi^2 f^2}\left\{\bar{l}_1(M_\pi^2) + 2\bar{l}_2(M_\pi^2) - \frac{3}{8}\bar{l}_3(M_\pi^2) + \frac{3}{8}\right\} - k_1\frac{W_0 a}{f^2}\right) - \frac{2c_2a^2}{16\pi f^2}. \tag{31}$$

As expected, the results reduce to the continuum one-loop result plus analytic corrections of order $M_\pi^2 a$ and a^2.

E. Practical remarks

An important application of WChPT is to provide formulae that can be used to fit lattice data and thereby allow the chiral extrapolation to the physical pion mass. As a by-product one also obtains estimates for the Gasser-Leutwyler coefficients involved in these formulae. The results for the scattering lengths of the previous sections serve exactly this purpose, but the way we have written them is not practical. In order to compare and cross check our results with continuum ChPT we have parametrized the chiral logarithms in terms of $\bar{l}_i$ and $\bar{\xi}_i$, defined in Eqs. (23) and (24). Introducing the scale independent coefficients $\bar{l}_i$ is useful in continuum ChPT, since the pion mass is constant in nature; consequently, the coefficients $\bar{l}_i$ are constants too. In lattice simulations we are free to choose the quark and pion mass, and it is this freedom that eventually enables us to compute Gasser-Leutwyler coefficients. For this it seems more useful to introduce the (scale dependent) coefficients

$$l_i(\mu) = \bar{l}_i + \ln\left(\frac{M_\pi^2}{\mu^2}\right) = \ln\frac{\Lambda_i^2}{\mu^2}, \tag{32}$$

$$\xi_i(\mu) = \bar{\xi}_i + \ln\left(\frac{M_\pi^2}{\mu^2}\right) = \ln\frac{\Xi_i^2}{\mu^2}, \tag{33}$$

which are, up to irrelevant constants, the standard renormalized Gasser-Leutwyler coefficients defined in [24].[11] In terms of these coefficients the chiral logarithms are explicit and the results for the scattering lengths can be written in a more compact form.

For simplicity let us first assume that we are interested in analyzing data at one fixed lattice spacing. In this case various terms which depend only on powers of the lattice spacing but not on the pion mass can be combined to single unknown parameters. This reduces the number of fit parameters. Explicitly we can write[12]

$$a_0^0 = \frac{7M_\pi^2}{32\pi f^2}\left(\kappa_{01} - \frac{M_\pi^2}{32\pi^2 f^2}\left\{5\ln\frac{M_\pi^2}{\mu^2} - \frac{40}{21}l_{\pi\pi}^{I=0}\right\} + \frac{2c_2a^2}{32\pi^2 f^2}\left\{\frac{90}{7}\ln\frac{M_\pi^2}{\mu^2}\right\}\right) - \frac{5\cdot 2c_2a^2}{32\pi f^2} \times \left(\kappa_{02} + \frac{2c_2a^2}{32\pi^2 f^2}\left\{11\ln\frac{M_\pi^2}{\mu^2}\right\}\right), \tag{34}$$

$$a_0^2 = -\frac{M_\pi^2}{16\pi f^2}\left(\kappa_{21} + \frac{M_\pi^2}{16\pi^2 f^2}\left\{\frac{7}{2}\ln\frac{M_\pi^2}{\mu^2} - \frac{4}{3}l_{\pi\pi}^{I=2}\right\} + \frac{2c_2a^2}{16\pi^2 f^2}\left\{3\ln\frac{M_\pi^2}{\mu^2}\right\}\right) - \frac{2c_2a^2}{16\pi f^2}\left(\kappa_{22} + \frac{2c_2a^2}{16\pi^2 f^2} \times \left\{\frac{11}{2}\ln\frac{M_\pi^2}{\mu^2}\right\}\right). \tag{35}$$

The new parameters κ_{Ij} comprise the analytic terms through $O(a^2)$, hence these are constants for fixed a, except for the fact that they are scale dependent since they contain the parameters $\xi_i(\mu)$. In the limit $a \to 0$ they assume the value $\kappa_{Ij} = 1$. As a shorthand notation we introduced

[11] The constants are $\gamma_i/(32\pi^2)$. The γ_i are given in Eq. (9.6) of Ref. [24].

[12] The results for a_1^1 are summarized in Appendix C.

$$l_{\pi\pi}^{I=0} = l_1 + 2l_2 - \tfrac{3}{8}l_3 + \tfrac{21}{8}, \qquad l_{\pi\pi}^{I=2} = l_1 + 2l_2 - \tfrac{3}{8}l_3 + \tfrac{3}{8}, \tag{36}$$

for the combinations of LECs entering the scattering lengths. We emphasize again that we have expressed our results in terms of the decay constant in the chiral limit, and not in terms of f_π. If the latter had been used the LEC l_4 [24] would also appear in Eq. (36).

Each of the expressions Eqs. (34) and (35) contain five unknown parameters: the continuum parameters f and $l_{\pi\pi}^I$ as well as κ_{I1}, κ_{I2}, c_2, i.e. three more than the continuum result. This is already quite large, taking into account that one usually has data for a few pion masses only. In $O(a)$ improved theories we have $\kappa_{I1} = 1 + O(a^2)$, so in this case one may try to ignore the higher order corrections and set $\kappa_{I1} = 1$.

We remark that the ratio a_0^I/M_π^2 has the functional form

$$\frac{a_0^I}{M_\pi^2} = \frac{A_{00}}{M_\pi^2} + A_{10} + A_{20}M_\pi^2 + A_{30}M_\pi^2 \ln M_\pi^2 + A_{40}\ln M_\pi^2 + \tilde{A}_{40}\frac{\ln M_\pi^2}{M_\pi^2}. \tag{37}$$

The first two terms on the right-hand side correspond to the tree-level result in Eq. (11). The constants A_{00}–A_{40} represent the five independent fit parameters, while $\tilde{A}_{40}$ is not independent. The first three terms in (37) have already been used in analyzing numerical lattice data [41], but the data could not be fitted well. It might be interesting to repeat the analysis with the full result in (37), even though the data was obtained for heavy pion masses between 500 MeV and 1.1 GeV, and ChPT is not expected to be applicable.

If one wants to simultaneously analyze data for various lattice spacings one has to keep in mind that the coefficients κ_{Ij} are no longer constants but functions of the lattice spacing,

$$\kappa_{Ij} = 1 + \kappa_{Ij}^{(1)}a + \kappa_{Ij}^{(2)}a^2. \tag{38}$$

This increases the number of free parameters in each formula from five to seven for unimproved theories. In $O(a)$ improved theories we have $\kappa_{I1}^{(1)} = 0$ and the number of free parameters is increased by only one. Note that for unimproved theories the $O(a)$ corrections are not independent,

$$7\kappa_{01}^{(1)} = -5\kappa_{21}^{(1)}, \qquad \kappa_{02}^{(1)} = \kappa_{22}^{(1)}. \tag{39}$$

Hence, if data for both scattering lengths are available the parameters in a simultaneous fit are related.

The fit formulae for the GSM regime are obtained from Eqs. (34) and (35), by dropping the appropriate higher order terms, leading to

$$a_0^0 = \frac{7M_\pi^2}{32\pi f^2}\left(\kappa_{01} - \frac{M_\pi^2}{32\pi^2 f^2}\left\{5\ln\frac{M_\pi^2}{\mu^2} - \frac{40}{21}l_{\pi\pi}^{I=0}\right\}\right) - \frac{5\cdot 2c_2a^2}{32\pi f^2}, \tag{40}$$

$$a_0^2 = -\frac{M_\pi^2}{16\pi f^2}\left(\kappa_{21} + \frac{M_\pi^2}{16\pi^2 f^2}\left\{\frac{7}{2}\ln\frac{M_\pi^2}{\mu^2} - \frac{4}{3}l_{\pi\pi}^{I=2}\right\}\right) - \frac{2c_2a^2}{16\pi f^2}. \tag{41}$$

Here $\kappa_{Ij} = 1 + \kappa_{Ij}^{(1)}a$. The free fit parameters are f, c_2, and $\kappa_{Ij}^{(1)}$, and the latter vanish in $O(a)$ improved theories. These formulae lead to the general form

$$\frac{a_0^I}{M_\pi^2} = \frac{A_{00}}{M_\pi^2} + A_{10} + A_{20}M_\pi^2 + A_{30}M_\pi^2\ln M_\pi^2, \tag{42}$$

for the ratio a_0^I/M_π^2, in contrast to (37).

IV. CONCLUDING REMARKS

Present day lattice simulations are still done with quark masses much heavier than in nature. Therefore, a chiral extrapolation to the physical point is still necessary, and that is where the predictions of ChPT enter the analysis of numerical lattice data. However, the results of continuum ChPT get modified at nonzero lattice spacing. For pion scattering with Wilson fermions we essentially find two modifications. First, the $I = 0$, 2 scattering lengths do not vanish in the chiral limit, but rather assume a nonzero value of order a^2. Second, additional chiral logarithms proportional to a^2 appear in the one-loop results for these quantities. Ignoring these modifications and using the results of continuum ChPT is potentially dangerous, depending on the size of these extra contributions. One either introduces a systematic error in the chiral extrapolation or the data cannot be fitted at all with the continuum results.

Related problems may arise in the determination of the Gasser-Leutwyler coefficients associated with pion scattering. Experience shared by many lattice groups is that the lattice data does not show the characteristic curvature due to the continuum chiral logarithms. A possible explanation is the presence of additional chiral logarithms proportional to the lattice spacing. These can conspire with the continuum chiral logarithms such that the overall curvature of the data is diminished. A correct and precise determination of the Gasser-Leutwyler coefficients using the continuum results is very unlikely in that case. Using the expression derived here should help in that respect.

The formulae we presented in this paper involve the parameter c_2, which also determines the phase diagram of the theory. In particular the $I = 2$ scattering length may provide a handle to obtain an estimate of c_2. At least the sign of c_2 should be easily accessible, and this is what matters for the phase diagram.

We conclude with a remark on finite volume corrections. The numerical calculation of phase shifts and scattering lengths is usually done by employing the so-called Lüscher formula [42,43] in order to circumvent the Maiani-Testa no-go theorem [44]. This formula relates the two-pion energy eigenvalues in finite volume to the infinite volume scattering length of the two-pion scattering process.

In addition to the power law finite volume dependence of the two-pion energy eigenvalues, which one exploits to extract the infinite volume scattering lengths, there are exponentially suppressed finite volume corrections. These have been studied in Ref. [45] and it is straightforward to include these in our results. However, these corrections are expected to be very small on typical lattice sizes, much smaller than the corrections due to the nonzero lattice spacing. For example, for a pion mass of approximately 300 MeV and a finite volume with $L \simeq 2.5$ fm the finite volume correction to the $I = 2$ scattering length is about 1 to 2% [45].[13] On the other hand, taking $|2c_2a^2| \approx (185\ \text{MeV})^2$ at $a \approx 0.086$ fm found by the ETM collaboration at a charged pion mass of about 300 MeV [32,33], we obtain the rough estimate of about 35% for the $O(a^2)$ corrections in this channel. Although the numerical value for $2c_2a^2$ has a large error bar and can easily be a factor of 2 or 4 smaller, these numbers indicate that the finite volume corrections are most likely much smaller than the lattice spacing corrections.

ACKNOWLEDGMENTS

This work is supported in part by the Grants-in-Aid for Scientific Research from the Japanese Ministry of Education, Culture, Sports, Science and Technology (No. 20340047) and by the Deutsche Forschungsgemeinschaft (SFB/TR 09). B. B. acknowledges financial support from the *Cusanuswerk* .

APPENDIX A: HIGHER ORDER TERMS IN THE CHIRAL LAGRANGIAN

The terms required for one-loop calculations in the LCE regime are shown in (14). Among them are the NLO terms of continuum ChPT, which are given in Ref. [24]. The terms of $O(p^2a, ma, a^2)$ can be found in Refs. [15,22]. So far unknown are the contributions of order p^2a^2, ma^2, a^3, a^4. However, these missing terms are easily constructed with the spurion fields introduced in [22].

There are essentially two independent spurion fields, M and A. These stem from the two sources of explicit chiral symmetry breaking, the quark mass and the lattice spacing. Under chiral symmetry transformations these fields transform as

$$M \to LMR^\dagger, \qquad A \to LAR^\dagger. \tag{A1}$$

These fields together with the field Σ and its derivatives are used to write down the most general chiral Lagrangian that is compatible with chiral symmetry, parity, and charge conjugation. Once the terms in the chiral Lagrangian have been found the spurion fields are assigned to their physical values,

$$M \to \text{diag}(m_u, m_d) = mI, \qquad A \to aI, \tag{A2}$$

where I denotes the two dimensional unit matrix (recall that we ignore isospin violation and assume $m_u = m_d \equiv m$). The number of terms in the chiral Lagrangian can be reduced further by making use of the Cayley-Hamilton theorem.

Proceeding along these lines we find the following independent terms of $O(p^2a^2, ma^2)$:

$$\begin{aligned}\mathcal{L}_{[p^2a^2]} = {} & a_1a^2\langle\partial_\mu\Sigma\partial_\mu\Sigma^\dagger\rangle \\ & + a_2a^2\langle\partial_\mu\Sigma\partial_\mu\Sigma^\dagger\rangle\langle\Sigma + \Sigma^\dagger\rangle^2 \\ & + a_3a^2\langle\partial_\mu(\Sigma + \Sigma^\dagger)\rangle\langle\partial_\mu(\Sigma + \Sigma^\dagger)\rangle,\end{aligned} \tag{A3}$$

$$\mathcal{L}_{[ma^2]} = b_1ma^2\langle\Sigma + \Sigma^\dagger\rangle + b_2ma^2\langle\Sigma + \Sigma^\dagger\rangle^3. \tag{A4}$$

The coefficients a_j, b_j are undetermined LECs.

Since the spurion fields M and A transform identically under all symmetries we trivially obtain the $O(a^3)$ terms by replacing M with A in the $O(ma^2)$ terms. This leads to

$$\mathcal{L}_{[a^3]} = d_1a^3\langle\Sigma + \Sigma^\dagger\rangle + d_2a^3\langle\Sigma + \Sigma^\dagger\rangle^3. \tag{A5}$$

Finally, for the $O(a^4)$ terms we obtain

$$\mathcal{L}_{[a^4]} = e_1a^4\langle\Sigma + \Sigma^\dagger\rangle^2 + e_2a^4\langle\Sigma + \Sigma^\dagger\rangle^4. \tag{A6}$$

Here we have dropped the constant term e_0a^4, which is also admitted by the symmetries but does not contribute to the pion mass and scattering amplitude.

Note that we have obtained the $O(a^3, a^4)$ terms although the Symanzik effective action has not been constructed to these orders. However, any spurion field at these orders has to transform as an appropriate tensor product of the spurion field A and therefore gives rise to the terms in (A5) and (A6) only.

APPENDIX B: THE SCATTERING AMPLITUDE TO ONE LOOP

The form of the one-loop result for the scattering amplitude is defined in Eq. (20). The functions $B(s, t, u)$, $C(s, t, u)$ introduced in Eqs. (21) and (22), contain the one-loop corrections. The parts B_{cont}, C_{cont} are the contributions from continuum ChPT and read

[13] For this estimate we made the crude approximation $k \cot\delta \approx 1/a_0^2$.

$$B_{\text{cont}} = \frac{1}{96\pi^2 f^4}\{3(s^2 - M_0^4)F(s) + \{t(t-u) - 2M_0^2(t-2u) - 2M_0^4\}F(t) + \{u(u-t) - 2M_0^2(u-2t) - 2M_0^4)\}F(u)\},$$
$$C_{\text{cont}} = \frac{1}{96\pi^2 f^4}\{2(\bar{l}_1 + 2/3)(s - 2M_0^2)^2 + (\bar{l}_2 + 7/6)(s^2 + (t-u)^2) + M_0^4\}. \quad \text{(B1)}$$

The constants $\bar{l}_i$ are defined in Eq. (23), M_0^2 is the tree-level pion mass of Eq. (5), and the function $F(x)$ is given by

$$F(x) = -\sigma\left(\ln\frac{1+\sigma}{1-\sigma} - i\pi\right), \qquad \sigma = \sqrt{1 - \frac{4M_0^2}{x}}. \quad \text{(B2)}$$

These results agree with the ones in [39]. The only difference is the use of the function $\bar{J}(x)$ in [39], which is related to our $F(x)$ by

$$16\pi^2 \bar{J}(x) = F(x) + 2. \quad \text{(B3)}$$

This leads to some differences between our functions B_{cont}, C_{cont} and the ones in [39]. The result for the scattering amplitude $A(s, t, u)$, however, is the same.

For the $O(a^2)$ contributions we find

$$B_{a^2}(s,t,u) = \frac{1}{96\pi^2 f^4}\{(42c_2a^2 + 18M_0^2 - 24s)F(s) + (12c_2a^2 - 12M_0^2 + 6t)F(t) + (12c_2a^2 - 12M_0^2 + 6u)F(u)\}, \quad \text{(B4)}$$

$$C_{a^2}(s,t,u) = \frac{1}{96\pi^2 f^4}\{-30s(\bar{\xi}_4 + 1) + 3M_0^2(11\bar{\xi}_5 + 6) + 66c_2a^2(\bar{\xi}_6 + 1)\} + k_5\frac{W_0 a}{f^4}. \quad \text{(B5)}$$

The constants $\bar{\xi}_i = \bar{\xi}_i(M_0^2)$ are defined in Eq. (24) and k_5 is the LEC associated with the $O(a^3)$ terms [it is a combination of the c_j in (A5)]. As claimed in Sec. 9, these functions assume a finite value for $a \to 0$. Hence the scattering amplitude reduces to the continuum result in this limit [recall the additional factor $2c_2a^2$ in front of B_{a^2}, C_{a^2} in Eqs. (21) and (22)].

APPENDIX C: THE $I = 1$ SCATTERING LENGTH

With the result for the scattering amplitude of the previous section we can compute other quantities like the slope parameters b_l^I or the phase shifts δ_l^I. Here we only quote the one-loop result for the scattering length a_1^1 in the isospin one channel, because the corrections due to a nonzero lattice spacing are fewer than in the other two isospin channels.

Performing the partial wave expansion for the $I = 1$ case we straightforwardly obtain

$$a_1^1 = \frac{M_0^2}{24\pi f^2}\left(1 - \frac{M_0^2}{12\pi^2 f^2}\left\{\bar{l}_1(M_0^2) - \bar{l}_2(M_0^2) + \frac{65}{48}\right\} - \frac{2c_2a^2}{16\pi^2 f^2}\left\{5\bar{\xi}_4(M_0^2) - \frac{35}{6}\right\}\right) + \frac{2c_2a^2}{24\pi f^2}\left(\frac{2c_2a^2}{16\pi^2 f^2}\left\{\frac{5}{12}\right\}\right) \quad \text{(C1)}$$

for the scattering length. We recover the continuum result in Ref. [24] for a vanishing lattice spacing.

Note that the number of lattice spacing corrections is reduced compared to the results (25) and (26), for the other two isospin channels. There are no corrections proportional to a^2 and a^3 in the result for a_1^1. Also the $a^4 \ln M_0^2$ term is missing. The absence of these terms is a direct consequence of taking the difference $A(t, s, u) - A(u, t, s)$ for the $I = 1$ scattering amplitude. However, analytic corrections of $O(a^3)$ enter when we replace M_0^2 by M_π^2 and express the scattering length as a function of the pion mass:

$$a_1^1 = \frac{M_\pi^2}{24\pi f^2}\left(1 - \frac{M_\pi^2}{12\pi^2 f^2}\left\{\bar{l}_1(M_\pi^2) - \bar{l}_2(M_\pi^2) - \frac{3}{8}\bar{l}_3(M_\pi^2) + \frac{65}{48}\right\} - k_1\frac{W_0 a}{f^2} - \frac{2c_2a^2}{16\pi^2 f^2}\left\{-\frac{5}{2}\bar{\xi}_3(M_\pi^2) + 5\bar{\xi}_4(M_\pi^2) - \frac{35}{6}\right\}\right) - \frac{2c_2a^2}{24\pi f^2}\left(k_3\frac{W_0 a}{f^2} + k_4\frac{2c_2a^2}{f^2} - \frac{2c_2a^2}{16\pi^2 f^2}\left\{\frac{5}{12}\right\}\right). \quad \text{(C2)}$$

For completeness we also give the analogue of the fit formulae inSec. III E. Replacing the $\bar{l}_i$ and $\bar{\xi}_3$ using Eqs. (23) and (24) we can write

$$a_1^1 = \frac{M_\pi^2}{24\pi f^2}\left(\kappa_{11} - \frac{M_\pi^2}{24\pi^2 f^2}\left\{\frac{3}{4}\ln\frac{M_\pi^2}{\mu^2} + 2l_{\pi\pi}^{I=1}\right\} + \frac{2c_2a^2}{24\pi^2 f^2}\left\{\frac{15}{4}\ln\frac{M_\pi^2}{\mu^2}\right\}\right) - \frac{2c_2a^2}{24\pi f^2}\kappa_{12}, \quad \text{(C3)}$$

where we introduced the combination

$$l_{\pi\pi}^{I=1} = l_1 - l_2 - \tfrac{3}{8}l_3 + \tfrac{65}{48}. \quad \text{(C4)}$$

The coefficients κ_{1j} comprise the analytic terms through $O(a^2)$. They are of the form

$$\kappa_{11} = 1 + \kappa_{11}^{(1)}a + \kappa_{11}^{(2)}a^2, \qquad \kappa_{12} = \kappa_{12}^{(1)}a + \kappa_{12}^{(2)}a^2. \quad \text{(C5)}$$

These coefficients are constants for a fixed lattice spacing. The coefficient $\kappa_{11}^{(1)}$ is related to the corresponding coefficients for the other two isospin channels:

$$7\kappa_{01}^{(1)} = -5\kappa_{21}^{(1)} = -5\kappa_{11}^{(1)}. \quad \text{(C6)}$$

In the $O(a)$ improved theory all these coefficients vanish.

There is no relation for $\kappa_{12}^{(1)}$ since it does not involve the low-energy constant k_5. Note that κ_{12} vanishes for $a \to 0$, in contrast to the other two isospin channels.

Finally, in order to obtain the result for the GSM regime one has to drop the $a^2 M_\pi^2 \ln M_\pi^2$ term and sets $\kappa_{11} = 1$ and $\kappa_{12} = 0$. The resulting expression is simply the one-loop result of continuum ChPT.

[1] H. Leutwyler, arXiv:hep-ph/0612112.
[2] G. Colangelo, Proc. Sci., KAON (2006) 038.
[3] C. Aubin *et al.*, Phys. Rev. D **70**, 114501 (2004).
[4] L. Del Debbio *et al.*, J. High Energy Phys. 02 (2007) 056.
[5] P. Boucaud *et al.*, Phys. Lett. B **650**, 304 (2007).
[6] G. Colangelo, J. Gasser, and H. Leutwyler, Nucl. Phys. **B603**, 125 (2001).
[7] T. Yamazaki *et al.*, Phys. Rev. D **70**, 074513 (2004).
[8] S. R. Beane *et al.*, Phys. Rev. D **77**, 014505 (2008).
[9] S. R. Beane, P. F. Bedaque, K. Orginos, and M. J. Savage, Phys. Rev. D **73**, 054503 (2006).
[10] C. W. Bernard *et al.*, Phys. Rev. D **64**, 054506 (2001).
[11] O. Bär, G. Rupak, and N. Shoresh, Phys. Rev. D **67**, 114505 (2003).
[12] O. Bär, C. Bernard, G. Rupak, and N. Shoresh, Phys. Rev. D **72**, 054502 (2005).
[13] J.-W. Chen, D. O'Connell, and A. Walker-Loud, Phys. Rev. D **75**, 054501 (2007).
[14] S. R. Sharpe and R. L. Singleton, Phys. Rev. D **58**, 074501 (1998).
[15] G. Rupak and N. Shoresh, Phys. Rev. D **66**, 054503 (2002).
[16] M. I. Buchoff, Phys. Rev. D **77**, 114502 (2008).
[17] N. Kawamoto and J. Smit, Nucl. Phys. **B192**, 100 (1981).
[18] S. R. Sharpe, R. Gupta, and G. W. Kilcup, Nucl. Phys. **B383**, 309 (1992).
[19] R. Gupta, A. Patel, and S. R. Sharpe, Phys. Rev. D **48**, 388 (1993).
[20] K. Symanzik, Nucl. Phys. **B226**, 187 (1983).
[21] K. Symanzik, Nucl. Phys. **B226**, 205 (1983).
[22] O. Bär, G. Rupak, and N. Shoresh, Phys. Rev. D **70**, 034508 (2004).
[23] S. Aoki, Phys. Rev. D **68**, 054508 (2003).
[24] J. Gasser and H. Leutwyler, Ann. Phys. (N.Y.) **158**, 142 (1984).
[25] J. Gasser and H. Leutwyler, Nucl. Phys. **B250**, 465 (1985).
[26] S. R. Sharpe and J. M. S. Wu, Phys. Rev. D **70**, 094029 (2004).
[27] S. R. Sharpe and J. M. S. Wu, Phys. Rev. D **71**, 074501 (2005).
[28] S. Aoki and O. Bär, Phys. Rev. D **70**, 116011 (2004).
[29] S. Aoki, Phys. Rev. D **30**, 2653 (1984).
[30] R. Frezzotti, P. A. Grassi, S. Sint, and P. Weisz, J. High Energy Phys. 08 (2001) 058.
[31] L. Scorzato, Eur. Phys. J. C **37**, 445 (2004).
[32] C. Michael and C. Urbach, Proc. Sci., LAT2007 (2007) 122.
[33] C. Urbach, Proc. Sci., LATTICE2007 (2007) 022.
[34] S. Weinberg, Phys. Rev. Lett. **17**, 616 (1966).
[35] C. Bernard, Phys. Rev. D **65**, 054031 (2002).
[36] C. Aubin and C. Bernard, Phys. Rev. D **68**, 034014 (2003).
[37] C. Aubin and C. Bernard, Phys. Rev. D **68**, 074011 (2003).
[38] B. Biedermann, Diploma thesis, Humboldt University Berlin, 2008, http://edoc.hu-berlin.de.
[39] J. Gasser and H. Leutwyler, Phys. Lett. B **125**, 325 (1983).
[40] S. Aoki and O. Bär, Proc. Sci., LATTICE2007 (2006) 062.
[41] T. Yamazaki *et al.*, Nucl. Phys. B, Proc. Suppl. **129**, 191 (2004).
[42] M. Lüscher, Commun. Math. Phys. **105**, 153 (1986).
[43] M. Lüscher, Nucl. Phys. **B354**, 531 (1991).
[44] L. Maiani and M. Testa, Phys. Lett. B **245**, 585 (1990).
[45] P. F. Bedaque, I. Sato, and A. Walker-Loud, Phys. Rev. D **73**, 074501 (2006).

Published by IOP Publishing for SISSA

Received: *December 19, 2008*
Accepted: *February 4, 2009*
Published: *March 2, 2009*

The epsilon regime with Wilson fermions

Oliver Bär,[a] **Silvia Necco**[b] **and Stefan Schaefer**[a]

[a] *Institute of Physics, Humboldt University Berlin, Newtonstrasse 15, 12489 Berlin, Germany*
[b] *Instituto de Física Corpuscular, CSIC-Universitat de València, Apartado de Correos 22085, E-46071 Valencia, Spain*
E-mail: obaer@physik.hu-berlin.de, necco@ific.uv.es, sschaef@physik.hu-berlin.de

Abstract: We study the impact of explicit chiral symmetry breaking of Wilson fermions on mesonic correlators in the ϵ-regime using Wilson chiral perturbation theory (WChPT). We generalize the ϵ-expansion of continuum ChPT to nonzero lattice spacings for various quark mass regimes. It turns out that the corrections due to a nonzero lattice spacing are highly suppressed for typical quark masses of the order $a\Lambda_{\rm QCD}^2$. The lattice spacing effects become more pronounced for smaller quark masses and lead to non-trivial corrections of the continuum ChPT results at next-to-leading order. We compute these corrections for the standard current and density correlation functions. A fit to lattice data shows that these corrections are small, as expected.

Keywords: Lattice QCD, Chiral Lagrangians

ArXiv ePrint: 0812.2403

Contents

1 Introduction

The ϵ-regime of QCD [1, 2] offers various advantages for the numerical determination of the low-energy couplings (LECs) in chiral perturbation theory (ChPT), the low-energy effective theory of QCD. Only the leading order LECs, the pseudo scalar decay constant in the chiral limit F and the chiral condensate Σ, enter the predictions of ChPT through next-to-leading order (NLO) in the epsilon expansion. The Gasser-Leutwyler coefficients [3, 4] first appear at one order higher, thus making the ϵ-regime attractive for precise determinations of F and Σ.[1] In addition, gauge field topology plays an important role in the ϵ-regime [6]. ChPT makes predictions for correlation functions restricted to individual topological sectors, thus enlarging the number of observables that can be compared to numerical lattice QCD results.

The role of topology and spontaneous chiral symmetry breaking has led to the widespread conviction that overlap [7] or domain-wall fermions [8–10] are the preferred or even mandatory choice for lattice simulations in the ϵ-regime. Consequently, a fairly large number of quenched simulations with these fermions in the ϵ-regime can be found in the literature [11–19]. Even though the results were to a large extend promising, the main hurdle for progress in real QCD is the need for simulations with dynamical sea quarks, and these are extremely time-consuming.[2] So far only the JLQCD collaboration [21] has carried out a large scale dynamical simulation with overlap fermions in the ϵ-regime, and the computer resources that went into this simulation are enormous.

In contrast, fairly inexpensive simulations with tree-level improved Wilson fermions have been reported recently [22]. Reweighting as described in ref. [23] has been used to reach small enough quark masses in order to be in the ϵ-regime. The size of the box was $L \simeq 2.8$fm, much larger than in all the simulations mentioned before. Quite surprisingly, the data for the axial vector and pseudo scalar correlation functions are very well described by the corresponding ChPT predictions, although chiral symmetry is explicitly broken for Wilson fermions.

A similar observation has been made before by the ETM collaboration [24, 25]. Their data[3], obtained with a twisted mass term [27, 28], also suggests that the ϵ-regime can be reached with Wilson fermions. One might argue that automatic $\mathrm{O}(a)$ improvement at maximal twist [29–31] may suppress chiral symmetry breaking effects. Still, the data obtained with Wilson fermions raises the question if and how the results can be interpreted in the presence of the explicit chiral symmetry breaking by the Wilson term.

In this paper we study this question with Wilson ChPT [32, 33], the low-energy effective theory for lattice QCD with Wilson fermions. And indeed, our analysis suggests a natural answer to the question raised above. It turns out that the lattice spacing corrections are in general highly suppressed and show up at higher order in the epsilon expansion. For example, for quark masses $m \sim a\Lambda_{\mathrm{QCD}}^2$ the deviations from the continuum results due to the $\mathrm{O}(a)$ corrections enter first at next-to-next-to-leading order (NNLO). This is in contrast to the expansion in the p-regime, where the corrections already appear at next-to-leading

[1] For a recent review of the various estimates see [5].
[2] For a recent review see [20].
[3] A review of the ETM results can be found in ref. [26].

order. This suppression is completely analogous to the suppression of terms involving the Gasser-Leutwyler coefficients in continuum ChPT in the ϵ-regime.

However, the power counting in WChPT can be different, depending on the relative size of the quark mass m and the lattice spacing a. For this reason we also consider a different power counting where $m \sim a\Lambda_{\rm QCD}^2$ is no longer appropriate. In this case the lattice spacing corrections enter already at NLO. Interestingly, these corrections are entirely caused by the $\mathrm{O}(a^2)$ term in the chiral effective Lagrangian that also determines the phase diagram of the lattice theory [32]. The corrections linear in the lattice spacing, stemming from the effective Lagrangian and the effective operators, are still of higher order in the epsilon expansion. This is relevant in practice: The Wilson ChPT expressions contain only one more unknown LEC at this order, and the predictive power is not spoiled by a plethora of free fit parameters.

We also use our WChPT results derived here for an analysis of the data of ref. [22]. The corrections due to the nonzero lattice spacing turn out to be very small, supporting our theoretical analysis that these corrections are in general highly suppressed. This is very encouraging for lattice simulations with Wilson fermions. The impact of explicit chiral symmetry breaking for ϵ-regime simulations is much less severe than previously thought. This makes simulations with Wilson fermions a serious and efficient alternative to those with chiral fermions.

2 Wilson chiral perturbation theory (WChPT)

2.1 Chiral Lagrangian

The chiral effective Lagrangian of WChPT is expanded in powers of (small) pion momenta p^2, quark masses m and the lattice spacing a. Based on the symmetries of the underlying Symanzik action [34, 35] the chiral Lagrangian including all terms of $\mathrm{O}(p^4, p^2m, m^2, p^2a, ma)$ is given in ref. [33]. The $\mathrm{O}(a^2)$ contributions are constructed in ref. [36] and, independently, in ref. [37] for the two-flavor case.

In the following we will restrict ourselves to $N_f = 2$ with degenerate quark mass m. The continuum part of the chiral Lagrangian is the well-known Gasser-Leutwyler Lagrangian [3, 38]. With our notations the leading part reads (in Euclidean space-time)

$$\mathcal{L}_2 = \frac{F^2}{4}\mathrm{Tr}\left(\partial_\mu U \partial_\mu U^\dagger\right) - \frac{F^2 B}{2} m \mathrm{Tr}\left(U + U^\dagger\right). \tag{2.1}$$

The field U containing the pion fields is defined as usual,

$$U(x) = \exp\left(\frac{2i}{F}\xi(x)\right), \qquad \xi(x) = \xi^a(x) T^a. \tag{2.2}$$

The SU(2) generators are normalized such that $\mathrm{Tr}(T^a T^b) = \delta^{ab}/2$, so $T^a = \sigma^a/2$ in terms of the standard Pauli matrices σ^a. The coefficients B and F are the familiar leading order (LO) low-energy coefficients.[4] Higher order terms are collected in the next-to-leading order Lagrangian $\mathcal{L}_4$ [3], which we do not need in this work.

[4] With our normalization the pion decay constant in the chiral limit is $F \approx 93\mathrm{MeV}$.

The terms involving the lattice spacing are as follows:[5]

$$\mathcal{L}_a = \hat{a}W_{45}\mathrm{Tr}\left(\partial_\mu U\partial_\mu U^\dagger\right)\mathrm{Tr}\left(U+U^\dagger\right) - \hat{a}\hat{m}W_{68}\Big(\mathrm{Tr}\left(U+U^\dagger\right)\Big)^2, \tag{2.3}$$

$$\mathcal{L}_{a^2} = \frac{F^2}{16}c_2a^2\Big(\mathrm{Tr}\left(U+U^\dagger\right)\Big)^2. \tag{2.4}$$

W_{45}, W_{68} are LECs, similar to Gasser-Leutwyler coefficients in $\mathcal{L}_4$. The quark mass and lattice spacing enter through the combinations

$$\hat{m} = 2Bm\,, \qquad \hat{a} = 2W_0a\,, \tag{2.5}$$

where W_0 is another low-energy coefficient [33]. Its presence here is for dimensional reasons: W_0 is of dimension three and $\hat{a}$ therefore of dimension two. Hence, $\hat{a}$ has the same dimension as the familiar combination Bm.

We have chosen to parametrize the $\mathrm{O}(a^2)$ contribution in terms of the LEC c_2. This coefficient plays a prominent role since its sign determines the phase diagram of the theory [32]. We briefly come back to this after we have discussed the power counting in WChPT in section 2.3.

Note that the mass parameter m in eq. (2.1) is the so-called *shifted mass* [32]. Besides the dominant additive mass renormalization proportional to $1/a$ it also contains the leading correction of $\mathrm{O}(a)$. Consequently, the term $F^2\hat{a}\mathrm{Tr}\left(U+U^\dagger\right)/4$ is not explicitly present in the chiral Lagrangian since it is absorbed in the shifted mass [33]. Of course, physical results expressed by observables do not depend on what mass is used for the parametrization of the chiral Lagrangian.

2.2 Currents and densities

The expressions for the currents and densities in continuum ChPT are well known. For example, the LO expressions for the axial vector current and the pseudo scalar density read

$$A^a_{\mu,\mathrm{ct}} = i\frac{F^2}{2}\mathrm{Tr}\left(T^a(U^\dagger\partial_\mu U - U\partial_\mu U^\dagger)\right)\,, \tag{2.6}$$

$$P^a_{\mathrm{ct}} = i\frac{F^2B}{2}\mathrm{Tr}\left(T^a(U-U^\dagger)\right)\,. \tag{2.7}$$

In WChPT these expressions receive corrections proportional to the lattice spacing. The currents and densities in WChPT can be constructed by a standard spurion analysis, similarly to the construction of the chiral Lagrangian. One first writes down the most general current/density that is compatible with the symmetries using the chiral field U, its derivatives and the spurion fields. Then, in a second step, one imposes the appropriate Ward identities valid in the theory. For the vector and axial vector current this has been done in [40]. Alternatively one can introduce source terms for the currents and densities and constructs the generating functional, as has been done in ref. [39]. Carrying over the notation of this reference the axial vector current including the leading corrections of $\mathrm{O}(a)$ reads

$$A^a_{\mu,\mathrm{WChPT}} = A^a_{\mu,\mathrm{cont}}\left(1+\frac{4}{F^2}\hat{a}W_{45}\mathrm{Tr}\left(U+U^\dagger\right)\right) + 2\hat{a}W_{10}\partial_\mu\mathrm{Tr}\left(T^a(U-U^\dagger)\right)\,. \tag{2.8}$$

[5] We essentially adopt the notation of refs. [39] and [31].

This axial vector does not satisfy any specific renormalization condition. Imposing a particular renormalization condition leads to a finite renormalization. Explicitly, one introduces [40]

$$A^a_{\mu,\mathrm{ren}}(x) = Z_A A^a_{\mu,\mathrm{WChPT}}(x) \tag{2.9}$$

with a renormalization factor Z_A.[6] Now one can impose a renormalization condition and demands that it is satisfied by $A^a_{\mu,\mathrm{ren}}$; this determines Z_A. For instance, in ref. [40] the massless chiral Ward identity has been imposed.

Quite generally, Z_A has the form (up to $\mathrm{O}(a)$)

$$Z_A = 1 + \frac{16}{F^2}\hat{a}W_A \tag{2.10}$$

with an unknown coefficient W_A. This form reflects the fact that, by construction, the WChPT current reduces to the correct continuum current for $a \to 0$. Consequently, Z_A is equal to one in the continuum limit, and (2.10) is the leading generalization for $a \neq 0$. Hence, the general form of the renormalized current is, up to $\mathrm{O}(a)$,

$$\begin{aligned} A^a_{\mu,\mathrm{WChPT}} = A^a_{\mu,\mathrm{cont}} &\left(1 + \frac{4}{F^2}\hat{a}\left[W_{45}\mathrm{Tr}\left(U + U^\dagger\right) + 4W_A\right]\right) \\ &+2\hat{a}W_{10}\partial_\mu \mathrm{Tr}\left(T^a(U - U^\dagger)\right). \end{aligned} \tag{2.11}$$

For brevity we have dropped the subscript "ren" on the left hand side. Terms of $\mathrm{O}(am, a^2)$ will be present at higher order in the chiral expansion.

Analogously, we use the expression [39]

$$P^a_{\mathrm{WChPT}} = P^a_{\mathrm{Cont}}\left(1 + \frac{4}{F^2}\hat{a}\left[W_{68}\mathrm{Tr}\left(U^\dagger + U\right) + 4W_P\right]\right) \tag{2.12}$$

for the pseudo scalar density. The contribution involving the LEC W_P (not present in ref. [39]) stems from a general renormalization factor $Z_P = 1 + 16\hat{a}W_P/F^2$, which we also allow, even though the results derived in this paper will not depend on the details of the $\mathrm{O}(a)$ correction.

2.3 Power counting in infinite volume

In WChPT there are two parameters that break chiral symmetry explicitly, the quark mass m and the lattice spacing a. The power counting is determined by the relative size of these two parameters.

The literature [39, 41] distinguishes two quark mass regimes with different power countings: (i) the GSM regime[7] where $m \sim a\Lambda^2_{\mathrm{QCD}}$ and (ii) the Aoki regime where $m \sim a^2\Lambda^3_{\mathrm{QCD}}$. A priori one does not know in which regime one actually has performed a simulation. For this to decide one has to compare with the predictions of WChPT and check which expressions fit the data better. However, recalling how lattice simulations are typically done one

[6] Z_A is a renormalization factor in the effective theory and should not be confused with Z_A in the underlying lattice theory.

[7] GSM stands for *generically small masses*.

can easily imagine that one starts in the GSM regime and by lowering the quark mass at fixed lattice spacing one will eventually enter the Aoki regime.

Depending on the particular regime, the LO Lagrangian is different. Since $m \sim a^2\Lambda_{\rm QCD}^3$ in the Aoki regime, also the $\mathcal{L}_{a^2}$ part in (2.4) counts as LO [37]:

$$\begin{aligned} \text{GSM regime}: \quad & \mathcal{L}_{\rm LO} = \mathcal{L}_2\,, \\ \text{Aoki regime}: \quad & \mathcal{L}_{\rm LO} = \mathcal{L}_2 + \mathcal{L}_{a^2}\,. \end{aligned}$$

The effects due to a nonzero lattice spacing are much more pronounced in the Aoki regime. Non-trivial phase transitions become relevant [32] and additional chiral logarithms proportional to a^2 appear at one loop [37, 42].

2.4 The pion mass and the PCAC mass in infinite volume

It is useful to derive the pion mass and PCAC mass at LO.

We start with the calculation of the pion mass. Expanding the LO chiral Lagrangian to quadratic order in the pion fields we obtain

$$\text{GSM regime}: \quad M_0^2 = 2Bm\,, \tag{2.13}$$

$$\text{Aoki regime}: \quad M_0^2 = 2Bm - 2c_2a^2\,. \tag{2.14}$$

The sign of c_2 determines the phase diagram of the theory [32].[8] For $c_2 > 0$ there exists a second-order phase transition separating the Aoki phase [43]. The charged pions are massless in this phase due to the spontaneous breaking of the flavor symmetry. The pion mass vanishes at $m = c_2a^2/B$. For even smaller values of m the charged pions remain massless, while the neutral pion becomes massive again [32].

Negative values of c_2, on the other hand, imply a first order phase transition with a minimal non-vanishing pion mass. All three pions are massive for all quark masses, and the pion mass assumes its minimal value at $m = 0$, resulting in

$$M_{0,\rm min}^2 = 2|c_2|a^2\,. \tag{2.15}$$

Note that magnitude and the sign of c_2 are a priori unknown and depend on the details of the underlying lattice theory, i.e. what particular lattice action has been used.

The PCAC quark mass is defined by the ratio (no sum over a)

$$m_{\rm PCAC} = \frac{\langle \partial_\mu A_\mu^a(x) P^a(0)\rangle}{2\langle P^a(x)P^a(0)\rangle}\,, \tag{2.16}$$

where angled brackets indicate expectation values. Expanding the current and the density in eqs. (2.11) and (2.12) to $\mathrm{O}(\xi^a)$ we find

$$A_\mu^a(x) = -iF\partial_\mu\xi^a(x)\,(1 + ac_A)\,, \tag{2.17}$$

$$P^a(x) = iFB\xi^a(x)\,(1 + ac_P)\,. \tag{2.18}$$

[8] Note that our definition for c_2 differs by a factor F^2a^2 from the one in ref. [32].

where here and in the following we for simplicity no longer write the subscript "WChPT". We also introduced the short hand notation

$$c_A = \frac{16}{F^2} 2W_0[W_{45} + W_A - W_{10}/4]\,, \tag{2.19}$$

$$c_P = \frac{16}{F^2} 2W_0[W_{68} + W_P]\,, \tag{2.20}$$

for the combinations of LECs in the effective current and density at this order. The correlation functions in (2.16) are now easily computed at LO, yielding

$$m_{\rm PCAC} = \frac{M_0^2}{2B}\Big(1 + a(c_A - c_P)\Big)\,. \tag{2.21}$$

Using the tree-level pion mass obtained above we find

$$\text{GSM regime}: \qquad m_{\rm PCAC} = m\Big(1 + a(c_A - c_P)\Big)\,, \tag{2.22}$$

$$\text{Aoki regime}: \qquad m_{\rm PCAC} = \Big(m - \frac{c_2}{B}a^2\Big)\Big(1 + a(c_A - c_P)\Big)\,. \tag{2.23}$$

In the GSM regime the result is rather simple and the PCAC mass is equal to the shifted quark mass, up to corrections of $\mathrm{O}(ma)$. This is no longer true in the Aoki regime. Still, the contribution proportional to $(c_A - c_P)$ is subleading and can be ignored if one works to leading order in the quark mass.

Equations (2.22) and (2.23) allow to replace the shifted mass m, which is just a parameter in the chiral Lagrangian, with the PCAC quark mass. The latter is an observable which is often used in lattice simulations.

Note that the results above reproduce a well-known fact, namely that the PCAC mass depends on the particular renormalization conditions imposed on the axial vector current and the pseudo scalar density. Different renormalization conditions show up as different values for c_A and c_P.

3 WChPT in the epsilon regime

3.1 Continuum ChPT in finite volume

Consider continuum QCD with N_f degenerate quark masses in a hypercubic volume $V = TL^3$, with $T, L \gg 1/\Lambda_{\rm QCD}$. Finite-size effects can be systematically studied by means of the corresponding chiral effective theory [1, 2, 44]. In this section we summarize the main aspects of finite-volume chiral perturbation theory in the continuum.

If the pion Compton wavelength is much smaller than the size of the box, $M_\pi L \gg 1$, finite-volume effects can be treated in the chiral effective theory by adopting the standard p-expansion, where the power-counting in terms of the momentum p is given by

$$m \sim O(p^2), \quad 1/L,\ 1/T\,, \partial_\mu \sim O(p), \quad \xi \sim O(p). \tag{3.1}$$

For asymptotically large volumes, one expects the finite-volume effects to be exponentially suppressed by factors $\sim e^{-M_\pi L}$.

On the other hand, approaching the chiral limit by keeping $\mu = m\Sigma V \lesssim O(1)$ (but still $L \gg 1/\Lambda_{\rm QCD}$), where $\Sigma = F^2 B$ is the quark condensate in the chiral limit, one explores the domain where the pion wavelength is larger than the size of the box, $M_\pi L < 1$. In this case the pion zero-mode gives a contribution to the propagator proportional to $1/M_0^2 V$, which cannot be treated perturbatively but has to be computed exactly [1, 2]. This is achieved by factorizing the pseudo Nambu-Goldstone boson fields as

$$U(x) = \exp\left(\frac{2i}{F}\xi(x)\right) U_0\,, \tag{3.2}$$

where the constant $U_0 \in \mathrm{SU}(N_f)$ represents the collective zero-mode. The nonzero modes parametrized by ξ, on the other hand, can still be treated perturbatively and satisfy the condition

$$\int_V d^4x\, \xi(x) = 0, \tag{3.3}$$

since the constant mode has been separated.

The zero-mode contribution proportional to $1/M_0^2 V$ in the pion propagator diverges in the chiral limit and a reordering of the perturbation series that sums all graphs with an arbitrary number of zero-mode propagators is necessary [2]. This reordering is achieved with the power counting

$$m \sim O(\epsilon^4), \quad 1/L,\ 1/T\,, \partial_\mu \sim O(\epsilon), \quad \xi \sim O(\epsilon). \tag{3.4}$$

Mass effects are suppressed compared to the p-regime, while volume effects are enhanced and become polynomial in $(FL)^{-2}$. Since M_0^2 is proportional to m the combination $1/M_0^2 V$ now counts as ϵ^0. Consequently, all graphs that exclusively involve zero-mode propagators count as O(1) and are unsuppressed. The key point here is, that the counting of the quark mass is dictated by the counting of L by demanding $1/M_0^2 V = \mathrm{O}(\epsilon^0)$. We will use this in the next section in order to establish the counting rules in WChPT.

With the factorization given in eq. (3.2), the leading order continuum partition function in the ϵ-regime is given by

$$Z = \int_{\mathrm{SU}(N_f)} [dU_0] \int [d\xi] \exp\left\{\frac{1}{2}\int_V d^4x \mathrm{Tr}(\partial_\mu \xi \partial_\mu \xi) + \frac{m\Sigma V}{2}\mathrm{Tr}(U_0 + U_0^\dagger)\right\}. \tag{3.5}$$

The integration over the perturbative degrees of freedom $[d\xi]$ gives rise to the usual Wick contractions, while the zero-mode integrals over $[dU_0]$ must be computed exactly. Notice that by going to $O(\epsilon^2)$, by factoring out the constant zero-mode from the measure, one obtains

$$[dU] = [d\xi][dU_0]\left(1 + A(\xi) + O(\epsilon^4)\right), \tag{3.6}$$

with

$$A(\xi) = -\frac{2N_f}{3F^2}\frac{1}{V}\int_V d^4x\, \mathrm{Tr}(\xi^2(x)) \tag{3.7}$$

for a general value of N_f [2, 45].

3.2 Power countings for the epsilon regime in WChPT

Like the continuum effective theory, WChPT can also be formulated in a finite volume, in particular the ϵ-regime discussed in this section.

In WChPT we have additional low-energy constants and the lattice spacing as an additional expansion parameter. The main task is to decide how to count these in the epsilon expansion.

Just as the continuum LECs F and Σ, we count all the additional LECs associated with the lattice spacing to be of order ϵ^0,

$$c_2, c_A, c_P \sim \mathrm{O}(1). \tag{3.8}$$

The counting of the lattice spacing a is more complicated. The general strategy is to follow the infinite-volume procedure and determine the power counting depending on the relative size of m and a. At finite volume, once the counting of m is fixed by the counting of L, we obtain the counting of a.

We start with the GSM regime. The LO Lagrangian and the pion mass M_0^2 are as in the continuum ϵ-regime, so we conclude $m \sim \mathrm{O}(\epsilon^4)$ by the same arguments as in the previous section. Since the GSM regime is defined by $m \sim a\Lambda_{\mathrm{QCD}}^2$ we are immediately lead to $a \sim \mathrm{O}(\epsilon^4)$.

The Aoki regime is more subtle. According to our assumption, the pion mass M_0^2, given in (2.14), is now a sum of two terms of equal order. If $c_2 < 0$, it is a sum of two positive terms. Hence, a small pion mass of order $\mathrm{O}(\epsilon^4)$ implies that both terms, $2Bm$ and $2|c_2|a^2$ are small too and also of order $\mathrm{O}(\epsilon^4)$.

If c_2 is positive, the pion mass is the difference of two positive contributions. This leaves the possibility that M_0^2 is small, even though the individual terms $2Bm$ and $2|c_2|a^2$ may not be small and only their difference is. A pion mass of order ϵ^4 may be obtained by the difference of two order ϵ^2 or ϵ^3 terms, for example.

We do not think that this is a likely scenario. Present day lattice simulations are usually done with small lattice spacings less than 0.1 fm and the $\mathrm{O}(a^2)$ corrections are expected to be small in this case. Hence, we *assume* that $a^2 \sim \mathrm{O}(\epsilon^4)$ in the Aoki regime. This assumption, together with the requirement $M_0^2 \sim \mathrm{O}(\epsilon^4)$ then also leads to $m \sim \mathrm{O}(\epsilon^4)$, the same counting as for $c_2 < 0$.

The epsilon expansion allows us to introduce yet another regime where we count $a \sim \epsilon^3$. Just by the powers of ϵ this is an intermediate regime between the GSM and Aoki regime. One may think about it as the GSM regime but at a larger lattice spacing (or smaller quark mass). Its usefulness will become clear in the next section when we discuss the epsilon expansion of correlation functions.

All three countings we introduced are well defined and are appropriate for a particular relative size between m and a. In order to be able to refer to these regimes we introduce the following nomenclature:

$$\begin{aligned} \text{GSM regime}: &\quad a \sim \mathrm{O}(\epsilon^4)\,, \\ \text{GSM}^* \text{ regime}: &\quad a \sim \mathrm{O}(\epsilon^3)\,, \\ \text{Aoki regime}: &\quad a \sim \mathrm{O}(\epsilon^2)\,. \end{aligned} \tag{3.9}$$

For fixed values of m and a in a given regime, one can match for instance the time-dependence of current correlators with lattice QCD results in order to extract the corresponding LECs.

We stress that one a priori does not know which power counting to use in analyzing numerical lattice data. For this to decide one has to analyze the data with the WChPT results for different power countings and see which one describes the data.

3.3 Epsilon expansion of correlation functions

We will be interested in correlators of the pseudo scalar density and the axial vector current. These correlators have been calculated before through NNLO in continuum ChPT [45]. In powers of ϵ this corresponds to $O(\epsilon^4)$ for the $\langle P^a(x)P^a(0)\rangle$ correlator and $O(\epsilon^8)$ for $\langle A^a_\mu(x)A^a_\mu(0)\rangle$.

In order to discuss the epsilon expansion in WChPT let us split an arbitrary operator and the action in WChPT into the continuum part and a remainder proportional to powers of a,

$$O(x) = O_{\rm ct}(x) + \delta O(x)\,, \tag{3.10}$$

$$S = S_{\rm ct} + \delta S\,. \tag{3.11}$$

Expectation values are generically defined as

$$\langle O\rangle = \frac{1}{Z}\int [dU] e^{-S} O, \tag{3.12}$$

where Z is the partition function

$$Z = \int [dU] e^{-S}. \tag{3.13}$$

The two-point correlator $\langle O_1(x)O_2(0)\rangle = \langle O_1 O_2\rangle$ (for notational simplicity we suppress the dependence on x) can then be written according to

$$\langle O_1 O_2\rangle_W = \langle O_{1,\rm ct} O_{2,\rm ct}\rangle + \delta\langle O_1 O_2\rangle\,, \tag{3.14}$$

$$\delta\langle O_1 O_2\rangle = \langle O_{1,\rm ct}\delta O_2 + \delta O_1 O_{2,\rm ct}\rangle - \langle O_{1,\rm ct} O_{2,\rm ct}\delta S\rangle + \langle O_{1,\rm ct} O_{2,\rm ct}\rangle\langle\delta S\rangle\,. \tag{3.15}$$

Here we have approximated $\exp(-\delta S) \approx 1 - \delta S$ and we dropped all higher corrections. Note that the expectation value on the left hand side of (3.14), labelled with a subscript "W", is defined with the full action S in the Boltzmann factor, while on the right hand side it is defined with $S_{\rm ct}$ only (for notational simplicity we suppress a subscript "ct").

The discretization corrections for the pseudo scalar and the axial vector can be read off from (2.11) and (2.12). For what matters here we can simplify these expressions. We are interested in the power counting for the epsilon expansion, and for this we can ignore all constants which count as O(1). Therefore, we write

$$\delta P^a \propto a\Big(\mathrm{Tr}\left(U + U^\dagger\right) + 1\Big) P^a_{\rm ct}\,. \tag{3.16}$$

δP^a is proportional to the continuum density itself. As mentioned before, the epsilon expansion of $P^a_{\rm ct}$ starts with $\mathrm{O}(\epsilon^0)$. The "scalar density" $\mathrm{Tr}(U+U^\dagger)$ also starts at $\mathrm{O}(\epsilon^0)$. Hence, by considering the continuum contribution at LO, the leading correction in the epsilon expansion due to lattice terms is completely determined by how we count the lattice spacing a. In the last section we defined three different countings, so for now we leave it unspecified, write $a \sim \epsilon^{n_a}$ where n_a counts the epsilon powers for a, and obtain

$$\delta P^a \sim \epsilon^{n_a}. \tag{3.17}$$

Note that the symbol $\sim$ stands here just for the leading lattice contribution in the epsilon expansion.

Analogously, we find for the axial vector (dropping again irrelevant constants)

$$\delta A^a_\mu \propto a\left[\left(\mathrm{Tr}\left(U+U^\dagger\right)+1\right)A^a_{\mu,\rm ct} + \partial_\mu \mathrm{Tr}\left(T^a(U-U^\dagger)\right)\right]. \tag{3.18}$$

Both, $A^a_{\mu,\rm ct}$ and $\partial_\mu \mathrm{Tr}\left(T^a(U-U^\dagger)\right)$ have an open Lorentz index and, therefore, contain at least one derivative acting on at least one power of $\xi(x)$. Hence, their continuum epsilon expansion starts at $\mathrm{O}(\epsilon^2)$ and we find for the leading lattice corrections

$$\delta A^a_\mu \sim \epsilon^{n_a+2}. \tag{3.19}$$

Finally, we have to take into account the lattice corrections due to the contribution δS. It will be useful to split them into two parts. The first one, denoted by δS_a, contains the terms of $\mathcal{L}_a$ in (2.3). These terms start at $\mathrm{O}(\epsilon^{n_a})$ (having taken into account ϵ^{-4} from the integration over space-time),

$$\delta S_a \sim \epsilon^{n_a}. \tag{3.20}$$

The second contribution, δS_{a^2}, contains only the a^2 term proportional to c_2. Therefore, it counts as

$$\delta S_{a^2} \sim \epsilon^{2n_a-4}. \tag{3.21}$$

After these preparations we can determine at which order the lattice spacing effects enter the PP and the AA correlator.

3.3.1 GSM regime

In the GSM regime we set $n_a = 4$ and find

$$\delta\langle P^a(x)P^a(0)\rangle \sim \mathrm{O}(\epsilon^4), \tag{3.22}$$

$$\delta\langle A^a_\mu(x)A^a_\mu(0)\rangle \sim \mathrm{O}(\epsilon^8). \tag{3.23}$$

The corrections due to the lattice spacing first affect both correlators at NNLO. Up to NLO the results obtained in continuum ChPT are the appropriate ones. This is quite remarkable and may explain why numerical data generated recently [22] could be fitted very well using the NLO continuum expressions. Note that this suppression to NNLO holds for the unimproved theory. The reason is that the terms linear in a are accompanied by at least one additional power of m or $\partial_\mu\xi$, and are therefore of higher order.

3.3.2 GSM* regime

Here we have $n_a = 3$ and obtain

$$\delta\langle P^a(x)P^a(0)\rangle \sim \mathrm{O}(\epsilon^2)\,, \tag{3.24}$$

$$\delta\langle A^a_\mu(x)A^a_\mu(0)\rangle \sim \mathrm{O}(\epsilon^6)\,, \tag{3.25}$$

hence the corrections enter at NLO. Interestingly, the dominant term here comes only from the correction δS_{a^2}. The other corrections from the $\mathrm{O}(a)$ contributions in the currents, densities and δS_a start at ϵ^3 and ϵ^7, respectively. Therefore, they are of higher order in the epsilon expansion, even though they are still lower than the NNLO contributions, which start at ϵ^4 and ϵ^8, respectively.

Notice that in the GSM and GSM* regimes the leading order partition function is like the continuum one given in eq. (3.5). In particular, the exact zero-mode integrals are computed with respect to the same Boltzmann factor as in continuum ChPT.

3.3.3 Aoki regime

The modifications in the Aoki regime are more pronounced than in the previously discussed regimes. Here, cut-off effects show up already at LO. Even worse, the corrections can no longer be linearly added to the continuum result. The reason is the correction δS_{a^2}, which gives a zero-mode contribution of order ϵ^0. Hence, it is no longer justified to expand completely the exponential $\exp(-S_{a^2}) \approx 1 - S_{a^2}$. The zero-mode contribution of order ϵ^0 has to be included in the leading order Boltzmann factor. That is, the partition function becomes

$$Z_{\text{Aoki}} = \int_{\mathrm{SU}(2)} [dU_0] \int [d\xi] \exp\left\{ \frac{1}{2}\int_V d^4x \mathrm{Tr}(\partial_\mu\xi\partial_\mu\xi) + \frac{m\Sigma V}{2}\mathrm{Tr}(U_0 + U_0^\dagger) \right. \tag{3.26}$$
$$\left. - \frac{c_2 F^2 a^2 V}{16}(\mathrm{Tr}(U_0 + U_0^\dagger))^2 \right\}.$$

This modification affects all constant integrals and probably leads to non-trivial changes of the continuum results. Note that the other $\mathrm{O}(a)$ corrections (from δO and δS_a) are of order ϵ^2 and show up at NLO only.

3.4 Comment on O(a) improvement

The results in the previous section are valid for unimproved Wilson fermions. It is natural to ask how (non-perturbative) $\mathrm{O}(a)$–improvement changes these results.

If the theory is non-perturbatively improved the corrections δO and δS_a are absent, and modifications are caused by δS_{a^2} only. We have seen that this term is the dominant correction and the others are subleading. Consequently, the epsilon expansion is essentially unaltered for the improved theory, since only subleading terms vanish.

4 Leading correction in the GSM* regime

We already mentioned in the introduction that the epsilon expansion is advantageous for the determination of F and Σ, since the Gasser-Leutwyler coefficients first enter the ChPT

formulae at NNLO. The same is true for WChPT in the GSM regime, where the additional lattice spacing contributions enter at NNLO too. In other words, working through NLO the results for the GSM regime are the same as those in continuum ChPT.

The first non-trivial modification of the continuum NLO results appears in the GSM* regime, and in this section we compute the leading correction to the PP and AA correlator; the results for some other correlators are given in appendix C. This correction is caused by the constant term of the δS_{a^2} contribution,

$$\delta\langle O_1(x)O_2(y)\rangle\Big|_{\text{leading}} = -\langle O^{\text{LO}}_{1,\text{ct}}(x)O^{\text{LO}}_{2,\text{ct}}(y)\delta S_{a^2}\rangle + \langle O^{\text{LO}}_{1,\text{ct}}(x)O^{\text{LO}}_{2,\text{ct}}(y)\rangle\langle\delta S_{a^2}\rangle\,, \quad (4.1)$$

where

$$\delta S_{a^2} = \frac{\rho}{16}(\text{Tr}(U_0+U_0))^2. \quad (4.2)$$

The superscript "LO" refers to leading order in the ϵ-expansion and we have introduced the dimensionless quantity

$$\rho = F^2 c_2 a^2 V. \quad (4.3)$$

Notice that if $\langle O^{\text{LO}}_{1,\text{ct}}(x)O^{\text{LO}}_{2,\text{ct}}(y)\delta S_{a^2}\rangle = \langle O^{\text{LO}}_{1,\text{ct}}(x)O^{\text{LO}}_{2,\text{ct}}(y)\rangle\langle\delta S_{a^2}\rangle$, i.e for disconnected insertions, the leading correction in eq. (4.1) vanishes. This happens for instance for left handed (V-A) current correlators [46], and more general for correlators which do not get zero-mode contributions at leading order.

Since chiral symmetry is explicitly broken in Lattice QCD with Wilson fermions, a natural definition for the topological charge does not exist at non-zero lattice spacing. Moreover, a WChPT analysis of topology and its cut-off effects has not been done so far. For this reason we will only give results for observables where the sum over all topological sectors has been performed, even though the projection onto topological sectors via a Fourier transform [6] seems to be possible.

4.1 Preliminaries

Calculations of mesonic 2-point functions in the ϵ-regime have been pioneered in ref. [45]. The integration over the non-constant modes $\xi(x)$ is done perturbatively as in ordinary chiral perturbation theory in the p-regime. We summarize the corresponding propagators and other useful properties in appendix A.

The integral over the constant mode U_0 has to be done exactly. In our particular case with $N_f = 2$ we encounter integrals of the type

$$\langle g(U_0)\rangle = \frac{1}{Z_0}\int_{\text{SU}(2)}[dU_0]\, g(U_0)\, e^{\frac{\mu}{2}\text{Tr}(U_0+U_0^\dagger)}\,, \quad (4.4)$$

where Z_0 is the continuum partition function associated to the zero modes,

$$Z_0 = \int_{\text{SU}(2)}[dU_0] e^{\frac{\mu}{2}\text{Tr}(U_0+U_0^\dagger)}\,, \quad (4.5)$$

and μ denotes the standard combination

$$\mu = m\Sigma V\,. \tag{4.6}$$

Quite generally, the integral (4.4) leads, at least for the types of g we are considering, to expressions involving modified Bessel functions $I_n(z)$ with integer index n. They satisfy numerous recursion relations [47], and all integrals can be expressed in terms of two Bessel functions, which we choose to be I_2 and I_1. In appendix B we collect various integrals that one encounters in calculating the PP and AA correlator in the GSM* regime.

As an example let us consider the expectation value of the quantity δS_{a^2}, defined in eq. (4.2), that is part of the correction in (4.1). By using the integrals given in the appendix we obtain

$$\langle \delta S_{a^2} \rangle = \rho \left(1 - \frac{3}{2\mu}\frac{I_2(2\mu)}{I_1(2\mu)}\right)\,. \tag{4.7}$$

4.2 The PP correlator

For the PP correlator we introduce the definition

$$\langle P^a(x) P^b(y)\rangle = \delta^{ab} C_{PP}(x-y)\,, \tag{4.8}$$

which takes into account translation invariance and the trivial dependence on the flavor indices. In the GSM* regime, $C_{PP}(x-y)$ can be written through NLO as the sum of the continuum correlator and a correction proportional to a^2,

$$C_{PP}(x-y) = C_{PP,\mathrm{ct}}(x-y) + C_{PP,a^2}(x-y)\,. \tag{4.9}$$

The continuum correlator for generic N_f at NLO (which corresponds to $O(\epsilon^2)$) is given by [45] (see also [48])

$$C_{PP,\mathrm{ct}}(x-y) = C_P + \alpha_P \bar{G}(x-y), \tag{4.10}$$

where $\bar{G}(x-y)$ is the finite-volume massless scalar propagator defined in eq. (A.1) and

$$C_P = -\frac{\Sigma_{\mathrm{eff}}^2}{8(N_f^2-1)}\left[\langle \mathrm{Tr}[(U_0 - U_0^\dagger)^2]\rangle_{\mathrm{eff}} - \frac{1}{N_f}\langle [\mathrm{Tr}(U_0 - U_0^\dagger)]^2\rangle_{\mathrm{eff}}\right], \tag{4.11}$$

$$\alpha_P = \frac{\Sigma^2}{4F^2(N_f^2-1)}\Bigg[2N_f^2 - 4 - \frac{2}{N_f}\langle \mathrm{Tr}(U_0^2) + \mathrm{Tr}(U_0^{\dagger 2})\rangle + \frac{2}{N_f^2}\langle \mathrm{Tr}(U_0)\mathrm{Tr}(U_0^\dagger)\rangle + \left(\frac{N_f^2+1}{N_f^2}\right)\langle (\mathrm{Tr}U_0)^2 + (\mathrm{Tr}U_0^\dagger)^2\rangle\Bigg]. \tag{4.12}$$

The expectation values with the subscript "eff" are defined like in eq. (4.4) with μ replaced by

$$\mu_{\mathrm{eff}} = m\Sigma_{\mathrm{eff}} V, \tag{4.13}$$

where Σ_{eff} is the quark condensate at one loop [45]

$$\Sigma_{\mathrm{eff}} = \Sigma\left(1 + \frac{N_f^2-1}{N_f}\frac{1}{F^2}\frac{\beta_1}{\sqrt{V}}\right). \tag{4.14}$$

β_1 is a so-called *shape factor* and is defined in eq. (A.5).

For the particular case $N_f = 2$, after the explicit computation of the zero-mode integrals according to appendix B, one gets

$$C_P = \frac{\Sigma_{\text{eff}}^2}{2\mu_{\text{eff}}} \frac{I_2(2\mu_{\text{eff}})}{I_1(2\mu_{\text{eff}})}, \tag{4.15}$$

$$\alpha_P = \frac{\Sigma^2}{2F^2} \left[2 - \frac{1}{\mu} \frac{I_2(2\mu)}{I_1(2\mu)} \right]. \tag{4.16}$$

For the leading lattice correction to the continuum result, as given in eq. (4.1), we find the $O(\epsilon^2)$ contribution

$$C_{PP,a^2} = \rho \frac{\Sigma^2}{2} \Delta_{PP}, \tag{4.17}$$

with

$$\Delta_{PP} = \frac{5\mu I_1^2(2\mu) - 10 I_1(2\mu) I_2(2\mu) - 3\mu I_2^2(2\mu)}{2\mu^3 I_1^2(2\mu)}. \tag{4.18}$$

Interestingly, the correction Δ_{PP} is finite in the limit $\mu \to 0$, as is easily checked using the leading order Taylor expansions for the Bessel functions [47], $I_1(2\mu) \sim \mu$ and $I_2(2\mu) \sim \mu^2/2$. We are not aware of a rigorous argument that Δ_{PP} has to be regular at vanishing μ, since this correction ceases to be valid for small enough quark mass where one enters the Aoki regime. A singularity at $\mu = 0$ would have been a clear signal for this breakdown of our calculation, however, this signal is not present in the result, at least not at the order in the chiral expansion we are working here.

For the matching with numerical results obtained in lattice simulations we are interested in the correlation function integrated over the spatial components,

$$C_{PP}(t) = \int d^3\vec{x}\, C_{PP}(x-y)\Big|_{y=0} = C_{PP,\text{ct}}(t) + \frac{L^3\Sigma^2}{2} \rho \Delta_{PP}, \tag{4.19}$$

where

$$C_{PP,\text{ct}}(t) = \frac{L^3}{2} \frac{\Sigma_{\text{eff}}^2}{\mu_{\text{eff}}} \frac{I_2(2\mu_{\text{eff}})}{I_1(2\mu_{\text{eff}})} + \frac{T\Sigma^2}{2F^2} h_1(t/T) \left[2 - \frac{1}{\mu} \frac{I_2(2\mu)}{I_1(2\mu)} \right]. \tag{4.20}$$

The time dependence is given by the parabolic function h_1 defined in eq. (A.9).

4.3 The AA correlator

The AA correlator is computed along the same lines. For simplicity we consider the time-component correlator and we define

$$\langle A_0^a(x) A_0^b(y) \rangle = \delta^{ab} C_{AA}(x-y). \tag{4.21}$$

Similarly to the PP correlator we split C_{AA} at NLO into a continuum part and a correction proportional to the lattice spacing,

$$C_{AA}(x-y) = C_{AA,\text{ct}}(x-y) + C_{AA,a^2}(x-y). \tag{4.22}$$

The continuum contribution at $O(\epsilon^6)$ for $x \neq y$ and generic N_f has been calculated before [45] (see also [49]) and is given by

$$C_{AA,\mathrm{ct}}(x-y) = \alpha_A \partial_{x_0}\partial_{y_0}\bar{G}(x-y) + \beta_A K_{00}(x-y) + \gamma_A \partial_{x_0}\partial_{y_0} H(x-y), \tag{4.23}$$

where the following short hand notation has been introduced:

$$\alpha_A = \frac{F^2}{2}\langle \mathcal{J}_0\rangle_{\mathrm{eff}} + \frac{N_f}{2}\frac{\beta_1}{\sqrt{V}}\langle \mathcal{J}_0\rangle\,, \tag{4.24}$$

$$\beta_A = \frac{N_f}{2}\left(2 - \langle \mathcal{J}_0\rangle\right)\,, \tag{4.25}$$

$$\gamma_A = \langle \mathrm{Tr}(U_0 + U_0^\dagger)\rangle \frac{\mu}{N_f}. \tag{4.26}$$

The functions $K_{\mu\nu}$ and H are given in eqs. (A.7) and (A.8). Moreover, we have introduced the quantity

$$\mathcal{J}_0 = \frac{1}{N_f^2 - 1}\left[\mathrm{Tr}U_0 \mathrm{Tr}U_0^\dagger + N_f^2 - 2\right]. \tag{4.27}$$

Like for the PP correlator, the subscript "eff" refers to the substitution $\mu \to \mu_{\mathrm{eff}}$ in the zero-mode integrals. For the particular case we are considering, $N_f = 2$, the results (4.24)–(4.26) reduce to

$$\alpha_A = F^2\left[1 - \frac{I_2(2\mu_{\mathrm{eff}})}{\mu_{\mathrm{eff}} I_1(2\mu_{\mathrm{eff}})}\right] + 2\frac{\beta_1}{\sqrt{V}}\left[1 - \frac{I_2(2\mu)}{\mu I_1(2\mu)}\right]\,, \tag{4.28}$$

$$\beta_A = \frac{2}{\mu}\frac{I_2(2\mu)}{I_1(2\mu)}\,, \tag{4.29}$$

$$\gamma_A = \frac{2\mu I_2(2\mu)}{I_1(2\mu)}. \tag{4.30}$$

In analogy to the PP correlator, the $O(a^2)$ contribution can be computed according to eq. (4.1), and we obtain

$$C_{AA,a^2}(x-y) = \frac{F^2}{2}\partial_{x_0}\partial_{y_0}\bar{G}(x-y)\rho\Delta_{AA}\,, \tag{4.31}$$

with

$$\Delta_{AA} = \frac{-5\mu I_1^2(2\mu) + 10 I_1(2\mu) I_2(2\mu) + 3\mu I_2(2\mu)^2}{\mu^3 I_1^2(2\mu)} = -2\Delta_{PP}\,. \tag{4.32}$$

Note that this correction affects only the coefficient α_A in eq. (4.28), which will be modified by the presence of lattice artifacts.

The $\mathrm{O}(a^2)$ correction is, up to a sign and a factor two, the same as the correction for the PP correlator. As far as we can see there is no deeper reason for this. It is simply a consequence of the fact that the zero-mode integrals for the leading order continuum PP and AA correlator are very similar, both lead to the same contribution involving the ratio $I_2(2\mu)/\mu I_1(2\mu)$.

By integrating over the spatial coordinates and using the properties listed in appendix A, we obtain for $t \neq 0$

$$C_{AA}(t) = \int d^3\vec{x}\, C_{AA}(x-y)|_{y=0} = C_{AA,\mathrm{ct}}(t) - \frac{F^2}{2T}\rho\Delta_{AA}, \tag{4.33}$$

where the continuum result for $N_f = 2$ explicitly reads

$$\begin{aligned} C_{AA,\mathrm{ct}}(t) &= -\frac{1}{T}\alpha_A + \frac{T}{V}k_{00}\beta_A - \frac{T}{V}\gamma_A h_1\left(\frac{t}{T}\right) = \\ &= -\frac{F^2}{T}\left(1 - \frac{I_2(2\mu_{\mathrm{eff}})}{\mu_{\mathrm{eff}} I_1(2\mu_{\mathrm{eff}})}\right) - \frac{2\beta_1}{T\sqrt{V}}\left(1 - \frac{I_2(2\mu)}{\mu I_1(2\mu)}\right) + \\ &\quad + \frac{2T}{V}k_{00}\frac{I_2(2\mu)}{\mu I_1(2\mu)} - \frac{2T}{V}h_1(t/T)\frac{\mu I_2(2\mu)}{I_1(2\mu)}\,. \end{aligned} \tag{4.34}$$

Here k_{00} is another shape factor defined in the appendix, eq. (A.6).

4.4 The PCAC mass

The correlators in the previous section are given as functions of m, the shifted mass. This is the mass parameter in the chiral Lagrangian and a priori not an observable. Here we compute the PCAC mass, defined in (2.16), and use it in the next section to replace m with m_{PCAC}.

We have already calculated the denominator of (2.16), and the numerator can be done analogously. Let us define

$$\langle \partial_\mu A^a_\mu(x) P^b(y)\rangle = \delta^{ab} C_{\partial AP}(x-y)\,. \tag{4.35}$$

To leading order in the epsilon expansion we find the result

$$C_{\partial AP,\mathrm{ct}}(x-y) = \frac{\Sigma}{V}\frac{I_2(2\mu)}{I_1(2\mu)}\,. \tag{4.36}$$

Dividing this by the leading order result of $2C_{PP,\mathrm{ct}}$ in eq. (4.10) we obtain

$$m_{\mathrm{PCAC}} = \frac{\mu}{\Sigma V} = m\,. \tag{4.37}$$

This is just the result of continuum ChPT, where it is not surprising because the PCAC mass stems from the PCAC Ward identity. Note, however, that both numerator and denominator contain non-trivial Bessel functions which cancel in the ratio. This cancellation will no longer happen with the lattice spacing corrections included, since the PCAC relation no longer holds.

The leading correction to the numerator in the GSM* regime is given by (4.1) with $O_1 = \partial_\mu A^a(x)$ and $O_2 = P^a(y)$ (no sum over a). The computation is straightforward as the ones in the previous sections and we find

$$C_{\partial AP}(x-y) = \frac{\Sigma}{V}\frac{I_2(2\mu)}{I_1(2\mu)}\left[1 - \frac{3\rho}{2\mu^2}\left(2 - \frac{\mu I_1(2\mu)}{I_2(2\mu)} + \frac{\mu I_2(2\mu)}{I_1(2\mu)}\right)\right]. \tag{4.38}$$

Dividing by $2C_{PP}$ given in (4.9) we obtain the leading $O(a^2)$ corrections to the PCAC mass:

$$m_{\rm PCAC} = m\left[1+\rho\left(\frac{2}{\mu^2}-\frac{I_1(2\mu)}{\mu I_2(2\mu)}\right)\right]. \tag{4.39}$$

The key observation here is that the PCAC mass is equal to m, up to a correction of $\mathrm{O}(ma^2V)$, which is ϵ^2 higher in the epsilon expansion in the GSM* regime.

4.5 The correlators as a function of the PCAC mass

The final step we have to do is to replace m by $m_{\rm PCAC}$ in the correlators. We first invert result (4.39),

$$\mu = \tilde{\mu}\left[1-\rho\left(\frac{2}{\tilde{\mu}^2}-\frac{I_1(2\tilde{\mu})}{\tilde{\mu}I_2(2\tilde{\mu})}\right)\right], \tag{4.40}$$

where

$$\tilde{\mu} = m_{\rm PCAC}\Sigma V. \tag{4.41}$$

In the NLO contributions of the correlators we can simply replace $m = m_{\rm PCAC}$, $\mu = \tilde{\mu}$, since the corrections are higher than this order. In the LO term, however, we have to use the full expression (4.40), which gives rise to additional corrections proportional to ρ.

Eq. (4.40) has to be inserted into the Bessel functions $I_n(2\mu)$. Since the correction proportional to ρ is ϵ^2 higher in the epsilon expansion we can Taylor-expand,

$$I_n(2\mu) = I_n(2\tilde{\mu}) - 2\rho\tilde{\mu}I_n'(2\tilde{\mu})\left(\frac{2}{\tilde{\mu}^2}-\frac{I_1(2\tilde{\mu})}{\tilde{\mu}I_2(2\tilde{\mu})}\right)+\ldots \tag{4.42}$$

and drop the higher order terms. The final results for the correlators can be brought into the form

$$C_{PP}(t) = C_{PP,\rm ct}(t) + \frac{L^3\Sigma^2}{2}\rho\Delta_{a^2}, \tag{4.43}$$

$$C_{AA}(t) = C_{AA,\rm ct}(t) + \frac{F^2}{T}\rho\Delta_{a^2}, \tag{4.44}$$

where the continuum correlators are as in (4.20) and (4.34), but with the replacements $\mu\to\tilde{\mu}$ and $\mu_{\rm eff}\to\tilde{\mu}_{\rm eff}$, with

$$\tilde{\mu}_{\rm eff} = m_{\rm PCAC}\Sigma_{\rm eff}V. \tag{4.45}$$

The correction Δ_{a^2}, which depends on $\tilde{\mu}$, captures the lattice spacing artifacts and reads

$$\Delta_{a^2} = \frac{4\tilde{\mu}^2I_1^3(2\tilde{\mu}) - 11\tilde{\mu}I_1^2(2\tilde{\mu})I_2(2\tilde{\mu}) + 2(3-2\tilde{\mu}^2)I_1(2\tilde{\mu})I_2^2(2\tilde{\mu}) + 5\tilde{\mu}I_2^3(2\tilde{\mu})}{2\tilde{\mu}^3I_1^2(2\tilde{\mu})I_2(2\tilde{\mu})}. \tag{4.46}$$

Note that it is regular at $\tilde{\mu}=0$.

Eqs. (4.43) and (4.44) are our final results for the GSM* regime. (In appendix C we also give the corresponding expression for the vector current correlator.) These results are remarkable and perhaps surprising in two ways: (i) The $\tilde{\mu}$ dependence of the $\mathrm{O}(a^2)$

correction is identical for both correlation functions. (ii) Besides the continuum LECs F and Σ only one more unknown LEC enters these expression, the parameter c_2. The second feature is very advantageous in practice when our results are used to fit numerical lattice data.

A different question is the actual size of the $\mathrm{O}(a^2)$ correction, which is directly proportional to c_2. In the next section we try to give at least a rough answer to this question.

5 Numerical tests

5.1 General considerations

For the pseudo scalar and axial vector correlators, the leading $\mathrm{O}(a^2)$ correction in the GSM* regime is just a shift of the constant part. The question is how big this correction is in a typical ϵ-regime simulation. As a measure for the correction we study the ratio

$$R_{\mathrm{XX}} = \left| \frac{C_{\mathrm{XX}}(T/2) - C_{\mathrm{XX,ct}}(T/2)}{C_{\mathrm{XX,ct}}(T/2)} \right| , \tag{5.1}$$

i.e. the relative shift of the correlators at $T/2$. The main unknown here is the coefficient c_2. Even though it plays a decisive role in the phase diagram of the theory [32], it is difficult to obtain in numerical simulations. So far only the ETM collaboration has obtained an estimate from their simulations with a twisted mass term [26, 50]. The data for the pion mass splitting together with the LO ChPT prediction gives the rough estimate $-2c_2a^2 \approx (185\mathrm{MeV})^2$ at $a \approx 0.086\mathrm{fm}$, which translates into $|c_2| \approx (550\mathrm{MeV})^4$. The error, however, is fairly large because of the large statistical error in the determination of the neutral pion mass. In addition, this value for c_2 was obtained with the tree-level Symanzik improved gauge action and the standard Wilson fermion action, and any change in this setup can and probably will lead to a different value for c_2.[9] Nevertheless, for lack of a better estimate we use $|c_2| = (500\mathrm{MeV})^4$ in the following.

For the other parameters we use $F = 90\mathrm{MeV}$, $a = 0.08\mathrm{fm}$ and a hypercubic lattice with $N_T = N_L = 24$, which corresponds to a box size $L = 1.92\mathrm{fm}$. This implies $\rho \approx 0.75$. Even though this is slightly large we may still count this as $\mathrm{O}(\epsilon^2)$ as it should in order to be in the GSM* regime.

Figure 1 shows R_{PP} and R_{AA} for $\tilde{\mu}$ values in the ϵ-regime. For $\tilde{\mu} = 1.0$ we find $R_{PP} = 2.8\%$ and it decreases to less than 1% for $\tilde{\mu}$ larger than 2. The correction is maximal (less than 5%) at vanishing $\tilde{\mu}$. However, for $\tilde{\mu} \sim \rho$ we enter the Aoki regime and our formulae are no longer valid. The values for R_{AA} are very similar. For instance, $R_{AA} = 2.1\%$ at $\tilde{\mu} = 1.0$.

Figure 1 also shows $\Delta_{a^2}(\tilde{\mu})$, which is, up to the factor ρ, the numerator in (5.1). It looks very similar to the ratios itself, since the denominator in (5.1) is of $\mathrm{O}(1)$ and varies only mildly for the $\tilde{\mu}$ values considered her. So the correction to the correlators is essentially $\Delta_{a^2}(\tilde{\mu})$, which happens to be of the order of 10^{-2}.

[9] An analysis [51] of quenched twisted mass lattice data led to a value $c_2 \approx (300\mathrm{MeV})^4$.

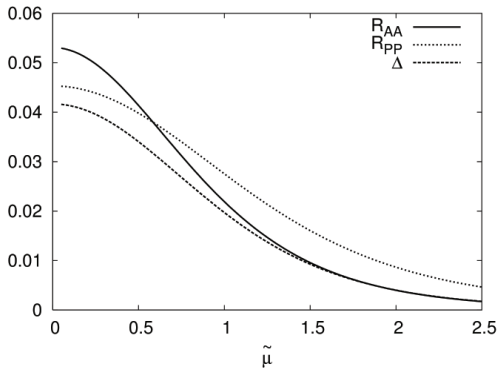

Figure 1. R_{PP} (dotted) and R_{AA} (solid) as a function of $\tilde{\mu}$. Both ratios are smaller than 3.5% for $\tilde{\mu} \geq 0.75$. The dashed curve represents $\Delta_{a^2}(\tilde{\mu})$.

The main conclusion we can draw from this exercise is that for our choice of parameters the $O(a^2)$ corrections to the correlators are at the few percent level, a comfortably small value.

Using a bigger box improves the epsilon expansion since the expansion parameter $1/(FL)^2$ is smaller. However, a bigger box also leads to larger ρ values and one easily enters the Aoki regime at moderately large volumes. For instance, with $N_L = 32$ and the other parameters unchanged we get $L = 2.4\,\text{fm}$ and $\rho \approx 2.4$, a value that is certainly not $O(\epsilon^2)$.[10]

5.2 Reanalysis of recent lattice data

In this section we investigate the impact of c_2 on the extraction of the continuum low energy constants F and Σ from lattice data. The data is taken from refs. [22, 52]. It is generated with $N_f = 2$ flavors of dynamical improved NHYP Wilson fermions [53] at a fairly small quark mass. From there, a reweighting procedure allows to access even smaller sea quark masses [23]. This procedure is exact and does not introduce systematic uncertainties but allows to compute correlators at very small quark masses at moderate cost. The lattice spacing is $a \approx 0.115\text{fm}$ from the measurement of the Sommer parameter r_0 taken to be 0.49fm [54]. We have two volumes available, one at $L = 16a \approx 1.84\text{fm}$ and a larger one with $L = 24a \approx 2.8\text{fm}$. The former serves mainly as a cross check whereas the latter has sufficient size for our NLO formulae to be applicable. Some parameters of the simulation are given in table 1.

The theoretical formulae for the pseudo scalar and axial vector correlator both have the form constant plus parabola. The coefficient c_2 only contributes to the constant term in both cases. The curvature itself is rather small at the parameter values simulated, in particular compared to the statistical uncertainties, see figure 2. Therefore, at a fixed mass,

[10] It may seem counterintuitive at first that a change in the volume may bring us into a different regime. However, increasing the volume requires that we need to decrease the mass in order to stay in the ϵ-regime with fixed $\tilde{\mu}$. Hence we have to decrease a as well in order to preserve the relative size between the mass and the lattice spacing terms.

L/a	κ	am_{PCAC}	μ
24	0.128150	0.0019(4)	2.1
	0.128125	0.0024(3)	2.7
	0.128100	0.0030(3)	3.4
	0.128050	0.0044(3)	5.0
16	0.128100	0.0028(11)	0.7
	0.128050	0.0047(9)	1.1
	0.128000	0.0058(7)	1.4
	0.127900	0.0088(5)	2.1
	0.127800	0.0117(3)	2.9

Table 1. Parameters of the simulation. L/a is the extend of the box, κ the hopping parameters, the PCAC quark mass and an approximate values of $\mu = m\Sigma V$, where we use the central value of Σ.

each of the two correlators effectively is a constant from which it is difficult to constrain three parameters. As already discussed, the theory predicts a particular and relatively strong $\tilde{\mu}$ dependence of the term multiplied by c_2. This gives a handle on the extraction of this coefficient. Therefore we simultaneously fit the axial vector and pseudo scalar correlators for all available quark masses. From a fit to $t \in [6, 18]$ we get $\Sigma^{1/3} = 249(4)\mathrm{MeV}$, $F = 88(3)\mathrm{MeV}$ and $c_2 = 0.02(8)\mathrm{GeV}^4$. The data, along with the theoretical curves can be found in figure 2. Here we used $Z_P^{\overline{\mathrm{MS}}}(2\mathrm{GeV}) = 0.90(2)$ and $Z_A = 0.99(2)$ from ref. [22]. The errors from the renormalization factors are not included in the uncertainties of the LECs. The value of c_2 is compatible with zero within errors and the one sigma band lies within the range of reasonable values for a low energy constant. Since the data points are highly correlated, we cannot give a good estimate for the quality of the fit; we find $\chi^2/\mathrm{dof} = 0.3(1)$ without the correlations taken into account. We also remark that the results are independent of the fit range once $t_{\mathrm{min}}/a > 4$. Another concern are the relatively large values of $\tilde{\mu}$. Therefore we repeated the analysis leaving the $\tilde{\mu} \approx 5$ data out. We get from the same fit range $\Sigma^{1/3} = 250(4)\mathrm{MeV}$, $F = 87(3)\mathrm{MeV}$ and $c_2 = -0.01(8)\mathrm{GeV}^4$. The differences to the previous values are well within the statistical uncertainties. This is encouraging. Even with the additional constant the errors of the continuum LECs are reasonably small.

Is the value we find for c_2 large or not? To gauge the impact of this term, we repeat the fit by setting $c_2 = 0$. The results are virtually unchanged within errors: $\Sigma^{1/3} = 249(4)\mathrm{MeV}$, $F = 88(3)\mathrm{MeV}$. This is very good news. The cut-off effects are so small that they do not impact the extraction of the low energy constants beyond the level of the statistical uncertainties.

As a cross check we repeated this analysis on the smaller volume, at the same lattice spacing and $L/a = 16$. We obtain $\Sigma^{1/3} = 257(4)\mathrm{MeV}$, $F = 83(2)\mathrm{MeV}$ and $c_2 = 0.06(14)\mathrm{GeV}^4$. However, the (uncorrelated) $\chi^2/\mathrm{dof} = 1.3$ might indicate that the NLO formulae are no longer applicable. These results agree with the findings of ref. [22].

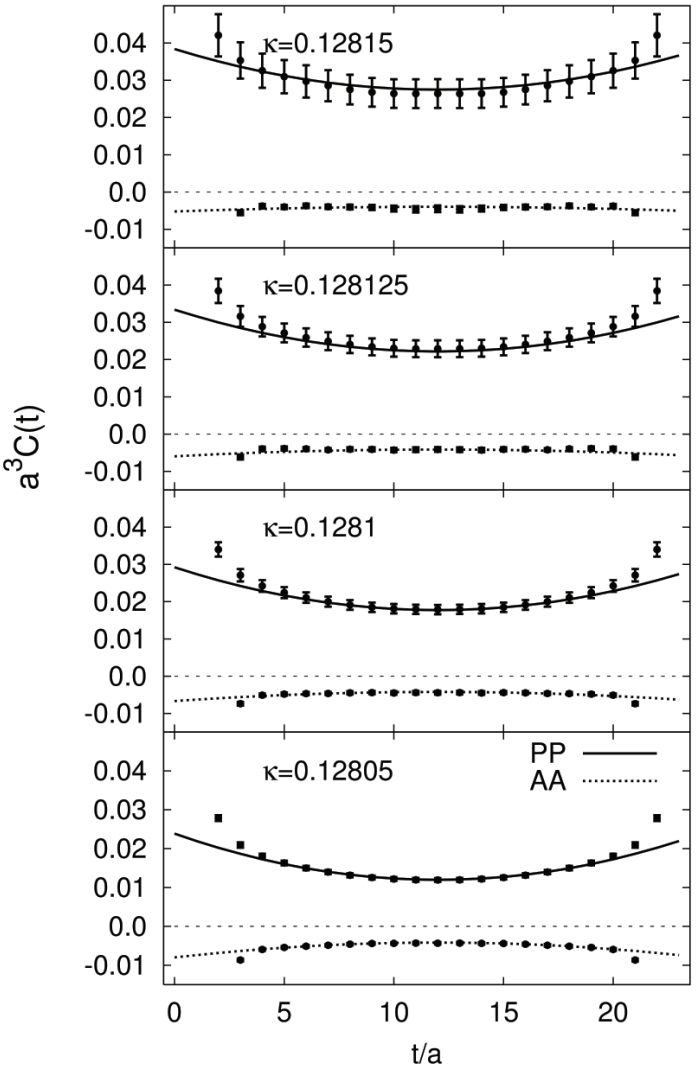

Figure 2. Fit of the WChPT predictions to lattice data. All data points within the fit range of $t/a \in [6, 18]$ for the four sea quark masses are included in the combined fit. The axial vector correlator is multiplied by a factor 50 for better visibility.

6 Conclusions

We have shown that the corrections due to the explicit chiral symmetry breaking of Wilson fermions are highly suppressed. For typical quark masses these corrections enter at either NNLO (GSM regime) or at NLO (GSM* regime). The reason for this suppression can be traced back to the fact that the lattice spacing corrections in the chiral effective action and the effective operators are either quadratic in a or they come with an additional power of either m or p^2. There is no explicit term with a single power of a only, since such a term

solely contributes to the additive mass renormalization which is absorbed in the quark mass. Hence, the lattice spacing corrections are suppressed in the chiral expansion, similar to the terms in the Gasser-Leutwyler Lagrangian $\mathcal{L}_4$.

In the Aoki regime the modifications are more substantial, affecting the correlators already at LO. The main complication in this regime are the zero mode integrals, which are no longer the known Bessel functions.

We tested our formulae against recent lattice data. We found that the additional terms which come from the broken chiral symmetry have very little impact on the extracted values of F and Σ whereas the low-energy constant associated with the breaking is hard to determine precisely.

Our results derived here can be generalized in various ways, for example to the case with a twisted mass term or to an arbitrary number of flavors. The details of the calculation will change, but our various power countings can be carried over with almost no modification. Perhaps most interesting from a practical point of view is an extension along the lines of ref. [55], where one considers a mixed setup with some quarks in the ϵ-regime and some others in the p-regime.

However, the main conclusion one can draw is that the effects due to explicit chiral symmetry breaking of Wilson fermions in the ϵ-regime are less severe than anticipated before. In view of the results of ref. [22] and the ones presented here, simulations with Wilson fermions seem to be a viable alternative to the daunting task of dynamical simulations with chiral fermions.

Note added. After this paper was completed we received a paper by A. Shindler which also deals with Wilson fermions in the ϵ-regime and comes to essentially the same conclusions [56]. Our result for the $O(a^2)$ correction to the PP correlator in the GSM* regime agrees with the one in [56] (the AA correlator has not been computed in that reference).

Acknowledgments

We would like to thank A. Hasenfratz and P. Hernández for fruitful discussions and A. Hasenfratz for reading the manuscript.

S.N. is supported by Marie Curie Fellowship MEIF-CT-2006-025673, and thanks the Physics Institute of the Humboldt University (Berlin) for hospitality during the preparation of this work.

This work is partially supported by EC Sixth Framework Program under the contract MRTN-CT-2006-035482 (FLAVIAnet), by the Deutsche Forschungsgemeinschaft (SFB/TR 09) and the Ministerio de Ciencia e Innovación under Grant No. FPA2007-60323 and by CPAN (Grant No. CSD2007-00042).

A Some results for the epsilon regime

In this appendix we summarize formulae which are relevant for the computation of correlation functions in the ϵ-regime of chiral perturbation theory.

Starting from the leading order continuum chiral Lagrangian of eq. (2.1) and by introducing the parametrization of eq. (3.2), we can read off the finite-volume scalar propagator for the nonzero modes:

$$\bar{G}(x) = \frac{1}{V} \sum_{p \neq 0} \frac{e^{ipx}}{p^2}, \tag{A.1}$$

with

$$p = 2\pi \left(\frac{n_0}{T}, \frac{\vec{n}}{L} \right).$$

The propagator $\bar{G}(x)$ satisfies the following properties:

$$\int_V d^4x \, \bar{G}(x) = 0\,, \tag{A.2}$$

$$\partial_\mu \bar{G}(0) = 0\,, \tag{A.3}$$

$$\Box \bar{G}(x) = -\delta(x) + \frac{1}{V}. \tag{A.4}$$

UV divergencies, if present, are treated in dimensional regularization.
We define [45, 57]

$$\bar{G}(0) \equiv -\frac{\beta_1}{\sqrt{V}}\,, \tag{A.5}$$

$$T \frac{d}{dT} \bar{G}(0) \equiv \frac{T^2 k_{00}}{V}, \tag{A.6}$$

where β_1 and k_{00} are finite dimensionless *shape coefficients* which depend on the geometry of the box. They can be evaluated numerically: for instance, for a symmetric box with $L = T$ one has $\beta_1 = 0.140461$ and $k_{00} = \beta_1/2$ (see also [46]).

In order to obtain time correlators one has to perform integrals over the spatial components of given functions of the propagators $\bar{G}(x)$. In particular we define [45, 57] [11]

$$\begin{aligned} K_{\mu\nu}(x-y) &= \bar{G}(x-y)\partial_{x_\mu}\partial_{y_\nu}\bar{G}(x-y) - \partial_{x_\mu}\bar{G}(x-y)\partial_{y_\nu}\bar{G}(x-y) + \\ &+ \partial_{x_\mu}\partial_{y_\nu} H(x-y), \end{aligned} \tag{A.7}$$

$$H(x-y) = -\frac{1}{V}\int_V d^4z \bar{G}(x-z)\bar{G}(z-y). \tag{A.8}$$

The integrals that we need for this work are ($x_0 = t$):

$$\int d^3\vec{x}\, \bar{G}(x-y)|_{y=0} = T h_1\left(\frac{t}{T}\right) = \frac{T}{2}\left[\left(\left|\frac{t}{T}\right| - \frac{1}{2}\right)^2 - \frac{1}{12}\right], \tag{A.9}$$

$$\int d^3\vec{x}\, K_{00}(x-y)|_{y=0} = \frac{T}{V} k_{00}, \tag{A.10}$$

$$\partial_{x_0}\partial_{y_0} \int d^3\vec{x}\, H(x-y)|_{y=0} = -\frac{T}{V} h_1\left(\frac{t}{T}\right). \tag{A.11}$$

[11] In the original definition of [45, 57], $K_{\mu\nu}(x-y)$ contains also contact terms, which we do not consider in our computation since we are interested in the correlators for $x \neq y$.

Finally, we recall the SU(N_f) completeness relations which are used for the computation of correlation functions. Given the SU(N_f) generators T^a, with $a = 1, \ldots, N_f^2 - 1$ and the convention

$$\mathrm{Tr}[T^a T^b] = \frac{1}{2}\delta^{ab},$$

one obtains

$$\mathrm{Tr}(T^a A T^a B) = -\frac{1}{2N_f}\mathrm{Tr}(AB) + \frac{1}{2}\mathrm{Tr}(A)\mathrm{Tr}(B), \tag{A.12}$$

$$\mathrm{Tr}(T^a A)\mathrm{Tr}(T^a B) = -\frac{1}{2N_f}\mathrm{Tr}(A)\mathrm{Tr}(B) + \frac{1}{2}\mathrm{Tr}(AB). \tag{A.13}$$

B SU(2) integrals

In the case $N_f = 2$, the partition function related to the zero-mode integrals in eq. (4.5) is given by

$$Z_0 = \int_{\mathrm{SU}(2)} [dU_0] e^{\frac{\mu}{2}\mathrm{Tr}(U_0 + U_0^\dagger)} = \frac{I_1(2\mu)}{\mu}, \tag{B.1}$$

where I_n is the modified Bessel function of the first kind. The normalization

$$\int_{\mathrm{SU}(2)} [dU_0] = 1 \tag{B.2}$$

has been adopted. Expectation values of arbitrary integer powers of $\mathrm{Tr}(U_0)$ can be obtained by computing derivatives of Z_0. In particular, for this work we need

$$\langle \mathrm{Tr} U_0 \rangle = \frac{1}{Z_0}\frac{\partial Z_0}{\partial \mu} = 2\frac{I_2(2\mu)}{I_1(2\mu)}, \tag{B.3}$$

$$\langle (\mathrm{Tr} U_0)^2 \rangle = \frac{1}{Z_0}\frac{\partial^2 Z_0}{\partial \mu^2} = 4 - \frac{6}{\mu}\frac{I_2(2\mu)}{I_1(2\mu)}, \tag{B.4}$$

$$\langle (\mathrm{Tr} U_0)^3 \rangle = \frac{1}{Z_0}\frac{\partial^3 Z_0}{\partial \mu^3} = -\frac{12}{\mu} + \frac{8(3+\mu^2)I_2(2\mu)}{\mu^2 I_1(2\mu)}, \tag{B.5}$$

$$\langle (\mathrm{Tr} U_0)^4 \rangle = \frac{1}{Z_0}\frac{\partial^4 Z_0}{\partial \mu^4} = 16 + \frac{60}{\mu^2} - \frac{24(5+2\mu^2)I_2(2\mu)}{\mu^3 I_1(2\mu)}. \tag{B.6}$$

Other integrals needed in this work can be related to the previous ones, for instance:

$$\langle \mathrm{Tr} U_0^2 \rangle = 2 - \frac{3}{\mu}\langle \mathrm{Tr} U_0 \rangle = 2 - \frac{6}{\mu}\frac{I_2(2\mu)}{I_1(2\mu)}, \tag{B.7}$$

$$\begin{aligned}\langle \mathrm{Tr} U_0^2 \, (\mathrm{Tr} U_0)^2 \rangle &= -\frac{6}{\mu^3}\langle \mathrm{Tr} U_0 \rangle + 2\left(1 + \frac{3}{\mu^2}\right)\langle (\mathrm{Tr} U_0)^2 \rangle - \frac{3}{\mu}\langle (\mathrm{Tr} U_0)^3 \rangle \\ &= \frac{4(15+2\mu^2)}{\mu^2} - \frac{12(10+3\mu^2)I_2(2\mu)}{\mu^3 I_1(2\mu)}.\end{aligned} \tag{B.8}$$

C Other correlators

Here we summarize the GSM* results for some other correlators. We start with the correlation function of the time component of two vector currents,

$$\langle V_0^a(x)V_0^b(y)\rangle = \delta^{ab}C_{VV}(x-y)\,, \tag{C.1}$$

which we again split into a continuum part and a correction proportional to the lattice spacing,

$$C_{VV}(x-y) = C_{VV,\mathrm{ct}}(x-y) + C_{VV,a^2}(x-y)\,. \tag{C.2}$$

In our notation the leading order vector current in the chiral effective theory reads

$$V^a_{\mu,\mathrm{ct}} = -i\frac{F^2}{2}\mathrm{Tr}\left(T^a(U^\dagger\partial_\mu U + U\partial_\mu U^\dagger)\right)\,. \tag{C.3}$$

The continuum contribution at $O(\epsilon^6)$ for generic N_f has been calculated before by Hansen [45] (see also [49]). After integrating over the spatial coordinates one gets

$$C^{ab}_{VV}(t) = \delta^{ab}\left[-\frac{1}{T}\alpha_V + \frac{T}{V}k_{00}\beta_V\right], \tag{C.4}$$

with

$$\alpha_V = \frac{F^2}{2}(2-\langle\mathcal{J}_0\rangle_{\mathrm{eff}}) + \frac{N_f}{2}\frac{\beta_1}{\sqrt{V}}(2-\langle\mathcal{J}_0\rangle), \tag{C.5}$$

$$\beta_V = \frac{N_f}{2}\langle\mathcal{J}_0\rangle. \tag{C.6}$$

The function $\mathcal{J}_0$ has been defined in eq. 4.27. In particular, for $N_f = 2$ the result explicitly reads

$$C^{ab}_{VV}(t) = -\frac{F^2}{T}\left(\frac{I_2(2\mu_{\mathrm{eff}})}{\mu_{\mathrm{eff}}I_1(2\mu_{\mathrm{eff}})}\right) - \frac{2\beta_1}{T\sqrt{V}}\left(\frac{I_2(2\mu)}{\mu I_1(2\mu)}\right) + \frac{2T}{V}k_{00}\left(1-\frac{1}{\mu}\frac{I_2(2\mu)}{I_1(2\mu)}\right). \tag{C.7}$$

The $\mathrm{O}(a^2)$ correction in terms of the PCAC mass is given by

$$C_{VV,a^2}(t) = -\frac{F^2}{T}\rho\Delta_{a^2}\,, \tag{C.8}$$

where Δ_{a^2} is defined in eq. (4.46). Comparing this with the result for the AA correlator in (4.44) we observe that the lattice spacing corrections in these two correlators are, up to a sign, identical.

With both the AA and the VV correlator at hand we can trivially obtain the correlation functions of right- and left-handed currents. For example, with $L^a_\mu = [V^a_\mu - A^a_\mu]/2$ we find

$$C_{LL}(t) = \frac{1}{4}\Big(C_{VV}(t) + C_{AA}(t)\Big)\,, \tag{C.9}$$

and the $\mathrm{O}(a^2)$ corrections cancel in the sum on the right hand side, i.e.

$$C_{LL,a^2}(t) = 0 \tag{C.10}$$

while the continuum part is given by [45, 46]

$$C_{LL,ct}(t) = \frac{1}{4}\left[-\frac{F^2}{T} - \frac{N_f}{T}\frac{\beta_1}{\sqrt{V}} + N_f\frac{T}{V}k_{00} - \frac{T}{V}\langle \mathrm{Tr}(U_0 + U_0^\dagger)\rangle \frac{\tilde{\mu}}{N_f} h_1\left(\frac{t}{T}\right)\right]$$
$$= \frac{1}{2}\left[-\frac{F^2}{2T} - \frac{1}{T}\frac{\beta_1}{\sqrt{V}} + \frac{T}{V}k_{00} - \frac{T}{V}\frac{\tilde{\mu} I_2(2\tilde{\mu})}{I_1(2\tilde{\mu})} h_1\left(\frac{t}{T}\right)\right]. \tag{C.11}$$

The same result can be obtained by a direct calculation of the correlator, of course.

Finally, the scalar correlator

$$\langle S^a(x) S^b(y)\rangle = \delta^{ab} C_{SS}(x-y) \tag{C.12}$$

vanishes identically in the chiral effective theory for $N_f = 2$, as one can check either by explicit calculation or by using G-parity.

References

[1] J. Gasser and H. Leutwyler, *Light quarks at low temperatures*, *Phys. Lett.* **B 184** (1987) 83 [SPIRES].

[2] J. Gasser and H. Leutwyler, *Thermodynamics of chiral symmetry*, *Phys. Lett.* **B 188** (1987) 477 [SPIRES].

[3] J. Gasser and H. Leutwyler, *Chiral perturbation theory to one loop*, *Ann. Phys.* **158** (1984) 142 [SPIRES].

[4] J. Gasser and H. Leutwyler, *Chiral perturbation theory: expansions in the mass of the strange quark*, *Nucl. Phys.* **B 250** (1985) 465 [SPIRES].

[5] S. Necco, *Determining QCD low-energy couplings from lattice simulations*, PoS(LATTICE 2007)021 [arXiv:0710.2444].

[6] H. Leutwyler and A.V. Smilga, *Spectrum of Dirac operator and role of winding number in QCD*, *Phys. Rev.* **D 46** (1992) 5607 [SPIRES].

[7] H. Neuberger, *Exactly massless quarks on the lattice*, *Phys. Lett.* **B 417** (1998) 141 [hep-lat/9707022] [SPIRES].

[8] D.B. Kaplan, *A Method for simulating chiral fermions on the lattice*, *Phys. Lett.* **B 288** (1992) 342 [hep-lat/9206013] [SPIRES].

[9] Y. Shamir, *Chiral fermions from lattice boundaries*, *Nucl. Phys.* **B 406** (1993) 90 [hep-lat/9303005] [SPIRES].

[10] V. Furman and Y. Shamir, *Axial symmetries in lattice QCD with Kaplan fermions*, *Nucl. Phys.* **B 439** (1995) 54 [hep-lat/9405004] [SPIRES].

[11] P. Hernández, K. Jansen and L. Lellouch, *Finite-size scaling of the quark condensate in quenched lattice QCD*, *Phys. Lett.* **B 469** (1999) 198 [hep-lat/9907022] [SPIRES].

[12] MILC collaboration, T.A. DeGrand, *Another determination of the quark condensate from an overlap action*, *Phys. Rev.* **D64** (2001) 117501 [hep-lat/0107014] [SPIRES].

[13] P. Hasenfratz, S. Hauswirth, T. Jorg, F. Niedermayer and K. Holland, *Testing the fixed-point QCD action and the construction of chiral currents*, *Nucl. Phys.* **B 643** (2002) 280 [hep-lat/0205010] [SPIRES].

[14] W. Bietenholz, T. Chiarappa, K. Jansen, K.I. Nagai and S. Shcheredin, *Axial correlation functions in the ϵ-regime: a numerical study with overlap fermions*, *JHEP* **02** (2004) 023 [hep-lat/0311012] [SPIRES].

[15] L. Giusti, P. Hernández, M. Laine, P. Weisz and H. Wittig, *Low-energy couplings of QCD from current correlators near the chiral limit*, *JHEP* **04** (2004) 013 [hep-lat/0402002] [SPIRES].

[16] H. Fukaya, S. Hashimoto and K. Ogawa, *Low-lying mode contribution to the quenched meson correlators in the ϵ-regime*, *Prog. Theor. Phys.* **114** (2005) 451 [hep-lat/0504018] [SPIRES].

[17] W. Bietenholz and S. Shcheredin, *Overlap hypercube fermions in QCD simulations near the chiral limit*, *Nucl. Phys.* **B 754** (2006) 17 [hep-lat/0605013] [SPIRES].

[18] L. Giusti and S. Necco, *Spontaneous chiral symmetry breaking in QCD: a finite-size scaling study on the lattice*, *JHEP* **04** (2007) 090 [hep-lat/0702013] [SPIRES].

[19] L. Giusti et. al., *Testing chiral effective theory with quenched lattice QCD*, *JHEP* **05** (2008) 024 [arXiv:0803.2772] [SPIRES].

[20] S. Schaefer, *Algorithms for dynamical overlap fermions*, PoS(LAT2006)020.

[21] JLQCD collaboration, H. Fukaya et. al., *Lattice study of meson correlators in the ϵ-regime of two-flavor QCD*, *Phys. Rev.* **D77** (2008) 074503 [arXiv:0711.4965] [SPIRES].

[22] A. Hasenfratz, R. Hoffmann and S. Schaefer, *Low energy chiral constants from ϵ-regime simulations with improved Wilson fermions*, *Phys. Rev.* **D78** (2008) 054511 [arXiv:0806.4586] [SPIRES].

[23] A. Hasenfratz, R. Hoffmann and S. Schaefer, *Reweighting towards the chiral limit*, *Phys. Rev.* **D 78** (2008) 014515 [arXiv:0805.2369] [SPIRES].

[24] K. Jansen et al., *Exploring the epsilon regime with twisted mass fermions*, PoS(LATTICE 2007)084 [arXiv:0711.1871].

[25] K. Jansen, A. Nube and A. Shindler, *Wilson twisted mass fermions in the ϵ-regime*, arXiv:0810.0300 [SPIRES].

[26] C. Urbach, *Lattice QCD with two light Wilson quarks and maximally twisted mass*, PoS(LATTICE 2007)022 [arXiv:0710.1517].

[27] Alpha collaboration, R. Frezzotti, P.A. Grassi, S. Sint and P. Weisz, *Lattice QCD with a chirally twisted mass term*, *JHEP* **08** (2001) 058 [hep-lat/0101001] [SPIRES].

[28] ALPHA collaboration, R. Frezzotti, S. Sint and P. Weisz, *$O(a)$ improved twisted mass lattice QCD*, *JHEP* **07** (2001) 048 [hep-lat/0104014] [SPIRES].

[29] R. Frezzotti and G.C. Rossi, *Chirally improving Wilson fermions. I: $O(a)$ improvement*, *JHEP* **08** (2004) 007 [hep-lat/0306014] [SPIRES].

[30] S. Aoki and O. Bär, *Twisted-mass QCD, $O(a)$ improvement and Wilson chiral perturbation theory*, *Phys. Rev.* **D 70** (2004) 116011 [hep-lat/0409006] [SPIRES].

[31] S. Aoki and O. Bär, *Automatic $O(a)$ improvement for twisted-mass QCD in the presence of spontaneous symmetry breaking*, *Phys. Rev.* **D74** (2006) 034511 [hep-lat/0604018] [SPIRES].

[32] S.R. Sharpe and J. Singleton, Robert L., *Spontaneous flavor and parity breaking with Wilson fermions*, *Phys. Rev.* **D58** (1998) 074501 [hep-lat/9804028] [SPIRES].

[33] G. Rupak and N. Shoresh, *Chiral perturbation theory for the Wilson lattice action*, *Phys. Rev.* **D 66** (2002) 054503 [hep-lat/0201019] [SPIRES].

[34] K. Symanzik, *Continuum Limit and Improved Action in Lattice Theories. 1. Principles and ϕ^4 theory*, *Nucl. Phys.* **B 226** (1983) 187 [SPIRES].

[35] K. Symanzik, *Continuum Limit and improved action in lattice theories. 2. $O(N)$ nonlinear σ-model in perturbation theory*, *Nucl. Phys.* **B 226** (1983) 205 [SPIRES].

[36] O. Bär, G. Rupak and N. Shoresh, *Chiral perturbation theory at $O(a^2)$ for lattice QCD*, *Phys. Rev.* **D 70** (2004) 034508 [hep-lat/0306021] [SPIRES].

[37] S. Aoki, *Chiral perturbation theory with Wilson-type fermions including a**2 effects: n(f) = 2 degenerate case*, *Phys. Rev.* **D68** (2003) 054508 [hep-lat/0306027] [SPIRES].

[38] S. Weinberg, *Phenomenological lagrangians*, *Physica* **A 96** (1979) 327 [SPIRES].

[39] S.R. Sharpe and J.M.S. Wu, *Twisted mass chiral perturbation theory at next-to-leading order*, *Phys. Rev.* **D 71** (2005) 074501 [hep-lat/0411021] [SPIRES].

[40] S. Aoki and O. Bär, *The vector and axial vector current in Wilson ChPT*, PoS(LATTICE 2007)062.

[41] S.R. Sharpe and J.M.S. Wu, *The phase diagram of twisted mass lattice QCD*, *Phys. Rev.* **D 70** (2004) 094029 [hep-lat/0407025] [SPIRES].

[42] S. Aoki, O. Bär and B. Biedermann, *Pion scattering in Wilson ChPT*, arXiv:0806.4863 [SPIRES].

[43] S. Aoki, *New phase structure for lattice QCD with wilson fermions*, *Phys. Rev.* **D30** (1984) 2653 [SPIRES].

[44] J. Gasser and H. Leutwyler, *Spontaneously broken symmetries: eeffective lagrangians at finite volume*, *Nucl. Phys.* **B 307** (1988) 763 [SPIRES].

[45] F.C. Hansen, *Finite size effects in spontaneously broken* $\mathrm{SU}(N) \times \mathrm{SU}(N)$ *theories*, *Nucl. Phys.* **B 345** (1990) 685 [SPIRES].

[46] P. Hernández and M. Laine, *Correlators of left charges and weak operators in finite volume chiral perturbation theory*, *JHEP* **01** (2003) 063 [hep-lat/0212014] [SPIRES].

[47] I. Gradshteyn and I. Ryzhik, *Table of integrals, series and products*, 4^{th} edition, Academic PRess, U.S.A. (1983).

[48] P.H. Damgaard, M.C. Diamantini, P. Hernández and K. Jansen, *Finite-size scaling of meson propagators*, *Nucl. Phys.* **B 629** (2002) 445 [hep-lat/0112016] [SPIRES].

[49] P.H. Damgaard, P. Hernández, K. Jansen, M. Laine and L. Lellouch, *Finite-size scaling of vector and axial current correlators*, *Nucl. Phys.* **B 656** (2003) 226 [hep-lat/0211020] [SPIRES].

[50] C. Michael and C. Urbach, *Neutral mesons and disconnected diagrams in twisted mass QCD*, PoS(LATTICE 2007)122.

[51] S. Aoki and O. Bär, *WChPT analysis of twisted mass lattice data*, *Eur. Phys. J.* **A 31** (2007) 481 [hep-lat/0610085] [SPIRES].

[52] A. Hasenfratz, R. Hoffmann and S. Schaefer, *Epsilon regime calculations with reweighted clover fermions*, in the proceedings of *LATTICE 2008*, July 14–19, Williamsburg, Virginia, U.S.A. (2008) [arXiv:0810.0496].

[53] A. Hasenfratz, R. Hoffmann and S. Schaefer, *Hypercubic smeared links for dynamical fermions*, *JHEP* **05** (2007) 029 [hep-lat/0702028] [SPIRES].

[54] R. Sommer, *A new way to set the energy scale in lattice gauge theories and its applications to the static force and α_s in* SU(2) *Yang-Mills theory*, *Nucl. Phys.* **B 411** (1994) 839 [hep-lat/9310022] [SPIRES].

[55] F. Bernardoni, P.H. Damgaard, H. Fukaya and P. Hernández, *Finite volume scaling of pseudo Nambu-Goldstone bosons in QCD*, *JHEP* **10** (2008) 008 [arXiv:0808.1986] [SPIRES].

[56] A. Shindler, *Observations on the Wilson fermions in the ϵ-regime*, *Phys. Lett.* **B 672** (2009) 82 [arXiv:0812.2251] [SPIRES].

[57] P. Hasenfratz and H. Leutwyler, *Goldstone boson related finite size effects in field theory and critical phenomena with $O(N)$ symmetry*, *Nucl. Phys.* **B 343** (1990) 241 [SPIRES].

PHYSICAL REVIEW D **80,** 014506 (2009)

Vector and axial currents in Wilson chiral perturbation theory

Sinya Aoki,[1,2] Oliver Bär,[3] and Stephen R. Sharpe[4]

[1]*Graduate School of Pure and Applied Sciences, University of Tsukuba, Tsukuba 305-8571, Ibaraki Japan*
[2]*Riken BNL Research Center, Brookhaven National Laboratory, Upton, New York 11973, USA*
[3]*Institute of Physics, Humboldt University Berlin, Newtonstrasse 15, 12489 Berlin, Germany*
[4]*Physics Department, University of Washington, Seattle, Washington 98195-1560, USA*

(Received 20 May 2009; published 20 July 2009)

We reconsider the construction of the vector and axial-vector currents in Wilson Chiral Perturbation Theory, the low-energy effective theory for lattice QCD with Wilson fermions. We discuss in detail the finite renormalization of the currents that has to be taken into account in order to properly match the currents. We explicitly show that imposing the chiral Ward identities on the currents does, in general, affect the axial-vector current at $O(a)$. As an application of our results we compute the pion decay constant to one loop in the two-flavor theory. Our result differs from previously published ones.

DOI: 10.1103/PhysRevD.80.014506 PACS numbers: 11.15.Ha, 12.39.Fe, 12.38.Gc

I. INTRODUCTION

Chiral perturbation theory (ChPT) is widely regarded to be an important tool for lattice QCD. It provides analytic guidance for the chiral extrapolation of the lattice data obtained at quark masses heavier than in nature. Standard ChPT, as formulated in Refs. [1,2], is based on the symmetries and the particular symmetry breaking of continuum QCD. The generalization to lattice QCD with Wilson fermions, taking into account the explicit chiral symmetry breaking of Wilson's fermion discretization [3], was given in Ref. [4]. The resulting low-energy effective theory, often called Wilson chiral perturbation theory (WChPT), is a double expansion in the quark mass and the lattice spacing, the two parameters of explicit chiral symmetry breaking.

Massless continuum QCD is invariant under various nonsinglet chiral transformations. This invariance implies the existence of conserved currents (which are obtained by the Noether theorem) and various chiral Ward identities. ChPT is constructed in such a way that these Ward identities are correctly reproduced, order by order in the chiral expansion. And since conserved currents do not renormalize it is straightforward to maintain the normalization of the currents.

The construction of WChPT is slightly more complicated compared to continuum ChPT. Because of the explicit breaking of chiral symmetry by the Wilson term there does not exist a conserved axial-vector current for vanishing bare quark mass. And even though a conserved vector current exists for degenerate quark masses, it is often not used in practice. The local, nonconserved vector current is employed instead, even though it requires the computation of a renormalization constant Z_V. The renormalization constant Z_A is also needed for the axial-vector current.

The explicit breaking of chiral symmetry and the need for renormalizing the currents raises the question how to construct the effective currents in Wilson ChPT. The ''Noether link'' does not hold anymore. Also the renormalization of the currents has to be taken into account for a proper matching of the effective theory to the fundamental lattice theory.

Some results concerning the currents can be found in the literature [5,6], but they are in conflict. Reference [5] calculates the pion decay constant using the current obtained by the naive Noether procedure as the axial-vector current [7]. Reference [6] introduces source terms for the currents as in continuum ChPT, and constructs the generating functional for correlation functions of the currents. The resulting axial-vector current contains an additional $O(a)$ contribution that is not present in the Noether current. Consequently, the resultant f_π contains an extra term and differs from that of Ref. [5].

Besides this discrepancy the issue of renormalization has not been properly taken into account in either work. No particular renormalization condition for the axial-vector current has been imposed as is necessary for a proper matching of the currents. It has been argued in Ref. [6] that the results for the currents derived there should hold for any choice of lattice operators which are correctly normalized in the continuum limit. However, the validity of this expectation has not been shown so far.

In this paper we reconsider the construction and mapping of the vector and axial-vector currents in WChPT to $O(a)$.[1] We proceed in two steps. First, we write down the most general expressions for the currents which are compatible with locality and the symmetries of the underlying lattice theory. With this procedure we reproduce the results of Ref. [6] (which are more fully justified in Ref. [9]). In the second step we impose the chiral Ward identities as particular renormalization conditions for the currents. This choice, suggested in Refs. [10–12], is widely used in practice. We find that this renormalization condition does have an impact at $O(a)$ on the axial-vector current. Consequently, our current differs from the ones in

[1]Preliminary results have already been presented in Ref. [8]. Details have changed, but the overall conclusions are unaltered.

Refs. [5,6]. As an application of our results we finally compute the pion decay constant to one loop, including the $O(a)$ correction to the chiral logarithm, which also differs from the results in [5,6].

This paper is organized as follows. In Sec. II we first summarize some definitions of the lattice theory with two flavors of Wilson quarks, in particular, the various vector and axial-vector currents used in numerical simulations. This is followed by the Symanzik expansion of the currents close to the continuum limit. The currents in the Symanzik effective theory are then mapped to their counterparts in the chiral effective theory. Section III discusses the renormalization of the vector and axial-vector currents in the lattice theory and how this is carried over to the effective theory. The results for the decay constant are given in Sec. IV, followed by some concluding remarks in Sec. V. Appendix A is devoted to an alternative but equivalent derivation of the currents based on the generating functional, while Appendix B consists of details concerning the calculation of Z_A in the effective theory.

II. CURRENTS IN WCHPT

A. Definitions in the lattice theory

We consider lattice QCD with Wilson fermions on a hypercubic lattice with lattice spacing a. For simplicity we study $N_f = 2$ quarks with equal quark mass. The fermion action is of the form

$$S_f = S_W + c_{\rm SW} S_{\rm clover}, \tag{1}$$

where the first part denotes the standard Wilson action [3] with bare quark mass m_0. We also allow for a clover-leaf term with coefficient $c_{\rm SW}$. The details of the gauge action are not important in the following so we leave it unspecified.

It is common to use the local expressions for the vector and axial-vector currents in numerical simulations,

$$V^a_{\mu,\rm Loc}(x) = \bar\psi(x)\gamma_\mu T^a \psi(x), \tag{2}$$

$$A^a_{\mu,\rm Loc}(x) = \bar\psi(x)\gamma_\mu\gamma_5 T^a \psi(x). \tag{3}$$

The T^a are the Hermitian $SU(N_f)$ generators, normalized according to $\mathrm{tr}(T^a T^b) = \delta^{ab}/2$. In the case of $N_f = 2$, the one we are considering, this normalization corresponds to $T^a = \sigma^a/2$, where σ^a are the usual Pauli matrices.

For degenerate quark masses the fermion action (1) is invariant under $SU(N_f)$ flavor transformations. The associated conserved vector current differs from (2) and reads [10]

$$\begin{aligned} V^a_{\mu,\rm Con}(x) = \frac{1}{2}\{&\bar\psi(x+a\hat\mu)\gamma_\mu T^a U_\mu(x)\psi(x) \\ &+ \bar\psi(x)\gamma_\mu T^a U^\dagger_\mu(x)\psi(x+a\hat\mu) \\ &+ \bar\psi(x+a\hat\mu) T^a U_\mu(x)\psi(x) \\ &- \bar\psi(x) T^a U^\dagger_\mu(x)\psi(x+a\hat\mu)\}. \end{aligned} \tag{4}$$

No conserved axial-vector current exists due to the explicit chiral symmetry breaking by the Wilson term in S_W.

In on-shell $O(a)$-improved lattice theories with degenerate quarks one defines improved currents by adding terms involving lattice derivatives to the local currents [13,14],

$$\begin{aligned} V^a_{\mu,\rm Imp}(x) = &(1 + b_V am) \\ &\times \left[V^a_{\mu,\rm Loc}(x) + c_V \frac{1}{2}(\nabla^+_\nu + \nabla_\nu) T^a_{\mu\nu}(x) \right], \end{aligned} \tag{5}$$

$$\begin{aligned} A^a_{\mu,\rm Imp}(x) = &(1 + b_A am) \\ &\times \left[A^a_{\mu,\rm Loc}(x) + c_A \frac{1}{2}(\nabla^+_\mu + \nabla_\mu) P^a(x) \right], \end{aligned} \tag{6}$$

where

$$\begin{aligned} T^a_{\mu\nu,\rm Loc}(x) &= \bar\psi(x) i\sigma_{\mu\nu} T^a \psi(x) \quad \text{and} \\ P^a_{\rm Loc}(x) &= \bar\psi(x)\gamma_5 T^a \psi(x). \end{aligned} \tag{7}$$

The coefficients $b_{V,A}$ and $c_{V,A}$—together with $c_{\rm SW}$—can be nonperturbatively tuned such that the cutoff effects are of $O(a^2)$ instead of linear in a.[2]

In order to correctly approach the continuum limit the nonconserved currents need to be renormalized. Thus one introduces

$$V^a_{\mu,\rm ren,Loc} = Z_{V,\rm Loc} V^a_{\mu,\rm Loc}, \qquad V^a_{\mu,\rm ren,Imp} = Z_{V,\rm Imp} V^a_{\mu,\rm Imp}, \tag{8}$$

$$A^a_{\mu,\rm ren,Loc} = Z_{A,\rm Loc} A^a_{\mu,\rm Loc}, \qquad A^a_{\mu,\rm ren,Imp} = Z_{A,\rm Imp} A^a_{\mu,\rm Imp}. \tag{9}$$

In the following, we will often use $Z_{V,A}$ generically, without specifying the underlying current.

The Z-factors (which depend not only on the choice of currents but also on the action) can be fixed by imposing chiral Ward identities [10–12]. We will come back to this important issue in Sec. III. The Z-factor for the conserved vector current is 1, of course.

[2]Note that the mass m in Eqs. (5) and (6) denotes the renormalized mass containing the additive mass renormalization proportional to $1/a$ and the renormalization factor: $m = Z_m(m_0 - m_{\rm cr})/a$. The factors of $(1 + b_{V,A} am)$ can also be considered to be part of the renormalization factor, but it is notationally convenient here to include them in the bare currents.

B. The Symanzik effective theory

According to Symanzik the lattice theory can be described by an effective continuum theory provided one is close to the continuum limit [15,16]. This effective theory is defined by an effective action and effective operators, and both are strongly restricted by the locality and the symmetries of the underlying lattice theory. The leading terms are, by construction, the familiar expressions of continuum QCD. Lattice artifacts appear as higher dimensional operators multiplied by appropriate powers of the lattice spacing. The effective action, for example, reads [17]

$$S_{\rm Sym} = S_{\rm ct} + a\bar{c}_{\rm SW}\int d^4x\,\bar{\psi}(x) i\sigma_{\mu\nu}F_{\mu\nu}(x)\psi(x) + O(a^2). \tag{10}$$

The first term is just the continuum QCD action for two flavors with degenerate quark mass. The leading cutoff effects are described by a single correction term, a Pauli term containing the field strength tensor $F_{\mu\nu}(x)$ multiplied by an unknown coefficient (''low-energy constant'') $\bar{c}_{\rm SW}$. Many more terms appear at $O(a^2)$ [17].

The mapping of the bare local currents of Eqs. (2) and (3) into the Symanzik theory is [13,14]:

$$V^a_{\mu,\rm Loc} \simeq V^a_{\mu,\rm Sym,Loc} = \frac{1}{Z^0_V}(1+\bar{b}_V am)(V^a_{\mu,\rm ct} + a\bar{c}_V\partial_\nu T^a_{\mu\nu,\rm ct}) + O(a^2), \tag{11}$$

$$A^a_{\mu,\rm Loc} \simeq A^a_{\mu,\rm Sym,Loc} = \frac{1}{Z^0_A}(1+\bar{b}_A am)(A^a_{\mu,\rm ct} + a\bar{c}_A\partial_\mu P^a_{\rm ct}) + O(a^2) \tag{12}$$

$$P^a_{\rm Loc} \simeq P^a_{\rm Sym,Loc} = \frac{1}{Z^0_P}(1+\bar{b}_P am)P^a_{\rm ct} + O(a) \tag{13}$$

$$T^a_{\mu\nu,\rm Loc} \simeq T^a_{\mu\nu,\rm Sym,Loc} = \frac{1}{Z^0_T}(1+\bar{b}_T am)T^a_{\mu\nu,\rm ct} + O(a) \tag{14}$$

where the continuum bilinears take their usual forms

$$\begin{aligned} V^a_{\mu,\rm ct} &= \bar{\psi}\gamma_\mu T^a\psi, \qquad & T^a_{\mu\nu,\rm ct} &= \bar{\psi}\sigma_{\mu\nu}T^a\psi, \\ A^a_{\mu,\rm ct} &= \bar{\psi}\gamma_\mu\gamma_5 T^a\psi, \qquad & P^a_{\rm ct} &= \bar{\psi}\gamma_5 T^a\psi. \end{aligned} \tag{15}$$

The mapping of operators between effective theories,

$$O_{\rm Lat} \simeq O_{\rm Sym}, \tag{16}$$

is defined so that

$$\langle O_{\rm Lat}(x)O(\psi^{\rm Lat},\bar{\psi}^{\rm Lat},A^{\rm Lat}_\mu,\mathbf{y})\rangle_{S_{\rm Lat}} = \langle O_{\rm Sym}(x)O(\psi^{\rm Sym},\bar{\psi}^{\rm Sym},A^{\rm Sym}_\mu,\mathbf{y})\rangle_{S_{\rm Sym}}. \tag{17}$$

Here $O(\psi^{\rm Lat},\bar{\psi}^{\rm Lat},A^{\rm Lat}_\mu,\mathbf{y})$ and $O(\psi^{\rm Sym},\bar{\psi}^{\rm Sym},A^{\rm Sym}_\mu,\mathbf{y})$ are arbitrary multilocal operators consisting of quark and gluon fields at positions $\mathbf{y} = y_1, y_2, \cdots$ which all differ from x. The above vacuum expectation values are calculated with $S_{\rm Lat}$ on the left-hand-side and $S_{\rm Sym}$ on the right-hand-side. We note that the equations of motion have been used in order to reduce the number of $O(a)$ terms on the right-hand sides of (10)–(12). This is legitimate as long as we consider the Symanzik theory as an on-shell effective theory, set up to reproduce physical quantities like masses, decay constants, etc..

We stress that the currents $V^a_{\mu,\rm Sym,Loc}$ and $A^a_{\mu,\rm Sym,Loc}$ are the result of matching the *bare* lattice currents into the Symanzik theory, and thus must include the renormalization constants $Z^0_{V,A}$. These have perturbative expansions of the form $Z^0_{V,A} = 1 + O[g(a)^2]$, but do not contain any contributions of $O(a)$, since all $O(a)$ terms are explicitly accounted for. They are completely determined in principle once one has specified the action and $g(a)$, but are only known approximately in practice. This will not present a problem, since we ultimately will normalize the currents nonperturbatively and all dependence on $Z^0_{V,A}$ will cancel. The superscript ''0,'' which indicates that this quantity is of 0'th order in an expansion in a, distinguishes these Z-factors from the nonperturbatively determined renormalization constants $Z_{V,A}$ introduced before. The latter, as we will see, depend linearly on a.

We can also map the renormalized currents of Eqs. (8) and (9) into the Symanzik theory. For $V_{\mu,\rm ren,Loc}$ and $A_{\mu,\rm ren,Loc}$, the result will be the same as in (11) and (12) except for multiplication by overall factors of (the to-be-determined quantities) $Z_{V,\rm Loc}$ and $Z_{A,\rm Loc}$, respectively.

The results (11) and (12) also hold for improved currents of the form of Eqs. (5) and (6), although the coefficients $Z^0_{V,A}$ and $\bar{c}_{V,A}$ will differ. It is important to keep in mind that these coefficients, as well as $\bar{c}_{\rm SW}$, are *a priori* unknown, their values depending on the details of the lattice theory. If all these parameters vanish we say that the lattice theory and current matrix elements are $O(a)$–improved. For this to happen the parameters c_X and b_X of the lattice theory need to be tuned to appropriate nonzero values.[3]

The vector current in (11) is the effective current into which the local lattice current is mapped. The conserved lattice vector current is mapped onto the most general conserved effective vector current. This current $V^a_{\mu,\rm Sym,Con}$ can be obtained by starting from (11) (with an *a priori* different coefficient $\bar{c}_V$ in front of the tensor term, and with $Z^0_V = 1$, $\bar{b}_V = 0$) and then imposing current

[3]Explicitly, $c_V = -(Z^0_T/Z^0_V)\bar{c}_V$, $c_A = -(Z^0_P/Z^0_A)\bar{c}_A$, $b_V = -\bar{b}_V$, and $b_A = -\bar{b}_A$.

conservation. The current in (11) is, however, already conserved,

$$\partial_\mu V^a_{\mu,\mathrm{Sym,Loc}} = 0, \tag{18}$$

which is a consequence of the particular structure of the $O(a)$ correction (total derivative of an antisymmetric tensor). Hence, both lattice currents are mapped onto the same form of effective current at this order in the Symanzik expansion. Violations of current conservation which imply a difference between the local and the conserved current are expected to show up at $O(a^2)$.

We mention two special cases of the Symanzik effective theory at $O(a)$ that we will need in the next section for the mapping to the chiral effective theory. Let us first consider the Symanzik effective theory in which $\bar{c}_{\mathrm{SW}}$ is nonzero but $\bar{c}_{V,A}$ and $\bar{b}_{V,A}$ vanish, and $Z^0_{V,A} = 1$. In this case the Symanzik currents coincide with the continuum QCD currents. These transform into each other under infinitesimal $SU(2)$ axial rotations $\delta\psi = \omega^a T^a \gamma_5 \psi$, $\delta\bar{\psi} = \omega^a \bar{\psi}\gamma_5 T^a$:

$$\delta V^a_\mu = i\epsilon^{abc}\omega^b A^c_\mu, \qquad \delta A^a_\mu = i\epsilon^{abc}\omega^b V^c_\mu. \tag{19}$$

This leads to various chiral Ward identities, schematically written as $\langle \delta S_{\mathrm{Sym}} \mathcal{O}_{\mathrm{Sym}}\rangle = \langle \delta \mathcal{O}_{\mathrm{Sym}}\rangle$, where $\mathcal{O}_{\mathrm{Sym}}$ denotes some product of vector and axial-vector currents. The form of these Ward identities is as in continuum QCD, since the right-hand side reads $\langle \delta \mathcal{O}_{\mathrm{Sym}}\rangle = \langle \delta \mathcal{O}_{\mathrm{ct}}\rangle$. The only difference is the appearance of an extra term proportional to $a\bar{c}_{\mathrm{SW}}$ in the variation of the effective action, caused by the Pauli term in S_{Sym}. Note, however, that these simple QCD-like Ward identities only hold at $O(a)$, and are violated at $O(a^2)$ by the terms of this order in the effective action and effective currents.

The second special case is obtained by setting $\bar{c}_{\mathrm{SW}} = 0$, $\bar{b}_{V,A} = 0$ and $Z^0_{V,A} = 1$, in which case $O(a)$ corrections stem entirely from the $\bar{c}_{V,A}$ terms in the effective currents. This implies, for example, that the correlation function of two axial-vector currents reads

$$\begin{aligned}\langle A^a_{\mu,\mathrm{Sym}}(x) A^a_{\nu,\mathrm{Sym}}(y)\rangle = {} & \langle A^a_{\mu,\mathrm{ct}}(x) A^a_{\nu,\mathrm{ct}}(y)\rangle \\ & + a\bar{c}_A \langle A^a_{\mu,\mathrm{ct}}(x)\partial_\nu P^a_{\mathrm{ct}}(y) \\ & + \partial_\mu P^a_{\mathrm{ct}}(x) A^a_{\nu,\mathrm{ct}}(y)\rangle.\end{aligned} \tag{20}$$

Here the expectation values are defined with Boltzmann factor $\exp(-S_{\mathrm{ct}})$ only. Hence, the $O(a)$ correction is given by the correlation function between the axial-vector current and the derivative of the pseudoscalar density. Again, this result will be violated as soon as one includes the corrections of $O(a^2)$.

C. Matching to ChPT

The appropriate chiral effective theory is obtained by writing down the most general chiral effective Lagrangian and effective currents which are compatible with the symmetries of the underlying Symanzik theory. A standard spurion analysis is employed in order to properly incorporate explicit symmetry breaking terms. For example, the Symanzik effective action is invariant under the chiral symmetry group G, parity P and charge conjugation C, provided both the mass and the coefficient $a\bar{c}_{\mathrm{SW}}$ are promoted to space-time dependent external fields M and A, which are postulated to transform according to [4,5,18]

$$\begin{aligned} & M \xrightarrow{G} LMR^\dagger, \qquad M \xrightarrow{P} M^\dagger, \qquad M \xrightarrow{C} M^T, \\ & A \xrightarrow{G} LAR^\dagger, \qquad A \xrightarrow{P} A^\dagger, \qquad A \xrightarrow{C} A^T. \end{aligned} \tag{21}$$

The "physical" values are obtained by setting $M \to m$ and $A \to a\bar{c}_{\mathrm{SW}}$. In an intermediate step, however, the spurion fields M and A are used together with the standard field

$$\Sigma(x) = \exp\left(\frac{2i}{f}\pi^a(x)T^a\right) \tag{22}$$

in order to write down the most general scalar that is invariant under G, P and C. This has been done in Refs. [5,18], and part of the result reads (in Euclidean space-time)

$$\begin{aligned}\mathcal{L}_{\mathrm{chiral}} = {} & \frac{f^2}{4}\langle \partial_\mu \Sigma (\partial_\mu \Sigma)^\dagger\rangle - \frac{f^2}{4} 2Bm\langle \Sigma^\dagger + \Sigma\rangle \\ & + L_{45} 2Bm \langle \partial_\mu \Sigma (\partial_\mu \Sigma)^\dagger\rangle \langle \Sigma^\dagger + \Sigma\rangle \\ & + W_{45}\hat{a}\bar{c}_{\mathrm{SW}} \langle \partial_\mu \Sigma (\partial_\mu \Sigma)^\dagger\rangle \langle \Sigma^\dagger + \Sigma\rangle \\ & - W_{68} 2Bm\hat{a}\bar{c}_{\mathrm{SW}} \langle \Sigma + \Sigma^\dagger\rangle^2 + \ldots.\end{aligned} \tag{23}$$

Here the angled brackets denote traces in flavor space.[4] The lattice spacing appears in the combination

$$\hat{a} = 2W_0 a, \tag{24}$$

which is of dimension two.[5] We have dropped a number of terms of $O(p^4)$ and $O(a^2)$, which we will not need in the following. Note that we have absorbed the term $f^2 W_0 a\bar{c}_{\mathrm{SW}}\langle \Sigma^\dagger + \Sigma\rangle/2$ in the definition of the mass, so m in (23) corresponds already to the so-called shifted mass [4,6].

Taking the naive continuum limit $a \to 0$ we recover the correct terms of the continuum chiral Lagrangian with the familiar low-energy coefficients f, B and $L_{45} = L_4 + L_5/2$ of continuum ChPT [1,2]. W_0 and $W_{45} = W_4 + W_5/2$ are low-energy constants associated with breaking terms due to the nonzero lattice spacing [5].[6]

[4] In the last section we used the same notation for correlation functions. The context usually tells unambiguously what is meant by $\langle \ldots \rangle$.

[5] W_0, a LEC that enters the chiral Lagrangian at $O(a)$, is of dimension three [5].

[6] Our notation for the low-energy coefficients differs slightly compared to the notation in other references, since our m is already the shifted mass: our $W_{45}\bar{c}_{\mathrm{SW}}$ and $W_{68}\bar{c}_{\mathrm{SW}}$ correspond to the combinations $W_{45} - L_{45}$ and $W_{68} - 2L_{68}$ in Ref. [5]. These combinations are abbreviated to $\tilde{W}$ and W in Ref. [6].

We now apply the same procedure to derive expressions for the effective operators. The currents in the Symanzik effective theory are given in Eqs. (11) and (12)—forms which, as noted above, hold for all the lattice currents of interest. To simplify the following discussion, we will map the Symanzik currents *without* overall Z-factors and b_X corrections into the chiral effective theory. These factors can be added at the end. Thus we consider the mappings

$$V^a_{\mu,\mathrm{ct}} + a\bar{c}_V \partial_\nu T^a_{\mu\nu,\mathrm{ct}} \to V^a_{\mu,\mathrm{eff}}, \tag{25}$$

$$A^a_{\mu,\mathrm{ct}} + a\bar{c}_A \partial_\mu P^a_{\mathrm{ct}} \to A^a_{\mu,\mathrm{eff}}. \tag{26}$$

The leading contributions are just the continuum expressions for the currents,

$$V^a_{\mu,\mathrm{ct}} = \bar{\psi}_R \gamma_\mu T^a \psi_R + \bar{\psi}_L \gamma_\mu T^a \psi_L, \tag{27}$$

$$A^a_{\mu,\mathrm{ct}} = \bar{\psi}_R \gamma_\mu T^a \psi_R - \bar{\psi}_L \gamma_\mu T^a \psi_L, \tag{28}$$

where we decomposed the currents into chiral fields. The vector current is just the sum of the right- and left-handed current, the axial-vector current is given by the difference.

The $O(a)$ corrections couple fields with opposite chirality, and the currents in the Symanzik theory do not transform under chiral rotations as continuum vector and axial-vector currents. However, the continuum transformation behavior can be enforced by promoting the coefficients $\bar{c}_V$, $\bar{c}_A$ to spurion fields C_V and C_A with nontrivial transformation behavior under G, P and C:

$$C_X \xrightarrow{G} L C_X R^\dagger, \qquad C_X \xrightarrow{P} C_X^\dagger, \qquad C_X \xrightarrow{C} C_X^T, \qquad X = V, A. \tag{29}$$

Note that these transformation laws are identical to the ones of the other $O(a)$ spurion A, cf. (21).

It is now easily checked that the $O(a)$ corrections written in the form

$$\begin{aligned} V^a_{\mu,a\text{-corr}} = {} & (\partial_\nu \bar{\psi}_L) i\sigma_{\mu\nu} C_V T^a \psi_R + \bar{\psi}_L i\sigma_{\mu\nu} T^a C_V \partial_\nu \psi_R \\ & + (\partial_\nu \bar{\psi}_R) i\sigma_{\mu\nu} C_V^\dagger T^a \psi_L + \bar{\psi}_R i\sigma_{\mu\nu} T^a C_V^\dagger \partial_\nu \psi_L, \end{aligned} \tag{30}$$

$$\begin{aligned} A^a_{\mu,a\text{-corr}} = {} & (\partial_\mu \bar{\psi}_L) \gamma_5 C_A T^a \psi_R + \bar{\psi}_L \gamma_5 T^a C_A \partial_\mu \psi_R \\ & + (\partial_\mu \bar{\psi}_R) \gamma_5 C_A^\dagger T^a \psi_L + \bar{\psi}_R \gamma_5 T^a C_A^\dagger \partial_\mu \psi_L, \end{aligned} \tag{31}$$

transform as the continuum currents. Setting the spurion field to its physical value, $C_V \to a\bar{c}_V$ and $C_A \to a\bar{c}_A$, one recovers the desired Symanzik currents.

The currents in the chiral effective theory are now obtained by writing down the most general vector and axial-vector current built of the chiral field Σ, its derivatives and the spurion fields. The spurions necessary for the construction of the vector current are M and A, the ones we already encountered in the construction of the effective action, and C_V. For the axial-vector C_A must be used instead.

In order to write down the currents we first recall that our effective theory has to reproduce continuum ChPT if we send $a \to 0$. This requirement implies that the continuum part of the currents are just the expressions given by Gasser and Leutwyler. At leading order these read

$$V^a_{\mu,\mathrm{LO}} = \frac{f^2}{2} \langle T^a (\Sigma^\dagger \partial_\mu \Sigma + \Sigma \partial_\mu \Sigma^\dagger) \rangle, \tag{32}$$

$$A^a_{\mu,\mathrm{LO}} = \frac{f^2}{2} \langle T^a (\Sigma^\dagger \partial_\mu \Sigma - \Sigma \partial_\mu \Sigma^\dagger) \rangle. \tag{33}$$

Obviously these expressions transform as vector and axial-vector currents under G, P and C. Moreover, these currents are properly normalized in order to satisfy the current algebra.

In order to construct the leading $O(a)$ corrections we need at least one power of either A or C_X and one partial derivative of Σ. It is easily checked that the following terms transform as desired:

$$\begin{aligned} &V1) \quad V^a_{\mu,\mathrm{LO}} \langle \Sigma^\dagger A + \Sigma A^\dagger \rangle, \\ &V2) \quad V^a_{\mu,\mathrm{LO}} \langle \Sigma^\dagger C_V + \Sigma C_V^\dagger \rangle, \\ &V3) \quad \langle T^a (\partial_\mu \Sigma^\dagger A - A \partial_\mu \Sigma^\dagger + \partial_\mu \Sigma A^\dagger - A^\dagger \partial_\mu \Sigma) \rangle, \\ &V4) \quad \langle T^a (\partial_\mu \Sigma^\dagger C_V - C_V \partial_\mu \Sigma^\dagger + \partial_\mu \Sigma C_V^\dagger - C_V^\dagger \partial_\mu \Sigma) \rangle, \end{aligned} \tag{34}$$

for the vector current, and

$$\begin{aligned} &A1) \quad A^a_{\mu,\mathrm{LO}} \langle \Sigma^\dagger A + \Sigma A^\dagger \rangle, \\ &A2) \quad A^a_{\mu,\mathrm{LO}} \langle \Sigma^\dagger C_A + \Sigma C_A^\dagger \rangle, \\ &A3) \quad \langle T^a (\partial_\mu \Sigma^\dagger A + A \partial_\mu \Sigma^\dagger - \partial_\mu \Sigma A^\dagger + A^\dagger \partial_\mu \Sigma) \rangle, \\ &A4) \quad \langle T^a (\partial_\mu \Sigma^\dagger C_A + C_A \partial_\mu \Sigma^\dagger - \partial_\mu \Sigma C_A^\dagger + C_A^\dagger \partial_\mu \Sigma) \rangle, \end{aligned} \tag{35}$$

for the axial-vector current. Setting the external fields to their final value, $C_X \to a\bar{c}_X$, we obtain the following expressions for the currents in the effective theory:

$$V^a_\mu = V^a_{\mu,\mathrm{LO}} \left(1 + \frac{4}{f^2} \hat{a} (W_{V1} \bar{c}_{\mathrm{SW}} + W_{V2} \bar{c}_V) \langle \Sigma + \Sigma^\dagger \rangle \right), \tag{36}$$

$$\begin{aligned} A^a_\mu = {} & A^a_{\mu,\mathrm{LO}} \left(1 + \frac{4}{f^2} \hat{a} (W_{A1} \bar{c}_{\mathrm{SW}} + W_{A2} \bar{c}_A) \langle \Sigma + \Sigma^\dagger \rangle \right) \\ & + 4\hat{a} (W_{A3} \bar{c}_{\mathrm{SW}} + W_{A4} \bar{c}_A) \partial_\mu \langle T^a (\Sigma - \Sigma^\dagger) \rangle. \end{aligned} \tag{37}$$

The coefficients W_X are unknown low-energy constants (LECs). In order to make W_{X1}, W_{X2} dimensionless we included the factor $4/f^2$. Note that the second line in (37) is proportional to the continuum pseudoscalar density, $P^a_{\mathrm{ct}} = f^2 B \langle T^a (\Sigma - \Sigma^\dagger) \rangle / 2$.

The number of unknown LECs in the currents can be reduced using the freedom of field redefinition [6,19]. Explicitly, performing $\Sigma \to \Sigma + \delta\Sigma$ with

$$\delta\Sigma = \frac{4\hat{a}}{f^2}\bar{c}_{\rm SW}\Delta W(\Sigma^2 - 1), \tag{38}$$

we obtain the same effective Lagrangian and currents with the transformed coefficients

$$\begin{aligned} &W_{45} \to W_{45} + \Delta W, \qquad W_{68} \to W_{68} + \Delta W/2, \\ &W_{V1} \to W_{V1} + \Delta W, \qquad W_{A1} \to W_{A1} + \Delta W, \\ &W_{A3} \to W_{A3} - \Delta W. \end{aligned} \tag{39}$$

Therefore, depending on the particular choice for ΔW we may make one LEC vanish. In the following we choose this to be W_{A3} in the expression for the axial-vector current.

So far the expressions in (36) and (37) are the most general currents compatible with the symmetries that have the correct continuum limit. In order to match the currents properly we have to impose the constraints that these currents have to obey at $O(a)$, for instance current conservation for the vector current. This will relate some of the LECs W_X to those in the effective action.

In order to discuss this we first derive the EOM corresponding to the Lagrangian in Eq. (23) without the continuum NLO term proportional to L_{45} and without the $O(am)$ correction proportional to W_{68}.[7] Using the shorthand notation $\chi = 2Bm$, $\rho = 2W_{45}W_0 a\bar{c}_{\rm SW}$ and

$$R = \frac{4}{f^2}\langle\Sigma + \Sigma^\dagger\rangle, \qquad T = \frac{4}{f^2}\langle\partial_\mu\Sigma\partial_\mu\Sigma^\dagger\rangle, \tag{40}$$

the leading order EOM reads

$$\begin{aligned} &[\Sigma(\partial_\mu\partial_\mu\Sigma^\dagger) - (\partial_\mu\partial_\mu\Sigma)\Sigma^\dagger](1 + \rho R) \\ &\quad - [\Sigma - \Sigma^\dagger](\chi + \rho T) \\ &= 2\lambda + [\partial_\mu\Sigma\Sigma^\dagger - \Sigma\partial_\mu\Sigma^\dagger]\rho\partial_\mu R. \end{aligned} \tag{41}$$

The parameter λ is the Lagrange multiplier associated with the constraint $\det\Sigma = 1$. Setting the lattice spacing to zero (i.e. $\rho = 0$) Eq. (41) reproduces the EOM in continuum ChPT [2].

Using (41) we find the condition

$$\partial_\mu V^a_\mu = 0 \Leftrightarrow W_{V1} = W_{45} \quad \text{and} \quad W_{V2} = 0. \tag{42}$$

Therefore, the conserved vector current in the chiral effective theory is given by

$$V^a_{\mu,\rm eff} = V^a_{\mu,\rm LO}\left(1 + \frac{4}{f^2}\hat{a}W_{45}\bar{c}_{\rm SW}\langle\Sigma + \Sigma^\dagger\rangle\right). \tag{43}$$

This expression agrees with the one in Ref. [6] obtained from the generating functional. Note that at this order this current coincides with the Noether current associated with vector transformations. This will, however, no longer be true at higher order in the chiral expansion.[8]

Note that there is no term proportional to $\bar{c}_V$ in (43), which is a consequence of the $\partial_\nu T^a_{\mu\nu}$ structure of the $O(a)$ correction. We need three partial derivatives in order to construct such a term in the chiral effective theory. Hence, this correction is of $O(ap^3)$, which is of higher order than we consider here.

In order to obtain the proper result for the axial-vector current we have to make sure that the properties (19) and (20) of the underlying theory are correctly reproduced. The result (43) for the vector current together with (19) (for $\bar{c}_V = \bar{c}_A = 0$) immediately implies $W_{A1} = W_{45}$. On the other hand, setting $\bar{c}_{\rm SW} = 0$ and demanding (20) leads to $W_{A2} = 0$. So the final result for the axial-vector current reads

$$\begin{aligned} A^a_{\mu,\rm eff} = A^a_{\mu,\rm LO}&\left(1 + \frac{4}{f^2}\hat{a}W_{45}\bar{c}_{\rm SW}\langle\Sigma + \Sigma^\dagger\rangle\right) \\ &+ 4\hat{a}W_A\bar{c}_A\partial_\mu\langle T^a(\Sigma - \Sigma^\dagger)\rangle, \end{aligned} \tag{44}$$

where we abbreviated $W_{A4} = W_A$. This expression also agrees with the result in Ref. [6].[9]

So far we have discussed the currents at leading order in the chiral expansion including the first correction of $O(a)$. Higher-order contributions to the currents can be derived in the same fashion. The terms without factors of the lattice spacing are the familiar contributions of continuum ChPT,

$$\begin{aligned} \delta V^a_{\mu,\rm eff} = &\frac{f^2}{2}\langle T^a(\Sigma^\dagger\partial_\mu\Sigma + \Sigma\partial_\mu\Sigma^\dagger)\rangle \\ &\times\left(\frac{4}{f^2}2BmL_{45}\langle\Sigma + \Sigma^\dagger\rangle\right), \end{aligned} \tag{45}$$

$$\begin{aligned} \delta A^a_{\mu,\rm eff} = &\frac{f^2}{2}\langle T^a(\Sigma^\dagger\partial_\mu\Sigma - \Sigma\partial_\mu\Sigma^\dagger)\rangle \\ &\times\left(\frac{4}{f^2}2BmL_{45}\langle\Sigma + \Sigma^\dagger\rangle\right). \end{aligned} \tag{46}$$

In order to construct the first subleading $O(a)$ corrections we have to form vector and axial-vector currents with one power of either A or C_X, and either three derivatives (corresponding to the $O(ap^2$ contributions), or one derivative and one power of the mass spurion field M (the $O(am)$ contributions). Simple examples for such terms are

[7] These can and need to be included if the NLO terms of $O(p^2m)$ and $O(p^2ma)$ are included in the current.

[8] At higher order in the chiral expansion the currents receive contributions which are not present in the Noether current. The vector current contribution proportional to L_9 [2], which captures the dominant contribution of the pion form factor, is an example for this. We thank J. Bijnens for pointing this out to us.

[9] The result in Ref. [6] is obtained by setting $W_{10} = 2W_A\bar{c}_A$ and $\tilde{W} = 2W_{45}\bar{c}_{\rm SW}$.

products of the leading $O(a)$ terms in (34) and (35) with either $\langle \Sigma M^\dagger + M\Sigma^\dagger \rangle$ or $\langle \partial_\mu \Sigma (\partial_\mu \Sigma)^\dagger \rangle$. An example is the correction

$$\delta A^a_{\mu,\text{eff}} = \frac{f^2}{2} \langle T^a (\Sigma^\dagger \partial_\mu \Sigma - \Sigma \partial_\mu \Sigma^\dagger) \rangle (X \bar{c}_A \hat{a} m \langle \Sigma + \Sigma^\dagger \rangle^2), \tag{47}$$

with X being the low-energy constant associated with this correction.

There are more terms possible and it is a straightforward but tedious exercise to find all possible terms contributing to the currents. For the rest of this paper, however, we do not need these higher-order terms.

We conclude this section by discussing the pseudoscalar density, which we need later on for the computation of the PCAC mass. In the Symanzik effective theory the pseudoscalar density is given by P^a_{ct}. The corresponding expression in the chiral effective theory is constructed in the same way as the currents. Since the density in the Symanzik theory has no $O(a)$ term, we only have the spurion A for the construction of the density, and we find[10]

$$P^a_{\text{eff}} = \frac{f^2 B}{2} \langle T^a (\Sigma^\dagger - \Sigma) \rangle \left(1 + \frac{4}{f^2} \hat{a} W_{68} \bar{c}_{\text{SW}} \langle \Sigma + \Sigma^\dagger \rangle \right). \tag{48}$$

As already mentioned, our expressions for the effective currents agree with the results in Ref. [6], although the two calculations use different methods. In the approach of Ref. [6], which follows the procedure used by Gasser and Leutwyler in continuum ChPT [1], sources for the currents are introduced and the generating functional is constructed. The currents are then obtained from the generating functional by taking derivatives with respect to the sources. The analysis is complicated, however, by the presence in the Symanzik theory of $O(a)$ violations of the local gauge invariance used to restrict the mapping to the chiral effective theory. This complication, missed in Ref. [6], was noted in Ref. [9], and an appropriate extension outlined. The outcome of this extension was that the form of the results of Ref. [6] still holds after a redefinition of the LECs. Since a systematic and complete treatment of the impact of the $O(a)$ effects in the generating functional method has not been presented, however, we provide such a treatment in Appendix A. In particular, we show that the same results (43) and (44) are obtained using this method.

III. RENORMALIZATION

We now return to the issue of the normalization of the currents. The results of the previous section allow us to determine the form that a given lattice current will have when mapped into WChPT. For example, putting back the overall factors, the renormalized local vector and axial-vector currents of Eqs. (8) and (9) map as

$$V_{\mu,\text{ren,Loc}} \simeq \frac{Z_{V,\text{Loc}}}{Z^0_V} (1 + \bar{b}_V a m) V^a_{\mu,\text{eff}}, \tag{49}$$

$$A_{\mu,\text{ren,Loc}} \simeq \frac{Z_{A,\text{Loc}}}{Z^0_A} (1 + \bar{b}_A a m) A^a_{\mu,\text{eff}}, \tag{50}$$

with $V^a_{\mu,\text{eff}}$ and $A^a_{\mu,\text{eff}}$ given by Eqs. (43) and (44), respectively. In the lattice theory, the renormalization factors are determined by imposing particular conditions at nonzero lattice spacing. Hence, in order to properly match the effective currents we should impose the same conditions in the effective theory.

A. Renormalization of the lattice currents

Since the conserved vector current does not need to be renormalized it can be used to normalize the local current and to define $Z_{V,\text{Loc}}$ (at the lattice level) according to [20,21]

$$Z_{V,\text{Loc}} = \frac{\langle f | V^a_{\mu,\text{Con}} | i \rangle}{\langle f | V^a_{\mu,\text{Loc}} | i \rangle}. \tag{51}$$

Here i and f denote arbitrary initial and final states, though it is convenient to choose zero-momentum pseudoscalar states. Note that the dependence of $Z_{V,\text{Loc}}$ on the particular states can be sizable, in particular, if the theory is not $O(a)$-improved [20].

An alternative definition for $Z_{V,\text{Loc}}$, which does not use the conserved current, is given by [20–22]

$$Z_{V,\text{Loc}} \langle \pi^a(\vec{p}) | V^b_{0,\text{Loc}} | \pi^c(\vec{p}) \rangle = \epsilon^{abc} 2E. \tag{52}$$

The matrix element on the left-hand side can be obtained in the usual way by calculating the ratio of two correlation functions, where pseudoscalar sources are used to project onto the pion states. Although we have specified initial and final pion states, the renormalization factor still depends on the momenta of the pions [20]. For massive pions one usually chooses zero spatial momentum, $\vec{p} = 0$.

The two renormalization conditions (51) and (52) do not specify the renormalization condition completely, since the matrix elements still depend on the quark mass. Theoretically preferable are mass independent renormalization schemes, in which the renormalization condition is imposed at zero quark mass. This implies some technical difficulties, because numerical simulations cannot be performed directly for vanishing quark masses. One way to circumvent this technical limitation is to calculate the Z-factors for various small quark masses and extrapolate

[10]This agrees with the result of Ref. [6], with W_{68} related to W of that reference by $W = W_{68} \bar{c}_{\text{SW}}$.

the results to the massless limit. This may introduce some extrapolation error, but in principle is a viable procedure.

A different strategy to define and compute the renormalization factors makes use of Schrödinger functional boundary conditions [23]. With this setup it is possible to compute $Z_{V,\mathrm{Loc}}$ and other renormalization factors for a vanishing partially conserved axial-vector current (PCAC) quark mass. Even though the renormalization conditions are imposed at vanishing quark mass, they now depend on details of the Schrödinger functional setup, e.g. the size and geometry of the finite volume. This dependence can, in principle, be removed by extrapolating to infinite volume.

Being able to work at vanishing quark mass has another advantage: chiral Ward identities involving the axial-vector current simplify significantly. In Ref. [24], for example, the Ward identity

$$\int_{\partial R} d\sigma_\mu(x)\epsilon^{abc}\langle f|A^a_{\mu,\mathrm{ren}}(x)A^b_{\nu,\mathrm{ren}}(y)|i\rangle = 2i\langle f|V^c_{\nu,\mathrm{ren}}(y)|i\rangle \tag{53}$$

is imposed. This identity is the Euclidean analogue of the current algebra relation stating that the commutator of two axial-vector currents is equal to the vector current [25]. The region R is chosen to be the space-time volume between two hyper-planes at $x_0 = y_0 \pm t$. The equation for $\nu = 0$ between pseudoscalar states has been used to determine the renormalization factor Z_A. For more details see Ref. [24].

B. Renormalization of the effective currents

Having chosen particular renormalization conditions for the lattice currents, we have to impose the same conditions in the chiral effective theory.

Some conditions are harder to implement than others. For example, matrix elements between the vacuum and a vector meson state in Eq. (51) are not easily accessible in standard mesonic ChPT, since the vector meson is not a degree of freedom in the chiral effective theory. Conditions involving quark states (the so-called ''RIMOM'' scheme [26]) are also out of reach. In practice, only conditions involving pseudoscalar states can be treated in the chiral effective theory.

In the following we carry out the matching for one particular class of renormalization conditions. For the vector current we assume that either the condition (51) or (52) is imposed with single pion states at zero spatial momentum and at vanishing bare PCAC mass. For the axial-vector current we assume that condition (53) is employed to fix Z_A. We impose these conditions in infinite volume. Finite volume can also be considered, but it does not make a difference at the order in the chiral expansion to which we work.

As a first step we have to calculate the PCAC mass and set it to zero. The PCAC mass is defined by

$$m_{\mathrm{PCAC}} = \frac{\langle 0|\partial_\mu A^a_{\mu,\mathrm{eff}}|\pi^a\rangle}{2\langle 0|P^a_{\mathrm{eff}}|\pi^a\rangle}. \tag{54}$$

Expanding the Σ fields in (44) and (48), keeping only one power of π^a, the ratio of expectation values on the right-hand side is easily obtained[11]

$$m_{\mathrm{PCAC}} = \frac{M_\pi^2}{2B}\left(1 + \frac{8}{f^2}\hat{a}[2(W_{45} - W_{68})\bar{c}_{\mathrm{SW}} + W_A\bar{c}_A]\right), \tag{55}$$

in agreement with Ref. [6]. The PCAC quark mass is proportional to the pion mass, which is given by [6]

$$M_\pi^2 = 2Bm\left(1 + \frac{16}{f^2}\hat{a}(2W_{68} - W_{45})\bar{c}_{\mathrm{SW}}\right). \tag{56}$$

Recall that m denotes the shifted mass including the leading $O(a)$ shift.

At higher order in the chiral expansion the right-hand side of (56) contains an additional correction of $O(a^2)$ [4]. A vanishing pion mass therefore corresponds to $m = O(a^2)$. Since we ignore $O(a^2)$ corrections, we conclude that a vanishing PCAC quark mass is equivalent to $m = 0$, and in the following we assume this condition for the shifted mass.[12]

The next step is the determination of $Z_{V,\mathrm{Loc}}$ using either (51) or (52). Both conditions are easily calculated using the chiral effective theory ''image'' of the local lattice current, Eq. (49) with $m = 0$, and the expression (43). In both cases we find[13]

$$Z_{V,\mathrm{Loc}} = Z^0_V. \tag{57}$$

Even though the result is the same for both renormalization conditions, the way it arises differs in the two cases. The result for the first condition is obviously trivial since both the local and the conserved effective vector currents have the same form in the effective theory [cf. (43)], differing only by overall factors. In (52), on the other hand, the two-

[11] In practice, to calculate m_{PCAC} requires knowledge of the renormalization constants of the lattice axial-vector current and pseudoscalar density, which can, as the present work shows, introduce additional $O(a)$ corrections. These do not, however, change the key result being derived here, namely, that $m_{\mathrm{PCAC}} \propto m$ up to $O(a^2)$ corrections.

[12] The $O(a^2)$ correction implies a nontrivial phase structure of the theory with two qualitatively different scenarios [4]. One of these is characterized by a first-order phase transition and the pion mass is nonzero for all values of m. For $m = 0$, however, the pion mass assumes its minimal value $M^2_{\pi,\mathrm{min}} = O(a^2)$. Since here we ignore the $O(a^2)$ corrections we also find for this scenario that a vanishing PCAC mass is given by a vanishing shifted mass, at least to the order we are working.

[13] It is a simple matter to restore the mass dependence, in which case (57) would read $Z_{V,\mathrm{Loc}} = Z^0_V(1 + \bar{b}_V am)$.

pion states contribute a wave function renormalization factor Z_π, which reads[14]

$$Z_\pi = 1 - \frac{16}{f^2}\hat{a}W_{45}\bar{c}_{\mathrm{SW}}, \tag{58}$$

and which exactly cancels the $O(a)$ correction coming from the current.

Let us consider higher-order corrections to the result (57). Expanding the Σ fields in the vector current (43) the first correction terms contain four pion fields. Two of these need to be contracted and form a loop. Hence the result will be proportional to $M_\pi^2 \ln M_\pi^2$, which vanishes for $m_{\mathrm{PCAC}} = 0$. Higher-order analytic parts, on the other hand, will contribute corrections of $O(a^2)$, which we do not consider here.

The implication of Eq. (57) is that, after one or other of the renormalization conditions has been enforced, the renormalized local vector current maps simply into $V^a_{\mu,\mathrm{eff}}$, since the prefactors on the right-hand side of Eq. (49) cancel. The same holds true for any lattice vector current which is renormalized in this way.

We now proceed to the local axial-vector current, whose normalization $Z_{A,\mathrm{Loc}}$ is to be fixed by imposing the Ward identity (53), using external one-pion states having definite (nonzero) momenta. Following Ref. [24] we choose the region R to be the space-time volume between two hyperplanes at $x_0 = y_0 \pm t$ with some finite time separation t. The equation for $\nu = 0$ can be brought into the form [24]

$$\int d\vec{x}\epsilon^{abc}\epsilon^{cde}\langle\pi^d(\vec{p})|[A^a_{0,\mathrm{ren}}(y_0+t,\vec{x}) - A^a_{0,\mathrm{ren}}(y_0-t,\vec{x})] \times A^b_{0,\mathrm{ren}}(y)|\pi^e(\vec{q})\rangle = 2i\epsilon^{cde}\langle\pi^d(\vec{p})|V^c_{0,\mathrm{ren}}(y)|\pi^e(\vec{q})\rangle. \tag{59}$$

The matrix element on the right-hand side of this equation is essentially the one in (52) that we used to fix $Z_{V,\mathrm{Loc}}$. Imposing (59) thus provides a condition for $Z_{A,\mathrm{Loc}}$: simply compute the two sides in the effective theory and set them equal. The calculation is straightforward but rather technical. For this reason we defer the details of the calculation to Appendix B. The final result is (recall that $m = 0$ so there is no $\bar{b}_A$ term)

$$\frac{Z_{A,\mathrm{Loc}}}{Z^0_A} = 1 - \frac{4\hat{a}}{f^2}(W_{45}\bar{c}_{\mathrm{SW}} + W_A\bar{c}_A)z_A(t), \tag{60}$$

$$z_A(t) = 1 - \cosh[t(|\vec{p}| - |\vec{q}|)]\exp[-|t||\vec{p} - \vec{q}|]. \tag{61}$$

Since this result is determined by a ratio of physical correlation functions in which the axial currents are separated, it must depend on the physical combination of LECs $W_{45}\bar{c}_{\mathrm{SW}} + W_A\bar{c}_A$ [6]. This point is also explained at the end of Appendix A, and provides a check of our result. We emphasize that (60) is the complete result to $O(a)$, there are no corrections of $O(am)$ since we work at zero quark mass. The next correction to (60) is of $O(a^2)$, which we do not consider here.

In contrast to the vector current we do find a nonvanishing correction of $O(a)$. That this correction depends on the separation between the axial currents, t, and upon the external state, is as expected. The t dependence is proportional to an integral (a sum on the lattice) of the divergence of the axial current, which does not vanish at $O(a)$, even when $m = 0$. The dependence of the external state is a generic feature of $O(a)$ corrections in an unimproved theory.

Using Eqs. (50) and (60) we find that the renormalized local axial-vector current maps into WChPT as

$$A^a_{\mu,\mathrm{ren,Loc}} \simeq A^a_{\mu,\mathrm{ren,Loc,eff}} = \left[1 - \frac{4\hat{a}}{f^2}(W_{45}\bar{c}_{\mathrm{SW}} + W_A\bar{c}_A)z_A(t)\right]A^a_{\mu,\mathrm{eff}}. \tag{62}$$

This is the main new result of this paper. We see that the a dependence of $A^a_{\mu,\mathrm{eff}}$, derived using symmetries and given in Eq. (44), is supplemented by an additional discretization error resulting from the application of the normalization condition at nonzero a.

Note that the quantity Z^0_A appears only in the combination $Z_{A,\mathrm{Loc}}/Z^0_A$ in Eqs. (50) and (60), and the individual value of Z^0_A is not necessary. This factor is needed only when expressing the bare lattice current in the intermediate Symanzik theory. In fact, the combination $Z_{A,\mathrm{Loc}}/Z^0_A$, and also the analogue for the vector current, $Z_{V,\mathrm{Loc}}/Z^0_V$, may be interpreted as renormalization constants $Z_{A,\mathrm{eff}}$ and $Z_{V,\mathrm{eff}}$ in the chiral effective theory [8].

We also remark that the *form* of $A^a_{\mu,\mathrm{ren,Loc,eff}}$ applies to any lattice current—local or improved. These cases only differ in the values of the LECs. Thus in the following we will drop the subscript "Loc" on the renormalized current in the chiral effective theory.

We close this section by investigating the dependence of $z_A(t)$ on t, $\vec{p}$ and $\vec{q}$. There turn out to be three distinct cases (recalling that $\vec{p}, \vec{q} \neq 0$):

(i) $\vec{p} = \vec{q}$. This is the simplest case to implement practically, and leads to $z_A(t) = 0$. Thus it turns out that, in this case, there are no additional $O(a)$ terms introduced by the current normalization.

(ii) $\vec{p}$ parallel to $\vec{q}$. Then, for $|t| \gg 1/|\vec{p} - \vec{q}|$, the product of cosh and exponential becomes $1/2$, and so $z_A \to 1/2$.

(iii) All other nonvanishing $\vec{p}$ and $\vec{q}$. Here, for $|t| \gg 1/|\vec{p} - \vec{q}|$, the exponential overwhelms the cosh and $z_A \to 1$.

We stress, however, that in both the second and third cases z_A depends on t for nonasymptotic values of t.

[14]Note that there are no terms proportional to the quark mass in the chiral Lagrangian (23), since we have set m to zero.

IV. APPLICATION: PION DECAY CONSTANT

At this point we have completed the construction and matching of the effective currents. Now we can proceed and compute correlation functions involving these currents. As a simple but important example we calculate the pion decay constant. Given the presence of the $z_A(t)$ contribution, our result differs, in general, from previously published ones.

The literature usually distinguishes two quark mass regimes: (i) the GSM regime with $m \sim a\Lambda_{\rm QCD}^2$ and (ii) the regime with $m \sim a^2\Lambda_{\rm QCD}^3$, sometimes called LCE regime.[15] Each of these regimes has its associated power-counting. In this section we do not, however, work within either regime, but rather calculate to one-loop order keeping terms of $O(a)$, but not $O(m)$, in the tree-level result. This choice is made for simplicity, and because we aim only to illustrate the impact of using the correctly normalized currents, and not to provide a compendium of results. In particular, we do not include correction of $O(a^2)$, which are required for an NLO result in the LCE regime. The NLO result for the GSM regime can, however, be obtained from our formulae by dropping some higher-order terms.

A. Decay constant at tree level

Expanding the renormalized axial-vector current in powers of the pion fields we obtain to leading order the expression

$$A^a_{\mu,\text{ren,eff}} = if\frac{\partial_\mu \pi^a}{\sqrt{Z_\pi}} \times \left(1 + \frac{4}{f^2}\hat{a}(W_{45}\bar{c}_{\rm SW} + W_A\bar{c}_A)[2 - z_A(t)]\right). \tag{63}$$

This depends, as required, only on the physical combination $W_{45}\bar{c}_{\rm SW} + W_A\bar{c}_A$ of LECs. We can immediately read off the following expression for the tree-level decay constant:

$$f_{\pi,\text{tree}} = f\left(1 + \frac{4}{f^2}\hat{a}(W_{45}\bar{c}_{\rm SW} + W_A\bar{c}_A)[2 - z_A(t)]\right). \tag{64}$$

We see that the $O(a)$ corrections depend not only on the form of the underlying lattice action and currents (through the LECs) but also on the choice of renormalization condition [through $z_A(t)$]. The $z_A(t)$ term always reduces the size of these corrections, although by no more than a factor of 2 (which happens in the third case discussed at the end of the previous section). The decay constant is free of $O(a)$ corrections only if both the action and the axial-vector current are improved, i.e. for $\bar{c}_{\rm SW} = \bar{c}_A = 0$, in accordance with what we know from the Symanzik effective theory.

[15]GSM stands for *generically small quark masses* [6] and LCE for *large cutoff effects* [27].

We want to comment on the origin of discrepancies between (64) and previously published results for the decay constant. Reference [5] finds[16]

$$f^{\rm RS}_{\pi,\text{tree}} = f\left(1 + \frac{8}{f^2}\hat{a}W_{45}\bar{c}_{\rm SW}\right). \tag{65}$$

There is no correction proportional to $W_A\bar{c}_A$ since their calculation used the Noether current as the axial-vector current [7]. This misses the $O(a)$ correction in (12), and cannot be correct since the result (65) is $O(a)$ improved if only the action (and not the current) is improved.

Reference [6] finds the same form as (64) except without the $z_A(t)$ contribution. These authors assumed that a nonperturbative renormalization condition had been applied, but did not include the impact of applying the condition at nonvanishing lattice spacing.

B. Decay constant to one loop

It is straightforward to compute the leading correction to the tree-level result (64). Expanding the axial-vector current in Eq. (37) to higher powers of the pion fields one obtains the one-loop contributions to f_π. The integrals that appear can be regularized using dimensional regularization. The counterterms for the divergences are provided by the tree-level contribution of the NLO terms in the axial-vector current, c.f. (46) and (47). Even though we have not explicitly given all possible NLO corrections of $O(am, ap^2)$, it is easy to convince oneself that all contributing tree-level terms with one partial derivative are of the form $if\partial_\mu\pi^a \cdot am$. Expressing m by the tree-level pion mass according to (56), we obtain the counterterm

$$A^a_\mu[aM^2_\pi]_{\rm CT} = if\partial_\mu\pi^a\tilde{W}_{A3}\hat{a}M^2_\pi/f^4. \tag{66}$$

For simplicity we have absorbed the coefficients $\bar{c}_{\rm SW}$ and $\bar{c}_A$, and the contribution proportional to $z_A(t)$, in the LEC $\tilde{W}_{A3}$, since in practice these and the W coefficients are difficult to disentangle. The additional factor $1/f^4$ is introduced for convenience, since it leads to a dimensionless coefficient $\tilde{W}_{A3}$.

The final one-loop result for f_π is then given by

$$f_{\pi,\text{1-loop}} = f\left(1 + \frac{\hat{a}}{f^2}\tilde{W}_{A1} - \frac{1}{16\pi^2 f^2}\left[1 + \frac{\hat{a}}{f^2}\tilde{W}_{A2}\right] \times M^2_\pi \ln\frac{M^2_\pi}{\mu^2} + \frac{8}{f^2}M^2_\pi\left[L_{45} + \frac{\hat{a}}{f^2}\tilde{W}_{A3}\right]\right). \tag{67}$$

The coefficients are $\tilde{W}_{A1} = 4(W_{45}\bar{c}_{\rm SW} + W_A\bar{c}_A) \times [2 - z_A(t)]$ (as above) and $\tilde{W}_{A2} = 4(W_{45}\bar{c}_{\rm SW} + W_A\bar{c}_A) \times [1 - z_A(t)]$. Note that both coefficients depend on the physical combination of LECs, as expected.

[16]Ref. [5] quotes explicitly the three-flavor result, which we changed to the corresponding two-flavor result to make the comparison. We also dropped the one-loop correction.

A couple of comments concerning (67) are in order. In the continuum limit we reproduce the familiar result for f_π from continuum ChPT for $N_f = 2$ [1]. Away from the continuum limit the result is modified by terms of $O(a)$, $O(aM_\pi^2)$ and $O(aM_\pi^2 \ln M_\pi^2)$. Dropping the latter two, i.e. setting $\tilde{W}_{A2} = \tilde{W}_{A3} = 0$, we obtain the NLO result for the GSM regime. Taking in addition $z_A(t) = 0$ we reproduce the NLO result in Ref. [6].

The coefficients $\tilde{W}_{A1}$ and $\tilde{W}_{A2}$ are in general not independent. For example, the first case discussed at the end of the last section has $\tilde{W}_{A1} = 2\tilde{W}_{A2}$ (for asymptotically large t values). For the third case we even find $\tilde{W}_{A2} = 0$, so the coefficient of the chiral logarithm is free of $O(a)$ artifacts. Since in this case also $\tilde{W}_{A1}$ assumes its minimal value this is the theoretically preferred renormalization condition.

Except for the special case with $\tilde{W}_{A2} = 0$ the coefficient of the chiral logarithm receives an $O(a)$ correction in the form of the factor $[1 + \hat{a}\tilde{W}_{A2}/f^2]$. Consequently, the coefficient of the chiral logarithm is, in contrast to continuum ChPT, not a universal coefficient depending on f (and N_f) only, but on the (nonuniversal) lattice artifacts too. This fact has previously been stressed in Ref. [28].

Note that the combination L_{45} appears effectively in the lattice spacing dependent combination $L_{45}^{\text{eff}}(a) = L_{45} + \hat{a}\tilde{W}_{A3}/f^2$. Determinations of L_{45} based on simulations at one lattice spacing only are potentially dangerous because the size of the contribution $\hat{a}\tilde{W}_{A3}/f^2$ is *a priori* unknown.

V. CONCLUDING REMARKS

In this paper we have reconsidered the construction of the vector and axial-vector currents in WChPT. Because of the explicit chiral symmetry breaking in lattice QCD with Wilson fermions two aspects need to be taken into account which are not present in continuum ChPT.

First, the local lattice currents are not conserved, and in general they do not map onto the conserved currents in WChPT. In particular, the WChPT currents are not the Noether currents associated with the chiral symmetries, not even at leading order in the chiral expansion. The reason is that the currents in the Symanzik theory have $O(a)$ corrections which are not related to the effective action.

Second, the matching of the currents needs to take into account the finite renormalization of the local lattice currents. In order to properly match the currents the same renormalization conditions that have been employed for the lattice currents must be imposed on the WChPT currents.

Depending on the particular choice for the renormalization conditions the expressions for the renormalized currents differ by terms of $O(a)$. As a result, the WChPT predictions for matrix elements of the currents are different as well. Consequently, a result for an observable like f_π should make reference to the renormalization condition one has adopted. This has to be so at some level, since the lattice data differs too depending on the condition one has chosen. What we find is that the dependence enters at $O(a)$.

At a technical level, our result does not change the number of low-energy coefficients that enter into WChPT predictions at $O(a)$. In particular, as stressed in Ref. [6], there are only two combinations of the LECs that can enter into physical quantities, allowing their $O(a)$ corrections to be related. What changes is the nature of these relations, which now depend on the choice of normalization condition.

The considerations of this paper apply more generally. Another example from WChPT is the ratio of the renormalization factors for pseudoscalar and scalar densities. This must be determined nonperturbatively, e.g. by enforcing Ward identities, and will presumably receive $O(a)$ corrections similar to those for the axial current, although we have not worked out the details. The combination mS is, however, protected by exact lattice WTIs.

More generally still, our results emphasize the (perhaps rather obvious) point that nonperturbative renormalization conditions generically introduce additional discretization errors. These must be (and in practice usually are being) accounted for when extrapolating to the continuum limit.

ACKNOWLEDGMENTS

O. B. acknowledges useful discussions with Johan Bijnens, Maarten Golterman and Rainer Sommer. We also thank Rainer Sommer for feedback on a first draft of this paper. This work is supported in part by the Grants-in-Aid for Scientific Research from the Ministry of Education, Culture, Sports, Science and Technology (Nos. 20340047, 20105001, 20105003), by the Deutsche Forschungsgemeinschaft (SFB/TR 09) and by the U.S. Department of Energy.

APPENDIX A: THE GENERATING FUNCTIONAL METHOD

In Sec. II C we constructed the effective currents in a rather direct way. We first wrote down the most general currents that transform as vector and axial-vector currents. In a second step we imposed appropriate Ward identities that these currents must obey, and this led to various constraints on the LECs in these currents.

We already mentioned at the end of Sec. II C that this is not the way one proceeds in continuum ChPT [1,2]. Instead, there one sets up the generating functional for correlation functions involving the currents (and the scalar and pseudoscalar density), and matches this to the analogous generating functional in the chiral effective theory. In this way the currents are obtained by functional derivatives with respect to the sources.

A crucial link in the matching is the invariance under local chiral transformations, which plays the role of a

gauge symmetry. The local invariance implies that the sources enter the chiral Lagrangian in a very restricted way, namely, in form of a gauge-covariant derivative.

One may ask if the same procedure is also possible once we include the lattice spacing corrections. In order to answer this question we derive in detail the generating functional for the Symanzik effective theory and match it to the one in WChPT. We will see that we indeed obtain the same currents as the ones in (43) and (44). However, we will also see that it is more complicated to maintain the invariance under local chiral transformations.

The ''generating functional method'' has been used before in WChPT in Ref. [6]. However, as discussed in Ref. [9], the generating functional of Ref. [6] violates the invariance under local chiral transformations at nonzero lattice spacing; only the leading (continuum) part respects this symmetry. Consequently, the construction of the axial-vector current requires some care: part of the $O(a)$ corrections have to be mapped separately into the effective theory [9]. The final result found in [9] for the currents turns out, however, to have the form given in Ref. [6], as we derive here in a systematic way.

1. Generating functional in continuum QCD and ChPT

In order to prepare our discussion we first give a brief review of the construction in continuum ChPT, mainly to introduce our notation. We start by defining a (Euclidean) QCD Lagrangian including a part that includes sources for the currents and densities,

$$\mathcal{L} = \mathcal{L}_{\mathrm{QCD}} - i\mathcal{L}_{\mathrm{Source}}, \tag{A1}$$

where $\mathcal{L}_{\mathrm{QCD}}$ is the usual massless QCD Lagrangian, while the second part

$$\begin{aligned}\mathcal{L}_{\mathrm{Source}} = {} & \bar{\psi}\gamma_\mu[v_\mu(x) + \gamma_5 a_\mu(x)]\psi \\ & + \bar{\psi}[s(x) + \gamma_5 p(x)]\psi\end{aligned} \tag{A2}$$

contains sources for the vector and axial-vector currents (v_μ, a_μ) and for the scalar and pseudoscalar densities (s, p). These sources are matrix valued fields, given by

$$\begin{aligned} v_\mu(x) &= v_\mu^a(x)T^a, & a_\mu(x) &= a_\mu^a(x)T^a, \\ s(x) &= s^a(x)T^a, & p(x) &= p^a(x)T^a, \end{aligned} \tag{A3}$$

where T^a are the Hermitian $SU(N_f)$ generators, normalized according to $\mathrm{tr}(T^aT^b) = \delta^{ab}/2$. We are interested in $N_f = 2$, for which $T^a = \sigma^a/2$, with σ^a the usual Pauli matrices.

After integrating over space-time we obtain the action in the presence of the sources, $S = \int d^4x\mathcal{L}(x)$. By taking functional derivatives with respect to the sources we obtain the vector and axial-vector current and the scalar and pseudoscalar densities:

$$i\frac{\delta S}{\delta v_\mu^a(x)} = \bar{\psi}(x)\gamma_\mu T^a\psi(x) = V_\mu^a(x), \tag{A4}$$

$$i\frac{\delta S}{\delta a_\mu^a(x)} = \bar{\psi}(x)\gamma_\mu\gamma_5 T^a\psi(x) = A_\mu^a(x), \tag{A5}$$

$$i\frac{\delta S}{\delta s^a(x)} = \bar{\psi}(x)T^a\psi(x) = S^a(x), \tag{A6}$$

$$i\frac{\delta S}{\delta p^a(x)} = \bar{\psi}(x)\gamma_5 T^a\psi(x) = P^a(x). \tag{A7}$$

The key observation is that the Lagrangian (A1) is invariant under *local* $SU(N_f)_R \times SU(N_f)_L$ transformations, which act on the fermion fields according to

$$\begin{aligned}\psi(x) &\to \psi'(x) = R(x)P_+\psi(x) + L(x)P_-\psi(x), \\ \bar{\psi}(x) &\to \bar{\psi}'(x) = \bar{\psi}(x)P_+L^\dagger(x) + \bar{\psi}(x)P_-R^\dagger(x).\end{aligned} \tag{A8}$$

The projectors are defined in the usual way, $P_\pm = (1 \pm \gamma_5)/2$, and project onto fields with definite chirality,

$$\begin{aligned}\psi_R &= P_+\psi, & \psi_L &= P_-\psi, \\ \bar{\psi}_R &= \bar{\psi}P_-, & \bar{\psi}_L &= \bar{\psi}P_+.\end{aligned} \tag{A9}$$

Crucial for the local invariance is the nontrivial transformation of the source fields

$$v_\mu + a_\mu \to v'_\mu + a'_\mu = R(v_\mu + a_\mu)R^\dagger + iR\partial_\mu R^\dagger, \tag{A10}$$

$$v_\mu - a_\mu \to v'_\mu - a'_\mu = L(v_\mu - a_\mu)L^\dagger + iL\partial_\mu L^\dagger, \tag{A11}$$

$$s + p \to s' + p' = L(s + p)R^\dagger, \tag{A12}$$

$$s - p \to s' - p' = R(s - p)L^\dagger. \tag{A13}$$

(For notational simplicity we drop from now on the argument x). The invariance is more easily seen if we express the Lagrangian in terms of left- and right-handed fields,

$$\begin{aligned}\mathcal{L}_{\mathrm{Source}} = {} & \bar{\psi}_R\gamma_\mu[v_\mu + a_\mu]\psi_R + \bar{\psi}_L\gamma_\mu[v_\mu - a_\mu]\psi_L \\ & + \bar{\psi}_L[s + p]\psi_R + \bar{\psi}_R[s - p]\psi_L,\end{aligned} \tag{A14}$$

which obviously is invariant under global transformations. Note that global transformations leave $\mathcal{L}_{\mathrm{QCD}}$ and $\mathcal{L}_{\mathrm{Source}}$ independently invariant. Under local transformations the derivative part of $\mathcal{L}_{\mathrm{QCD}}$ produces extra terms which are cancelled by the derivative terms in (A10) and (A11). The reason why this cancellation works is related to the fact that the currents are the conserved Noether currents associated with chiral transformations and hence stem from local variations of the derivative term in the Lagrangian.

The Lagrangian $\mathcal{L}$ can be conveniently rewritten in a form that makes the local invariance more transparent.

First, the source term in (A14) suggests to introduce sources for right- and left-handed currents,

$$r_\mu = v_\mu + a_\mu, \qquad l_\mu = v_\mu - a_\mu, \tag{A15}$$

which transform according to

$$\begin{aligned} r_\mu &\to r'_\mu = R r_\mu R^\dagger + iR\partial_\mu R^\dagger, \\ l_\mu &\to l'_\mu = L l_\mu L^\dagger + iL\partial_\mu L^\dagger. \end{aligned} \tag{A16}$$

Vector and axial-vector currents are then obtained by

$$V^a_\mu(x) = i\left[\frac{\delta S}{\delta r^a_\mu(x)} + \frac{\delta S}{\delta l^a_\mu(x)}\right], \tag{A17}$$

$$A^a_\mu(x) = i\left[\frac{\delta S}{\delta r^a_\mu(x)} - \frac{\delta S}{\delta l^a_\mu(x)}\right]. \tag{A18}$$

The right- and left-handed sources allow the definition of covariant derivatives

$$D^R_\mu = D^{\text{color}}_\mu - ir_\mu, \qquad D^L_\mu = D^{\text{color}}_\mu - il_\mu, \tag{A19}$$

where D^{color}_μ is the covariant derivative with respect to local $SU(3)$ color transformations. By construction, $D^R_\mu \psi_R$, $D^L_\mu \psi_L$ transform as the chiral fields themselves, and $\mathcal{L}$ is simply given by

$$\mathcal{L} = \bar\psi_R \gamma_\mu D^R_\mu \psi_R + \bar\psi_L \gamma_\mu D^L_\mu \psi_L + \mathcal{L}_{\text{Gauge}}, \tag{A20}$$

where $\mathcal{L}_{\text{Gauge}}$ is the gauge field part of the QCD Lagrangian containing the gluon fields $G^a_\mu(x)$. Obviously, (A20) is invariant under local chiral transformations.

Having $\mathcal{L}$ in hand we can now define a generating functional for correlation functions involving the currents and densities,

$$Z_{\text{QCD}}[r_\mu, l_\mu, s, p] = \frac{1}{Z_0}\int \mathcal{D}[G_\mu, \bar\psi, \psi] e^{-\int d^4x \mathcal{L}[r_\mu, l_\mu, s, p]}, \tag{A21}$$

where Z_0 denotes the partition function, i.e. Z_{QCD} for vanishing sources.[17] Taking functional derivatives with respect to the sources one generates all possible correlation functions involving the currents and densities; the generating functional for connected correlation functions can be defined as usual by the logarithm of Z_{QCD}.

The matching to the chiral effective theory is now done by requiring that the generating functional in the chiral effective theory is the same as the one in the fundamental theory,

$$Z_{\text{QCD}}[r_\mu, l_\mu, s, p] = Z_{\text{chiral}}[r_\mu, l_\mu, s, p], \tag{A22}$$

$$Z_{\text{chiral}}[r_\mu, l_\mu, s, p] = \frac{1}{Z_0}\int \mathcal{D}[\pi] e^{-\int d^4x \mathcal{L}_{\text{chiral}}[r_\mu, l_\mu, s, p]}. \tag{A23}$$

The equality in (A22) is meant in the sense that the two sides coincide order by order in a low-energy expansion, where the long-distance correlation functions are dominated by the pion pole [29]. Correlation functions in the effective theory are obtained by the same functional derivatives as in the underlying theory. Provided the generating functionals, as functions of the sources, are the same, arbitrary correlation functions also agree. Moreover, the QCD symmetries are carried over to the effective theory, i.e. the Ward identities of QCD are correctly reproduced by the effective theory. Consequently, the right-hand side must also be invariant under local chiral transformations, and this invariance provides one constraint in the construction of $\mathcal{L}_{\text{chiral}}$. Other constraints are provided by parity (P) and charge conjugation (C).

The effective Lagrangian $\mathcal{L}_{\text{chiral}}[r_\mu, l_\mu, s, p]$ is obtained in a systematic low-energy expansion, and it has been derived by Gasser and Leutwyler through next-to-leading order [1,2]. We do not repeat their result here but emphasize that the local chiral invariance implies that the sources for the right- and left-handed currents can only enter the effective Lagrangian through the covariant derivative

$$D_\mu \Sigma = \partial_\mu \Sigma + i\Sigma r_\mu - i l_\mu \Sigma \tag{A24}$$

on the usual chiral field Σ, and through the field strength tensors

$$\begin{aligned} r_{\mu\nu} &= \partial_\mu r_\nu - \partial_\nu r_\mu + i[r_\mu, r_\nu], \\ l_{\mu\nu} &= \partial_\mu l_\nu - \partial_\nu l_\mu + i[l_\mu, l_\nu]. \end{aligned} \tag{A25}$$

The transformation behavior of these objects is as expected, taking into account $\Sigma \to L\Sigma R^\dagger$,

$$\begin{gathered} D_\mu \Sigma \to L(D_\mu \Sigma)R^\dagger, \qquad r_{\mu\nu} \to R r_{\mu\nu} R^\dagger, \\ l_{\mu\nu} \to L l_{\mu\nu} L^\dagger. \end{gathered} \tag{A26}$$

2. Generating functional in the Symanzik effective theory

Following the development in the continuum, we want to define a generating functional in the Symanzik effective theory, which may then be matched to the chiral effective theory. As before we want to obtain the currents and densities by taking derivatives with respect to the source fields. As we will see this is not as straightforward as in continuum QCD. For simplicity we will deal here only with the currents and ignore the densities. This reveals the main obstacles in the procedure.

As in the continuum case we want to define a source term in the Lagrangian, such that taking the derivatives with respect to sources produce the Symanzik currents, given in (11) and (12). In addition, we want to do this in a

[17] Strictly speaking, the scalar source should not vanish but be set to the physical quark mass.

way that maintains invariance under local chiral transformations, since this symmetry provides one of the links in the matching to the chiral effective theory.

It is illustrative to first show that the naive generalization of the continuum case fails in this respect. Suppose we write down a source term that directly couples source fields to the vector and axial-vector current,

$$\mathcal{L}_{\text{Source,Sym}} = v^a(x) V^a_{\mu,\text{Sym,Loc}}(x) + a^a_\mu(x) A^a_{\mu,\text{Sym,Loc}}(x). \tag{A27}$$

Just as in the continuum—cf. Eqs. (A4) and (A5)—functional derivatives with respect to $v^a(x)$, $a^a(x)$ produce the desired currents. However, local invariance is lost: The $O(a)$ corrections in the currents and the derivative terms in (A10) and (A11), generate $O(a)$ terms under local chiral transformations that are not cancelled by the variation of the Symanzik effective action in (10). That is of course no surprise; it simply reflects the fact that chiral symmetry is explicitly broken in the Symanzik effective theory and that the currents in (11) and (12) are not Noether currents associated with exact chiral symmetries.

In order to maintain local chiral invariance we proceed differently and introduce separate sources fields for the $O(a)$ corrections in the currents. Our source Lagrangian has the form

$$\mathcal{L}_{\text{Source,Sym}} = \mathcal{L}_{\text{Source,ct}} + \mathcal{L}_{\text{Source},a}. \tag{A28}$$

The first term with subscript "ct" is the familiar one from continuum QCD, defined in (A2). As before, one can rewrite it in terms of right- and left-handed sources using (A15). The second part reads

$$\begin{aligned}\mathcal{L}_{\text{Source},a} = {} & (D^L_\nu \bar\psi_L) i\sigma_{\mu\nu} C_V r_{V,\mu} \psi_R + \bar\psi_L i\sigma_{\mu\nu} l_{V,\mu} C_V D^R_\nu \psi_R + (D^R_\nu \bar\psi_R) i\sigma_{\mu\nu} C_V^\dagger l_{V,\mu} \psi_L + \bar\psi_R i\sigma_{\mu\nu} r_{V,\mu} C_V^\dagger D^L_\nu \psi_L \\ & + (D^L_\mu \bar\psi_L)\gamma_5 C_A r_{A,\mu} \psi_R + \bar\psi_L \gamma_5 l_{A,\mu} C_A D^R_\mu \psi_R + (D^R_\mu \bar\psi_R)\gamma_5 C_A^\dagger l_{A,\mu} \psi_L + \bar\psi_R \gamma_5 r_{A,\mu} C_A^\dagger D^L_\mu \psi_L.\end{aligned} \tag{A29}$$

This is essentially nothing but a source term for the $O(a)$ corrections to the currents as given in (30) and (31). We have introduced sources $r^a_{X,\mu}$, $l^a_{X,\mu}$, $X = V$ or A, which transform according to

$$r_{X,\mu} \to r'_{X,\mu} = R r_{X,\mu} R^\dagger \qquad l_{X,\mu} \to l'_{X,\mu} = L l_{X,\mu} L^\dagger. \tag{A30}$$

Note that this is the transformation law under *local* transformations even though there are no terms involving derivatives of L and R. Note also that $\mathcal{L}_{\text{Source},a}$ contains the covariant derivatives D^R_μ, D^L_μ, defined in (A19), which involve the sources l_μ, r_μ for the continuum parts in the Symanzik currents.

It is easily checked that the source term (A29) is invariant under local chiral transformations (taking into account the transformation laws for C_V, C_A given in (29)). Therefore, also the total Lagrangian

$$\mathcal{L} = \mathcal{L}_{\text{Sym}} - i\mathcal{L}_{\text{Source,Sym}} \tag{A31}$$

is locally invariant. The currents are then obtained from $S = \int d^4x \mathcal{L}(x)$ according to

$$V^a_{\mu,\text{Sym}}(x) = i\left[\frac{\delta S}{\delta r^a_\mu(x)} + \frac{\delta S}{\delta l^a_\mu(x)} + \frac{\delta S}{\delta r^a_{V,\mu}(x)} + \frac{\delta S}{\delta l^a_{V,\mu}(x)}\right], \tag{A32}$$

$$A^a_{\mu,\text{Sym}}(x) = i\left[\frac{\delta S}{\delta r^a_\mu(x)} - \frac{\delta S}{\delta l^a_\mu(x)} + \frac{\delta S}{\delta r^a_{A,\mu}(x)} - \frac{\delta S}{\delta l^a_{A,\mu}(x)}\right], \tag{A33}$$

which is a generalization of the prescription in the continuum, (A17) and (A18). Note that we implicitly assume here that the spurion fields A, C_V, C_A are set to their physical values $a\bar c_{\text{SW}}$, $a\bar c_V$, $a\bar c_A$ after the derivatives have been taken.

So far we focused on the invariance under local chiral transformations. For the matching to the chiral effective theory the discrete symmetries P and C are also needed. In addition, there is one property in the source term that we also have to preserve. The source term in (A29) depends on the sources and the spurion fields C_V and C_A. The dependence is such that the vector current sources r_V, l_V only couple to C_V and the axial-vector sources only to C_A. A mixed term, involving $C_A r_{V,\mu}$ for example, is not present. It is mandatory to preserve this feature, otherwise the vector current in the effective theory may end up with a contribution proportional to $\bar c_A$, which is certainly not the case. In order to achieve this we choose to generalize the source term without changing the results for the currents derived from it.

Instead of one spurion field C_V we introduce two of them, $C_{V,1}$ and $C_{V,2}$, and make the replacements

$$C_V r_{V,\mu} \to C_{V,1} r_{V,\mu} \qquad l_{V,\mu} C_V \to l_{V,\mu} C_{V,2}. \tag{A34}$$

The symmetry properties of $\mathcal{L}_{\text{Source},a}$ remain unchanged if both $C_{V,1}$ and $C_{V,2}$ transform as C_V, and if both have the same physical value $a\bar c_V$. However, the source term is now invariant under more general symmetry transformations, namely

$$\begin{aligned} r_{V,\mu} &\to H_V r_{V,\mu} R^\dagger, & C_{V,1} &\to L C_{V,1} H_V^\dagger, \\ l_{V,\mu} &\to L l_{V,\mu} G_V^\dagger, & C_{V,2} &\to G_V C_{V,2} R^\dagger, \end{aligned} \tag{A35}$$

where H_V and G_V are two independent local $SU(2)$ matrices. The origin of these two *hidden local symmetries* is the fact that the right- and left-handed sources and the spurions

$C_{V,i}$ only appear next to each other in the source term. Note that we recover the previously discussed transformation laws with $H_V = R$ and $G_V = L$.

The same generalization can be done with the axial-vector part in the source term after we have introduced $C_{A,1}$ and $C_{A,2}$ and postulated the transformation behavior

$$\begin{aligned} r_{A,\mu} &\to H_A r_{A,\mu} R^\dagger, \qquad C_{A,1} \to L C_{A,1} H_A^\dagger, \\ l_{A,\mu} &\to L l_{A,\mu} G_A^\dagger, \qquad C_{A,2} \to G_A C_{A,2} R^\dagger. \end{aligned} \tag{A36}$$

Since the symmetries H_A, G_A are independent of the ones in the vector current part we can no longer form invariants with vector current sources and axial-vector spurions $C_{A,i}$ and vice-versa. This will become important in the next section where we construct the currents in the chiral effective theory.

In analogy to (A21) we can now define a generating functional in the Symanzik effective theory. The number of external fields, however, has grown significantly,

$$\begin{aligned} Z_{\mathrm{Sym}} = Z_{\mathrm{Sym}}[&r_\mu, l_\mu, r_{V,\mu}, l_{V,\mu}, r_{A,\mu}, l_{A,\mu}, A, C_{V,1}, \\ &C_{V,2}, C_{A,1}, C_{A,2}], \end{aligned} \tag{A37}$$

and here we still have not included any sources associated with the scalar and pseudoscalar density. Apparently, the method of constructing correlation functions via a generating functional loses its simplicity away from the continuum limit. In the naive continuum limit (A37) reduces to Z_{QCD} with its dependence on r_μ, l_μ only.

3. Matching to WChPT

Similarly to the continuum case we now match the Symanzik effective theory to Wilson ChPT by demanding that the generating functionals in both theories agree

$$Z_{\mathrm{Sym}} = Z_{\mathrm{chiral}}, \tag{A38}$$

where the right-hand side is defined in analogy to (A23). For simplicity we have dropped the dependence on the large number of external fields, specified in (A37).

The effective Lagrangian entering the right-hand side in (A38) is built in terms of the pseudoscalar field Σ and its covariant derivative $D_\mu \Sigma$ as well as all external fields. Many terms have already been constructed and can be found in the literature. First, one finds the familiar Gasser-Leutwyler Lagrangian [1,2], which provides the continuum part. Terms involving the spurion field A are given in Ref. [6]. Hence we focus here on the new contributions stemming from the $O(a)$ terms in the currents, i.e. those involving the fields $r_{V,\mu}$, $l_{V,\mu}$, $r_{A,\mu}$, $l_{A,\mu}$, $C_{V,i}$, $C_{A,i}$.

It will be useful to introduce the following combinations:

$$\begin{aligned} S_{V,\mu} &= i(C_{V,1} r_{V,\mu} + l_{V,\mu} C_{V,2}), \\ S_{A,\mu} &= i(C_{A,1} r_{A,\mu} + l_{A,\mu} C_{A,2}), \\ A_{V,\mu} &= i(C_{V,1} r_{V,\mu} - l_{V,\mu} C_{V,2}), \\ A_{A,\mu} &= i(C_{A,1} r_{A,\mu} - l_{A,\mu} C_{A,2}). \end{aligned} \tag{A39}$$

These combinations are automatically invariant under the four hidden symmetries involving H_X, G_X with $X = V, A$. The factor i is just convention, inspired by the observation that the terms involving the continuum sources also always include an i. For convenience we have summarized the transformation behavior of these quantities in Table I. We also list the transformation rules under parity and charge conjugation, which one also needs for the construction of invariants under all symmetries.

We are now in the position to construct the terms of $O(a)$ that will contribute to the currents. For this we need invariants involving one power of the sources in (A39). Lorentz invariance then requires one covariant derivative D_μ. The simplest invariants that can be formed are

$$\langle D_\mu \Sigma A_{X,\mu}^\dagger + A_{X,\mu} (D_\mu \Sigma)^\dagger \rangle, \qquad X = V, A. \tag{A40}$$

Analogous invariants involving $S_{X,\mu}$ cannot be built since they violate charge conjugation.

We do not need to consider any invariants involving $D_\mu S_{X,\mu}$, $D_\mu A_{X,\mu}$ or terms quadratic in $S_{X,\mu}$ or $A_{X,\mu}$. Even though there exist nonvanishing invariants they will not give contributions to the vector or axial-vector current. The reason is that all these terms contain more than one source field and derivatives of C_X. Setting in the end the sources to zero and C_X to its constant final value all these terms vanish. We also do not consider the terms involving $\langle \Sigma^\dagger D_\mu \Sigma \pm \Sigma (D_\mu \Sigma)^\dagger \rangle$ since

$$\mathrm{tr}\,(\Sigma^\dagger D_\mu \Sigma) = \partial_\mu \ln \det \Sigma = 0. \tag{A41}$$

It turns out that the two terms given in (A40) are the only independent invariants at the order we are interested in.

TABLE I. Summary of transformation properties. The shorthand notation $(-1)^\mu$ in the vector quantities represents the sign flip in the spatial components under parity.

Field	Chiral	Charge Conj. C	Parity P
Σ	$L\Sigma L^\dagger$	Σ^T	$\Sigma^\dagger$
$D_\mu \Sigma$	$L D_\mu \Sigma R^\dagger$	$(D_\mu \Sigma)^T$	$(-1)^\mu (D_\mu \Sigma)^\dagger$
A	$LAR^\dagger$	A^T	$A^\dagger$
$r_{X,\mu}$	$H_X r_{X,\mu} R^\dagger$	$-l_{X,\mu}^T$	$(-1)^\mu l_{X,\mu}$
$l_{X,\mu}$	$L r_{X,\mu} G_X^\dagger$	$-r_{X,\mu}^T$	$(-1)^\mu r_{X,\mu}$
$C_{X,1}$	$L C_X H_X^\dagger$	$C_{X,1}^T$	$C_{X,1}^\dagger$
$C_{X,2}$	$G_X C_X R^\dagger$	$C_{X,2}^T$	$C_{X,2}^\dagger$
$S_{X,\mu}$	$L S_{X,\mu} R^\dagger$	$-S_{X,\mu}^T$	$-(-1)^\mu S_{X,\mu}^\dagger$
$A_{X,\mu}$	$L A_{X,\mu} R^\dagger$	$A_{X,\mu}^T$	$(-1)^\mu A_{X,\mu}^\dagger$

In the last section we stressed the importance of the local hidden symmetries for the correct chiral Lagrangian. If instead of (A35) and (A36) we assume the weaker transformation laws (A30) and (29), we can construct the additional invariants

$$\langle \Sigma^\dagger D_\mu \Sigma r_{X,\mu} + \Sigma (D_\mu \Sigma)^\dagger l_{X,\mu} \rangle \langle C_X \Sigma^\dagger + \Sigma C_X^\dagger \rangle. \quad \text{(A42)}$$

These invariants require to "split" the right- and left-handed source fields from the $O(a)$ spurions C_X and build products of two trace terms, something that is forbidden by the transformation rule (A35) and (A36).

It is straightforward to compute the $O(a)$ corrections to the currents following from (A40). In the case of the vector current the correction vanishes. For the axial-vector current we find the correction

$$2a\bar{c}_A \partial_\mu \langle T^a(\Sigma - \Sigma^\dagger) \rangle. \quad \text{(A43)}$$

In order to derive the complete currents including all $O(a)$ corrections we also need other terms which have already been given by Ref. [6]. Carrying over their notation, the relevant terms in the Lagrangian are

$$\begin{aligned} \mathcal{L} = {} & \frac{f^2}{4} \langle D_\mu \Sigma (D_\mu \Sigma)^\dagger \rangle + W_{45} \langle D_\mu \Sigma (D_\mu \Sigma)^\dagger \rangle \\ & \times \langle A \Sigma^\dagger + \Sigma A^\dagger \rangle + W_{10} \langle D_\mu \Sigma (D_\mu A)^\dagger \\ & + D_\mu A (D_\mu \Sigma)^\dagger \rangle + 2 W_A \langle D_\mu \Sigma A_{A,\mu}^\dagger + A_{A,\mu} (D_\mu \Sigma)^\dagger \rangle. \end{aligned} \quad \text{(A44)}$$

The last term, coming with a new LEC W_A, is the one we found above. We do not include the term with $X = V$ since its contribution to the vector current vanishes anyway.

Before deriving the currents we are free to make a field redefinition in order to simplify $\mathcal{L}$. Following Ref. [6] we perform the change $\Sigma \to \Sigma + \delta\Sigma$ with

$$\delta\Sigma = \frac{4W_{10}}{f^2} (\Sigma A^\dagger \Sigma - A) \quad \text{(A45)}$$

and obtain $\mathcal{L}$ in (A44) with the modified coefficient $W_{45} \to W_{45} + W_{10}$. Therefore, without loss we can drop the W_{10} term in (A44), as long as we consider only physical quantities.

In fact, if we work only to linear order in the sources, it is easy to see that the W_A and W_{10} terms in (A44) are proportional, so that W_A can also be absorbed into W_{45} by a change of variables [9]. This holds as long as we consider only physical quantities *and* if all currents are placed at different space-time points. In order to avoid the latter restriction, and maintain generality, we do not make this change of variables. Nevertheless, for the quantities we calculate in this paper, which are both physical and involve separated currents, the possibility of this change of variables implies that the LECs must enter in the combination [6] $W_{45}\bar{c}_{\rm SW} + W_A \bar{c}_A$. This provides a check on the results.

We can now compute the vector and axial-vector current according to (A32) and (A33), and find exactly the same expressions given before in Eqs. (43) and (44). We therefore conclude that we obtain identical results for the currents with the generating functional as with our "direct method."

APPENDIX B: COMPUTATION OF $Z_{A,\rm Loc}$.

In this appendix we derive the result (60) for the renormalization constant $Z_{A,\rm Loc}$, which follows from imposing the Ward-Takahashi identity (WTI) in (59). It will be useful to first show that (59) is indeed an identity in (massless) continuum ChPT. The generalization to WChPT is then straightforward.

We start by establishing

$$\begin{aligned} & \int d\vec{x} \epsilon^{abc} \langle \{ A^a_{0,\rm LO}(y_0 + t, \vec{x}) - A^a_{0,\rm LO}(y - t, \vec{x}) \} A^b_{0,\rm LO}(y) \mathcal{O}_{\rm out} \rangle \\ & = 2i \langle V^c_{0,\rm LO}(y) \mathcal{O}_{\rm out} \rangle, \end{aligned} \quad \text{(B1)}$$

at leading order in continuum ChPT. The operator $\mathcal{O}_{\rm out}$ is composed of fields with support outside the time interval $[y_0 - t, y_0 + t]$. We will not need to specify $\mathcal{O}_{\rm out}$ in detail until we consider the $O(a)$ corrections; for now, we only assume that it creates an even number of pion fields, that the two-pion component occurs at LO in a chiral expansion, and that the two-pion component contains no zero-momentum pions.

Expanding the vector current to leading order in the pion fields,

$$\begin{aligned} V^a_{\mu,\rm LO} &= \frac{f^2}{2} \langle T^a (\Sigma^\dagger \partial_\mu \Sigma + \Sigma \partial_\mu \Sigma^\dagger \rangle \\ &= i \epsilon^{abc} \pi^b \pi^c_\mu + O(\pi^4), \end{aligned} \quad \text{(B2)}$$

(using abbreviation $\pi^a_\mu = \partial_\mu \pi^a$), the right-hand side of the identity we want to show is simply given by

$$\text{rhs}_{\rm LO} = 2i \langle V^c_{0,\rm LO}(y) \mathcal{O}_{\rm out} \rangle_{\rm LO} \quad \text{(B3)}$$

$$= -2 \epsilon^{cab} \langle \pi^a(y) \pi^b_0(y) \mathcal{O}_{\rm out} \rangle_{\rm LO} \quad \text{(B4)}$$

where $\langle \mathcal{O} \rangle_{\rm LO}$ denotes functional integrals with $\mathcal{L}^{\rm LO}_{\rm chiral} = \pi^2_\mu/2$ in the Boltzmann weight, and interactions, which stem from the expansion

$$\begin{aligned} \mathcal{L}_{\rm chiral} &= \frac{f^2}{4} \langle \partial_\mu \Sigma \partial_\mu \Sigma^\dagger \rangle \\ &= \frac{1}{2} \left[\pi^2_\mu + \frac{1}{3f^2} \{ (\pi \cdot \pi_\mu)^2 - \pi^2 \pi^2_\mu \} \right] + O(\pi^6), \end{aligned} \quad \text{(B5)}$$

used at the lowest order giving a nonvanishing result. In fact, to evaluate $\text{rhs}_{\rm LO}$ we need no interactions, given that $\mathcal{O}_{\rm out}$ has a LO two-pion component.

For the left-hand side we need the expansion of the axial-vector current,

$$A^a_{\mu,\mathrm{LO}} = \frac{f^2}{2}\langle T^a(\Sigma^\dagger\partial_\mu\Sigma - \Sigma\partial_\mu\Sigma^\dagger)\rangle = if\left[\pi^a_\mu + \frac{2}{3f^2}\{\pi^a(\pi\cdot\pi_\mu) - \pi^a_\mu\pi^2\}\right] + O(\pi^5). \tag{B6}$$

The contribution with the leading-order term in both axial-vector currents on the left-hand side vanishes,

$$-f^2\int d\vec{x}\langle\{\pi^a_0(y_0+t,\vec{x}) - \pi^a_0(y_0-t,\vec{x})\}\pi^b_0(y)\mathcal{O}_{\mathrm{out}}\rangle_{\mathrm{LO}} = 0, \tag{B7}$$

since $\mathcal{O}_{\mathrm{out}}$ does not contain zero-momentum pion fields.

The nonvanishing contribution to the left-hand side stems from the three-pion term in one of the axial-vector currents or the four-pion term in $\mathcal{L}_{\mathrm{chiral}}$.

We obtain the first contribution using the three-pion term in the current $A^b_0(y)$, finding

$$\mathrm{lhs}_{1,\mathrm{LO}} = -\frac{2}{3}\epsilon^{abc}\int d\vec{x}\langle\{\pi^a_0(y_0+t,\vec{x}) - \pi^a_0(y_0-t,\vec{x})\} \times\{\pi^b(\pi\cdot\pi_0)(y) - \pi^b_0\pi^2(y)\}\mathcal{O}_{\mathrm{out}}\rangle_{\mathrm{LO}}. \tag{B8}$$

Performing the Wick contractions this can be written as

$$\mathrm{lhs}_{1,\mathrm{LO}} = 2\epsilon^{cab}\langle\pi^a(y)\pi^b_0(y)\mathcal{O}_{\mathrm{out}}\rangle_{\mathrm{LO}} \times\int d\vec{x}\partial_0\{G(t,\vec{x}-\vec{y}) - G(-t,\vec{x}-\vec{y})\}, \tag{B9}$$

where G denotes the massless pion propagator,

$$\langle\pi^a(x)\pi^b(y)\rangle_{\mathrm{LO}} = \delta^{ab}G(x-y) = \delta^{ab}\int\frac{d^4p}{(2\pi)^4}\frac{1}{p^2}e^{ip(x-y)}. \tag{B10}$$

The integral over $\vec{x}$ is easily evaluated. Using

$$\int d\vec{x}\partial_0 G(x) = \begin{cases} -\frac{1}{2} & \text{for } x_0 > 0 \\ +\frac{1}{2} & \text{for } x_0 < 0 \end{cases} \tag{B11}$$

the integral reduces to -1 and we find that

$$\mathrm{lhs}_{1,\mathrm{LO}} = \mathrm{rhs}_{\mathrm{LO}}. \tag{B12}$$

We obtain the second contribution to the left-hand side using the three-pion term for $A^a_0(y_0 \pm t,\vec{x})$, yielding

$$\mathrm{lhs}_{2,\mathrm{LO}} = 2\epsilon^{abc}\int d\vec{x}\langle\{\pi^a(y_+)\pi^b_0(y_+)\partial_0 G(t,\vec{x}-\vec{y}) - \pi^a(y_-)\pi^b_0(y_-)\partial_0 G(-t,\vec{x}-\vec{y})\}\mathcal{O}_{\mathrm{out}}\rangle_{\mathrm{LO}}, \tag{B13}$$

where we introduced the shorthand notation $y_\pm = (y_0 \pm t,\vec{x})$.

The third contribution stems from the four-pion terms in the chiral Lagrangian (B5), and we find

$$\mathrm{lhs}_{3,\mathrm{LO}} = \frac{1}{6}\epsilon^{abc}\int d\vec{x}\left\langle\{\pi^a_0(y_+) - \pi^a_0(y_-)\} \times\int d^4z\{(\pi\cdot\pi_\mu)^2 - \pi^2\pi^2_\mu\}(z)\pi_0(y)\mathcal{O}_{\mathrm{out}}\right\rangle_{\mathrm{LO}}. \tag{B14}$$

This reduces to

$$\mathrm{lhs}_{3,\mathrm{LO}} = \epsilon^{abc}\int d^4z\,d\vec{x}\langle\pi^a(z)\pi^b_\mu(z)\{\partial_\mu\partial_0 G(y_+ - z) - \partial_\mu\partial_0 G(y_- - z) + \partial_0 G(y_+ - z)\partial_\mu - \partial_0 G(y_- - z)\partial_\mu\}\partial_0 G(z-y)\mathcal{O}_{\mathrm{out}}\rangle_{\mathrm{LO}}. \tag{B15}$$

Since

$$\int d\vec{x}\partial_\mu\partial_0 G(y_\pm - z) = -\delta_{\mu 0}\delta(y_0 \pm t - z_0), \tag{B16}$$

the first two terms in (B15) become

$$-\epsilon^{abc}\int d\vec{x}\langle\{\pi^a(y_+)\pi^b_0(y_+)\partial_0 G(t,\vec{x}-\vec{y}) - \pi^a(y_-)\pi^b_0(y_-)\partial_0 G(-t,\vec{x}-\vec{y})\}\mathcal{O}_{\mathrm{out}}\rangle_{\mathrm{LO}} \tag{B17}$$

where we renamed $\vec{z}$ as $\vec{x}$. Using (B11) for the integral over $\partial_0 G(y_\pm - z)$ the remaining two terms become

$$-\epsilon^{abc}\int_{y_0-t}^{y_0+t}dz_0\int d\vec{z}\langle\pi^a(z)\pi^b_\mu(z)\partial_\mu\partial_0 G(z-y)\mathcal{O}_{\mathrm{out}}\rangle_{\mathrm{LO}},$$

and after partial integration this can be written as

$$-\epsilon^{abc}\int d\vec{x}\langle\{\pi^a(y_+)\pi^b_0(y_+)\partial_0 G(t,\vec{x}-\vec{y}) - \pi^a(y_-)\pi^b_0(y_-)\partial_0 G(-t,\vec{x}-\vec{y})\}\mathcal{O}_{\mathrm{out}}\rangle_{\mathrm{LO}} + \epsilon^{abc}\int_{y_0-t}^{y_0+t}dz_0\int d\vec{z}\langle\pi^a(z)\partial_\mu\partial_\mu\pi^b(z)\partial_0 \times G(z-y)\mathcal{O}_{\mathrm{out}}\rangle_{\mathrm{LO}}.$$

Since $\partial^2_\mu\pi^b(z)$ is contracted with the on-shell fields in $\mathcal{O}_{\mathrm{out}}$ (recall our assumption!), the second line vanishes. The remaining first line is the same as in (B17). Hence, in total the third contribution reduces to

$$\mathrm{lhs}_{3,\mathrm{LO}} = -\mathrm{lhs}_{2,\mathrm{LO}}, \tag{B18}$$

so the second and third contributions cancel. This, together with Eq. (B12), proves the Ward-Takahashi identity (B1) to first nontrivial order in the chiral expansion.

Repeating this calculation with the lattice spacing corrections included is now straightforward. What changes are the expansions of the currents and the effective Lagrangian in terms of the pion fields:

$$\mathcal{L}_{\text{chiral}} = \frac{1}{2}(1+X_1)\pi_\mu^2 + \frac{1}{6f^2}[(1+X_1)(\pi\cdot\pi_\mu)^2 - (1+X_2)\pi^2\pi_\mu^2] + O(\pi^6), \tag{B19}$$

$$V^a_{\mu,\text{eff}} = i\epsilon^{abc}\pi^b\pi^c_\mu(1+X_1) + O(\pi^4), \tag{B20}$$

$$A^a_{\mu,\text{eff}} = if(1+Y_1)\pi^a_\mu + i\frac{2}{3f}[(1+Y_2)\pi^a(\pi\cdot\pi_\mu) - (1+Y_3)\pi^a_\mu\pi^2], \tag{B21}$$

where we introduced the coefficients

$$X_1 = \frac{16}{f^2}W_{45}\hat{a}\bar{c}_{\text{SW}}, \qquad X_2 = \frac{40}{f^2}W_{45}\hat{a}\bar{c}_{\text{SW}},$$
$$Y_1 = X_1 + \frac{8}{f^2}W_A\hat{a}\bar{c}_A, \qquad Y_2 = X_1 - \frac{4}{f^2}W_A\hat{a}\bar{c}_A, \tag{B22}$$
$$Y_3 = \frac{28}{f^2}W_{45}\hat{a}\bar{c}_{\text{SW}} + \frac{2}{f^2}W_A\hat{a}\bar{c}_A.$$

The modification of the kinetic term by the factor $1+X_1$ yields a slightly different pion propagator,

$$\langle\pi^a(x)\pi^b(y)\rangle_{\text{LO}(a)} = \frac{\delta^{ab}}{1+X_1}\langle\pi^a(x)\pi^b(y)\rangle_{\text{LO}} = \frac{\delta^{ab}}{1+X_1}G(x-y), \tag{B23}$$

with G defined in (B10) and $\langle\mathcal{O}\rangle_{\text{LO}(a)}$ denotes functional integrals with $\mathcal{L}^{\text{LO}}_{\text{chiral}} = (1+X_1)\pi_\mu^2/2$ in the Boltzmann weight. Notice that $1+X_1 = Z_\pi^{-1}$ [cf. (58)]. Hence, in terms of the renormalized pion fields

$$\tilde{\pi}^a(x) = Z_\pi^{-1/2}\pi^a(x) \tag{B24}$$

Eq. (B23) assumes its standard form

$$\langle\tilde{\pi}^a(x)\tilde{\pi}^b(y)\rangle_{\text{LO}(a)} = \delta^{ab}G(x-y). \tag{B25}$$

The right-hand side of the WTI now reads

$$\text{rhs}_{\text{LO}(a)} = -2\epsilon^{cab}(1+X_1)\langle\pi^a(y)\pi^b_\mu(y)\mathcal{O}_{\text{out}}\rangle_{\text{LO}(a)}, \tag{B26}$$

while the three contributions on the left-hand side are modified as follows:

$$\text{lhs}_{1,\text{LO}(a)} = \frac{[1+(3Y_1+Y_2+2Y_3)/3]}{(1+X_1)}(-2\epsilon^{cab}) \times\langle\pi^a(y)\pi^b_\mu(y)\mathcal{O}_{\text{out}}\rangle_{\text{LO}(a)}, \tag{B27}$$

$$\text{lhs}_{2,\text{LO}(a)} = \frac{[1+(3Y_1+Y_2+2Y_3)/3]}{(1+X_1)}(\text{lhs}_{2,+} - \text{lhs}_{2,-}), \tag{B28}$$

$$\text{lhs}_{2,\pm} = 2\epsilon^{abc}\int d\vec{x}\,\partial_0 G(\pm t, \vec{x}-\vec{y}) \times\langle\pi^a(y_\pm)\pi^b_0(y_\pm)\mathcal{O}_{\text{out}}\rangle_{\text{LO}(a)}, \tag{B29}$$

$$\text{lhs}_{3,\text{LO}(a)} = -\frac{[1+2Y_1+(X_1+2X_2)/3]}{(1+X_1)^2} \times(\text{lhs}_{2,+} - \text{lhs}_{2,-}). \tag{B30}$$

Here the factors in the numerator come from (B22) while those in the denominator arise from the presence of (one or two) pion propagators in the manipulations given earlier in the appendix.

To determine the renormalization constant we need the ratio of the two sides of the original WTI. It follows from (B26) and (B27) that

$$\frac{\text{lhs}_{1,\text{LO}(a)}}{\text{rhs}_{\text{LO}(a)}} = \frac{[1+(3Y_1+Y_2+2Y_3)/3]}{(1+X_1)^2}, \tag{B31}$$

independent of the detailed form of $\mathcal{O}_{\text{out}}$.

For the remaining ratios we need to specify the external fields. We take

$$\mathcal{O}^{\,c}_{\text{out}} = \epsilon^{cde}\tilde{\pi}^d(T,\vec{p})\tilde{\pi}^e(-T,-\vec{q}) \tag{B32}$$

with $\vec{p}, \vec{q} \neq \vec{0}$. Here $\tilde{\pi}^d(T,\vec{p})$ is the Fourier transform of $\tilde{\pi}^d(T,\vec{x})$ with respect to the three spatial coordinates. For this choice, the correlators we need are

$$\text{rhs}_{\text{LO}(a)} = -12\partial_0^T\{G(T-y_0,\vec{p})G(T+y_0,\vec{q})\}, \tag{B33}$$

$$\text{lhs}_{2,\pm} = 12\frac{\partial_0 G(\pm t,\vec{p}-\vec{q})}{(1+X_1)} \times\partial_0^T\{G(T-y_0\mp t,\vec{p})G(T+y_0\pm t,\vec{q})\}, \tag{B34}$$

where $\partial_0^T = \partial/\partial T$. For simplicity, and without loss of generality, we have set $\vec{y}=0$, which avoids an overall phase.

To evaluate these expressions we need the hybrid position-momentum pion propagator,

$$G(t,\vec{p}) = \int\frac{dp_0}{2\pi}\frac{e^{ip_0t}}{p_0^2+\vec{p}^2} = \frac{e^{-E_pt}}{2E_p}, \qquad t\geq 0, E_p = |\vec{p}|, \tag{B35}$$

using which we find

$$\text{rhs}_{\text{LO}(a)} = \frac{3(E_p+E_q)}{E_pE_q}e^{[-(E_p+E_q)T+y_0(E_p-E_q)]}, \tag{B36}$$

$$\text{lhs}_{2,\pm} = \frac{\pm 1}{(1+X_1)} \times\frac{3(E_p+E_q)}{2E_pE_q}e^{[-|t|E_{p-q}-(E_p+E_q)T+(y_0\pm t)(E_p-E_q)]}, \tag{B37}$$

where $E_{p-q} = |\vec{p} - \vec{q}|$. Inserting these results into Eqs. (B26), (B28), and (B30) we obtain

$$\frac{\mathrm{lhs}_{2,\mathrm{LO}(a)}}{\mathrm{rhs}_{\mathrm{LO}(a)}} = \frac{[1 + (3Y_1 + Y_2 + 2Y_3)/3]}{(1 + X_1)^2} \times \cosh[t(|\vec{p}| - |\vec{q}|)]\exp[-|t||\vec{p} - \vec{q}|], \quad \text{(B38)}$$

$$\frac{\mathrm{lhs}_{3,\mathrm{LO}(a)}}{\mathrm{rhs}_{\mathrm{LO}(a)}} = -\frac{[1 + 2Y_1 + (X_1 + 2X_2)/3]}{(1 + X_1)^3} \times \cosh[t(|\vec{p}| - |\vec{q}|)]\exp[-|t||\vec{p} - \vec{q}|], \quad \text{(B39)}$$

and thus, finally,

$$\frac{\mathrm{lhs}_{\mathrm{LO}(a)}}{\mathrm{rhs}_{\mathrm{LO}(a)}} = \frac{\mathrm{lhs}_{1,\mathrm{LO}(a)} + \mathrm{lhs}_{2,\mathrm{LO}(a)} + \mathrm{lhs}_{3,\mathrm{LO}(a)}}{\mathrm{rhs}_{\mathrm{LO}(a)}} \quad \text{(B40)}$$

$$= 1 + \frac{8\hat{a}}{f^2}(W_{45}\bar{c}_{\mathrm{SW}} + W_A\bar{c}_A)\{1 - \cosh[t(|\vec{p}| - |\vec{q}|)] \times \exp[-|t||\vec{p} - \vec{q}|]\}. \quad \text{(B41)}$$

This ratio should be unity when multiplied by the renormalization factor $(Z_{A,\mathrm{Loc}}/Z_A^0)^2$, leading to the result (60) in the main text.

[1] J. Gasser and H. Leutwyler, Ann. Phys. (N.Y.) **158**, 142 (1984).
[2] J. Gasser and H. Leutwyler, Nucl. Phys. **B250**, 465 (1985).
[3] K. G. Wilson, Phys. Rev. D **10**, 2445 (1974).
[4] S. R. Sharpe and R. L. Singleton, Jr., Phys. Rev. D **58**, 074501 (1998).
[5] G. Rupak and N. Shoresh, Phys. Rev. D **66**, 054503 (2002).
[6] S. R. Sharpe and J. M. S. Wu, Phys. Rev. D **71**, 074501 (2005).
[7] N. Shoresh (private communication).
[8] S. Aoki and O. Bär, Proc. Sci., LAT2007 (2007) 062.
[9] S. R. Sharpe, *Lectures Given at the Nara Workshop* (Nara, Japan, 2005).
[10] L. H. Karsten and J. Smit, Nucl. Phys. **B183**, 103 (1981).
[11] M. Bochicchio *et al.*, Nucl. Phys. **B262**, 331 (1985).
[12] L. Maiani and G. Martinelli, Phys. Lett. B **178**, 265 (1986).
[13] M. Lüscher, S. Sint, R. Sommer, and P. Weisz, Nucl. Phys. **B478**, 365 (1996).
[14] S. Sint and P. Weisz, Nucl. Phys. **B502**, 251 (1997).
[15] K. Symanzik, Nucl. Phys. **B226**, 187 (1983).
[16] K. Symanzik, Nucl. Phys. **B226**, 205 (1983).
[17] B. Sheikholeslami and R. Wohlert, Nucl. Phys. **B259**, 572 (1985).
[18] O. Bär, G. Rupak, and N. Shoresh, Phys. Rev. D **70**, 034508 (2004).
[19] S. Scherer and H. W. Fearing, Phys. Rev. D **52**, 6445 (1995).
[20] G. Martinelli, C. T. Sachrajda, and A. Vladikas, Nucl. Phys. **B358**, 212 (1991).
[21] G. Martinelli, S. Petrarca, C. T. Sachrajda, and A. Vladikas, Phys. Lett. B **311**, 241 (1993).
[22] D. S. Henty, R. D. Kenway, B. J. Pendleton, and J. I. Skullerud, Phys. Rev. D **51**, 5323 (1995).
[23] K. Jansen *et al.*, Phys. Lett. B **372**, 275 (1996).
[24] M. Lüscher, S. Sint, R. Sommer, and H. Wittig, Nucl. Phys. **B491**, 344 (1997).
[25] M. Lüscher, arXiv:hep-lat/9802029.
[26] G. Martinelli *et al.*, Nucl. Phys. **B445**, 81 (1995).
[27] S. Aoki, O. Bär, and B. Biedermann, Phys. Rev. D **78**, 114501 (2008).
[28] S. Aoki, Phys. Rev. D **68**, 054508 (2003).
[29] H. Leutwyler, Ann. Phys. (N.Y.) **235**, 165 (1994).

Published for SISSA by Springer

Received: *February 23, 2010*
Accepted: *March 21, 2010*
Published: *April 13, 2010*

The epsilon regime with twisted mass Wilson fermions

Oliver Bär,[a] **Silvia Necco**[b] **and Andrea Shindler**[c]

[a] *Institut für Physik, Humboldt Universität zu Berlin, Newtonstrasse 15, 12489 Berlin, Germany*
[b] *CERN, Physics Departement, 1211 Geneva 23, Switzerland*
[c] *Instituto de Física Teórica UAM/CSIC, Universidad Autónoma de Madrid, Cantoblanco E-28049 Madrid, Spain*

E-mail: obaer@physik.hu-berlin.de, necco@mail.cern.ch, andrea.shindler@uam.es

Abstract: We investigate the leading lattice spacing effects in mesonic two-point correlators computed with twisted mass Wilson fermions in the epsilon-regime. By generalizing the procedure already introduced for the untwisted Wilson chiral effective theory, we extend the continuum chiral epsilon expansion to twisted mass WChPT. We define different regimes, depending on the relative power counting for the quark masses and the lattice spacing. We explicitly compute, for arbitrary twist angle, the leading $O(a^2)$ corrections appearing at NLO in the so-called GSM* regime. As in untwisted WChPT, we find that in this situation the impact of explicit chiral symmetry breaking due to lattice artefacts is strongly suppressed. Of particular interest is the case of maximal twist, which corresponds to the setup usually adopted in lattice simulations with twisted mass Wilson fermions. The formulae we obtain can be matched to lattice data to extract physical low energy couplings, and to estimate systematic uncertainties coming from discretization errors.

Keywords: Lattice QCD, Lattice Gauge Field Theories, Chiral Lagrangians, Lattice Quantum Field Theory

ArXiv ePrint: 1002.1582

Contents

---

1 Introduction

A precise matching of results obtained in lattice QCD with the predictions of the chiral effective theory is an important test of strong dynamics at low energies. In particular, it provides a way to check if chiral symmetry is spontaneously broken according to the expected pattern and eventually to extract from first principles the low-energy couplings which parametrize the effective theory.

With many recent calculations with $N_f = 2, 2+1$ getting close to the physical point (see the plenary talks [1, 2] presented at the 2009 lattice conference and references therein) this

goal starts now to be realistic, although a reliable estimation of systematic uncertainties is still problematic. In particular, approaching the chiral limit in a finite box implies a detailed control over finite-size effects. The chiral effective theory provides information also on the volume dependence of physical observables: in the asymptotic region, where $M_\pi L \gg 1$, volume effects are expected to be exponentially suppressed. For practical purposes, for instance for the extraction of the pion decay constant, the empirical criterion $M_\pi L \gtrsim 4$ seems to be necessary in order to keep effects well below the statistical error typically present.

An alternative approach is to study QCD in a different kinematic corner, namely the ϵ-regime [3, 4]: here finite-volume effects are polynomial instead of exponentially suppressed, and one can exploit the finite-size scaling properties of given observables in order to extract information about infinite-volume quantities. Since the chiral expansion obeys a different power counting with respect to the infinite volume, higher order corrections will be different: the matching of the chiral effective theory with lattice QCD will then provide low energy couplings which will be affected by different systematic uncertainties. A general agreement among those independent determinations is a good check on the validity of the approach.

Many quenched simulations in the ϵ-regime have been performed [5–13], using Dirac operators which satisfy the Ginsparg-Wilson relation [14]. More recently, ϵ-regime calculations with Ginsparg-Wilson fermions have been carried out also in the dynamical case, with $N_f = 2$ [15–20] and $N_f = 2 + 1$ [21, 22]. Since the Ginsparg-Wilson relation ensures exact chiral symmetry at finite lattice spacing [23], it guarantees many theoretical advantages, for instance the possibility to reach arbitrarily small quark masses and a continuum-like renormalization pattern. The price to pay is the high computational cost, which makes these simulations very challenging. In particular, approaching the continuum limit or exploring a broad range of physical volumes requires very big efforts.

Recently it has been realized that simulations in the ϵ-regime are feasible also for Wilson-type fermions. In [24–26] first results obtained with Wilson twisted mass fermions have been presented. The use of a PHMC algorithm combined with an exact reweighting of a few low modes of the lattice operator turned out to be an important ingredient in this study. Analogously, in [27, 28] a reweighting algorithm has been proposed and successfully applied to simulate nHYP improved Wilson fermions in the ϵ-regime (see also ref. [29]). In both cases continuum chiral perturbation theory (ChPT) describes the lattice data very well, although chiral symmetry is explicitly broken for Wilson-type fermions. Even though a scaling study would be necessary to systematically investigate lattice artifacts, this suggests that the impact of chiral symmetry breaking is mild and that it can be legitimate to match lattice results with the expressions of continuum ChPT.

We address this issue by means of Wilson Chiral perturbation theory (WChPT) [30, 31], which can be generalized to the twisted mass case [32–37]. In refs. [38, 39] we extended untwisted WChPT to the ϵ-regime.[1]

The relevant issue is the relative power counting of the quark mass and the lattice

[1] Recently, WChPT in the ϵ-regime has been adopted also to study the spectral density of the Wilson Dirac Operator at fixed topology [40].

spacing (in units of $\Lambda_{\rm QCD}$). It turns out that for $m \sim a\Lambda^2_{\rm QCD}$ (GSM regime) the explicit breaking of chiral symmetry is still dominated by the quark mass, and lattice artifacts are highly suppressed. For mesonic two-point functions, the lattice spacing corrections start to appear at NNLO. On the other hand, if $m \sim a^2\Lambda^3_{\rm QCD}$ (Aoki regime), lattice artifacts compete with the quark mass, and corrections are substantial since they contribute already at LO.

In refs. [38, 39] we also introduced an intermediate regime (GSM*), where discretization effects appear at NLO, and for this case we computed the leading corrections for several correlators. An important observation is that in this intermediate regime only one additional low energy coupling appears, namely c_2 [30]. In this paper we extend this study to the twisted mass case. While there will be many features in common to the untwisted case, some new aspects arise and will be discussed.

The paper is organized as follows: in section 2 we define the chiral Lagrangian of twisted WChPT, currents and densities, and we recall the main related properties and definitions in an infinite volume; in section 3 we define the effective theory in the ϵ-regime, we discuss the power counting and the rôle of the vacuum; in section 4 we compute leading corrections in the GSM* regime for several 2-point correlators and we give numerical estimates for these corrections. Finally, we draw our conclusions in section 5.

2 Chiral perturbation theory for twisted mass Wilson fermions

2.1 The chiral Lagrangian

Correlation functions computed with lattice simulations are affected by discretization errors, which can be analyzed using effective field theory. To obtain the correct form of the effective Lagrangian one proceeds in two steps [30]. First, one matches the lattice action used in the simulations with the appropriate Symanzik effective action. The Symanzik action is subsequently matched to a chiral Lagrangian which contains the standard continuum terms and appropriate additional operators that transform under chiral symmetry as the operators of the Symanzik effective theory. These additional operators describe the effects of the nonzero lattice spacing a.[2]

In this paper we are interested in lattice actions with Wilson twisted mass fermions [43]. These actions are sometimes called Wilson-type fermions because they represent a simple generalization of the standard Wilson action. Their explicit form will not be needed in this paper (see ref. [44] for a review). We just recall that in our analysis we consider the lattice action with $N_f = 2$ degenerate flavours, and bare mass parameters m_0 and $\mu_{\rm q}$. The untwisted quark mass $m_{\rm R} = Z_m(m_0 - m_{\rm cr})$ and the twisted quark mass $\mu_{\rm R} = Z_{\rm P}^{-1}\mu_{\rm q}$ are renormalized with renormalization factors computed in a mass independent scheme, and $m_{\rm cr}$ denotes the critical mass. Wilson twisted mass lattice QCD in the continuum limit is then equivalent to QCD [43] with a physical quark mass $m_{\rm P} = \sqrt{m_{\rm R}^2 + \mu_{\rm R}^2}$. From now on we will drop the subscript R and all the quark masses are considered, unless specified differently, as renormalized in a mass independent scheme.

[2] For introductory lecture notes see ref. [41, 42].

The chiral Lagrangian in twisted mass WChPT is essentially the same as for the untwisted case [33, 35–37, 45]. The only difference is a mass matrix that contains, besides an untwisted mass m, the twisted mass μ.

In WChPT there are two sources of explicit chiral symmetry breaking, the quark masses m, μ and the lattice spacing a. The power counting is determined by the relative size of these parameters. The literature [34, 36] distinguishes two regimes with different power counting: (i) the *generically small quark mass* (GSM) regime where the quark mass is $\sim a\Lambda_{\rm QCD}^2$ and (ii) the Aoki regime where the quark mass is $\sim a^2\Lambda_{\rm QCD}^3$. Depending on the particular regime, the LO Lagrangian differs. Explicitly, in the GSM regime at leading order the chiral Lagrangian reads

$$\mathcal{L}_2 = \frac{F^2}{4}\mathrm{Tr}(\partial_\mu U \partial_\mu U^\dagger) - \frac{\Sigma}{2}\mathrm{Tr}(\mathcal{M}^\dagger U + U^\dagger \mathcal{M})\,. \tag{2.1}$$

F and Σ are the familiar low energy couplings (LECs) appearing at LO in the continuum chiral Lagrangian and U contains the pion fields in the usual way (see below). The mass matrix $\mathcal{M}$ is defined by (σ^a denotes the Pauli matrices)

$$\mathcal{M} = (m\mathbb{I} + i\mu\sigma^3)\,. \tag{2.2}$$

The field U and the matrix $\mathcal{M}$ are written in the so called twisted basis. There is no $\mathrm{O}(a)$ contribution in the chiral Lagrangian $\mathcal{L}_2$, since we have absorbed it in the definition of m, which therefore represents the so-called *shifted mass* [30].[3]

Eq. (2.2) can be used to define the *polar mass* $m_{\rm P}$ and a *twist angle* ω_0 by

$$\mathcal{M} = m_{\rm P} e^{i\omega_0\sigma^3}\,, \tag{2.3}$$

or, directly in terms of m and μ:

$$m_{\rm P} = \sqrt{m^2+\mu^2}\,, \qquad \tan\omega_0 = \frac{\mu}{m}\,. \tag{2.4}$$

The subscript '0' serves as a reminder that the angle ω_0 relates the two mass parameters in the chiral Lagrangian.[4] We emphasize that ω_0 is related to but not identical with the twist angle ω that we define in section 2.3.

We can easily go the so-called *physical basis*, where the quark mass matrix takes the standard form proportional to the identity, $\widetilde{\mathcal{M}} = m_{\rm P}\mathbb{I}$, by performing the following non-anomalous field transformation:

$$U = W\widetilde{U}W \qquad \text{with} \qquad W = \exp\left(i\frac{\omega_0\sigma^3}{2}\right). \tag{2.5}$$

Here $\widetilde{U}$ denotes the field in the physical basis.

[3] The shifted mass is sometimes denoted by m'. Here we drop the prime since we exclusively work with the shifted mass and we will never need the original mass parameter.

[4] Since we use the shifted mass to parametrize the chiral Lagrangian, the angle ω_0 defined in (2.4) does not coincide with the one in ref. [35].

If we move to the Aoki regime we have to add to the Lagrangian (2.1) the $O(a^2)$ corrections [46, 47]

$$\delta\mathcal{L}_{a^2} = \frac{F^2}{16} c_2 a^2 \left(\mathrm{Tr}(U + U^\dagger)\right)^2, \tag{2.6}$$

since these contribute already at LO in this regime. Therefore, we expect the corrections due to a nonzero lattice spacing to be much more pronounced in the Aoki regime. Additional chiral logarithms proportional to a^2 appear in one-loop results of various observables like the pion mass and pion scattering lengths [47, 48]. Moreover, in infinite volume nontrivial phase transitions become relevant, and the sign of the LEC c_2 plays a decisive rôle for the phase diagram of the theory [30].

The NLO terms linear in a can be found in refs. [31, 36], but these terms will not be needed in the following.

2.2 Currents and densities

The currents and densities in the effective theory can be computed by adding appropriate source terms to the partition function of the theory and differentiating the resulting generating functional with respect to the sources [36, 49]. Alternatively, the currents and densities can be obtained using a standard spurion analysis, as described in [49]. Both methods have been discussed in detail in the literature. Here we simply summarize what is relevant for our computation with Wilson twisted mass fermions.

We assume the following definitions for the currents and densities at the quark level:

$$S^0(x) = \overline{\psi}(x)\psi(x), \qquad P^a(x) = i\overline{\psi}(x)\gamma_5 T^a \psi(x), \tag{2.7}$$

$$A^a_\mu(x) = i\overline{\psi}(x)\gamma_\mu\gamma_5 T^a \psi(x), \qquad V^a_\mu(x) = i\overline{\psi}(x)\gamma_\mu T^a \psi(x). \tag{2.8}$$

$T^a, a = 1, \ldots, N_f^2 - 1$ are the Hermitean $\mathrm{SU}(N_f)$ generators satisfying the property $\mathrm{Tr}(T^a T^b) = \delta^{ab}/2$. For $N_f = 2$, $T^a = \sigma^a/2$. The corresponding currents and densities at LO in the chiral effective theory read

$$\mathcal{S}^0(x) = -\frac{\Sigma}{2}\mathrm{Tr}\left[U(x) + U^\dagger(x)\right], \tag{2.9}$$

$$\mathcal{P}^a(x) = i\frac{\Sigma}{2}\mathrm{Tr}\left[T^a(U(x) - U^\dagger(x))\right], \tag{2.10}$$

$$\mathcal{A}^a_\mu(x) = i\frac{F^2}{2}\mathrm{Tr}\left[T^a(U(x)^\dagger\partial_\mu U(x) - U(x)\partial_\mu U^\dagger(x))\right], \tag{2.11}$$

$$\mathcal{V}^a_\mu(x) = -i\frac{F^2}{2}\mathrm{Tr}\left[T^a(U(x)^\dagger\partial_\mu U(x) + U(x)\partial_\mu U^\dagger(x))\right]. \tag{2.12}$$

These are the familiar expressions from LO continuum ChPT. The leading corrections of $O(a)$ can be found in [36, 49]. They are of higher order and we will not need them explicitly in the following.

2.3 The PCAC mass and the twist angle

There are various ways to define a twist angle. A popular way that has often been used is by the ratio

$$\tan\omega = \frac{\mu}{m_{\mathrm{PCAC}}}. \tag{2.13}$$

The denominator is given by the PCAC mass, which is an observable, instead of the shifted mass m. The former is defined as usual by

$$m_{\mathrm{PCAC}} = \frac{\langle \partial_\mu A^a_\mu(x) P^a(y)\rangle}{2\langle P^a(x) P^a(y)\rangle}\,. \tag{2.14}$$

In the classical continuum limit the PCAC mass is equal to m, and therefore $\omega = \omega_0$. For nonzero lattice spacings this is true only at LO, but violated at higher order, as we will derive in section 4.2. Hence, usually we have $\omega \neq \omega_0$.

Quite generally, m_{PCAC} is a function of m, μ, the lattice spacing a and the volume V. In principle this function can be "inverted" to obtain the shifted mass m as function of the other parameters,

$$m_{\mathrm{PCAC}} = m_{\mathrm{PCAC}}(m,\mu,a,V) \quad \Rightarrow \quad m = m(m_{\mathrm{PCAC}},\mu,a,V)\,. \tag{2.15}$$

In practice this relation can be computed perturbatively in the chiral expansion. Once it is known it allows us to express other observables as functions of the measurable quantity m_{PCAC} instead of m. This will be the way we present our results in the latter sections.

A particularly interesting value for the twist angle is maximal twist, $\omega = \pi/2$, where automatic $\mathrm{O}(a)$ improvement is guaranteed [50]. According to our definition (2.13) maximal twist is given by a vanishing PCAC mass.

3 Effective theory in the epsilon regime

3.1 Epsilon expansion and power counting

The discussion on the power counting in the previous section assumed an infinite volume. Finite-size effects due to a finite volume $V = TL^3$ with $L, T \gg 1/\Lambda_{\mathrm{QCD}}$ can be systematically studied within ChPT [3, 4, 51]. If the pion Compton wavelength is much smaller than the size of the volume, $M_\pi L \gg 1$, finite-volume effects can be treated in the chiral effective theory by adopting the standard p-expansion, where the inverse box extensions are treated as small expansion parameters of the same order as the typical momenta: $1/L,\ 1/T \sim O(p)$. For asymptotically large volumes the finite-volume corrections are exponentially suppressed by factors $\exp(-M_\pi L)$.

On the other hand, for pion masses such that $M_\pi L \lesssim 1$ one probes the so-called ϵ-regime of QCD [52–54]. In this regime the pion zero mode contribution $1/M_\pi^2 V$ to the pion propagator will eventually diverge in the chiral limit. Hence its contribution cannot be treated perturbatively but has to be computed exactly. This is achieved by a reordering of the chiral expansion by means of summing up all Feynman graphs with an arbitrary number of zero modes propagators. In the ϵ-expansion one parametrizes the chiral field U according to

$$U(x) = U_0 \exp\left(\frac{i}{F}\xi^a(x)\sigma^a\right)\,, \tag{3.1}$$

where the constant $U_0 \in \mathrm{SU}(N_f)$ represents the collective zero-mode. The nonzero modes parametrized by ξ^a are still treated perturbatively. These satisfy the condition

$$\int_V d^4x\, \xi^a(x) = 0, \tag{3.2}$$

since the constant mode has been separated. The ϵ-expansion is now defined by using the counting rules

$$M_\pi^2 \sim \mathrm{O}(\epsilon^4), \quad 1/L,\ 1/T\ , \partial_\mu \sim \mathrm{O}(\epsilon), \quad \xi^a \sim \mathrm{O}(\epsilon). \tag{3.3}$$

With these counting rules the product $M_\pi^2 V$ counts as ϵ^0, just as its inverse. Consequently, all Feynman graphs that exclusively involve zero-mode propagators count as O(1) and are unsuppressed.

Once the counting for the pion mass is fixed, it determines the counting of the quark mass. In continuum ChPT the tree-level result $M_\pi^2 = 2Bm$, with $B = \Sigma/F^2$, fixes the counting $m \sim \mathrm{O}(\epsilon^4)$. The same line of argument has been applied to WChPT for untwisted masses m, and one obtains the same counting [38, 39]. Here we use it to deduce the counting for the polar mass m_{P} and the twisted mass μ. The continuum tree-level pion mass for twisted mass QCD is $M_\pi^2 = 2Bm_{\mathrm{P}}$. Counting the pion mass squared as $O(\epsilon^4)$ we immediately find

$$m_{\mathrm{P}} \sim O(\epsilon^4)\,. \tag{3.4}$$

This is the result that we would naively expect. With Wilson twisted mass fermions m_{P} plays the rôle of the physical quark mass, so the counting should be as for m in the untwisted case.[5] In terms of m and μ this corresponds to have either both masses of $\mathrm{O}(\epsilon^4)$ or at least one of them of $\mathrm{O}(\epsilon^4)$ and the other of even higher order (in case one of the two masses is significantly smaller than the other).

In our computations we will keep both masses to be of $\mathrm{O}(\epsilon^4)$. This choice allows us to keep the computation general and our final formulæ, expressed in terms of rescaled masses $z_m = m\Sigma V$ and $z_\mu = \mu\Sigma V$, are valid for arbitrary twist angles. In particular, our final results will account for the special cases $\omega = \pi/2$ (maximal twist) as well as for $\omega = 0$, where we reproduce the results for standard Wilson fermions obtained in [38, 39].

The counting rule for the lattice spacing a is now easily fixed. Quite generally, as in infinite volume, the power counting is determined by the relative size of a and the quark mass. Since the counting of m_{P} is fixed we obtain the counting for a. The arguments are just as in WChPT with untwisted masses [38, 39], in particular, we carry over the definitions for three different regimes:

$$\begin{aligned} \text{GSM regime}: &\quad a \sim \mathrm{O}(\epsilon^4)\,, \\ \text{GSM}^* \text{ regime}: &\quad a \sim \mathrm{O}(\epsilon^3)\,, \\ \text{Aoki regime}: &\quad a \sim \mathrm{O}(\epsilon^2)\,. \end{aligned} \tag{3.5}$$

[5] Notice that in the Aoki regime the situation can be more complicated, since the standard LO relation between the pion mass and the polar mass is modified by $\mathrm{O}(a^2)$ corrections.

Depending on the relative size of a and $m_{\rm P}$ one of these counting rules is applicable. The GSM and the Aoki regimes have also been introduced in infinite volume WChPT. The ϵ-expansion allows the introduction of the intermediate GSM* regime [39], which defines the "transition region" between the other two regimes [38].

In the ϵ-regime the topological charge plays a relevant rôle [55] and predictions in sectors of fixed topology can be given in the chiral effective theory. For Wilson-like fermions there is no unambiguous definition of the topological charge because the space of lattice gauge fields is connected and hence a division into topological sectors is somehow arbitrary. It is maybe possible, using the small real part of the eigenvalues of the Wilson operator, to have an operative definition of topology which leads to the correct continuum limit. Nevertheless in this work we concentrate on correlators where all sectors have been summed up also because numerical simulations are up to now not done at fixed topological charge.

3.2 Vacuum state and epsilon regime

A slightly unusual feature in twisted mass WChPT is the non-trivial ground state U_V, that is determined by a gap equation [35, 37]. U_V depends on the parameters m, μ and a, and this dependence affects observables when computed perturbatively. The reason is that U_V enters the calculation if we compute correlation functions perturbatively by a saddle point expansion of the path integral around U_V. In the following we want to argue that U_V is no longer needed in ϵ-regime calculations where one integrates exactly over the collective constant mode.

In chiral perturbation theory (continuum or on the lattice, with a twisted or untwisted mass) we are interested in correlation functions defined by a functional integral,

$$\langle \mathcal{O} \rangle \,=\, \frac{1}{\mathcal{Z}} \int \mathcal{D}[U]\, \mathcal{O}[U] e^{-S_\chi[U]}\,, \tag{3.6}$$

where S_χ is the effective action and $\mathcal{O}$ an effective (local) operator at a given order. $\mathcal{D}[U]$ denotes the measure for the path integral that needs to be properly defined [56, 57].

Suppose the effective action assumes its minimum for the constant field configuration $U = U_V$ and the integrand in (3.6) is strongly peaked around it. In this case we perform the standard saddle point expansion around U_V. We expand the field U by the familiar ansatz

$$U(x) \,=\, U_V \exp(i\pi^a(x)\sigma^a/F)\,, \tag{3.7}$$

and the measure is given by the formal product measure

$$\mathcal{D}[U] \,=\, \mathcal{D}[\pi], \tag{3.8}$$

leading to standard Gaussian integrals involving the propagator for the pion fields.

Alternatively, we may parametrize the U field by isolating the collective zero-mode field as it is done in ϵ-regime calculations. In this case we write

$$U(x) \,=\, U_V U_0 \exp(i\xi^a(x)\sigma^a/F)\,, \tag{3.9}$$

where the integration over U_0 is done exactly. The measure for this parametrization then reads [4, 52]

$$\mathcal{D}[U] = \mathrm{d}[U_0]\mathcal{D}[\xi][1 - B(\xi)]\,. \tag{3.10}$$

The measure factorizes and the correction $[1 - B(\xi)]$ can be exponentiated to give an effective action $S_{\mathrm{meas}}[\xi]$. In appendix A we give the explicit expression of $B(\xi)$ at $O(\epsilon^2)$. The main point here is that the measure $\mathrm{d}[U_0]$ for the constant mode is the standard Haar measure over the group manifold $\mathrm{SU}(N_f)$. Since it is left-invariant we can use $\mathrm{d}[U_0] = \mathrm{d}[U_V U_0]$ in computing the path integral. This implies, since we integrate over all constant fields, that the particular field U_V is irrelevant, and instead of (3.9) we can directly parametrize the fields according to

$$U(x) = U_0 \exp(i\xi^a(x)\sigma^a/F)\,, \tag{3.11}$$

just as one does in calculations with an untwisted mass term [38, 39]. To summarize: In contrast to twisted mass WChPT in infinite volume (or in the p-regime) the ground state and the gap equation do not play a special rôle in the epsilon regime.

3.3 Epsilon expansion of correlation functions

In the following sections we mainly use the notation of ref. [39]. In appendix C we briefly discuss how the final formulæ should be written using the notation of ref. [38].

The discussion of the ϵ-expansion of correlation functions can be carried over from ref. [38, 39]. It is based entirely on dimensional arguments and once m is replaced by m_{P} the entire discussion holds true for the twisted mass case. For this reason we do not repeat the arguments here but simply summarize the main results.

Correlation functions $\langle O_1(x)O_2(y)\rangle = \langle O_1 O_2\rangle$ (for notational simplicity we suppress the dependence on x, y) in WChPT are written as the sum of the corresponding continuum correlator plus a correction stemming from the nonzero lattice spacing,

$$\langle O_1 O_2\rangle_{\mathrm{WChPT}} = \langle O_1 O_2\rangle_{\mathrm{ct}} + \delta\langle O_1 O_2\rangle. \tag{3.12}$$

The correction $\delta\langle O_1 O_2\rangle$ receives contributions from both the effective action and the effective operator.

This correction is proportional to powers of the lattice spacing. At which order it contributes depends on the regime, cf. eq. (3.5).

In the GSM regime the correction starts with ϵ^4 higher than the continuum contribution. In other words, the lattice spacing first affects the correlators at NNLO. Working to NLO one can ignore the correction and the continuum results are the appropriate ones.

In the GSM* regime the lattice spacing corrections enter at NLO. However, at this order only the $\mathrm{O}(a^2)$ correction proportional to c_2 contributes. The corrections linear in a, stemming from the corrections in both the action and the effective operators, are suppressed by one more power of ϵ.[6]

[6] These corrections of $\mathrm{O}(am)$ for Wilson fermions have been computed in ref. [38] for the pseudoscalar and scalar two point functions.

Most pronounced are the corrections in the Aoki regime, where they contribute already to LO. In addition, the $O(a^2)$ correction in the chiral Lagrangian cannot be completely expanded, it provides a zero-mode contribution of order ϵ^0 that has to be treated exactly. As a result, the integrals over the constant mode are no longer the standard Bessel functions that one usually encounters in ϵ-regime calculations.

Notwithstanding the complications in the Aoki regime, the main conclusion one can draw is that the lattice spacing corrections are typically suppressed, in the GSM regime to NNLO. This suppression of the lattice spacing corrections is one of the main reasons for the belief that Wilson fermions (twisted or not) are still a good choice for ϵ-regime simulations despite their explicit chiral symmetry breaking.

4 Leading correction in the GSM* regime

4.1 Basic definitions

Lattice spacing corrections to correlation functions enter at NLO in the GSM* regime. As mentioned in the previous section, only the $O(a^2)$ term in the effective action contributes, and the NLO correction explicitly reads

$$\delta\langle O_1(x)O_2(y)\rangle\Big|_{\mathrm{GSM}^*,\mathrm{NLO}} = -\langle O^{\mathrm{LO}}_{1,\mathrm{ct}}(x)O^{\mathrm{LO}}_{2,\mathrm{ct}}(y)\delta S_{a^2}\rangle + \langle O^{\mathrm{LO}}_{1,\mathrm{ct}}(x)O^{\mathrm{LO}}_{2,\mathrm{ct}}(y)\rangle\langle\delta S_{a^2}\rangle\,. \quad (4.1)$$

The superscript "LO" in (4.1) refers to leading order in the ϵ-expansion. In the twisted basis the $O(a^2)$ term takes the same form as for standard Wilson fermions

$$\delta S_{a^2} = \frac{\rho}{16}(\mathrm{Tr}(U_0 + U_0^\dagger))^2\,, \quad (4.2)$$

where we introduced the dimensionless quantity

$$\rho = F^2 c_2 a^2 V\,. \quad (4.3)$$

The angled brackets in (4.1) stand for the functional integral over the non-constant fields $\xi^a(x)$ and the constant mode U_0. The integrals over the first ones are done perturbatively. This part is completely analogous to the untwisted case in ref. [38, 39], and we refer to appendix A for a collection of useful properties of the propagators.

The integral over the constant mode has to be done exactly, and here differences appear because of the twisted mass term μ. The integrals we encounter in the twisted basis are of the type

$$\langle g(U_0)\rangle = \frac{1}{Z_0}\int_{\mathrm{SU}(2)} \mathrm{d}[U_0]\, g(U_0)\, e^{\frac{z_m}{2}\mathrm{Tr}[U_0+U_0^\dagger]-i\frac{z_\mu}{2}\mathrm{Tr}[\sigma^3(U_0-U_0^\dagger)]}\,, \quad (4.4)$$

where Z_0 is the partition function, obtained with $g(U_0)\equiv 1$. The parameters z_m and z_μ are defined as[7]

$$z_m = m\Sigma V\,, \qquad z_\mu = \mu\Sigma V\,. \quad (4.5)$$

[7] z_m is the standard combination familiar from continuum ChPT, where it is usually denoted by μ. In order to avoid confusion with the twisted mass we had to change this notation.

For $z_\mu = 0$ the integral (4.4) reduces to the standard one for an untwisted mass term. In this case it leads to expressions involving modified Bessel functions $I_n(x)$ with integer index n.

The same is true for $z_\mu \neq 0$, although the integral looks superficially rather different. This is immediately seen after performing a field redefinition to the physical basis. Performing the axial rotation (2.5) and using the invariance of the Haar measure, $\mathrm{d}[U_0] = \mathrm{d}[WU_0W]$, eq. (4.4) can be written as

$$\langle g(U_0)\rangle = \frac{1}{Z_0}\int_{\mathrm{SU}(2)} \mathrm{d}[\widetilde{U_0}]\, g(W\widetilde{U_0}W)\, e^{\frac{z}{2}\mathrm{Tr}[\widetilde{U_0}+\widetilde{U_0}^\dagger]} \equiv \langle g(W\widetilde{U_0}W)\rangle_{\mathrm{phys}}\,, \tag{4.6}$$

where z in the exponent is now given by

$$z = m_{\mathrm{P}}\Sigma V = \sqrt{z_m^2 + z_\mu^2}. \tag{4.7}$$

The Boltzmann factor in the integrand assumes now the standard form with the polar mass m_{P} entering the exponent, hence the index 'phys' on the r.h.s of eq. (4.6). The representation (4.6) is particularly useful for doing actual calculations, since many results for integrals with untwisted masses can be taken over to the twisted mass case.

Note that twisted mass Wilson fermions break the SU(2) isospin symmetry to a residual U(1). This implies that completeness relations for SU(N_f) generators, which are repeatedly used in standard ϵ-regime calculations [52], cannot be applied in our case. This poses a slight computational nuisance but no serious difficulty. In appendix D we give an example for the computation of zero mode integrals in presence of isospin breaking.

We calculated the correction (4.1) for a variety of mesonic correlation functions. For the presentation of our results we find it useful to introduce the following notation. First, translation invariance allows us to write

$$\langle X^a(x)Y^b(y)\rangle = C^{ab}_{XY}(x-y)\,, \tag{4.8}$$

where X^a and Y^a represent one of the densities or currents listed in (2.9)–(2.12). We suppress the spacetime index in the currents and only make the isospin index explicit. The vector and axial correlators we consider in section 4.3.2 refer to the temporal component of the currents.

In the GSM* regime, $C^{ab}_{XY}(x-y)$ can be written through NLO as the sum of the continuum correlator and a correction proportional to a^2,

$$C^{ab}_{XY}(x-y) = C^{ab}_{XY,\mathrm{ct}}(x-y) + C^{ab}_{XY,a^2}(x-y)\,. \tag{4.9}$$

The continuum correlator (for generic N_f) at NLO can be found in the literature [52] (see also refs. [58] and [39]). Since we present our final results in the twisted basis, for the reader's convenience we collect a few relevant formulae and the expressions for the continuum parts of the correlation functions in the twisted basis in appendix B.

For the matching with numerical results obtained in lattice simulations one is often interested in the correlation function integrated over the spatial components,

$$C^{ab}_{XY}(t) = \int d^3\vec{x}\, C^{ab}_{XY}(x-y)\Big|_{y=0} = C^{ab}_{XY,\mathrm{ct}}(t) + C^{ab}_{XY,a^2}\,, \tag{4.10}$$

To the order we are working here the correction C^{ab}_{XY,a^2} is independent of t and only shifts the constant part of the continuum result.

4.2 The PCAC mass in the GSM* regime

The first observable we compute is the PCAC mass defined in (2.14). This allows us to express the results for other correlators as a function of $m_{\rm PCAC}$ instead of m (or, equivalently, as a function of ω instead of ω_0).

In the chiral effective theory we write the numerator in (2.14) as (no summation over the flavor index a, with a restricted to 1,2)

$$\begin{aligned}\langle \partial_\mu \mathcal{A}^a_\mu(x)\mathcal{P}^a(0)\rangle &= C_{\partial AP}(x)\,,\\ C_{\partial AP}(x) &= C_{\partial AP,\rm ct}(x) + C_{\partial AP,a^2}(x)\,,\end{aligned} \tag{4.11}$$

and similarly for $\langle \mathcal{P}^a(x)\mathcal{P}^a(0)\rangle$. To leading order in the ϵ-expansion we find

$$C_{\partial AP,\rm ct}(x) = \frac{\Sigma}{V}\frac{I_2(2z)}{I_1(2z)}\cos\omega_0\,, \tag{4.12}$$

$$C_{PP,\rm ct}(x) = \frac{\Sigma^2}{2}\frac{I_2(2z)}{zI_1(2z)}\,, \tag{4.13}$$

where z is defined in (4.7). Hence, for the PCAC mass we find the expected result

$$m^{\rm LO}_{\rm PCAC} = m_{\rm P}\cos\omega_0 = m\,. \tag{4.14}$$

Defining maximal twist by a vanishing PCAC mass is therefore equivalent to $m = 0$, at least to this order in the chiral expansion.

The leading correction in the GSM* regime is given by (4.1). The NLO result for the PCAC mass is then found to be

$$m^{\rm NLO}_{\rm PCAC} = m_{\rm P}\cos\omega_0\,(1+\rho\Delta_m) = m\,(1+\rho\Delta_m)\,, \tag{4.15}$$

$$\Delta_m = \frac{2}{z^2} - \frac{I_1(2z)}{zI_2(2z)}\,. \tag{4.16}$$

The main observation we can make is that the PCAC mass is still proportional to m. Consequently, maximal twist, given by a vanishing PCAC mass, is still equivalent to $m = 0$. This is perhaps better seen if we reformulate (4.16) in terms of the twist angles,

$$\tan\omega = (1-\rho\Delta_m)\,\tan\omega_0\,. \tag{4.17}$$

This implies that $\omega = \pi/2$ is equivalent to $\omega_0 = \pi/2$ at NLO. This is another way of saying that $m^{\rm NLO}_{\rm PCAC}$ vanishes if $m = 0$. Note that $\omega = \omega_0$ only for angles $\pm\pi/2$ and 0. For all other values full use of (4.17) has to be made.

Eq. (4.15) can be inverted to obtain m as a function of $m_{\rm PCAC}$,

$$m = m_{\rm PCAC}\,[1-\rho\Delta_m]\,, \tag{4.18}$$

where in the correction Δ_m we can use the LO result (4.14) and replace m by $m_{\rm PCAC}$. This is the result we already anticipated in eq. (2.15). In the following we will use it to express correlators as functions of $m_{\rm PCAC}$ instead of m.

4.3 Results

Our results are presented in terms of

$$z_m = m_{\rm PCAC}\Sigma V, \qquad z_\mu = \mu\Sigma V. \tag{4.19}$$

For z_m we keep the same symbol as in eq. (4.5), but we now substitute m with $m_{\rm PCAC}$ given in eq. (4.18). In order to make our formulae more readable we also use

$$z = \sqrt{z_\mu^2 + z_m^2}. \tag{4.20}$$

4.3.1 Scalar and pseudoscalar correlators

It is convenient to write the $\mathrm{O}(a^2)$ correction to the time correlator in eq. (4.10) in the form

$$C^{ab}_{PP,a^2} = \rho\frac{L^3\Sigma^2}{2}\Delta^{ab}_{PP}, \qquad C^{00}_{SS,a^2} = \rho\frac{L^3\Sigma^2}{2}\Delta^{00}_{SS}. \tag{4.21}$$

For the pseudoscalar correlator we obtain

$$\begin{aligned}\Delta^{11,22}_{PP} = \frac{1}{2z^5 I_1(2z)^2 I_2(2z)}\Big\{ & 4{z_m}^2\left({z_\mu}^2+{z_m}^2\right) I_1(2z)^3 + \\ & -z\left({z_\mu}^2+11{z_m}^2\right) I_2(2z)\, I_1(2z)^2 + \\ & +2\left(-2{z_m}^4+3{z_m}^2+{z_\mu}^2\left(1-2{z_m}^2\right)\right) I_2(2z)^2\, I_1(2z) + \\ & +z\left({z_\mu}^2+5{z_m}^2\right) I_2(2z)^3\Big\},\end{aligned} \tag{4.22}$$

$$\begin{aligned}\Delta^{33}_{PP} = \frac{1}{2z^7 I_1(2z)^2 I_2(2z)}\Big\{ & -4\left(-{z_m}^6+4{z_\mu}^2{z_m}^4+5{z_\mu}^4{z_m}^2\right) I_1(2z)^3 + \\ & +z\left(5{z_\mu}^4+42{z_m}^2{z_\mu}^2-11{z_m}^4\right) I_2(2z)\, I_1(2z)^2 + \\ & +2\left(-2{z_m}^6+3{z_m}^4+5{z_\mu}^4\left(2{z_m}^2-1\right)+{z_\mu}^2\left(8{z_m}^4-2{z_m}^2\right)\right) I_2(2z)^2\, I_1(2z) + \\ & +z\left(-3{z_\mu}^4-14{z_m}^2{z_\mu}^2+5{z_m}^4\right) I_2(2z)^3\Big\}.\end{aligned} \tag{4.23}$$

The Wilson untwisted case corresponds to $z_\mu = 0$. In this limit we obtain

$$\begin{aligned}\Delta^{ab}_{PP}\Big|_{\omega=0} = \frac{\delta^{ab}}{2z_m^3 I_1(2z_m)^2 I_2(2z_m)}\Big\{ & 4z_m^2 I_1(2z_m)^3 - 11 z_m I_2(2z_m) I_1(2z_m)^2 + \\ & +2\left(3-2z_m^2\right) I_2(2z_m)^2 I_1(2z_m) + 5 z_m I_2(2z_m)^3\Big\},\end{aligned} \tag{4.24}$$

which reproduces the result reported in [39] (eq. (4.46)) and [38] (eq. (4.4)).

The most interesting case is maximal twist, which is obtained for $z_m = 0$. In this case the results simplify to

$$\Delta^{11,22}_{PP}\Big|_{\omega=\pi/2} = \frac{-z_\mu I_1(2z_\mu)^2 + 2 I_2(2z_\mu) I_1(2z_\mu) + z_\mu I_2(2z_\mu)^2}{2{z_\mu}^3 I_1(2z_\mu)^2}, \tag{4.25}$$

$$\Delta^{33}_{PP}\Big|_{\omega=\pi/2} = \frac{5 z_\mu I_1(2z_\mu)^2 - 10 I_2(2z_\mu) I_1(2z_\mu) - 3 z_\mu I_2(2z_\mu)^2}{2 z_\mu^3 I_1(2z_\mu)^2}. \tag{4.26}$$

Notice that both corrections $\Delta_{PP}^{11,22}$ and Δ_{PP}^{33} are finite in the limit $z_\mu \to 0$.

The $\mathrm{O}(a^2)$ corrections for the scalar singlet and pseudoscalar correlators are related by

$$\frac{\Delta_{SS}^{00}}{4} + \sum_{a=1}^{3} \Delta_{PP}^{aa} = 0, \tag{4.27}$$

which is valid for generic twist angle, at least to this order in the chiral expansion. This result leads to a generalization of what has already been found for untwisted masses [38]: The combination

$$\frac{C_{SS}^{00}(t)}{4} + \sum_{a=1}^{3} C_{PP}^{aa}(t) \tag{4.28}$$

of correlation functions is free from $\mathrm{O}(a^2)$ corrections.

4.3.2 Axial and vector correlators

For the $\mathrm{O}(a^2)$ correction in eq. (4.10) to the time-component axial and vector correlators we find

$$C_{XY,a^2}^{ab} = -\rho \frac{F^2}{2T} \Delta_{XY}^{ab}, \qquad X, Y = A, V\,, \tag{4.29}$$

where Δ_{AA}^{ab} is given by

$$\begin{aligned}
\Delta_{AA}^{11,22} = \frac{1}{z^7 I_1(2z)^2 I_2(2z)} \Big\{ & 4\left(-{z_m}^6 + {z_\mu}^2 {z_m}^4 + 2{z_\mu}^4 {z_m}^2\right) I_1(2z)^3 + \\
& + z\left(-2{z_\mu}^4 - 15{z_m}^2 {z_\mu}^2 + 11{z_m}^4\right) I_2(2z)\, I_1(2z)^2 + \\
& - 2\left(-2{z_m}^6 + 3{z_m}^4 + {z_\mu}^4\left(4{z_m}^2 - 2\right) + {z_\mu}^2\left(2{z_m}^4 + {z_m}^2\right)\right) I_2(2z)^2\, I_1(2z) + \\
& + z\left({z_\mu}^4 + 4{z_m}^2 {z_\mu}^2 - 5{z_m}^4\right) I_2(2z)^3 \Big\},
\end{aligned} \tag{4.30}$$

$$\begin{aligned}
\Delta_{AA}^{33} = \frac{1}{z^5 I_1(2z)^2 I_2(2z)} \Big\{ & -4{z_m}^2 z^2 I_1(2z)^3 + z\left({z_\mu}^2 + 11{z_m}^2\right) I_2(2z)\, I_1(2z)^2 + \\
& + 2\left(\left(2{z_m}^2 - 1\right){z_\mu}^2 + {z_m}^2\left(2{z_m}^2 - 3\right)\right) I_2(2z)^2\, I_1(2z) - z\left({z_\mu}^2 + 5{z_m}^2\right) I_2(2z)^3 \Big\}.
\end{aligned} \tag{4.31}$$

Also in this case one can verify that for $z_\mu = 0$ one obtains the Wilson untwisted formula [39]

$$\Delta_{AA}^{ab}\Big|_{\omega=0} = -2\Delta_{PP}^{ab}\Big|_{\omega=0}. \tag{4.32}$$

At maximal twist we obtain

$$\Delta_{AA,\omega=\pi/2}^{11,22} = \frac{-2z_\mu I_1(2z_\mu)^2 + 4I_2(2z_\mu) I_1(2z_\mu) + z_\mu I_2(2z_\mu)^2}{z_\mu^3 I_1(2z_\mu)^2}, \tag{4.33}$$

$$\Delta_{AA,\omega=\pi/2}^{33} = \frac{z_\mu I_1(2z_\mu)^2 - 2I_2(2z_\mu) I_1(2z_\mu) - z_\mu I_2(2z_\mu)^2}{z_\mu^3 I_1(2z_\mu)^2}. \tag{4.34}$$

The $O(a^2)$ correction for the vector correlator is, up to a sign, the same as for the axial vector correlator,

$$\Delta^{ab}_{VV,a^2} = -\Delta^{ab}_{AA,a^2} \,. \tag{4.35}$$

This identity holds for generic twist angles and generalizes the result for untwisted masses [39]. An obvious consequence is that for correlation functions of right- and left-handed currents $J^a_{\mu,L,R} = \frac{1}{2}(V^a_\mu \pm A^a_\mu)$ the leading $O(a^2)$ corrections cancel. This follows from the fact that these currents do not contain zero modes at LO, hence the connected and disconnected contributions in eq. (4.1) cancel among each others.

4.4 Numerical estimates

For the correlators considered, the leading $O(a^2)$ correction in the GSM* regime is just a shift of the constant part. In order to get estimates for the size of these corrections in typical present-day simulations we look at the ratios

$$R^{ab}_{XY} = \left| \frac{C^{ab}_{XY,a^2}(T/2)}{C^{ab}_{XY,\mathrm{ct}}(T/2)} \right| . \tag{4.36}$$

These ratios are the relative shift of the correlators at the midpoint $t = T/2$.

Approximate values for the parameters entering the correlators are taken from the simulations of the ETM collaboration [26, 59]. We use $F = 90\,\mathrm{MeV}$ and $a = 0.063\,\mathrm{fm}$. For simplicity we assume a hypercubic lattice with $N_T = N_L = 24$, which corresponds to a box size $L = 1.512\,\mathrm{fm}$. This is rather small and the ϵ-expansion might not converge well, but here we are interested only in an estimate about the order of magnitude for the lattice spacing corrections.

The coefficient c_2 is estimated from the pion mass splitting together with the LO ChPT prediction $-2c_2a^2 = m^2_{\pi^\pm} - m^2_{\pi^0}$ [36]. The data for the charged and neutral pion masses in ref. [59] translates into $|c_2| \approx (600\ \mathrm{MeV})^4$. The error, however, is quite large because of the large statistical uncertainty in the determination of the neutral pion mass.[8] $|c_2| \approx (600\ \mathrm{MeV})^4$ implies $\rho \approx 0.75$. Although this is slightly large it is smaller than 1 and we may still count this as $O(\epsilon^2)$, as we should in the GSM* regime.

Figure 1 shows $R^{11,22}_{PP}, R^{33}_{PP}, R^{11,22}_{VV}$ and R^{33}_{VV} for maximal twist ($z_m = 0$) and $z = z_\mu$ values in the ϵ-regime. For $z_\mu = 1.0$ we find values less than 2.5 percent, decreasing to less than 2 percent for $z_\mu = 2.5$. The ratios for flavor index $a = b = 1, 2$ and $a = b = 3$ assume the same value for vanishing z_μ, since for vanishing twisted mass we restore isospin symmetry. At $z_\mu = 0$ the corrections are maximal but for small values z_μ we eventually enter the Aoki regime and our formulae cease to be valid.

The curves in figure 1 look qualitatively very similar to the ones for untwisted masses shown in ref. [39], although the decrease of the ratios for growing z_μ is slightly faster in the untwisted case.

[8] Note that the value for c_2 is not universal but depends on all the details of the lattice action chosen in the simulation. An analysis [60] of quenched twisted mass lattice data led to the value $c_2 \approx (300\ \mathrm{MeV})^4$.

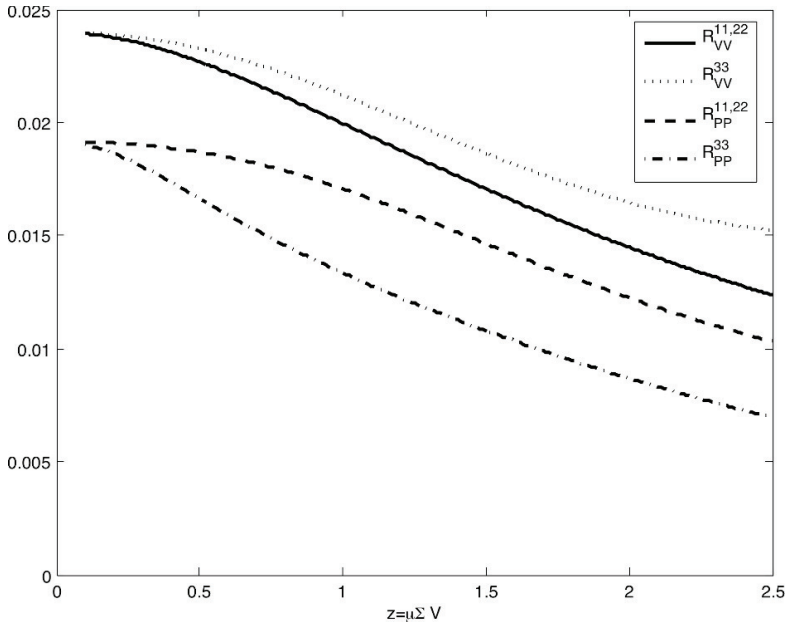

Figure 1. Ratios for the pseudoscalar and vector current correlators as a function of $z = z_\mu = \mu\Sigma V$.

Figure 2 shows the ratios involving the axial vector current, $R_{AA}^{11,22}$ and R_{AA}^{33}. The ratio R_{AA}^{33} shows a behavior similar to the ratios plotted in figure 1. In contrast, $R_{AA}^{11,22}$ increases with increasing z_μ, up to about 6 percent for $z_\mu = 2.5$. The reason for this somewhat odd feature is not that the $\mathrm{O}(a^2)$ corrections are larger for this particular correlator. The origin for the increase in $R_{AA}^{11,22}$ is the continuum correlator in the denominator of the ratio. $C_{AA,\mathrm{ct}}^{11,22}$ deceases much more rapidly with increasing z_μ than $C_{AA,a^2}^{11,22}$ in the numerator, leading to an increasing ratio $R_{AA}^{11,22}$. In fact, the result for $R_{AA}^{11,22}$ will eventually diverge for large z_μ where the continuum correlator has a zero. Notice that this happens in a region where $z \gg 1$ (at fixed volume), which is not expected to be in the domain of validity of the ϵ-expansion. Figure 3 shows directly the correlators $C_{AA}^{11,22}(T/2)$ and $C_{AA,\mathrm{ct}}^{11,22}(T/2)$, both divided by $(-F^2/T)$ in order to get dimensionless quantities. Obviously, the correlators are well behaved and $\mathrm{O}(a^2)$ correction gives a small and almost constant shift of the continuum result.

We conclude that, for our choice of parameters, the $\mathrm{O}(a^2)$ corrections to the correlators are at the few percent level, a small and probably negligible correction.

5 Concluding remarks

We have extended the framework of the $N_f = 2$ Wilson chiral effective theory in the ϵ-regime to the case of a twisted mass. By keeping the same power counting for the untwisted mass m and for the twisted mass μ, we have defined different regimes along the same lines as in the pure Wilson case [38, 39]. For quark masses of the order $a\Lambda_{\mathrm{QCD}}^2$ (GSM regime), the explicit breaking of chiral symmetry induced by the lattice spacing is strongly suppressed, and lattice artefacts appear only at NNLO in the epsilon expansion. On the other hand, if

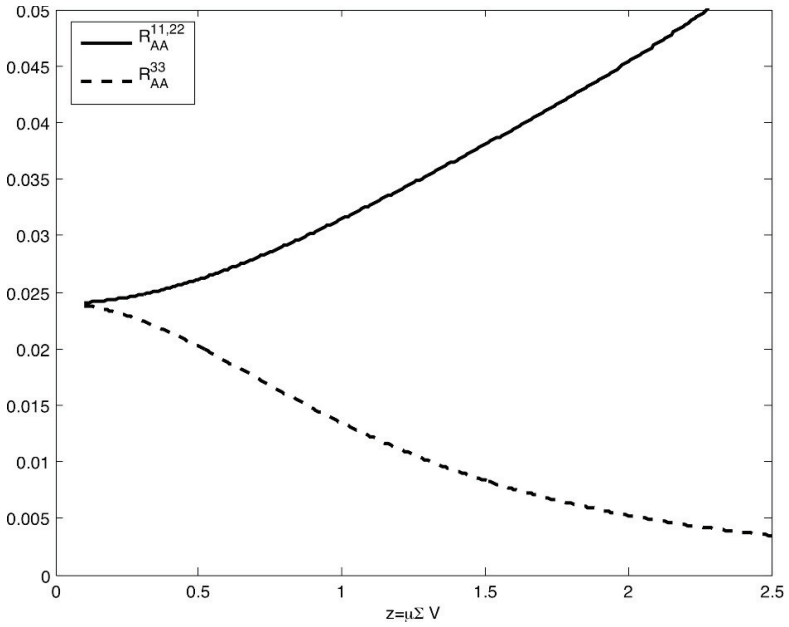

Figure 2. Ratios for the axial vector correlators as a function of $z = z_\mu = \mu\Sigma V$.

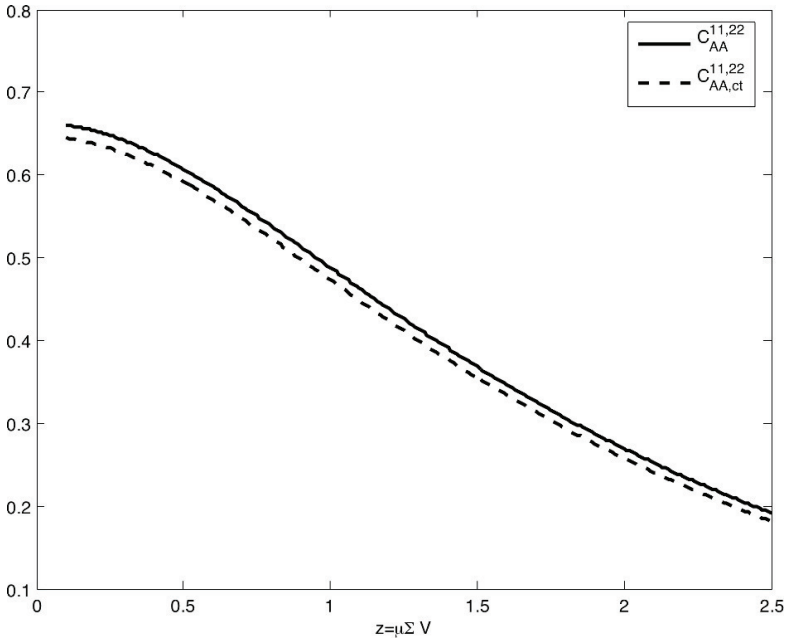

Figure 3. The axial vector correlator with $a = 1, 2$ (normalized by $-F^2/T$) as a function of $z = z_\mu = \mu\Sigma V$.

the quark masses are of order $a^2\Lambda^3_{\rm QCD}$ (Aoki regime), discretization effects appear already at LO. In this paper we have focused on the intermediate (GSM*) regime, where lattice artefacts start to contribute at NLO, which is the order at which the matching between lattice data and the chiral effective theory is usually performed. We have computed those

leading effects for several mesonic two-point functions (pseudoscalar, scalar singlet, axial and vector). The interesting feature of this regime is that only the $O(a^2)$ corrections in the chiral Lagrangian contribute. There is no proliferation of unknown couplings: apart from the continuum leading order couplings Σ and F, only an extra constant c_2 appears.

We have computed the leading $O(a^2)$ corrections to the PCAC quark mass and expressed the correlators as a function of the dimensionless variables $z_m = m_{\rm PCAC}\Sigma V$ and $z_\mu = \mu\Sigma V$. We have adopted the so-called twisted basis, where isospin breaking for non-zero twist angle explicitly shows up.

The final formulae we quote are valid for an arbitrary twist angle, and hence reproduce also the untwisted Wilson case considered in [38, 39], for $\omega = 0$ (equivalent to $\mu = 0$). A particularly interesting setup is maximal twist $\omega = \pi/2$, here defined by $m_{\rm PCAC} = 0$, where automatic $O(a)$ improvement occurs [50]. The numerical investigations performed in section 4.4 suggest that, like for untwisted Wilson fermions, for typical lattice parameters adopted in present-day simulations, the $O(a^2)$ corrections remain at the few percent level. This result supports the possibility to extract low-energy couplings with twisted mass Wilson fermions simulations in the ϵ-regime with controlled systematic errors. Notice, however, that it is not possible to predict a priori in which particular regime (GSM, Aoki) one actually has performed a simulation, and a scaling study is advocated.

We finally remark that a determination of the twist angle in the ϵ-regime might be numerically not so easy. To determine the actual value of ω with a reasonable accuracy the statistical and systematic uncertainties on the PCAC mass have to be ideally much smaller than the value of the twisted mass μ. In the ϵ-regime, where the value of the twisted mass could become comparable to the errors associated with the PCAC mass, this task could become extremely difficult. This fact could induce large uncertainties in the determination of the twist angle. A realistic procedure is to determine the twist angle from p-regime simulations [59, 61] where it is possible to keep the uncertainty on the twist angle well under control. The bare parameters tuned in the p-regime are then used in the ϵ regime. We expect that this choice will induce $O(a)$ corrections to the PCAC mass, which will not spoil automatic $O(a)$ improvement and the validity of the formulae given in this paper. An alternative procedure is to use correlation functions which are ω independent at the classical level. As we have seen in section 4.3 (cf. eqs. (4.27) and (4.35)) these particular linear combinations are ω independent also at NLO in the GSM* regime and additionally they are free from $O(a^2)$ corrections. This is an alternative procedure to analyze lattice data which is free from the uncertainties stemming from the determination of the twist angle and free from the $O(a^2)$ corrections affecting the standard correlation functions.

Acknowledgments

This work is partially supported by EC Sixth Framework Program under the contract MRTN-CT-2006-035482 (FLAVIAnet) and by the Deutsche Forschungsgemeinschaft (SFB/TR 09). A.S. acknowledges discussions with K. Jansen and C. Michael. A.S. would like to thank for the pleasant and stimulating atmosphere all the members of the Theoretical Division of the University of Liverpool, where a big part of this work has been done.

A.S. also acknowledges financial support from Spanish Consolider-Ingenio 2010 Programme CPAN (CSD 2007-00042) and from Comunidad Autónoma de Madrid, CAM under grant HEPHACOS P-ESP-00346.

A Selected formulae and definitions for the epsilon regime

In this appendix we briefly summarize formulae which are relevant for the computation of correlation functions in the ϵ-regime of chiral perturbation theory. For more details the reader can refer to [38, 39]. The pseudo Nambu-Goldstone bosons propagators for the nonzero modes is defined as

$$\bar{G}(x) = \frac{1}{V}\sum_{p\neq 0}\frac{e^{ipx}}{p^2}. \tag{A.1}$$

Following refs. [52, 54] we define

$$\bar{G}(0) \equiv -\frac{\beta_1}{\sqrt{V}}, \tag{A.2}$$

$$T\frac{d}{dT}\bar{G}(0) \equiv \frac{T^2 k_{00}}{V}, \tag{A.3}$$

where β_1 and k_{00} are finite dimensionless *shape coefficients* which depend on the geometry and can be evaluated numerically.

The integral over spatial components of the propagators $\bar{G}(x)$ yields the parabolic function $h_1(t/T)$:

$$\int d^3\vec{x}\,\bar{G}(x) = T h_1\left(\frac{t}{T}\right) = \frac{T}{2}\left[\left(\left|\frac{t}{T}\right| - \frac{1}{2}\right)^2 - \frac{1}{12}\right]. \tag{A.4}$$

Another quantity which appears frequently is the quark condensate at one loop, which for $N_f = 2$ is given by [52]

$$\Sigma_{\text{eff}} = \Sigma\left(1 + \frac{3}{2F^2}\frac{\beta_1}{\sqrt{V}}\right). \tag{A.5}$$

In the calculation of the NLO continuum correlators the measure factor in eq. (3.10) is needed at $O(\epsilon^2)$ [4, 52]:

$$B(\xi) = \frac{4}{3F^2V}\frac{1}{2}\int d^4x \mathrm{Tr}(\xi^a T^a \xi^b T^b). \tag{A.6}$$

B Continuum correlators in the twisted basis

In this appendix we summarize continuum formulæ for two-point functions in the twisted basis. For simplicity we introduce the function

$$L(x) = \frac{I_2(2x)}{xI_1(2x)}. \tag{B.1}$$

The results are given in terms of the variables

$$z_\mu = \mu\Sigma V, \quad z_m = m_{\text{PCAC}}\Sigma V, \quad z = \sqrt{z_\mu^2 + z_m^2}. \tag{B.2}$$

The pure Wilson case corresponds to $z_\mu = 0, z = z_m$, while the maximal twist is verified for $z_m = 0$, $z = z_\mu$. Each correlator consists of a constant part and on a time-dependent contribution; the time-dependence is represented by the function h_1 defined in eq. (A.4).

B.1 Scalar and pseudoscalar correlators

We write the continuum scalar singlet correlator as

$$C^{00}_{SS,ct}(t) = L^3 C^{00}_S + \alpha^{00}_S T h_1(t/T), \tag{B.3}$$

while for the pseudoscalar correlator we have

$$C^{ab}_{PP,ct}(t) = L^3 C^{ab}_P + \alpha^{ab}_P T h_1(t/T). \tag{B.4}$$

The coefficients C_{S^0}, α_{S^0},C^{ab}_P and α^{ab}_P are given by

$$C^{00}_S = 4\Sigma^2_{\text{eff}} \left[\frac{z_m^2}{z^2} - \frac{L(z_{\text{eff}})}{2} \left(1 - \frac{2(z_\mu^2 - z_m^2)}{z^2} \right) \right], \tag{B.5}$$

$$\alpha^{00}_S = 4\frac{\Sigma^2}{F^2} \left[\frac{z_\mu^2}{z^2} + \frac{L(z)}{2} \left(1 - \frac{2(z_\mu^2 - z_m^2)}{z^2} \right) \right], \tag{B.6}$$

$$C^{11,22}_P = \Sigma^2_{\text{eff}} \frac{L(z_{\text{eff}})}{2}, \tag{B.7}$$

$$C^{33}_P = \Sigma^2_{\text{eff}} \left[\frac{z_\mu^2}{z^2} - \frac{L(z_{\text{eff}})}{2} \left(1 + \frac{2(z_\mu^2 - z_m^2)}{z^2} \right) \right], \tag{B.8}$$

$$\alpha^{11,22}_P = \frac{\Sigma^2}{F^2} \left[1 - \frac{L(z)}{2} \right], \tag{B.9}$$

$$\alpha^{33}_P = \frac{\Sigma^2}{F^2} \left[\frac{z_m^2}{z^2} + \frac{L(z)}{2} \left(1 + \frac{2(z_\mu^2 - z_m^2)}{z^2} \right) \right]. \tag{B.10}$$

The subscript "eff" in z_{eff} indicates that Σ must be substituted by the one-loop corrected quark condensate Σ_{eff} given in eq. (A.5).

B.2 Axial and vector correlators

The continuum vector and axial correlators are given by

$$C^{ab}_{AA,VV,ct}(x-y) = -\frac{\alpha^{ab}_{A,V}}{T} + \frac{T}{V}\beta^{ab}_{A,V} k_{00} - \frac{T}{V}\gamma^{ab}_{A,V} h_1(t/T). \tag{B.11}$$

Here β_1 and k_{00} are familiar shape factors which depend on the geometry of the space-time volume. They are defined in eqs.(A.2), (A.3).

Explicit results for the coefficients are:

$$\alpha_A^{11,22} = F^2\left(\frac{z_m^2}{z^2} - \frac{z_m^2 - z_\mu^2}{z^2}L(z_{\text{eff}})\right) + \frac{2\beta_1}{\sqrt{V}}\left(\frac{z_m^2}{z^2} - \frac{z_m^2 - z_\mu^2}{z^2}L(z)\right), \tag{B.12}$$

$$\alpha_A^{33} = F^2\left(1 - L(z_{\text{eff}})\right) + \frac{2\beta_1}{\sqrt{V}}\left(1 - L(z)\right), \tag{B.13}$$

$$\beta_A^{11,22} = 2\left(\frac{z_\mu^2}{z^2} + \frac{z_m^2 - z_\mu^2}{z^2}L(z)\right), \tag{B.14}$$

$$\beta_A^{33} = 2L(z), \tag{B.15}$$

$$\gamma_A^{11,22} = 2z_m^2 L(z), \tag{B.16}$$

$$\gamma_A^{33} = 2z^2 L(z), \tag{B.17}$$

$$\alpha_V^{11,22} = F^2\left(\frac{z_\mu^2}{z^2} + \frac{z_m^2 - z_\mu^2}{z^2}L(z_{\text{eff}})\right) + \frac{2\beta_1}{\sqrt{V}}\left(\frac{z_\mu^2}{z^2} + \frac{z_m^2 - z_\mu^2}{z^2}L(z)\right), \tag{B.18}$$

$$\alpha_V^{33} = F^2 L(z_{\text{eff}}) + \frac{2\beta_1}{\sqrt{V}}L(z), \tag{B.19}$$

$$\beta_V^{11,22} = 2\left(\frac{z_m^2}{z^2} - \frac{z_m^2 - z_\mu^2}{z^2}L(z)\right), \tag{B.20}$$

$$\beta_V^{33} = 2\left(1 - L(z)\right), \tag{B.21}$$

$$\gamma_V^{11,22} = 2z_\mu^2 L(z), \tag{B.22}$$

$$\gamma_V^{33} = 0. \tag{B.23}$$

Also in this case, the subscript "eff" in z_{eff} indicates that Σ must be substituted by the one-loop corrected quark condensate Σ_{eff} given in eq. (A.5).

C Notations for comparison with ref. [38]

In ref. [38] a slightly different notation has been used in comparison with this work. Here we give a short summary of the main differences. In ref. [38] the variables z and z_2 have been introduced. They correspond respectively to $z_m/2$ (cf. eq. (4.5)) and $-\rho$ (cf. eq. (4.3)).

In the following for the z variables we will use the same notation adopted in the main text given in eqs. (4.19) and (4.20). The Bessel functions $I_n(x)$ translate to the function $X_n(x)$ used in [38] as

$$I_n = \frac{(x/2)^n}{\sqrt{\pi}\Gamma\left(n + 1/2\right)}X_n\,. \tag{C.1}$$

As examples we give here few ratios which typically appear in correlation functions

$$\frac{I_2}{I_1} = \frac{2z}{3}\frac{X_2}{X_1} = \frac{X_1'}{X_1}\,, \qquad \frac{I_3}{I_1} = \frac{4z^2}{15}\frac{X_2}{X_1}\,, \tag{C.2}$$

To conclude we find it useful to write the following correlation function

$$C_{PP}^{11}(t) = C_{PP,\text{ct}}^{11}(t) + C_{PP,a^2}^{11}\,. \tag{C.3}$$

with the notations of ref. [38]. We have

$$C^{11}_{PP,\mathrm{ct}}(t) = \frac{\Sigma^2_{\mathrm{eff}}}{3}\left\{\frac{X_2}{X_1} + \frac{3}{F^2}\left[1 - \frac{1}{3}\frac{X_2}{X_1}\right]\frac{T}{L^3}h_1(t/T)\right\} \tag{C.4}$$

and

$$\begin{aligned} C^{11}_{PP,a^2} = \frac{z_2 L^3\Sigma^2}{3}\Bigg\{ & 48\frac{z_m^2}{z^4} - \left(64\frac{z_m^2}{z^4} - 2\frac{z_m^2}{z^2}\right)\left(\frac{X_2}{X_1}\right) - \left(\frac{32}{3z^2} + \frac{z_m^2}{z^2} - \frac{z_\mu^2}{3z^2}\right)\left(\frac{X_2}{X_1}\right)^2 \\ & - 9\frac{z_m^2}{z^4}\left(\frac{X_1}{X_2}\right) - \left(\frac{z_m^2}{z^2} - \frac{z_\mu}{5z^2}\right)\left(\frac{X_3}{X_1}\right)\Bigg\} \end{aligned} \tag{C.5}$$

where $X_n = X_n(2z)$ with z defined in eq. (4.20).

D Example of group integrals with isospin breaking

In this appendix we show one of the procedures we have used to perform the zero-modes integrals with isospin breaking integrands. We use the example of calculating the expectation value $\langle \delta S_{a^2}\rangle$, which is part of the correction (4.1) we are interested in. To simplify the calculation we restrict ourselves to the case of maximal twist with $m = 0$, which nevertheless demonstrates the main idea. In this case the integral we have to perform reads (c.f. eqs. (4.2) and (4.4))

$$\langle \delta S_{a^2}\rangle = \frac{\rho}{16Z_0}\int \mathrm{d}[U_0](\mathrm{Tr}(U_0 + U_0^\dagger))^2 e^{-i\frac{z_\mu}{2}\mathrm{Tr}[\sigma^3(U_0 - U_0^\dagger)]}\,. \tag{D.1}$$

Performing the change of variables $U_0 \to i\sigma^3 U_0$ (which is equivalent to the rotation (2.5) with $\omega_0 = \pi/2$) this translates into

$$\langle \delta S_{a^2}\rangle = -\frac{\rho}{16Z_0}\int \mathrm{d}[U_0](\mathrm{Tr}(\sigma^3[U_0 - U_0^\dagger]))^2 e^{\frac{z_\mu}{2}\mathrm{Tr}[U_0 + U_0^\dagger]}\,. \tag{D.2}$$

If we use the parametrization

$$U_0 = \exp[i\phi\vec{n}\cdot\vec{\sigma}/2]\,, \tag{D.3}$$

($\phi \in [0, 2\pi]\,, |\vec{n}| = 1$) for the constant mode, the Haar measure reads

$$\mathrm{d}[U_0] = \frac{1}{4\pi^2}\mathrm{d}\phi\mathrm{d}\Omega\sin^2\frac{\phi}{2}\,, \tag{D.4}$$

with $\mathrm{d}\Omega = \mathrm{d}\Omega(\vec{n})$ being the measure of the 2-sphere, and the integral turns into

$$\langle \delta S_{a^2}\rangle = \rho\frac{1}{Z_0}\int \mathrm{d}[U_0] e^{2z_\mu\cos\phi}\sin^2\frac{\phi}{2}n_3^2\,. \tag{D.5}$$

The factor n_3^2 in the integrand is a remnant of isospin breaking. Without isospin breaking the integrals one faces involve functions of ϕ only, at least if various completeness relations for the group generators are used [52]. In this case the integration $\int \mathrm{d}\Omega$ gives a trivial

factor 4π and the remaining integral over ϕ leads to expressions involving modified Bessel functions. In order to make contact to these known integrals we write

$$\int_{S^2} \mathrm{d}\Omega\, n_3^2 = \frac{1}{3}\int_{S^2} \mathrm{d}\Omega, \tag{D.6}$$

and the integral we are interested in turns into

$$\langle \delta S_{a^2} \rangle = \frac{\rho}{3}\frac{1}{Z_0}\int \mathrm{d}[U_0] e^{2z_\mu \cos\phi} \sin^2\frac{\phi}{2}\,. \tag{D.7}$$

For the remaining integration over ϕ we write $\sin^2(\phi/2) = 1 - \cos^2(\phi/2) = 1 - (\mathrm{Tr}U_0)^2/4$, and we finally obtain

$$\langle \delta S_{a^2} \rangle = \frac{\rho}{3}\left[\langle 1\rangle_{\mathrm{phys}} - \frac{1}{4}\langle (\mathrm{Tr}U_0)^2\rangle_{\mathrm{phys}}\right]. \tag{D.8}$$

This is our desired result: The right hand side involves familiar integrals with the standard Boltzmann weight, c.f. (4.6) (as indicated by the subscript "phys"). A useful collection of relevant integrals is given in appendix B of ref. [39], which can be used to express (D.8) as

$$\langle \delta S_{a^2} \rangle = \rho \frac{1}{2z_\mu}\frac{I_2(2z_\mu)}{I_1(2z_\mu)}\,. \tag{D.9}$$

The same steps can be carried out in the calculation of correlators $\langle O_1^a O_2^b\rangle$. The integrand will be a product $f(\phi)p(n_3)$, where f is a function of ϕ only and p denotes a polynomial in n_3. Generalizing eq. (D.6), the integration over S^2 is trivial and gives a simple factor c_p,

$$\int_{S^2} \mathrm{d}\Omega\, p(n_3) = c_p \int_{S^2} \mathrm{d}\Omega. \tag{D.10}$$

The remaining integral can be expressed in terms of familiar integrals known from continuum ϵ-regime calculations without isospin breaking.

References

[1] E.E. Scholz, *Light hadron masses and decay constants*, arXiv:0911.2191 [SPIRES].

[2] C. Jung, *Status of dynamical ensemble generation*, arXiv:1001.0941 [SPIRES].

[3] J. Gasser and H. Leutwyler, *Light quarks at low temperatures*, *Phys. Lett.* **B 184** (1987) 83 [SPIRES].

[4] J. Gasser and H. Leutwyler, *Thermodynamics of chiral symmetry*, *Phys. Lett.* **B 188** (1987) 477 [SPIRES].

[5] P. Hernández, K. Jansen and L. Lellouch, *Finite-size scaling of the quark condensate in quenched lattice QCD*, *Phys. Lett.* **B 469** (1999) 198 [hep-lat/9907022] [SPIRES].

[6] MILC collaboration, T.A. DeGrand, *Another determination of the quark condensate from an overlap action*, *Phys. Rev.* **D 64** (2001) 117501 [hep-lat/0107014] [SPIRES].

[7] P. Hasenfratz, S. Hauswirth, T. Jörg, F. Niedermayer and K. Holland, *Testing the fixed-point QCD action and the construction of chiral currents*, *Nucl. Phys.* **B 643** (2002) 280 [hep-lat/0205010] [SPIRES].

[8] W. Bietenholz, T. Chiarappa, K. Jansen, K.I. Nagai and S. Shcheredin, *Axial correlation functions in the ϵ-regime: a numerical study with overlap fermions*, *JHEP* **02** (2004) 023 [hep-lat/0311012] [SPIRES].

[9] L. Giusti, P. Hernández, M. Laine, P. Weisz and H. Wittig, *Low-energy couplings of QCD from current correlators near the chiral limit*, *JHEP* **04** (2004) 013 [hep-lat/0402002] [SPIRES].

[10] H. Fukaya, S. Hashimoto and K. Ogawa, *Low-lying mode contribution to the quenched meson correlators in the ϵ-regime*, *Prog. Theor. Phys.* **114** (2005) 451 [hep-lat/0504018] [SPIRES].

[11] W. Bietenholz, T. Chiarappa, K. Jansen, K.I. Nagai and S. Shcheredin, *Simulating chiral quarks in the ϵ-regime of QCD*, *Nucl. Phys.* **A 755** (2005) 641 [hep-lat/0501012] [SPIRES].

[12] L. Giusti and S. Necco, *Spontaneous chiral symmetry breaking in QCD: a finite-size scaling study on the lattice*, *JHEP* **04** (2007) 090 [hep-lat/0702013] [SPIRES].

[13] L. Giusti et al., *Testing chiral effective theory with quenched lattice QCD*, *JHEP* **05** (2008) 024 [arXiv:0803.2772] [SPIRES].

[14] P.H. Ginsparg and K.G. Wilson, *A remnant of chiral symmetry on the lattice*, *Phys. Rev.* **D 25** (1982) 2649 [SPIRES].

[15] T. DeGrand, Z. Liu and S. Schaefer, *Quark condensate in two-flavor QCD*, *Phys. Rev.* **D 74** (2006) 094504 [*Erratum ibid.* **D 74** (2006) 099904] [hep-lat/0608019] [SPIRES].

[16] C.B. Lang, P. Majumdar and W. Ortner, *The condensate for two dynamical chirally improved quarks in QCD*, *Phys. Lett.* **B 649** (2007) 225 [hep-lat/0611010] [SPIRES].

[17] T. DeGrand and S. Schaefer, *Parameters of the lowest order chiral Lagrangian from fermion eigenvalues*, *Phys. Rev.* **D 76** (2007) 094509 [arXiv:0708.1731] [SPIRES].

[18] JLQCD collaboration, H. Fukaya et al., *Two-flavor lattice QCD simulation in the ϵ-regime with exact chiral symmetry*, *Phys. Rev. Lett.* **98** (2007) 172001 [hep-lat/0702003] [SPIRES].

[19] H. Fukaya et al., *Two-flavor lattice QCD in the ϵ-regime and chiral Random Matrix theory*, *Phys. Rev.* **D 76** (2007) 054503 [arXiv:0705.3322] [SPIRES].

[20] JLQCD collaboration, H. Fukaya et al., *Lattice study of meson correlators in the ϵ-regime of two-flavor QCD*, *Phys. Rev.* **D 77** (2008) 074503 [arXiv:0711.4965] [SPIRES].

[21] P. Hasenfratz et al., *2+1 flavor QCD simulated in the ϵ-regime in different topological sectors*, *JHEP* **11** (2009) 100 [arXiv:0707.0071] [SPIRES].

[22] JLQCD collaboration, H. Fukaya et al., *Determination of the chiral condensate from 2+1-flavor lattice QCD*, *Phys. Rev. Lett.* **104** (2010) 122002 [arXiv:0911.5555] [SPIRES].

[23] M. Lüscher, *Exact chiral symmetry on the lattice and the Ginsparg-Wilson relation*, *Phys. Lett.* **B 428** (1998) 342 [hep-lat/9802011] [SPIRES].

[24] K. Jansen, A. Nube, A. Shindler, C. Urbach and U. Wenger, *Exploring the ϵ-regime with twisted mass fermions*, PoS(LATTICE 2007)084 [arXiv:0711.1871] [SPIRES].

[25] K. Jansen, A. Nube and A. Shindler, *Wilson twisted mass fermions in the ϵ-regime*, PoS(LATTICE 2008)083 [arXiv:0810.0300] [SPIRES].

[26] K. Jansen and A. Shindler, *The ϵ-regime of chiral perturbation theory with Wilson-type fermions*, arXiv:0911.1931 [SPIRES].

[27] A. Hasenfratz, R. Hoffmann and S. Schaefer, *Reweighting towards the chiral limit*, *Phys. Rev.* **D 78** (2008) 014515 [arXiv:0805.2369] [SPIRES].

[28] A. Hasenfratz, R. Hoffmann and S. Schaefer, *Low energy chiral constants from ϵ-regime simulations with improved Wilson fermions*, *Phys. Rev.* **D 78** (2008) 054511 [arXiv:0806.4586] [SPIRES].

[29] M. Lüscher and F. Palombi, *Fluctuations and reweighting of the quark determinant on large lattices*, PoS(LATTICE 2008)049 [arXiv:0810.0946] [SPIRES].

[30] S.R. Sharpe and R.L. Singleton, Jr, *Spontaneous flavor and parity breaking with Wilson fermions*, *Phys. Rev.* **D 58** (1998) 074501 [hep-lat/9804028] [SPIRES].

[31] G. Rupak and N. Shoresh, *Chiral perturbation theory for the Wilson lattice action*, *Phys. Rev.* **D 66** (2002) 054503 [hep-lat/0201019] [SPIRES].

[32] G. Münster and C. Schmidt, *Chiral perturbation theory for lattice QCD with a twisted mass term*, *Europhys. Lett.* **66** (2004) 652 [hep-lat/0311032] [SPIRES].

[33] L. Scorzato, *Pion mass splitting and phase structure in twisted mass QCD*, *Eur. Phys. J.* **C 37** (2004) 445 [hep-lat/0407023] [SPIRES].

[34] S.R. Sharpe and J.M.S. Wu, *The phase diagram of twisted mass lattice QCD*, *Phys. Rev.* **D 70** (2004) 094029 [hep-lat/0407025] [SPIRES].

[35] S. Aoki and O. Bär, *Twisted-mass QCD, O(a) improvement and Wilson chiral perturbation theory*, *Phys. Rev.* **D 70** (2004) 116011 [hep-lat/0409006] [SPIRES].

[36] S.R. Sharpe and J.M.S. Wu, *Twisted mass chiral perturbation theory at next-to-leading order*, *Phys. Rev.* **D 71** (2005) 074501 [hep-lat/0411021] [SPIRES].

[37] S. Aoki and O. Bär, *Automatic O(a) improvement for twisted-mass QCD in the presence of spontaneous symmetry breaking*, *Phys. Rev.* **D 74** (2006) 034511 [hep-lat/0604018] [SPIRES].

[38] A. Shindler, *Observations on the Wilson fermions in the ϵ-regime*, *Phys. Lett.* **B 672** (2009) 82 [arXiv:0812.2251] [SPIRES].

[39] O. Bär, S. Necco and S. Schaefer, *The ϵ-regime with Wilson fermions*, *JHEP* **03** (2009) 006 [arXiv:0812.2403] [SPIRES].

[40] P.H. Damgaard, K. Splittorff and J.J.M. Verbaarschot, *Microscopic spectrum of the Wilson dirac operator*, arXiv:1001.2937 [SPIRES].

[41] S.R. Sharpe, *Applications of chiral perturbation theory to lattice QCD*, lectures given at *the Nara workshop*, October 31 — December 11 (2005), Nara, Japan hep-lat/0607016 [SPIRES].

[42] M. Golterman, *Applications of chiral perturbation theory to lattice QCD*, lectures given at *the 2009 Les Houches Summer School 'Modern perspectives in lattice QCD: Quantum field theory and high performance computing'*, arXiv:0912.4042 [SPIRES].

[43] ALPHA collaboration, R. Frezzotti, P.A. Grassi, S. Sint and P. Weisz, *Lattice QCD with a chirally twisted mass term*, *JHEP* **08** (2001) 058 [hep-lat/0101001] [SPIRES].

[44] A. Shindler, *Twisted mass lattice QCD*, *Phys. Rept.* **461** (2008) 37 [arXiv:0707.4093] [SPIRES].

[45] G. Münster, *On the phase structure of twisted mass lattice QCD*, *JHEP* **09** (2004) 035 [hep-lat/0407006] [SPIRES].

[46] O. Bär, G. Rupak and N. Shoresh, *Chiral perturbation theory at $O(a^2)$ for lattice QCD*, *Phys. Rev.* **D 70** (2004) 034508 [hep-lat/0306021] [SPIRES].

[47] S. Aoki, *Chiral perturbation theory with Wilson-type fermions including a^2 effects: $N_f = 2$ degenerate case*, *Phys. Rev.* **D 68** (2003) 054508 [hep-lat/0306027] [SPIRES].

[48] S. Aoki, O. Bär and B. Biedermann, *Pion scattering in Wilson ChPT*, *Phys. Rev.* **D 78** (2008) 114501 [arXiv:0806.4863] [SPIRES].

[49] S. Aoki, O. Bär and S.R. Sharpe, *Vector and axial currents in Wilson chiral perturbation theory*, *Phys. Rev.* **D 80** (2009) 014506 [arXiv:0905.0804] [SPIRES].

[50] R. Frezzotti and G.C. Rossi, *Chirally improving Wilson fermions. I: O(a) improvement*, *JHEP* **08** (2004) 007 [hep-lat/0306014] [SPIRES].

[51] J. Gasser and H. Leutwyler, *Spontaneously broken symmetries: effective Lagrangians at finite volume*, *Nucl. Phys.* **B 307** (1988) 763 [SPIRES].

[52] F.C. Hansen, *Finite size effects in spontaneously broken* $\mathrm{SU}(N) \times \mathrm{SU}(N)$ *theories*, *Nucl. Phys.* **B 345** (1990) 685 [SPIRES].

[53] F.C. Hansen and H. Leutwyler, *Charge correlations and topological susceptibility in QCD*, *Nucl. Phys.* **B 350** (1991) 201 [SPIRES].

[54] P. Hasenfratz and H. Leutwyler, *Goldstone boson related finite size effects in field theory and critical phenomena with O(N) symmetry*, *Nucl. Phys.* **B 343** (1990) 241 [SPIRES].

[55] H. Leutwyler and A.V. Smilga, *Spectrum of Dirac operator and role of winding number in QCD*, *Phys. Rev.* **D 46** (1992) 5607 [SPIRES].

[56] H. Leutwyler, *On the foundations of chiral perturbation theory*, *Ann. Phys.* **235** (1994) 165 [hep-ph/9311274] [SPIRES].

[57] D. Espriu and J. Matias, *Renormalization and the equivalence theorem: on-shell scheme*, *Phys. Rev.* **D 52** (1995) 6530 [hep-ph/9501279] [SPIRES].

[58] P.H. Damgaard, M.C. Diamantini, P. Hernández and K. Jansen, *Finite-size scaling of meson propagators*, *Nucl. Phys.* **B 629** (2002) 445 [hep-lat/0112016] [SPIRES].

[59] ETM collaboration, R. Baron et al., *Light meson physics from maximally twisted mass lattice QCD*, arXiv:0911.5061 [SPIRES].

[60] S. Aoki and O. Bär, *WChPT analysis of twisted mass lattice data*, *Eur. Phys. J.* **A 31** (2007) 481 [hep-lat/0610085] [SPIRES].

[61] ETM collaboration, P. Boucaud et al., *Dynamical twisted mass fermions with light quarks: simulation and analysis details*, *Comput. Phys. Commun.* **179** (2008) 695 [arXiv:0803.0224] [SPIRES].